



Universiteit
Leiden
The Netherlands

Illuminating N-acylethanolamine biosynthesis with new chemical tools

Mock, E.D.

Citation

Mock, E. D. (2019, November 6). *Illuminating N-acylethanolamine biosynthesis with new chemical tools*. Retrieved from <https://hdl.handle.net/1887/80154>

Version: Publisher's Version

License: [Licence agreement concerning inclusion of doctoral thesis in the Institutional Repository of the University of Leiden](#)

Downloaded from: <https://hdl.handle.net/1887/80154>

Note: To cite this publication please use the final published version (if applicable).

**Illuminating *N*-acylethanolamine biosynthesis
with new chemical tools**

PROEFSCHRIFT

ter verkrijging van

de graad van Doctor aan de Universiteit Leiden,

op gezag van Rector Magnificus prof. mr. C.J.J.M. Stolker,

volgens het besluit van het College voor Promoties

te verdedigen op woensdag 6 november 2019

klokke 15:00 uur

door

Elliot David Mock

geboren te Amsterdam in 1989

Promotiecommissie

Promotores: Prof. dr. M. van der Stelt
Prof. dr. C.A.A. van Boeckel

Overige leden: Prof. dr. H.S. Overkleeft
Prof. dr. J.M.F.G. Aerts
Prof. dr. C.J. Hillard
Medical College of Wisconsin, USA
Prof. dr. C.J. Schofield
Oxford University, UK
Dr. G.J.P. van Westen

The cover depicts the inhibitor **LEI-401** docked in a crystal structure of the enzyme NAPE-PLD (PDB: 4QN9).
Adapted from Magotti *et al.*, *Structure* (2015).

Sapere aude

Table of contents

| | |
|--|------------|
| Chapter 1 | 7 |
| Therapeutic opportunities of modulating the endogenous <i>N</i> -acylethanolamine tone | |
| Chapter 2 | 45 |
| High-throughput screening delivers new inhibitors for NAPE-PLD | |
| Chapter 3 | 63 |
| Optimization of pyrimidine-4-carboxamide NAPE-PLD inhibitors affords LEI-401 | |
| Chapter 4 | 131 |
| Photoaffinity probes for NAPE-PLD confirm LEI-401 target engagement | |
| Chapter 5 | 175 |
| LEI-401 is an <i>in vivo</i> active NAPE-PLD inhibitor that reduces brain anandamide levels and pain behavior | |
| Chapter 6 | 201 |
| Discovery and optimization of α -ketoamide inhibitors for the <i>N</i> -acyltransferase PLAAT2 | |
| Chapter 7 | 239 |
| Summary and future prospects | |
| Nederlandse Samenvatting | 264 |
| List of publications | 272 |
| Curriculum Vitae | 274 |
| Nawoord | 275 |

Chapter 1

Therapeutic opportunities of modulating the endogenous *N*-acylethanolamine tone

Over the past decades, lipids have emerged as important signaling molecules in health and disease. Lipid messengers come in a range of shapes and sizes and are classified in seven different categories: fatty acyls, glycerolipids, glycerophospholipids, sphingolipids, sterol lipids, prenol lipids, saccharolipids and polyketides.¹ Signaling lipids often exert their bioactivities through activation of various proteins, including G protein-coupled receptors (GPCRs), ion channels and nuclear receptors. Within the class of fatty acyl lipids, the *N*-acylethanolamines (NAEs) have garnered attention as a family of bioactive fatty acid amides with diverse roles in inflammation, neurotransmission, appetite, fertility, stress and anxiety. The NAEs incorporate saturated, mono- or polyunsaturated fatty acyl groups in their structures, which determines their signaling function. The most frequently occurring NAEs are *N*-palmitoylethanolamine (PEA), *N*-stearoylethanolamine (SEA), *N*-oleoylethanolamine (OEA), *N*-linoleoylethanolamine (LEA), *N*-arachidonoylethanolamine (AEA) and *N*-docosahexaenoylethanolamine (DHEA) (Table 1). At present, many outstanding questions exist with regard to the biological actions of NAEs. In this chapter,

an overview is provided of NAE biosynthesis and degradation, current understanding of their physiological functions and potential therapeutic applications of modulating the NAE tone.

Table 1. *N*-acylethanolamine (NAE) family members and their reported biological activities.

| Name | Structure | Receptor | Bioactivity |
|----------------------------|-----------|---|--|
| PEA (16:0) | | PPAR- α ² GPR55 ³ GPR119 ⁴ | Anti-inflammatory ⁵ Neuroprotective ⁶ Anti-epileptic ⁷ Analgesic ⁸ Anorectic ⁹ |
| SEA (18:0) | | GPR119 ⁴ | Anti-inflammatory ¹⁰ Anorectic ¹¹ |
| OEA (18:1- ω 9) | | PPAR- α ¹² GPR119 ⁴ | Anti-inflammatory ¹³ Anorectic ⁹ Analgesic ¹⁴ Neuroprotective ¹⁵ |
| LEA (18:2- ω 6) | | PPAR- α ¹⁶ GPR119 ¹⁷ | Anorectic ¹⁸ Neuroprotective ¹⁹ |
| AEA (20:4- ω 6) | | CB ₁ ²⁰ CB ₂ ²¹ TRPV1 ²² | Neurotransmission ²³ Orexigenic ²⁴ Analgesic ²⁵ Anxiolytic ²⁶ Memory formation ²⁷ Neuroprotective ²⁸ Fertility ²⁹ |
| DHEA (22:6- ω 3) | | GPR110 ³⁰ | Neurogenesis ³¹ Anti-inflammatory ³² |

Abbreviations: PEA = *N*-palmitoylethanolamine; SEA = *N*-stearoylethanolamine; OEA = *N*-oleoylethanolamine; LEA = *N*-linoleoylethanolamine; AEA = *N*-arachidonoylethanolamine; DHEA = *N*-docosahexaenoylethanolamine; PPAR- α = peroxisome proliferator-activated receptor α ; GPR55, 110 or 119 = G-protein coupled receptor 55, 110 or 119; CB_{1/2} = cannabinoid receptor 1 or 2; TRPV1 = transient receptor potential vanilloid 1.

1.1 NAE metabolism

In 1979, Schmid and co-workers reported the accumulation of NAEs in infarcted dog heart.³³ Shortly hereafter, the same lab showed that *N*-acylphosphatidylethanolamines (NAPEs), a previously unknown lipid class, were equally upregulated.³⁴ Due to the structural similarities of NAPEs and NAEs, a precursor-product relationship was

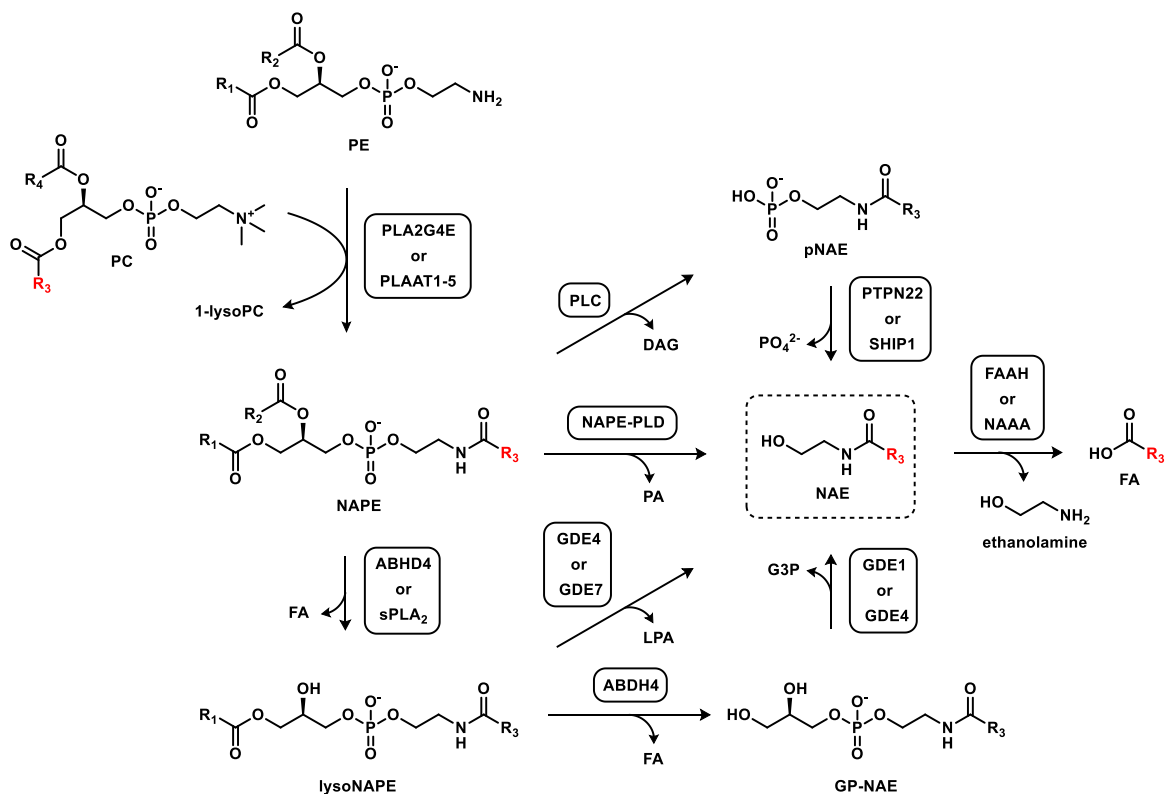


Figure 1. Biosynthetic pathways of *N*-acylethanolamines (NAEs). In total, four different enzymatic routes have been reported that can produce NAEs.³⁷ In the canonical pathway, *N*-acylphosphatidylethanolamine (NAPE) is formed from phosphatidylethanolamine (PE) and phosphatidylcholine (PC) catalyzed by phospholipase A₂ group IV E (PLA2G4E). This is followed by NAPE phospholipase D (NAPE-PLD)-mediated hydrolysis to NAE. Fatty acid amide hydrolase (FAAH) catabolizes NAEs into fatty acids (FAs) and ethanolamine. Abbreviations: PLAAT1-5 = phospholipase and acyltransferase 1-5; ABHD4 = α,β -hydrolase domain 4; GDE1, 4 or 7 = glycerophosphodiesterase 1, 4 or 7; PLC = phospholipase C; PTPN22 = protein tyrosine phosphatase non receptor type 22; SHIP1 = phosphatidylinositol 3,4,5-trisphosphate 5-phosphatase 1; NAAA = *N*-acylethanolamine acid amidase; GP-NAE = glycerophospho-*N*-acylethanolamine; 1-LPC = 1-lysophosphatidylcholine; LPA = lysophosphatidic acid; PA = phosphatidic acid; DAG = diacylglycerol; G3P = glycerol-3-phosphate; pNAE = phospho-*N*-acylethanolamine.

proposed.³⁵ Ensuing studies revealed that NAPEs are produced by the transfer of the sn-1 acyl group of phosphatidylcholine (PC) to the amine of phosphatidylethanolamine (PE), forming NAPE and 1-lysoPC (Figure 1).³⁶ Next, the phosphodiester bond of NAPE is hydrolyzed to generate NAE and phosphatidic acid (PA). Finally, the NAE is degraded to fatty acid (FA) and ethanolamine.

1.1.1 NAPE biosynthesis

The canonical acyl transfer reaction that produces NAPEs, is carried out by a Ca^{2+} -dependent *N*-acyltransferase (Ca-NAT). High Ca-NAT enzymatic activities were found in heart, brain and testis tissues.^{35,38,39} Remaining elusive for more than two decades, the serine hydrolase phospholipase A2 group IV E (PLA2G4E) was recently identified as a NAPE-generating Ca-NAT in cells, matching the reported expression and activity profile.⁴⁰ Also plasmalogen-type PEs, which incorporates a vinyl ether at the sn-1 position, were found to be suitable substrates for PLA2G4E, thereby producing plasmalogen-NAPEs (pNAPEs).⁴¹ pNAPEs are considered to be an important source of NAEs in the brain. In mouse brain, the total pNAPE amount was 4-fold higher than the NAPE content.⁴² In contrast, NAPEs were almost exclusively observed in the mucosal layer of rat jejunum, while in the serosal layer both NAPE and pNAPE species were abundant.⁴³ Interestingly, in rat brain lysate, Ca-NAT activity preferably generated *N*-arachidonoyl-containing (p)NAPEs with polyunsaturated acyl groups at the sn-2 position.⁴⁴ This may indicate that the Ca^{2+} -dependent generation of AEA favors polyunsaturated (p)NAPEs as precursors.⁴⁴

A second family of NATs was discovered that can produce NAPEs in a Ca^{2+} -independent manner, termed phospholipase and acyl transferase (PLAAT) 1-5.⁴⁵⁻⁵⁰ These enzymes belong to the cysteine hydrolases and show expression in the central nervous system (CNS) as well in peripheral tissues. In particular, PLAAT2 showed high *N*-acyltransferase activity, comparable to PLA2G4E.^{41,50} Also PLAAT2 accepted both PE and plasmalogen-type PE as substrates.⁴¹ Expression of PLAAT2 was found to be high in the liver, kidney, small intestine, colon, testis and trachea.^{47,51} This suggests that PLAAT2 may be involved in NAE biosynthesis in the gut. Notably, PLAAT2 expression was absent in rodents.⁴⁷ So far, no genetic or pharmacological tools have been described for the PLAAT family members. To what extent the Ca^{2+} -independent pathway contributes to NAPE and pNAPE biosynthesis *in vivo*, is therefore still unclear.³⁷

1.1.2 NAE biosynthesis

In 2004, the enzyme that produces NAEs in a single step from NAPEs or pNAPEs was identified as *N*-acylphosphatidylethanolamine phospholipase D (NAPE-PLD) (Figure 1).⁵² A crystal structure revealed that NAPE-PLD forms a membrane-bound homodimer with two Zn^{2+} -ions in its active site.⁵³ NAPE-PLD is classified as a metallo- β -lactamase and is distinct

from the PLD family.⁵² Brain, kidney and testis tissues were found to abundantly express NAPE-PLD.⁵² Interestingly, NAPE-PLD did not display any substrate preference *in vitro*.⁵⁴ Furthermore, PE increased the NAPE-PLD enzymatic activity, suggesting that the enzyme is constitutively active.⁵⁵ *In vitro*, NAPE-PLD activity was found to be elevated by specific bile acids, as well as polyamines such as spermine and spermidine.^{53,56,57} Multiple NAPE-PLD knockout (KO) studies described a significant reduction of saturated and unsaturated NAEs in the brains of mice.^{42,58,59} In accordance, NAPE and pNAPE precursors were greatly enhanced.^{42,58} However, levels of ω -6 and ω -3 polyunsaturated NAEs – AEA and DHEA, respectively – were not decreased in all KO strains.⁵⁸ It was therefore proposed that genetic deletion of NAPE-PLD stimulated compensatory mechanisms which counteract the reduction of AEA and DHEA content.⁵⁸ In peripheral organs such as heart, kidney, liver and jejunum, NAPE-PLD KO mice did not present decreased NAE levels, although NAPE concentrations were highly elevated, except for jejunum.⁶⁰ At present, the study of NAPE-PLD is hampered by a lack of *in vivo* active inhibitors which are needed to elucidate its role in NAE biosynthesis.

Three additional pathways have been discovered that can also produce NAEs (Figure 1). Firstly, two phospholipases were reported that can hydrolyze the fatty acyl esters of NAPEs. Three isoforms of secretory phospholipase A2 (sPLA₂-IB, IIA and V) were described to exclusively cleave the NAPE sn-2 ester to form lysoNAPE and a fatty acid.⁶¹ The serine hydrolase α , β -hydrolase domain 4 (ABHD4) performed the same reaction, but did not show any specificity towards the sn-1 or sn-2 ester.⁶² In addition, ABHD4 could hydrolyze the fatty acyl ester of lysoNAPE, generating glycerophospho-NAE (GP-NAE). This lipid species is converted by glycerophosphodiesterase 1 and 4 (GDE1/4) to afford NAE and glycerol-3-phosphate (G3P).^{63,64} A second pathway involves cleavage of the lysoNAPE phosphodiester by GDE4 or GDE7 in a lysoPLD-type reaction, producing NAE and lysophosphatidic acid (LPA).^{64,65} Expression of ABHD4 was found to be high in brain and testis, but not in heart.⁶² ABHD4 KO mice displayed decreased levels of GP-NAE and lyso-(p)NAPE in the brain, however NAE content, including AEA, was not reduced.⁶⁶ The activity of GDE1 was stimulated by Mg²⁺-ions and high protein expression levels were found in brain, testis, liver and kidney tissues.⁶³ Genetic deletion of GDE1 in mice also did not afford a significant decrease of brain NAE levels, therefore the physiological importance of this pathway for the formation of brain NAEs is still under debate.⁶⁷ The recently reported GDE4 and GDE7 enzymes, as well as the sPLA₂s have yet to be further characterized in KO models to establish their role in NAE biosynthesis *in vivo*.³⁷ It is interesting to note that the second product of the lysoPLD pathway is LPA, a bona fide signaling lipid in the CNS involved in cell proliferation and synaptic transmission.⁶⁸

A third NAE biosynthetic pathway was described to be important in macrophages, where lipopolysaccharide (LPS) induced elevation of AEA in a NAPE-PLD-independent manner.^{69,70} It was proposed that a yet unknown PLC-type enzyme hydrolyzes the phosphodiester of NAPE to produce phosphoNAE and diacylglycerol (DAG). Two phosphatases were identified, protein tyrosine phosphatase non-receptor type 22 (PTPN22) and phosphatidylinositol 3,4,5-trisphosphate 5-phosphatase 1 (SHIP1), that can catalyze the dephosphorylation of phosphoNAE to NAE and phosphate.^{69,71} Both PTPN22 and SHIP1 were induced in macrophages upon LPS stimulation. Incubation of phosphoNAE with brain tissue from PTPN22 KO mice demonstrated reduced conversion to AEA compared to wild-type (WT), that could indicate a possible role *in vivo*.⁶⁹

1.1.3 NAE degradation

The hydrolysis of NAE to fatty acid and ethanolamine can be performed by several enzymes (Figure 2).⁷² Fatty acid amide hydrolase (FAAH) displays specificity towards AEA over saturated and mono-unsaturated NAEs and has high expression in human brain, but is absent in heart tissue.⁷³ Genetic or pharmacological blockade of FAAH resulted in a large increase of brain AEA levels in mice, as well as smaller but significant increases of PEA and OEA.⁷⁴⁻⁷⁶ FAAH is therefore regarded as the primary AEA metabolizing enzyme in the brain. Surprisingly, in the liver, FAAH was found to catalyze the reverse reaction during liver regeneration which could be attributed to highly increased arachidonic acid levels, but not ethanolamine.⁷⁷ A second fatty acid amidase (FAAH-2) was identified that shares 20% sequence identity with FAAH.⁷⁸ FAAH-2 is specific for higher mammals including primates and marsupials and does not occur in rats or mice. It is expressed in peripheral organs such as heart and ovary. Whereas FAAH localizes to the endoplasmic reticulum in cells, FAAH-2 was reported to be enriched in lipid droplets.⁷⁹ Contrary to FAAH, FAAH-2 preferred primary fatty acid amides (*e.g.* oleamide) over NAEs as substrates.⁷⁸ A third NAE-hydrolyzing enzyme was described to be active in cells of the immune system.⁸⁰ *N*-acyl ethanolamine acid amidase (NAAA) is lysosomally located and preferentially hydrolyzes saturated NAE species.⁸¹ NAAA is an *N*-terminal cysteine hydrolase and shares no homology with FAAH (a serine hydrolase). Pharmacological inhibition of NAAA in mice induced significant elevations of brain PEA and OEA, but not AEA levels.⁸² The development of NAAA KO mice is necessary to confirm these findings.

Besides hydrolysis of the amide bond, polyunsaturated NAEs such as AEA and DHEA can undergo oxygenation of the double bonds which produces eicosanoid-type lipids (Figure 2). Each of these oxygenated products have reported lipid signaling functions of their own.^{83,84} Cyclooxygenase (COX)-2 was described to convert AEA to various prostaglandin-ethanolamides (PG-EA), a lipid class designated as prostamides.^{85,86} For

example, AEA cyclooxygenation by COX-2 followed by consecutive action of a PGF synthase produces $\text{PGF}_{2\alpha}$ -EA. Both these enzymes occur in the CNS and it is suggested that $\text{PGF}_{2\alpha}$ -EA is involved in inflammatory pain *in vivo*.^{87,88} Also lipoxygenases (LOX) are able to use AEA as a substrate, generating for example 12-hydroxyeicosatetraenoic acid-ethanolamide (12-HETE-EA).^{89,90} These oxygenated AEA derivatives inhibit FAAH and could therefore prolong NAE signaling.⁹¹ Lastly, epoxidation of AEA by cytochrome P450 enzymes can produce different epoxides such as 5,6-epoxyeicosatrienoic acid-ethanolamide (5,6-EET-EA).^{92,93} Since AEA is primarily hydrolyzed by FAAH and generally has low endogenous concentrations in most tissues, the biological importance of many of these oxygenated products is still unknown.⁸⁴

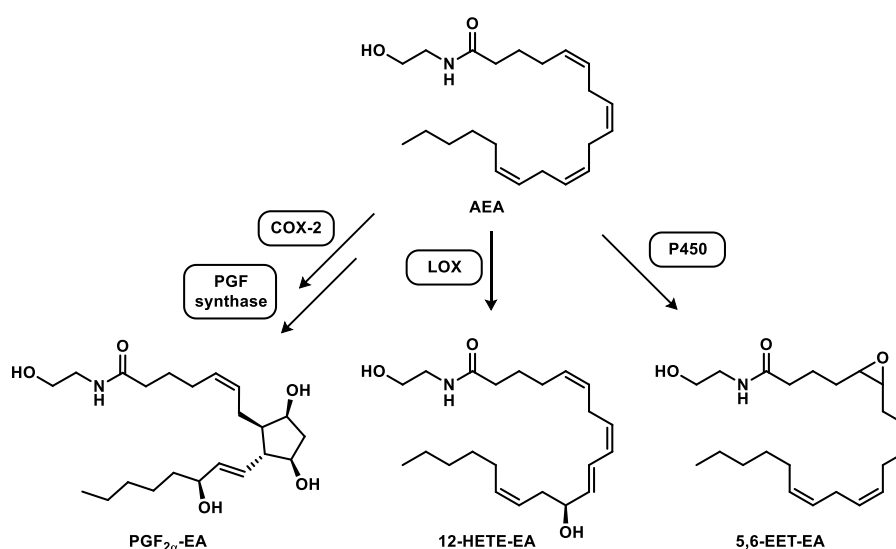


Figure 2. Oxidative degradation pathways of anandamide showing representative products. Cyclooxygenase 2 (COX-2) and prostaglandin synthases (*e.g.* PGF synthase) can convert AEA into prostamide-type lipids such as prostaglandin- $\text{F}_{2\alpha}$ -ethanolamide ($\text{PGF}_{2\alpha}$ -EA). Lipoxygenases (LOX) enzymes can hydroxylate AEA to form for example 12-hydroxyeicosatetraenoic acid-ethanolamide (12-HETE-EA). Cytochrome P450-type enzymes can produce various epoxygenated AEA derivatives such as 5,6-epoxyeicosatrienoic acid-ethanolamide (5,6-EET-EA).

1.2 Physiological functions of NAEs and (p)NAPEs

1.2.1 NAPE and pNAPE

NAPEs and pNAPEs are primarily considered to be precursors of NAEs. However, recent overviews have highlighted that (p)NAPEs may have biological functions of their own.^{94,95} These include putative roles in neuroprotection, anti-inflammation and satiety. During

cellular injury, NAPEs accumulate in damaged tissue, presumably due to an influx of calcium ions.^{96,97} This phenomenon has been observed in ischemia of the brain, heart and testis in various mammals such as mice, rats, dogs and humans.^{34,98-103} Also in plants NAPEs increase under cellular stress.^{94,104,105} Importantly, NAPE levels are higher than their corresponding NAE congeners in brain ischemia, which may suggest a neuroprotective function.¹⁰⁶ Conversion of PE to NAPE has a proposed membrane stabilizing role, possibly due to hydrogen bonding of the newly formed amide.^{107,108} NAPE-enriched liposomes were found to be less prone to dye leakage.¹⁰⁹ Furthermore, NAPEs induced membrane fusion in the presence of Ca²⁺-ions.^{110,111} This effect was found to be NAPE-specific as other anionic phospholipids such as phosphatidylserine (PS) and phosphatidylglycerol (PG) did not stimulate membrane fusion.¹¹⁰ The fusogenic properties of NAPE-liposomes have been exploited for drug delivery: liposomes incorporating the neuroprotective ganglioside GM1 were enriched in the brains of treated rats.¹¹² *N*-palmitoyl-PE-enriched liposomes decreased phagocytosis in mouse macrophages, thereby contributing to the termination of inflammation.¹¹³ In the rat jejunum, NAPE levels, specifically *N*-oleoyl-PE, were increased after feeding.^{43,114} NAPE has been described as a lipid hormone that can decrease food intake, while exogenous NAPE was able to induce weight loss in mice.¹¹⁵ However, following reports have contested this claim and point towards NAE metabolites as the cause of the observed anorectic effect.^{116,117} Collectively, these studies provide evidence for a putative biological role of NAPEs in neurodegeneration and inflammation. The molecular mechanisms through which NAPEs exert its bioactivities should therefore be addressed. Genetic or pharmacological tools that enable modulation of NAPE metabolic enzymes may help to answer these questions.

1.2.2 PEA

In the 1950s, PEA was the first member of the NAE family to be identified in egg yolk, soybean lecithin and later in mammalian tissues.^{118,119} It was immediately noted that PEA possessed anti-allergic and anti-inflammatory properties in a guinea pig model of anaphylactic arthritis.¹¹⁸ Following reports revealed that PEA also produces anti-epileptic, neuroprotective, analgesic and anorectic effects.^{7,9,120-123} During acute brain ischemia in rats, PEA levels increased 30-fold specifically in damaged brain areas.¹²⁴ Exogenous administration of PEA showed to be neuroprotective in various disease models such as traumatic brain injury, Parkinson's and Alzheimer's disease.¹²² Multiple biological targets have been identified for PEA that can explain its pharmacological effects.^{123,125} The nuclear receptor peroxisome proliferator-activated receptor (PPAR)- α was found to mediate the anti-inflammatory and analgesic effects of PEA.^{6,126} Furthermore, PEA displayed affinity for GPR119, a fat sensor in the gut, although OEA is regarded as a more potent agonist *in vivo*.^{4,127} Another receptor through which PEA can exert its bioactive

effects is GPR55, however these findings have been questioned in later studies.^{3,128} Today, PEA is marketed as a dietary supplement as well as a skin cream in many countries. Numerous clinical trials have been conducted with PEA for the treatment of pain, demonstrating that, overall, PEA produces few unwanted side effects and shows promise as an analgesic.⁸

1.2.3 SEA

Although SEA and PEA differ just two carbons in chain length, SEA has been studied far less extensively. This may be due to the fact that unlike PEA, SEA did not present affinity for PPAR- α .² Nevertheless, SEA showed affinity for GPR119 and shares several bioactivities with PEA.⁴ SEA produced anti-inflammatory effects in a mouse cutaneous anaphylaxis model.¹⁰ In rat brain, SEA levels were similar to PEA and showed a comparable 30-fold increase upon brain ischemia.¹²⁴ Furthermore, oral administration of SEA in mice produced an anorectic effect, presumably through increase of liver stearoyl-CoA desaturase-1 (SCD-1) mRNA expression.¹¹ These findings indicate that SEA may have therapeutic properties and the exclusion of this lipid species from NAE studies is unjustified. It is therefore recommended to include SEA in the standard NAE lipid panel to elucidate its biological role.

1.2.4 OEA

OEA is a well-studied member of the NAE family, especially in the gastrointestinal system. Upon oral administration in mice, OEA demonstrated anorectic effects that are mediated by peripheral PPAR- α .^{12,129,130} Of the NAE members, OEA showed the highest potency for PPAR- α .¹⁶ Endogenous OEA levels in the small intestine were markedly reduced in starved mice and significantly increased after refeeding compared to free-feeding mice.^{9,43,131} As such, OEA is regarded as a satiety factor that is released upon food intake.^{114,132} However, both short-term and chronic high fat diets were found to decrease levels of OEA in rat jejunum, but not in other tissues such as brain and liver.^{16,133} It was proposed that reduction in OEA levels may cause the reduced satiety and hyperphagia as seen in obesity.^{125,132} OEA also showed *in vitro* affinity for GPR119, a receptor that modulates feeding behavior.⁴ Nevertheless, OEA produced anorectic effects in both GPR119 WT and KO mice, indicating that *in vivo*, this activity is not required for satiety.¹³⁴ Similar to PEA, administration of OEA in rodents was reported to generate anti-inflammatory, neuroprotective and analgesic effects.¹³⁻¹⁵ These are likely mediated by activation of PPAR- α , although also PPAR- α -independent mechanisms have been described.^{126,135,136} In rat brain, OEA concentrations were found to be roughly one-third of PEA and SEA levels and showed a comparable 30-fold increase upon cerebral ischemia.¹²⁴ A putative

neuroprotective role for the NAE family was therefore hypothesized, acting via multiple molecular mechanisms.^{122,137}

1.2.5 LEA

LEA has received less attention compared to the other NAE family members, even though it possesses similar bioactivities as OEA and PEA. Importantly, endogenous levels of LEA in rat jejunum were found to be 4 to 6-fold higher than OEA, PEA and SEA upon fasting and refeeding.¹³¹ Intraperitoneal (i.p.) administration of LEA in rats elicited a reduction of food intake, which was dependent on PPAR- α activation and was comparable to OEA and PEA.^{9,16} Because of the high intestinal levels of LEA, it was proposed that the anorectic effect could also in part be mediated through GPR119, for which LEA shows equal activity as OEA.¹⁷ This has yet to be confirmed in genetically deleted GPR119 rodents. In a rat stroke model, treatment with exogenous LEA demonstrated a neuroprotective effect.¹⁹ Although endogenous LEA levels in rat brain accumulated 30-fold upon brain ischemia similar to PEA and SEA, the absolute concentrations were just 1% to 5% of saturated NAEs, suggesting only a minor role in the brain *in vivo*.¹²⁴

1.2.6 AEA

AEA or anandamide has been studied most extensively of all the NAE family members. In most tissues, AEA levels are 10 to 100 times lower than PEA, SEA and OEA.^{138,139} However, unlike other NAEs, AEA can activate the cannabinoid (CB₁)-receptor.²⁰ The CB₁ receptor is one of the most abundant GPCRs in the mammalian brain and is activated by (-)- Δ^9 -tetrahydrocannabinol (THC), the psychoactive component of cannabis. As a result, anandamide and 2-arachidonoylglycerol (2-AG), a second endogenous CB₁ receptor agonist, are termed endogenous cannabinoids or endocannabinoids. AEA is regarded as a tonic neuromodulator – *i.e.*, it continuously signals in the basal state – which is released by neurons upon Ca²⁺-stimulation and is quickly degraded by FAAH.^{23,140-142} Although AEA was initially described as a retrograde neurotransmitter, NAPE-PLD is localized presynaptically and FAAH postsynaptically, suggesting that AEA may function as an anterograde signaling lipid.¹⁴³ AEA can also act as an intracellular messenger, formed upon an influx of Ca²⁺-ions via activation of the G_q-pathway.¹⁴⁴

The word '*ananda*' – meaning bliss in Sanskrit – was aptly chosen, as increased AEA signaling produces analgesic, anxiolytic and anti-depressant effects through CB₁ receptor signaling in the brain.^{26,145,146} Conversely, acute and repeated stress exposure in rats afforded a decrease in AEA content in the amygdala, mediated by enhanced FAAH activity.¹⁴⁷ Stressed rats showed an inverse correlation between amygdalar AEA and plasma stress hormone levels (corticosterone).¹⁴⁸ Diminished brain AEA signaling upon repeated stress increased secretion of corticosterone.¹⁴⁹ In contrast, repeated stress

elevated amygdalar 2-AG levels, which attenuated hypothalamic-pituitary-adrenal (HPA) axis activation. AEA and 2-AG are therefore hypothesized to be the effectors of HPA-axis signaling in the brain, while having functionally distinct roles.^{149,150} In addition to its roles in modulating fear and stress behavior, AEA was reported to promote neuroprotection, memory formation and food intake via brain CB₁ receptor activation.^{27,28,151,152} Pharmacological studies in mice showed that exogenous AEA produces cannabimimetic responses, which are rapid in onset, but shorter and less potent than THC, presumably due to its fast metabolism.¹⁵³ Correspondingly, FAAH KO mice were supersensitive to AEA treatment.⁷⁴ Exogenous AEA administration in rats generated a central CB₁-receptor-dependent orexigenic (appetite-stimulating) effect similar to THC.²⁴

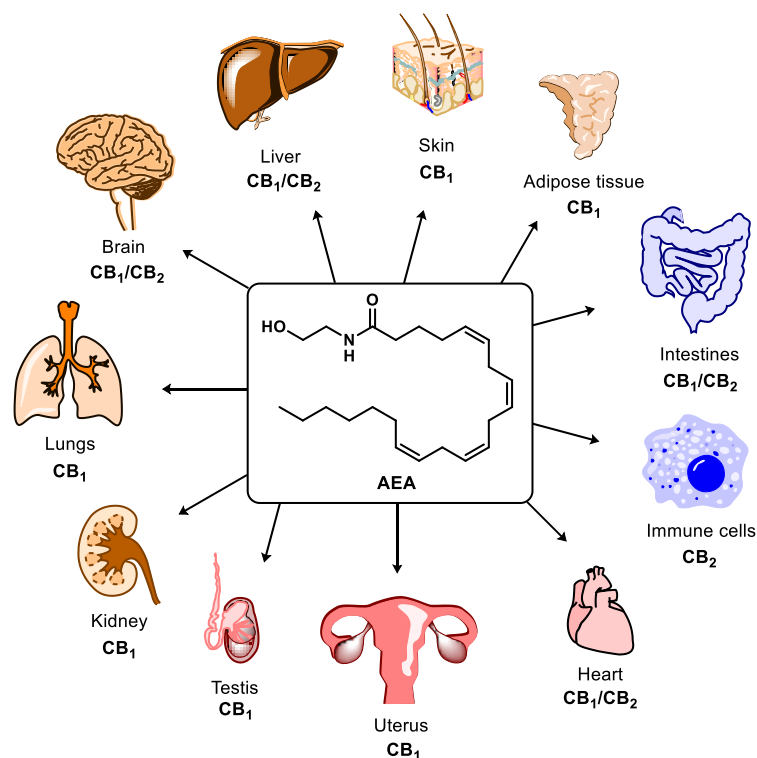


Figure 3. AEA is involved in cannabinoid receptor 1 and 2 (CB₁ and CB₂) signaling in both central and peripheral organs, of which several are depicted.¹⁵⁴

Anandamide has also been linked to CB₁ receptor signaling in the periphery, for instance in adipocytes, the female reproductive system and skin tissue where it is involved in energy expenditure, implantation and epidermal differentiation, respectively (Figure 3).^{154,155} Interestingly, peripheral CB₁ receptor activation is implicated in food intake as well, and intestinal AEA levels were found to be highly increased in starved mice.¹⁵⁶ Also

the analgesic effects of AEA were observed in the periphery, as peripheral blockade of FAAH produced antinociception via a CB₁ receptor-dependent mechanism.¹⁵⁷ Notably, the antinociceptive effect of AEA increased synergistically when combined with PEA in a mouse model of peripheral pain.²⁵

AEA has additionally been described as a partial agonist for the CB₂ receptor, which is primarily expressed in the immune system and is involved in the inflammatory response.^{21,158-160} Typically, AEA levels are 10- to 1000-fold lower compared to 2-AG in most tissues.¹³⁸ 2-AG has therefore been suggested to be the true endogenous CB₂ receptor ligand.¹⁶¹ Nevertheless, AEA was reported to modulate inflammation via activation of the CB₂ receptor by reducing pro-inflammatory cytokines in cells.^{154,162}

Besides the cannabinoid receptors, AEA also activates the transient receptor potential vanilloid 1 (TRPV1) ion channel.²² AEA has therefore been termed an endovanilloid.^{163,164} TRPV1, also known as the capsaicin receptor, is an important player in pain perception and is localized at peripheral sensory neurons.¹⁶⁵ Evidence is accumulating that TRPV1 is expressed in the CNS as well.^{166,167} The activation of TRPV1 by AEA causes an cellular influx of Ca²⁺-ions and has been linked to locomotor depression, hyperalgesia under inflammatory conditions, vasodilation and hypothermia.^{144,165}

1.2.7 DHEA

Over the past ten years, DHEA has come into view as a member of the NAE family with unique properties in neuronal signaling.³¹ As such, the name synaptamide was coined for its ability to induce neurogenesis.¹⁶⁸ Recently, DHEA was found to have nanomolar affinity for GPR110, an adhesion-type GPCR highly expressed in the hippocampus.³⁰ DHEA generated neurite outgrowth and synapse formation in neurons derived from WT mice, but not from GPR110 KO littermates. GPR110 KO mice showed reduced spatial memory and object recognition, but have yet to be profiled completely. DHEA has also been reported to have anti-inflammatory properties.^{32,169} In LPS-treated microglia and macrophage cells, DHEA reduced pro-inflammatory cytokines or eicosanoids, respectively.^{32,139} In addition, LPS-induced neuroinflammation in mice was significantly decreased after i.p. administration of DHEA. Brain DHEA levels are generally 2- to 10-fold higher than AEA, while the opposite is true for plasma.^{58,59,138,170} Furthermore, brain DHEA concentrations are linked directly with brain content of docosahexaenoic acid (DHA, 22:6), an ω -3 polyunsaturated fatty acid.¹⁷¹⁻¹⁷³ DHA is preferably acquired from the diet, but can also be synthesized from the essential fatty acid α -linolenic acid (18:3- ω 3).¹⁷⁴ The biosynthesis of DHEA is considered to follow the same route as other NAEs via formation of NAPE and hydrolysis by NAPE-PLD, which was confirmed in two NAPE-PLD KO mouse strains.^{42,59} A third NAPE-PLD KO mouse strain did not show a reduction of brain DHEA and

displayed elevated levels of brain DHEA upon administration of a fish oil diet rich in DHA.^{58,175} This suggests that alternative pathways are also involved in DHEA production in the brain.

Few studies have looked at the physiological role of DHEA in the periphery. It has been reported that under normal conditions, peripheral tissue levels of DHEA often exceed AEA, for example in the heart, kidney, jejunum and skin.^{60,176} GPR110 was found to be expressed in various peripheral organs including kidney, prostate and lung, which points to a possible role of DHEA signaling in these tissues.¹⁷⁷

1.3 Pharmacological modulation of NAE metabolism

As outlined in the prior section, NAEs possess desirable bioactivities that may be used for therapeutic intervention. Moreover, in certain pathological conditions NAE levels are disrupted, for example in cancer, obesity and neurodegenerative diseases and have been linked to disease progression and severity.¹⁷⁸⁻¹⁸⁰ Modulating the NAE tone could therefore be a viable treatment strategy for these pathologies. However, due to the polypharmacology of NAEs acting on multiple receptors that can have opposing outcomes, it is not always clear whether NAE levels should be enhanced or reduced.¹⁸¹ In the following section, a brief overview will be provided of the therapeutic potential of blockade of NAE degradation as well as its biosynthesis.

1.3.1 Inhibition of NAE degradation

After the discovery of the NAE-hydrolyzing enzyme FAAH in 1995, it became apparent that increasing NAE levels by genetic or pharmacological disruption of FAAH had profound effects on ECS signaling.¹⁸² To date, multiple research groups and pharmaceutical companies have developed *in vivo* active and brain penetrant FAAH inhibitors (Figure 4A).¹⁸³ Upon administration in rats or mice, the irreversible FAAH inhibitors URB597, PF-3845 and PF-04457845 increased AEA levels with 3- to 7-fold in brain and plasma, while PEA and OEA were also enhanced with 8- to 20-fold in the same tissues.^{26,75,184} Limited data is available of other NAE levels after FAAH inhibition, although one study reported that PF-3845 could similarly elevate SEA, LEA and DHEA levels with 5- to 20-fold in the brain, but in plasma only LEA and DHEA were increased.¹⁸⁵ Pre-clinical research in rodents revealed that inhibition of FAAH may be exploited for treatment of inflammatory or neuropathic pain, acting via central or peripheral CB₁ and CB₂ receptor activation.^{75,157,186,187} Furthermore, pharmacological FAAH disruption has shown promise for treating anxiety²⁶, depression¹⁴⁵, post-traumatic stress disorder¹⁸⁸, Parkinson's

disease¹⁸⁹, nausea¹⁹⁰, skin inflammation¹⁹¹, pruritus¹⁹², inflammatory bowel disease¹⁹², glaucoma¹⁹³, hypertension¹⁹⁴, traumatic brain injury¹⁹⁵, HIV-associated neurocognitive disorders¹⁹⁶ and multiple sclerosis-associated spasticity¹⁹⁷. Several FAAH inhibitors have been tested in Phase I and II clinical trials with mixed success.^{198,199} The selective inhibitor PF-04457845 was found to be well tolerated in healthy volunteers, completely blocked plasma FAAH activity and increased plasma AEA (10-fold), LEA (9-fold), OEA (6-fold) and PEA (3.5-fold) concentrations.²⁰⁰ However, in a subsequent Phase II clinical trial for osteoarthritic pain of the knee, PF-04457845 did not produce analgesia.²⁰¹ Recently, PF-04457845 was reported to be efficacious for the treatment of cannabis withdrawal symptoms in a Phase II clinical study.²⁰²

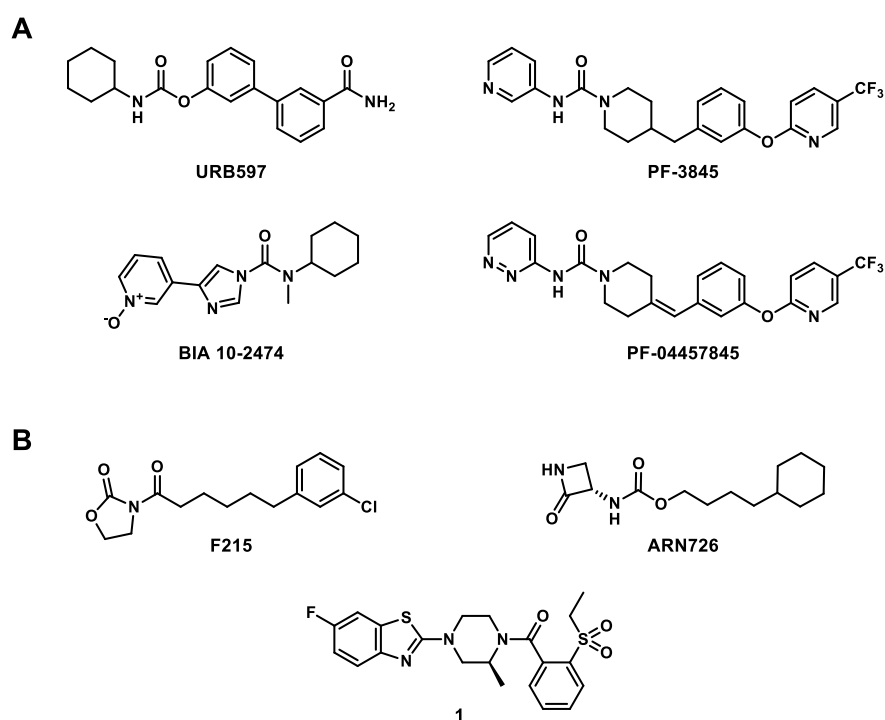


Figure 4. Structures of selected *in vivo* active inhibitors of **A)** fatty acid amide hydrolase (FAAH) or **B)** N-acyl ethanolamine acid amidase (NAAA).

In 2016, the covalent FAAH inhibitor BIA 10-2474 (Figure 4A) was tested in healthy volunteers in a Phase I clinical study, which led to the tragic death of one individual and mild-to-severe neurological symptoms in four others.²⁰³ It was later revealed that BIA 10-2474 displayed off-target activities against multiple serine hydrolases in the CNS, whereas PF-04457845 was highly selective for FAAH and did not present adverse effects in

multiple clinical studies.²⁰⁴ Accordingly, the observed neurotoxic side effects of BIA 10-2474 are presumed not to be caused by inhibition of FAAH.¹⁹⁹

Due to the limited success of FAAH inhibitors in the clinic, in recent years, inhibitors of the other NAE-hydrolyzing enzyme NAAA have come to the foreground.²⁰⁵ Several *in vivo* active NAAA inhibitors have been reported, showing encouraging results for the treatment of inflammatory and neuropathic pain, allergic dermatitis and multiple sclerosis.^{82,206-208} Considerable evidence point towards a PPAR- α -mediated mechanism.^{198,207,209} First generation irreversible NAAA inhibitors ARN276 and F215 (Figure 4B) were able to increase PEA and OEA concentrations 2- to 4-fold in lungs of mice after an inflammatory stimulus, but not in naïve mice.^{208,210} It is possible that these compounds elicit an inflammation-specific effect, although their low plasma stability and fast clearance could also explain the observed results.¹⁸³ Importantly, the increase of OEA illustrates the difference between *in vivo* and *in vitro* NAAA activity, since in the latter case NAAA showed high preference towards hydrolysis of PEA.⁸¹ A second generation reversible NAAA inhibitor (**1**, Figure 4B) presented improved drug-like properties and was able to elevate brain PEA and OEA levels (2-fold) of healthy mice, but not AEA.⁸² It is anticipated that the newly reported crystal structure of NAAA will aide future inhibitor design.²¹¹ In addition, the therapeutic exploitation of NAAA blockade will require KO mice to confirm the effects observed with pharmacological inhibitors.

1.3.2 Inhibition of NAE biosynthesis

Blocking NAE biosynthesis by pharmacological agents is an underdeveloped strategy in endocannabinoid research and so far no selective and *in vivo* active inhibitors have been described.²¹² Nevertheless, there is substantial evidence that reducing the NAE tone could be beneficial in pathological conditions such as obesity, metabolic syndrome, cancer and liver cirrhosis.¹⁸¹ The potential net effect of inhibiting NAE production would be indirect antagonism of the respective NAE receptors. Because the cannabinoid receptors, PPAR- α , TRPV1, GPR55, GPR110 and GPR119 have additional endogenous agonists besides the NAEs, this will likely lead to only partial receptor deactivation.¹⁹⁹ Here, different conditions are outlined where decreasing NAE levels could be of therapeutic value.

Obesity and metabolic syndrome

The endocannabinoid system is a key player in energy balance and food intake, both in the CNS and the periphery.²¹³ The centrally active CB₁ receptor antagonist rimonabant (Acomplia®, Figure 5) was clinically approved for treatment of obesity and metabolic syndrome, as it induced significant weight-loss, decreased food intake and improved insulin resistance.²¹⁴⁻²¹⁶ Unfortunately, patients treated with rimonabant suffered from depression-like side effects leading to its withdrawal from the market.^{217,218} Peripherally

restricted CB₁ receptor antagonists have shown comparable pre-clinical efficacy and are currently being pursued as potential anti-obesity drugs without psychiatric side effects.^{219,220} Alternatively, inhibiting NAE biosynthesis could be a possible therapeutic strategy. It has become increasingly clear from human studies and animal models that endocannabinoid and NAE signaling is disrupted during diet-induced obesity and metabolic disease.¹⁸⁰ Mice receiving a high fat diet for 18 weeks showed sustained elevation of plasma NAE levels including AEA, as well as increased expression of the NAE biosynthetic enzyme NAPE-PLD in brown adipose tissue.²²¹ In adipocytes, CB₁ receptor activation is associated with energy storage by increasing fatty acid uptake and lipogenesis and decreasing mitochondrial biogenesis, resulting in attenuated browning of white adipose tissue.^{213,222} In the liver, mice fed a high fat diet for 3 weeks developed steatosis and showed greatly increased hepatic AEA levels, but not 2-AG.²²³ This was credited to reduced FAAH activity, although NAPE-PLD activity was not determined. In the small intestine of rodents administered a high fat diet for 1 week, normal OEA mobilization after feeding was disrupted, possibly explaining the diminished satiety and hyperphagia observed in diet-induced obesity.^{16,125,133} Sham feeding of a lipid-based meal to rats for 5 days resulted in an increase of jejunal AEA and 2-AG levels, which was dependent on signaling of the vagus nerve.²²⁴ Enhanced NAPE-PLD and reduced FAAH activities in the jejunum were reported, yet interestingly, OEA levels were not affected. Peripheral CB₁ receptor blockade (URB447, Figure 5) attenuated fat sham feeding, which supports the hypothesis that endocannabinoids are released upon high fat food consumption and drive a positive feedback loop via CB₁ receptor signaling.²²⁴ In pancreatic islets, AEA content and NAPE-PLD gene expression was enhanced in fatty diabetic versus lean rats.²²⁵ It was shown that AEA induced apoptosis of insulin producing beta cells via peripheral CB₁ receptor activation, thereby enabling the progression of type II diabetes. Accordingly, chronic treatment with the peripherally restricted CB₁ receptor antagonist

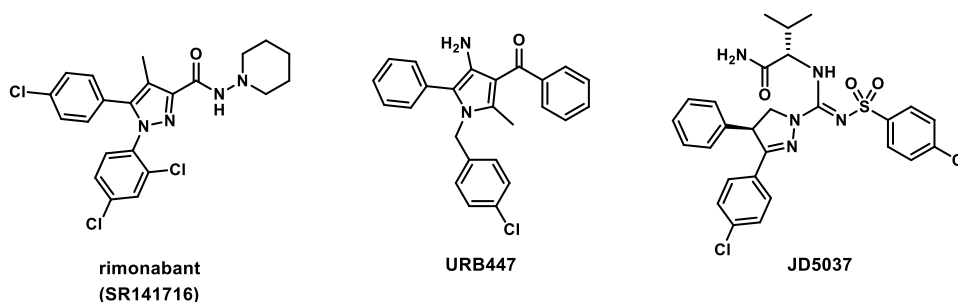


Figure 5. Structures of selected central (rimonabant) or peripherally restricted (URB447, JD5037) CB₁ receptor antagonists.

JD5037 (Figure 5) reversed islet elevation of AEA levels and NAPE-PLD expression and restored blood glucose levels to normal in overweight diabetic rats, although they remained insulin resistant.²²⁵

In humans, an analogous relationship between NAEs and obesity has been described. In a small human study (24 subjects), circulating AEA levels, but not 2-AG, peaked before a meal and significantly decreased postprandially in lean, but not in obese individuals.²²⁶ A larger human study (328 subjects) revealed that obesity is associated with an increased AEA tone in plasma, as well as altered circulatory PEA/AEA and OEA/AEA ratios, indicative of enhanced appetite and diminished satiety.²²⁷ In the same cohort, plasma 2-AG levels were not found to be upregulated in obese individuals.²²⁸ In another large human trial (997 subjects), circulating AEA concentrations were also associated with BMI.²²⁹ Furthermore, AEA correlated with non-alcoholic steatohepatitis (NASH) disease severity and was therefore proposed as a biomarker.²²⁹ These combined clinical and pre-clinical data suggest that lowering plasma AEA concentrations may offer a therapeutic opportunity for treatment of obesity, metabolic syndrome, type II diabetes and liver steatosis. At the same time, it is not yet known which organs contribute to circulatory NAEs, which needs to be addressed.²³⁰

Several studies have looked at the role of NAPE-PLD in energy metabolism. In a large human cohort, a common NAPE-PLD haplotype was described to be protective against severe obesity.²³¹ Mice with a genetic deletion of NAPE-PLD presented a reduced food intake and overall leaner phenotype than their WT littermates.¹⁷⁵ Of note, these effects were not observed in a different NAPE-PLD KO strain.²³² On the other hand, FAAH ablation in mice increased energy storage, body weight and adipose tissue and promoted the appetite-stimulating effect of AEA, rather than the OEA-induced satiety.²³³ These studies suggest that inhibition of NAPE-PLD may constitute as a potential treatment for metabolic syndrome. However, mice with a specific deletion of NAPE-PLD in adipose tissue had a predisposition for obesity while receiving a normal diet.²³⁴ When administered a high fat diet for 8 weeks, adipocyte NAPE-PLD KO mice showed increased body weight gain compared to WT. Notably, in both diets levels of the anorectic OEA, PEA and SEA were decreased in NAPE-PLD KO adipose tissue, but not of orexigenic AEA. A similar NAE profile was observed in WT mice receiving a high fat versus a control diet.²³⁴ Conditional KO of intestinal NAPE-PLD in mice induced hyperphagia upon initial high fat diet administration and exacerbated fat mass accumulation compared to WT mice.²³⁵ When receiving a normal diet, intestinal NAPE-PLD KO mice displayed reduced intestinal levels of AEA, OEA, PEA and SEA. In contrast, after 16 weeks of high fat diet, jejunal NAE concentrations in WT and intestinal NAPE-PLD KO mice did not significantly differ.²³⁵ Collectively, these data

indicate that NAPE-PLD functioning in the gut and adipose tissue is altered during obese conditions. It remains to be determined what the effect of global or peripheral pharmacological NAPE-PLD blockade will be on energy balance and food intake in metabolic syndrome and obesity.

Cancer

Multiple studies have reported disrupted NAE levels in cancer and associations between NAE receptors and tumor proliferation. Hepatic CB₁ receptor and NAPE-PLD expression as well as AEA concentrations were found to be elevated in hepatocellular carcinoma (HCC) both in humans and mice.²³⁶ Treatment with the peripherally restricted CB₁ receptor antagonist JD5037 or CB₁ receptor KO mice demonstrated suppressed tumor growth. These findings were underscored in a second study, showing that AEA acts as a tumor promotor in HCC via the CB₁ receptor.²³⁷ Accordingly, FAAH KO mice displayed a worsened tumor progression. In addition, human hepatic tumor tissue exhibited reduced FAAH expression.²³⁷ In chronic lymphocytic leukemia (CLL) patients, plasma levels of OEA were upregulated and correlated with the number of circulating tumor cells.²³⁸ After treatment with the chemotherapy drug lenalidomide, patients in clinical remission presented significantly reduced plasma OEA. Patient derived CLL cells expressed NAPE-PLD and a role for overproduction of OEA by these cells was proposed.²³⁸ Importantly, PPAR- α expression was found to be elevated in CLL patients and associated with an advanced disease stage.²³⁹ Furthermore, a PPAR- α antagonist was able to reduce tumor burden in a mouse model of CLL.²⁴⁰ Taken together, these studies suggest that targeting NAE biosynthetic enzymes, in particular NAPE-PLD, could have beneficial therapeutic effects in leukemia or hepatic cancer.

Chronic liver disease

Besides hepatic cancer and steatosis, also cirrhosis has been implicated in aberrant NAE signaling.²⁴¹⁻²⁴³ Liver cirrhosis is most often caused by alcohol abuse, hepatitis or steatosis and has a high mortality rate. In monocytes derived from humans and rats with cirrhotic liver, AEA levels were found to be elevated.^{244,245} Similar findings were observed in another study, reporting increased circulatory AEA, OEA and PEA levels in cirrhotic patients, which correlated with advanced disease stage.²⁴⁶ Hypertension of the portal vein is a major complication of advanced cirrhosis as a result of intrahepatic vascular resistance due to excessive scarring (fibrosis) and vasodilation in mesenteric arteries.²⁴³ AEA induced vasodilation in mesenteric vessels from cirrhotic rats, whereas control samples were less sensitive to AEA.²⁴⁷ Antagonists for the CB₁ receptor (rimonabant) or TRPV1 (capsazepine) blocked this effect.²⁴⁷ Accordingly, administration of rimonabant in cirrhotic rats decreased mesenteric blood flow and portal hypertension.²⁴⁵ CB₁ receptor expression is

low in healthy human liver, but it was upregulated in fibrotic and cirrhotic samples.²⁴⁸ Genetic deletion or pharmacological blockade of CB₁ receptors (rimonabant) reduced hepatic fibrogenesis in three different fibrotic rat models.²⁴⁸ This was extended to advanced cirrhotic rats, where treatment with rimonabant for two weeks reversed fibrosis.²⁴⁹

The relevant biosynthetic pathway of circulatory AEA in cirrhosis is still unknown. It is well established that cirrhotic patients have elevated plasma levels of endotoxins and increased hepatic macrophages.²⁵⁰⁻²⁵² LPS was reported to induce AEA production in mouse macrophages, which was dependent on the PLC/phosphatase biosynthetic pathway.^{69,71} In addition, pro-inflammatory stimuli such as LPS were found to downregulate NAPE-PLD expression in mouse macrophages, thereby reducing anti-inflammatory PEA concentrations.⁷⁰ To summarize, the described studies point towards pathological signaling of AEA in hepatic fibrosis and cirrhosis and suggest that blocking CB₁ receptor activation or AEA biosynthesis, possibly via the PLC/phosphatase pathway, could be of potential therapeutic benefit.

Reducing NAE levels in the brain?

In neurodegenerative diseases, for example multiple sclerosis and Parkinson's disease, AEA levels were found to be elevated in human cerebrospinal fluid.^{253,254} It is proposed that the AEA increase does not induce disease progression, but rather provides neuroprotection via CB₁ or CB₂ receptor activation as a result of the neuroinflammatory component of these diseases.^{179,255} Substantial evidence has been collected for the beneficial effects of CB₁ and CB₂ receptor signaling in CNS injury, however, several studies also point to a positive effect of CB₁ receptor inhibition.²⁵⁵ For example, CB₁ receptor blockade with rimonabant was neuroprotective in various rodent models of brain injury and enhanced AEA levels were harmful.^{124,256,257} OEA and PEA, which are more abundant in the brain, have neuroprotective or anti-inflammatory effects acting in part via PPAR- α .^{6,126} In a mouse model of cerebral ischemia, activation of brain PPAR- α by OEA reduced infarct volume.²⁵⁸ Currently, different strategies are being investigated that activate the cannabinoid and PPAR receptors by enhancing the NAE tone (*e.g.* FAAH inhibition) or by using CB₁/CB₂ agonists as therapeutic treatment for neurological conditions.¹⁹⁹ Recently, a frameshift variant of NAPE-PLD in several dog breeds was reported to be a risk factor for leukoencephalomyelopathy, a myelination disorder.²⁵⁹ The impact of this NAPE-PLD variant on the enzymatic activity or brain NAE concentrations, has yet to be determined.

NAE signaling in the brain is involved in numerous physiological processes, such as memory formation, stress and anxiety.¹⁵⁰ At present, the potential benefits of reducing NAE levels in the CNS are unclear.²⁶⁰ The depressive side effects associated with brain CB₁

receptor antagonism, suggest that depletion of tonic AEA signaling could have a similar negative outcome. Recently, two reports looked at selective overexpression of the AEA degrading enzyme FAAH in specific brain regions using a viral vector. In the hippocampus, this afforded an elevation of anxiety-like behavior and a deficit in object recognition memory and in extinction of aversive memory.²⁶¹ Interestingly, reduced NAE levels were observed for AEA and PEA, but not OEA. In contrast, FAAH overexpression in the amygdala produced an anxiolytic effect and decreased conditioned fear responses.²⁶² These studies indicate that depleting the brain NAE tone can have brain region-specific outcomes. The neurophysiological behavior of mice with a genetic deletion in one of the NAE-producing enzymes such as NAPE-PLD, ABHD4 and GDE1 have not yet been profiled, since brain AEA concentrations were not unambiguously reduced.³⁷ This highlights the need for centrally active NAE biosynthesis inhibitors, to expose the primary pathway of NAE and AEA generation, and to establish the effect of decreased NAE signaling.

1.4 Aim and outline of this thesis:

Selective and *in vivo* active pharmacological tools that modulate NAE biosynthetic enzymes are necessary to elucidate the importance of these pathways. Furthermore, reducing the NAE tone may hold promise for the treatment of several pathological conditions. So far, no inhibitors have been described that can decrease NAE levels in cells or live animals. The aim of this thesis work is the discovery and application of new chemical tools for two NAE-generating enzymes: NAPE-PLD and PLAAT2.

To obtain new molecules that can inhibit NAPE-PLD, in **Chapter 2**, a fluorescence-based activity assay for NAPE-PLD was optimized to enable high-throughput screening for hit identification. A library of ~350,000 compounds was screened. After multiple deselection rounds, five hit compounds were obtained with (sub)micromolar potency and reasonable physicochemical properties. Resynthesis and testing of the most promising hit – a pyrimidine-4-carboxamide – confirmed its activity for NAPE-PLD and provided a suitable starting point for the development of *in vivo* active NAPE-PLD inhibitors.

In **Chapter 3**, a library of pyrimidine-4-carboxamides was generated to increase the potency of the HTS-hit compound for NAPE-PLD and to improve its physicochemical properties. By modifying different substituents one at a time, a structure-activity relationship map was created. This afforded the optimized NAPE-PLD inhibitor **LEI-401** with nanomolar potency and favorable physicochemical features.

In drug discovery and development, establishing target engagement of a drug candidate and its intended protein target is an essential step for success in pre-clinical and clinical research. To assess whether **LEI-401** can bind to NAPE-PLD in live cells, in **Chapter 4**, a photoaffinity labeling approach was investigated. First, photoaffinity probes were synthesized that allowed visualization of NAPE-PLD using gel-based fluorescent labeling or chemical proteomics. Finally, cellular target engagement of **LEI-401** with NAPE-PLD was confirmed by performing competition experiments in the photoaffinity assay.

In **Chapter 5**, the NAPE-PLD inhibitor **LEI-401** was profiled in cellular and *in vivo* models to characterize its effect on NAE biosynthesis. In neuronal cells, **LEI-401** produced a marked reduction of multiple NAEs, including AEA, among a broad lipid panel. This effect was dependent on NAPE-PLD protein expression. Intraperitoneal administration in mice showed that **LEI-401** exhibited a good pharmacokinetic profile and passed the blood-brain barrier. A significant time- and dose-dependent decrease of AEA was observed in the brain, but not of other NAEs. Behavioral profiling in mice indicated that **LEI-401** produced hypomotility, antinociception and hypothermia. Also in a mouse model of inflammatory pain **LEI-401** elicited an analgesic effect. In short, **LEI-401** was identified as an *in vivo* active NAPE-PLD inhibitor, capable of decreasing brain AEA levels.

PLAAT2 is a Ca^{2+} -independent *N*-acyltransferase that was reported to produce high levels of NAEs in cells. In **Chapter 6**, α -ketoamide inhibitors were identified as PLAAT2 inhibitors through library screening with an activity-based probe. A structure-activity relationship analysis was performed, which yielded **LEI-301** as a nanomolar potent PLAAT2 inhibitor. **LEI-301** was able to significantly reduce NAE levels including AEA after PLAAT2 overexpression in cells.

Chapter 7 summarizes the work described in this thesis and provides new avenues for future research.

References

1. Fahy, E., Subramaniam, S., Murphy, R.C., Nishijima, M., Raetz, C.R.H., Shimizu, T., Spener, F., van Meer, G., Wakelam, M.J.O. & Dennis, E.A. Update of the LIPID MAPS comprehensive classification system for lipids. *Journal of Lipid Research* **50**, S9-S14 (2009).
2. Lo Verme, J., Fu, J., Astarita, G., La Rana, G., Russo, R., Calignano, A. & Piomelli, D. The nuclear receptor peroxisome proliferator-activated receptor- α mediates the anti-inflammatory actions of palmitoylethanolamide. *Molecular Pharmacology* **67**, 15-19 (2005).
3. Ryberg, E., Larsson, N., Sjögren, S., Hjorth, S., Hermansson, N.-O., Leonova, J., Elebring, T., Nilsson, K., Drmota, T. & Greasley, P.J. The orphan receptor GPR55 is a novel cannabinoid receptor. *British Journal of Pharmacology* **152**, 1092-1101 (2007).
4. Overton, H.A., Babbs, A.J., Doel, S.M., Fyfe, M.C.T., Gardner, L.S., Griffin, G., Jackson, H.C., Procter, M.J., Rasamison, C.M., Tang-Christensen, M., Widdowson, P.S., Williams, G.M. & Reynet, C. Deorphanization of a G protein-coupled receptor for oleoylethanolamide and its use in the discovery of small-molecule hypophagic agents. *Cell Metabolism* **3**, 167-175 (2006).
5. Didier, M.L., Severine, V., Kent-Olov, J. & Christopher, J.F. The palmitoylethanolamide family: a new class of anti-inflammatory agents? *Current Medicinal Chemistry* **9**, 663-674 (2002).
6. Hansen, H.S. Palmitoylethanolamide and other anandamide congeners. Proposed role in the diseased brain. *Experimental Neurology* **224**, 48-55 (2010).
7. Lambert, D.M., Vandevoorde, S., Diependaele, G., Govaerts, S.J. & Robert, A.R. Anticonvulsant activity of *N*-palmitoylethanolamide, a putative endocannabinoid, in mice. *Epilepsia* **42**, 321-327 (2001).
8. Gabrielsson, L., Mattsson, S. & Fowler, C.J. Palmitoylethanolamide for the treatment of pain: pharmacokinetics, safety and efficacy. *British Journal of Clinical Pharmacology* **82**, 932-942 (2016).
9. Rodríguez de Fonseca, F., Navarro, M., Gómez, R., Escuredo, L., Nava, F., Fu, J., Murillo-Rodríguez, E., Giuffrida, A., LoVerme, J., Gaetani, S., Kathuria, S., Gall, C. & Piomelli, D. An anorexic lipid mediator regulated by feeding. *Nature* **414**, 209-212 (2001).
10. Dalle Carbonare, M., Del Giudice, E., Stecca, A., Colavito, D., Fabris, M., D'Arrigo, A., Bernardini, D., Dam, M. & Leon, A. A saturated *N*-acylethanolamine other than *N*-palmitoyl ethanolamine with anti-inflammatory properties: a neglected story.... *Journal of Neuroendocrinology* **20**, 26-34 (2008).
11. Terrazzino, S., Berto, F., Carbonare, M.D., Fabris, M., Guiotto, A., Bernardini, D. & Leon, A. Stearoylethanolamide exerts anorexic effects in mice via down-regulation of liver stearoyl-coenzyme A desaturase-1 mRNA expression. *The FASEB Journal* **18**, 1580-1582 (2004).
12. Fu, J., Gaetani, S., Oveisi, F., Lo Verme, J., Serrano, A., Rodríguez de Fonseca, F., Rosengarth, A., Luecke, H., Di Giacomo, B., Tarzia, G. & Piomelli, D. Oleylethanolamide regulates feeding and body weight through activation of the nuclear receptor PPAR- α . *Nature* **425**, 90 (2003).
13. Rodríguez de Fonseca, F., Leza, J.C., Sayd, A., Antón, M., García-Bueno, B., Alén, F., Pavón, J., Caso, J.R. & Orío, L. Systemic administration of oleoylethanolamide protects from neuroinflammation and anhedonia induced by LPS in rats. *International Journal of Neuropsychopharmacology* **18** (2015).
14. Suardíaz, M., Estivill-Torrús, G., Goicoechea, C., Bilbao, A. & Rodríguez de Fonseca, F. Analgesic properties of oleoylethanolamide (OEA) in visceral and inflammatory pain. *PAIN* **133**, 99-110 (2007).
15. Gonzalez-Aparicio, R., Blanco, E., Serrano, A., Pavon, F.J., Parsons, L.H., Maldonado, R., Robledo, P., Fernandez-Espejo, E. & de Fonseca, F.R. The systemic administration of oleoylethanolamide exerts neuroprotection of the nigrostriatal system in experimental Parkinsonism. *International Journal of Neuropsychopharmacology* **17**, 455-468 (2014).
16. Artmann, A., Petersen, G., Hellgren, L.I., Boberg, J., Skonberg, C., Nellemann, C., Hansen, S.H. & Hansen, H.S. Influence of dietary fatty acids on endocannabinoid and *N*-acylethanolamine levels in rat brain, liver and small intestine. *Biochimica et Biophysica Acta (BBA) - Molecular and Cell Biology of Lipids* **1781**, 200-212 (2008).

17. Syed, S.K., Bui, H.H., Beavers, L.S., Farb, T.B., Ficorilli, J., Chesterfield, A.K., Kuo, M.-S., Bokvist, K., Barrett, D.G. & Efanov, A.M. Regulation of GPR119 receptor activity with endocannabinoid-like lipids. *American Journal of Physiology-Endocrinology and Metabolism* **303**, E1469-E1478 (2012).
18. Diep, T.A., Madsen, A.N., Holst, B., Kristiansen, M.M., Wellner, N., Hansen, S.H. & Hansen, H.S. Dietary fat decreases intestinal levels of the anorectic lipids through a fat sensor. *The FASEB Journal* **25**, 765-774 (2011).
19. Garg, P., Duncan, R.S., Kaja, S., Zabaneh, A., Chapman, K.D. & Koulen, P. Lauroylethanolamide and linoleoylethanolamide improve functional outcome in a rodent model for stroke. *Neuroscience Letters* **492**, 134-138 (2011).
20. Devane, W., Hanus, L., Breuer, A., Pertwee, R., Stevenson, L., Griffin, G., Gibson, D., Mandelbaum, A., Etinger, A. & Mechoulam, R. Isolation and structure of a brain constituent that binds to the cannabinoid receptor. *Science* **258**, 1946-1949 (1992).
21. Soethoudt, M., Grether, U., Fingerle, J., Grim, T.W., Fezza, F., de Petrocellis, L., Ullmer, C., Rothenhäusler, B., Perret, C., van Gils, N., Finlay, D., MacDonald, C., Chicca, A., Gens, M.D., Stuart, J., de Vries, H., Mastrangelo, N., Xia, L., Alachouzos, G., Baggelaar, M.P., Martella, A., Mock, E.D., Deng, H., Heitman, L.H., Connor, M., Di Marzo, V., Gertsch, J., Lichtman, A.H., Maccarrone, M., Pacher, P., Glass, M. & van der Stelt, M. Cannabinoid CB₂ receptor ligand profiling reveals biased signalling and off-target activity. *Nature Communications* **8**, 13958 (2017).
22. Zygmunt, P.M., Petersson, J., Andersson, D.A., Chuang, H.-h., Sjørgård, M., Di Marzo, V., Julius, D. & Högestätt, E.D. Vanilloid receptors on sensory nerves mediate the vasodilator action of anandamide. *Nature* **400**, 452-457 (1999).
23. Katona, I. & Freund, T.F. Multiple functions of endocannabinoid signaling in the brain. *Annual Review of Neuroscience* **35**, 529-558 (2012).
24. Williams, C.M. & Kirkham, T.C. Anandamide induces overeating: mediation by central cannabinoid (CB₁) receptors. *Psychopharmacology* **143**, 315-317 (1999).
25. Calignano, A., Rana, G.L., Giuffrida, A. & Piomelli, D. Control of pain initiation by endogenous cannabinoids. *Nature* **394**, 277-281 (1998).
26. Kathuria, S., Gaetani, S., Fegley, D., Valiño, F., Duranti, A., Tontini, A., Mor, M., Tarzia, G., Rana, G.L., Calignano, A., Giustino, A., Tattoli, M., Palmery, M., Cuomo, V. & Piomelli, D. Modulation of anxiety through blockade of anandamide hydrolysis. *Nature Medicine* **9**, 76 (2002).
27. Morena, M., Roozendaal, B., Trezza, V., Ratano, P., Peloso, A., Hauer, D., Atsak, P., Trabace, L., Cuomo, V., McGaugh, J.L., Schelling, G. & Campolongo, P. Endogenous cannabinoid release within prefrontal- limbic pathways affects memory consolidation of emotional training. *Proceedings of the National Academy of Sciences* **111**, 18333-18338 (2014).
28. Marsicano, G., Goodenough, S., Monory, K., Hermann, H., Eder, M., Cannich, A., Azad, S.C., Cascio, M.G., Gutiérrez, S.O., van der Stelt, M., López-Rodríguez, M.L., Casanova, E., Schütz, G., Zieglgänsberger, W., Di Marzo, V., Behl, C. & Lutz, B. CB₁ cannabinoid receptors and on-demand defense against excitotoxicity. *Science* **302**, 84-88 (2003).
29. Fernando, C., Manuel, L.W., Paula, V., Julieta, A. & Ana María, F. Endocannabinoid system and pregnancy. *Reproduction* **152**, R191-R200 (2016).
30. Lee, J.-W., Huang, B.X., Kwon, H., Rashid, M.A., Kharebava, G., Desai, A., Patnaik, S., Marugan, J. & Kim, H.-Y. Orphan GPR110 (ADGRF1) targeted by *N*-docosahexaenoylethanolamine in development of neurons and cognitive function. *Nature Communications* **7**, 13123 (2016).
31. Kim, H.-Y. & Spector, A.A. *N*-Docosahexaenoylethanolamine: A neurotrophic and neuroprotective metabolite of docosahexaenoic acid. *Molecular Aspects of Medicine* **64**, 34-44 (2018).
32. Park, T., Chen, H., Kevala, K., Lee, J.-W. & Kim, H.-Y. *N*-Docosahexaenoylethanolamine ameliorates LPS-induced neuroinflammation via cAMP/PKA-dependent signaling. *Journal of Neuroinflammation* **13**, 284 (2016).

33. Epps, D.E., Schmid, P.C., Natarajan, V. & Schmid, H.H.O. *N*-acylethanolamine accumulation in infarcted myocardium. *Biochemical and Biophysical Research Communications* **90**, 628-633 (1979).
34. Epps, D.E., Natarajan, V., Schmid, P.C. & Schmid, H.H.O. Accumulation of *N*-acylethanolamine glycerophospholipids in infarcted myocardium. *Biochimica et Biophysica Acta (BBA) - Lipids and Lipid Metabolism* **618**, 420-430 (1980).
35. Schmid, H.H.O., Schmid, P.C. & Natarajan, V. *N*-Acylated glycerophospholipids and their derivatives. *Progress in Lipid Research* **29**, 1-43 (1990).
36. Schmid, H.H.O. Pathways and mechanisms of *N*-acylethanolamine biosynthesis: can anandamide be generated selectively? *Chemistry and Physics of Lipids* **108**, 71-87 (2000).
37. Hussain, Z., Uyama, T., Tsuboi, K. & Ueda, N. Mammalian enzymes responsible for the biosynthesis of *N*-acylethanolamines. *Biochimica et Biophysica Acta (BBA) - Molecular and Cell Biology of Lipids* **1862**, 1546-1561 (2017).
38. Natarajan, V., Schmid, P.C., Reddy, P.V., Zuzarte-Augustin, M.L. & Schmid, H.H.O. Biosynthesis of *N*-acylethanolamine phospholipids by dog brain preparations. *Journal of Neurochemistry* **41**, 1303-1312 (1983).
39. Reddy, P.V., Natarajan, V., Schmid, P.C. & Schmid, H.H.O. *N*-acylation of dog heart ethanolamine phospholipids by transacylase activity. *Biochimica et Biophysica Acta (BBA) - Lipids and Lipid Metabolism* **750**, 472-480 (1983).
40. Ogura, Y., Parsons, W.H., Kamat, S.S. & Cravatt, B.F. A calcium-dependent acyltransferase that produces *N*-acyl phosphatidylethanolamines. *Nature Chemical Biology* **12**, 669 (2016).
41. Hussain, Z., Uyama, T., Kawai, K., Binte Mustafiz, S.S., Tsuboi, K., Araki, N. & Ueda, N. Phosphatidylserine-stimulated production of *N*-acyl-phosphatidylethanolamines by Ca²⁺-dependent *N*-acyltransferase. *Biochimica et Biophysica Acta (BBA) - Molecular and Cell Biology of Lipids* **1863**, 493-502 (2018).
42. Tsuboi, K., Okamoto, Y., Ikematsu, N., Inoue, M., Shimizu, Y., Uyama, T., Wang, J., Deutsch, D.G., Burns, M.P., Ulloa, N.M., Tokumura, A. & Ueda, N. Enzymatic formation of *N*-acylethanolamines from *N*-acylethanolamine plasmalogen through *N*-acylphosphatidylethanolamine-hydrolyzing phospholipase D-dependent and -independent pathways. *Biochimica et Biophysica Acta (BBA) - Molecular and Cell Biology of Lipids* **1811**, 565-577 (2011).
43. Fu, J., Astarita, G., Gaetani, S., Kim, J., Cravatt, B.F., Mackie, K. & Piomelli, D. Food intake regulates oleoylethanolamide formation and degradation in the proximal small intestine. *Journal of Biological Chemistry* **282**, 1518-1528 (2007).
44. Astarita, G., Ahmed, F. & Piomelli, D. Identification of biosynthetic precursors for the endocannabinoid anandamide in the rat brain. *Journal of Lipid Research* **49**, 48-57 (2008).
45. Jin, X.-H., Okamoto, Y., Morishita, J., Tsuboi, K., Tonai, T. & Ueda, N. Discovery and characterization of a Ca²⁺-independent phosphatidylethanolamine *N*-acyltransferase generating the anandamide precursor and its congeners. *Journal of Biological Chemistry* **282**, 3614-3623 (2007).
46. Jin, X.-H., Uyama, T., Wang, J., Okamoto, Y., Tonai, T. & Ueda, N. cDNA cloning and characterization of human and mouse Ca²⁺-independent phosphatidylethanolamine *N*-acyltransferases. *Biochimica et Biophysica Acta (BBA) - Molecular and Cell Biology of Lipids* **1791**, 32-38 (2009).
47. Uyama, T., Jin, X.-H., Tsuboi, K., Tonai, T. & Ueda, N. Characterization of the human tumor suppressors TIG3 and HRASLS2 as phospholipid-metabolizing enzymes. *Biochimica et Biophysica Acta (BBA) - Molecular and Cell Biology of Lipids* **1791**, 1114-1124 (2009).
48. Ueda, N., Tsuboi, K. & Uyama, T. Enzymological studies on the biosynthesis of *N*-acylethanolamines. *Biochimica et Biophysica Acta (BBA) - Molecular and Cell Biology of Lipids* **1801**, 1274-1285 (2010).
49. Shinohara, N., Uyama, T., Jin, X.-H., Tsuboi, K., Tonai, T., Houchi, H. & Ueda, N. Enzymological analysis of the tumor suppressor A-C1 reveals a novel group of phospholipid-metabolizing enzymes. *Journal of Lipid Research* **52**, 1927-1935 (2011).

50. Uyama, T., Ikematsu, N., Inoue, M., Shinohara, N., Jin, X.-H., Tsuboi, K., Tonai, T., Tokumura, A. & Ueda, N. Generation of *N*-acylphosphatidylethanolamine by members of the phospholipase A/acyltransferase (PLA/AT) family. *Journal of Biological Chemistry* **287**, 31905-31919 (2012).
51. Shyu, R.-Y., Hsieh, Y.-C., Tsai, F.-M., Wu, C.-C. & Jiang, S.-Y. Cloning and functional characterization of the HRASLS2 gene. *Amino Acids* **35**, 129-137 (2008).
52. Okamoto, Y., Morishita, J., Tsuboi, K., Tonai, T. & Ueda, N. Molecular characterization of a phospholipase D generating anandamide and its congeners. *Journal of Biological Chemistry* **279**, 5298-5305 (2004).
53. Magotti, P., Bauer, I., Igarashi, M., Babagoli, M., Marotta, R., Piomelli, D. & Garau, G. Structure of human *N*-acylphosphatidylethanolamine-hydrolyzing phospholipase D: regulation of fatty acid ethanolamide biosynthesis by bile acids. *Structure* **23**, 598-604 (2015).
54. Wang, J., Okamoto, Y., Morishita, J., Tsuboi, K., Miyatake, A. & Ueda, N. Functional analysis of the purified anandamide-generating phospholipase D as a member of the metallo- β -lactamase family. *Journal of Biological Chemistry* **281**, 12325-12335 (2006).
55. Wang, J., Okamoto, Y., Tsuboi, K. & Ueda, N. The stimulatory effect of phosphatidylethanolamine on *N*-acylphosphatidylethanolamine-hydrolyzing phospholipase D (NAPE-PLD). *Neuropharmacology* **54**, 8-15 (2008).
56. Margheritis, E., Castellani, B., Magotti, P., Peruzzi, S., Romeo, E., Natali, F., Mostarda, S., Gioiello, A., Piomelli, D. & Garau, G. Bile acid recognition by NAPE-PLD. *ACS Chemical Biology* **11**, 2908-2914 (2016).
57. Liu, Q., Tonai, T. & Ueda, N. Activation of *N*-acylethanolamine-releasing phospholipase D by polyamines. *Chemistry and Physics of Lipids* **115**, 77-84 (2002).
58. Leung, D., Saghatelian, A., Simon, G.M. & Cravatt, B.F. Inactivation of *N*-acyl phosphatidylethanolamine phospholipase D reveals multiple mechanisms for the biosynthesis of endocannabinoids. *Biochemistry* **45**, 4720-4726 (2006).
59. Leishman, E., Mackie, K., Luquet, S. & Bradshaw, H.B. Lipidomics profile of a NAPE-PLD KO mouse provides evidence of a broader role of this enzyme in lipid metabolism in the brain. *Biochimica et Biophysica Acta (BBA) - Molecular and Cell Biology of Lipids* **1861**, 491-500 (2016).
60. Inoue, M., Tanaka, T., Okamoto, Y., Tokumura, A., Tsuboi, K., Ueda, N., Uyama, T., Hidaka, M. & Tsutsumi, T. Peripheral tissue levels and molecular species compositions of *N*-acyl-phosphatidylethanolamine and its metabolites in mice lacking *N*-acyl-phosphatidylethanolamine-specific phospholipase D. *The Journal of Biochemistry* **162**, 449-458 (2017).
61. Sun, Y.X., Tsuboi, K., Okamoto, Y., Tonai, T., Murakami, M., Kudo, I. & Ueda, N. Biosynthesis of anandamide and *N*-palmitoylethanolamine by sequential actions of phospholipase A(2) and lysophospholipase D. *Biochemical Journal* **380**, 749-756 (2004).
62. Simon, G.M. & Cravatt, B.F. Endocannabinoid biosynthesis proceeding through glycerophospho-*N*-acyl ethanolamine and a role for α/β -hydrolase 4 in this pathway. *Journal of Biological Chemistry* **281**, 26465-26472 (2006).
63. Simon, G.M. & Cravatt, B.F. Anandamide biosynthesis catalyzed by the phosphodiesterase GDE1 and detection of glycerophospho-*N*-acyl ethanolamine precursors in mouse brain. *Journal of Biological Chemistry* **283**, 9341-9349 (2008).
64. Tsuboi, K., Okamoto, Y., Rahman, I.A.S., Uyama, T., Inoue, T., Tokumura, A. & Ueda, N. Glycerophosphodiesterase GDE4 as a novel lysophospholipase D: a possible involvement in bioactive *N*-acylethanolamine biosynthesis. *Biochimica et Biophysica Acta (BBA) - Molecular and Cell Biology of Lipids* **1851**, 537-548 (2015).
65. Rahman, I.A.S., Tsuboi, K., Hussain, Z., Yamashita, R., Okamoto, Y., Uyama, T., Yamazaki, N., Tanaka, T., Tokumura, A. & Ueda, N. Calcium-dependent generation of *N*-acylethanolamines and lysophosphatidic acids by glycerophosphodiesterase GDE7. *Biochimica et Biophysica Acta (BBA) - Molecular and Cell Biology of Lipids* **1861**, 1881-1892 (2016).

66. Lee, H.-C., Simon, G.M. & Cravatt, B.F. ABHD4 regulates multiple classes of *N*-acyl phospholipids in the mammalian central nervous system. *Biochemistry* **54**, 2539-2549 (2015).
67. Simon, G.M. & Cravatt, B.F. Characterization of mice lacking candidate *N*-acyl ethanolamine biosynthetic enzymes provides evidence for multiple pathways that contribute to endocannabinoid production in vivo. *Molecular BioSystems* **6**, 1411-1418 (2010).
68. Yung, Yun C., Stoddard, Nicole C., Mirendil, H. & Chun, J. Lysophosphatidic acid signaling in the nervous system. *Neuron* **85**, 669-682 (2015).
69. Liu, J., Wang, L., Harvey-White, J., Osei-Hyiaman, D., Razdan, R., Gong, Q., Chan, A.C., Zhou, Z., Huang, B.X., Kim, H.-Y. & Kunos, G. A biosynthetic pathway for anandamide. *Proceedings of the National Academy of Sciences* **103**, 13345-13350 (2006).
70. Zhu, C., Solorzano, C., Sahar, S., Realini, N., Fung, E., Sassone-Corsi, P. & Piomelli, D. Proinflammatory stimuli control *N*-acylphosphatidylethanolamine-specific phospholipase D expression in macrophages. *Molecular Pharmacology* **79**, 786-792 (2011).
71. Liu, J., Wang, L., Harvey-White, J., Huang, B.X., Kim, H.-Y., Luquet, S., Palmiter, R.D., Krystal, G., Rai, R., Mahadevan, A., Razdan, R.K. & Kunos, G. Multiple pathways involved in the biosynthesis of anandamide. *Neuropharmacology* **54**, 1-7 (2008).
72. Ahn, K., McKinney, M.K. & Cravatt, B.F. Enzymatic pathways that regulate endocannabinoid signaling in the nervous system. *Chemical Reviews* **108**, 1687-1707 (2008).
73. Giang, D.K. & Cravatt, B.F. Molecular characterization of human and mouse fatty acid amide hydrolases. *Proceedings of the National Academy of Sciences* **94**, 2238-2242 (1997).
74. Cravatt, B.F., Demarest, K., Patricelli, M.P., Bracey, M.H., Giang, D.K., Martin, B.R. & Lichtman, A.H. Supersensitivity to anandamide and enhanced endogenous cannabinoid signaling in mice lacking fatty acid amide hydrolase. *Proceedings of the National Academy of Sciences* **98**, 9371-9376 (2001).
75. Ahn, K., Johnson, D.S., Mileni, M., Beidler, D., Long, J.Z., McKinney, M.K., Weerapana, E., Sadagopan, N., Liimatta, M., Smith, S.E., Lazerwith, S., Stiff, C., Kamtekar, S., Bhattacharya, K., Zhang, Y., Swaney, S., Van Becelaere, K., Stevens, R.C. & Cravatt, B.F. Discovery and characterization of a highly selective FAAH inhibitor that reduces inflammatory pain. *Chemistry & Biology* **16**, 411-420 (2009).
76. Saghatelian, A., Trauger, S.A., Want, E.J., Hawkins, E.G., Siuzdak, G. & Cravatt, B.F. Assignment of endogenous substrates to enzymes by global metabolite profiling. *Biochemistry* **43**, 14332-14339 (2004).
77. Mukhopadhyay, B., Cinar, R., Yin, S., Liu, J., Tam, J., Godlewski, G., Harvey-White, J., Mordi, I., Cravatt, B.F., Lotersztajn, S., Gao, B., Yuan, Q., Schuebel, K., Goldman, D. & Kunos, G. Hyperactivation of anandamide synthesis and regulation of cell-cycle progression via cannabinoid type 1 (CB₁) receptors in the regenerating liver. *Proceedings of the National Academy of Sciences* **108**, 6323-6328 (2011).
78. Wei, B.Q., Mikkelsen, T.S., McKinney, M.K., Lander, E.S. & Cravatt, B.F. A second fatty acid amide hydrolase with variable distribution among placental mammals. *Journal of Biological Chemistry* **281**, 36569-36578 (2006).
79. Kaczocha, M., Glaser, S.T., Chae, J., Brown, D.A. & Deutsch, D.G. Lipid droplets are novel sites of *N*-acylethanolamine inactivation by fatty acid amide hydrolase-2. *Journal of Biological Chemistry* **285**, 2796-2806 (2010).
80. Ueda, N., Yamanaka, K. & Yamamoto, S. Purification and characterization of an acid amidase selective for *N*-palmitoylethanolamine, a putative endogenous anti-inflammatory substance. *Journal of Biological Chemistry* **276**, 35552-35557 (2001).
81. Tsuboi, K., Sun, Y.-X., Okamoto, Y., Araki, N., Tonai, T. & Ueda, N. Molecular characterization of *N*-acylethanolamine-hydrolyzing acid amidase, a novel member of the cholesteryl glycerophosphorylcholine hydrolase family with structural and functional similarity to acid ceramidase. *Journal of Biological Chemistry* **280**, 11082-11092 (2005).
82. Migliore, M., Pontis, S., Fuentes de Arriba, A.L., Realini, N., Torrente, E., Armirotti, A., Romeo, E., Di Martino, S., Russo, D., Pizzirani, D., Summa, M., Lanfranco, M., Ottonello, G., Busquet, P., Jung, K.-M.,

- Garcia-Guzman, M., Heim, R., Scarpelli, R. & Piomelli, D. Second-generation non-covalent NAAA inhibitors are protective in a model of multiple sclerosis. *Angewandte Chemie International Edition* **55**, 11193-11197 (2016).
83. Rouzer, C.A. & Marnett, L.J. Endocannabinoid oxygenation by cyclooxygenases, lipoxygenases, and cytochromes P450: cross-talk between the eicosanoid and endocannabinoid signaling pathways. *Chemical Reviews* **111**, 5899-5921 (2011).
 84. Urquhart, P., Nicolaou, A. & Woodward, D.F. Endocannabinoids and their oxygenation by cyclooxygenases, lipoxygenases and other oxygenases. *Biochimica et Biophysica Acta (BBA) - Molecular and Cell Biology of Lipids* **1851**, 366-376 (2015).
 85. Yu, M., Ives, D. & Ramesha, C.S. Synthesis of prostaglandin E2 ethanolamide from anandamide by cyclooxygenase-2. *Journal of Biological Chemistry* **272**, 21181-21186 (1997).
 86. Kozak, K.R., Crews, B.C., Morrow, J.D., Wang, L.-H., Ma, Y.H., Weinander, R., Jakobsson, P.-J. & Marnett, L.J. Metabolism of the endocannabinoids, 2-arachidonylethanolamide and anandamide, into prostaglandin, thromboxane, and prostacyclin glycerol esters and ethanolamides. *Journal of Biological Chemistry* **277**, 44877-44885 (2002).
 87. Moriuchi, H., Koda, N., Okuda-Ashitaka, E., Daiyasu, H., Ogasawara, K., Toh, H., Ito, S., Woodward, D.F. & Watanabe, K. Molecular characterization of a novel type of prostamide/prostaglandin F synthase, belonging to the thioredoxin-like superfamily. *Journal of Biological Chemistry* **283**, 792-801 (2008).
 88. Gatta, L., Piscitelli, F., Giordano, C., Boccella, S., Lichtman, A., Maione, S. & Di Marzo, V. Discovery of prostamide F2 α and its role in inflammatory pain and dorsal horn nociceptive neuron hyperexcitability. *PLOS ONE* **7**, e31111 (2012).
 89. Hampson, A.J., Hill, W.A.G., Zan-Phillips, M., Makriyannis, A., Leung, E., Eglen, R.M. & Bornheim, L.M. Anandamide hydroxylation by brain lipoxygenase: metabolite structures and potencies at the cannabinoid receptor. *Biochimica et Biophysica Acta (BBA) - Lipids and Lipid Metabolism* **1259**, 173-179 (1995).
 90. Ueda, N., Yamamoto, K., Yamamoto, S., Tokunaga, T., Shirakawa, E., Shinkai, H., Ogawa, M., Sato, T., Kudo, I., Inoue, K., Takizawa, H., Nagano, T., Hirobe, M., Matsuki, N. & Saito, H. Lipoxygenase-catalyzed oxygenation of arachidonylethanolamide, a cannabinoid receptor agonist. *Biochimica et Biophysica Acta (BBA) - Lipids and Lipid Metabolism* **1254**, 127-134 (1995).
 91. van der Stelt, M., van Kuik, J.A., Bari, M., van Zadelhoff, G., Leeflang, B.R., Veldink, G.A., Finazzi-Agrò, A., Vliegthart, J.F.G. & Maccarrone, M. Oxygenated metabolites of anandamide and 2-arachidonylethanolamide: conformational analysis and interaction with cannabinoid receptors, membrane transporter, and fatty acid amide hydrolase. *Journal of Medicinal Chemistry* **45**, 3709-3720 (2002).
 92. Bornheim, L.M., Kim, K.Y., Chen, B.L. & Correia, M.A. The effect of cannabidiol on mouse hepatic microsomal cytochrome P450-dependent anandamide metabolism. *Biochemical and Biophysical Research Communications* **197**, 740-746 (1993).
 93. Snider, N.T., Nast, J.A., Tesmer, L.A. & Hollenberg, P.F. A cytochrome P450-derived epoxygenated metabolite of anandamide is a potent cannabinoid receptor 2-selective agonist. *Molecular Pharmacology* **75**, 965-972 (2009).
 94. Coulon, D., Faure, L., Salmon, M., Wattedet, V. & Bessoule, J.-J. Occurrence, biosynthesis and functions of *N*-acylphosphatidylethanolamines (NAPE): Not just precursors of *N*-acylethanolamines (NAE). *Biochimie* **94**, 75-85 (2012).
 95. Wellner, N., Diep, T.A., Janfelt, C. & Hansen, H.S. *N*-Acylation of phosphatidylethanolamine and its biological functions in mammals. *Biochimica et Biophysica Acta (BBA) - Molecular and Cell Biology of Lipids* **1831**, 652-662 (2013).
 96. Cadas, H., Gaillet, S., Beltramo, M., Venance, L. & Piomelli, D. Biosynthesis of an endogenous cannabinoid precursor in neurons and its control by calcium and cAMP. *The Journal of Neuroscience* **16**, 3934-3942 (1996).

97. Hansen, H.S., Lauritzen, L., Strand, A.M., Vinggaard, A.M., Frandsen, A. & Schousboe, A. Characterization of glutamate-induced formation of *N*-acylphosphatidylethanolamine and *N*-acylethanolamine in cultured neocortical neurons. *Journal of Neurochemistry* **69**, 753-761 (1997).
98. Natarajan, V., Schmid, P.C. & Schmid, H.H.O. *N*-Acylethanolamine phospholipid metabolism in normal and ischemic rat brain. *Biochimica et Biophysica Acta (BBA) - Lipids and Lipid Metabolism* **878**, 32-41 (1986).
99. Moesgaard, B., Petersen, G., Jaroszewski, J.W. & Hansen, H.S. Age dependent accumulation of *N*-acyl-ethanolamine phospholipids in ischemic rat brain: a ³¹P NMR and enzyme activity study. *Journal of Lipid Research* **41**, 985-990 (2000).
100. Hansen, H.H., Ikonomidou, C., Bittigau, P., Hansen, S.H. & Hansen, H.S. Accumulation of the anandamide precursor and other *N*-acylethanolamine phospholipids in infant rat models of in vivo necrotic and apoptotic neuronal death. *Journal of Neurochemistry* **76**, 39-46 (2001).
101. Moesgaard, B., Hansen, H.H., Hansen, S.L., Hansen, S.H., Petersen, G. & Hansen, H.S. Brain levels of *N*-acylethanolamine phospholipids in mice during pentylenetetrazol-induced seizure. *Lipids* **38**, 387-390 (2003).
102. Janfelt, C., Wellner, N., Leger, P.-L., Kokesch-Himmelreich, J., Hansen, S.H., Charriaut-Marlangue, C. & Hansen, H.S. Visualization by mass spectrometry of 2-dimensional changes in rat brain lipids, including *N*-acylphosphatidylethanolamines, during neonatal brain ischemia. *The FASEB Journal* **26**, 2667-2673 (2012).
103. Basit, A., Pontis, S., Piomelli, D. & Armirotti, A. Ion mobility mass spectrometry enhances low-abundance species detection in untargeted lipidomics. *Metabolomics* **12**, 50 (2016).
104. Rawlyer, A.J. & Braendle, R.A. *N*-Acylphosphatidylethanolamine accumulation in potato cells upon energy shortage caused by anoxia or respiratory inhibitors. *Plant Physiology* **127**, 240-251 (2001).
105. Gao, Y., Vasilyev, D.V., Goncalves, M.B., Howell, F.V., Hobbs, C., Reisenberg, M., Shen, R., Zhang, M.-Y., Strassle, B.W., Lu, P., Mark, L., Piesla, M.J., Deng, K., Kouranova, E.V., Ring, R.H., Whiteside, G.T., Bates, B., Walsh, F.S., Williams, G., Pangalos, M.N., Samad, T.A. & Doherty, P. Loss of retrograde endocannabinoid signaling and reduced adult neurogenesis in diacylglycerol lipase knock-out mice. *The Journal of Neuroscience* **30**, 2017-2024 (2010).
106. Hansen, H.H., Schmid, P.C., Bittigau, P., Lastres-Becker, I., Berrendero, F., Manzanares, J., Ikonomidou, C., Schmid, H.H.O., Fernández-Ruiz, J.J. & Hansen, H.S. Anandamide, but not 2-arachidonoylglycerol, accumulates during in vivo neurodegeneration. *Journal of Neurochemistry* **78**, 1415-1427 (2001).
107. Domingo, J.C., Mora, M. & Africa de Madariaga, M. Role of headgroup structure in the phase behaviour of *N*-acylethanolamine phospholipids: hydrogen-bonding ability and headgroup size. *Chemistry and Physics of Lipids* **69**, 229-240 (1994).
108. Swamy, M.J., Tarafdar, P.K. & Kamlekar, R.K. Structure, phase behaviour and membrane interactions of *N*-acylethanolamines and *N*-acylphosphatidylethanolamines. *Chemistry and Physics of Lipids* **163**, 266-279 (2010).
109. Domingo, J.C., Mora, M. & Africa de Madariaga, M. Incorporation of *N*-acylethanolamine phospholipids into egg phosphatidylcholine vesicles: characterization and permeability properties of the binary systems. *Biochimica et Biophysica Acta (BBA) - Biomembranes* **1148**, 308-316 (1993).
110. Shangguan, T., Pak, C.C., Ali, S., Janoff, A.S. & Meers, P. Cation-dependent fusogenicity of an *N*-acyl phosphatidylethanolamine. *Biochimica et Biophysica Acta (BBA) - Biomembranes* **1368**, 171-183 (1998).
111. Mora, M., Mir, F., de Madariaga, M.A. & Sagrista, M.L. Aggregation and fusion of vesicles composed of *N*-palmitoyl derivatives of membrane phospholipids. *Lipids* **35**, 513-524 (2000).
112. Mora, M., Sagristá, M.-L., Trombetta, D., Bonina, F.P., De Pasquale, A. & Saija, A. Design and characterization of liposomes containing long-chain *N*-acylPEs for brain delivery: penetration of liposomes incorporating GM1 into the rat brain. *Pharmaceutical Research* **19**, 1430-1438 (2002).

113. Ichiki, M., Sugimoto, N., Ueda, N., Okamoto, Y., Takuwa, Y., Nakanishi, Y. & Shiratsuchi, A. Inhibitory effect of *N*-palmitoylphosphatidylethanolamine on macrophage phagocytosis through inhibition of Rac1 and Cdc42. *The Journal of Biochemistry* **145**, 43-50 (2008).
114. Piomelli, D. A fatty gut feeling. *Trends in Endocrinology & Metabolism* **24**, 332-341 (2013).
115. Gillum, M.P., Zhang, D., Zhang, X.-M., Erion, D.M., Jamison, R.A., Choi, C., Dong, J., Shanabrough, M., Duenas, H.R., Frederick, D.W., Hsiao, J.J., Horvath, T.L., Lo, C.M., Tso, P., Cline, G.W. & Shulman, G.I. *N*-Acylphosphatidylethanolamine, a gut- derived circulating factor induced by fat ingestion, inhibits food intake. *Cell* **135**, 813-824 (2008).
116. Wellner, N., Tsuboi, K., Madsen, A.N., Holst, B., Diep, T.A., Nakao, M., Tokumura, A., Burns, M.P., Deutsch, D.G., Ueda, N. & Hansen, H.S. Studies on the anorectic effect of *N*-acylphosphatidylethanolamine and phosphatidylethanolamine in mice. *Biochimica et Biophysica Acta (BBA) - Molecular and Cell Biology of Lipids* **1811**, 508-512 (2011).
117. Chen, Z., Zhang, Y., Guo, L., Dosoky, N., de Ferra, L., Peters, S., Niswender, K.D. & Davies, S.S. Leptogenic effects of NAPE require activity of NAPE-hydrolyzing phospholipase D. *Journal of Lipid Research* **58**, 1624-1635 (2017).
118. Kuehl, F.A., Jacob, T.A., Ganley, O.H., Ormond, R.E. & Meisinger, M.A.P. The identification of *N*-(2-hydroxyethyl)-palmitamide as a naturally occurring anti-inflammatory agent. *Journal of the American Chemical Society* **79**, 5577-5578 (1957).
119. Bachur, N.R., Masek, K., Melmon, K.L. & Udenfriend, S. Fatty acid amides of ethanolamine in mammalian tissues. *Journal of Biological Chemistry* **240**, 1019-1024 (1965).
120. Skaper, S.D., Buriani, A., Dal Toso, R., Petrelli, L., Romanello, S., Facci, L. & Leon, A. The ALIAmide palmitoylethanolamide and cannabinoids, but not anandamide, are protective in a delayed postglutamate paradigm of excitotoxic death in cerebellar granule neurons. *Proceedings of the National Academy of Sciences* **93**, 3984-3989 (1996).
121. Calignano, A., La Rana, G. & Piomelli, D. Antinociceptive activity of the endogenous fatty acid amide, palmitoylethanolamide. *European Journal of Pharmacology* **419**, 191-198 (2001).
122. Esposito, E., Cordaro, M. & Cuzzocrea, S. Roles of fatty acid ethanolamides (FAE) in traumatic and ischemic brain injury. *Pharmacological Research* **86**, 26-31 (2014).
123. Petrosino, S. & Di Marzo, V. The pharmacology of palmitoylethanolamide and first data on the therapeutic efficacy of some of its new formulations. *British Journal of Pharmacology* **174**, 1349-1365 (2017).
124. Berger, C., Schmid, P.C., Schabitz, W.-R., Wolf, M., Schwab, S. & Schmid, H.H.O. Massive accumulation of *N*-acylethanolamines after stroke. Cell signalling in acute cerebral ischemia? *Journal of Neurochemistry* **88**, 1159-1167 (2004).
125. Hansen, H.S. & Vana, V. Non-endocannabinoid *N*-acylethanolamines and 2-monoacylglycerols in the intestine. *British Journal of Pharmacology* **176**, 1443-1454 (2019).
126. O'Sullivan, S.E. An update on PPAR activation by cannabinoids. *British Journal of Pharmacology* **173**, 1899-1910 (2016).
127. Hansen, H.S., Rosenkilde, M.M., Holst, J.J. & Schwartz, T.W. GPR119 as a fat sensor. *Trends in Pharmacological Sciences* **33**, 374-381 (2012).
128. Lauckner, J.E., Jensen, J.B., Chen, H.-Y., Lu, H.-C., Hille, B. & Mackie, K. GPR55 is a cannabinoid receptor that increases intracellular calcium and inhibits M current. *Proceedings of the National Academy of Sciences* **105**, 2699-2704 (2008).
129. Nielsen, M.J., Petersen, G., Astrup, A. & Hansen, H.S. Food intake is inhibited by oral oleoylethanolamide. *Journal of Lipid Research* **45**, 1027-1029 (2004).
130. Oveisi, F., Gaetani, S., Eng, K.T.-P. & Piomelli, D. Oleoylethanolamide inhibits food intake in free-feeding rats after oral administration. *Pharmacological Research* **49**, 461-466 (2004).
131. Petersen, G., Sørensen, C., Schmid, P.C., Artmann, A., Tang-Christensen, M., Hansen, S.H., Larsen, P.J., Schmid, H.H.O. & Hansen, H.S. Intestinal levels of anandamide and oleoylethanolamide in food-

- deprived rats are regulated through their precursors. *Biochimica et Biophysica Acta (BBA) - Molecular and Cell Biology of Lipids* **1761**, 143-150 (2006).
132. Bowen, K.J., Kris-Etherton, P.M., Shearer, G.C., West, S.G., Reddivari, L. & Jones, P.J.H. Oleic acid-derived oleoylethanolamide: A nutritional science perspective. *Progress in Lipid Research* **67**, 1-15 (2017).
 133. Igarashi, M., DiPatrizio, N.V., Narayanaswami, V. & Piomelli, D. Feeding-induced oleoylethanolamide mobilization is disrupted in the gut of diet-induced obese rodents. *Biochimica et Biophysica Acta (BBA) - Molecular and Cell Biology of Lipids* **1851**, 1218-1226 (2015).
 134. Hong, L., Galya, V., Aaron, C., Li, L., Hana, B., Andrei, G., Susan, J.A., Weiwen, H., Shijun, Y., Yun, N., Robert, A.D.V., Frederique, P., Maureen, L., Eric, L.G., Joseph, A.H. & Timothy, J.K. GPR119 is required for physiological regulation of glucagon-like peptide-1 secretion but not for metabolic homeostasis. *Journal of Endocrinology* **201**, 219-230 (2009).
 135. Iannotti, F.A., Di Marzo, V. & Petrosino, S. Endocannabinoids and endocannabinoid-related mediators: Targets, metabolism and role in neurological disorders. *Progress in Lipid Research* **62**, 107-128 (2016).
 136. Orio, L., Alen, F., Pavón, F.J., Serrano, A. & García-Bueno, B. Oleoylethanolamide, neuroinflammation, and alcohol abuse. *Frontiers in Molecular Neuroscience* **11** (2019).
 137. Hansen, H.S., Moesgaard, B., Petersen, G. & Hansen, H.H. Putative neuroprotective actions of *N*-acyl-ethanolamines. *Pharmacology & Therapeutics* **95**, 119-126 (2002).
 138. Gouveia-Figueira, S. & Nording, M.L. Validation of a tandem mass spectrometry method using combined extraction of 37 oxylipins and 14 endocannabinoid-related compounds including prostamides from biological matrices. *Prostaglandins & Other Lipid Mediators* **121**, 110-121 (2015).
 139. Hansen, H.S. & Diep, T.A. *N*-Acylethanolamines, anandamide and food intake. *Biochemical Pharmacology* **78**, 553-560 (2009).
 140. Di Marzo, V., Fontana, A., Cadas, H., Schinelli, S., Cimino, G., Schwartz, J.-C. & Piomelli, D. Formation and inactivation of endogenous cannabinoid anandamide in central neurons. *Nature* **372**, 686 (1994).
 141. Beltramo, M., Stella, N., Calignano, A., Lin, S.Y., Makriyannis, A. & Piomelli, D. Functional role of high-affinity anandamide transport, as revealed by selective inhibition. *Science* **277**, 1094-1097 (1997).
 142. Wilson, R.I. & Nicoll, R.A. Endogenous cannabinoids mediate retrograde signalling at hippocampal synapses. *Nature* **410**, 588-592 (2001).
 143. Nyilas, R., Dudok, B., Urbán, G.M., Mackie, K., Watanabe, M., Cravatt, B.F., Freund, T.F. & Katona, I. Enzymatic machinery for endocannabinoid biosynthesis associated with calcium stores in glutamatergic axon terminals. *The Journal of Neuroscience* **28**, 1058-1063 (2008).
 144. van der Stelt, M., Trevisani, M., Vellani, V., De Petrocellis, L., Schiano Moriello, A., Campi, B., McNaughton, P., Geppetti, P. & Di Marzo, V. Anandamide acts as an intracellular messenger amplifying Ca^{2+} influx via TRPV1 channels. *The EMBO Journal* **24**, 3026-3037 (2005).
 145. Gobbi, G., Bambico, F.R., Mangieri, R., Bortolato, M., Campolongo, P., Solinas, M., Cassano, T., Morgese, M.G., Debonnel, G., Duranti, A., Tontini, A., Tarzia, G., Mor, M., Trezza, V., Goldberg, S.R., Cuomo, V. & Piomelli, D. Antidepressant-like activity and modulation of brain monoaminergic transmission by blockade of anandamide hydrolysis. *Proceedings of the National Academy of Sciences of the United States of America* **102**, 18620-18625 (2005).
 146. Hohmann, A.G., Suplita, R.L., Bolton, N.M., Neely, M.H., Fegley, D., Mangieri, R., Krey, J.F., Michael Walker, J., Holmes, P.V., Crystal, J.D., Duranti, A., Tontini, A., Mor, M., Tarzia, G. & Piomelli, D. An endocannabinoid mechanism for stress-induced analgesia. *Nature* **435**, 1108-1112 (2005).
 147. Morena, M., Patel, S., Bains, J.S. & Hill, M.N. Neurobiological interactions between stress and the endocannabinoid system. *Neuropsychopharmacology* **41**, 80 (2015).
 148. Hill, M.N., McLaughlin, R.J., Morrish, A.C., Viau, V., Floresco, S.B., Hillard, C.J. & Gorzalka, B.B. Suppression of amygdalar endocannabinoid signaling by stress contributes to activation of the hypothalamic–pituitary–adrenal axis. *Neuropsychopharmacology* **34**, 2733 (2009).

149. Hill, M.N., McLaughlin, R.J., Bingham, B., Shrestha, L., Lee, T.T.Y., Gray, J.M., Hillard, C.J., Gorzalka, B.B. & Viau, V. Endogenous cannabinoid signaling is essential for stress adaptation. *Proceedings of the National Academy of Sciences* **107**, 9406-9411 (2010).
150. Lutz, B., Marsicano, G., Maldonado, R. & Hillard, C.J. The endocannabinoid system in guarding against fear, anxiety and stress. *Nature Reviews Neuroscience* **16**, 705 (2015).
151. Jamshidi, N. & Taylor, D.A. Anandamide administration into the ventromedial hypothalamus stimulates appetite in rats. *British Journal of Pharmacology* **134**, 1151-1154 (2001).
152. van der Stelt, M., Veldhuis, W.B., van Haften, G.W., Fezza, F., Bisogno, T., Bär, P.R., Veldink, G.A., Vliegthart, J.F.G., Di Marzo, V. & Nicolay, K. Exogenous anandamide protects rat brain against acute neuronal injury *in vivo*. *The Journal of Neuroscience* **21**, 8765-8771 (2001).
153. Smith, P.B., Compton, D.R., Welch, S.P., Razdan, R.K., Mechoulam, R. & Martin, B.R. The pharmacological activity of anandamide, a putative endogenous cannabinoid, in mice. *Journal of Pharmacology and Experimental Therapeutics* **270**, 219-227 (1994).
154. Maccarrone, M., Bab, I., Bíró, T., Cabral, G.A., Dey, S.K., Di Marzo, V., Konje, J.C., Kunos, G., Mechoulam, R., Pacher, P., Sharkey, K.A. & Zimmer, A. Endocannabinoid signaling at the periphery: 50 years after THC. *Trends in Pharmacological Sciences* **36**, 277-296 (2015).
155. van Eenige, R., van der Stelt, M., Rensen, P.C.N. & Kooijman, S. Regulation of adipose tissue metabolism by the endocannabinoid system. *Trends in Endocrinology & Metabolism* **29**, 326-337 (2018).
156. Gómez, R., Navarro, M., Ferrer, B., Trigo, J.M., Bilbao, A., Del Arco, I., Cippitelli, A., Nava, F., Piomelli, D. & Rodríguez de Fonseca, F. A peripheral mechanism for CB₁ cannabinoid receptor-dependent modulation of feeding. *The Journal of Neuroscience* **22**, 9612-9617 (2002).
157. Clapper, J.R., Moreno-Sanz, G., Russo, R., Guijarro, A., Vacondio, F., Duranti, A., Tontini, A., Sanchini, S., Sciolino, N.R., Spradley, J.M., Hohmann, A.G., Calignano, A., Mor, M., Tarzia, G. & Piomelli, D. Anandamide suppresses pain initiation through a peripheral endocannabinoid mechanism. *Nature Neuroscience* **13**, 1265 (2010).
158. Munro, S., Thomas, K.L. & Abu-Shaar, M. Molecular characterization of a peripheral receptor for cannabinoids. *Nature* **365**, 61-65 (1993).
159. Pertwee, R.G., Howlett, A.C., Abood, M.E., Alexander, S.P.H., Di Marzo, V., Elphick, M.R., Greasley, P.J., Hansen, H.S., Kunos, G., Mackie, K., Mechoulam, R. & Ross, R.A. International Union of Basic and Clinical Pharmacology. LXXIX. Cannabinoid receptors and their ligands: beyond CB₁ and CB₂. *Pharmacological Reviews* **62**, 588-631 (2010).
160. Turcotte, C., Blanchet, M.-R., Laviolette, M. & Flamand, N. The CB₂ receptor and its role as a regulator of inflammation. *Cellular and Molecular Life Sciences* **73**, 4449-4470 (2016).
161. Di Marzo, V. & De Petrocellis, L. Why do cannabinoid receptors have more than one endogenous ligand? *Philosophical Transactions of the Royal Society B: Biological Sciences* **367**, 3216-3228 (2012).
162. Turcotte, C., Chouinard, F., Lefebvre Julie, S. & Flamand, N. Regulation of inflammation by cannabinoids, the endocannabinoids 2-arachidonoyl-glycerol and arachidonoyl-ethanolamide, and their metabolites. *Journal of Leukocyte Biology* **97**, 1049-1070 (2015).
163. Stelt, M.v.d. & Marzo, V.D. Endovanilloids. *European Journal of Biochemistry* **271**, 1827-1834 (2004).
164. Di Marzo, V. & De Petrocellis, L. Endocannabinoids as regulators of transient receptor potential (TRP) channels: a further opportunity to develop new endocannabinoid-based therapeutic drugs. *Current Medicinal Chemistry* **17**, 1430-1449 (2010).
165. Tóth, A., Blumberg, P.M. & Boczán, J. Anandamide and the vanilloid receptor (TRPV1), in *Vitamins & Hormones*, Vol. 81 389-419 (Academic Press, 2009).
166. Martins, D., Tavares, I. & Morgado, C. "Hotheaded": The role of TRPV1 in brain functions. *Neuropharmacology* **85**, 151-157 (2014).
167. Marrone, M.C., Morabito, A., Giustizieri, M., Chiurchiù, V., Leuti, A., Mattioli, M., Marinelli, S., Riganti, L., Lombardi, M., Murana, E., Totaro, A., Piomelli, D., Ragozzino, D., Oddi, S., Maccarrone, M., Verderio,

- C. & Marinelli, S. TRPV1 channels are critical brain inflammation detectors and neuropathic pain biomarkers in mice. *Nature Communications* **8**, 15292 (2017).
168. Kim, H.-Y., Spector, A.A. & Xiong, Z.-M. A synaptogenic amide *N*-docosahexaenoylethanolamide promotes hippocampal development. *Prostaglandins & Other Lipid Mediators* **96**, 114-120 (2011).
169. Meijerink, J., Poland, M., Balvers, M.G.J., Plastina, P., Lute, C., Dwarkasing, J., van Norren, K. & Witkamp, R.F. Inhibition of COX-2-mediated eicosanoid production plays a major role in the anti-inflammatory effects of the endocannabinoid *N*-docosahexaenoylethanolamine (DHEA) in macrophages. *British Journal of Pharmacology* **172**, 24-37 (2015).
170. Kim, J., Carlson, M.E., Kuchel, G.A., Newman, J.W. & Watkins, B.A. Dietary DHA reduces downstream endocannabinoid and inflammatory gene expression and epididymal fat mass while improving aspects of glucose use in muscle in C57BL/6J mice. *International Journal Of Obesity* **40**, 129 (2015).
171. Berger, A., Crozier, G., Bisogno, T., Cavaliere, P., Innis, S. & Di Marzo, V. Anandamide and diet: Inclusion of dietary arachidonate and docosahexaenoate leads to increased brain levels of the corresponding *N*-acylethanolamines in piglets. *Proceedings of the National Academy of Sciences* **98**, 6402-6406 (2001).
172. Wood, J.T., Williams, J.S., Pandarinathan, L., Janero, D.R., Lammi-Keefe, C.J. & Makriyannis, A. Dietary docosahexaenoic acid supplementation alters select physiological endocannabinoid-system metabolites in brain and plasma. *Journal of Lipid Research* **51**, 1416-1423 (2010).
173. Kim, H.-Y., Moon, H.-S., Cao, D., Lee, J., Kevala, K., Jun, Sang B., Lovinger, David M., Akbar, M. & Huang, Bill X. *N*-Docosahexaenoylethanolamide promotes development of hippocampal neurons. *Biochemical Journal* **435**, 327-336 (2011).
174. Lacombe, R.J.S., Chouinard-Watkins, R. & Bazinet, R.P. Brain docosahexaenoic acid uptake and metabolism. *Molecular Aspects of Medicine* **64**, 109-134 (2018).
175. Lin, L., Metherel, A.H., Kitson, A.P., Alashmali, S.M., Hopperton, K.E., Trépanier, M.-O., Jones, P.J. & Bazinet, R.P. Dietary fatty acids augment tissue levels of *N*-acylethanolamines in *N*-acylphosphatidylethanolamine phospholipase D (NAPE-PLD) knockout mice. *The Journal of Nutritional Biochemistry* **62**, 134-142 (2018).
176. Kendall, A.C., Pilkington, S.M., Massey, K.A., Sassano, G., Rhodes, L.E. & Nicolaou, A. Distribution of bioactive lipid mediators in human skin. *Journal of Investigative Dermatology* **135**, 1510-1520 (2015).
177. Lum, A.M., Wang, B.B., Beck-Engeser, G.B., Li, L., Channa, N. & Wabl, M. Orphan receptor GPR110, an oncogene overexpressed in lung and prostate cancer. *BMC Cancer* **10**, 40 (2010).
178. Pisanti, S., Picardi, P., D'Alessandro, A., Laezza, C. & Bifulco, M. The endocannabinoid signaling system in cancer. *Trends in Pharmacological Sciences* **34**, 273-282 (2013).
179. Chiurchiù, V., van der Stelt, M., Centonze, D. & Maccarrone, M. The endocannabinoid system and its therapeutic exploitation in multiple sclerosis: Clues for other neuroinflammatory diseases. *Progress in Neurobiology* **160**, 82-100 (2018).
180. Mazier, W., Saucisse, N., Gatta-Cherifi, B. & Cota, D. The endocannabinoid system: pivotal orchestrator of obesity and metabolic disease. *Trends in Endocrinology & Metabolism* **26**, 524-537 (2015).
181. Di Marzo, V. Targeting the endocannabinoid system: to enhance or reduce? *Nature Reviews Drug Discovery* **7**, 438 (2008).
182. Blankman, J.L. & Cravatt, B.F. Chemical probes of endocannabinoid metabolism. *Pharmacological Reviews* **65**, 849-871 (2013).
183. Tuo, W., Leleu-Chavain, N., Spencer, J., Sansook, S., Millet, R. & Chavatte, P. Therapeutic potential of fatty acid amide hydrolase, monoacylglycerol lipase, and *N*-acylethanolamine acid amidase inhibitors. *Journal of Medicinal Chemistry* **60**, 4-46 (2017).
184. Ahn, K., Smith, S.E., Liimatta, M.B., Beidler, D., Sadagopan, N., Dudley, D.T., Young, T., Wren, P., Zhang, Y., Swaney, S., Van Becelaere, K., Blankman, J.L., Nomura, D.K., Bhattachar, S.N., Stiff, C., Nomanbhoy, T.K., Weerapana, E., Johnson, D.S. & Cravatt, B.F. Mechanistic and pharmacological characterization of PF-04457845: a highly potent and selective fatty acid amide hydrolase inhibitor that reduces

- inflammatory and noninflammatory pain. *Journal of Pharmacology and Experimental Therapeutics* **338**, 114-124 (2011).
185. Long, J.Z., LaCava, M., Jin, X. & Cravatt, B.F. An anatomical and temporal portrait of physiological substrates for fatty acid amide hydrolase. *Journal of Lipid Research* **52**, 337-344 (2011).
 186. Donvito, G., Nass, S.R., Wilkerson, J.L., Curry, Z.A., Schurman, L.D., Kinsey, S.G. & Lichtman, A.H. The endogenous cannabinoid system: a budding source of targets for treating inflammatory and neuropathic pain. *Neuropsychopharmacology* **43**, 52 (2017).
 187. Booker, L., Kinsey, S.G., Abdullah, R.A., Blankman, J.L., Long, J.Z., Ezzili, C., Boger, D.L., Cravatt, B.F. & Lichtman, A.H. The fatty acid amide hydrolase (FAAH) inhibitor PF-3845 acts in the nervous system to reverse LPS-induced tactile allodynia in mice. *British Journal of Pharmacology* **165**, 2485-2496 (2012).
 188. Hill, M.N., Campolongo, P., Yehuda, R. & Patel, S. Integrating endocannabinoid signaling and cannabinoids into the biology and treatment of posttraumatic stress disorder. *Neuropsychopharmacology* **43**, 80 (2017).
 189. Celorrio, M., Fernández-Suárez, D., Rojo-Bustamante, E., Echeverry-Alzate, V., Ramírez, M.J., Hillard, C.J., López-Moreno, J.A., Maldonado, R., Oyarzábal, J., Franco, R. & Aymerich, M.S. Fatty acid amide hydrolase inhibition for the symptomatic relief of Parkinson's disease. *Brain, Behavior, and Immunity* **57**, 94-105 (2016).
 190. Rock, E.M., Limebeer, C.L., Mechoulam, R., Piomelli, D. & Parker, L.A. The effect of cannabidiol and URB597 on conditioned gaping (a model of nausea) elicited by a lithium-paired context in the rat. *Psychopharmacology* **196**, 389-395 (2008).
 191. Oláh, A., Ambrus, L., Nicolussi, S., Gertsch, J., Tubak, V., Kemény, L., Soeberdt, M., Abels, C. & Bíró, T. Inhibition of fatty acid amide hydrolase exerts cutaneous anti-inflammatory effects both in vitro and in vivo. *Experimental Dermatology* **25**, 328-330 (2016).
 192. Schlosburg, J.E., Boger, D.L., Cravatt, B.F. & Lichtman, A.H. Endocannabinoid modulation of scratching response in an acute allergenic model: a new prospective neural therapeutic target for pruritus. *Journal of Pharmacology and Experimental Therapeutics* **329**, 314-323 (2009).
 193. Nucci, C., Gasperi, V., Tartaglione, R., Cerulli, A., Terrinoni, A., Bari, M., De Simone, C., Agrò, A.F., Morrone, L.A., Corasaniti, M.T., Bagetta, G. & Maccarrone, M. Involvement of the endocannabinoid system in retinal damage after high intraocular pressure-induced ischemia in rats. *Investigative Ophthalmology & Visual Science* **48**, 2997-3004 (2007).
 194. Bátkai, S., Pacher, P., Osei-Hyiaman, D., Radaeva, S., Liu, J., Harvey-White, J., Offertáler, L., Mackie, K., Rudd, M.A., Bukoski, R.D. & Kunos, G. Endocannabinoids acting at cannabinoid-1 receptors regulate cardiovascular function in hypertension. *Circulation* **110**, 1996-2002 (2004).
 195. Tchantchou, F., Tucker, L.B., Fu, A.H., Bluett, R.J., McCabe, J.T., Patel, S. & Zhang, Y. The fatty acid amide hydrolase inhibitor PF-3845 promotes neuronal survival, attenuates inflammation and improves functional recovery in mice with traumatic brain injury. *Neuropharmacology* **85**, 427-439 (2014).
 196. Hermes, D.J., Xu, C., Poklis, J.L., Niphakis, M.J., Cravatt, B.F., Mackie, K., Lichtman, A.H., Ignatowska-Jankowska, B.M. & Fitting, S. Neuroprotective effects of fatty acid amide hydrolase catabolic enzyme inhibition in a HIV-1 Tat model of neuroAIDS. *Neuropharmacology* **141**, 55-65 (2018).
 197. Pryce, G., Cabranes, A., Fernández-Ruiz, J., Bisogno, T., Di Marzo, V., Long, J., Cravatt, B., Giovannoni, G. & Baker, D. Control of experimental spasticity by targeting the degradation of endocannabinoids using selective fatty acid amide hydrolase inhibitors. *Multiple Sclerosis Journal* **19**, 1896-1904 (2013).
 198. Toczek, M. & Malinowska, B. Enhanced endocannabinoid tone as a potential target of pharmacotherapy. *Life Sciences* **204**, 20-45 (2018).
 199. Di Marzo, V. New approaches and challenges to targeting the endocannabinoid system. *Nature Reviews Drug Discovery* **17**, 623 (2018).
 200. Li, G.L., Winter, H., Arends, R., Jay, G.W., Le, V., Young, T. & Huggins, J.P. Assessment of the pharmacology and tolerability of PF-04457845, an irreversible inhibitor of fatty acid amide hydrolase-1, in healthy subjects. *British Journal of Clinical Pharmacology* **73**, 706-716 (2012).

201. Huggins, J.P., Smart, T.S., Langman, S., Taylor, L. & Young, T. An efficient randomised, placebo-controlled clinical trial with the irreversible fatty acid amide hydrolase-1 inhibitor PF-04457845, which modulates endocannabinoids but fails to induce effective analgesia in patients with pain due to osteoarthritis of the knee. *PAIN* **153**, 1837-1846 (2012).
202. D'Souza, D.C., Cortes-Briones, J., Creatura, G., Bluez, G., Thurnauer, H., Deaso, E., Bielen, K., Surti, T., Radhakrishnan, R., Gupta, A., Gupta, S., Cahill, J., Sherif, M.A., Makriyannis, A., Morgan, P.T., Ranganathan, M. & Skosnik, P.D. Efficacy and safety of a fatty acid amide hydrolase inhibitor (PF-04457845) in the treatment of cannabis withdrawal and dependence in men: a double-blind, placebo-controlled, parallel group, phase 2a single-site randomised controlled trial. *The Lancet Psychiatry* **6**, 35-45 (2019).
203. Kerbrat, A., Ferré, J.-C., Fillatre, P., Ronzière, T., Vannier, S., Carsin-Nicol, B., Lavoué, S., Vérin, M., Gauvrit, J.-Y., Le Tulzo, Y. & Edan, G. Acute neurologic disorder from an inhibitor of fatty acid amide hydrolase. *New England Journal of Medicine* **375**, 1717-1725 (2016).
204. van Esbroeck, A.C.M., Janssen, A.P.A., Cognetta, A.B., Ogasawara, D., Shpak, G., van der Kroeg, M., Kantae, V., Baggelaar, M.P., de Vrij, F.M.S., Deng, H., Allarà, M., Fezza, F., Lin, Z., van der Wel, T., Soethoudt, M., Mock, E.D., den Dulk, H., Baak, I.L., Florea, B.I., Hendriks, G., De Petrocellis, L., Overkleeft, H.S., Hankemeier, T., De Zeeuw, C.I., Di Marzo, V., Maccarrone, M., Cravatt, B.F., Kushner, S.A. & van der Stelt, M. Activity-based protein profiling reveals off-target proteins of the FAAH inhibitor BIA 10-2474. *Science* **356**, 1084-1087 (2017).
205. Botteman, P., Muccioli, G.G. & Alhouayek, M. *N*-Acylethanolamine hydrolyzing acid amidase inhibition: tools and potential therapeutic opportunities. *Drug Discovery Today* **23**, 1520-1529 (2018).
206. Sasso, O., Moreno-Sanz, G., Martucci, C., Realini, N., Dionisi, M., Mengatto, L., Duranti, A., Tarozzo, G., Tarzia, G., Mor, M., Bertorelli, R., Reggiani, A. & Piomelli, D. Antinociceptive effects of the *N*-acylethanolamine acid amidase inhibitor ARN077 in rodent pain models. *PAIN* **154**, 350-360 (2013).
207. Bonezzi, F.T., Sasso, O., Pontis, S., Realini, N., Romeo, E., Ponzano, S., Nuzzi, A., Fiasella, A., Bertozzi, F. & Piomelli, D. An important role for *N*-acylethanolamine acid amidase in the complete Freund's adjuvant rat model of arthritis. *Journal of Pharmacology and Experimental Therapeutics* **356**, 656-663 (2016).
208. Li, Y., Zhou, P., Chen, H., Chen, Q., Kuang, X., Lu, C., Ren, J. & Qiu, Y. Inflammation-restricted anti-inflammatory activities of a *N*-acylethanolamine acid amidase (NAAA) inhibitor F215. *Pharmacological Research* **132**, 7-14 (2018).
209. Solorzano, C., Zhu, C., Battista, N., Astarita, G., Lodola, A., Rivara, S., Mor, M., Russo, R., Maccarrone, M., Antonietti, F., Duranti, A., Tontini, A., Cuzzocrea, S., Tarzia, G. & Piomelli, D. Selective *N*-acylethanolamine-hydrolyzing acid amidase inhibition reveals a key role for endogenous palmitoylethanolamide in inflammation. *Proceedings of the National Academy of Sciences* **106**, 20966-20971 (2009).
210. Ribeiro, A., Pontis, S., Mengatto, L., Armirotti, A., Chiurchiù, V., Capurro, V., Fiasella, A., Nuzzi, A., Romeo, E., Moreno-Sanz, G., Maccarrone, M., Reggiani, A., Tarzia, G., Mor, M., Bertozzi, F., Bandiera, T. & Piomelli, D. A potent systemically active *N*-acylethanolamine acid amidase inhibitor that suppresses inflammation and human macrophage activation. *ACS Chemical Biology* **10**, 1838-1846 (2015).
211. Gorelik, A., Gebai, A., Illes, K., Piomelli, D. & Nagar, B. Molecular mechanism of activation of the immunoregulatory amidase NAAA. *Proceedings of the National Academy of Sciences* **115**, E10032-E10040 (2018).
212. Maccarrone, M. Metabolism of the endocannabinoid anandamide: open questions after 25 years. *Frontiers in Molecular Neuroscience* **10** (2017).
213. Piazza, P.V., Cota, D. & Marsicano, G. The CB₁ receptor as the cornerstone of exostasis. *Neuron* **93**, 1252-1274 (2017).
214. Després, J.-P., Golay, A. & Sjöström, L. Effects of rimonabant on metabolic risk factors in overweight patients with dyslipidemia. *New England Journal of Medicine* **353**, 2121-2134 (2005).

215. Van Gaal, L.F., Rissanen, A.M., Scheen, A.J., Ziegler, O. & Rössner, S. Effects of the cannabinoid-1 receptor blocker rimonabant on weight reduction and cardiovascular risk factors in overweight patients: 1-year experience from the RIO-Europe study. *The Lancet* **365**, 1389-1397 (2005).
216. Pi-Sunyer, F.X., Aronne, L.J., Heshmati, H.M., Devin, J., Rosenstock, J. & RIO-North America Study Group, f.t. Effect of rimonabant, a cannabinoid-1 receptor blocker, on weight and cardiometabolic risk factors in overweight or obese patientsrio-north america: a randomized controlled trial. *JAMA* **295**, 761-775 (2006).
217. Christensen, R., Kristensen, P.K., Bartels, E.M., Bliddal, H. & Astrup, A. Efficacy and safety of the weight-loss drug rimonabant: a meta-analysis of randomised trials. *The Lancet* **370**, 1706-1713 (2007).
218. Topol, E.J., Bousser, M.-G., Fox, K.A.A., Creager, M.A., Despres, J.-P., Easton, J.D., Hamm, C.W., Montalescot, G., Steg, P.G., Pearson, T.A., Cohen, E., Gaudin, C., Job, B., Murphy, J.H. & Bhatt, D.L. Rimonabant for prevention of cardiovascular events (CRESCENDO): a randomised, multicentre, placebo-controlled trial. *The Lancet* **376**, 517-523 (2010).
219. Shrestha, N., Cuffe, J.S.M., Hutchinson, D.S., Headrick, J.P., Perkins, A.V., McAinch, A.J. & Hryciw, D.H. Peripheral modulation of the endocannabinoid system in metabolic disease. *Drug Discovery Today* **23**, 592-604 (2018).
220. Tam, J., Hinden, L., Drori, A., Udi, S., Azar, S. & Baraghithy, S. The therapeutic potential of targeting the peripheral endocannabinoid/CB₁ receptor system. *European Journal of Internal Medicine* **49**, 23-29 (2018).
221. Kuipers, E.N., Kantae, V., Maarse, B.C.E., van den Berg, S.M., van Eenige, R., Nahon, K.J., Reifel-Miller, A., Coskun, T., de Winther, M.P.J., Lutgens, E., Kooijman, S., Harms, A.C., Hankemeier, T., van der Stelt, M., Rensen, P.C.N. & Boon, M.R. High fat diet increases circulating endocannabinoids accompanied by increased synthesis enzymes in adipose tissue. *Frontiers in Physiology* **9** (2019).
222. Cota, D., Marsicano, G., Tschöp, M., Grübler, Y., Flachskamm, C., Schubert, M., Auer, D., Yassouridis, A., Thöne-Reineke, C., Ortman, S., Tomassoni, F., Cervino, C., Nisoli, E., Linthorst, A.C.E., Pasquali, R., Lutz, B., Stalla, G.K. & Pagotto, U. The endogenous cannabinoid system affects energy balance via central orexigenic drive and peripheral lipogenesis. *The Journal of Clinical Investigation* **112**, 423-431 (2003).
223. Osei-Hyiaman, D., DePetrillo, M., Pacher, P., Liu, J., Radaeva, S., Bátkai, S., Harvey-White, J., Mackie, K., Offertáler, L., Wang, L. & Kunos, G. Endocannabinoid activation at hepatic CB₁ receptors stimulates fatty acid synthesis and contributes to diet-induced obesity. *The Journal of Clinical Investigation* **115**, 1298-1305 (2005).
224. DiPatrizio, N.V., Astarita, G., Schwartz, G., Li, X. & Piomelli, D. Endocannabinoid signal in the gut controls dietary fat intake. *Proceedings of the National Academy of Sciences* **108**, 12904-12908 (2011).
225. Jourdan, T., Godlewski, G., Cinar, R., Bertola, A., Szanda, G., Liu, J., Tam, J., Han, T., Mukhopadhyay, B., Skarulis, M.C., Ju, C., Aouadi, M., Czech, M.P. & Kunos, G. Activation of the Nlrp3 inflammasome in infiltrating macrophages by endocannabinoids mediates beta cell loss in type 2 diabetes. *Nature Medicine* **19**, 1132 (2013).
226. Gatta-Cherifi, B., Matias, I., Vallée, M., Tabarin, A., Marsicano, G., Piazza, P.V. & Cota, D. Simultaneous postprandial deregulation of the orexigenic endocannabinoid anandamide and the anorexigenic peptide YY in obesity. *International Journal Of Obesity* **36**, 880 (2011).
227. Fanelli, F., Mezzullo, M., Repaci, A., Belluomo, I., Ibarra Gasparini, D., Di Dalmazi, G., Mastroberto, M., Vicennati, V., Gambineri, A., Morselli-Labate, A.M., Pasquali, R. & Pagotto, U. Profiling plasma *N*-acylethanolamine levels and their ratios as a biomarker of obesity and dysmetabolism. *Molecular Metabolism* **14**, 82-94 (2018).
228. Fanelli, F., Mezzullo, M., Belluomo, I., Di Lallo, V.D., Baccini, M., Ibarra Gasparini, D., Casadio, E., Mastroberto, M., Vicennati, V., Gambineri, A., Morselli-Labate, A.M., Pasquali, R. & Pagotto, U. Plasma 2-arachidonoylglycerol is a biomarker of age and menopause related insulin resistance and dyslipidemia in lean but not in obese men and women. *Molecular Metabolism* **6**, 406-415 (2017).

229. Kimberly, W.T., O'Sullivan, J.F., Nath, A.K., Keyes, M., Shi, X., Larson, M.G., Yang, Q., Long, M.T., Vasan, R., Peterson, R.T., Wang, T.J., Corey, K.E. & Gerszten, R.E. Metabolite profiling identifies anandamide as a biomarker of nonalcoholic steatohepatitis. *JCI Insight* **2** (2017).
230. Hillard, C.J. Circulating endocannabinoids: from whence do they come and where are they going? *Neuropsychopharmacology* **43**, 155 (2017).
231. Wangensteen, T., Akselsen, H., Holmen, J., Undlien, D. & Retterstøl, L. A common haplotype in NAPEPLD is associated with severe obesity in a Norwegian population-based cohort (the HUNT study). *Obesity* **19**, 612-617 (2011).
232. Powell, D.R., Gay, J.P., Wilganowski, N., Doree, D., Savelieva, K.V., Lanthorn, T.H., Read, R., Vogel, P., Hansen, G.M., Brommage, R., Ding, Z.-M., Desai, U. & Zambrowicz, B. Diacylglycerol lipase α knockout mice demonstrate metabolic and behavioral phenotypes similar to those of cannabinoid receptor 1 knockout mice. *Frontiers in Endocrinology* **6** (2015).
233. Touriño, C., Oveisi, F., Lockney, J., Piomelli, D. & Maldonado, R. FAAH deficiency promotes energy storage and enhances the motivation for food. *International Journal Of Obesity* **34**, 557 (2009).
234. Geurts, L., Everard, A., Van Hul, M., Essaghir, A., Duparc, T., Matamoros, S., Plovier, H., Castel, J., Denis, R.G.P., Bergiers, M., Druart, C., Alhouayek, M., Delzenne, N.M., Muccioli, G.G., Demoulin, J.-B., Luquet, S. & Cani, P.D. Adipose tissue NAPE-PLD controls fat mass development by altering the browning process and gut microbiota. *Nature Communications* **6**, 6495 (2015).
235. Everard, A., Plovier, H., Rastelli, M., Van Hul, M., de Wouters d'Oplinter, A., Geurts, L., Druart, C., Robine, S., Delzenne, N.M., Muccioli, G.G., de Vos, W.M., Luquet, S., Flamand, N., Di Marzo, V. & Cani, P.D. Intestinal epithelial *N*-acylphosphatidylethanolamine phospholipase D links dietary fat to metabolic adaptations in obesity and steatosis. *Nature Communications* **10**, 457 (2019).
236. Mukhopadhyay, B., Schuebel, K., Mukhopadhyay, P., Cinar, R., Godlewski, G., Xiong, K., Mackie, K., Lizak, M., Yuan, Q., Goldman, D. & Kunos, G. Cannabinoid receptor 1 promotes hepatocellular carcinoma initiation and progression through multiple mechanisms. *Hepatology* **61**, 1615-1626 (2015).
237. Suk, K.-T., Mederacke, I., Gwak, G.-Y., Cho, S.W., Adeyemi, A., Friedman, R. & Schwabe, R.F. Opposite roles of cannabinoid receptors 1 and 2 in hepatocarcinogenesis. *Gut* **65**, 1721-1732 (2016).
238. Masoodi, M., Lee, E., Eiden, M., Bahlo, A., Shi, Y., Ceddia, R.B., Baccei, C., Prasit, P. & Spaner, D.E. A role for oleoylethanolamide in chronic lymphocytic leukemia. *Leukemia* **28**, 1381 (2014).
239. Spaner, D.E., Lee, E., Shi, Y., Wen, F., Li, Y., Tung, S., McCaw, L., Wong, K., Gary-Gouy, H., Dalloul, A., Ceddia, R. & Gorzcyński, R. PPAR- α is a therapeutic target for chronic lymphocytic leukemia. *Leukemia* **27**, 1090 (2012).
240. Messmer, D., Lorrain, K., Stebbins, K., Bravo, Y., Stock, N., Cabrera, G., Correa, L., Chen, A., Jacintho, J., Chiorazzi, N., Yan, X.J., Spaner, D., Prasit, P. & Lorrain, D. A selective novel peroxisome proliferator-activated receptor (PPAR)- α antagonist induces apoptosis and inhibits proliferation of CLL cells *in vitro* and *in vivo*. *Molecular Medicine* **21**, 410-419 (2015).
241. Moezi, L., Gaskari, S.A. & Lee, S.S. Endocannabinoids and liver disease. V. Endocannabinoids as mediators of vascular and cardiac abnormalities in cirrhosis. *American Journal of Physiology-Gastrointestinal and Liver Physiology* **295**, G649-G653 (2008).
242. Ying-Ying, Y. & Lin, H.-C. Endocannabinoids and non-endocannabinoid fatty acid amides in cirrhosis. *Liver International* **30**, 780-781 (2010).
243. Baldassarre, M., Giannone, F.A., Napoli, L., Tovoli, A., Ricci, C.S., Tufoni, M. & Caraceni, P. The endocannabinoid system in advanced liver cirrhosis: pathophysiological implication and future perspectives. *Liver International* **33**, 1298-1308 (2013).
244. Ros, J., Clària, J., To-Figueras, J., Planagumà, A., Cejudo-Martín, P., Fernández-Varo, G., Martín-Ruiz, R., Arroyo, V., Rivera, F., Rodés, J. & Jiménez, W. Endogenous cannabinoids: A new system involved in the homeostasis of arterial pressure in experimental cirrhosis in the rat. *Gastroenterology* **122**, 85-93 (2002).

245. Bátkai, S., Járjai, Z., Wagner, J.A., Goparaju, S.K., Varga, K., Liu, J., Wang, L., Mirshahi, F., Khanolkar, A.D., Makriyannis, A., Urbaschek, R., Garcia Jr, N., Sanyal, A.J. & Kunos, G. Endocannabinoids acting at vascular CB₁ receptors mediate the vasodilated state in advanced liver cirrhosis. *Nature Medicine* **7**, 827 (2001).
246. Caraceni, P., Viola, A., Piscitelli, F., Giannone, F., Berzigotti, A., Cescon, M., Domenicali, M., Petrosino, S., Giampalma, E., Riili, A., Grazi, G., Golfieri, R., Zoli, M., Bernardi, M. & Di Marzo, V. Circulating and hepatic endocannabinoids and endocannabinoid-related molecules in patients with cirrhosis. *Liver International* **30**, 816-825 (2010).
247. Domenicali, M., Ros, J., Fernández-Varo, G., Cejudo-Martín, P., Crespo, M., Morales-Ruiz, M., Briones, A.M., Campistol, J.-M., Arroyo, V., Vila, E., Rodés, J. & Jiménez, W. Increased anandamide induced relaxation in mesenteric arteries of cirrhotic rats: role of cannabinoid and vanilloid receptors. *Gut* **54**, 522-527 (2005).
248. Teixeira-Clerc, F., Julien, B., Grenard, P., Van Nhieu, J.T., Deveaux, V., Li, L., Serriere-Lanneau, V., Ledent, C., Mallat, A. & Lotersztajn, S. CB₁ cannabinoid receptor antagonism: a new strategy for the treatment of liver fibrosis. *Nature Medicine* **12**, 671 (2006).
249. Giannone, F.A., Baldassarre, M., Domenicali, M., Zaccherini, G., Trevisani, F., Bernardi, M. & Caraceni, P. Reversal of liver fibrosis by the antagonism of endocannabinoid CB₁ receptor in a rat model of CCl₄-induced advanced cirrhosis. *Laboratory Investigation* **92**, 384 (2011).
250. Lumsden, A.B., Henderson, J.M. & Kutner, M.H. Endotoxin levels measured by a chromogenic assay in portal, hepatic and peripheral venous blood in patients with cirrhosis. *Hepatology* **8**, 232-236 (1988).
251. Lin, R.-S., Lee, F.-Y., Lee, S.-D., Tsai, Y.-T., Lin, H.C., Rei-Hwa, L., Wan-Ching, H., Cheng-Chun, H., Sun-Sang, W. & Kwang-Juei, L. Endotoxemia in patients with chronic liver diseases: relationship to severity of liver diseases, presence of esophageal varices, and hyperdynamic circulation. *Journal of Hepatology* **22**, 165-172 (1995).
252. Ju, C. & Tacke, F. Hepatic macrophages in homeostasis and liver diseases: from pathogenesis to novel therapeutic strategies. *Cellular And Molecular Immunology* **13**, 316 (2016).
253. Centonze, D., Bari, M., Rossi, S., Prosperetti, C., Furlan, R., Fezza, F., De Chiara, V., Battistini, L., Bernardi, G., Bernardini, S., Martino, G. & Maccarrone, M. The endocannabinoid system is dysregulated in multiple sclerosis and in experimental autoimmune encephalomyelitis. *Brain* **130**, 2543-2553 (2007).
254. Pisani, V., Madeo, G., Tassone, A., Sciamanna, G., Maccarrone, M., Stanzione, P. & Pisani, A. Homeostatic changes of the endocannabinoid system in Parkinson's disease. *Movement Disorders* **26**, 216-222 (2011).
255. Gowran, A., Noonan, J. & Campbell, V.A. The multiplicity of action of cannabinoids: implications for treating neurodegeneration. *CNS Neuroscience & Therapeutics* **17**, 637-644 (2011).
256. Hansen, H.H., Azcoitia, I., Pons, S., Romero, J., García-Segura, L.M., Ramos, J.A., Hansen, H.S. & Fernández-Ruiz, J. Blockade of cannabinoid CB₁ receptor function protects against *in vivo* disseminating brain damage following NMDA-induced excitotoxicity. *Journal of Neurochemistry* **82**, 154-158 (2002).
257. Muthian, S., Rademacher, D.J., Roelke, C.T., Gross, G.J. & Hillard, C.J. Anandamide content is increased and CB₁ cannabinoid receptor blockade is protective during transient, focal cerebral ischemia. *Neuroscience* **129**, 743-750 (2004).
258. Sun, Y., Alexander, S.P.H., Garle, M.J., Gibson, C.L., Hewitt, K., Murphy, S.P., Kendall, D.A. & Bennett, A.J. Cannabinoid activation of PPAR α ; a novel neuroprotective mechanism. *British Journal of Pharmacology* **152**, 734-743 (2007).
259. Minor, K.M., Letko, A., Becker, D., Drögemüller, M., Mandigers, P.J.J., Bellekom, S.R., Leegwater, P.A.J., Stassen, Q.E.M., Putschbach, K., Fischer, A., Flegel, T., Matiasek, K., Ekenstedt, K.J., Furrow, E., Patterson, E.E., Platt, S.R., Kelly, P.A., Cassidy, J.P., Shelton, G.D., Lucot, K., Bannasch, D.L., Martineau, H., Muir, C.F., Priestnall, S.L., Henke, D., Oevermann, A., Jagannathan, V., Mickelson, J.R. &

- Drögemüller, C. Canine NAPEPLD-associated models of human myelin disorders. *Scientific Reports* **8**, 5818 (2018).
260. Morena, M. & Hill, M.N. Buzzkill: the consequences of depleting anandamide in the hippocampus. *Neuropsychopharmacology* (2019).
261. Zimmermann, T., Bartsch, J.C., Beer, A., Lomazzo, E., Guggenhuber, S., Lange, M.D., Bindila, L., Pape, H.-C. & Lutz, B. Impaired anandamide/palmitoylethanolamide signaling in hippocampal glutamatergic neurons alters synaptic plasticity, learning, and emotional responses. *Neuropsychopharmacology* (2018).
262. Morena, M., Aukema, R.J., Leitl, K.D., Rashid, A.J., Vecchiarelli, H.A., Josselyn, S.A. & Hill, M.N. Upregulation of anandamide hydrolysis in the basolateral complex of amygdala reduces fear memory expression and indices of stress and anxiety. *The Journal of Neuroscience* **39**, 1275-1292 (2019).

Chapter 2

High-throughput screening delivers new inhibitors for NAPE-PLD

2.1 Introduction

N-acylphosphatidylethanolamine phospholipase D (NAPE-PLD) is an enzyme that produces a family of bioactive signaling lipids called *N*-acylethanolamines (NAEs) from *N*-acylphosphatidylethanolamines (NAPEs). The enzyme has a metallo- β -lactamase fold and cannot perform transphosphatidylation, making it distinct from the PLD enzyme family.¹ A crystal structure of NAPE-PLD showed that the active site contains two Zn^{2+} -ions bridged by one hydrolytic water molecule, all coordinated by several histidine and aspartic acid residues (Figure 1A).²

The NAE products exert their biological effects through multiple protein classes, including G protein-coupled receptors (*e.g.* cannabinoid receptors type 1 and type 2, GPR55), ion channels (*e.g.* transient receptor potential vanilloid 1) and nuclear receptors (*e.g.* peroxisome proliferator-activated receptor (PPAR)- α) that are involved in a multitude of biological processes, such as neurotransmission, immunomodulation, energy balance, motor coordination, addiction, pain sensation, appetite, inflammation,

neurodegeneration and anxiety.³ Better understanding of the physiological role of NAPE-PLD and the NAEs products has been hampered by a lack of pharmacological tools that allow acute modulation of the enzyme in live animals. These tools are essential to effectively perturb NAE signaling, as different NAPE-PLD knock-out (KO) mice studies have shown inconsistent results, with NAE levels not reduced in all cases, possibly due to long-term compensatory effects.⁴⁻⁸

So far, few inhibitors for NAPE-PLD have been reported. Out of a small library of NAPE substrate mimics, phosphoramidate AHP-71B was described as an inhibitor with micromolar potency ($IC_{50} \sim 10 \mu M$) (Figure 1B).⁹ Other reported active compounds are β -lactamase substrate nitrocefin⁹, desketoraloxifene analog 17b¹⁰, which also targets phospholipase D1 (PLD1), and sulfonamide ARN19874¹¹. All compounds showed poor to moderate potency for NAPE-PLD *in vitro*. Of note, ARN19874 was able to increase NAPE levels in HEK293 cells, but did not affect most NAE levels.¹¹ Therefore, new and more potent chemotypes are required to target NAPE-PLD *in vivo*.

Over the past three decades, the discovery of new first-in-class drugs has primarily relied on target-based approaches.¹² High-throughput screening (HTS) has been the predominant method for identifying new chemical entities, while fragment-based screening, virtual screening and structure-based design have also been successfully employed.¹³ To start a HTS campaign a biochemical assay needs to be developed that allows the testing of 10,000 to 100,000 compounds per day.¹⁴ Most of the currently available NAPE-PLD activity assays use thin-layer chromatography (TLC) or mass

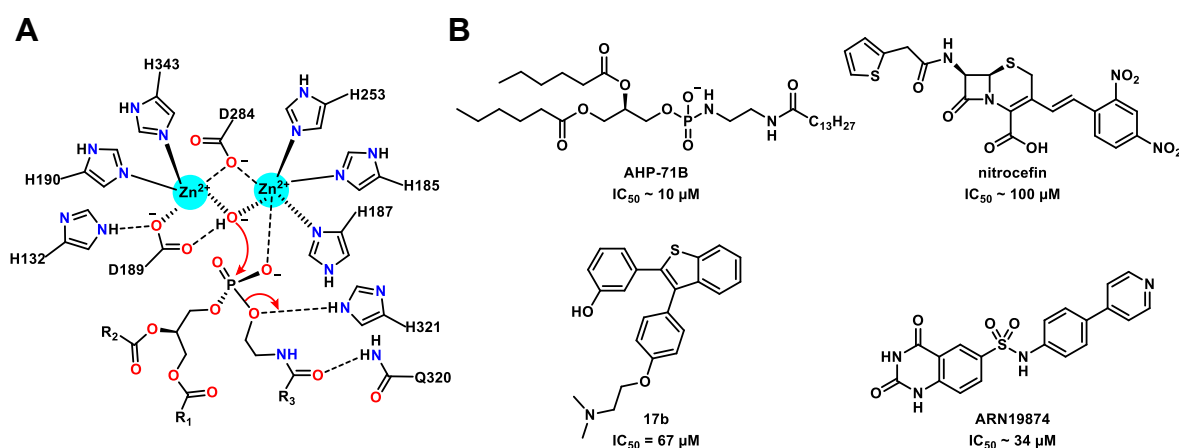


Figure 1. A) Model of the NAPE-PLD active site mechanism based on the published crystal structure.² B) Reported inhibitors for NAPE-PLD.

spectrometry (MS) as a read-out and are therefore not compatible with high-throughput screening.^{1,4,11} In this chapter the optimization of a recently reported fluorescent NAPE-PLD activity assay¹⁵ and its successful application in the screening of the Joint European Compound Library (JECL) as part of the European Lead Factory¹⁶ (ELF) is described. Four new chemotypes were discovered of which the most promising scaffold was confirmed as a selective, submicromolar potent inhibitor for NAPE-PLD.

2.2 Results

A previously reported fluorescent NAPE-PLD activity assay¹⁵ using the surrogate substrate *N*-((6-(2,4-dinitrophenyl)amino)hexanoyl)-2-(4,4-difluoro-5,7-dimethyl-4-bora-3a,4a-diaza-*s*-indacene-3-pentanoyl)-1-hexa-decanoyl-*sn*-glycero-3-phosphoethanolamine triethylammonium salt (PED6) was converted to a HTS-compatible format. The assay principle relies on the cleavage of the phosphodiester bond of PED6 by NAPE-PLD, thereby liberating the fluorescent BODIPY from the dinitroaniline quencher, which is proportional to the enzymatic activity (Figure 2A). Firstly, the assay was altered to accommodate membrane fractions of NAPE-PLD overexpressing cells as an enzyme source instead of purified NAPE-PLD. This circumvents the need for laborious protein purification. Human embryonic kidney (HEK293T) cells were transiently transfected with a pcDNA3.1 plasmid containing human NAPE-PLD-FLAG. After 72 hours the cells were lysed, membrane

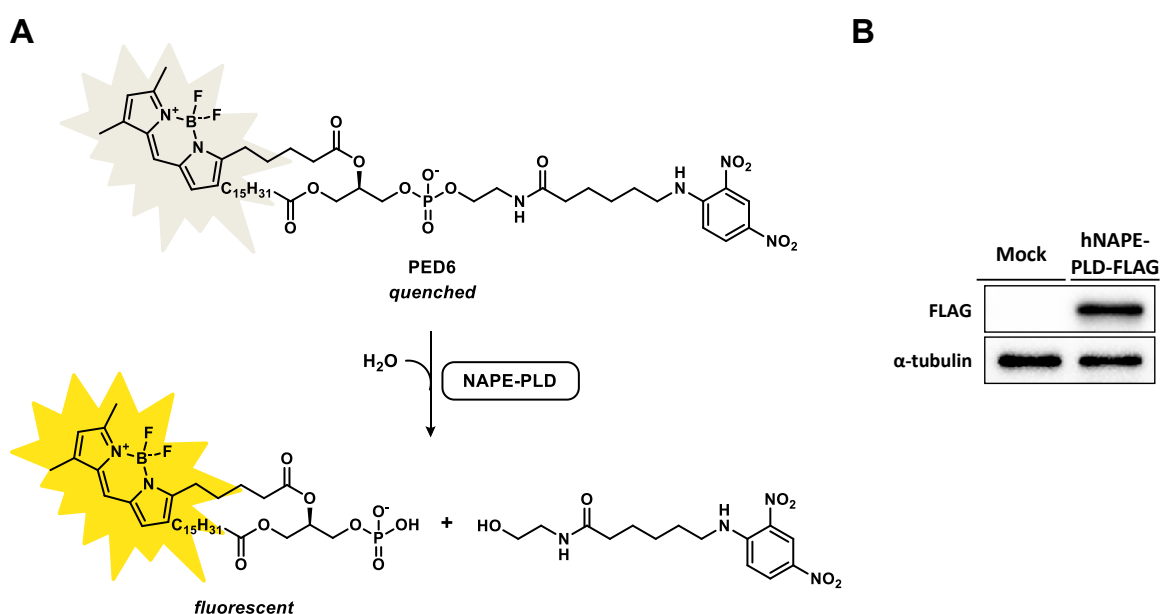


Figure 2. A) NAPE-PLD PED6 assay principle. B) Western blot of the membrane fraction from mock or hNAPE-PLD transfected HEK293T cells. α -Tubulin was used as a loading control.

fractions were prepared and the protein expression was confirmed by Western blot using anti-FLAG antibodies (Figure 2B).

Next, the optimal assay conditions were determined in a 96-well plate. The enzyme activity was linear between 0.01 and 0.5 $\mu\text{g}/\mu\text{L}$ membrane lysate (Figure 3A). The signal-to-background (S/B)-ratio was determined between 0.02 and 0.05 $\mu\text{g}/\mu\text{L}$, minimizing the amount of lysate required, which gave 0.04 $\mu\text{g}/\mu\text{L}$ as the optimal concentration (Figure 3B). The NAPE-PLD activity was highest at pH 7.5 (Figure 3C). Triton X-100 was employed as a rate enhancing non-ionic detergent¹⁷⁻¹⁹, with optimal activity and S/B-ratio at 0.02% (v/v) (Figure 3D). Screening various salts showed that NaCl, KCl and MgCl_2 enhanced the enzymatic activity, giving an optimal 2.5-fold increase for 150 mM NaCl (Figure 3E). ZnCl_2 was inhibitory with an IC_{50} of 60 μM (95% confidence interval (CI): 46-78 μM), confirming previous findings for purified rat NAPE-PLD in a radioactive natural substrate assay.¹⁹⁻²¹ Although purified NAPE-PLD has been reported to be stimulated by millimolar CaCl_2

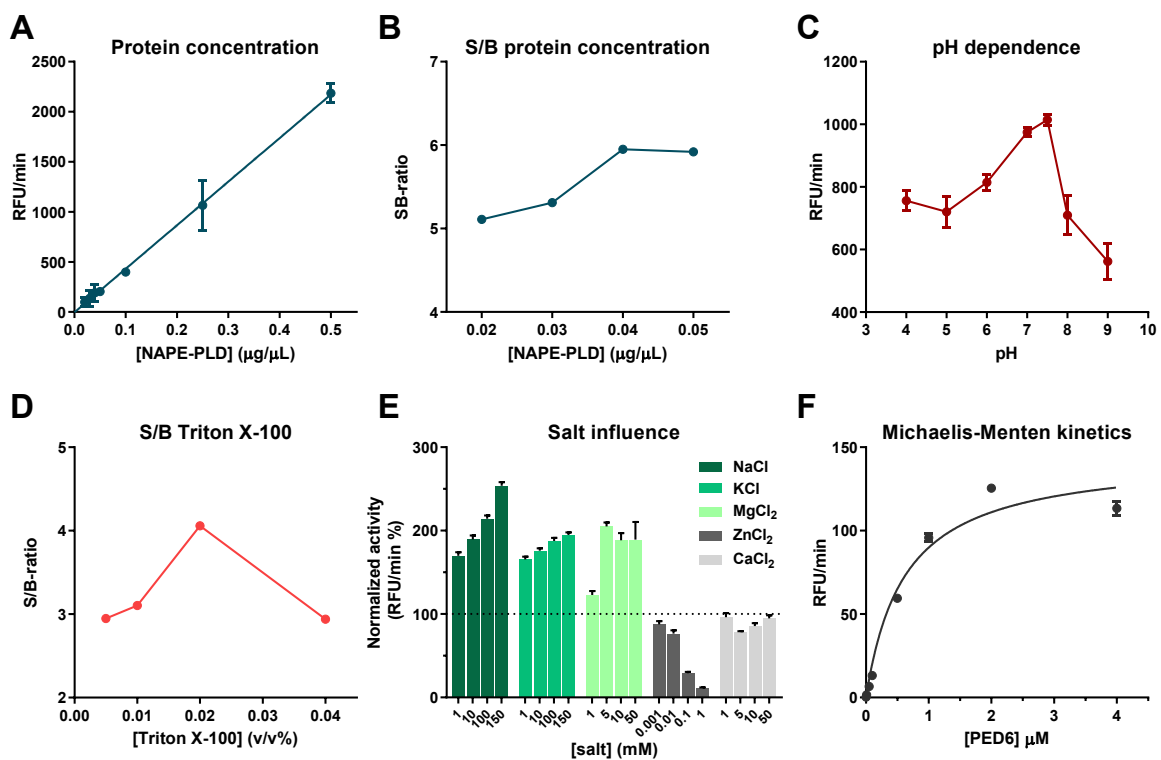


Figure 3. Optimization of the NAPE-PLD PED6 surrogate substrate assay. **A)** Protein concentration vs. enzyme rate was linear between 0.01 and 0.5 $\mu\text{g}/\mu\text{L}$. **B)** Optimal S/B-ratio at 0.04 $\mu\text{g}/\mu\text{L}$ membrane lysate. **C)** Optimal enzyme activity at pH 7.5. **D)** Optimal S/B-ratio at 0.02% Triton X-100. **E)** NaCl (150 mM) increases the enzyme activity 2.5 fold. **F)** Michaelis-Menten plot ($K_M = 0.59 \pm 0.08 \mu\text{M}$, $V_{\text{max}} = 145 \text{ RFU}/\text{min}$). Data represent mean values \pm SD ($n = 2-4$).

concentrations²⁰, in this assay CaCl_2 did not affect the NAPE-PLD activity. A prior study reported that the presence of phosphatidylethanolamine (PE) in the membrane fraction of NAPE-PLD transfected COS-7 cells constitutively activate NAPE-PLD, thereby mitigating the Ca^{2+} -induced stimulatory effect.²¹ A Michaelis-Menten constant (K_M) of $0.59 \pm 0.08 \mu\text{M}$ was determined for PED6 using the optimized assay conditions (Figure 3F). The intra-plate variability of the assay, measured as the coefficient of variance (CV), was 3.3%. This indicated that the assay is robust and compatible for high-throughput screening, which according to the ELF screening requirements should be a $\text{CV} < 10\%$.²² Next, the assay was miniaturized to a 384-well format to allow compatibility with the ELF program. This afforded a S/B-ratio of 5.4 and statistical effect size Z' of 0.89, well within the ELF limits for a HTS-compatible assay ($\text{S/B-ratio} > 3$ and $Z' > 0.6$).²²

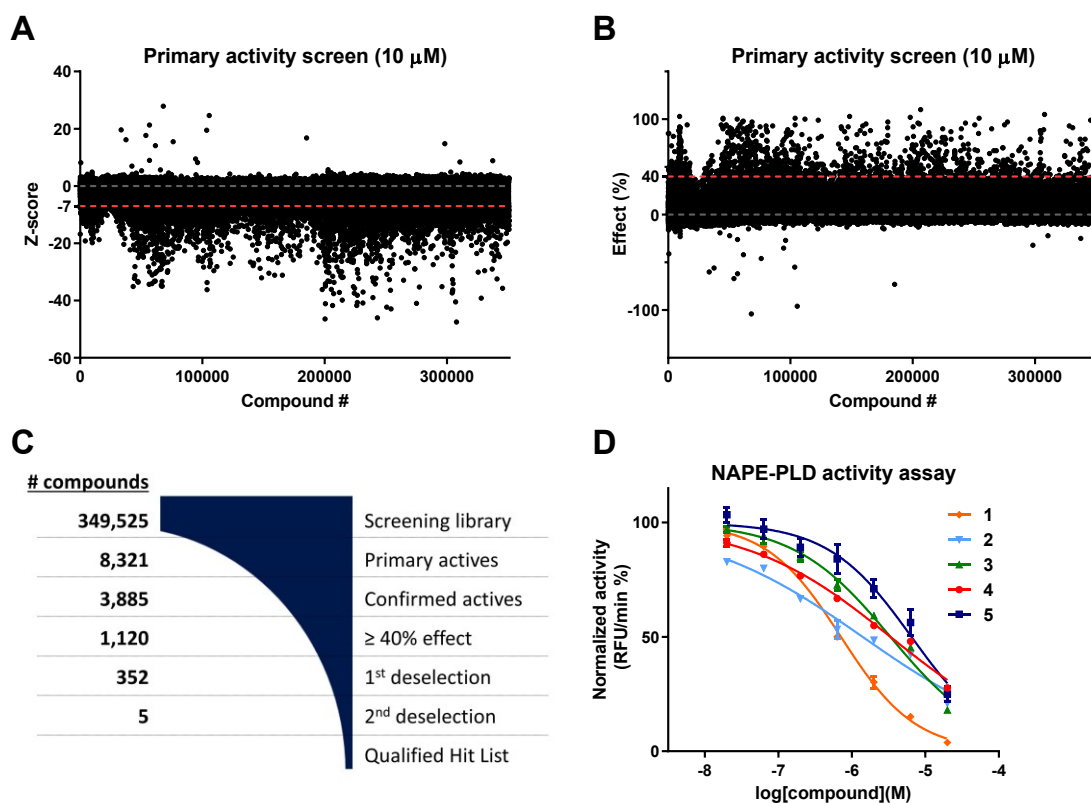


Figure 4. A) Primary activity screen plotted as Z-score. B) Primary activity screen plotted as effect %. C) Hit triage of the high-throughput campaign. D) Dose-response curves of hit compounds 1-5. Data represent mean values \pm SEM ($n = 2$).

Further assay miniaturization was performed by the Pivot Park Screening Centre to afford a 1,536-well assay. This resulted in a robust assay with $Z' = 0.87$, S/B-ratio = 6.7 and

CV = 3.3%. Approximately 350,000 compounds at a single concentration (10 μM) were screened in 294 plates in 3 days, affording 8321 actives using the cut-off value of Z-score ≤ -7 ($> 20\%$ -30% effect) (Figure 4A,C). Hit validation at the same concentration gave 3885 confirmed actives. To reduce the number of compounds, the percent effect on the enzyme activity ($\geq 40\%$) was utilized to obtain a list of 1120 actives (Figure 4B,C). Next, dose-response curves were generated in the presence and absence of ZnSO_4 (100 μM) to remove promiscuous Zn^{2+} -ion chelators, which yielded 352 hits. ZnCl_2 demonstrated an IC_{50} of 60 μM (Figure 3E), however the S/B-ratio (8.2) and Z' (0.68) of the leftover NAPE-PLD activity was sufficient to obtain reliable dose-response curves. Visual inspection of the 352 compounds revealed the presence of potential assay interfering compounds that absorbed light within the visible wavelength, therefore a second deselection assay was

Table 1. NAPE-PLD activity and physicochemical parameters of HTS hit compounds 1-5.

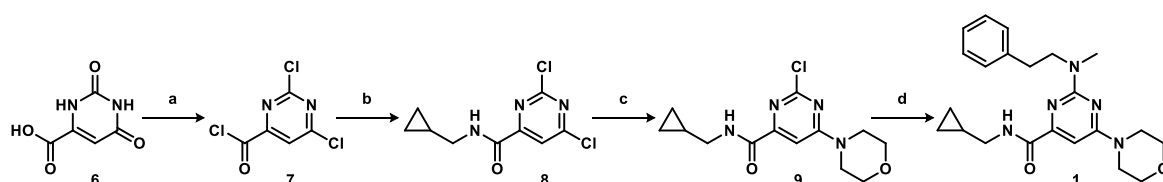
| ID | Structure | pIC_{50} \pm SEM | K_i (μM) | Desel. 1 pIC_{50} (+ ZnSO_4) | Desel. 2 pIC_{50} (quenching) | MW ^a (Da) | cLogP ^b | LipE ^c | tPSA ^b (\AA^2) |
|----|-----------|--------------------------------|----------------------------|---|--|-------------------------|--------------------|-------------------|---|
| 1 | | 6.14 \pm 0.02 | 0.26 | 6.15 | <4.7 | 396 | 3.84 | 2.30 | 69.5 |
| 2 | | 5.86 \pm 0.06 | 0.51 | 5.44 | 4.73 | 449 | 4.63 | 1.23 | 76.9 |
| 3 | | 5.46 \pm 0.04 | 1.3 | 5.21 | 5.08 | 398 | 3.42 | 2.04 | 96.2 |
| 4 | | 5.48 \pm 0.04 | 1.2 | 5.62 | <4.7 | 464 | 6.23 | -0.75 | 66.5 |
| 5 | | 5.20 \pm 0.05 | 2.3 | 5.14 | <4.7 | 431 | 5.75 | -0.55 | 71.8 |

^a MW: molecular weight; ^b cLogP and topological polar surface area (tPSA) were calculated using Chemdraw 15; ^c Lipophilic efficiency (LipE) = pIC_{50} - cLogP.

developed. The substrate PED6 was incubated with lysate to obtain the maximum fluorescent signal, followed by incubation with different concentrations of the confirmed actives to determine the ability of the compounds to quench the fluorescent signal under the primary assay conditions. Only compounds that demonstrated no effect ($pIC_{50} < 5$) in the second deselection assay were selected. Notably, nitrocefin was identified as a false positive inhibitor using this procedure. The compounds were checked for purity ($> 85\%$) and correct molecular weight (MW) by liquid chromatography-mass spectrometry (LC-MS) analysis. This afforded a qualified hit list of 5 compounds with four different chemotypes (Table 1, Figure 4D).

Compound **1** (*N*-(cyclopropylmethyl)-2-(methyl(phenethyl)amino)-6-morpholino-pyrimidine-4-carboxamide) displayed the most optimal biological and physicochemical characteristics (MW = 396, $cLogP = 3.84$, LipE = 2.30) (Table 2). Resynthesis of **1** was achieved by chlorination of orotic acid **6**, followed by three sequential chemoselective substitution reactions with cyclopropylmethanamine, morpholine and *N*-methylphenethylamine, respectively, affording **1** (Scheme 1). After chemical analysis and retesting in the NAPE-PLD activity assay, the identity and submicromolar potency ($pIC_{50} \pm SE = 6.09 \pm 0.04$, $K_i = 0.30 \mu M$, 95% CI = 0.22 - 0.38 μM) of hit compound **1** was confirmed.

Subsequently, the selectivity of **1** for the proteins of the endocannabinoid system was evaluated. Compound **1** did not show any significant inhibitory activities at 10 μM at the cannabinoid receptors type 1 and type 2 (Table 2) as well as for the other proteins involved in anandamide biosynthesis and degradation, such as phospholipase A2 group 4E (PLA2G4E) and fatty acid amide hydrolase (FAAH), respectively (Table 3, Figure 5). Furthermore, **1** did not inhibit the enzymes involved in the biosynthesis and degradation of the endocannabinoid 2-arachidonoylglycerol (2-AG), including diacylglycerol lipases (DAGL α/β), monoacylglycerol lipase (MAGL) and α,β -hydrolase domain containing 6 (ABHD6) (Table 3, Figure 5).



Scheme 1. Synthesis of hit compound **1**. Reagents and conditions: a) $POCl_3$, DMF, reflux, 60%; b) cyclopropylmethanamine, Et_3N , DCM, $-78^\circ C$ to $0^\circ C$, 80%; c) morpholine, DiPEA, MeOH, $0^\circ C$, 89%; d) *N*-methylphenethylamine, DiPEA, *n*-BuOH, μW , $160^\circ C$, 50%.

Table 2. **1** shows no significant inhibitory activity for the CB₁ and CB₂ receptors.

| Radioligand displacement at 10 μ M 1 (% \pm SD) | |
|---|------------------|
| hCB ₁ | hCB ₂ |
| 39 \pm 6 | 40 \pm 6 |

>50% is considered a target

Table 3. No inhibitory activities were found for **1** for the metabolic enzymes of the ECS. Activities were measured using surrogate or natural substrate assays for DAGL α / β and MAGL, or activity-based protein profiling for PLA2G4E.

| Remaining enzyme activity at 10 μ M 1 (% \pm SD) | | | |
|---|---------------|------------|--------------|
| hDAGL α | mDAGL β | hMAGL | hPLA2G4E |
| 103 \pm 9 | 86 \pm 13 | 74 \pm 7 | 118 \pm 17 |

< 50% is considered a target.

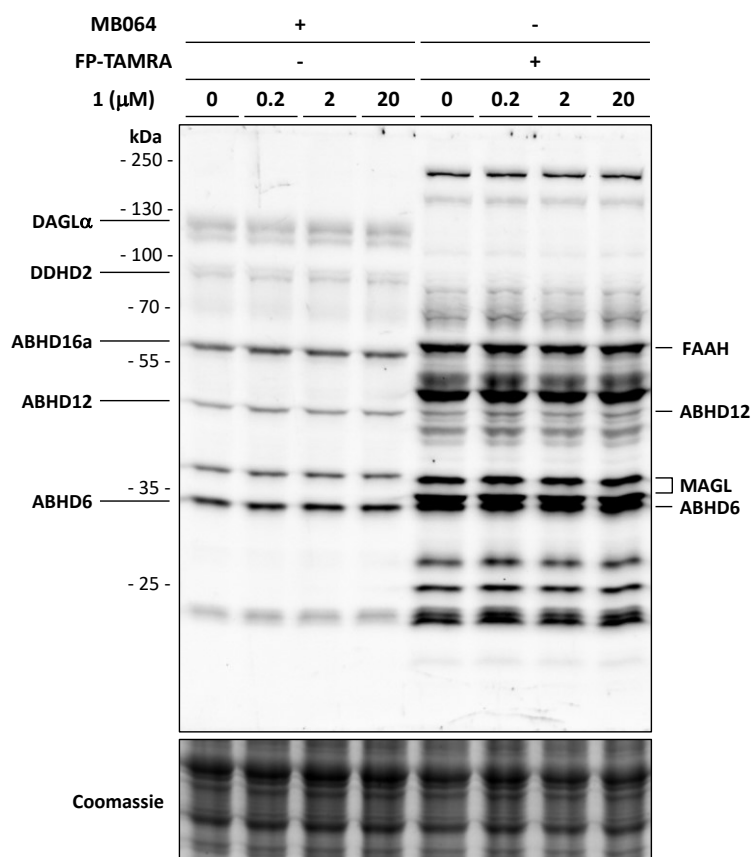


Figure 5. Competitive activity-based protein profiling of **1** in mouse brain membrane fractions using broad-spectrum lipase probes MB064²³ (0.25 μ M) and FP-TAMRA (0.5 μ M). No probe targets were competed by **1**. Structures of MB064 and FP-TAMRA in Supplementary Figure 1.

2.3 Conclusion

In this chapter, the successful optimization of a NAPE-PLD fluorescent surrogate substrate assay and high-throughput screening of the Joint European Compound Library is described. This provided five hits from four new chemotypes: two dihydropyrrolo[2,1-a]isoquinoline-1-carboxylate esters and three singletons. On the basis of its favorable potency and physicochemical properties, pyrimidine-4-carboxamide **1** was selected for resynthesis. The submicromolar activity of **1** could be confirmed, making it the most potent NAPE-PLD inhibitor to date. In addition, **1** was selective over the receptors and enzymes of the endocannabinoid system. It is anticipated that these new chemical scaffolds, in particular compound **1**, may provide a useful starting point for the discovery of *in vivo* active NAPE-PLD inhibitors.

Acknowledgements

The research leading to these results has received support from the Innovative Medicines Initiative Joint Undertaking under grant agreement n°115489, resources of which are composed of financial contribution from the European Union's Seventh Framework Programme (FP7/2007-2013) and EFPIA companies. Anouk van der Gracht and Ioli Kotsogianni are kindly acknowledged for their contributions with regard to the NAPE-PLD assay development and compound synthesis. Marjolein Soethoudt, Ming Jiang, Tom van der Wel, Timo Wendel and Anthe Janssen are acknowledged for performing biochemical assays. Jesse Wat, Helma van den Hurk, Stan van Boeckel and the Pivot Park Screening Centre are kindly acknowledged for conducting the high-throughput screen.

2.4 Experimental Methods

A. Biological Procedures

Cloning of plasmid DNA

Full length human cDNA of human NAPE-PLD (obtained from Natsuo Ueda¹), hDAGL α , mDAGL β , hMAGL and hPLA2G4E was cloned into mammalian expression vector pcDNA3.1, containing a C-terminal FLAG-tag and genes for ampicillin and neomycin resistance. All plasmids were grown in XL-10 Z-competent cells and prepped (Maxi Prep, Qiagen). Constructs were verified by Sanger sequencing (Macrogen).

Cell culture

HEK293T were cultured at 37 °C and 7% CO₂ in DMEM (Sigma Aldrich, D6546) with GlutaMax (2 mM), penicillin (100 µg/ml, Duchefa), streptomycin (100 µg/ml, Duchefa) and 10% newborn calf serum (Thermo Fisher). Cells were passaged twice a week to appropriate confluence by thorough pipetting.

Transient transfection

One day before transfection 10^7 cells were seeded in 15 cm petri dishes. Two hours before transfection the medium was refreshed with 13 mL medium. Transfection was performed with polyethyleneimine (PEI, 60 μ g per dish) in a ratio of 3:1 with plasmid DNA (20 μ g per dish). PEI and plasmid DNA were incubated in serum free medium (2 mL per dish) at rt for 15 min, followed by dropwise addition to the cells. Transfection with the empty pcDNA3.1 vector was used to generate mock control samples. The medium was refreshed after 24 hours and cells were harvested after 48 or 72 hours in cold PBS. Cells were centrifuged (10 min, 200 g , 4 $^{\circ}$ C) and the supernatant was removed. The cell pellets were flash frozen in liquid N_2 and stored at -80 $^{\circ}$ C.

Cell lysate preparation

Cell pellets were resuspended in lysis buffer: 20 mM HEPES pH 7.2, 2 mM DTT, 0.25 M sucrose, 1 mM $MgCl_2$, 2.5 U/mL benzonase and incubated on ice for 30 minutes. The cells were homogenized with a Heidolph SilentCrusher S (5F, 20,000 rpm, 3 x 7s). The cytosolic fraction (supernatant) was separated from the membranes by ultra-centrifugation (30 min, 100,000 g , 4 $^{\circ}$ C, Beckman Coulter, Ti 70.1 rotor). The pellet (membrane fraction) was resuspended in storage buffer (20 mM HEPES pH 7.2, 2 mM DTT) and homogenized with a Heidolph SilentCrusher S (5F, 20,000 rpm, 3 x 7s). Protein concentrations were determined using a Quick Start™ Bradford protein assay (Bio-Rad). All samples were stored at -80 $^{\circ}$ C.

Mouse brain lysate preparation

Mouse brain lysate was prepared as described previously.²⁴ Mouse brains (C57BL/6) were isolated according to guidelines approved by the ethical committee of Leiden University (DEC#13191), frozen in liquid N_2 and stored at -80 $^{\circ}$ C. Tissues were thawed on ice, dounce homogenized in cold lysis buffer (20 mM HEPES pH 7.2, 2 mM DTT, 1 mM $MgCl_2$, 25 U/mL benzonase) and incubated on ice (15 min), followed by low-speed centrifugation (2,500 g , 3 min, 4 $^{\circ}$ C) to remove debris. After high-speed centrifugation (100,000 g , 45 min, 4 $^{\circ}$ C) the supernatant was collected as the cytosol fraction. The pellet was resuspended in cold storage buffer (20 mM HEPES pH 7.2, 2 mM DTT). Protein concentrations were determined by a Quick Start™ Bradford protein assay (Bio-Rad) or Qubit™ protein assay (Invitrogen). Samples were flash frozen in liquid N_2 and stored at -80 $^{\circ}$ C.

Western blot

Cell lysates were denatured with 4x Laemmli buffer (stock concentrations: 240 mM Tris-HCl pH 6.8, 8% w/v SDS, 40% v/v glycerol, 5% v/v β -mercaptoethanol, 0.04% v/v bromophenol blue, 30 min, RT) and 10-20 μ g per sample was resolved on a 10% acrylamide SDS-PAGE gel (180 V, 75 min). Proteins were transferred from the gel to a 0.2 μ m PVDF membrane using a Trans-Blot® Turbo (Bio-Rad). The membranes were washed with TBS (50 mM Tris-HCl pH 7.5, 150 mM NaCl) and blocked with 5% milk in TBST (50 mM Tris-HCl pH 7.5, 150 mM NaCl, 0.05% Tween 20) 1 h at rt or overnight at 4 $^{\circ}$ C. Primary antibodies against FLAG-tagged proteins (Sigma Aldrich, F3165, 1:5000 in 5% milk in TBST) or α -tubulin (Genetex, GTX76511, 1:5000 in 5% milk in TBST) were incubated 1 h at rt or overnight at 4 $^{\circ}$ C. Membranes were washed with TBST and incubated with secondary antibodies: for FLAG-tagged proteins, goat-anti-mouse-HRP (Santa Cruz, sc-2005, 1:5000 in 5% milk in TBST); for α -tubulin, goat-anti-rat (Santa Cruz, sc-2032, 1:5000 in 5% milk in TBST). All secondary antibodies were incubated for 1 h at rt. Membranes were washed with TBST and TBS. The blot was developed in the dark using a luminal solution (10 mL, 1.4 mM luminal in Tris-HCl pH 8.8), ECL enhancer (100 μ L, 6.7 mM *para*-hydroxycoumaric acid in DMSO) and H_2O_2 (3 μ L, 30% w/w in H_2O). Chemiluminescence was visualized using a ChemiDoc™ Imaging System (Bio-Rad). Band intensity is normalized to α -tubulin using ImageLab software (Bio-Rad).

Surrogate substrate-based fluorescence assay NAPE-PLD

The NAPE-PLD activity assay was based on a previously reported method with small alterations.¹⁵ The membrane fraction from transient overexpression of human NAPE-PLD in HEK293T cells was diluted to 0.4 μ g/ μ L in assay buffer (50 mM Tris-HCl pH 7.5, 150 mM NaCl, 0.02% Triton X-100). The substrate PED6

(Invitrogen, D23739) 1 mM stock in DMSO was consecutively diluted in DMSO (10x) and in assay buffer (10x) to make a 10 μ M working solution. Relevant concentrations of compound (100x working solution) were prepared in DMSO. The assay was performed in a dark Greiner 96-well plate (flat bottom), final volume 100 μ L. The compound or DMSO was incubated with membrane protein lysate (final concentration 0.04 μ g/ μ L) for 30 minutes at 37 $^{\circ}$ C. Then, substrate PED6 was added (final concentration 1 μ M) and the measurement was started immediately on a TECAN infinite M1000 pro at 37 $^{\circ}$ C (excitation 485 nm, emission 535 nm, gain = 100), scanning every 2 minutes for 1 h. Mock membrane lysate with DMSO was used for background subtraction. The slope of $t = 4$ min to $t = 14$ min was used as the enzymatic rate (RFU/min), which was normalized to generate IC_{50} curves using Graphpad Prism v6 (log(inhibitor) vs. normalized response with variable slope). K_i values were calculated from the Cheng-Prusoff equation $K_i = IC_{50}/(1+([S]/K_M))$ where $K_M = 0.59$ μ M. All measurements were performed in $N = 2$, $n = 2$ or $N = 2$, $n = 4$ for controls, with $Z' \geq 0.6$.

High-throughput screening of NAPE-PLD activity assay

High-throughput screening of the NAPE-PLD activity assay was performed at Pivot Park Screening Centre B.V. Assay buffer with Triton-X100 (prepared on the day of the assay): 1x assay buffer (50 mM Tris-HCl pH 7.5, 150 mM NaCl, 0.02% Triton-X100 (Sigma-Aldrich)). In a black 1536-well plate (Corning, Cat# 3724, Lot# 19214025) was added 10 nL of 4 mM compound (final compound concentration 10 μ M and final DMSO concentration 0.25%). 10 nL of DMSO was added to the min wells or 10 nL of 40 mM nitrocefin (Millipore) to the max wells (final nitrocefin concentration 100 μ M and final DMSO concentration 0.25%). 2 μ L of 0.08 μ g/ μ L hNAPE-PLD membrane lysate in assay buffer was added (final concentration 0.04 μ g/ μ L), followed by incubation for 30 minutes at rt. Then 2 μ L of 1 μ M PED6 in assay buffer (final concentration 0.5 μ M) was added and the plate was incubated for 1 h at rt. Fluorescence intensity signal (excitation 485 nm, emission 535 nm) was measured on a Envision reader. For dispensing an Echo-555 was used for 10 nL compounds, nitrocefin or DMSO. A Multidrop Combi was used for dispensing 2 μ L hNAPE-PLD lysate and a BioRAPTR for dispensing 2 μ L PED6. In this manner the Joint European Compound Library (JECL) consisting of 349,525 compounds was screened in 294 plates with a S/B ratio between 5.48-7.08 and Z' between 0.66-0.91. As a hit criterium a Z-score ≤ -7 was used ($Z\text{-score} = (X - \mu)/\sigma$ where X = measured effect, μ = mean effect, σ = standard deviation). This gave a hit rate of 2.4% (8,321 primary actives). The primary actives were screened again at 10 μ M (single point) giving 3,885 confirmed actives. Due to the large number of compounds the cut-off score was changed to ≥ 40 effect %, giving 1,120 hits. Dose-response curves (7 equidistant concentration steps from 20 μ M to 20 nM, $n = 2$) were performed with or without 100 μ M ZnSO₄ to remove promiscuous zinc chelators, which gave 352 compounds. A second deselection to remove fluorescence quenchers was performed: first the maximum fluorescence signal was obtained by incubating PED6 with hNAPE-PLD membrane lysate, then the compounds were added in a similar dose-response concentration curve ($n = 2$). Five compounds (1-5) demonstrating no effect ($pIC_{50} < 5$) in the second deselection assay were selected (Table 1).

Natural substrate-based fluorescence assay DAGL α

The hDAGL α natural substrate assay was performed as reported previously.²⁵ Standard assay conditions: 0.2 U/mL glycerol kinase (GK), glycerol-3-phosphate oxidase (GPO) and horseradish peroxidase (HRP), 0.125 mM ATP, 10 μ M Amplifu™Red, 5% DMSO in a total volume of 200 μ L. The assay additionally contained 5 μ g/mL hMAGL overexpressing membranes, 100 μ M SAG and 0.0075% (w/v) Triton X-100, with a final protein concentration of 50 μ g/mL. All measurements were performed in $N = 2$, $n = 2$ or $N = 2$, $n = 4$ for controls, with $Z' \geq 0.6$.

Surrogate substrate-based fluorescence assay DAGL β

The biochemical mDAGL β assay was performed as reported previously.²³ In brief, the biochemical mDAGL β activity assay is based on the hydrolysis of *para*-nitrophenylbutyrate (PNP-butyrate) by membrane preparations from HEK293T cells transiently transfected with mDAGL β . Reactions were performed in 50 mM

HEPES pH 7.2 buffer with 0.05 $\mu\text{g}/\mu\text{L}$ mDAGL β transfected membrane fractions (final protein concentration). All measurements were performed in $N = 2$, $n = 2$ or $N = 2$, $n = 4$ for controls, with $Z' \geq 0.6$.

Natural substrate-based fluorescence assay MAGL

The MAGL activity assay is based on the production of glycerol from 2-arachidonoylglycerol (2-AG) hydrolysis by hMAGL overexpressing membrane preparations from transiently transfected HEK293T cells, as previously reported.²⁶ Glycerol is formed during the reaction and is coupled to the oxidation of commercially available Amplifu™Red via a multi-enzyme cascade, resulting in a fluorescent signal from resorufin. Standard assays were performed in HEMNB buffer (50 mM HEPES pH 7.4, 1 mM EDTA, 5 mM MgCl_2 , 100 mM NaCl, 0.5% w/v BSA) in black, flat bottom 96-wells plates. Final protein concentration of membrane preparations from overexpressing hMAGL HEK293T cells was 1.5 $\mu\text{g}/\text{mL}$ (0.3 μg per well). Inhibitors were added from 40x concentrated DMSO stocks. After 20 min incubation, 100 μL assay mix containing glycerol kinase (GK), glycerol-3-phosphate oxidase (GPO), horse radish peroxidase (HRP), adenosine triphosphate (ATP), Amplifu™Red and 2-arachidonoylglycerol (2-AG) was added and fluorescence was measured in 5 min intervals for 60 min on a plate reader. Final assay concentrations: 0.2 U/mL GK, GPO and HRP, 0.125 mM ATP, 10 μM Amplifu™Red, 25 μM 2-AG, 5% DMSO, 0.5% ACN in a total volume of 200 μL . All measurements were performed in $N = 2$, $n = 2$ or $N = 2$, $n = 4$ for controls, with $Z' \geq 0.6$. For IC_{50} determination, slopes of corrected fluorescence in time were determined in the linear interval of $t = 10$ to $t = 35$ min and then scaled to the corrected positive control of hMAGL-overexpressing membranes treated with vehicle (DMSO) as a 100% activity reference point. The data was exported to GraphPad Prism v6 and analyzed in a non-linear dose-response analysis with variable slope.

Radioligand displacement assays CB₁ and CB₂ receptor

[³H]CP55940 displacement assays to determine the affinity for the cannabinoid CB₁ and CB₂ were performed as previously described.²⁷ Membrane aliquots containing 5 μg (CHOK1hCB₁_bgal) or 1.5 μg (CHOK1hCB₂_bgal) of membrane protein were incubated in a total volume of 100 μL assay buffer (50 mM Tris-HCl pH 7.4, 5 mM MgCl_2 and 0.1% BSA) at 25 °C for 2 hours in presence of ~3 nM or ~1.5 nM [³H]CP55940, respectively. NAPE-PLD inhibitors were added at 50, 10 or 1 μM (final concentration) and nonspecific binding was determined in the presence of 10 μM rimonabant (CHOK1hCB₁_bgal) or 10 μM AM630 (CHOK1hCB₂_bgal). Incubations were terminated by harvesting the samples on 96-well GF/C filters, precoated with 25 μL 0.25% (v/v) PEI per well, with rapid vacuum filtration, to separate the bound and free radioligand, using a Perkin Elmer 96-well harvester (Perkin Elmer, Groningen, The Netherlands). Filters were subsequently washed ten times with ice-cold assay buffer on the 96-well plate and 5 times on a wash plate. Filter plates were dried at 55 °C for ~45 min, then 25 μL Microscint was added per well (Perkin Elmer, Groningen, The Netherlands). After 3 hours, the filter-bound radioactivity was determined by scintillation spectrometry using a Microbeta2® 2450 microplate counter (Perkin Elmer, Boston, MA).

Activity based protein profiling for FAAH, ABHD6, ABHD12 and PLA2G4E activity

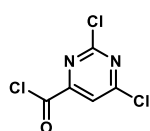
Gel-based activity based protein profiling (ABPP) was performed as previously described.²³ In brief, mouse brain membrane proteome or hPLA2G4E overexpressing cytosol lysate (9.5 μL , 2 or 1 $\mu\text{g}/\mu\text{L}$, respectively) was pre-incubated with vehicle or inhibitor (0.5 μL 40x inhibitor stock in DMSO, 30 min, rt) followed by incubation with the activity based probe MB064 (250 nM, prepared in house) or FP-TAMRA (500 nM, Invitrogen) for mouse brain lysate (15 min, rt) or FP-TAMRA (50 nM) for PLA2G4E overexpressing lysate (5 min, rt). Final concentrations for the inhibitors are indicated in the main text and figure legends. Proteins were denatured with 4x Laemmli buffer (3.5 μL , stock concentrations: 240 mM Tris-HCl pH 6.8, 8% w/v SDS, 40% v/v glycerol, 5% v/v β -mercaptoethanol, 0.04% v/v bromophenol blue, 30 min, rt). The samples (10 μL per slot) were resolved by SDS-PAGE (respectively, 10% or 8% acrylamide for mouse brain or PLA2G4E lysate, 180 V, 75 min). Gels were scanned using Cy3 and Cy5 multichannel settings (605/50 and 695/55

filters, respectively) on a ChemiDoc™ Imaging System (Bio-Rad). Fluorescence was normalized to Coomassie staining and quantified with Image Lab (Bio-Rad).

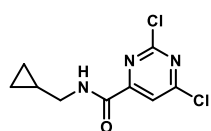
B. Synthetic Procedures

General

All chemicals (Sigma-Aldrich, Fluka, Acros, Merck, Combi-Blocks, Fluorochem, TCI) were used as received. All solvents used for reactions were of analytical grade. THF, Et₂O, DMF, CH₃CN and DCM were dried over activated 4 Å molecular sieves, MeOH over 3 Å molecular sieves. Flash chromatography was performed on silica gel (Screening Devices BV, 40-63 μm, 60 Å). The eluent EtOAc was of technical grade and distilled before use. Reactions were monitored by thin layer chromatography (TLC) analysis using Merck aluminium sheets (Silica gel 60, F₂₅₄). Compounds were visualized by UV-absorption (254 nm) and spraying for general compounds: KMnO₄ (20 g/L) and K₂CO₃ (10 g/L) in water, or for amines: ninhydrin (0.75 g/L) and acetic acid (12.5 mL/L) in ethanol, followed by charring at ~150 °C. ¹H and ¹³C NMR experiments were recorded on a Bruker AV-400 (400/101 MHz), Bruker DMX-400 (400/101 MHz) and Bruker AV-500 (500/126 MHz). Chemical shifts are given in ppm (δ) relative to tetramethylsilane or CDCl₃ as internal standards. Multiplicity: s = singlet, br s = broad singlet, d = doublet, dd = doublet of doublet, t = triplet, q = quartet, p = pentet, m = multiplet. Coupling constants (*J*) are given in Hz. LC-MS measurements were performed on a Thermo Finnigan LCQ Advantage MAX ion-trap mass spectrometer (ESI⁺) coupled to a Surveyor HPLC system (Thermo Finnigan) equipped with a standard C18 (Gemini, 4.6 mm D x 50 mm L, 5 μm particle size, Phenomenex) analytical column and buffers A: H₂O, B: CH₃CN, C: 0.1% aq. TFA. High resolution mass spectra were recorded on a LTQ Orbitrap (Thermo Finnigan) mass spectrometer or a Synapt G2-Si high definition mass spectrometer (Waters) equipped with an electrospray ion source in positive mode (source voltage 3.5 kV, sheath gas flow 10 mL min⁻¹, capillary temperature 250 °C) with resolution *R* = 60000 at *m/z* 400 (mass range *m/z* = 150-2000) and dioctylphthalate (*m/z* = 391.28428) as a lock mass. Preparative HPLC was performed on a Waters Acquity Ultra Performance LC with a C18 column (Gemini, 150 x 21.2 mm, Phenomenex). All final compounds were determined to be >95% pure by integrating UV intensity recorded via HPLC.

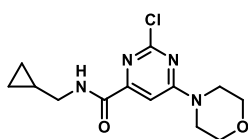


2,6-Dichloropyrimidine-4-carbonyl chloride (7). In a 500 mL round bottom flask orotic acid (15.6 g, 100 mmol, 1 eq) was dissolved in phosphorous oxychloride (46 mL, 500 mmol, 5 eq) and 10 drops of DMF were added. The mixture was heated to reflux and stirred for 19 h. *n*-Hexane (250 mL) was added and the mixture was stirred vigorously for 10 min and then transferred to a separatory funnel containing 100 mL H₂O. The flask was washed with 50 mL hexane. After shaking, the aqueous layer was removed and the hexane was washed with brine (1 x 100 mL), dried with MgSO₄ and concentrated under reduced pressure to yield the product (12.8 g, 60.4 mmol, 60%). ¹H NMR (500 MHz, CDCl₃) δ 8.00 (s, 1H). ¹³C NMR (126 MHz, CDCl₃) δ 167.17, 165.27, 161.56, 158.19, 119.70.

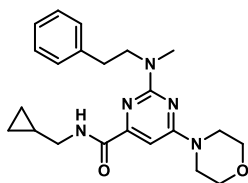


2,6-Dichloro-*N*-(cyclopropylmethyl)pyrimidine-4-carboxamide (8). A round bottom flask was charged with 2,6-dichloropyrimidine-4-carbonyl chloride **7** (0.63 mL, 5.0 mmol, 1 eq) and dry DCM (50 mL) and cooled to -78 °C. Et₃N (0.91 mL, 6.5 mmol, 1.3 eq) and cyclopropylmethanamine (0.44 mL, 5.1 mmol, 1.025 eq) were added and the mixture was stirred for 3.5 h while letting the acetone bath warm up to 0 °C. The mixture was transferred to a separatory funnel and the organic layer was washed with H₂O (2 x 50 mL) and brine (1 x 75 mL), dried (Na₂SO₄), filtered and concentrated under reduced pressure. Silica gel column chromatography (5% → 20% EtOAc/pentane) afforded the product (0.99 g, 4.0 mmol, 80%). TLC: *R*_f = 0.8 (20% EtOAc/pentane). ¹H NMR (400 MHz, CDCl₃) δ 8.11 (s, 1H), 7.96 (br s, 1H), 3.44 – 3.27 (m, 2H), 1.20 – 1.03 (m, 1H), 0.68 – 0.52 (m, 2H),

0.32 (q, $J = 4.8$ Hz, 2H). ^{13}C NMR (101 MHz, CDCl_3) δ 164.74, 160.44, 160.04, 159.77, 118.22, 44.72, 10.57, 3.67. HRMS [$\text{C}_9\text{H}_{10}\text{Cl}_2\text{N}_3\text{O} + \text{H}$] $^+$: 246.0195 calculated, 246.0196 found.



2-Chloro-*N*-(cyclopropylmethyl)-6-morpholinopyrimidine-4-carboxamide (9). A round bottom flask was charged with dichloropyrimidine **8** (1.7 g, 7.1 mmol, 1 eq) and dry MeOH (71 mL) and cooled to 0 °C. DiPEA (1.9 mL, 11 mmol, 1.5 eq) and morpholine (0.64 mL, 7.4 mmol, 1.05 eq) were added and the mixture was stirred for 2 h at 0 °C. The solvents were evaporated under reduced pressure and the crude material was purified by silica gel column chromatography (30% → 60% EtOAc/pentane), affording the product (1.7 g, 6.3 mmol, 89%). $R_f = 0.5$ in 40% EtOAc/pentane. ^1H NMR (400 MHz, CDCl_3) δ 7.94 (t, $J = 5.9$ Hz, 1H), 7.28 (s, 1H), 3.87 – 3.63 (m, 8H), 3.33 – 3.25 (m, 2H), 1.12 – 1.00 (m, 1H), 0.61 – 0.52 (m, 2H), 0.32 – 0.24 (m, 2H). ^{13}C NMR (101 MHz, CDCl_3) δ 163.83, 162.21, 159.84, 157.90, 99.36, 66.35, 44.45, 10.65, 3.64. Regioselectivity was confirmed by NOESY analysis. HRMS [$\text{C}_{13}\text{H}_{17}\text{ClN}_4\text{O}_2 + \text{H}$] $^+$: 297.1113 calculated, 297.1116 found.



***N*-(Cyclopropylmethyl)-2-(methyl(phenethyl)amino)-6-morpholino-pyrimidine-4-carboxamide (1).** A microwave vial with a magnetic stir bar was charged with 2-chloropyrimidine **9** (59 mg, 0.20 mmol, 1 eq), *N*-methylphenethylamine hydrobromide (66 mg, 0.30 mmol, 1.5 eq), DiPEA (140 μL , 0.80 mmol, 4 eq) and *n*-BuOH (1 mL). The tube was capped, flushed with N_2 and heated to 160 °C in a microwave reactor (Biotage, 75 W) for 8 h. The reaction showed complete conversion as measured by LC/MS. The mixture was transferred to a round-bottom flask, concentrated under reduced pressure and coevaporated with toluene (2x). The residue was purified by silica gel column chromatography (40% → 60% EtOAc/pentane), affording the product (40 mg, 0.10 mmol, 50%). TLC: $R_f = 0.3$ (40% EtOAc/pentane). ^1H NMR (400 MHz, CDCl_3) δ 8.03 (br s, 1H), 7.34 – 7.25 (m, 2H), 7.25 – 7.12 (m, 3H), 6.72 (s, 1H), 3.88 – 3.72 (m, 6H), 3.72 – 3.55 (m, 4H), 3.30 (t, $J = 6.5$ Hz, 2H), 3.13 (s, 3H), 2.90 (t, $J = 7.7$ Hz, 2H), 1.14 – 0.99 (m, 1H), 0.64 – 0.44 (m, 2H), 0.38 – 0.19 (m, 2H). ^{13}C NMR (101 MHz, CDCl_3) δ 164.66, 163.97, 160.86, 156.78, 139.92, 128.95, 128.58, 126.29, 90.08, 66.74, 51.68, 44.50, 44.11, 35.70, 33.93, 10.88, 3.48. HRMS [$\text{C}_{22}\text{H}_{29}\text{N}_5\text{O}_2 + \text{H}$] $^+$: 396.2394 calculated, 396.2387 found.

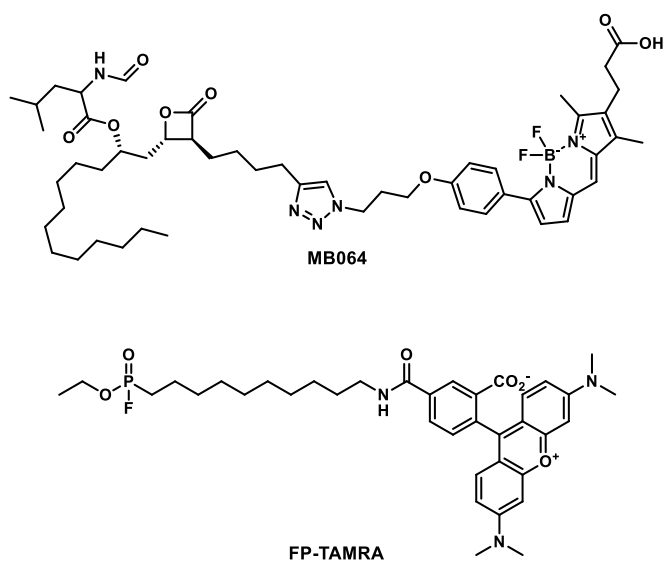
References

- Okamoto, Y., Morishita, J., Tsuboi, K., Tonai, T. & Ueda, N. Molecular characterization of a phospholipase D generating anandamide and its congeners. *Journal of Biological Chemistry* **279**, 5298-5305 (2004).
- Magotti, P., Bauer, I., Igarashi, M., Babagoli, M., Marotta, R., Piomelli, D. & Garau, G. Structure of human *N*-acylphosphatidylethanolamine-hydrolyzing phospholipase D: regulation of fatty acid ethanolamide biosynthesis by bile acids. *Structure* **23**, 598-604 (2015).
- Hussain, Z., Uyama, T., Tsuboi, K. & Ueda, N. Mammalian enzymes responsible for the biosynthesis of *N*-acylethanolamines. *Biochimica et Biophysica Acta (BBA) - Molecular and Cell Biology of Lipids* **1862**, 1546-1561 (2017).
- Leung, D., Saghatelian, A., Simon, G.M. & Cravatt, B.F. Inactivation of *N*-acyl phosphatidylethanolamine phospholipase D reveals multiple mechanisms for the biosynthesis of endocannabinoids. *Biochemistry* **45**, 4720-4726 (2006).
- Simon, G.M. & Cravatt, B.F. Endocannabinoid biosynthesis proceeding through glycerophospho-*N*-acyl ethanolamine and a role for α/β -hydrolase 4 in this pathway. *Journal of Biological Chemistry* **281**, 26465-26472 (2006).

6. Simon, G.M. & Cravatt, B.F. Characterization of mice lacking candidate *N*-acyl ethanolamine biosynthetic enzymes provides evidence for multiple pathways that contribute to endocannabinoid production *in vivo*. *Molecular BioSystems* **6**, 1411-1418 (2010).
7. Tsuboi, K., Okamoto, Y., Ikematsu, N., Inoue, M., Shimizu, Y., Uyama, T., Wang, J., Deutsch, D.G., Burns, M.P., Ulloa, N.M., Tokumura, A. & Ueda, N. Enzymatic formation of *N*-acylethanolamines from *N*-acylethanolamine plasmalogen through *N*-acylphosphatidylethanolamine-hydrolyzing phospholipase D-dependent and -independent pathways. *Biochimica et Biophysica Acta (BBA) - Molecular and Cell Biology of Lipids* **1811**, 565-577 (2011).
8. Leishman, E., Mackie, K., Luquet, S. & Bradshaw, H.B. Lipidomics profile of a NAPE-PLD KO mouse provides evidence of a broader role of this enzyme in lipid metabolism in the brain. *Biochimica et Biophysica Acta (BBA) - Molecular and Cell Biology of Lipids* **1861**, 491-500 (2016).
9. Petersen, G., Pedersen, A.H., Pickering, D.S., Begtrup, M. & Hansen, H.S. Effect of synthetic and natural phospholipids on *N*-acylphosphatidylethanolamine-hydrolyzing phospholipase D activity. *Chemistry and Physics of Lipids* **162**, 53-61 (2009).
10. Scott, S.A., Spencer, C.T., O'Reilly, M.C., Brown, K.A., Lavieri, R.R., Cho, C.-H., Jung, D.-I., Larock, R.C., Brown, H.A. & Lindsley, C.W. Discovery of desketoraloxifene analogues as inhibitors of mammalian, *Pseudomonas aeruginosa*, and NAPE phospholipase D enzymes. *ACS Chemical Biology* **10**, 421-432 (2015).
11. Castellani, B., Diamanti, E., Pizzirani, D., Tardia, P., Maccesi, M., Realini, N., Magotti, P., Garau, G., Bakkum, T., Rivara, S., Mor, M. & Piomelli, D. Synthesis and characterization of the first inhibitor of *N*-acylphosphatidylethanolamine phospholipase D (NAPE-PLD). *Chemical Communications* **53**, 12814-12817 (2017).
12. Eder, J., Sedrani, R. & Wiesmann, C. The discovery of first-in-class drugs: origins and evolution. *Nature Reviews Drug Discovery* **13**, 577 (2014).
13. Macarron, R., Banks, M.N., Bojanic, D., Burns, D.J., Cirovic, D.A., Garyantes, T., Green, D.V.S., Hertzberg, R.P., Janzen, W.P., Paslay, J.W., Schopfer, U. & Sittampalam, G.S. Impact of high-throughput screening in biomedical research. *Nature Reviews Drug Discovery* **10**, 188 (2011).
14. Inglese, J., Johnson, R.L., Simeonov, A., Xia, M., Zheng, W., Austin, C.P. & Auld, D.S. High-throughput screening assays for the identification of chemical probes. *Nature Chemical Biology* **3**, 466 (2007).
15. Peppard, J.V., Mehdi, S., Li, Z. & Duguid, M.S. WO 2008/150832 A1.
16. Karawajczyk, A., Orrling, K.M., de Vlieger, J.S.B., Rijnders, T. & Tzalis, D. The European Lead Factory: a blueprint for public-private partnerships in early drug discovery. *Frontiers in Medicine* **3** (2017).
17. Schmid, P.C., Reddy, P.V., Natarajan, V. & Schmid, H.H. Metabolism of *N*-acylethanolamine phospholipids by a mammalian phosphodiesterase of the phospholipase D type. *Journal of Biological Chemistry* **258**, 9302-9306 (1983).
18. Natarajan, V., Schmid, P.C., Reddy, P.V. & Schmid, H.H.O. Catabolism of *N*-Acylethanolamine phospholipids by dog brain preparations. *Journal of Neurochemistry* **42**, 1613-1619 (1984).
19. Ueda, N., Liu, Q. & Yamanaka, K. Marked activation of the *N*-acylphosphatidylethanolamine-hydrolyzing phosphodiesterase by divalent cations. *Biochimica et Biophysica Acta (BBA) - Molecular and Cell Biology of Lipids* **1532**, 121-127 (2001).
20. Wang, J., Okamoto, Y., Morishita, J., Tsuboi, K., Miyatake, A. & Ueda, N. Functional analysis of the purified anandamide-generating phospholipase D as a member of the metallo- β -lactamase family. *Journal of Biological Chemistry* **281**, 12325-12335 (2006).
21. Wang, J., Okamoto, Y., Tsuboi, K. & Ueda, N. The stimulatory effect of phosphatidylethanolamine on *N*-acylphosphatidylethanolamine-hydrolyzing phospholipase D (NAPE-PLD). *Neuropharmacology* **54**, 8-15 (2008).
22. European Lead Factory assay requirements: <https://www.europeanleadfactory.eu/how-submit/drug-target-assays/requirements>.

23. Baggelaar, M.P., Janssen, F.J., van Esbroeck, A.C.M., den Dulk, H., Allarà, M., Hoogendoorn, S., McGuire, R., Florea, B.I., Meeuwenoord, N., van den Elst, H., van der Marel, G.A., Brouwer, J., Di Marzo, V., Overkleeft, H.S. & van der Stelt, M. Development of an activity-based probe and *in silico* design reveal highly selective inhibitors for diacylglycerol lipase- α in brain. *Angewandte Chemie International Edition* **52**, 12081-12085 (2013).
24. Baggelaar, M.P., Chameau, P.J.P., Kantae, V., Hummel, J., Hsu, K.L., Janssen, F., van der Wel, T., Soethoudt, M., Deng, H., den Dulk, H., Allara, M., Florea, B.I., Di Marzo, V., Wadman, W.J., Kruse, C.G., Overkleeft, H.S., Hankemeier, T., Werkman, T.R., Cravatt, B.F. & van der Stelt, M. Highly selective, reversible inhibitor identified by comparative chemoproteomics modulates diacylglycerol lipase activity in neurons. *J. Am. Chem. Soc.* **137**, 8851-8857 (2015).
25. van der Wel, T., Janssen, F.J., Baggelaar, M.P., Deng, H., den Dulk, H., Overkleeft, H.S. & van der Stelt, M. A natural substrate-based fluorescence assay for inhibitor screening on diacylglycerol lipase α . *Journal of Lipid Research* **56**, 927-935 (2015).
26. Navia-Paldanius, D., Savinainen, J.R. & Laitinen, J.T. Biochemical and pharmacological characterization of human α/β -hydrolase domain containing 6 (ABHD6) and 12 (ABHD12). *Journal of Lipid Research* **53**, 2413-2424 (2012).
27. Soethoudt, M., Grether, U., Fingerle, J., Grim, T.W., Fezza, F., de Petrocellis, L., Ullmer, C., Rothenhäusler, B., Perret, C., van Gils, N., Finlay, D., MacDonald, C., Chicca, A., Gens, M.D., Stuart, J., de Vries, H., Mastrangelo, N., Xia, L., Alachouzos, G., Baggelaar, M.P., Martella, A., Mock, E.D., Deng, H., Heitman, L.H., Connor, M., Di Marzo, V., Gertsch, J., Lichtman, A.H., Maccarrone, M., Pacher, P., Glass, M. & van der Stelt, M. Cannabinoid CB₂ receptor ligand profiling reveals biased signalling and off-target activity. *Nature Communications* **8**, 13958 (2017).

Supplementary Information



Supplementary Figure 1. Structures of serine hydrolase activity-based probes MB064²³ and FP-TAMRA.

Chapter 3

Optimization of pyrimidine-4-carboxamide NAPE-PLD inhibitors affords LEI-401

3.1 Introduction

N-acylphosphatidylethanolamine phospholipase D (NAPE-PLD) is considered to be the principal enzyme in the brain that produces *N*-acylethanolamines (NAEs), a family of signaling lipids.¹ NAPE-PLD catalyzes the hydrolysis of *N*-acylphosphatidylethanolamines (NAPEs) to NAEs, which includes the endocannabinoid anandamide.² Through activation of the cannabinoid receptors 1 and 2 (CB₁ and CB₂), as well as the ion channel transient receptor potential vanilloid 1 (TRPV1), anandamide regulates various physiological processes such as appetite, pain, fertility, stress and anxiety.³

Decreased levels of saturated, mono- and poly-unsaturated NAEs have been observed in the brains of various strains of NAPE-PLD knock-out mice, although anandamide levels were not affected in all genetic mouse models.⁴⁻⁷ This suggested the existence of compensatory mechanisms in animals with long-term ablation of NAPE-PLD activity and has spurred the discovery of alternative NAE biosynthetic pathways.^{1,8} These genetic models highlight the necessity of a complementary approach to modulate anandamide

biosynthesis in an acute manner. Thus, there is a need for pharmacological tools that inhibit the function of NAPE-PLD. Previously, several NAPE-PLD inhibitors have been described, but they lack the potency, selectivity or physicochemical properties to function as *in situ* or *in vivo* active NAPE-PLD inhibitors.⁹⁻¹¹

In Chapter 2, pyrimidine-4-carboxamides were identified as a novel chemotype of NAPE-PLD inhibitors in a high-throughput screening (HTS) campaign. Here, the structure-activity relationship (SAR) of a library of NAPE-PLD inhibitors is described. Starting from HTS hit **1** (Figure 1) a hit optimization program led to the discovery of **LEI-401**. Modification of the *N*-methylphenethylamine and morpholine substituents of compound **1**, provided **LEI-401** as a NAPE-PLD inhibitor with nanomolar activity and good physicochemical properties.

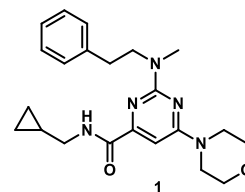


Figure 1. Structure of HTS lead hit **1**.

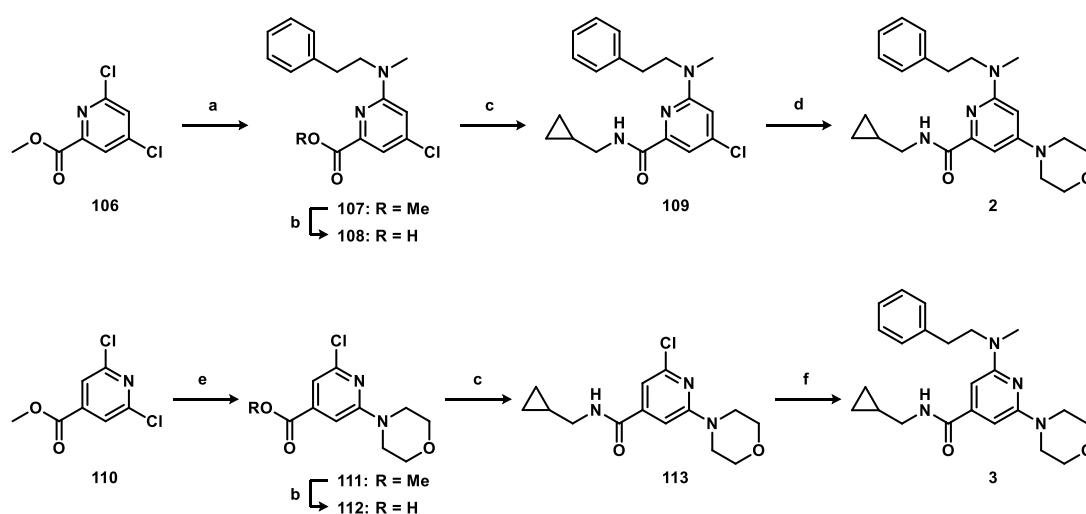
3.2 Results

To study the SAR of hit **1**, different synthetic routes were employed that allowed systematic variation of the amide, morpholine and phenethylamine substituents as well as the pyrimidine scaffold. This led to the synthesis of compounds **2-105**.

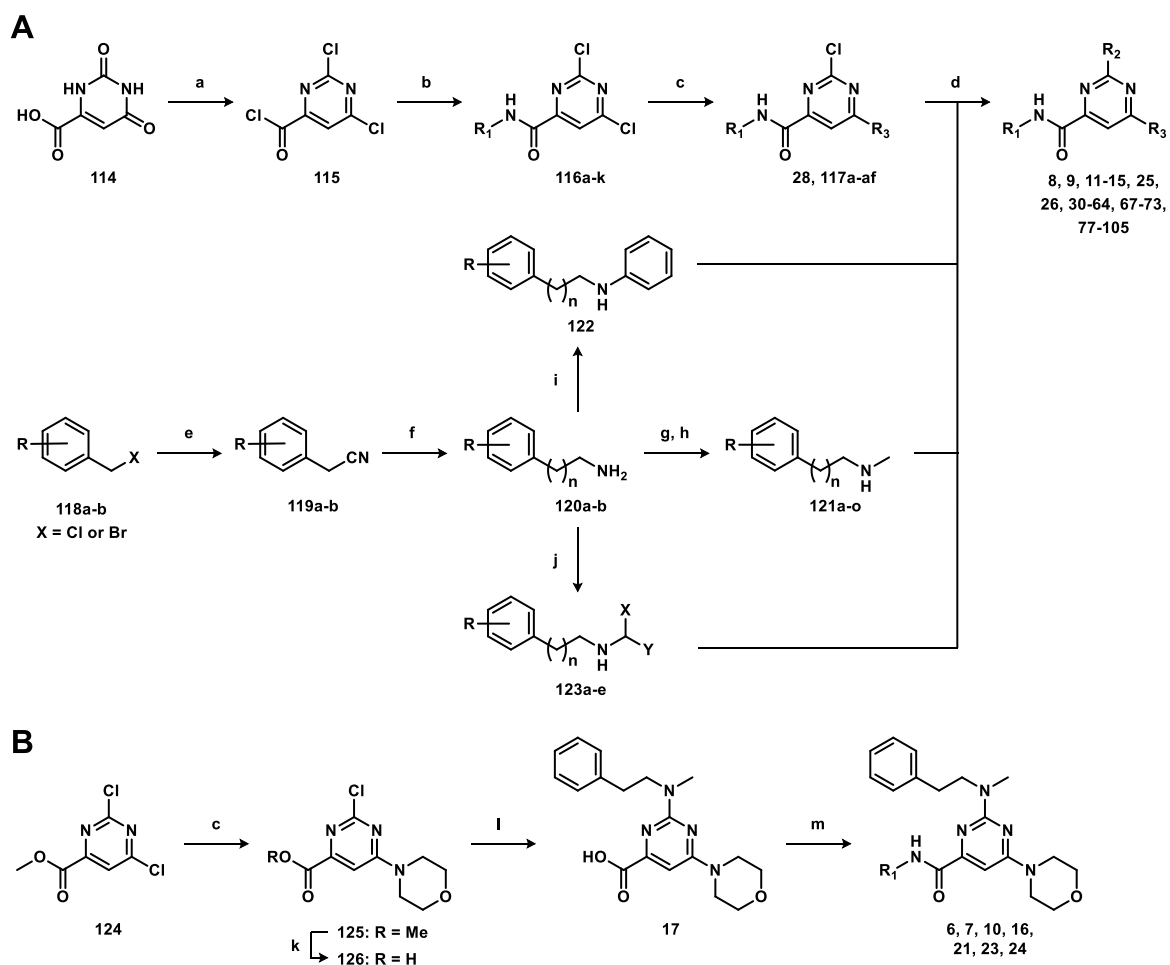
The influence of the nitrogen atoms in the pyrimidyl ring was investigated with pyridyl analogues **2** and **3** (Scheme 1). The synthesis of compound **2** commenced with the regioselective nucleophilic aromatic substitution (S_NAr) of dichloride **106** with *N*-methylphenethylamine, which gave **107** (confirmed by 1H , ^{13}C -HMBC and 1H -NOESY 2D NMR). Subsequent ester hydrolysis and amide coupling afforded **109**, which was converted to **2** with morpholine using Buchwald-Hartwig amination conditions.¹² Isomer **3** was synthesized in four steps from symmetric dichloride **110**: S_NAr with morpholine, ester hydrolysis and amide coupling giving **113**, followed by similar Pd-catalyzed amination with *N*-methylphenethylamine.

Next, the systematic synthesis of amide, morpholine and phenethylamine analogues of **1** was performed. Amide derivatives were made via two general four-step sequences, which either produced the amide in the second or final step (Scheme 2A,B). The primary route depicted in Scheme 2A started with orotic acid (**114**), which was converted to acyl chloride **115** using phosphorous oxychloride. Cold addition (-78 °C to 0 °C) of various primary amines gave amides **116a-k**. The more electrophilic 4-chloro substituent of the

dichloropyrimidine was regioselectively substituted with morpholine analogues to afford **117a-af** (confirmed by $^1\text{H-NOESY}$ 2D NMR). Finally, high temperature and/or microwave irradiation was used to couple different phenethylamine derivatives to the 2-chloropyrimidine scaffold, which provided the desired products. Non-commercially available *N*-methylphenethylamines were synthesized from benzylic halides **118a-b**, that were converted to the corresponding nitrile (**119a-b**) followed by hydrogenation affording the primary amine (**120a-b**). Mono-*N*-methylation was achieved by carbamoylation and subsequent LiAlH_4 reduction, giving the *N*-methylphenethylamines **121a-o**. Alternatively, phenethylamine was converted to the *N*-phenyl analogue **122** via Chan-Lam coupling¹³ or to *N*-alkyl derivatives **123a-e** by reductive amination with aldehydes or ketones. The secondary route for introduction of the amide in the final step consisted of regioselective substitution of dichloropyrimidine **124** to give **125** (Scheme 2B). Then, ester hydrolysis followed by coupling with *N*-methylphenethylamine gave carboxylic acid **17**, which was condensed with various amines. Molecules (**2**, **5**, **18-21**, **27**, **28**, **65**, **66**, **74-77**) not listed in Scheme 1 or 2 were synthesized according to the routes described in the Supplementary Information (Supplementary Scheme 1-8).



Scheme 1. Synthesis of pyridyl analogues **2** and **3**. Reagents and conditions: a) *N*-methylphenethylamine, DiPEA, MeOH, rt, 40%; b) NaOH, THF, H₂O, rt, for **108**: 90%, for **112**: 99%; c) cyclopropylmethanamine, EDC-HCl, HOBT, DCM, rt, for **109**: 24%, for **113**: 77%; d) morpholine, RuPhos-Pd-G3, NaOtBu, THF, toluene, 110 °C, 37%; e) morpholine, K₂CO₃, CH₃CN, reflux, 65%; f) *N*-methylphenethylamine, RuPhos-Pd-G3, NaOtBu, THF, toluene, 110 °C, 41%.

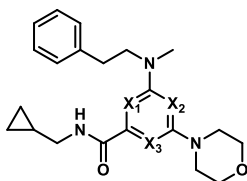


Scheme 2. A) General synthetic route for compound **1** analogues. B) Alternative synthetic route for amide analogues. Reagents and conditions: a) POCl_3 , DMF, reflux, 60%; b) R_1NH_2 , Et_3N , DCM, $-78\text{ }^\circ\text{C}$ to $0\text{ }^\circ\text{C}$, 78% – 99%; c) (cyclo)alkylNH, DiPEA, MeOH, $0\text{ }^\circ\text{C}$, 32% – 99%, or (hetero)arylOH or heteroarylNH, K_2CO_3 , DMF, rt, 51% – 76%; d) **121a-o** or **122** or **123a-e**, DiPEA, *n*-BuOH, μW , $160\text{ }^\circ\text{C}$ or oil bath, $120\text{ }^\circ\text{C}$, 21% – 97%; e) KCN, EtOH, dioxane, H_2O , reflux, 84% – 99%; f) H_2 , Pd/C, HCl, EtOH, rt, 98% – 99%; g) methyl chloroformate, DiPEA, DCM, $0\text{ }^\circ\text{C}$ to rt; h) LiAlH_4 , THF, $0\text{ }^\circ\text{C}$ to reflux, 40% – 94% over 2 steps; i) phenylboronic acid, $\text{Cu}(\text{OAc})_2 \cdot \text{H}_2\text{O}$, 4 \AA MS, O_2 , DCE, rt, 32%; j) aldehyde or ketone, $\text{NaB}(\text{OAc})_3\text{H}$, AcOH, DCM, rt, 18% – 63%. k) NaOH, THF, MeOH, H_2O , rt, 99%; l) *N*-methylphenethylamine, DiPEA, *n*-BuOH, $120\text{ }^\circ\text{C}$, 51%; m) R_1NH_2 , PyBOP, DiPEA, DMF, $0\text{ }^\circ\text{C}$ to rt, 43% – 55%.

A fluorescent NAPE-PLD activity assay was performed to measure the half maximum inhibitory concentration (IC_{50}) of inhibitors (**2-105**), as described previously (Chapter 2). The data are reported in Tables 1-7 as the $\text{pIC}_{50} \pm \text{SEM}$ ($N = 2$, $n = 2$). First, to identify the essential pharmacophore of the scaffold, pyridyl analogues **2** and **3** and pyrimidyl regioisomer **4** were evaluated (Table 1). The removal of the X_2 -nitrogen (compound **2**),

but not X_1 (compound **3**), resulted in a ten-fold drop in potency. This suggested that the X_2 -nitrogen may form an important *H*-bond interaction with the protein, while the electron withdrawing effect seems less important. A significant decrease in potency was also observed for regioisomer **4**, indicating that the scaffold of the hit was most optimal.

Table 1. Activity data for hit **1** and scaffold analogues **2-4**.



| ID | X_1 | X_2 | X_3 | $pIC_{50} \pm SEM$ | $cLogP^a$ |
|----------|-------|-------|-------|--------------------|-----------|
| 1 | N | N | CH | 6.09 ± 0.04 | 3.84 |
| 2 | N | CH | CH | 4.98 ± 0.03 | 4.25 |
| 3 | CH | N | CH | 5.84 ± 0.03 | 3.90 |
| 4 | CH | N | N | 5.39 ± 0.11 | 3.84 |

^a $cLogP$ was calculated using Chemdraw 15.

Next, the influence of the amide R_1 -substituent was investigated. Methylation of the amide in compound **1** resulted in complete loss of potency (compound **5**, Table 2), suggesting that the amide may form another hydrogen bond, or, alternatively that the methyl group has a steric clash with the enzyme. Removal of the methylene group (**6**) reduced the activity, whereas linear alkylamides **7-12** showed optimal inhibition with a propyl chain. Branching of the alkyl substituent, introduction of heteroatoms or larger aromatic groups were less favorable (compounds **13**, **14**, **16**, **24-26**). The ten-fold drop in potency for isobutylamide **13** may be attributed to the increased size of the isobutyl group or lack of π -character compared to the cyclopropyl moiety.¹⁴ Of note, propargylamide **15** was equally active compared to the hit. Substituting the lipophilic amide for more polar analogues did not result in increased activities (compounds **17-23**), although glycine methyl ester **19** showed to be equipotent to **1**. The amide bioisostere imidazole **27** displayed a substantial decrease in potency. In conclusion, the cyclopropylmethylamide of **1** is the most optimal R_1 -substituent and the SAR suggests that it occupies a small lipophilic pocket in NAPE-PLD.

To assess the influence of the *N*-methylphenethylamine moiety on the inhibitory activity, a large number of structural analogues (**28-67**) were evaluated (Tables 3-5).

Analogues **28-50** demonstrated that the *N*-methylphenethylamine is important for inhibitory activity as its complete removal resulted in inactive compounds (**28** and **29**) (Table 3). *N*-Methyl was found to be preferred over the hydrogen of **30**. A similar trend

Table 2. Structure-activity relationship analysis of amide analogues **5-27**.

| ID | R ₁ : | pIC ₅₀ ± SEM | cLogP ^a | ID | R ₁ : | pIC ₅₀ ± SEM | cLogP ^a |
|----|------------------|-------------------------|--------------------|----|------------------|-------------------------|--------------------|
| 1 | | 6.09 ± 0.04 | 3.84 | 17 | | <4.3 | 3.29 |
| 5 | | <4.3 | 2.71 | 18 | | <4.3 | 2.66 |
| 6 | | 5.43 ± 0.07 | 3.45 | 19 | | 6.08 ± 0.03 | 2.87 |
| 7 | | 4.75 ± 0.08 | 2.52 | 20 | | 4.77 ± 0.06 | 2.01 |
| 8 | | 4.87 ± 0.07 | 2.87 | 21 | | 5.30 ± 0.04 | 2.31 |
| 9 | | 5.34 ± 0.11 | 3.40 | 22 | | 4.96 ± 0.03 | 3.07 |
| 10 | | 5.74 ± 0.09 | 3.93 | 23 | | 4.51 ± 0.02 | 2.27 |
| 11 | | 5.17 ± 0.08 | 4.45 | 24 | | 4.49 ± 0.03 | 3.18 |
| 12 | | 4.46 ± 0.10 | 5.51 | 25 | | 4.63 ± 0.07 | 4.84 |
| 13 | | 5.15 ± 0.09 | 4.32 | 26 | | <4.3 | 6.72 |
| 14 | | 4.67 ± 0.08 | 4.72 | 27 | | 4.39 ± 0.05 | 3.94 |
| 15 | | 6.04 ± 0.06 | 3.29 | | | | |
| 16 | | 4.48 ± 0.07 | 3.66 | | | | |

^a cLogP was calculated using Chemdraw 15.

was apparent for benzylic amines **31** and **32**. Reducing (**31**) or increasing the alkyl chain length (**33**, **34**) decreased the potency, indicating that the two methylene chain length is optimal. Various large substituents (*e.g.* phenyl) on the phenyl group were tolerated, but

Table 3. Structure-activity relationship analysis of *N*-methylphenethylamine analogues **28-50**.

| ID | R ₂ : | pIC ₅₀ ± SEM | cLogP ^a | ID | R ₂ : | pIC ₅₀ ± SEM | cLogP ^a |
|----|------------------|-------------------------|--------------------|----|------------------|-------------------------|--------------------|
| 1 | | 6.09 ± 0.04 | 3.84 | 39 | | 6.05 ± 0.07 | 4.29 |
| 28 | | <4.3 | 1.58 | 40 | | 5.46 ± 0.07 | 3.76 |
| 29 | | <4.3 | 0.84 | 41 | | 6.11 ± 0.04 | 3.76 |
| 30 | | 5.56 ± 0.06 | 3.76 | 42 | | 5.21 ± 0.08 | 4.72 |
| 31 | | 5.04 ± 0.08 | 3.51 | 43 | | 5.52 ± 0.10 | 5.94 |
| 32 | | 4.64 ± 0.10 | 3.11 | 44 | | 5.46 ± 0.08 | 5.94 |
| 33 | | 5.50 ± 0.07 | 4.22 | 45 | | 6.22 ± 0.06 | 5.94 |
| 34 | | 5.00 ± 0.04 | 4.75 | 46 | | 6.31 ± 0.10 | 5.43 |
| 35 | | 5.20 ± 0.08 | 4.55 | 47 | | 4.94 ± 0.07 | 2.34 |
| 36 | | 5.61 ± 0.14 | 4.55 | 48 | | 4.97 ± 0.10 | 2.34 |
| 37 | | 6.01 ± 0.07 | 4.55 | 49 | | 4.89 ± 0.04 | 2.34 |
| 38 | | 5.74 ± 0.07 | 4.34 | 50 | | 5.97 ± 0.03 | 3.49 |

^a cLogP was calculated using Chemdraw 15.

only at the *ortho* position, (compounds **35-46**), suggesting that there is space in the binding pocket. Heteroatoms in the phenyl ring were not favorable (**47-50**), while the thiophene isostere **50** displayed similar potency compared to **1**. *N*-Alkyl analogues **51-56** demonstrated that larger groups than methyl are allowed (Table 4). In particular, isopropyl derivative **52** displayed a two-fold increase in activity, albeit with a significant lipophilicity penalty. Next, several cyclic phenethylamine derivatives were evaluated (compounds **57-67**), to study the effect of conformational restriction by reducing the number of rotatable bonds (Table 5). A two-fold activity improvement was observed for both 3-phenylpiperidine **59** and 2-benzylpyrrolidine **60**. Introduction of heteroatoms in the piperidine ring was not favored as witnessed by morpholine **64** and piperazine **65**, but the activity could be recovered by introducing a *N*-benzyl-group in the piperazine analogue **66**.

Table 4. Structure-activity relationship analysis of *N*-methylphenethylamine analogues **51-56**.

| ID | R ₂ : | pIC ₅₀ ± SEM | cLogP ^a |
|-----------|------------------|-------------------------|--------------------|
| 1 | | 6.09 ± 0.04 | 3.84 |
| 51 | | 6.19 ± 0.08 | 4.37 |
| 52 | | 6.55 ± 0.07 | 4.68 |
| 53 | | 5.96 ± 0.07 | 4.42 |
| 54 | | 5.95 ± 0.09 | 5.61 |
| 55 | | 6.13 ± 0.06 | 4.50 |
| 56 | | 6.28 ± 0.16 | 5.79 |

^a cLogP was calculated using Chemdraw 15.

Table 5. Structure-activity relationship analysis of *N*-methylphenethylamine analogues **57-67**.

| ID | R ₂ : | pIC ₅₀ ± SEM | cLogP ^a | ID | R ₂ : | pIC ₅₀ ± SEM | cLogP ^a |
|-----------|------------------|-------------------------|--------------------|-----------|------------------|-------------------------|--------------------|
| 1 | | 6.09 ± 0.04 | 3.84 | 62 | | 4.60 ± 0.10 | 5.59 |
| 57 | | 5.65 ± 0.09 | 3.08 | 63 | | 5.59 ± 0.09 | 3.76 |
| 58 | | 5.66 ± 0.10 | 3.42 | 64 | | 5.91 ± 0.03 | 2.59 |
| 59 | | 6.42 ± 0.11 | 3.97 | 65 | | 5.11 ± 0.06 | 2.58 |
| 60 | | 6.42 ± 0.09 | 3.94 | 66 | | 6.00 ± 0.12 | 5.02 |
| 61 | | 6.13 ± 0.06 | 4.50 | 67 | | 5.49 ± 0.11 | 5.49 |

^a cLogP was calculated using Chemdraw 15.

To study the SAR of the R₃-substituent, inhibitors **68-97** were evaluated (Table 6). Substitution of the morpholine for a more hydrophobic piperidine (**68**) was allowed, while the 3,3-difluoropiperidine **69** increased the potency two-fold. The 4-position of the morpholine ring was less favorable for substitution (compounds **70-77**). Replacing the morpholine with a dimethylamine **78** increased the activity two-fold, suggesting that the morpholine **1** is too polar or may experience steric hindrance in the pocket. Several other small alkylamines were tested (**79-84**). Pyrrolidine **84** was the most effective with almost a four-fold increase in potency. Substitutions on the pyrrolidine ring were investigated (compounds **85-91**), revealing that hydroxylation on the 3-position (**86**) resulted in similar potency as pyrrolidine **84**, while decreasing the cLogP with more than one log unit. Both enantiomers of the 3-hydroxypyrrolidine (**87** and **88**) were equally active. Of note, introduction of aromatic substituents was allowed (**91-97**), but did not improve the potency of the inhibitors.

Table 6. Structure-activity relationship analysis of morpholine analogues 68-97.

| ID | R ₃ : | pIC ₅₀ ± SEM | cLogP ^a | ID | R ₃ : | pIC ₅₀ ± SEM | cLogP ^a |
|----|------------------|-------------------------|--------------------|----|------------------|-------------------------|--------------------|
| 1 | | 6.09 ± 0.04 | 3.84 | 83 | | 5.78 ± 0.03 | 3.68 |
| 68 | | 6.19 ± 0.08 | 5.22 | 84 | | 6.65 ± 0.09 | 4.66 |
| 69 | | 6.41 ± 0.12 | 5.51 | 85 | | 5.93 ± 0.10 | 4.95 |
| 70 | | 5.05 ± 0.08 | 4.61 | 86 | | 6.65 ± 0.04 | 3.33 |
| 71 | | 5.58 ± 0.08 | 4.67 | 87 | | 6.52 ± 0.03 | 3.33 |
| 72 | | <4.3 | 2.87 | 88 | | 6.63 ± 0.05 | 3.33 |
| 73 | | 5.80 ± 0.04 | 4.40 | 89 | | 6.15 ± 0.11 | 4.09 |
| 74 | | 5.27 ± 0.07 | 3.83 | 90 | | 5.02 ± 0.03 | 4.28 |
| 75 | | 5.92 ± 0.05 | 4.55 | 91 | | 5.85 ± 0.08 | 6.22 |
| 76 | | 5.11 ± 0.09 | 5.01 | 92 | | 5.96 ± 0.05 | 6.32 |
| 77 | | 4.89 ± 0.09 | 6.74 | 93 | | 6.81 ± 0.06 | 6.65 |
| 78 | | 6.54 ± 0.05 | 4.55 | 94 | | 5.92 ± 0.08 | 4.09 |
| 79 | | 6.07 ± 0.06 | 4.47 | 95 | | 5.65 ± 0.04 | 3.64 |
| 80 | | 6.00 ± 0.03 | 3.81 | 96 | | 4.95 ± 0.11 | 5.74 |
| 81 | | 6.30 ± 0.10 | 5.61 | 97 | | 5.28 ± 0.05 | 4.25 |
| 82 | | 6.37 ± 0.05 | 4.10 | | | | |

^a cLogP was calculated using Chemdraw 15.

Table 7. Structure-activity relationship analysis of optimized analogues **98-105**.

| ID | R ₂ : | R ₃ : | pIC ₅₀ ± SEM | | cLogP ^a | LipE ^b (hNAPE-PLD) |
|------------------|------------------|------------------|-------------------------|-------------|--------------------|----------------------------------|
| | | | hNAPE-PLD | mNAPE-PLD | | |
| 1 | | | 6.09 ± 0.04 | 5.48 ± 0.04 | 3.84 | 2.31 |
| 78 | | | 6.54 ± 0.05 | n.d. | 4.55 | 1.99 |
| 98 | | | 6.95 ± 0.10 | 6.41 ± 0.10 | 4.68 | 2.26 |
| 99 | | | 6.39 ± 0.11 | n.d. | 4.68 | 1.71 |
| 100 | | | 6.68 ± 0.09 | 6.24 ± 0.09 | 3.97 | 2.70 |
| 101 | | | 4.76 ± 0.08 | 5.02 ± 0.08 | 3.01 | 1.75 |
| 102 (LEI-401) | | | 7.14 ± 0.04 | 6.35 ± 0.04 | 3.46 | 3.68 |
| 103 | | | 6.96 ± 0.04 | 6.42 ± 0.04 | 3.46 | 3.50 |
| 104 | | | 6.60 ± 0.05 | 5.74 ± 0.05 | 3.46 | 3.13 |
| 105 | | | 6.49 ± 0.04 | 5.90 ± 0.04 | 3.46 | 3.02 |

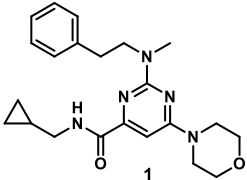
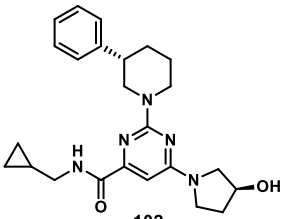
^a cLogP was calculated using Chemdraw 15; ^b Lipophilic efficiency (LipE) = pIC₅₀ – cLogP.

Combination of the optimal R₁ (cyclopropylmethylamide), R₂ ((*R/S*)-3-phenylpiperidine) and various R₃ substituents (dimethylamine, morpholine or (*R/S*)-3-hydroxyproline)

resulted in compounds **98-105** (Table 7). It was found that the combination of (*S*)-3-phenylpiperidine with (*S*)-3-hydroxypyrrolidine afforded the most potent compound (**102**, $pIC_{50} = 7.14 \pm 0.04$), having a ten-fold increase in activity compared to **1**. Interestingly, its (*R,R*)-enantiomer (compound **107**) showed a three-fold reduced activity. In addition, the significant reduction of the cLogP for **102** resulted in the highest lipophilic efficiency (LipE = 3.68). In view of the inhibitory activity and optimal LipE it was decided to select compound **102** (termed **LEI-401**) as the lead compound for further biological profiling (Chapters 4-5).

Since the biological profiling of NAPE-PLD inhibitors is mostly performed in mouse models, it was assessed whether **LEI-401** showed any species difference using recombinant mouse NAPE-PLD expressed in HEK293T cells. Despite high homology between human and mouse NAPE-PLD (89%), it was found that **LEI-401** showed somewhat lower potency ($pIC_{50} = 6.35 \pm 0.04$) for mouse NAPE-PLD, although optimal activity compared to other inhibitors was retained (Table 7).

Table 8. hNAPE-PLD activity data and physicochemical parameters of **1** and **103 (LEI-401)**.

| Compound | pIC_{50} \pm SEM | K_i (μ M) 95% CI ^a | cLogP ^b | LipE ^c | MW ^d (Da) | tPSA ^b (\AA^2) | HBD ^e | HBA ^f | RB ^g |
|--|-------------------------|---|--------------------|-------------------|-------------------------|---|------------------|------------------|-----------------|
|  1 | 6.09 \pm 0.04 | 0.30 0.22-0.38 | 3.84 | 2.31 | 396 | 69.5 | 1 | 6 | 9 |
|  102 (LEI-401) | 7.14 \pm 0.04 | 0.027 0.021- 0.033 | 3.46 | 3.68 | 422 | 80.5 | 2 | 6 | 7 |

^a CI: Confidence interval; ^b cLogP and topological polar surface area (tPSA) were calculated using Chemdraw 15; ^c Lipophilic efficiency (LipE) = $pIC_{50} - cLogP$; ^d MW: molecular weight; ^e HBD: H-bond donors; ^f HBA: H-bond acceptors; ^g RB: rotatable bonds.

A summary of the activity data and the physicochemical parameters of **1** and **LEI-401** is shown in Table 8. Using the Cheng-Prusoff equation, the K_i of **LEI-401** was determined ($K_i = 27$ nM), making **LEI-401** the first nanomolar potent inhibitor for NAPE-PLD.

Furthermore, **LEI-401** shows promise as a lead candidate since its properties fall within the Rule of Five for drug-like molecules (MW < 500, HBD < 5, HBA < 10, cLogP < 5) as well as the Veber rules (tPSA < 140 Å²; RB < 10).^{15,16} Due to a polar surface area below 90 Å², **LEI-401** is expected to cross the blood-brain barrier (BBB), which will allow targeting of NAPE-PLD in the central nervous system.¹⁷

3.3 Conclusion

In this chapter, the optimization of pyrimidine-4-carboxamide NAPE-PLD inhibitors is described. A map displaying an overview of the SAR is presented in Figure 2. Conformational restriction of the *N*-methylphenethylamine of hit compound **1** by introduction of a (*S*)-3-phenylpiperidine afforded a three-fold potency increase. Exchange of the morpholine for the smaller and more polar (*S*)-3-hydroxypyrrolidine gave a synergistic ten-fold increase in activity. This provided the nanomolar potent NAPE-PLD inhibitor **LEI-401** (K_i = 27 nM), possessing favorable drug-like properties.

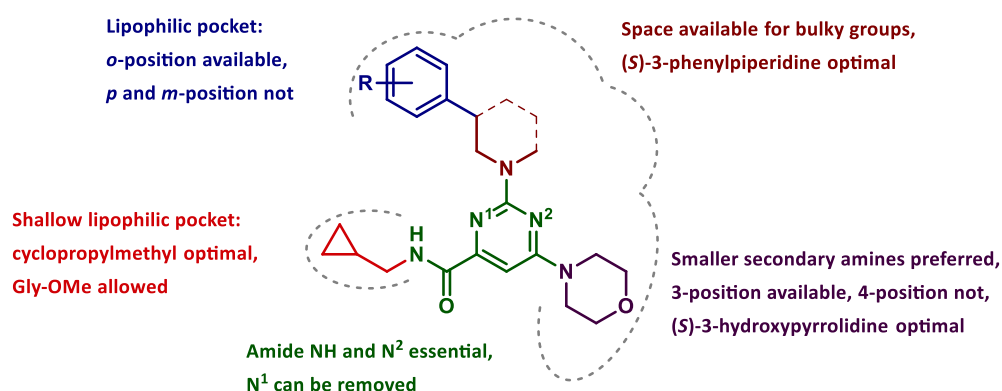


Figure 2. Structure activity map for the pyrimidine-4-carboxamide NAPE-PLD inhibitor library.

Acknowledgements

Ioli Kotsogianni, Jelle Vooijs and Carmen Fonseca are kindly acknowledged for their contributions with regard to compound synthesis and biochemical testing. Hans den Dulk is kindly thanked for generating NAPE-PLD plasmids. Hans van den Elst, Sebastian Grimm and Rian van den Nieuwendijk are kindly acknowledged for HPLC purification and optical rotation measurements.

3.4 Experimental section

A. Biological Procedures

NAPE-PLD surrogate substrate activity assay

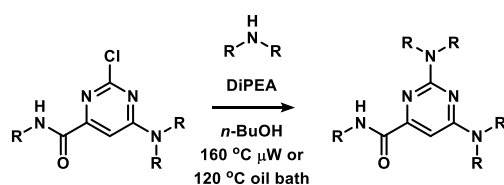
The NAPE-PLD activity assay was performed as described in Chapter 2.

B. Synthetic Procedures

General

All chemicals (Sigma-Aldrich, Fluka, Acros, Merck, Combi-Blocks, Fluorochem, TCI) were used as received. All solvents used for reactions were of analytical grade. THF, Et₂O, DMF, CH₃CN and DCM were dried over activated 4 Å molecular sieves, MeOH over 3 Å molecular sieves. Flash chromatography was performed on silica gel (Screening Devices BV, 40-63 μm, 60 Å). The eluent EtOAc was of technical grade and distilled before use. Reactions were monitored by thin layer chromatography (TLC) analysis using Merck aluminium sheets (Silica gel 60, F₂₅₄). Compounds were visualized by UV-absorption (254 nm) and spraying for general compounds: KMnO₄ (20 g/L) and K₂CO₃ (10 g/L) in water, or for amines: ninhydrin (0.75 g/L) and acetic acid (12.5 mL/L) in ethanol, followed by charring at ~150 °C. ¹H and ¹³C NMR experiments were recorded on a Bruker AV-300 (300/75 MHz), Bruker AV-400 (400/101 MHz), Bruker DMX-400 (400/101 MHz), Bruker AV-500 (500/126 MHz) and Bruker AV-600 (600/151 MHz). Chemical shifts are given in ppm (δ) relative to tetramethylsilane or CDCl₃ as internal standards. Multiplicity: s = singlet, br s = broad singlet, d = doublet, dd = doublet of doublet, t = triplet, q = quartet, p = pentet, m = multiplet. Coupling constants (*J*) are given in Hz. LC-MS measurements were performed on a Thermo Finnigan LCQ Advantage MAX ion-trap mass spectrometer (ESI⁺) coupled to a Surveyor HPLC system (Thermo Finnigan) equipped with a standard C18 (Gemini, 4.6 mm D x 50 mm L, 5 μm particle size, Phenomenex) analytical column and buffers A: H₂O, B: CH₃CN, C: 0.1% aq. TFA. High resolution mass spectra were recorded on a LTQ Orbitrap (Thermo Finnigan) mass spectrometer or a Synapt G2-Si high definition mass spectrometer (Waters) equipped with an electrospray ion source in positive mode (source voltage 3.5 kV, sheath gas flow 10 mL/min, capillary temperature 250 °C) with resolution *R* = 60000 at *m/z* 400 (mass range *m/z* = 150-2000) and dioctylphthalate (*m/z* = 391.28428) as a lock mass. Preparative HPLC was performed on a Waters Acquity Ultra Performance LC with a C18 column (Gemini, 150 x 21.2 mm, Phenomenex). All final compounds were determined to be > 95% pure by integrating UV intensity recorded via HPLC.

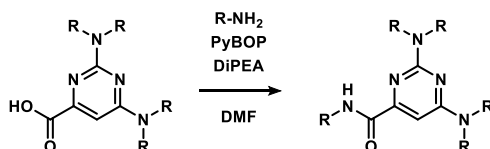
General procedure A:



A microwave tube with a magnetic stir bar was charged with the appropriate 2-chloropyrimidine (1 eq), *n*-BuOH (0.2 M), the appropriate amine (1.5 eq) and DiPEA (3-4 eq). The tube was capped, flushed with N₂ and heated to 160 °C in a microwave reactor (75 W) for 4-36 h or heated to 120 °C in an oil bath for 1-6 days. When the reaction was completed as judged by LC-MS, it was transferred to a round-bottom flask, concentrated under reduced pressure and coevaporated with toluene (2x). The residue was purified by silica

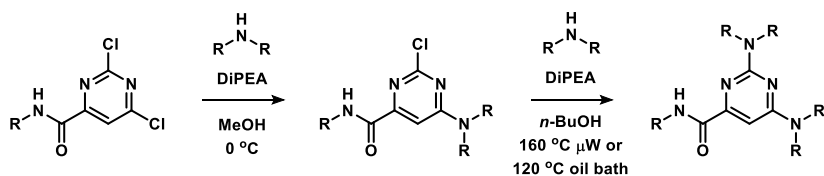
gel column chromatography affording the product, or alternatively by HPLC-MS purification yielding the TFA salt. The free base was generated by dissolving the TFA salt in EtOAc, followed by washing with sat. aq. NaHCO₃ (2x). The organic layer was dried (Na₂SO₄), filtered and concentrated under reduced pressure, affording the pure product.

General procedure B:



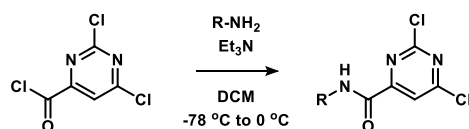
A round-bottom flask was charged with carboxylic acid (1 eq) and dissolved in dry DMF (0.2 M). PyBOP (1.2-1.5 eq), DiPEA (3-5 eq) and the appropriate amine (1.2-5 eq) were added and the mixture was stirred overnight at rt. Work-up involved dilution with EtOAc, washing with H₂O (1x) and brine (2x), drying (Na₂SO₄), filtering and concentration under reduced pressure. The residue was purified by silica gel column chromatography affording the pure product.

General procedure C:



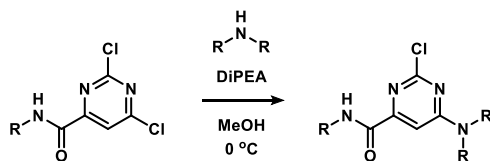
A microwave vial was charged with the dichloropyrimidine (1 eq) and dry MeOH (0.1 M) and cooled to 0 °C. DiPEA (1.5-2.5 eq) and the appropriate amine (1.05 eq) were added and the mixture was stirred for 1-2 h at 0 °C. The solvents were evaporated under reduced pressure. The vial was charged with *n*-BuOH (0.2 M), *N*-methylphenethylamine (1.5 eq) and DiPEA (3-4 eq). The tube was capped, flushed with N₂ and heated to 160 °C in a microwave reactor (75 W) for 4 h. When the reaction was completed as judged by LC-MS, it was transferred to a round-bottom flask, concentrated under reduced pressure and co-evaporated with toluene (2x). The residue was purified by silica gel column chromatography affording the product, or alternatively by HPLC-MS purification yielding the TFA salt. The free base was generated by dissolving the TFA salt in EtOAc, followed by washing with sat. aq. NaHCO₃ (2x). The organic layer was dried (Na₂SO₄), filtered and concentrated under reduced pressure, affording the pure product.

General procedure D:



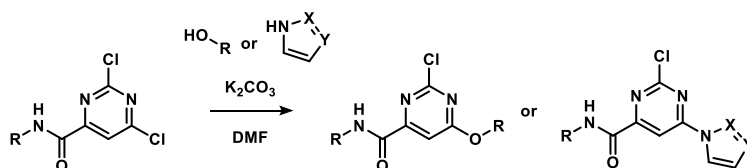
A round-bottom flask with dry DCM (0.1 M) was charged via syringe with 2,6-dichloropyrimidine-4-carbonyl chloride (1 eq) and cooled to -78 °C. Et₃N (1.3-2.3 eq) and the appropriate amine (1.025 eq) were added and the mixture was stirred, while letting the acetone bath warm up to 0 °C (3-4 h). The mixture was transferred to a separatory funnel and the organic layer was washed with H₂O (2x) and brine (1x), dried (Na₂SO₄), filtered and concentrated under reduced pressure. Silica gel column chromatography afforded the pure amide.

General procedure E:



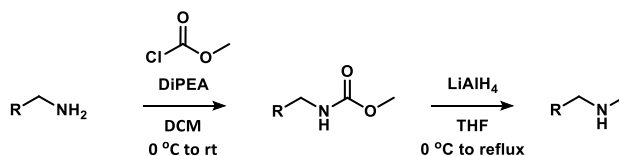
A round-bottom flask was charged with the dichloropyrimidine (1 eq) and dry MeOH (0.1 M) and cooled to 0 °C. DiPEA (1.5-2.5 eq) and the appropriate amine (1.05 eq) were added and the mixture was stirred for 1-2 h at 0 °C. The solvents were evaporated under reduced pressure and the crude material was purified by silica gel column chromatography, affording the pure product.

General procedure F:

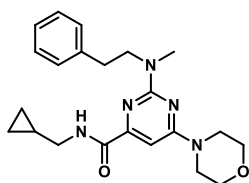


A round-bottom flask was charged with the dichloropyrimidine (1 eq) and dry DMF (0.1 M). K_2CO_3 (1.5 eq) and the appropriate phenol or heteroaryl (1.05 eq) were added and the mixture was stirred overnight at rt. H_2O was added and the mixture was extracted with EtOAc (3x). The organic layers were combined and washed with brine (2x), dried (Na_2SO_4) and concentrated under reduced pressure. The residue was purified by silica gel column chromatography, affording the pure product.

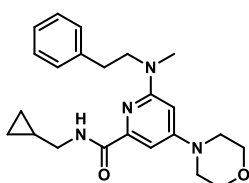
General procedure G:



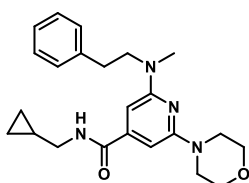
Carbamoylation: a round-bottom flask was charged with the primary amine (1 eq) and dry DCM (0.2 M). The solution was cooled to 0 °C and DiPEA (2 eq) and methylchloroformate (1.5 eq) were added. The reaction was stirred and allowed to warm up to room temperature over 1-2 h. Then the mixture was diluted with DCM and washed with sat. aq. $NaHCO_3$ (2x), brine (1x), dried ($MgSO_4$), filtered and concentrated under reduced pressure. The resulting crude material was purified by silica gel column chromatography affording the methyl carbamate. *Carbamate reduction:* a round-bottom flask was charged with the methyl carbamate (1 eq) and dry THF (0.15 M). The solution was cooled to 0 °C and $LiAlH_4$ (2 M in THF solution, 1.6 eq) was added dropwise. The reaction was then stirred at reflux for 1-2 h. Fieser workup involved dilution of the reaction mixture with Et_2O (3x) and cooling to 0 °C, followed by the sequential addition of water (1 μ L for every 1 mg of $LiAlH_4$), $NaOH$ (aq) 15% (1 μ L for every 1 mg of $LiAlH_4$) and water (3 μ L for every 1 mg of $LiAlH_4$). The mixture was allowed to warm to room temperature and stirred for 15 min. Then it was dried ($MgSO_4$), filtered and concentrated under reduced pressure to afford the product as a clear oil, which was used without further purification or purified by silica gel chromatography.



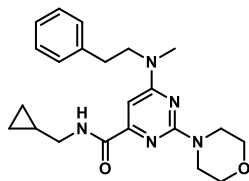
N-(Cyclopropylmethyl)-2-(methyl(phenethyl)amino)-6-morpholino-pyrimidine-4-carboxamide (1). The title compound was prepared according to general procedure A using 2-chloropyrimidine **28** (59 mg, 0.20 mmol, 1 eq), *N*-methylphenethylamine HBr salt (66 mg, 0.30 mmol, 1.5 eq) and DiPEA (140 μ L, 0.80 mmol, 4 eq). Total heating time: 8 h at 160 $^{\circ}$ C with μ W irradiation. Column chromatography (40% \rightarrow 60% EtOAc/pentane) afforded the product (40 mg, 0.10 mmol, 50%). TLC: R_f = 0.3 (40% EtOAc/pentane). ^1H NMR (400 MHz, CDCl_3) δ 8.03 (br s, 1H), 7.34 – 7.25 (m, 2H), 7.25 – 7.12 (m, 3H), 6.72 (s, 1H), 3.88 – 3.72 (m, 6H), 3.72 – 3.55 (m, 4H), 3.30 (t, J = 6.5 Hz, 2H), 3.13 (s, 3H), 2.90 (t, J = 7.7 Hz, 2H), 1.14 – 0.99 (m, 1H), 0.64 – 0.44 (m, 2H), 0.38 – 0.19 (m, 2H). ^{13}C NMR (101 MHz, CDCl_3) δ 164.66, 163.97, 160.86, 156.78, 139.92, 128.95, 128.58, 126.29, 90.08, 66.74, 51.68, 44.50, 44.11, 35.70, 33.93, 10.88, 3.48. HRMS [$\text{C}_{22}\text{H}_{29}\text{N}_5\text{O}_2 + \text{H}$] $^+$: 396.2394 calculated, 396.2387 found.



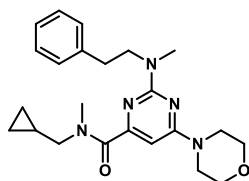
N-(Cyclopropylmethyl)-6-(methyl(phenethyl)amino)-4-morpholino-picolinamide (2). A microwave vial with a magnetic stir bar under N_2 was charged with 4-chloropyridine **109** (30 mg, 87 μ mol, 1 eq), morpholine (9 μ L, 0.10 mmol, 1.2 eq) and dry toluene (87 μ L). The vial was capped and the solution purged with N_2 . This was followed by the addition of RuPhosPd G3 (0.01 M THF solution, 237 μ L, 2.37 μ mol, 0.027 eq) and NaOtBu (2 M THF solution, 97 μ L, 0.19 mmol, 2.2 eq) and the mixture was purged again with N_2 and stirred in a preheated oil bath at 110 $^{\circ}$ C for 44 h. The mixture was filtered through a plug of Celite and the filtrate concentrated under reduced pressure. The crude material was purified by silica gel column chromatography (30% \rightarrow 60% EtOAc/pentane) affording the product (5 mg, 13 μ mol, 15%). TLC: R_f = 0.2 (30% EtOAc/pentane) and recovered starting material (11 mg, 32 μ mol, 37%). ^1H NMR (500 MHz, CDCl_3) δ 8.03 (t, J = 5.7 Hz, 1H), 7.29 (t, J = 7.3 Hz, 2H), 7.24 – 7.13 (m, 4H), 5.77 (d, J = 2.0 Hz, 1H), 3.91 – 3.81 (m, 4H), 3.63 (t, J = 7.4 Hz, 2H), 3.51 – 3.40 (m, 4H), 3.34 – 3.29 (m, 2H), 2.92 – 2.83 (m, 5H), 1.11 – 1.05 (m, 1H), 0.58 – 0.50 (m, 2H), 0.29 (q, J = 4.7 Hz, 2H). ^{13}C NMR (126 MHz, CDCl_3) δ 165.54, 160.20, 156.01, 148.69, 139.16, 129.00, 128.80, 126.61, 99.04, 90.28, 66.98, 54.09, 46.37, 44.16, 38.55, 33.55, 11.08, 3.57. HRMS [$\text{C}_{23}\text{H}_{30}\text{N}_4\text{O}_2 + \text{H}$] $^+$: 395.2442 calculated, 395.2438 found.



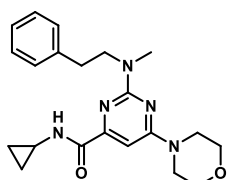
N-(Cyclopropylmethyl)-2-(methyl(phenethyl)amino)-6-morpholino-isonicotinamide (3). A microwave vial with a magnetic stir bar under N_2 was charged with 2-chloropyridine **113** (31 mg, 0.10 mmol, 1 eq), *N*-methylphenethylamine HBr salt (28 mg, 0.13 mmol, 1.3 eq) and dry toluene (0.1 mL). The vial was capped and the solution purged with N_2 . This was followed by the addition of RuPhosPd G3 (0.01 M THF solution, 100 μ L, 1 μ mol, 0.01 eq) and NaOtBu (2 M THF solution, 120 μ L, 0.24 mmol, 2.4 eq) and the mixture was purged again with N_2 and stirred in a preheated oil bath at 110 $^{\circ}$ C. After 24 h the reaction was complete as judged by LC-MS. The mixture was filtered through a plug of Celite and the filtrate concentrated under reduced pressure to provide the crude material. Purification by HPLC (C18 reverse phase, 45% \rightarrow 55% $\text{CH}_3\text{CN}/\text{H}_2\text{O} + 0.2\%$ TFA, RT 12.3 min) afforded the product (16 mg, 40 μ mol, 41%). TLC: R_f = 0.5 (60% EtOAc/pentane). ^1H NMR (400 MHz, CDCl_3) δ 7.35 – 7.24 (m, 2H), 7.25 – 7.14 (m, 3H), 6.24 – 6.13 (m, 2H), 6.10 (s, 1H), 3.87 – 3.78 (m, 4H), 3.78 – 3.67 (m, 2H), 3.59 – 3.47 (m, 4H), 3.28 (dd, J = 7.2, 5.4 Hz, 2H), 2.98 (s, 3H), 2.93 – 2.82 (m, 2H), 1.15 – 0.95 (m, 1H), 0.64 – 0.48 (m, 2H), 0.35 – 0.19 (m, 2H). ^{13}C NMR (101 MHz, CDCl_3) δ 168.07, 159.06, 157.76, 145.86, 140.05, 128.98, 128.60, 126.26, 92.90, 91.48, 66.94, 52.51, 45.80, 44.97, 36.87, 33.92, 10.82, 3.68. HRMS [$\text{C}_{23}\text{H}_{30}\text{N}_4\text{O}_2 + \text{H}$] $^+$: 395.2442 calculated, 395.2434 found.



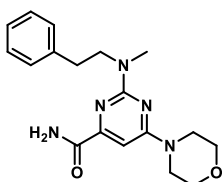
N-(Cyclopropylmethyl)-6-(methyl(phenethyl)amino)-2-morpholinopyrimidine-4-carboxamide (4). The title compound was prepared according to general procedure A using 4-chloropyrimidine **127** (21 mg, 70 μ mol, 1.0 eq), *N*-methylphenethylamine HBr salt (16 mg, 70 μ mol, 1 eq) and DiPEA (36.6 μ L, 0.21 mmol, 3 eq) in MeOH. Total heating time: 6 h at 70 $^{\circ}$ C. Column chromatography (30% \rightarrow 60% EtOAc/pentane) afforded the product (20 mg, 50 μ mol, 71%). TLC: R_f = 0.4 (30% EtOAc/pentane). ^1H NMR (400 MHz, CDCl_3) δ 8.44 (br s, 1H), 7.33 – 7.27 (m, 2H), 7.25 – 7.13 (m, 3H), 6.84 (s, 1H), 3.79 (br s, 10H), 3.38 – 3.22 (m, 2H), 3.02 (s, 3H), 2.90 (t, J = 7.4 Hz, 2H), 1.14 – 1.00 (m, 1H), 0.62 – 0.46 (m, 2H), 0.36 – 0.21 (m, 2H). ^{13}C NMR (101 MHz, CDCl_3) δ 162.97, 159.05, 128.91, 128.82, 126.75, 93.22, 66.81, 44.92, 44.69, 10.71, 3.65. HRMS [$\text{C}_{22}\text{H}_{29}\text{N}_5\text{O}_2 + \text{H}$] $^+$: 396.2394 calculated, 396.2385 found.



N-(Cyclopropylmethyl)-N-methyl-2-(methyl(phenethyl)amino)-6-morpholinopyrimidine-4-carboxamide (5). A round-bottom flask was charged with amide **1** (36 mg, 90 μ mol, 1 eq), dry DMF (1.5 mL) and cooled to 0 $^{\circ}$ C. NaH (60% in mineral oil, 4 mg, 0.10 mmol, 1.1 eq) was added and the mixture was stirred for 30 min followed by addition of methyl iodide (11 μ L, 0.18 mmol, 2 eq). The reaction was allowed to warm to rt while stirring overnight. The reaction was quenched with H_2O (20 mL) followed by extraction with EtOAc (3 x 20 mL). The combined organic layers were washed with brine (1 x 50 mL), dried (MgSO_4), filtered and concentrated under reduced pressure. The residue was purified by silica gel column chromatography (50 \rightarrow 80% EtOAc/pentane) affording the product (18 mg, 40 μ mol, 44%). TLC: R_f = 0.3 (60% EtOAc/pentane). ^1H NMR analysis showed two rotamers in 6:4 ratio in CDCl_3 at 298 K, which was confirmed by high temperature ^1H NMR experiments. ^1H NMR (400 MHz, CDCl_3) δ 7.32 – 7.24 (m, 2H), 7.23 – 7.16 (m, 3H), 6.07 – 6.02 (m, 1H), 3.83 – 3.71 (m, 6H), 3.62 – 3.55 (m, 4H), 3.43 – 3.23 (m, 2H), 3.16 – 3.10 (m, 3H), 3.10 – 3.02 (m, 3H), 2.92 – 2.83 (m, 2H), 1.14 – 1.01 (m, 1H), 0.60 – 0.43 (m, 2H), 0.36 – 0.12 (m, 2H). ^{13}C NMR (101 MHz, CDCl_3) δ 163.34, 162.35, 160.82, 156.31, 140.05, 128.91, 128.52, 126.20, 90.43, 66.76, 55.26, 51.57, 44.33, 35.80, 33.94, 33.10, 10.33, 3.66. HRMS [$\text{C}_{23}\text{H}_{31}\text{N}_5\text{O}_2 + \text{H}$] $^+$: 410.2551 calculated, 410.2545 found.

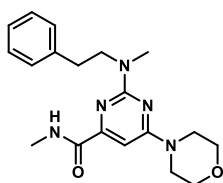


N-Cyclopropyl-2-(methyl(phenethyl)amino)-6-morpholinopyrimidine-4-carboxamide (6). The title compound was prepared according to general procedure B using carboxylic acid **17** (34 mg, 0.10 mmol, 1 eq), DiPEA (52 μ L, 0.30 mmol, 3 eq), PyBOP (78 mg, 0.12 mmol, 1.2 eq) and cyclopropylamine (8.3 μ L, 0.12 mmol, 1.2 eq). Column chromatography (50% \rightarrow 80% EtOAc/pentane) afforded the product (8 mg, 21 μ mol, 21%). TLC: R_f = 0.3 (60% EtOAc/pentane). ^1H NMR (400 MHz, CDCl_3) δ 7.92 (br s, 1H), 7.34 – 7.27 (m, 2H), 7.25 – 7.15 (m, 3H), 6.70 (s, 1H), 3.84 – 3.72 (m, 6H), 3.66 (br s, 4H), 3.09 (s, 3H), 2.94 – 2.82 (m, 3H), 1.36 – 1.21 (m, 1H), 0.92 – 0.82 (m, 2H), 0.67 – 0.58 (m, 2H). ^{13}C NMR (101 MHz, CDCl_3) δ 166.25, 163.97, 160.84, 156.51, 139.98, 128.84, 128.64, 126.34, 89.86, 66.78, 51.67, 44.52, 35.72, 33.98, 22.53, 6.78. HRMS [$\text{C}_{21}\text{H}_{27}\text{N}_5\text{O}_2 + \text{H}$] $^+$: 382.2238 calculated, 382.2241 found.

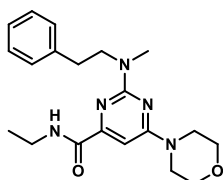


2-(Methyl(phenethyl)amino)-6-morpholinopyrimidine-4-carboxamide (7). The title compound was prepared according to general procedure B using carboxylic acid **17** (27 mg, 79 μ mol, 1 eq), DiPEA (56 μ L, 0.32 mmol, 4 eq), PyBOP (62 mg, 0.12 mmol, 1.5 eq), HOBt (16 mg, 0.12 mmol, 1.5 eq) and ammonium chloride (15 mg, 0.32 mmol, 3.5 eq). Column chromatography (80% \rightarrow 100% EtOAc/pentane) afforded the product (20 mg, 59 μ mol, 75%). TLC: R_f = 0.5 (80% EtOAc/pentane). ^1H NMR (400 MHz, CDCl_3) δ 7.74 (br s, 1H), 7.34 – 7.25 (m, 2H), 7.25 – 7.16 (m, 3H), 6.71 (br s, 1H), 5.83 (s, 1H), 3.86 – 3.72 (m, 6H), 3.66 (br s, 4H), 3.09 (s, 3H), 2.90 (t, J = 7.1 Hz, 2H). ^{13}C NMR (101 MHz, CDCl_3) δ 167.46, 163.96,

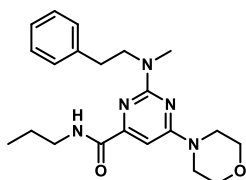
161.04, 156.27, 139.93, 128.86, 128.62, 126.31, 90.17, 66.74, 51.60, 44.50, 35.77, 33.97. HRMS $[C_{18}H_{23}N_5O_2 + H]^+$: 342.1925 calculated, 342.1934 found.



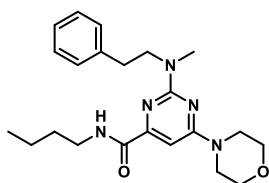
N-Methyl-2-(methyl(phenethyl)amino)-6-morpholinopyrimidine-4-carboxamide TFA salt (8). The title compound was prepared according to general procedure A using 2-chloropyrimidine **117a** (8.5:1 mixture of regioisomers) (51 mg, 0.20 mmol, 1 eq), DiPEA (139 μ L, 0.80 mmol, 4 eq) and *N*-methylphenethylamine HBr salt (65 mg, 0.30 mmol, 1.5 eq). Total heating time: 4 h at 160 $^{\circ}$ C with μ W irradiation. Purification by preparative HPLC (C18 reverse phase, 25% to 35% CH_3CN/H_2O + 0.2% TFA, RT = 8.77) afforded the product as the TFA salt (83 mg, 0.18 mmol, 88%) TLC: R_f = 0.3 (50% EtOAc/pentane). 1H NMR (400 MHz, MeOD) δ 7.30 – 7.12 (m, 5H), 6.90 (s, 1H), 3.92 (t, J = 7.0 Hz, 2H), 3.85 – 3.69 (m, 8H), 3.18 (s, 3H), 3.00 – 2.88 (m, 5H). ^{13}C NMR (101 MHz, MeOD) δ 162.45, 162.16 (q, J = 35.8 Hz), 154.95, 147.48, 139.88, 129.99, 129.67, 127.62, 117.79 (q, J = 291.3 Hz), 94.22, 67.37, 53.01, 46.62, 36.22, 34.27, 26.90. HRMS $[C_{19}H_{25}N_5O_2 + H]^+$: 356.2081 calculated, 356.2079 found.



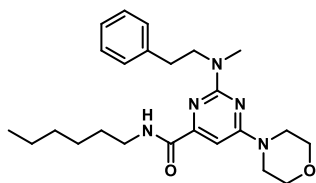
N-Ethyl-2-(methyl(phenethyl)amino)-6-morpholinopyrimidine-4-carboxamide (9). The title compound was prepared according to general procedure A using 2-chloropyrimidine **117b** (54 mg, 0.20 mmol, 1 eq), DiPEA (139 μ L, 0.80 mmol, 4 eq) and *N*-methylphenethylamine HBr salt (65 mg, 0.30 mmol, 1.5 eq). Total heating time: 4 h at 160 $^{\circ}$ C with μ W irradiation. Column chromatography (50% -> 70% EtOAc/pentane) afforded the product (64 mg, 0.17 mmol, 86%). TLC: R_f = 0.3 (50% EtOAc/pentane). 1H NMR (500 MHz, $CDCl_3$) δ 7.88 (s, 1H), 7.32 – 7.26 (m, 2H), 7.24 – 7.16 (m, 3H), 6.71 (s, 1H), 3.84 – 3.77 (m, 2H), 3.77 – 3.73 (m, 4H), 3.69 – 3.62 (m, 4H), 3.50 – 3.42 (m, 2H), 3.11 (s, 3H), 2.94 – 2.84 (m, 2H), 1.25 (t, J = 7.3 Hz, 3H). ^{13}C NMR (126 MHz, $CDCl_3$) δ 164.65, 163.98, 160.88, 156.82, 139.99, 128.83, 128.59, 126.29, 90.02, 66.74, 51.63, 44.51, 35.71, 34.26, 33.98, 14.94. HRMS $[C_{20}H_{27}N_5O_2 + H]^+$: 370.2238 calculated, 370.2236 found.



N-Propyl-2-(methyl(phenethyl)amino)-6-morpholino-pyrimidine-4-carboxamide (10). The title compound was prepared according to general procedure B using carboxylic acid **17** (23 mg, 67 μ mol, 1 eq), DiPEA (60 μ L, 0.34 mmol, 3 eq), PyBOP (52 mg, 0.10 mmol, 1.5 eq) and propylamine HCl salt (8 mg, 80 μ mol, 1.2 eq). Column chromatography (40% -> 60% EtOAc/pentane) afforded the product (17 mg, 44 μ mol, 66%). TLC: R_f = 0.3 (50% EtOAc/pentane). 1H NMR (400 MHz, $CDCl_3$) δ 7.99 (br s, 1H), 7.37 – 7.28 (m, 2H), 7.28 – 7.19 (m, 3H), 6.74 (s, 1H), 3.90 – 3.75 (m, 6H), 3.69 (br s, 4H), 3.42 (q, J = 6.7 Hz, 2H), 3.13 (s, 3H), 2.92 (t, J = 7.5 Hz, 2H), 1.71 – 1.62 (m, 2H), 1.02 (t, J = 7.3 Hz, 3H). ^{13}C NMR (101 MHz, $CDCl_3$) δ 164.80, 164.01, 160.86, 156.82, 139.98, 128.85, 128.61, 126.31, 90.06, 66.77, 51.65, 44.52, 41.08, 35.73, 33.98, 23.01, 11.61. HRMS $[C_{21}H_{29}N_5O_2 + H]^+$: 384.2394 calculated, 384.2394 found.

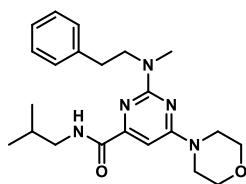


N-Butyl-2-(methyl(phenethyl)amino)-6-morpholinopyrimidine-4-carboxamide (11). The title compound was prepared according to general procedure A using 2-chloropyrimidine **117c** (30 mg, 0.10 mmol, 1 eq), DiPEA (70 μ L, 0.40 mmol, 4 eq) and *N*-methylphenethylamine HBr salt (32 mg, 0.15 mmol, 1.5 eq). Total heating time: 45 h at 120 $^{\circ}$ C. Column chromatography (40% -> 60% EtOAc/pentane) afforded the product (29 mg, 73 μ mol, 73%). TLC: R_f = 0.6 (50% EtOAc/pentane). 1H NMR (400 MHz, $CDCl_3$) δ 7.94 (br s, 1H), 7.33 – 7.25 (m, 2H), 7.24 – 7.16 (m, 3H), 6.72 (s, 1H), 3.84 – 3.72 (m, 6H), 3.66 (br s, 4H), 3.42 (q, J = 6.6 Hz, 2H), 3.11 (s, 3H), 2.95 – 2.84 (m, 2H), 1.60 (p, J = 7.1 Hz, 2H), 1.42 (h, J = 7.3 Hz, 2H), 0.96 (t, J = 7.3 Hz, 3H). ^{13}C NMR (101 MHz, $CDCl_3$) δ 164.74, 164.00, 160.86, 156.83, 139.97, 128.84, 128.60, 126.31, 90.05, 66.76, 51.64, 44.52, 39.12, 35.72, 33.97, 31.81, 20.30, 13.94. HRMS $[C_{22}H_{31}N_5O_2 + H]^+$: 398.2551 calculated, 398.2560 found.



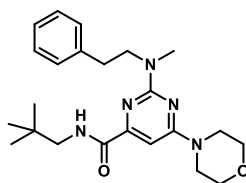
N-Hexyl-2-(methyl(phenethyl)amino)-6-morpholinopyrimidine-4-carboxamide (12). The title compound was prepared according to general procedure A using 2-chloropyrimidine **117d** (33 mg, 0.10 mmol, 1 eq), DiPEA (70 μ L, 0.40 mmol, 4 eq) and *N*-methylphenethylamine HBr salt (32 mg, 0.15 mmol, 1.5 eq). Total heating time: 3 d at 120 $^{\circ}$ C. Column chromatography (40% \rightarrow 50% EtOAc/ pentane) afforded the product (36 mg, 85 μ mol, 85%).

TLC: R_f = 0.6 (50% EtOAc/pentane). ^1H NMR (400 MHz, CDCl_3) δ 7.94 (s, 1H), 7.33 – 7.25 (m, 2H), 7.25 – 7.17 (m, 3H), 6.72 (s, 1H), 3.83 – 3.73 (m, 6H), 3.71 – 3.62 (m, 4H), 3.41 (q, J = 6.9 Hz, 2H), 3.10 (s, 3H), 2.95 – 2.85 (m, 2H), 1.61 (p, J = 7.6, 7.2 Hz, 2H), 1.44 – 1.27 (m, 6H), 0.94 – 0.84 (m, 3H). ^{13}C NMR (101 MHz, CDCl_3) δ 164.71, 164.01, 160.86, 156.85, 139.97, 128.84, 128.60, 126.30, 90.05, 66.76, 51.65, 44.53, 39.43, 35.73, 33.98, 31.63, 29.68, 26.78, 22.67, 14.14. HRMS [$\text{C}_{24}\text{H}_{35}\text{N}_5\text{O}_2 + \text{H}$] $^+$: 426.2864 calculated, 426.2857 found.



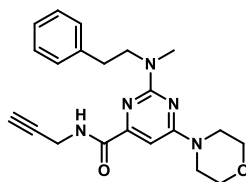
N-Isobutyl-2-(methyl(phenethyl)amino)-6-morpholinopyrimidine-4-carboxamide (13). The title compound was prepared according to general procedure A using 2-chloropyrimidine **117e** (30 mg, 0.10 mmol, 1 eq), DiPEA (70 μ L, 0.40 mmol, 4 eq) and *N*-methylphenethylamine HBr salt (32 mg, 0.15 mmol, 1.5 eq). Total heating time: 3 d at 120 $^{\circ}$ C. Column chromatography (40% \rightarrow 60% EtOAc/pentane) afforded the product (29 mg, 73 μ mol, 73%). TLC: R_f = 0.7 (50% EtOAc/pentane). ^1H NMR

(400 MHz, CDCl_3) δ 8.04 (br s, 1H), 7.33 – 7.25 (m, 2H), 7.25 – 7.16 (m, 3H), 6.72 (s, 1H), 3.88 – 3.73 (m, 6H), 3.73 – 3.62 (m, 4H), 3.26 (t, J = 6.5 Hz, 2H), 3.10 (s, 3H), 2.96 – 2.85 (m, 2H), 1.97 – 1.82 (m, 1H), 0.98 (d, J = 6.7 Hz, 6H). ^{13}C NMR (101 MHz, CDCl_3) δ 164.77, 164.01, 160.84, 156.84, 139.94, 128.84, 128.58, 126.29, 90.07, 66.75, 51.63, 46.65, 44.52, 35.72, 33.98, 28.80, 20.28. HRMS [$\text{C}_{22}\text{H}_{31}\text{N}_5\text{O}_2 + \text{H}$] $^+$: 398.2551 calculated, 398.2552 found.



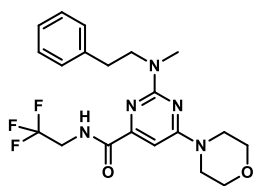
N-Neopentyl-2-(methyl(phenethyl)amino)-6-morpholinopyrimidine-4-carboxamide (14). The title compound was prepared according to general procedure A using 2-chloropyrimidine **117f** (31 mg, 0.10 mmol, 1 eq), DiPEA (70 μ L, 0.40 mmol, 4 eq) and *N*-methylphenethylamine HBr salt (32 mg, 0.15 mmol, 1.5 eq). Total heating time: 3 d at 120 $^{\circ}$ C. Column chromatography (20% \rightarrow 50% EtOAc/pentane) afforded the product (30 mg, 73 μ mol, 73%). TLC: R_f = 0.6 (40%

EtOAc/pentane). ^1H NMR (400 MHz, CDCl_3) δ 8.14 (br s, 1H), 7.32 – 7.25 (m, 2H), 7.24 – 7.17 (m, 3H), 6.73 (s, 1H), 3.85 – 3.78 (m, 2H), 3.78 – 3.73 (m, 4H), 3.71 – 3.61 (m, 4H), 3.23 (d, J = 6.6 Hz, 2H), 3.10 (s, 3H), 2.95 – 2.86 (m, 2H), 0.97 (s, 9H). ^{13}C NMR (101 MHz, CDCl_3) δ 164.82, 164.03, 160.82, 156.82, 139.89, 128.85, 128.59, 126.30, 90.15, 66.76, 51.62, 50.57, 44.53, 35.72, 33.99, 32.28, 27.38. HRMS [$\text{C}_{23}\text{H}_{33}\text{N}_5\text{O}_2 + \text{H}$] $^+$: 412.2707 calculated, 412.2710 found.

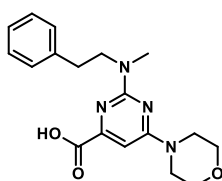


2-(Methyl(phenethyl)amino)-6-morpholino-N-(prop-2-yn-1-yl)pyrimidine-4-carboxamide (15). The title compound was prepared according to general procedure A using 2-chloropyrimidine **117g** (42 mg, 0.15 mmol, 1 eq), DiPEA (105 μ L, 0.60 mmol, 4 eq) and *N*-methylphenethylamine HBr salt (49 mg, 0.225 mmol, 1.5 eq). Total heating time: 45 h at 120 $^{\circ}$ C. Column chromatography (30% \rightarrow 50% EtOAc/pentane) afforded the product (43 mg, 0.11 mmol, 73%). TLC: R_f = 0.7 (50%

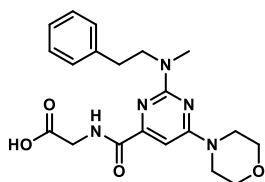
EtOAc/pentane). ^1H NMR (400 MHz, CDCl_3) δ 8.03 (br s, 1H), 7.33 – 7.25 (m, 2H), 7.25 – 7.17 (m, 3H), 6.69 (s, 1H), 4.22 (dd, J = 5.6, 2.5 Hz, 2H), 3.86 – 3.72 (m, 6H), 3.72 – 3.60 (m, 4H), 3.11 (s, 3H), 2.96 – 2.85 (m, 2H), 2.29 (t, J = 2.4 Hz, 1H). ^{13}C NMR (101 MHz, CDCl_3) δ 164.60, 163.89, 160.88, 156.03, 139.91, 128.90, 128.60, 126.30, 90.15, 79.57, 71.67, 66.72, 51.70, 44.50, 35.75, 33.98, 29.21. HRMS [$\text{C}_{21}\text{H}_{25}\text{N}_5\text{O}_2 + \text{H}$] $^+$: 380.2081 calculated, 380.2089 found.



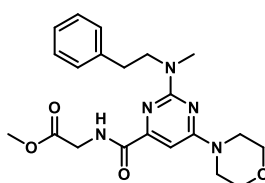
***N*-(2,2-Trifluoroethyl)-2-(methyl(phenethyl)amino)-6-morpholinopyrimidine-4-carboxamide (16).** The title compound was prepared according to general procedure B using carboxylic acid **17** (25 mg, 73 μ mol, 1 eq), DiPEA (51 μ L, 0.29 mmol, 4 eq), PyBOP (57 mg, 0.11 mmol, 1.5 eq) and 2,2,2-trifluoroethylamine HCl salt (12 mg, 88 μ mol, 1.2 eq). Column chromatography (30% \rightarrow 40% EtOAc/pentane) afforded the product (17 mg, 40 μ mol, 55%). TLC: R_f = 0.8 (50% EtOAc/pentane). ^1H NMR (500 MHz, CDCl_3) δ 8.20 (br s, 1H), 7.32 – 7.26 (m, 2H), 7.23 – 7.17 (m, 3H), 6.70 (s, 1H), 4.12 – 4.02 (m, 2H), 3.83 – 3.78 (m, 2H), 3.78 – 3.74 (m, 4H), 3.71 – 3.59 (m, 4H), 3.11 (s, 3H), 2.92 – 2.86 (m, 2H). ^{13}C NMR (126 MHz, CDCl_3) δ 165.31, 163.88, 160.92, 155.42, 139.85, 128.86, 128.65, 126.37, 124.31 (q, J = 278.4 Hz), 90.45, 66.75, 51.70, 44.58, 40.89 (q, J = 34.8 Hz), 35.77, 34.04. HRMS [$\text{C}_{20}\text{H}_{24}\text{F}_3\text{N}_5\text{O}_2 + \text{H}$] $^+$: 424.1955 calculated, 424.1958 found.



2-(Methyl(phenethyl)amino)-6-morpholinopyrimidine-4-carboxylic acid (17). *Ester hydrolysis:* a round-bottom flask was charged with methyl ester **125** (680 mg, 2.64 mmol, 1 eq) in 12.5 mL THF/MeOH (4:1). A 1.5 M aqueous NaOH solution (1.76 mL, 2.64 mmol, 1 eq) was added together with 0.75 mL H_2O . The reaction was stirred overnight at rt after which the solvents were evaporated yielding the product as the Na^+ salt (**126**) which was used without further purification (779 mg, 2.64 mmol, quant.). *$S_N\text{Ar}$ reaction:* the title compound was prepared according to general procedure A using 2-chloropyrimidine **126** (244 mg, 1.0 mmol, 1 eq), DiPEA (0.52 mL, 3.0 mmol, 3 eq) and *N*-methylphenethylamine (189 μ L, 1.3 mmol, 1.3 eq). Total heating time: 6 d at 120 $^\circ\text{C}$. Column chromatography (2.5% \rightarrow 15% MeOH/DCM) afforded the product (175 mg, 0.51 mmol, 51%). TLC: R_f = 0.5 (100% EtOAc with 3 drops of AcOH). ^1H NMR (400 MHz, MeOD + CDCl_3) δ 7.35 – 7.26 (m, 2H), 7.26 – 7.15 (m, 3H), 6.87 (s, 1H), 3.91 (t, J = 7.0 Hz, 2H), 3.81 (br s, 8H), 3.17 (s, 3H), 2.97 (t, J = 7.0 Hz, 2H). ^{13}C NMR (101 MHz, MeOD + CDCl_3) δ 161.70, 152.17, 148.40, 137.57, 133.96, 128.50, 128.38, 126.57, 93.89, 66.02, 51.86, 45.10, 33.13. HRMS [$\text{C}_{18}\text{H}_{22}\text{N}_4\text{O}_3 + \text{H}$] $^+$: 343.1765 calculated, 343.1772 found.

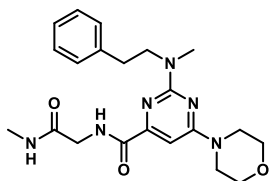


2-(Methyl(phenethyl)amino)-6-morpholinopyrimidine-4-carbonyl)glycine (18). The title compound was prepared according to general procedure A using 2-chloropyrimidine **128** (150 mg, 0.50 mmol, 1 eq), DiPEA (0.43 mL, 2.5 mmol, 5 eq) and *N*-methylphenethylamine HBr salt (162 mg, 0.76 mmol, 1.5 eq). Total heating time: 6 h at 160 $^\circ\text{C}$ with μW irradiation. Purification by HPLC (C18 reverse phase, 10% to 70% $\text{CH}_3\text{CN}/\text{H}_2\text{O} + 50$ mM NH_4HCO_3) afforded the product (40 mg, 0.10 mmol, 20%). TLC: R_f = 0.3 (5% MeOH/DCM). ^1H NMR (500 MHz, MeOD + CDCl_3) δ 7.32 – 7.14 (m, 5H), 6.65 (s, 1H), 4.01 (s, 2H), 3.83 (t, J = 7.3 Hz, 2H), 3.80 – 3.75 (m, 4H), 3.73 – 3.60 (m, 4H), 3.11 (s, 3H), 2.91 (t, J = 7.4 Hz, 2H). ^{13}C NMR (126 MHz, MeOD + CDCl_3) δ 173.63, 164.96, 163.55, 160.59, 155.89, 139.54, 128.50, 128.00, 125.67, 89.33, 66.26, 51.10, 49.06, 43.96, 42.64, 39.58, 35.05, 33.47, 20.71. HRMS [$\text{C}_{20}\text{H}_{25}\text{N}_5\text{O}_4 + \text{H}$] $^+$: 400.1979 calculated, 400.1984 found.

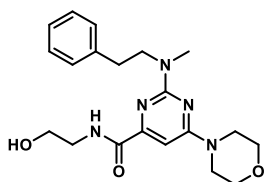


Methyl 2-(methyl(phenethyl)amino)-6-morpholinopyrimidine-4-carbonyl)glycinate (19). A round-bottom flask was charged with carboxylic acid **18** (28 mg, 70 μ mol, 1 eq) in dry DCM (1.5 mL). This was followed by addition of HOBT (15 mg, 0.11 mmol, 1.5 eq), EDC-HCl (20 mg, 0.11 mmol, 1.5 eq). The reaction was stirred for 1 h at rt after which MeOH (11 μ L, 0.28 mmol, 4 eq) was added and then stirred overnight at rt. The reaction was diluted with EtOAc (25 mL), washed with sat. aq. NaHCO_3 (2 x 25 mL), dried (Na_2SO_4), filtered and concentrated under reduced pressure. The residue was purified using silica gel column chromatography (60% \rightarrow 80% EtOAc/pentane) affording the product (18 mg, 44 μ mol, 62%). TLC: R_f = 0.3 (70% EtOAc/pentane). ^1H NMR (400 MHz, CDCl_3) δ 8.40 (br s, 1H), 7.39 – 7.13 (m, 5H), 6.69 (s, 1H), 4.22 (d, J = 5.5 Hz, 2H), 3.86 – 3.71 (m, 9H), 3.71 – 3.59 (m, 4H), 3.11 (s,

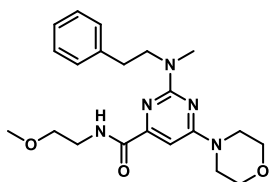
3H), 2.96 – 2.85 (m, 2H). ^{13}C NMR (101 MHz, CDCl_3) δ 170.25, 165.14, 163.91, 160.92, 155.99, 139.96, 128.98, 128.58, 126.27, 90.13, 66.75, 52.52, 51.68, 44.51, 41.37, 35.79, 34.01. HRMS [$\text{C}_{21}\text{H}_{27}\text{N}_5\text{O}_4 + \text{H}$] $^+$: 414.2136 calculated, 414.2144 found.



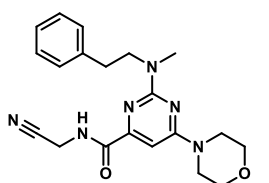
***N*-(2-(Methylamino)-2-oxoethyl)-2-(methyl(phenethyl)amino)-6-morpholinopyrimidine-4-carboxamide (20).** The title compound was prepared according to general procedure B using carboxylic acid **18** (12 mg, 30 μmol , 1 eq), DiPEA (21 μL , 120 μmol , 4 eq), PyBOP (19 mg, 45 μmol , 1.5 eq) and methylamine HCl salt (3 mg, 36 μmol , 1.2 eq). Column chromatography (2.5% \rightarrow 10% MeOH/DCM) afforded the product (6 mg, 15 μmol , 50%). TLC: R_f = 0.4 (5% MeOH/DCM). ^1H NMR (500 MHz, CDCl_3) δ 8.43 (br s, 1H), 7.32 – 7.26 (m, 2H), 7.23 – 7.16 (m, 3H), 6.69 (br s, 1H), 6.22 (br s, 1H), 4.08 (d, J = 6.1 Hz, 2H), 3.86 – 3.79 (m, 2H), 3.79 – 3.73 (m, 4H), 3.67 (br s, 4H), 3.10 (s, 3H), 2.93 – 2.86 (m, 2H), 2.84 (d, J = 4.9 Hz, 3H). ^{13}C NMR (126 MHz, CDCl_3) δ 169.58, 165.74, 163.84, 160.90, 155.66, 139.91, 128.93, 128.65, 126.36, 90.21, 66.75, 51.65, 44.60, 43.84, 35.86, 34.06, 26.41. HRMS [$\text{C}_{21}\text{H}_{28}\text{N}_6\text{O}_3 + \text{H}$] $^+$: 413.2296 calculated, 413.2294 found.



***N*-(2-Hydroxyethyl)-2-(methyl(phenethyl)amino)-6-morpholinopyrimidine-4-carboxamide (21).** The title compound was prepared according to general procedure B using carboxylic acid **17** (39 mg, 0.11 mmol, 1 eq), DiPEA (60 μL , 0.34 mmol, 3 eq), PyBOP (89 mg, 0.17 mmol, 1.5 eq) and ethanolamine (34 μL , 0.57 mmol, 5 eq). Column chromatography (70% \rightarrow 100% EtOAc/pentane to 5% MeOH/EtOAc) afforded the product (25 mg, 65 μmol , 59%). TLC: R_f = 0.3 (80% EtOAc/pentane). ^1H NMR (400 MHz, CDCl_3) δ 8.29 (br s, 1H), 7.33 – 7.27 (m, 2H), 7.24 – 7.16 (m, 3H), 6.70 (s, 1H), 3.87 – 3.78 (m, 4H), 3.78 – 3.74 (m, 4H), 3.70 – 3.62 (m, 4H), 3.62 – 3.55 (m, 2H), 3.10 (s, 3H), 2.98 – 2.80 (m, 3H). ^{13}C NMR (101 MHz, CDCl_3) δ 166.19, 163.93, 160.87, 156.29, 139.96, 128.89, 128.61, 126.32, 90.14, 66.74, 62.71, 51.61, 44.51, 42.71, 35.77, 33.98. HRMS [$\text{C}_{20}\text{H}_{27}\text{N}_5\text{O}_3 + \text{H}$] $^+$: 386.2187 calculated, 386.2191 found.

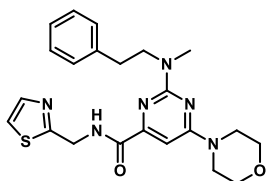


***N*-(2-Methoxyethyl)-2-(methyl(phenethyl)amino)-6-morpholinopyrimidine-4-carboxamide (22).** A round-bottom flask was charged with alcohol **21** (17 mg, 44 μmol , 1 eq) in dry DMF (1 mL) and cooled to 0 $^\circ\text{C}$. NaOtBu (2 M in THF, 33 μL , 66 μmol , 1.5 eq) and methyl iodide (3.1 μL , 49 μmol , 1.1 eq) were added. The reaction was allowed to warm to rt while stirring overnight. EtOAc (25 mL) was added followed by washing with H_2O (1 x 25 mL) and brine (2 x 25 mL), drying (Na_2SO_4), filtering and concentration under reduced pressure. The residue was purified by silica gel column chromatography (70 \rightarrow 80% EtOAc/pentane) affording the product (5 mg, 13 μmol , 30%). TLC: R_f = 0.4 (80% EtOAc/pentane). ^1H NMR (400 MHz, CDCl_3) δ 8.26 (br s, 1H), 7.33 – 7.27 (m, 2H), 7.25 – 7.16 (m, 3H), 6.71 (s, 1H), 3.85 – 3.71 (m, 6H), 3.72 – 3.59 (m, 6H), 3.59 – 3.51 (m, 2H), 3.38 (s, 3H), 3.11 (s, 3H), 2.95 – 2.83 (m, 2H). ^{13}C NMR (101 MHz, CDCl_3) δ 164.96, 163.98, 160.89, 156.67, 139.95, 128.93, 128.62, 126.29, 90.08, 71.38, 66.78, 59.02, 51.72, 44.53, 39.25, 35.77, 33.96. HRMS [$\text{C}_{21}\text{H}_{29}\text{N}_5\text{O}_3 + \text{H}$] $^+$: 400.2343 calculated, 400.2345 found.

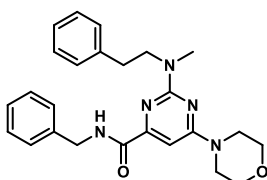


***N*-(Cyanomethyl)-2-(methyl(phenethyl)amino)-6-morpholinopyrimidine-4-carboxamide (23).** The title compound was prepared according to general procedure B using carboxylic acid **17** (21 mg, 61 μmol , 1 eq), DiPEA (53 μL , 0.31 mmol, 5 eq), PyBOP (48 mg, 92 μmol , 1.5 eq) and aminoacetonitrile bisulfate (11 mg, 73 μmol , 1.2 eq). Column chromatography (50% \rightarrow 70% EtOAc/pentane) afforded the product (10 mg, 26 μmol , 43%). TLC: R_f = 0.6 (60% EtOAc/pentane). ^1H NMR (400 MHz, CDCl_3) δ 8.12 (br s, 1H), 7.35 – 7.27 (m, 2H), 7.25 – 7.14 (m, 3H), 6.67 (s, 1H), 4.34 (d, J =

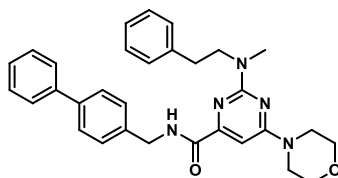
6.1 Hz, 2H), 3.86 – 3.79 (m, 2H), 3.79 – 3.74 (m, 4H), 3.66 (br s, 4H), 3.10 (s, 3H), 2.95 – 2.84 (m, 2H). ^{13}C NMR (101 MHz, CDCl_3) δ 165.12, 163.72, 160.92, 154.96, 139.94, 128.88, 128.68, 126.41, 115.95, 90.37, 66.71, 51.58, 44.50, 35.86, 34.05, 27.52. HRMS [$\text{C}_{20}\text{H}_{24}\text{N}_6\text{O}_2 + \text{H}$] $^+$: 381.2034 calculated, 381.2042 found.



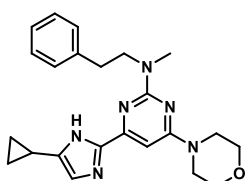
***N*-(Thiazol-2-ylmethyl)-2-(methyl(phenethyl)amino)-6-morpholinopyrimidine-4-carboxamide (24)**. The title compound was prepared according to general procedure B using carboxylic acid **17** (27 mg, 79 μmol , 1 eq), DiPEA (82 μL , 0.47 mmol, 6 eq), PyBOP (62 mg, 0.12 mmol, 1.5 eq) and 2-aminomethylthiazole double HCl salt (19 mg, 0.10 mmol, 1.3 eq). Purification by preparative HPLC (C18 reverse phase, 34% to 37% $\text{CH}_3\text{CN}/\text{H}_2\text{O} + 0.2\%$ TFA) afforded the product (11 mg, 25 μmol , 32%). TLC: $R_f = 0.3$ (80% EtOAc/pentane). ^1H NMR (400 MHz, CDCl_3) δ 8.61 (br s, 1H), 7.73 (d, $J = 3.3$ Hz, 1H), 7.29 (d, $J = 3.3$ Hz, 1H), 7.28 – 7.22 (m, 2H), 7.21 – 7.14 (m, 3H), 6.74 (s, 1H), 4.94 (d, $J = 6.2$ Hz, 2H), 3.85 – 3.71 (m, 6H), 3.71 – 3.59 (m, 4H), 3.09 (s, 3H), 2.93 – 2.81 (m, 2H). ^{13}C NMR (101 MHz, CDCl_3) δ 167.81, 165.37, 164.19, 161.18, 156.27, 142.95, 140.22, 129.23, 128.91, 126.61, 120.05, 90.65, 67.07, 51.97, 44.85, 41.38, 36.13, 34.31. HRMS [$\text{C}_{22}\text{H}_{26}\text{N}_6\text{O}_2\text{S} + \text{H}$] $^+$: 439.1911 calculated, 439.1913 found.



***N*-Benzyl-2-(methyl(phenethyl)amino)-6-morpholinopyrimidine-4-carboxamide (25)**. The title compound was prepared according to general procedure A using 2-chloropyrimidine **117i** (67 mg, 0.20 mmol, 1 eq), DiPEA (139 μL , 0.80 mmol, 4 eq) and *N*-methylphenethylamine HBr salt (65 mg, 0.30 mmol, 1.5 eq). Total heating time: 4 h at 160 $^\circ\text{C}$ with μW irradiation. Column chromatography (40% -> 60% EtOAc/pentane) afforded the product (75 mg, 0.17 mmol, 87%). TLC: $R_f = 0.8$ (60% EtOAc/pentane). ^1H NMR (400 MHz, CDCl_3) δ 8.25 (br s, 1H), 7.39 – 7.33 (m, 4H), 7.33 – 7.26 (m, 1H), 7.24 – 7.14 (m, 3H), 7.14 – 7.04 (m, 2H), 6.76 (s, 1H), 4.63 (d, $J = 6.1$ Hz, 2H), 3.80 – 3.71 (m, 6H), 3.71 – 3.62 (m, 4H), 3.08 (s, 3H), 2.89 – 2.80 (m, 2H). ^{13}C NMR (101 MHz, CDCl_3) δ 164.83, 163.90, 160.82, 156.52, 139.79, 138.35, 128.80, 128.77, 128.54, 127.69, 127.51, 126.20, 90.17, 66.70, 51.63, 44.46, 43.37, 35.68, 33.88. HRMS [$\text{C}_{25}\text{H}_{29}\text{N}_5\text{O}_2 + \text{H}$] $^+$: 432.2394 calculated, 432.2390 found.

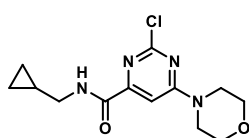


***N*-([1,1'-Biphenyl]-4-ylmethyl)-2-(methyl(phenethyl)amino)-6-morpholinopyrimidine-4-carboxamide (26)**. The title compound was prepared according to general procedure A using 2-chloropyrimidine **117j** (41 mg, 0.10 mmol, 1 eq), DiPEA (70 μL , 0.40 mmol, 4 eq) and *N*-methylphenethylamine HBr salt (32 mg, 0.15 mmol, 1.5 eq). Total heating time: 4 h at 160 $^\circ\text{C}$ with μW irradiation. Column chromatography (40% -> 60% EtOAc/pentane) afforded the product (40 mg, 79 μmol , 79%). TLC: $R_f = 0.5$ (50% EtOAc/pentane). ^1H NMR (400 MHz, CDCl_3) δ 8.29 (br s, 1H), 7.57 (d, $J = 7.9$ Hz, 4H), 7.47 – 7.39 (m, 4H), 7.38 – 7.30 (m, 1H), 7.23 – 7.07 (m, 5H), 6.77 (s, 1H), 4.68 (d, $J = 6.1$ Hz, 2H), 3.81 – 3.72 (m, 6H), 3.71 – 3.61 (m, 4H), 3.08 (s, 3H), 2.90 – 2.81 (m, 2H). ^{13}C NMR (101 MHz, CDCl_3) δ 164.92, 163.94, 160.86, 156.54, 140.84, 140.51, 139.82, 137.43, 128.88, 128.79, 128.56, 128.17, 127.56, 127.42, 127.17, 126.24, 90.22, 66.73, 51.65, 44.50, 43.12, 35.73, 33.91. HRMS [$\text{C}_{31}\text{H}_{33}\text{N}_5\text{O}_2 + \text{H}$] $^+$: 508.2707 calculated, 508.2704 found.



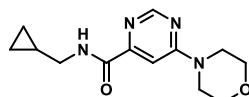
4-(5-Cyclopropyl-1H-imidazol-2-yl)-*N*-methyl-6-morpholino-*N*-phenethylpyrimidin-2-amine (27). *Acyloxymethylketone synthesis*: a round-bottom flask was charged with carboxylic acid **17** (53 mg, 0.15 mmol, 1 eq) in dry DMF (1 mL). Cs_2CO_3 (91 mg, 0.28 mmol, 1.8 eq) and 2-bromocyclopropylethanone (16 μL , 0.16 mmol, 1.05 eq) were added and the mixture was stirred for 1.5 h. The reaction was diluted with EtOAc (25 mL) and the mixture was washed with H_2O (1 x 25 mL) and brine (2 x 25 mL), dried (Na_2SO_4), filtered and concentrated under reduced pressure. The residue was purified by silica gel column chromatography (30% -> 50% EtOAc/pentane) affording the

acyloxymethylketone **131** (34 mg, 80 μ mol, 53%). ^1H NMR (400 MHz, CDCl_3) δ 7.36 – 7.12 (m, 5H), 6.63 (s, 1H), 5.04 (s, 2H), 3.87 – 3.78 (m, 2H), 3.78 – 3.72 (m, 4H), 3.71 – 3.53 (m, 4H), 3.14 (s, 3H), 2.97 – 2.80 (m, 2H), 2.16 – 2.00 (m, 1H), 1.22 – 1.08 (m, 2H), 1.04 – 0.88 (m, 2H). ^{13}C NMR (101 MHz, CDCl_3) δ 203.64, 165.50, 163.61, 161.85, 154.67, 139.97, 128.93, 128.50, 126.17, 93.17, 69.31, 66.69, 51.54, 44.41, 35.64, 33.77, 17.38, 11.70. *Imidazole synthesis*: a microwave vial was charged with acyloxymethylketone **131** (34 mg, 80 μ mol, 1 eq) and NH_4OAc (31 mg, 0.40 mmol, 5 eq) in xylene (0.7 mL). The vial was capped and stirred at 140 $^\circ\text{C}$ for 2 h. Purification by preparative HPLC (C18 reverse phase, 35% to 40% $\text{CH}_3\text{CN}/\text{H}_2\text{O}$ + 0.2% TFA) afforded the product (2 mg, 5 μ mol, 6%). TLC: R_f = 0.7 (40% EtOAc/pentane). ^1H NMR (850 MHz, CDCl_3) δ 9.89 (br s, 1H), 7.33 – 7.27 (m, 2H), 7.24 – 7.16 (m, 3H), 6.98 – 6.49 (m, 2H), 3.84 (s, 2H), 3.80 – 3.73 (m, 4H), 3.68 (br s, 4H), 3.14 (s, 3H), 2.97 – 2.83 (m, 2H), 1.91 (br s, 1H), 0.92 (br s, 2H), 0.74 (br s, 2H). ^{13}C NMR (214 MHz, CDCl_3) δ 163.48, 161.12, 154.40, 145.32, 140.18, 128.91, 128.66, 126.35, 111.74, 87.19, 66.84, 51.62, 44.66, 35.84, 34.08, 9.44, 7.18, 6.01. HRMS [$\text{C}_{23}\text{H}_{28}\text{N}_5\text{O} + \text{H}$] $^+$: 405.2397 calculated, 405.2403 found.



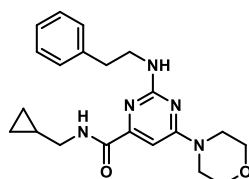
2-Chloro-*N*-(cyclopropylmethyl)-6-morpholinopyrimidine-4-carboxamide (28).

The title compound was prepared according to general procedure E using dichloropyrimidine **116a** (1.7 g, 7.1 mmol, 1 eq), DiPEA (1.9 mL, 10.6 mmol, 1.5 eq) and morpholine (0.64 mL, 7.4 mmol, 1.05 eq). Column chromatography (30% -> 60% EtOAc/pentane) afforded the product (1.7 g, 6.3 mmol, 89%). TLC: R_f = 0.5 in 40% EtOAc/pentane. ^1H NMR (400 MHz, CDCl_3) δ 7.94 (t, J = 5.9 Hz, 1H), 7.28 (s, 1H), 3.87 – 3.63 (m, 8H), 3.33 – 3.25 (m, 2H), 1.12 – 1.00 (m, 1H), 0.61 – 0.52 (m, 2H), 0.32 – 0.24 (m, 2H). ^{13}C NMR (101 MHz, CDCl_3) δ 163.83, 162.21, 159.84, 157.90, 99.36, 66.35, 44.45, 10.65, 3.64. Regioselectivity was confirmed by ^1H -NOESY NMR analysis. HRMS [$\text{C}_{13}\text{H}_{17}\text{ClN}_4\text{O}_2 + \text{H}$] $^+$: 297.1113 calculated, 297.1116 found. Regioisomer 6-chloro-*N*-(cyclopropylmethyl)-2-morpholinopyrimidine-4-carboxamide (**127**) was also obtained (99 mg, 0.33 mmol, 5%). R_f = 0.6 in 40% EtOAc/pentane. ^1H NMR (400 MHz, CDCl_3) δ 7.80 – 7.65 (m, 1H), 7.32 (s, 1H), 3.90 – 3.72 (m, 8H), 3.30 (t, J = 6.5 Hz, 2H), 1.14 – 0.98 (m, 1H), 0.69 – 0.46 (m, 2H), 0.39 – 0.17 (m, 2H). ^{13}C NMR (101 MHz, CDCl_3) δ 163.48, 162.31, 160.68, 158.86, 107.51, 66.64, 44.42, 44.30, 10.80, 3.55.



***N*-(Cyclopropylmethyl)-6-morpholinopyrimidine-4-carboxamide (29).**

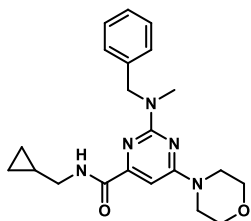
A round-bottom flask was charged with 2-chloropyrimidine **28** (24 mg, 80 μ mol, 1 eq), NaHCO_3 (8 mg, 0.10 mmol, 1.2 eq) and MeOH (0.5 mL). The solution was purged with N_2 followed by addition of Pd/C (10% w/w, 40 mg, 50 μ mol, 5 mol%), purged again with N_2 and then stirred overnight under an H_2 atmosphere (balloon). The mixture was filtered through a plug of Celite, which was washed with MeOH and the filtrate was concentrated under reduced pressure. The residue was purified by silica gel column chromatography (40% -> 70% EtOAc/pentane) to afford the product (20 mg, 76 μ mol, 95%). TLC: R_f = 0.2 (40% EtOAc/pentane). ^1H NMR (500 MHz, CDCl_3) δ 8.57 (s, 1H), 8.09 (t, J = 5.7 Hz, 1H), 7.36 (s, 1H), 3.80 – 3.77 (m, 4H), 3.76 – 3.67 (m, 4H), 3.33 – 3.28 (m, 2H), 1.10 – 1.02 (m, 1H), 0.59 – 0.54 (m, 2H), 0.32 – 0.26 (m, 2H). ^{13}C NMR (126 MHz, CDCl_3) δ 163.56, 163.02, 157.44, 155.78, 100.60, 66.59, 44.44, 44.37, 10.79, 3.65. HRMS [$\text{C}_{13}\text{H}_{18}\text{N}_4\text{O}_2 + \text{H}$] $^+$: 263.1503 calculated, 263.1502 found.



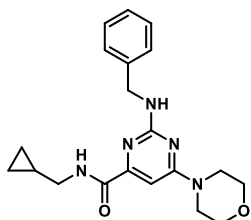
***N*-(Cyclopropylmethyl)-6-morpholino-2-(phenethylamino)pyrimidine-4-carboxamide (30).**

The title compound was prepared according to general procedure A using 2-chloropyrimidine **28** (59 mg, 0.20 mmol, 1 eq), 2-phenethylamine (30 μ L, 0.24 mmol, 1.2 eq) and DiPEA (70 μ L, 0.40 mmol, 2 eq). Total heating time: 8 h at 160 $^\circ\text{C}$ with μW irradiation. Column chromatography (2% -> 5% MeOH/DCM) afforded the product (40 mg, 0.10 mmol, 50%). TLC: R_f = 0.4 (4% MeOH/DCM). ^1H NMR (400 MHz, CDCl_3) δ 8.02 (br s, 1H), 7.39 – 7.28 (m, 2H), 7.28 – 7.15 (m, 3H), 6.78 (s, 1H), 4.96 (br s, 1H), 3.84 – 3.71 (m, 4H), 3.71 – 3.49 (m, 6H), 3.27 (t, J = 6.4 Hz, 2H), 2.92 (t, J = 7.2 Hz, 2H), 1.13 – 0.95 (m, 1H), 0.64 – 0.41 (m, 2H), 0.37 – 0.18 (m, 2H). ^{13}C NMR (101 MHz, CDCl_3) δ 164.46, 163.98,

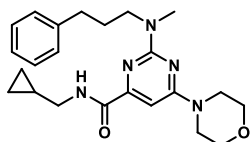
161.46, 156.84, 139.40, 128.89, 128.71, 126.53, 91.72, 66.68, 44.50, 43.00, 36.13, 10.79, 3.63. HRMS $[C_{21}H_{27}N_5O_2 + H]^+$: 382.2238 calculated, 382.2241 found.



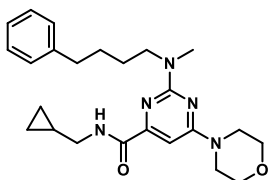
2-(Benzyl(methyl)amino)-N-(cyclopropylmethyl)-6-morpholinopyrimidine-4-carboxamide (31). The title compound was prepared according to general procedure A using 2-chloropyrimidine **28** (59 mg, 0.20 mmol, 1 eq), *N*-methylbenzylamine (38 μ L, 0.30 mmol, 1.5 eq) and DiPEA (140 μ L, 0.80 mmol, 4 eq). Total heating time: 8 h at 160 $^{\circ}$ C with μ W irradiation. Column chromatography (2% \rightarrow 5% MeOH/DCM) afforded the product (40 mg, 0.10 mmol, 50%). TLC: R_f = 0.5 (4% MeOH/DCM). 1H NMR (500 MHz, $CDCl_3$) δ 7.96 (br s, 1H), 7.34 – 7.28 (m, 2H), 7.28 – 7.21 (m, 3H), 6.75 (s, 1H), 4.85 (s, 2H), 3.82 – 3.69 (m, 4H), 3.69 – 3.54 (m, 4H), 3.26 (t, J = 6.5 Hz, 2H), 3.15 (s, 3H), 1.10 – 0.95 (m, 1H), 0.56 – 0.44 (m, 2H), 0.29 – 0.17 (m, 2H). ^{13}C NMR (101 MHz, $CDCl_3$) δ 164.58, 163.97, 161.35, 156.85, 139.11, 128.56, 127.34, 127.03, 90.41, 66.68, 52.76, 44.47, 44.00, 35.18, 10.85, 3.43. HRMS $[C_{21}H_{27}N_5O_2 + H]^+$: 382.2238 calculated, 382.2241 found.



N-(Cyclopropylmethyl)-2-(benzylamino)-6-morpholinopyrimidine-4-carboxamide (32). The title compound was prepared according to general procedure A using 2-chloropyrimidine **28** (59 mg, 0.20 mmol, 1 eq), DiPEA (0.14 mL, 0.80 mmol, 4 eq) and benzylamine (33 μ L, 0.30 mmol, 1.5 eq). Total heating time: 4 h at 160 $^{\circ}$ C with μ W irradiation. Column chromatography (2% \rightarrow 4% MeOH/DCM) afforded the product (19 mg, 50 μ mol, 25%). TLC: R_f = 0.5 (6% MeOH/DCM). 1H NMR (400 MHz, $CDCl_3$) δ 7.94 (br s, 1H), 7.41 – 7.19 (m, 5H), 6.78 (s, 1H), 5.24 (br s, 1H), 4.60 (d, J = 5.9 Hz, 2H), 3.76 – 3.69 (m, 4H), 3.69 – 3.60 (m, 4H), 3.25 (t, J = 7.1, 5.8 Hz, 2H), 1.09 – 0.95 (m, 1H), 0.57 – 0.48 (m, 2H), 0.29 – 0.22 (m, 2H). ^{13}C NMR (126 MHz, $CDCl_3$) δ 164.20, 164.03, 161.41, 156.91, 139.73, 128.65, 127.53, 127.27, 91.86, 66.67, 45.79, 44.48, 44.25, 10.78, 3.59. HRMS $[C_{20}H_{25}N_5O_2 + H]^+$: 368.2081 calculated, 368.2081 found.

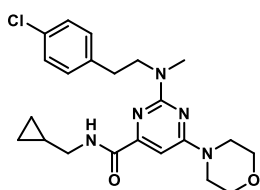


N-(Cyclopropylmethyl)-2-(methyl(3-phenylpropyl)amino)-6-morpholinopyrimidine-4-carboxamide (33). The title compound was prepared according to general procedure A using 2-chloropyrimidine **28** (39 mg, 0.13 mmol, 1 eq), amine **121b** (30 mg, 0.20 mmol, 1.5 eq) and DiPEA (87 μ L, 0.53 mmol, 4 eq). Total heating time: 48 h at 120 $^{\circ}$ C. Column chromatography (30% \rightarrow 60% EtOAc/pentane) afforded the product (38 mg, 93 μ mol, 72%). TLC: R_f = 0.4 (50% EtOAc/pentane). 1H NMR (400 MHz, $CDCl_3$) δ 7.98 (br s, 1H), 7.32 – 7.22 (m, 2H), 7.22 – 7.14 (m, 3H), 6.69 (s, 1H), 3.76 – 3.68 (m, 4H), 3.65 – 3.59 (m, 2H), 3.59 – 3.51 (m, 4H), 3.28 (t, J = 7.0, 5.9 Hz, 2H), 3.14 (s, 3H), 2.66 (t, J = 7.5 Hz, 2H), 1.95 (p, J = 9.0, 7.5 Hz, 2H), 1.10 – 0.98 (m, 1H), 0.57 – 0.49 (m, 2H), 0.30 – 0.24 (m, 2H). ^{13}C NMR (101 MHz, $CDCl_3$) δ 164.69, 163.93, 161.04, 156.75, 142.00, 128.49, 128.43, 125.93, 89.96, 66.73, 48.99, 44.42, 43.97, 35.31, 33.52, 28.92, 10.93, 3.43. HRMS $[C_{23}H_{31}N_5O_2 + H]^+$: 410.2551 calculated, 410.2548 found.



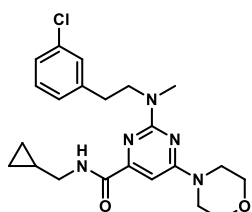
N-(Cyclopropylmethyl)-2-(methyl(4-phenylbutyl)amino)-6-morpholinopyrimidine-4-carboxamide (34). The title compound was prepared according to general procedure A using 2-chloropyrimidine **28** (30 mg, 0.10 mmol, 1 eq), amine **121c** (23 mg, 0.15 mmol, 1.5 eq) and DiPEA (70 μ L, 0.40 mmol, 4 eq). Total heating time: 24 h at 120 $^{\circ}$ C. Column chromatography (30% \rightarrow 60% EtOAc/pentane) afforded the product (40 mg, 94 μ mol, 94%). TLC: R_f = 0.5 (50% EtOAc/pentane). 1H NMR (400 MHz, $CDCl_3$) δ 8.03 (t, J = 5.8 Hz, 1H), 7.31 – 7.22 (m, 2H), 7.21 – 7.12 (m, 3H), 6.70 (s, 1H), 3.77 – 3.70 (m, 4H), 3.67 – 3.58 (m, 6H), 3.31 – 3.24 (m, 2H), 3.11 (s, 3H), 2.73 – 2.59 (m, 2H), 1.76 – 1.56 (m, J = 3.5, 2.9 Hz, 4H), 1.11 – 0.95 (m, 1H), 0.56 – 0.44 (m, 2H), 0.28 – 0.18 (m, 2H). ^{13}C NMR (101 MHz, $CDCl_3$) δ 164.70, 163.96, 161.10, 156.74, 142.44, 128.42, 128.40, 125.87, 89.89, 66.72,

49.12, 44.47, 44.00, 35.88, 35.32, 29.03, 27.20, 10.86, 3.39. HRMS $[C_{24}H_{33}N_5O_2 + H]^+$: 424.2707 calculated, 424.2706 found.

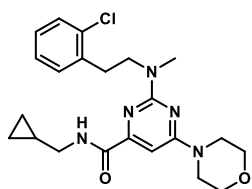


2-((4-Chlorophenethyl)(methyl)amino)-N-(cyclopropylmethyl)-6-morpholinopyrimidine-4-carboxamide (35). The title compound was prepared according to general procedure A using 2-chloropyrimidine **28** (30 mg, 0.10 mmol, 1 eq), amine **121d** (34 mg, 0.20 mmol, 2 eq) and DiPEA (70 μ L, 0.40 mmol, 4 eq). Total heating time: 25 h at 120 $^{\circ}$ C. Column chromatography (30% \rightarrow 70% EtOAc/pentane) afforded the product (10 mg, 30 μ mol, 30%). TLC:

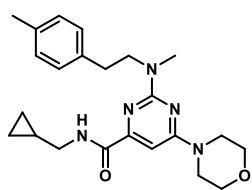
$R_f = 0.4$ (50% EtOAc/pentane). 1H NMR (400 MHz, $CDCl_3$) δ 7.98 (br s, 1H), 7.28 – 7.23 (m, 2H), 7.17 – 7.09 (m, 2H), 6.73 (s, 1H), 3.82 – 3.72 (m, 6H), 3.65 (t, $J = 4.8$ Hz, 4H), 3.35 – 3.24 (m, 2H), 3.09 (s, 3H), 2.94 – 2.82 (m, 2H), 1.12 – 1.01 (m, 1H), 0.60 – 0.49 (m, 2H), 0.36 – 0.23 (m, 2H). ^{13}C NMR (101 MHz, $CDCl_3$) δ 164.64, 163.98, 156.81, 138.45, 132.12, 130.22, 128.72, 90.28, 66.76, 51.50, 44.53, 44.15, 35.86, 33.39, 10.91, 3.51. HRMS $[C_{22}H_{28}ClN_5O_2 + H]^+$: 430.2004 calculated, 430.2004 found.



2-((3-Chlorophenethyl)(methyl)amino)-N-(cyclopropylmethyl)-6-morpholinopyrimidine-4-carboxamide (36). The title compound was prepared according to general procedure A using 2-chloropyrimidine **28** (20 mg, 70 μ mol, 1 eq), amine **121e** (20 mg, 0.12 mmol, 1.5 eq) and DiPEA (49 μ L, 0.28 mmol, 4 eq). Total heating time: 5 d at 120 $^{\circ}$ C. Column chromatography (30% \rightarrow 50% EtOAc/pentane) afforded the product (26 mg, 62 μ mol, 89%). TLC: $R_f = 0.6$ (40% EtOAc/pentane). 1H NMR (400 MHz, $CDCl_3$) δ 8.00 (t, $J = 5.9$ Hz, 1H), 7.25 – 7.14 (m, 3H), 7.14 – 7.02 (m, 1H), 6.73 (s, 1H), 3.86 – 3.72 (m, 6H), 3.66 (t, $J = 4.9$ Hz, 4H), 3.30 (dd, $J = 7.1, 5.8$ Hz, 2H), 3.12 (s, 3H), 2.93 – 2.83 (m, 2H), 1.12 – 1.01 (m, 1H), 0.60 – 0.50 (m, 2H), 0.33 – 0.24 (m, 2H). ^{13}C NMR (101 MHz, $CDCl_3$) δ 164.62, 163.98, 160.86, 156.78, 141.98, 134.32, 129.82, 128.99, 127.06, 126.50, 90.27, 66.74, 51.34, 44.51, 44.12, 35.72, 33.68, 10.90, 3.48. HRMS $[C_{22}H_{28}ClN_5O_2 + H]^+$: 430.2004 calculated, 430.2004 found.



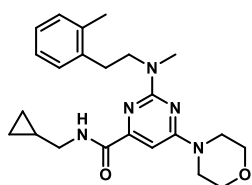
2-((2-Chlorophenethyl)(methyl)amino)-N-(cyclopropylmethyl)-6-morpholinopyrimidine-4-carboxamide (37). The title compound was prepared according to general procedure A using 2-chloropyrimidine **28** (30 mg, 0.10 mmol, 1 eq), amine **121f** (28 mg, 0.17 mmol, 1.7 eq) and DiPEA (70 μ L, 0.40 mmol, 4 eq). Total heating time: 3 d at 120 $^{\circ}$ C. Purification by HPLC (C18 reverse phase, 35% \rightarrow 45% $CH_3CN/H_2O + 0.2\%$ TFA, RT 10.8 min) afforded the product (31 mg, 70 μ mol, 70%). TLC: $R_f = 0.7$ (50% EtOAc/pentane). 1H NMR (500 MHz, $CDCl_3$) δ 8.06 (br s, 1H), 7.37 – 7.32 (m, 1H), 7.21 – 7.12 (m, 3H), 6.70 (s, 1H), 3.89 – 3.83 (m, 2H), 3.78 – 3.74 (m, 4H), 3.69 – 3.62 (m, 4H), 3.29 (dd, $J = 7.0, 5.9$ Hz, 2H), 3.14 (s, 3H), 3.06 – 3.02 (m, 2H), 1.13 – 1.01 (m, 1H), 0.59 – 0.51 (m, 2H), 0.31 – 0.27 (m, 2H). ^{13}C NMR (101 MHz, $CDCl_3$) δ 164.70, 163.95, 160.97, 156.79, 137.46, 134.14, 131.17, 129.60, 127.93, 127.01, 90.11, 66.78, 49.36, 44.51, 44.14, 35.52, 31.93, 10.97, 3.59. HRMS $[C_{22}H_{28}ClN_5O_2 + H]^+$: 430.2004 calculated, 430.2003 found.



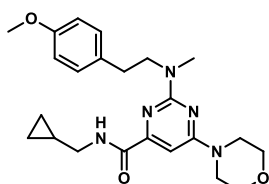
N-(Cyclopropylmethyl)-2-(methyl(4-methylphenethyl)amino)-6-morpholinopyrimidine-4-carboxamide (38). The title compound was prepared according to general procedure A using 2-chloropyrimidine **28** (30 mg, 0.10 mmol, 1 eq), amine **121g** (23 mg, 0.15 mmol, 1.5 eq) and DiPEA (70 μ L, 0.40 mmol, 4 eq). Total heating time: 3 d at 120 $^{\circ}$ C. Column chromatography (30% \rightarrow 50% EtOAc/pentane) afforded the product (16 mg, 40 μ mol, 40%). TLC: $R_f = 0.8$ (50%

EtOAc/pentane). 1H NMR (400 MHz, $CDCl_3$) δ 8.04 (t, $J = 5.8$ Hz, 1H), 7.11 (s, 4H), 6.72 (s, 1H), 3.82 – 3.72 (m, 6H), 3.66 (t, $J = 4.8$ Hz, 4H), 3.30 (dd, $J = 7.1, 5.8$ Hz, 2H), 3.13 (s, 3H), 2.90 – 2.82 (m, 2H), 2.33 (s, 3H), 1.14 – 0.99 (m, 1H), 0.61 – 0.49 (m, 2H), 0.33 – 0.25 (m, 2H). ^{13}C NMR (101 MHz, $CDCl_3$) δ 164.72, 164.01, 160.89,

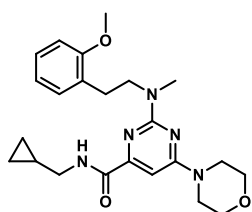
156.79, 136.81, 135.80, 129.28, 128.72, 90.06, 66.76, 51.81, 44.52, 44.12, 35.69, 33.46, 21.16, 10.90, 3.49. HRMS [C₂₃H₃₁N₅O₂ + H]⁺: 410.2551 calculated, 410.2549 found.



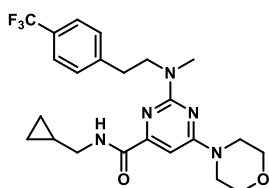
N-(Cyclopropylmethyl)-2-(methyl(2-methylphenethyl)amino)-6-morpholinopyrimidine-4-carboxamide (39). The title compound was prepared according to general procedure A using 2-chloropyrimidine **28** (30 mg, 0.10 mmol, 1 eq), amine **121h** (23 mg, 0.15 mmol, 1.5 eq) and DiPEA (70 μ L, 0.40 mmol, 4 eq). Total heating time: 4 d at 120 $^{\circ}$ C. Column chromatography (30% \rightarrow 60% EtOAc/pentane) afforded the product (39 mg, 95 μ mol, 95%). TLC: R_f = 0.4 (40% EtOAc/pentane). ¹H NMR (400 MHz, CDCl₃) δ 8.02 (t, *J* = 5.9 Hz, 1H), 7.23 – 7.06 (m, 4H), 6.73 (s, 1H), 3.85 – 3.71 (m, 6H), 3.66 (t, *J* = 4.8 Hz, 4H), 3.29 (dd, *J* = 7.1, 5.9 Hz, 2H), 3.15 (s, 3H), 2.97 – 2.83 (m, 2H), 2.39 (s, 3H), 1.15 – 0.98 (m, 1H), 0.62 – 0.47 (m, 2H), 0.34 – 0.22 (m, 2H). ¹³C NMR (101 MHz, CDCl₃) δ 164.69, 163.99, 160.91, 156.84, 137.97, 136.13, 130.38, 129.54, 126.51, 126.22, 90.12, 66.74, 50.23, 44.50, 44.12, 35.58, 31.31, 19.46, 10.91, 3.52. HRMS [C₂₃H₃₁N₅O₂ + H]⁺: 410.2551 calculated, 410.2546 found.



N-(Cyclopropylmethyl)-2-((4-methoxyphenethyl)(methyl)amino)-6-morpholinopyrimidine-4-carboxamide (40). The title compound was prepared according to general procedure A using 2-chloropyrimidine **28** (30 mg, 0.10 mmol, 1 eq), amine **121i** (36 mg, 0.20 mmol, 2 eq) and DiPEA (70 μ L, 0.40 mmol, 4 eq). Total heating time: 7 d at 120 $^{\circ}$ C. Column chromatography (30% \rightarrow 70% EtOAc/pentane) afforded the product (38 mg, 90 μ mol, 90%). TLC: R_f = 0.4 (30% EtOAc/pentane). ¹H NMR (400 MHz, CDCl₃) δ 8.04 (t, *J* = 5.6 Hz, 1H), 7.18 – 7.07 (m, 2H), 6.87 – 6.80 (m, 2H), 6.72 (s, 1H), 3.79 (s, 3H), 3.79 – 3.72 (m, 6H), 3.66 (t, *J* = 4.8 Hz, 4H), 3.30 (dd, *J* = 7.1, 5.8 Hz, 2H), 3.11 (s, 3H), 2.88 – 2.81 (m, 2H), 1.11 – 1.02 (m, 1H), 0.58 – 0.52 (m, 2H), 0.32 – 0.27 (m, 2H). ¹³C NMR (101 MHz, CDCl₃) δ 164.71, 164.00, 160.88, 158.16, 156.79, 131.97, 129.76, 114.01, 90.06, 66.76, 55.39, 51.86, 44.51, 44.11, 35.75, 33.01, 10.90, 3.49. HRMS [C₂₃H₃₁N₅O₃ + H]⁺: 426.2500 calculated, 426.2497 found.

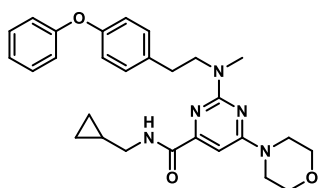


N-(Cyclopropylmethyl)-2-((2-methoxyphenethyl)(methyl)amino)-6-morpholinopyrimidine-4-carboxamide (41). The title compound was prepared according to general procedure A using 2-chloropyrimidine **28** (30 mg, 0.10 mmol, 1 eq), amine **121j** (24 mg, 0.15 mmol, 1.5 eq) and DiPEA (70 μ L, 0.40 mmol, 4 eq). Total heating time: 8 h at 160 $^{\circ}$ C with μ W irradiation. Column chromatography (30% \rightarrow 70% EtOAc/pentane) afforded the product (42 mg, 0.10 mmol, 99%). TLC: R_f = 0.3 (30% EtOAc/pentane). ¹H NMR (400 MHz, CDCl₃) δ 8.08 (t, *J* = 6.0 Hz, 1H), 7.20 (td, *J* = 7.8, 1.8 Hz, 1H), 7.13 (dd, *J* = 7.3, 1.7 Hz, 1H), 6.94 – 6.82 (m, 2H), 6.71 (s, 1H), 3.83 (s, 3H), 3.81 – 3.72 (m, 6H), 3.66 (t, *J* = 4.8 Hz, 4H), 3.30 (dd, *J* = 7.0, 5.9 Hz, 2H), 3.12 (s, 3H), 3.03 – 2.84 (m, 2H), 1.13 – 0.97 (m, 1H), 0.65 – 0.44 (m, 2H), 0.35 – 0.20 (m, 2H). ¹³C NMR (101 MHz, CDCl₃) δ 164.81, 163.99, 160.95, 157.81, 156.77, 130.55, 128.37, 127.64, 120.64, 110.48, 89.88, 66.79, 55.47, 49.93, 44.49, 44.04, 35.65, 28.70, 10.94, 3.47. HRMS [C₂₃H₃₁N₅O₃ + H]⁺: 426.2500 calculated, 426.2496 found.

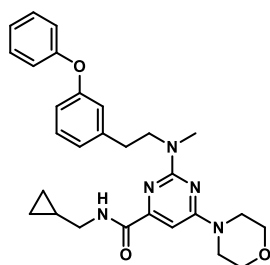


N-(Cyclopropylmethyl)-2-(methyl(4-(trifluoromethyl)phenethyl)amino)-6-morpholino-pyrimidine-4-carboxamide (42) The title compound was prepared according to general procedure A using 2-chloropyrimidine **28** (22 mg, 73 μ mol, 1 eq), amine **121k** (29 mg, 0.10 mmol, 1.5 eq) and DiPEA (51 μ L, 0.29 mmol, 4 eq). Total heating time: 25 h at 120 $^{\circ}$ C. Purification by HPLC (C18 reverse phase, 47% \rightarrow 55% CH₃CN/H₂O + 0.2% TFA, RT 12 min) afforded the product (9 mg, 20 μ mol, 27%). TLC: R_f = 0.4 (50% EtOAc/pentane). ¹H NMR (400 MHz, CDCl₃) δ 7.98 (br s, 1H), 7.54 (d, *J* = 8.0 Hz, 2H), 7.32 (d, *J* = 7.9 Hz, 2H), 6.73 (s, 1H), 3.87 – 3.79 (m, 2H), 3.79 – 3.71 (m, 4H), 3.65 (t, *J* = 4.8 Hz, 4H), 3.35 – 3.24 (m, 2H), 3.10 (s, 3H), 3.02 – 2.93 (m, 2H), 1.12 – 0.99 (m, 1H), 0.65 – 0.48 (m, 2H), 0.39 – 0.22 (m, 2H). ¹³C NMR (101 MHz, CDCl₃) δ 164.61, 163.98, 160.88, 156.81, 144.18 (q, *J* = 1.4 Hz), 129.21, 128.89,

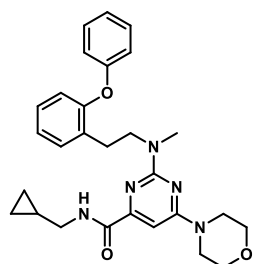
128.57, 125.73, 125.51 (q, $J = 3.7$ Hz), 123.03, 90.37, 66.75, 51.30, 44.51, 44.13, 35.87, 33.91, 10.92, 3.50. HRMS $[C_{23}H_{28}F_3N_5O_2 + H]^+$: 464.2268 calculated, 464.2267 found.



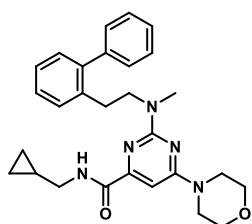
N-(Cyclopropylmethyl)-2-(methyl(4-phenoxyphenethyl)amino)-6-morpholinopyrimidine-4-carboxamide (43). The title compound was prepared according to general procedure A using 2-chloropyrimidine **28** (30 mg, 0.10 mmol, 1 eq), amine **121l** (34 mg, 0.15 mmol, 1.5 eq) and DiPEA (70 μ L, 0.40 mmol, 4 eq). Total heating time: 48 h at 120 $^{\circ}$ C. Column chromatography (30% \rightarrow 70% EtOAc/pentane) afforded the product (26 mg, 50 μ mol, 50%). TLC: $R_f = 0.4$ (50% EtOAc/pentane). 1H NMR (600 MHz, $CDCl_3$) δ 8.00 (br s, 1H), 7.35 – 7.28 (m, 2H), 7.19 – 7.13 (m, 2H), 7.10 – 7.06 (m, 1H), 6.99 – 6.89 (m, 4H), 6.72 (s, 1H), 3.84 – 3.78 (m, 2H), 3.78 – 3.73 (m, 4H), 3.69 – 3.63 (m, 4H), 3.31 – 3.26 (m, 2H), 3.13 (s, 3H), 2.93 – 2.86 (m, 2H), 1.11 – 0.98 (m, 1H), 0.56 – 0.51 (m, 2H), 0.29 – 0.25 (m, 2H). ^{13}C NMR (151 MHz, $CDCl_3$) δ 164.67, 164.00, 160.92, 157.63, 156.80, 155.60, 134.93, 130.09, 129.83, 123.17, 119.27, 118.63, 90.12, 66.75, 51.67, 44.54, 44.12, 35.73, 33.25, 10.90, 3.49. HRMS $[C_{28}H_{33}N_5O_3 + H]^+$: 488.2656 calculated, 488.2656 found.



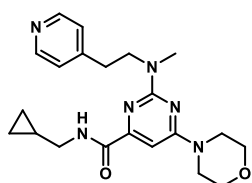
N-(Cyclopropylmethyl)-2-(methyl(3-phenoxyphenethyl)amino)-6-morpholinopyrimidine-4-carboxamide (44). The title compound was prepared according to general procedure A using 2-chloropyrimidine **28** (25 mg, 84 μ mol, 1 eq), amine **121m** (28 mg, 0.12 mmol, 1.5 eq) and DiPEA (60 μ L, 0.34 mmol, 4 eq). Total heating time: 5 d at 120 $^{\circ}$ C. Purification by HPLC (C18 reverse phase, 40% \rightarrow 50% $CH_3CN/H_2O + 0.2\%$ TFA, RT 11.2 min) afforded the product (14 mg, 29 μ mol, 35%). TLC: $R_f = 0.5$ (30% EtOAc/pentane). 1H NMR (400 MHz, $CDCl_3$) δ 8.00 (br s, 1H), 7.35 – 7.28 (m, 2H), 7.29 – 7.20 (m, 1H), 7.13 – 7.06 (m, 1H), 6.99 – 6.94 (m, 3H), 6.92 – 6.87 (m, 1H), 6.86 – 6.83 (m, 1H), 6.71 (s, 1H), 3.84 – 3.77 (m, 2H), 3.76 – 3.70 (m, 4H), 3.67 – 3.61 (m, 4H), 3.30 – 3.24 (m, 2H), 3.12 (s, 3H), 2.93 – 2.83 (m, 2H), 1.11 – 0.98 (m, 1H), 0.57 – 0.49 (m, 2H), 0.30 – 0.24 (m, 2H). ^{13}C NMR (101 MHz, $CDCl_3$) δ 164.67, 163.98, 160.89, 157.41, 157.32, 156.81, 142.03, 129.86, 123.91, 123.26, 119.57, 118.70, 116.91, 90.19, 66.75, 51.48, 44.52, 44.14, 35.69, 33.87, 10.90, 3.51. HRMS $[C_{28}H_{33}N_5O_3 + H]^+$: 488.2656 calculated, 488.2653 found.



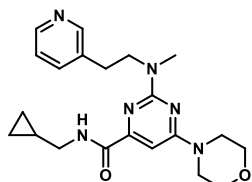
N-(Cyclopropylmethyl)-2-(methyl(2-phenoxyphenethyl)amino)-6-morpholinopyrimidine-4-carboxamide (45). The title compound was prepared according to general procedure A using 2-chloropyrimidine **28** (34 mg, 0.10 mmol, 1 eq), amine **121n** (37 mg, 0.16 mmol, 1.6 eq) and DiPEA (70 μ L, 0.40 mmol, 4 eq). Total heating time: 3 d at 120 $^{\circ}$ C. Column chromatography (30% \rightarrow 50% EtOAc/pentane) afforded the product (45 mg, 90 μ mol, 90%). TLC: $R_f = 0.5$ (40% EtOAc/pentane). 1H NMR (400 MHz, $CDCl_3$) δ 8.06 (t, $J = 5.4$ Hz, 1H), 7.34 – 7.28 (m, 2H), 7.26 (dd, $J = 7.4, 1.5$ Hz, 1H), 7.17 (td, $J = 7.8, 1.7$ Hz, 1H), 7.12 – 7.00 (m, 2H), 6.93 (dd, $J = 8.6, 0.9$ Hz, 2H), 6.86 (d, $J = 8.0$ Hz, 1H), 6.69 (s, 1H), 3.90 – 3.79 (m, 2H), 3.76 – 3.54 (m, 8H), 3.27 (t, $J = 6.4$ Hz, 2H), 3.07 (s, 3H), 2.99 – 2.88 (m, 2H), 1.11 – 0.98 (m, 1H), 0.60 – 0.44 (m, 2H), 0.27 (q, $J = 4.7$ Hz, 2H). ^{13}C NMR (101 MHz, $CDCl_3$) δ 164.74, 163.94, 160.90, 157.74, 156.72, 155.09, 131.31, 129.89, 127.84, 123.92, 122.99, 119.36, 118.07, 89.98, 66.70, 50.17, 44.44, 44.03, 35.57, 28.69, 10.92, 3.49. HRMS $[C_{28}H_{33}N_5O_3 + H]^+$: 488.2656 calculated, 488.2653 found.



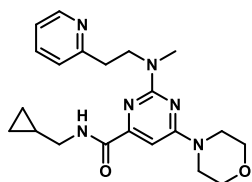
2-((2-([1,1'-Biphenyl]-2-yl)ethyl)(methylamino)-N-(cyclopropylmethyl)-6-morpholinopyrimidine-4-carboxamide (46). The title compound was prepared according to general procedure A using 2-chloropyrimidine **28** (29 mg, 96 μmol , 1 eq), amine **121o** (31 mg, 0.15 mmol, 1.5 eq) and DiPEA (70 μL , 0.40 mmol, 4 eq). Total heating time: 24 h at 160 $^{\circ}\text{C}$ with μW irradiation. Column chromatography (30% \rightarrow 60% EtOAc/pentane) afforded the product (43 mg, 91 μmol , 95%). TLC: $R_f = 0.4$ (30% EtOAc/pentane). ^1H NMR (400 MHz, CDCl_3) δ 7.97 (t, $J = 5.9$ Hz, 1H), 7.41 – 7.19 (m, 9H), 6.68 (s, 1H), 3.77 – 3.70 (m, 4H), 3.66 – 3.57 (m, 6H), 3.28 (dd, $J = 7.0, 5.8$ Hz, 2H), 2.94 – 2.89 (m, 2H), 2.77 (s, 3H), 1.10 – 1.00 (m, 1H), 0.59 – 0.49 (m, 2H), 0.31 – 0.25 (m, 2H). ^{13}C NMR (101 MHz, CDCl_3) δ 164.69, 163.87, 160.70, 156.65, 142.44, 141.63, 137.33, 130.26, 129.83, 129.28, 128.15, 127.56, 126.94, 126.29, 89.99, 66.72, 51.00, 44.44, 44.04, 35.31, 30.93, 10.90, 3.47. HRMS [$\text{C}_{28}\text{H}_{33}\text{N}_5\text{O}_2 + \text{H}$] $^+$: 472.2707 calculated, 472.2703 found.



N-(Cyclopropylmethyl)-2-(methyl(2-(pyridin-4-yl)ethyl)amino)-6-morpholinopyrimidine-4-carboxamide (47). The title compound was prepared according to general procedure A using 2-chloropyrimidine **28** (30 mg, 0.10 mmol, 1 eq), *N*-methyl-2-(pyridin-4-yl)ethan-1-amine (21 μL , 0.15 mmol, 1.5 eq) and DiPEA (70 μL , 0.40 mmol, 4 eq). Total heating time: 17 h at 120 $^{\circ}\text{C}$. Column chromatography (2% \rightarrow 6% MeOH/DCM) afforded the product (8 mg, 21 μmol , 21%). TLC: $R_f = 0.2$ (4% MeOH/DCM). ^1H NMR (400 MHz, CDCl_3) δ 8.51 (d, $J = 5.7$ Hz, 2H), 7.96 (br s, 1H), 7.15 (d, $J = 5.7$ Hz, 2H), 6.74 (s, 1H), 3.90 – 3.80 (m, 2H), 3.80 – 3.72 (m, 4H), 3.72 – 3.53 (m, 4H), 3.36 – 3.24 (m, 2H), 3.11 (s, 3H), 2.98 – 2.85 (m, 2H), 1.12 – 0.99 (m, 1H), 0.64 – 0.47 (m, 2H), 0.28 (q, $J = 4.7$ Hz, 2H). ^{13}C NMR (101 MHz, CDCl_3) δ 164.54, 163.96, 160.83, 156.80, 149.96, 148.99, 124.32, 90.46, 66.74, 50.59, 44.50, 44.13, 35.87, 33.44, 10.91, 3.51. HRMS [$\text{C}_{21}\text{H}_{28}\text{N}_6\text{O}_2 + \text{H}$] $^+$: 397.2347 calculated, 397.2345 found.

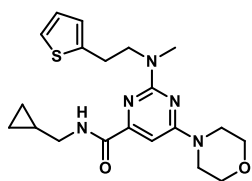


N-(Cyclopropylmethyl)-2-(methyl(2-(pyridin-3-yl)ethyl)amino)-6-morpholinopyrimidine-4-carboxamide (48). The title compound was prepared according to general procedure A using 2-chloropyrimidine **28** (30 mg, 0.10 mmol, 1 eq), *N*-methyl-2-(pyridin-3-yl)ethan-1-amine (21 μL , 0.15 mmol, 1.5 eq) and DiPEA (70 μL , 0.40 mmol, 4 eq). Total heating time: 17 h at 120 $^{\circ}\text{C}$. Column chromatography (2% \rightarrow 6% MeOH/DCM) afforded the product (11 mg, 29 μmol , 29%). TLC: $R_f = 0.15$ (4% MeOH/DCM). ^1H NMR (400 MHz, CDCl_3) δ 8.65 – 8.28 (m, 2H), 7.95 (br s, 1H), 7.51 (d, $J = 7.9$ Hz, 1H), 7.21 (dd, $J = 7.9, 4.8$ Hz, 1H), 6.72 (s, 1H), 3.89 – 3.69 (m, 6H), 3.69 – 3.53 (m, 4H), 3.29 (t, $J = 6.4$ Hz, 2H), 3.11 (s, 3H), 2.92 (t, $J = 7.4$ Hz, 2H), 1.12 – 0.99 (m, 1H), 0.66 – 0.45 (m, 2H), 0.36 – 0.19 (m, 2H). ^{13}C NMR (101 MHz, CDCl_3) δ 164.57, 163.95, 160.86, 156.77, 150.27, 147.86, 136.33, 135.30, 123.50, 90.36, 66.74, 51.19, 44.49, 44.15, 35.84, 31.23, 10.91, 3.51. HRMS [$\text{C}_{21}\text{H}_{28}\text{N}_6\text{O}_2 + \text{H}$] $^+$: 397.2347 calculated, 397.2345 found.

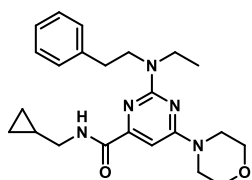


N-(Cyclopropylmethyl)-2-(methyl(2-(pyridin-2-yl)ethyl)amino)-6-morpholinopyrimidine-4-carboxamide (49). The title compound was prepared according to general procedure A using 2-chloropyrimidine **28** (30 mg, 0.10 mmol, 1 eq), *N*-methyl-2-(pyridin-2-yl)ethan-1-amine (21 μL , 0.15 mmol, 1.5 eq) and DiPEA (70 μL , 0.40 mmol, 4 eq). Total heating time: 8 h at 160 $^{\circ}\text{C}$ with μW irradiation. Column chromatography (3% \rightarrow 4% MeOH/DCM) afforded the product (26 mg, 66 μmol , 66%). TLC: $R_f = 0.3$ (3% MeOH/DCM). ^1H NMR (400 MHz, CDCl_3) δ 8.66 – 8.44 (m, 1H), 8.18 (br s, 1H), 7.58 (td, $J = 7.6, 1.7$ Hz, 1H), 7.21 – 7.03 (m, 2H), 6.72 (s, 1H), 3.99 (t, $J = 7.2$ Hz, 2H), 3.88 – 3.71 (m, 4H), 3.71 – 3.54 (m, 4H), 3.31 (t, $J = 6.4$ Hz, 2H), 3.21 – 3.03 (m, 5H), 1.16 – 1.00 (m, 1H), 0.62 – 0.43 (m, 2H), 0.29 (q, $J = 4.8$ Hz, 2H). ^{13}C NMR (101 MHz, CDCl_3) δ 164.62, 163.91, 160.79, 159.86, 156.60, 149.21,

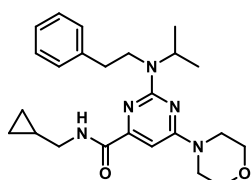
136.68, 123.60, 121.48, 90.12, 66.72, 49.98, 44.48, 44.01, 36.15, 35.62, 10.94, 3.45. HRMS [$C_{21}H_{28}N_6O_2 + H$] $^+$: 397.2347 calculated, 397.2345 found.



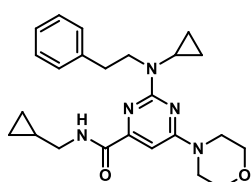
***N*-(Cyclopropylmethyl)-2-(methyl(2-(thiophen-2-yl)ethyl)amino)-6-morpholinopyrimidine-4-carboxamide (50).** The title compound was prepared according to general procedure A using 2-chloropyrimidine **28** (30 mg, 0.10 mmol, 1 eq), DiPEA (52 μ L, 0.30 mmol, 3 eq) and *N*-methyl-2-thiopheneethylamine (18 μ L, 0.13 mmol, 1.3 eq). Total heating time: 4 h at 160 $^{\circ}$ C with μ W irradiation. Column chromatography (40% \rightarrow 60% EtOAc/pentane) afforded the product (16 mg, 40 μ mol, 40%). TLC: R_f = 0.4 (50% EtOAc/pentane). 1 H NMR (400 MHz, $CDCl_3$) δ 8.04 (t, J = 5.3 Hz, 1H), 7.15 (dd, J = 5.1, 1.1 Hz, 1H), 6.94 (dd, J = 5.1, 3.4 Hz, 1H), 6.83 (d, J = 2.9 Hz, 1H), 6.73 (s, 1H), 3.88 – 3.80 (m, 2H), 3.80 – 3.72 (m, 4H), 3.71 – 3.62 (m, 4H), 3.33 – 3.26 (m, 2H), 3.20 – 3.08 (m, 5H), 1.13 – 0.99 (m, 1H), 0.60 – 0.48 (m, 2H), 0.28 (q, J = 4.7 Hz, 2H). ^{13}C NMR (101 MHz, $CDCl_3$) δ 164.62, 163.97, 160.84, 156.81, 142.18, 127.06, 125.03, 123.68, 90.26, 66.75, 51.90, 44.51, 44.13, 35.75, 27.94, 10.91, 3.55. HRMS [$C_{20}H_{27}N_5O_2S + H$] $^+$: 402.1958 calculated, 402.1956 found.



***N*-(Cyclopropylmethyl)-2-(ethyl(phenethyl)amino)-6-morpholinopyrimidine-4-carboxamide (51).** The title compound was prepared according to general procedure A using 2-chloropyrimidine **28** (28 mg, 93 μ mol, 1 eq), amine **123a** (21 mg, 0.15 mmol, 1.5 eq) and DiPEA (70 μ L, 0.40 mmol, 4 eq). Total heating time: 12 h at 160 $^{\circ}$ C with μ W irradiation. Column chromatography (20% \rightarrow 50% EtOAc/pentane) afforded the product (15 mg, 40 μ mol, 43%). TLC: R_f = 0.3 (30% EtOAc/pentane). 1 H NMR (400 MHz, $CDCl_3$) δ 8.04 (t, J = 5.9 Hz, 1H), 7.35 – 7.27 (m, 2H), 7.25 – 7.20 (m, 3H), 6.72 (s, 1H), 3.80 – 3.73 (m, 6H), 3.70 – 3.63 (m, 4H), 3.58 (q, J = 7.0 Hz, 2H), 3.30 (dd, J = 7.1, 5.8 Hz, 2H), 2.97 – 2.89 (m, 2H), 1.18 (t, J = 7.0 Hz, 3H), 1.11 – 1.01 (m, 1H), 0.59 – 0.51 (m, 2H), 0.31 – 0.25 (m, 2H). ^{13}C NMR (101 MHz, $CDCl_3$) δ 164.74, 164.12, 160.29, 156.86, 140.06, 128.83, 128.62, 126.32, 90.06, 66.78, 49.83, 44.53, 44.09, 43.04, 34.76, 13.24, 10.90, 3.44. HRMS [$C_{23}H_{31}N_5O_2 + H$] $^+$: 410.2551 calculated, 410.2549 found.

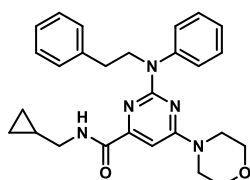


***N*-(Cyclopropylmethyl)-2-(isopropyl(phenethyl)amino)-6-morpholinopyrimidine-4-carboxamide (52).** The title compound was prepared according to general procedure A using 2-chloropyrimidine **28** (59 mg, 0.20 mmol, 1 eq), amine **123b** (50 mg, 0.30 mmol, 1.5 eq) and DiPEA (140 μ L, 0.80 mmol, 4 eq). Total heating time: 12 h at 160 $^{\circ}$ C with μ W irradiation. Column chromatography (50% \rightarrow 60% EtOAc/pentane) afforded the product (19 mg, 40 μ mol, 20%). TLC: R_f = 0.4 (50% EtOAc/pentane). 1 H NMR (400 MHz, $CDCl_3$) δ 8.05 (br s, 1H), 7.37 – 7.29 (m, 2H), 7.29 – 7.20 (m, 3H), 6.75 (s, 1H), 4.96 (hept, J = 6.8 Hz, 1H), 3.82 – 3.74 (m, 4H), 3.72 – 3.64 (m, 4H), 3.64 – 3.55 (m, 2H), 3.35 – 3.26 (m, 2H), 3.01 – 2.88 (m, 2H), 1.24 (d, J = 6.8 Hz, 6H), 1.11 – 1.00 (m, 1H), 0.60 – 0.49 (m, 2H), 0.33 – 0.23 (m, 2H). ^{13}C NMR (101 MHz, $CDCl_3$) δ 164.79, 164.06, 160.40, 156.81, 140.36, 128.68, 128.65, 126.35, 90.26, 66.77, 46.38, 44.57, 44.48, 44.17, 36.29, 20.65, 10.90, 3.51. HRMS [$C_{24}H_{33}N_5O_2 + H$] $^+$: 424.2707 calculated, 424.2705 found.

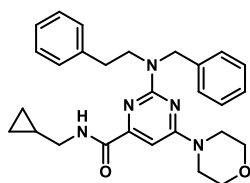


2-(Cyclopropyl(phenethyl)amino)-*N*-(cyclopropylmethyl)-6-morpholinopyrimidine-4-carboxamide (53). The title compound was prepared according to general procedure A using 2-chloropyrimidine **28** (30 mg, 0.10 mmol, 1 eq), amine **123c** (25 mg, 0.16 mmol, 1.6 eq) and DiPEA (115 μ L, 0.60 mmol, 6 eq). Total heating time: 36 h at 160 $^{\circ}$ C with μ W irradiation. Purification by HPLC (C18 reverse phase, 37% \rightarrow 47% $CH_3CN/H_2O + 0.2\%$ TFA) afforded the product (7 mg, 20 μ mol, 20%). TLC: R_f = 0.4 (40% EtOAc/pentane). 1 H NMR (400 MHz, $CDCl_3$) δ 8.17 (s, 1H), 7.34 – 7.24 (m, 3H),

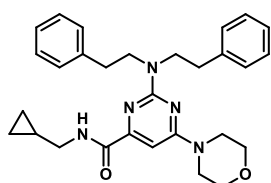
7.25 – 7.16 (m, 3H), 6.79 (s, 1H), 3.87 – 3.73 (m, 6H), 3.69 (t, $J = 4.7$ Hz, 4H), 3.30 (dd, $J = 7.1, 5.7$ Hz, 2H), 2.98 – 2.85 (m, 2H), 2.73 – 2.64 (m, 1H), 1.14 – 0.98 (m, 1H), 0.90 – 0.77 (m, 2H), 0.68 – 0.59 (m, 2H), 0.59 – 0.49 (m, 2H), 0.35 – 0.22 (m, 2H). ^{13}C NMR (101 MHz, CDCl_3) δ 164.62, 163.99, 162.12, 156.64, 140.18, 128.88, 128.59, 126.31, 91.08, 66.78, 50.52, 44.57, 44.11, 34.58, 30.41, 10.86, 8.67, 3.42. HRMS [$\text{C}_{24}\text{H}_{31}\text{N}_5\text{O}_2 + \text{H}$] $^+$: 422.2551 calculated, 422.2549 found.



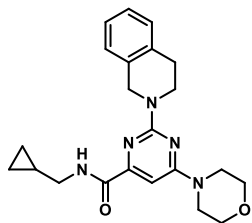
N-(Cyclopropylmethyl)-6-morpholino-2-(phenethyl(phenyl)amino)pyrimidine-4-carboxamide (54). A microwave vial with a magnetic stir bar under N_2 was charged with 2-chloropyrimidine **28** (29 mg, 98 μmol , 1 eq), amine **122** (24 mg, 0.12 mmol, 1.2 eq) and dry toluene (0.1 mL). The vial was capped and the solution purged with N_2 . This was followed by the addition of RuPhosPd G3 (0.01 M THF solution, 100 μL , 1 μmol , 0.01 eq) and NaOtBu (2 M THF solution, 60 μL , 0.12 mmol, 1.2 eq) and the mixture was purged again with N_2 and stirred in a preheated oil bath at 110 $^\circ\text{C}$. After 24 h the reaction was complete as judged by LC-MS. The mixture was filtered through a plug of Celite and the filtrate concentrated under reduced pressure to provide the crude material. Purification by HPLC (C18 reverse phase, 5% \rightarrow 50% $\text{CH}_3\text{CN}/\text{H}_2\text{O} + 0.2\%$ TFA, RT 12.0 min) afforded the product (12 mg, 26 μmol , 27%). TLC: $R_f = 0.4$ (40% EtOAc/pentane). ^1H NMR (400 MHz, CDCl_3) δ 7.79 (t, $J = 4.9$ Hz, 1H), 7.43 – 7.33 (m, 2H), 7.32 – 7.17 (m, 8H), 6.79 (s, 1H), 4.28 – 4.11 (m, 2H), 3.79 – 3.67 (m, 4H), 3.60 (t, $J = 4.8$ Hz, 4H), 3.20 (dd, $J = 7.1, 5.7$ Hz, 2H), 3.09 – 2.96 (m, 2H), 1.02 – 0.89 (m, 1H), 0.55 – 0.41 (m, 2H), 0.27 – 0.12 (m, 2H). ^{13}C NMR (101 MHz, CDCl_3) δ 164.24, 163.97, 160.50, 156.64, 144.67, 139.63, 128.84, 128.62, 127.72, 126.40, 125.73, 91.42, 66.71, 52.33, 44.51, 43.96, 34.64, 10.70, 3.34. HRMS [$\text{C}_{27}\text{H}_{31}\text{N}_5\text{O}_2 + \text{H}$] $^+$: 458.2551 calculated, 458.2547 found.



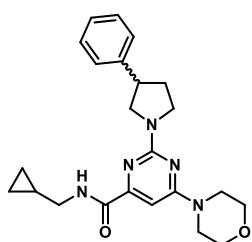
2-(Benzyl(phenethyl)amino)-N-(cyclopropylmethyl)-6-morpholinopyrimidine-4-carboxamide (55). The title compound was prepared according to general procedure A using 2-chloropyrimidine **28** (26 mg, 88 μmol , 1 eq), amine **123d** (28 mg, 0.13 mmol, 1.5 eq) and DiPEA (44 μL , 0.25 mmol, 3 eq). Total heating time: 7 d at 120 $^\circ\text{C}$. Column chromatography (30% \rightarrow 50% EtOAc/pentane) afforded the product (20 mg, 40 μmol , 45%). TLC: $R_f = 0.6$ (40% EtOAc/pentane). ^1H NMR (400 MHz, MeOD + CDCl_3) δ 7.36 – 7.04 (m, 10H), 6.67 (s, 1H), 4.74 (s, 2H), 3.91 – 3.50 (m, 10H), 3.19 (br s, 2H), 2.94 – 2.79 (m, 2H), 0.98 (br s, 1H), 0.50 (br s, 2H), 0.21 (br s, 2H). ^{13}C NMR (101 MHz, CDCl_3) δ 164.60, 164.09, 160.81, 156.93, 139.90, 139.50, 128.82, 128.62, 128.57, 127.31, 127.04, 126.34, 90.66, 66.72, 51.39, 49.88, 44.56, 44.13, 34.22, 10.84, 3.47. HRMS [$\text{C}_{28}\text{H}_{33}\text{N}_5\text{O}_2 + \text{H}$] $^+$: 472.2707 calculated, 472.2704 found.



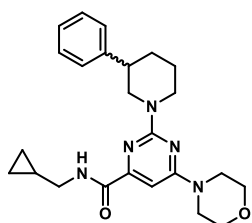
N-(Cyclopropylmethyl)-2-(diphenethylamino)-6-morpholinopyrimidine-4-carboxamide (56). The title compound was prepared according to general procedure A using 2-chloropyrimidine **28** (30 mg, 0.10 mmol, 1 eq), amine **123e** (37 mg, 0.16 mmol, 1.6 eq) and DiPEA (70 μL , 0.40 mmol, 4 eq). Total heating time: 12 h at 160 $^\circ\text{C}$ with μW irradiation. Column chromatography (20% \rightarrow 50% EtOAc/pentane) afforded the product (24 mg, 50 μmol , 50%). TLC: $R_f = 0.5$ (30% EtOAc/pentane). ^1H NMR (400 MHz, CDCl_3) δ 8.02 (t, $J = 5.8$ Hz, 1H), 7.34 – 7.26 (m, 4H), 7.24 – 7.15 (m, 6H), 6.75 (s, 1H), 3.83 – 3.60 (m, 12H), 3.30 (dd, $J = 7.1, 5.8$ Hz, 2H), 2.97 – 2.82 (m, 4H), 1.12 – 1.00 (m, 1H), 0.63 – 0.49 (m, 2H), 0.35 – 0.23 (m, 2H). ^{13}C NMR (101 MHz, CDCl_3) δ 164.66, 164.08, 160.34, 156.84, 139.91, 128.82, 128.62, 126.35, 90.34, 66.75, 50.69, 44.57, 44.23, 34.58, 10.86, 3.52. HRMS [$\text{C}_{29}\text{H}_{35}\text{N}_5\text{O}_2 + \text{H}$] $^+$: 486.2864 calculated, 486.2861 found.



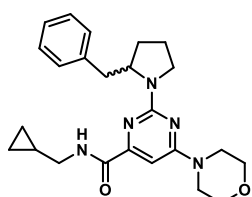
***N*-(Cyclopropylmethyl)-2-(3,4-dihydroisoquinolin-2(1H)-yl)-6-morpholinopyrimidine-4-carboxamide (57).** The title compound was prepared according to general procedure A using 2-chloropyrimidine **28** (29 mg, 97 μ mol, 1 eq), 1,2,3,4-tetrahydroisoquinoline (19 μ L, 0.15 mmol, 1.5 eq) and DiPEA (70 μ L, 0.40 mmol, 4 eq). Total heating time: 18 h at 120 $^{\circ}$ C. Column chromatography (20% \rightarrow 60% EtOAc/pentane) afforded the product (34 mg, 90 μ mol, 93%). TLC: R_f = 0.5 (50% EtOAc/pentane). ^1H NMR (400 MHz, CDCl_3) δ 8.04 (t, J = 6.0 Hz, 1H), 7.25 – 7.13 (m, 4H), 6.76 (s, 1H), 4.90 (s, 2H), 4.04 (t, J = 5.9 Hz, 2H), 3.81 – 3.62 (m, 8H), 3.36 – 3.28 (m, 2H), 2.93 (t, J = 5.8 Hz, 2H), 1.16 – 1.01 (m, 1H), 0.61 – 0.51 (m, 2H), 0.31 (dt, J = 6.1, 4.6 Hz, 2H). ^{13}C NMR (101 MHz, CDCl_3) δ 164.61, 163.99, 160.78, 156.88, 135.40, 134.49, 128.77, 126.58, 126.40, 126.23, 90.80, 66.76, 46.46, 44.54, 44.10, 41.63, 29.14, 10.99, 3.54. HRMS [$\text{C}_{22}\text{H}_{27}\text{N}_5\text{O}_2 + \text{H}$] $^+$: 394.2238 calculated, 394.2231 found.



(\pm)-*N*-(Cyclopropylmethyl)-6-morpholino-2-(3-phenylpyrrolidin-1-yl)pyrimidine-4-carboxamide (58). The title compound was prepared according to general procedure A using 2-chloropyrimidine **28** (30 mg, 0.10 mmol, 1 eq), (\pm)-3-phenylpyrrolidine (22 μ L, 0.15 mmol, 1.5 eq) and DiPEA (70 μ L, 0.40 mmol, 4 eq). Total heating time: 4 h at 160 $^{\circ}$ C with μ W irradiation. Column chromatography (30% \rightarrow 70% EtOAc/pentane) afforded the product (39 mg, 95 μ mol, 95%). TLC: R_f = 0.4 (40% EtOAc/pentane). ^1H NMR (500 MHz, CDCl_3) δ 8.09 (br s, 1H), 7.40 – 7.29 (m, 4H), 7.29 – 7.24 (m, 1H), 6.75 (s, 1H), 4.18 – 4.03 (m, 1H), 3.88 (t, J = 9.5 Hz, 1H), 3.79 – 3.71 (m, 4H), 3.71 – 3.59 (m, 5H), 3.58 – 3.51 (m, 1H), 3.51 – 3.43 (m, 1H), 3.35 – 3.20 (m, 2H), 2.43 – 2.33 (m, 1H), 2.18 – 2.06 (m, 1H), 1.13 – 0.97 (m, 1H), 0.61 – 0.44 (m, 2H), 0.34 – 0.20 (m, 2H). ^{13}C NMR (101 MHz, CDCl_3) δ 164.65, 163.89, 159.58, 156.77, 142.22, 128.70, 127.29, 126.84, 90.15, 66.73, 53.27, 46.49, 44.42, 44.19, 44.02, 33.28, 10.90, 3.49. HRMS [$\text{C}_{23}\text{H}_{29}\text{N}_5\text{O}_2 + \text{H}$] $^+$: 408.2394 calculated, 408.2391 found.

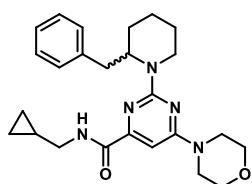


(\pm)-*N*-(Cyclopropylmethyl)-6-morpholino-2-(3-phenylpiperidin-1-yl)pyrimidine-4-carboxamide (59). The title compound was prepared according to general procedure A using 2-chloropyrimidine **28** (30 mg, 0.10 mmol, 1 eq), (\pm)-3-phenylpiperidine (24 μ L, 0.15 mmol, 1.5 eq) and DiPEA (70 μ L, 0.40 mmol, 4 eq). Total heating time: 4 h at 160 $^{\circ}$ C with μ W irradiation. Column chromatography (40% \rightarrow 70% EtOAc/pentane) afforded the product (37 mg, 88 μ mol, 88%). TLC: R_f = 0.3 (40% EtOAc/pentane). ^1H NMR (500 MHz, CDCl_3) δ 7.97 (t, J = 5.9 Hz, 1H), 7.35 (t, J = 7.5 Hz, 2H), 7.32 – 7.22 (m, 3H), 6.73 (s, 1H), 4.89 – 4.70 (m, 2H), 3.74 (t, J = 4.8 Hz, 4H), 3.69 – 3.56 (m, 4H), 3.37 – 3.16 (m, 2H), 2.97 – 2.83 (m, 2H), 2.76 (tt, J = 11.5, 3.7 Hz, 1H), 2.12 – 2.02 (m, 1H), 1.91 – 1.83 (m, 1H), 1.82 – 1.72 (m, 1H), 1.72 – 1.57 (m, 1H), 1.11 – 0.99 (m, 1H), 0.61 – 0.43 (m, 2H), 0.27 (q, J = 5.1 Hz, 2H). ^{13}C NMR (101 MHz, CDCl_3) δ 164.60, 164.07, 160.94, 156.93, 144.28, 128.65, 127.30, 126.66, 90.57, 66.71, 51.24, 44.67, 44.48, 44.04, 42.63, 32.27, 25.56, 10.94, 3.50, 3.48. HRMS [$\text{C}_{24}\text{H}_{31}\text{N}_5\text{O}_2 + \text{H}$] $^+$: 422.2551 calculated, 422.2548 found.

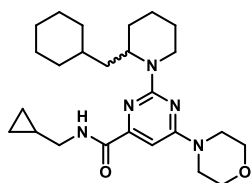


(\pm)-2-(2-Benzylpyrrolidin-1-yl)-*N*-(cyclopropylmethyl)-6-morpholinopyrimidine-4-carboxamide (60). The title compound was prepared according to general procedure A using 2-chloropyrimidine **28** (30 mg, 0.10 mmol, 1 eq), (\pm)-2-benzylpyrrolidine (24 μ L, 0.15 mmol, 1.5 eq) and DiPEA (70 μ L, 0.40 mmol, 4 eq). Total heating time: 3 d at 120 $^{\circ}$ C. Column chromatography (40% \rightarrow 60% EtOAc/pentane) afforded the product (42 mg, 0.10 mmol, 99%). TLC: R_f = 0.5 (50% EtOAc/pentane). ^1H NMR (400 MHz, CDCl_3) δ 8.11 (t, J = 5.8 Hz, 1H), 7.35 – 7.25 (m, 2H), 7.26 – 7.18 (m, 3H), 6.76 (s, 1H), 4.48 – 4.34 (m, 1H), 3.80 – 3.73 (m, 4H), 3.73 – 3.65 (m, 4H), 3.65 – 3.59 (m, 1H), 3.59 – 3.50 (m, 1H), 3.37 – 3.24 (m, 3H), 2.59 (dd, J = 13.1, 9.7 Hz, 1H), 1.91 – 1.82 (m, 4H), 1.14 – 0.98 (m, 1H), 0.65 – 0.46

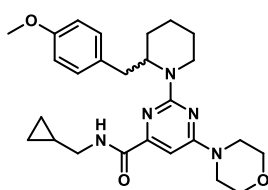
(m, 2H), 0.37 – 0.21 (m, 2H). ^{13}C NMR (101 MHz, CDCl_3) δ 164.71, 164.02, 159.56, 156.78, 139.83, 129.39, 128.49, 126.24, 90.22, 66.76, 59.06, 47.38, 44.54, 44.18, 39.30, 29.42, 23.16, 10.87, 3.51. HRMS [$\text{C}_{24}\text{H}_{31}\text{N}_5\text{O}_2 + \text{H}$] $^+$: 422.2551 calculated, 422.2549 found.



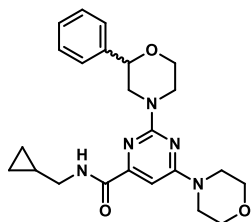
(±)-2-(2-Benzylpiperidin-1-yl)-N-(cyclopropylmethyl)-6-morpholinopyrimidine-4-carboxamide (61). The title compound was prepared according to general procedure A using 2-chloropyrimidine **28** (30 mg, 0.10 mmol, 1 eq), (±)-2-benzylpiperidine hydrochloride (52 mg, 0.24 mmol, 2.4 eq) and DiPEA (104 μL , 0.60 mmol, 6 eq). Total heating time: 6 d at 120 $^\circ\text{C}$. Column chromatography (30% \rightarrow 60% EtOAc/pentane) afforded the product (12 mg, 27 μmol , 27%). TLC: R_f = 0.4 (50% EtOAc/pentane). ^1H NMR (600 MHz, CDCl_3) δ 7.98 (t, J = 5.2 Hz, 1H), 7.26 (t, J = 7.4 Hz, 2H), 7.24 – 7.16 (m, 3H), 6.70 (s, 1H), 5.13 – 4.97 (m, 1H), 4.77 – 4.60 (m, 1H), 3.82 – 3.73 (m, 4H), 3.66 (br s, 4H), 3.40 – 3.21 (m, 2H), 3.07 – 2.98 (m, 1H), 2.95 (dd, J = 13.1, 10.0 Hz, 1H), 2.81 (dd, J = 13.1, 5.1 Hz, 1H), 1.85 – 1.73 (m, 2H), 1.73 – 1.67 (m, 2H), 1.57 – 1.46 (m, 2H), 1.13 – 1.04 (m, 1H), 0.63 – 0.53 (m, 2H), 0.31 (q, J = 4.7 Hz, 2H). ^{13}C NMR (151 MHz, CDCl_3) δ 164.75, 163.97, 160.84, 156.81, 140.16, 129.26, 128.47, 126.16, 90.34, 66.78, 52.27, 44.53, 44.24, 39.47, 35.32, 26.29, 25.82, 19.30, 10.95, 3.65, 3.61. HRMS [$\text{C}_{25}\text{H}_{33}\text{N}_5\text{O}_2 + \text{H}$] $^+$: 436.2707 calculated, 436.2706 found.



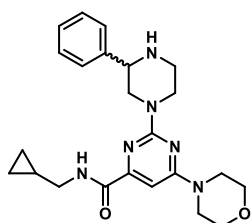
(±)-N-(Cyclopropylmethyl)-2-(2-(cyclohexylmethyl)piperidin-1-yl)-6-morpholinopyrimidine-4-carboxamide. The title compound was prepared according to general procedure A using 2-chloropyrimidine **28** (24 mg, 80 μmol , 1 eq), DiPEA (70 μL , 0.4 mmol, 5 eq) and (±)-2-(cyclohexylmethyl)piperidine (22 mg, 0.12 mmol, 1.5 eq). Total heating time: 24 h at 160 $^\circ\text{C}$ with μW irradiation. Column chromatography (10% \rightarrow 60% EtOAc/pentane) afforded the product (6 mg, 14 μmol , 18%). TLC: R_f = 0.6 (50% EtOAc/pentane). ^1H NMR (500 MHz, CDCl_3) δ 7.98 (s, 1H), 6.67 (s, 1H), 5.07 – 4.94 (m, 1H), 4.61 (dd, J = 13.8, 4.4 Hz, 1H), 3.81 – 3.70 (m, 4H), 3.70 – 3.56 (m, 4H), 3.37 – 3.17 (m, 2H), 2.90 (td, J = 13.1, 2.5 Hz, 1H), 1.80 (dd, J = 25.9, 12.9 Hz, 2H), 1.73 – 1.59 (m, 8H), 1.56 – 1.38 (m, 3H), 1.24 – 1.10 (m, 4H), 1.10 – 1.00 (m, 1H), 0.99 – 0.86 (m, 2H), 0.62 – 0.47 (m, 2H), 0.27 (q, J = 4.8 Hz, 2H). ^{13}C NMR (126 MHz, CDCl_3) δ 164.86, 164.07, 160.88, 156.90, 89.87, 66.82, 47.48, 44.55, 44.22, 38.83, 36.74, 34.55, 34.22, 33.47, 29.85, 28.23, 26.76, 26.48, 26.42, 25.94, 19.46, 10.90, 3.57, 3.54. HRMS [$\text{C}_{25}\text{H}_{39}\text{N}_5\text{O}_2 + \text{H}$] $^+$: 442.3177 calculated, 442.3174 found.



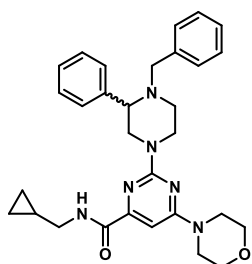
(±)-N-(Cyclopropylmethyl)-2-(2-(4-methoxybenzyl)piperidin-1-yl)-6-morpholinopyrimidine-4-carboxamide (63). The title compound was prepared according to general procedure A using 2-chloropyrimidine **28** (30 mg, 0.10 mmol, 1 eq), (±)-2-(4-methoxybenzyl)piperidine (46 mg, 0.22 mmol, 2.2 eq) and DiPEA (70 μL , 0.40 mmol, 4 eq). Total heating time: 28 h at 160 $^\circ\text{C}$ with μW irradiation. Purification by HPLC (C18 reverse phase, 5% \rightarrow 90% $\text{CH}_3\text{CN}/\text{H}_2\text{O} + 0.2\%$ TFA, RT 9.3 min) afforded the product (13 mg, 29 μmol , 29%). TLC: R_f = 0.3 (40% EtOAc/pentane). ^1H NMR (400 MHz, CDCl_3) δ 7.98 (t, J = 5.8 Hz, 1H), 7.16 – 7.10 (m, 2H), 6.85 – 6.75 (m, 2H), 6.69 (s, 1H), 5.00 (dt, J = 10.4, 4.9 Hz, 1H), 4.67 (dd, J = 13.5, 3.7 Hz, 1H), 3.84 – 3.72 (m, 7H), 3.65 (t, J = 4.8 Hz, 4H), 3.40 – 3.21 (m, 2H), 3.00 (td, J = 13.2, 2.8 Hz, 1H), 2.90 (dd, J = 13.2, 10.0 Hz, 1H), 2.74 (dd, J = 13.2, 5.1 Hz, 1H), 1.85 – 1.71 (m, 2H), 1.65 (s, 2H), 1.59 – 1.42 (m, 2H), 1.15 – 1.01 (m, 1H), 0.64 – 0.50 (m, 2H), 0.36 – 0.25 (m, 2H). ^{13}C NMR (101 MHz, CDCl_3) δ 164.78, 164.00, 160.88, 158.03, 156.84, 132.18, 130.15, 113.89, 90.31, 66.79, 55.40, 52.38, 44.54, 44.23, 39.47, 34.37, 26.18, 25.83, 19.29, 10.97, 3.65, 3.61. HRMS [$\text{C}_{26}\text{H}_{35}\text{N}_5\text{O}_3 + \text{H}$] $^+$: 466.2813 calculated, 466.2809 found.



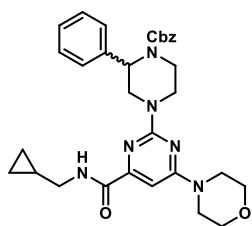
(±)-N-(Cyclopropylmethyl)-6-morpholino-2-(2-phenylmorpholino)pyrimidine-4-carboxamide (64). The title compound was prepared according to general procedure A using 2-chloropyrimidine **28** (30 mg, 0.10 mmol, 1 eq), DIPEA (52 μ L, 0.30 mmol, 3 eq) and (±)-2-phenylmorpholine (21 μ L, 0.13 mmol, 1.3 eq). Total heating time: 4 h at 160 °C with μ W irradiation. Column chromatography (40% \rightarrow 60% EtOAc/pentane) afforded the product (37 mg, 87 μ mol, 87%). TLC: R_f = 0.4 (50% EtOAc/pentane). ^1H NMR (400 MHz, CDCl_3) δ 7.92 (br s, 1H), 7.50 – 7.31 (m, 5H), 6.80 (s, 1H), 4.66 (d, J = 13.3 Hz, 1H), 4.59 – 4.48 (m, 2H), 4.20 – 4.13 (m, 1H), 3.80 (td, J = 11.8, 2.8 Hz, 1H), 3.77 – 3.70 (m, 4H), 3.70 – 3.59 (m, 4H), 3.36 – 3.22 (m, 2H), 3.22 – 3.12 (m, 1H), 2.97 (dd, J = 13.3, 10.6 Hz, 1H), 1.12 – 0.99 (m, 1H), 0.60 – 0.46 (m, 2H), 0.28 (q, J = 4.7 Hz, 2H). ^{13}C NMR (101 MHz, CDCl_3) δ 164.34, 163.92, 160.97, 156.85, 139.91, 128.62, 128.23, 126.51, 91.50, 78.26, 67.02, 66.67, 50.63, 44.47, 44.11, 43.99, 10.94, 3.53. HRMS $[\text{C}_{23}\text{H}_{29}\text{N}_5\text{O}_3 + \text{H}]^+$: 424.2343 calculated, 424.2340 found.



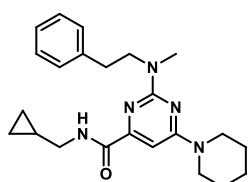
(±)-N-(Cyclopropylmethyl)-6-morpholino-2-(3-phenylpiperazin-1-yl)pyrimidine-4-carboxamide (65). A round-bottom flask was charged with Cbz-protected amine **67** (56 mg, 0.10 mmol, 1 eq) and MeOH (0.5 mL). The solution was purged with N_2 and Pd/C (10% w/w, 50 mg, 50 μ mol, 0.5 eq) was added. The mixture was purged with N_2 and then with H_2 and stirred for 2 h under an H_2 atmosphere (balloon). The mixture was filtered through a plug of Celite, washed with MeOH and the filtrate was concentrated under reduced pressure. The residue was purified by silica gel column chromatography (1% \rightarrow 4% MeOH/DCM) to afford the product (38 mg, 90 μ mol, 90%). TLC: R_f = 0.3 (2% MeOH/DCM). ^1H NMR (400 MHz, CDCl_3) δ 7.94 (t, J = 5.9 Hz, 1H), 7.51 – 7.44 (m, 2H), 7.43 – 7.30 (m, 3H), 6.76 (s, 1H), 4.69 (d, J = 12.5 Hz, 2H), 3.88 – 3.78 (m, 1H), 3.78 – 3.71 (m, 4H), 3.68 – 3.61 (m, 4H), 3.32 – 3.23 (m, 2H), 3.21 (d, J = 10.6 Hz, 1H), 3.13 – 2.94 (m, 2H), 2.90 (t, J = 11.7 Hz, 1H), 2.11 (br s, 1H), 1.09 – 1.00 (m, 1H), 0.57 – 0.47 (m, 2H), 0.30 – 0.24 (m, 2H). ^{13}C NMR (101 MHz, CDCl_3) δ 164.51, 163.99, 161.01, 156.89, 142.01, 128.73, 127.97, 127.32, 91.05, 66.72, 60.57, 51.48, 46.27, 44.49, 44.26, 44.10, 10.97, 3.55. HRMS $[\text{C}_{23}\text{H}_{30}\text{N}_6\text{O}_2 + \text{H}]^+$: 423.2503 calculated, 423.2501 found.



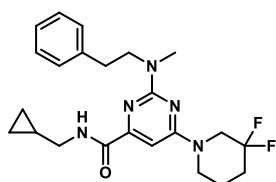
(±)-2-(4-Benzyl-3-phenylpiperazin-1-yl)-N-(cyclopropylmethyl)-6-morpholinopyrimidine-4-carboxamide (66). A round-bottom flask was charged with amine **65** (19 mg, 45 μ mol, 1 eq) in dry CH_3CN (0.5 mL). This was followed by DIPEA (16 μ L, 90 μ mol, 2 eq) and benzyl bromide (6.4 μ L, 54 μ mol, 1.2 eq). The reaction was stirred for 4 h at rt after which the solvents were concentrated under reduced pressure. The residue was purified by silica gel column chromatography (1 \rightarrow 5% MeOH/DCM) affording the product (17 mg, 33 μ mol, 73%). TLC: R_f = 0.5 (2% MeOH/DCM). ^1H NMR (400 MHz, CDCl_3) δ 7.90 (t, J = 5.7 Hz, 1H), 7.57 (d, J = 7.2 Hz, 2H), 7.41 (t, J = 7.4 Hz, 2H), 7.36 – 7.27 (m, 5H), 7.25 – 7.18 (m, 1H), 6.74 (s, 1H), 4.70 – 4.54 (m, 2H), 3.83 (d, J = 13.4 Hz, 1H), 3.77 – 3.67 (m, 4H), 3.66 – 3.54 (m, 4H), 3.35 (dd, J = 10.6, 3.1 Hz, 1H), 3.32 – 3.18 (m, 2H), 3.08 (td, J = 12.7, 2.7 Hz, 1H), 3.03 – 2.92 (m, 2H), 2.87 (d, J = 13.4 Hz, 1H), 2.17 (td, J = 11.8, 3.0 Hz, 1H), 1.09 – 0.95 (m, 1H), 0.57 – 0.44 (m, 2H), 0.25 (q, J = 4.6 Hz, 2H). ^{13}C NMR (101 MHz, CDCl_3) δ 164.48, 164.02, 160.74, 156.91, 141.70, 138.93, 128.92, 128.87, 128.29, 128.20, 127.87, 127.00, 90.97, 67.34, 66.71, 59.23, 51.90, 51.73, 44.47, 44.36, 44.08, 10.92, 3.53, 3.51. HRMS $[\text{C}_{30}\text{H}_{36}\text{N}_6\text{O}_2 + \text{H}]^+$: 513.2973 calculated, 513.2973 found.



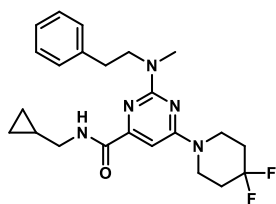
(±)-Benzyl 4-(4-((cyclopropylmethyl)carbamoyl)-6-morpholinopyrimidin-2-yl)-2-phenylpiperazine-1-carboxylate (67). The title compound was prepared according to general procedure A using 2-chloropyrimidine **28** (30 mg, 0.10 mmol, 1 eq), amine **130** (45 mg, 0.12 mmol, 1.2 eq) and DiPEA (70 μ L, 0.40 mmol, 4 eq). Total heating time: 41 h at 120 $^{\circ}$ C. Column chromatography (40% \rightarrow 70% EtOAc/pentane) afforded the product (56 mg, 0.10 mmol, 99%). TLC: R_f = 0.3 (50% EtOAc/pentane). ^1H NMR (400 MHz, CDCl_3) δ 7.90 (t, J = 5.9 Hz, 1H), 7.45 – 7.19 (m, 10H), 6.77 (s, 1H), 5.47 (br s, 1H), 5.31 – 5.12 (m, 2H), 5.04 (d, J = 13.8 Hz, 1H), 4.52 – 4.31 (m, 1H), 4.17 (d, J = 9.4 Hz, 1H), 3.75 (t, J = 4.8 Hz, 4H), 3.71 – 3.60 (m, 4H), 3.53 (d, J = 13.4 Hz, 1H), 3.29 (t, J = 6.5 Hz, 2H), 3.17 (d, J = 9.2 Hz, 2H), 1.13 – 0.97 (m, 1H), 0.61 – 0.46 (m, 2H), 0.34 – 0.21 (m, 2H). ^{13}C NMR (101 MHz, CDCl_3) δ 164.36, 163.88, 160.76, 156.82, 155.79, 139.31, 136.59, 128.68, 128.65, 128.23, 128.03, 127.44, 127.04, 91.44, 67.65, 66.70, 45.36, 44.54, 44.13, 43.82, 39.89, 10.93, 3.53. HRMS [$\text{C}_{31}\text{H}_{36}\text{N}_6\text{O}_4 + \text{H}$] $^+$: 557.2871 calculated, 557.2869 found.



N-(Cyclopropylmethyl)-2-(methyl(phenethyl)amino)-6-(piperidin-1-yl)pyrimidine-4-carboxamide (68). The title compound was prepared according to general procedure A using 2-chloropyrimidine **117k** (44 mg, 0.15 mmol, 1 eq), DiPEA (105 μ L, 0.60 mmol, 4 eq) and *N*-methylphenethylamine HBr salt (49 mg, 0.23 mmol, 1.5 eq). Total heating time: 4 h at 160 $^{\circ}$ C with μ W irradiation. Column chromatography (20% \rightarrow 50% EtOAc/pentane) afforded the product (37 mg, 94 μ mol, 63%). TLC: R_f = 0.4 (20% EtOAc/pentane). ^1H NMR (400 MHz, CDCl_3) δ 8.07 (t, J = 4.8 Hz, 1H), 7.35 – 7.16 (m, 5H), 6.76 (s, 1H), 3.84 – 3.75 (m, 2H), 3.67 (br s, 4H), 3.34 – 3.25 (m, 2H), 3.13 (s, 3H), 2.95 – 2.87 (m, 2H), 1.74 – 1.65 (m, 2H), 1.65 – 1.55 (m, 4H), 1.13 – 1.00 (m, 1H), 0.59 – 0.50 (m, 2H), 0.28 (q, J = 4.7 Hz, 2H). ^{13}C NMR (101 MHz, CDCl_3) δ 165.02, 163.41, 161.01, 156.35, 140.10, 128.88, 128.56, 126.22, 90.36, 51.80, 45.37, 44.07, 35.66, 33.94, 25.77, 24.95, 10.91, 3.48. HRMS [$\text{C}_{23}\text{H}_{31}\text{N}_5\text{O} + \text{H}$] $^+$: 394.2601 calculated, 394.2592 found.

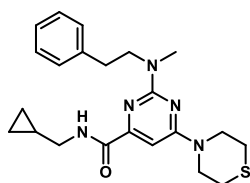


N-(Cyclopropylmethyl)-6-(3,3-difluoropiperidin-1-yl)-2-(methyl(phenethyl)amino)pyrimidine-4-carboxamide (69). The title compound was prepared according to general procedure A using 2-chloropyrimidine **117l** (50 mg, 0.15 mmol, 1 eq), DiPEA (78 μ L, 0.45 mmol, 3 eq) and *N*-methylphenethylamine (33 μ L, 0.27 mmol, 1.5 eq). Total heating time: 4 h at 160 $^{\circ}$ C with μ W irradiation. Column chromatography (10% \rightarrow 30% EtOAc/pentane) afforded the product (10 mg, 23 μ mol, 15%). TLC: R_f = 0.5 (20% EtOAc/pentane). ^1H NMR (400 MHz, CDCl_3) δ 8.02 (br s, 1H), 7.34 – 7.27 (m, 2H), 7.26 – 7.18 (m, 3H), 6.78 (s, 1H), 4.01 (t, J = 11.7 Hz, 2H), 3.86 – 3.73 (m, 2H), 3.71 – 3.58 (m, 2H), 3.35 – 3.25 (m, 2H), 3.13 (s, 3H), 2.95 – 2.86 (m, 2H), 2.17 – 2.03 (m, 2H), 1.88 – 1.78 (m, 2H), 1.12 – 1.01 (m, 1H), 0.61 – 0.50 (m, 2H), 0.29 (q, J = 4.7 Hz, 2H). ^{13}C NMR (101 MHz, CDCl_3) δ 164.61, 163.70, 160.80, 157.10, 139.92, 128.91, 128.63, 126.32, 119.79 (t, J = 244.2 Hz), 90.16, 51.89, 49.40 (t, J = 32.8 Hz), 44.14, 43.73, 35.80, 33.92, 33.03 (t, J = 23.5 Hz), 22.07 (t, J = 4.4 Hz), 10.91, 3.50. HRMS [$\text{C}_{23}\text{H}_{29}\text{F}_2\text{N}_5\text{O} + \text{H}$] $^+$: 430.2413 calculated, 430.2419 found.

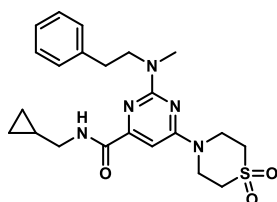


N-(Cyclopropylmethyl)-6-(4,4-difluoropiperidin-1-yl)-2-(methyl(phenethyl)amino)pyrimidine-4-carboxamide (70). The title compound was prepared according to general procedure A using 2-chloropyrimidine **117m** (45 mg, 0.14 mmol, 1 eq), DiPEA (73 μ L, 0.42 mmol, 3 eq) and *N*-methylphenethylamine (31 μ L, 0.21 mmol, 1.5 eq). Total heating time: 4 h at 160 $^{\circ}$ C with μ W irradiation. Column chromatography (5% \rightarrow 30% EtOAc/pentane) afforded the product (27 mg, 63 μ mol, 45%). TLC: R_f = 0.5 (15% EtOAc/pentane). ^1H NMR (400 MHz, CDCl_3) δ 8.03 (t, J = 5.2 Hz, 1H), 7.33 – 7.27 (m, 2H), 7.25 – 7.18 (m, 3H), 6.79 (s, 1H), 3.88 – 3.74 (m, 6H), 3.36 – 3.25 (m, 2H), 3.13 (s, 3H), 2.95 – 2.85 (m, 2H), 2.06 – 1.92 (m, 4H), 1.13 – 0.99 (m, 1H), 0.63 – 0.50 (m, 2H), 0.29 (q, J = 4.7 Hz, 2H). ^{13}C

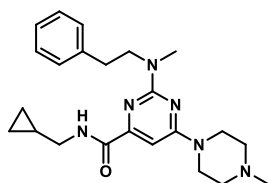
NMR (101 MHz, CDCl₃) δ 164.58, 163.23, 160.99, 157.16, 139.85, 128.83, 128.62, 126.35, 122.10 (t, J = 242.0 Hz), 90.06, 51.73, 44.13, 41.27, 35.74, 33.95, 33.84 (t, J = 23.0 Hz), 10.89, 3.49. HRMS [C₂₃H₂₉F₂N₅O + H]⁺: 430.2413 calculated, 430.2422 found.



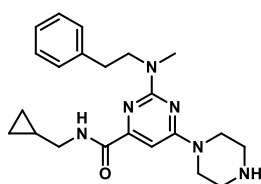
N-(Cyclopropylmethyl)-2-(methyl(phenethyl)amino)-6-thiomorpholinopyrimidine-4-carboxamide (71). The title compound was prepared according to general procedure A using 2-chloropyrimidine **117n** (41 mg, 0.13 mmol, 1 eq), DiPEA (91 μ L, 0.52 mmol, 4 eq) and *N*-methylphenethylamine HBr salt (43 mg, 0.20 mmol, 1.5 eq). Total heating time: 4 h at 160 °C with μ W irradiation. Column chromatography (10% -> 40% EtOAc/pentane) afforded the product (51 mg, 0.12 mmol, 92%). TLC: R_f = 0.4 (25% EtOAc/pentane). ¹H NMR (400 MHz, CDCl₃) δ 8.05 (br s, 1H), 7.33 – 7.27 (m, 2H), 7.25 – 7.18 (m, 3H), 6.73 (s, 1H), 4.03 (br s, 4H), 3.84 – 3.74 (m, 2H), 3.35 – 3.26 (m, 2H), 3.13 (s, 3H), 2.96 – 2.85 (m, 2H), 2.70 – 2.58 (m, 4H), 1.13 – 0.99 (m, 1H), 0.55 (q, J = 5.7 Hz, 2H), 0.29 (q, J = 4.9 Hz, 2H). ¹³C NMR (101 MHz, CDCl₃) δ 164.67, 163.05, 156.85, 139.87, 128.80, 128.58, 126.29, 90.34, 51.74, 47.24, 44.08, 35.71, 33.90, 26.68, 10.88, 3.47. HRMS [C₂₂H₂₉N₅OS + H]⁺: 412.2166 calculated, 412.2159 found.



N-(Cyclopropylmethyl)-6-(1,1-dioxidothiomorpholino)-2-(methyl(phenethyl)amino)pyrimidine-4-carboxamide (72). The title compound was prepared according to general procedure A using 2-chloropyrimidine **117o** (4:1 mixture of regioisomers) (35 mg, 0.10 mmol, 1 eq), DiPEA (70 μ L, 0.40 mmol, 4 eq) and *N*-methylphenethylamine HBr salt (32 mg, 0.15 mmol, 1.5 eq). Total heating time: 2 d at 120 °C. Column chromatography (40% -> 60% EtOAc/pentane) afforded the product (35 mg, 79 μ mol, 79%). TLC: R_f = 0.6 (60% EtOAc/pentane). ¹H NMR (400 MHz, CDCl₃) δ 7.99 (br s, 1H), 7.36 – 7.26 (m, 2H), 7.26 – 7.16 (m, 3H), 6.81 (s, 1H), 4.20 (br s, 4H), 3.83 (t, J = 7.5 Hz, 2H), 3.30 (t, J = 6.4 Hz, 2H), 3.13 (s, 3H), 3.04 (br s, 4H), 2.91 (t, J = 7.4 Hz, 2H), 1.14 – 1.00 (m, 1H), 0.66 – 0.49 (m, 2H), 0.37 – 0.24 (m, 2H). ¹³C NMR (101 MHz, CDCl₃) δ 164.04, 162.66, 160.94, 157.93, 139.56, 128.76, 128.68, 126.49, 89.88, 51.67, 51.54, 44.19, 43.04, 35.82, 33.95, 10.86, 3.50. HRMS [C₂₂H₂₉N₅O₃S + H]⁺: 444.2064 calculated, 444.2074 found.

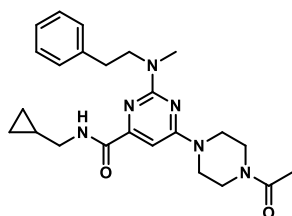


N-(Cyclopropylmethyl)-2-(methyl(phenethyl)amino)-6-(4-methylpiperazin-1-yl)pyrimidine-4-carboxamide (73). The title compound was prepared according to general procedure A using 2-chloropyrimidine **117p** (42 mg, 0.14 mmol, 1 eq), DiPEA (98 μ L, 0.56 mmol, 4 eq) and *N*-methylphenethylamine HBr salt (44 mg, 0.20 mmol, 1.5 eq). Total heating time: 45 h at 120 °C. Purification by preparative HPLC (C18 reverse phase, 25% to 35% CH₃CN/H₂O + 0.2% TFA, RT 8.98 min) afforded the product (21 mg, 51 μ mol, 36%). TLC: R_f = 0.3 (5% MeOH/DCM). ¹H NMR (400 MHz, CDCl₃) δ 8.03 (t, J = 5.4 Hz, 1H), 7.33 – 7.26 (m, 2H), 7.25 – 7.18 (m, 3H), 6.74 (s, 1H), 3.87 – 3.73 (m, 6H), 3.34 – 3.25 (m, 2H), 3.13 (s, 3H), 2.94 – 2.86 (m, 2H), 2.64 – 2.51 (m, 4H), 2.42 (s, 3H), 1.12 – 1.00 (m, 1H), 0.60 – 0.50 (m, 2H), 0.29 (q, J = 4.9 Hz, 2H). ¹³C NMR (101 MHz, CDCl₃) δ 164.70, 163.60, 160.91, 156.82, 139.95, 128.85, 128.60, 126.30, 90.22, 54.58, 51.72, 45.88, 44.12, 43.58, 35.71, 33.94, 10.89, 3.49. HRMS [C₂₃H₃₂N₆O + H]⁺: 409.2710 calculated, 409.2708 found.



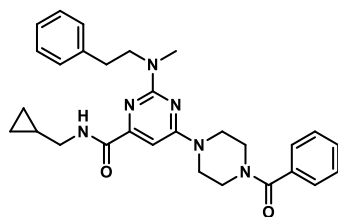
N-(Cyclopropylmethyl)-2-(methyl(phenethyl)amino)-6-(piperazin-1-yl)pyrimidine-4-carboxamide (74). A round-bottom flask was charged with Cbz-protected amine **77** (175 mg, 0.33 mmol, 1 eq), dry MeOH (3 mL) and AcOH (0.3 mL). The flask was purged with N₂, followed by addition of Pd/C (10% w/w, 18 mg, 0.02 mmol, 5 mol%) and then purging with H₂ (balloon). The reaction was stirred for 2 days, then filtered over a cellulose filter (Whatman) which was washed with MeOH. The filtrate was concentrated under reduced pressure and the residue was purified

using silica gel column chromatography (2.5% → 5% MeOH/DCM with 5% Et₃N) affording the product (82 mg, 0.21 mmol, 64%). ¹H NMR (400 MHz, CDCl₃) δ 8.05 (t, *J* = 5.5 Hz, 1H), 7.35 – 7.26 (m, 2H), 7.26 – 7.17 (m, 3H), 6.74 (s, 1H), 3.84 – 3.76 (m, 2H), 3.75 – 3.58 (m, 4H), 3.30 (t, *J* = 6.5 Hz, 2H), 3.13 (s, 3H), 2.96 – 2.85 (m, 6H), 1.96 (s, 1H), 1.13 – 1.00 (m, 1H), 0.61 – 0.47 (m, 2H), 0.28 (q, *J* = 4.7 Hz, 2H). ¹³C NMR (101 MHz, CDCl₃) δ 164.78, 163.74, 160.85, 156.51, 139.95, 128.80, 128.52, 126.20, 90.16, 51.66, 45.94, 45.26, 44.02, 35.62, 33.88, 10.84, 3.42. HRMS [C₂₂H₃₀N₆O + H]⁺: 395.2554 calculated, 395.2558 found.



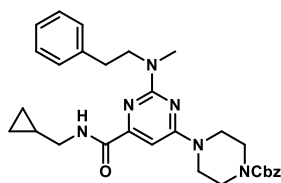
6-(4-Acetylpiperazin-1-yl)-N-(cyclopropylmethyl)-2-(methyl(phenethyl)amino)pyrimidine-4-carboxamide (75). A round-bottom flask was charged with amine **74** (22 mg, 56 μmol, 1 eq) in dry DCM (1.5 mL). This was followed by addition of DiPEA (49 μL, 0.28 mmol, 5 eq) and Ac₂O (10.5 μL, 0.11 mmol, 2 eq). The reaction was stirred for 3 h at rt after which it was diluted with EtOAc (25 mL). The organic layer was washed with sat. aq. NaHCO₃ (1 x 25 mL) and brine (1 x 25 mL), dried (MgSO₄), filtered and concentrated under reduced

pressure. The residue was purified by silica gel column chromatography (2.5% → 10% MeOH/DCM) affording the product (19 mg, 44 μmol, 79%). TLC: R_f = 0.8 (10% MeOH/DCM). ¹H NMR (400 MHz, CDCl₃) δ 8.02 (t, *J* = 5.3 Hz, 1H), 7.34 – 7.26 (m, 2H), 7.26 – 7.17 (m, 3H), 6.74 (s, 1H), 3.87 – 3.77 (m, 2H), 3.77 – 3.65 (m, 6H), 3.59 – 3.50 (m, 2H), 3.34 – 3.26 (m, 2H), 3.13 (s, 3H), 2.95 – 2.86 (m, 2H), 2.15 (s, 3H), 1.14 – 0.99 (m, 1H), 0.61 – 0.50 (m, 2H), 0.29 (q, *J* = 4.7 Hz, 2H). ¹³C NMR (101 MHz, CDCl₃) δ 169.32, 164.57, 163.63, 160.85, 156.97, 139.84, 128.82, 128.61, 126.33, 90.13, 51.70, 45.94, 44.12, 43.82, 41.12, 35.73, 33.92, 21.57, 10.87, 3.48. HRMS [C₂₄H₃₂N₆O₂ + H]⁺: 437.2660 calculated, 437.2661 found.



6-(4-Benzoylpiperazin-1-yl)-N-(cyclopropylmethyl)-2-(methyl(phenethyl)amino)pyrimidine-4-carboxamide (76). A round-bottom flask was charged with amine **74** (22 mg, 56 μmol, 1 eq) in dry DCM (1.5 mL). This was followed by Et₃N (16 μL, 0.11 mmol, 2 eq) and benzoyl chloride (8 μL, 67 μmol, 1.2 eq). The reaction was stirred for 3 h at rt after which it was diluted with EtOAc (25 mL). The organic layer was washed with sat. aq. NaHCO₃ (1 x 25 mL) and brine (1 x 25 mL), dried (Na₂SO₄), filtered and

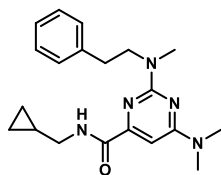
concentrated under reduced pressure. The residue was purified by silica gel column chromatography (60 → 80% EtOAc/pentane) affording the product (20 mg, 40 μmol, 71%). TLC: R_f = 0.3 (60% EtOAc/pentane). ¹H NMR (400 MHz, CDCl₃) δ 8.03 (br s, 1H), 7.49 – 7.40 (m, 5H), 7.32 – 7.25 (m, 2H), 7.25 – 7.17 (m, 3H), 6.75 (s, 1H), 3.95 – 3.74 (m, 6H), 3.66 (br s, 2H), 3.52 (br s, 2H), 3.36 – 3.25 (m, 2H), 3.12 (s, 3H), 2.94 – 2.82 (m, 2H), 1.14 – 0.99 (m, 1H), 0.63 – 0.48 (m, 2H), 0.29 (q, *J* = 4.7 Hz, 2H). ¹³C NMR (101 MHz, CDCl₃) δ 170.77, 164.61, 163.71, 160.87, 156.99, 139.85, 135.48, 130.14, 128.83, 128.76, 128.62, 128.49, 127.23, 126.34, 90.21, 51.70, 47.55, 44.16, 42.05, 35.75, 33.94, 10.88, 3.50. HRMS [C₂₉H₃₄N₆O₂ + H]⁺: 499.2816 calculated, 499.2825 found.



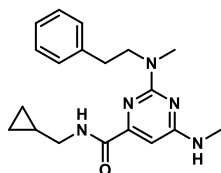
Benzyl 4-(6-((cyclopropylmethyl)carbamoyl)-2-(methyl(phenethyl)amino)pyrimidin-4-yl)piperazine-1-carboxylate (77). The title compound was prepared according to general procedure A using 2-chloropyrimidine **117q** (202 mg, 0.47 mmol, 1 eq), DiPEA (0.40 mL, 2.28 mmol, 5 eq) and *N*-methylphenethylamine HBr salt (161 mg, 0.74 mmol, 1.5 eq). Total heating time: 4 h at 160 °C with μW irradiation. Column chromatography (30% → 60%

EtOAc/pentane) afforded the product (199 mg, 0.38 mmol, 81%). TLC: R_f = 0.6 (50% EtOAc/pentane). ¹H NMR (400 MHz, CDCl₃) δ 8.02 (t, *J* = 5.4 Hz, 1H), 7.42 – 7.25 (m, 7H), 7.24 – 7.17 (m, 3H), 6.73 (s, 1H), 5.17 (s, 2H), 3.86 – 3.77 (m, 2H), 3.69 (br s, 4H), 3.62 – 3.53 (m, 4H), 3.34 – 3.26 (m, 2H), 3.12 (s, 3H), 2.94 – 2.85 (m, 2H), 1.12 – 1.00 (m, 1H), 0.61 – 0.50 (m, 2H), 0.28 (q, *J* = 4.7 Hz, 2H). ¹³C NMR (101 MHz, CDCl₃) δ 164.58, 163.64, 160.85, 156.90, 155.32, 139.84, 136.56, 128.79, 128.62, 128.56, 128.23, 128.08, 126.27, 90.16,

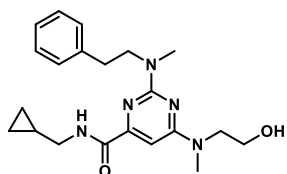
67.46, 51.66, 44.07, 43.86, 43.53, 35.67, 33.91, 10.85, 3.44. HRMS $[C_{30}H_{36}N_6O_3 + H]^+$: 529.2922 calculated, 529.2933 found.



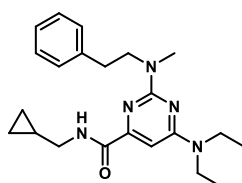
N-(Cyclopropylmethyl)-6-(dimethylamino)-2-(methyl(phenethyl)amino)pyrimidine-4-carboxamide (78). The title compound was prepared according to general procedure A using 2-chloropyrimidine **117r** (27 mg, 0.11 mmol, 1 eq), *N*-methylphenethylamine HBr salt (35 mg, 0.16 mmol, 1.6 eq) and DiPEA (92 μ L, 0.53 mmol, 5 eq). Total heating time: 8 h at 160 °C with μ W irradiation. Column chromatography (20% \rightarrow 50% EtOAc/pentane) afforded the product (32 mg, 90 μ mol, 82%). TLC: R_f = 0.6 (40% EtOAc/pentane). 1H NMR (400 MHz, $CDCl_3$) δ 8.08 (t, J = 5.8 Hz, 1H), 7.34 – 7.27 (m, 2H), 7.26 – 7.17 (m, 3H), 6.69 (s, 1H), 3.92 – 3.70 (m, 2H), 3.30 (dd, J = 7.1, 5.8 Hz, 2H), 3.23 – 3.01 (m, 9H), 3.00 – 2.80 (m, 2H), 1.17 – 0.98 (m, 1H), 0.64 – 0.46 (m, 2H), 0.36 – 0.22 (m, 2H). ^{13}C NMR (101 MHz, $CDCl_3$) δ 164.89, 164.01, 160.68, 155.88, 140.01, 128.79, 128.47, 126.12, 90.10, 51.66, 43.98, 37.16, 35.52, 33.84, 10.82, 3.39. HRMS $[C_{20}H_{27}N_5O + H]^+$: 354.2288 calculated, 354.2290 found.



N-(Cyclopropylmethyl)-2-(methyl(phenethyl)amino)-6-(methylamino)pyrimidine-4-carboxamide (79). The title compound was prepared according to general procedure A using 2-chloropyrimidine **117s** (25 mg, 0.10 mmol, 1 eq), DiPEA (52 μ L, 0.30 mmol, 3 eq) and *N*-methylphenethylamine (22 μ L, 0.15 mmol, 1.5 eq). Total heating time: 4 h at 160 °C with μ W irradiation. Column chromatography (50% \rightarrow 70% EtOAc/pentane) afforded the product (26 mg, 77 μ mol, 77%). TLC: R_f = 0.5 (50% EtOAc/pentane). 1H NMR (400 MHz, $CDCl_3$) δ 8.03 (br s, 1H), 7.33 – 7.27 (m, 2H), 7.26 – 7.18 (m, 3H), 6.54 (s, 1H), 5.13 – 4.72 (m, 1H), 3.93 – 3.66 (m, 2H), 3.34 – 3.24 (m, 2H), 3.13 (s, 3H), 2.98 (d, J = 4.9 Hz, 3H), 2.94 – 2.87 (m, 2H), 1.12 – 1.00 (m, 1H), 0.61 – 0.50 (m, 2H), 0.28 (q, J = 4.7 Hz, 2H). ^{13}C NMR (101 MHz, $CDCl_3$) δ 164.71, 161.06, 156.00, 140.05, 128.89, 128.55, 126.24, 92.54, 51.66, 44.06, 35.62, 33.93, 28.23, 10.89, 3.48. HRMS $[C_{19}H_{25}N_5O + H]^+$: 340.2132 calculated, 340.2138 found.

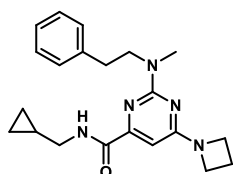


N-(Cyclopropylmethyl)-6-((2-hydroxyethyl)(methyl)amino)-2-(methyl(phenethyl)amino)pyrimidine-4-carboxamide (80). The title compound was prepared according to general procedure C using dichloropyrimidine **116a** (39 mg, 0.16 mmol, 1 eq), DiPEA (43 μ L, 0.24 mmol, 1.5 eq) and *N*-methylethanolamine (13 μ L, 0.16 mmol, 1.0 eq) in MeOH (1.6 mL), followed by concentration and addition of DiPEA (84 μ L, 0.48 mmol, 3 eq), *N*-methylphenethylamine (35 μ L, 0.24 mmol, 1.5 eq) and *n*-BuOH (0.75 mL). Total heating time: 4 h at 160 °C with μ W irradiation. Column chromatography (20% \rightarrow 40% EtOAc/pentane) afforded the product (15 mg, 33 μ mol, 21%). TLC: R_f = 0.4 (80% EtOAc/pentane). 1H NMR (400 MHz, $CDCl_3$) δ 8.02 (br s, 1H), 7.33 – 7.27 (m, 2H), 7.26 – 7.18 (m, 3H), 6.68 (s, 1H), 4.12 – 3.52 (m, 7H), 3.33 – 3.26 (m, 2H), 3.14 (s, 3H), 3.11 (s, 3H), 2.93 – 2.86 (m, 2H), 1.12 – 1.00 (m, 1H), 0.60 – 0.51 (m, 2H), 0.29 (q, J = 4.7 Hz, 2H). ^{13}C NMR (101 MHz, $CDCl_3$) δ 164.63, 160.52, 156.34, 139.80, 128.86, 128.60, 126.32, 90.28, 62.14, 52.62, 51.83, 44.12, 37.11, 35.91, 33.97, 10.86, 3.48. HRMS $[C_{21}H_{29}N_5O_2 + H]^+$: 384.2394 calculated, 384.2399 found.

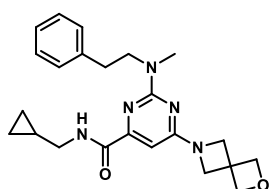


N-(Cyclopropylmethyl)-6-(diethylamino)-2-(methyl(phenethyl)amino)pyrimidine-4-carboxamide (81). The title compound was prepared according to general procedure A using 2-chloropyrimidine **177t** (37 mg, 0.13 mmol, 1 eq), DiPEA (68 μ L, 0.39 mmol, 3 eq) and *N*-methylphenethylamine (28 μ L, 0.20 mmol, 1.5 eq). Total heating time: 4 h at 160 °C with μ W irradiation. Column chromatography (20% \rightarrow 40% EtOAc/pentane) afforded the product (30 mg, 79 μ mol, 61%). TLC: R_f = 0.8 (50% EtOAc/pentane). 1H NMR (400 MHz, $CDCl_3$) δ 8.10 (br s, 1H), 7.40 – 7.14 (m, 5H), 6.65 (s, 1H), 3.92 – 3.71 (m, 2H), 3.54 (br s, 4H), 3.30 (t, J = 6.3 Hz, 2H), 3.14 (s, 3H), 3.02 – 2.85 (m, 2H), 1.20 (t, J = 6.9 Hz, 6H),

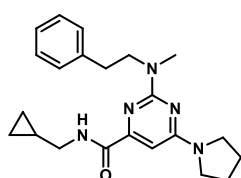
1.13 – 0.99 (m, 1H), 0.64 – 0.46 (m, 2H), 0.37 – 0.21 (m, 2H). ^{13}C NMR (101 MHz, CDCl_3) δ 165.05, 162.59, 160.96, 155.94, 140.12, 128.87, 128.55, 126.21, 90.19, 51.79, 44.03, 42.44, 35.60, 34.04, 13.26, 10.92, 3.46. HRMS [$\text{C}_{22}\text{H}_{31}\text{N}_5\text{O} + \text{H}$] $^+$: 382.2601 calculated, 382.2599 found.



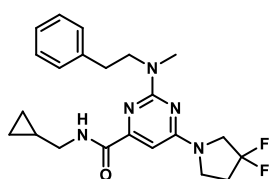
***N*-(Cyclopropylmethyl)-2-(methyl(phenethyl)amino)-6-(azetidin-1-yl)pyrimidine-4-carboxamide (82)**. The title compound was prepared according to general procedure A using 2-chloropyrimidine **117u** (27 mg, 0.10 mmol, 1 eq), DiPEA (52 μL , 0.30 mmol, 3 eq) and *N*-methylphenethylamine (22 μL , 0.15 mmol, 1.5 eq). Total heating time: 4 h at 160 $^\circ\text{C}$ with μW irradiation. Column chromatography (40% \rightarrow 60% EtOAc/pentane) afforded the product (25 mg, 68 μmol , 68%). TLC: R_f = 0.6 (50% EtOAc/pentane). ^1H NMR (400 MHz, CDCl_3) δ 8.04 (br s, 1H), 7.33 – 7.27 (m, 2H), 7.26 – 7.16 (m, 3H), 6.38 (s, 1H), 4.11 (t, J = 7.5 Hz, 4H), 3.85 – 3.71 (m, 2H), 3.35 – 3.26 (m, 2H), 3.13 (s, 3H), 2.94 – 2.84 (m, 2H), 2.40 (p, J = 7.5 Hz, 2H), 1.14 – 1.00 (m, 1H), 0.60 – 0.48 (m, 2H), 0.28 (q, J = 4.7 Hz, 2H). ^{13}C NMR (101 MHz, CDCl_3) δ 164.78, 164.75, 160.96, 155.60, 140.10, 128.90, 128.55, 126.22, 89.42, 51.73, 49.83, 44.07, 35.54, 33.88, 16.75, 10.90, 3.49. HRMS [$\text{C}_{21}\text{H}_{27}\text{N}_5\text{O} + \text{H}$] $^+$: 366.2288 calculated, 366.2296 found.



***N*-(Cyclopropylmethyl)-2-(methyl(phenethyl)amino)-6-(2-oxa-6-azaspiro[3.3]heptan-6-yl)pyrimidine-4-carboxamide (83)**. The title compound was prepared according to general procedure A using 2-chloropyrimidine **117v** (31 mg, 0.10 mmol, 1 eq), DiPEA (52 μL , 0.30 mmol, 3 eq) and *N*-methylphenethylamine (22 μL , 0.15 mmol, 1.5 eq). Total heating time: 4 h at 160 $^\circ\text{C}$ with μW irradiation. Column chromatography (70% \rightarrow 90% EtOAc/pentane) afforded the product (7 mg, 17 μmol , 17%). TLC: R_f = 0.4 (80% EtOAc/pentane). ^1H NMR (400 MHz, CDCl_3) δ 8.00 (br s, 1H), 7.35 – 7.27 (m, 2H), 7.26 – 7.19 (m, 3H), 6.39 (s, 1H), 4.85 (s, 4H), 4.24 (s, 4H), 3.84 – 3.71 (m, 2H), 3.36 – 3.22 (m, 2H), 3.12 (s, 3H), 2.94 – 2.82 (m, 2H), 1.13 – 0.98 (m, 1H), 0.60 – 0.48 (m, 2H), 0.28 (q, J = 4.7 Hz, 2H). ^{13}C NMR (101 MHz, CDCl_3) δ 164.68, 164.52, 160.91, 156.07, 139.97, 128.89, 128.62, 126.32, 89.61, 81.23, 59.40, 51.71, 44.12, 39.24, 35.61, 33.89, 10.90, 3.51. HRMS [$\text{C}_{23}\text{H}_{29}\text{N}_5\text{O}_2 + \text{H}$] $^+$: 408.2394 calculated, 408.2396 found.

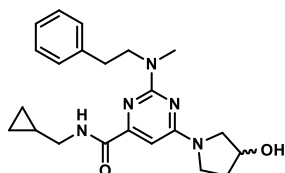


***N*-(Cyclopropylmethyl)-2-(methyl(phenethyl)amino)-6-(pyrrolidin-1-yl)pyrimidine-4-carboxamide (84)**. The title compound was prepared according to general procedure A using 2-chloropyrimidine **117w** (28 mg, 0.10 mmol, 1 eq), DiPEA (52 μL , 0.30 mmol, 3 eq) and *N*-methylphenethylamine (22 μL , 0.15 mmol, 1.5 eq). Total heating time: 4 h at 160 $^\circ\text{C}$ with μW irradiation. Column chromatography (30% \rightarrow 50% EtOAc/pentane) afforded the product (26 mg, 69 μmol , 69%). TLC: R_f = 0.7 (40% EtOAc/pentane). ^1H NMR (500 MHz, CDCl_3) δ 8.09 (t, J = 5.3 Hz, 1H), 7.33 – 7.27 (m, 2H), 7.27 – 7.18 (m, 3H), 6.54 (s, 1H), 3.89 – 3.71 (m, 2H), 3.62 (br s, 2H), 3.53 – 3.34 (m, 2H), 3.30 (dd, J = 6.9, 5.9 Hz, 2H), 3.14 (s, 3H), 2.97 – 2.85 (m, 2H), 2.15 – 1.85 (m, 4H), 1.12 – 1.01 (m, 1H), 0.63 – 0.47 (m, 2H), 0.35 – 0.22 (m, 2H). ^{13}C NMR (126 MHz, CDCl_3) δ 165.03, 161.92, 160.90, 155.49, 140.19, 128.89, 128.54, 126.18, 91.37, 51.73, 46.43, 44.05, 35.55, 33.95, 25.78, 25.01, 10.91, 3.47. HRMS [$\text{C}_{22}\text{H}_{29}\text{N}_5\text{O} + \text{H}$] $^+$: 380.2445 calculated, 380.2452 found.

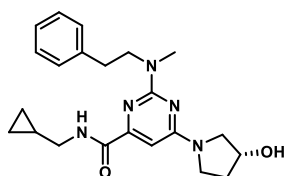


***N*-(Cyclopropylmethyl)-6-(3,3-difluoropyrrolidin-1-yl)-2-(methyl(phenethyl)amino)pyrimidine-4-carboxamide (85)**. The title compound was prepared according to general procedure A using 2-chloropyrimidine **117x** (32 mg, 0.10 mmol, 1 eq), DiPEA (52 μL , 0.30 mmol, 3 eq) and *N*-methylphenethylamine (22 μL , 0.15 mmol, 1.5 eq). Total heating time: 4 h at 160 $^\circ\text{C}$ with μW irradiation. Column chromatography (20% \rightarrow 40% EtOAc/pentane) afforded the product (34 mg, 82 μmol , 82%). TLC: R_f = 0.8 (40% EtOAc/pentane). ^1H NMR (400 MHz, CDCl_3) δ 8.03 (br s, 1H), 7.34 – 7.27 (m, 2H), 7.25 – 7.18 (m,

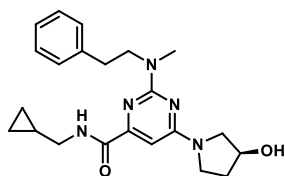
3H), 6.52 (br s, 1H), 3.89 (br s, 2H), 3.84 – 3.78 (m, 2H), 3.74 (br s, 2H), 3.37 – 3.22 (m, 2H), 3.13 (s, 3H), 2.97 – 2.83 (m, 2H), 2.56 – 2.37 (m, 2H), 1.14 – 1.00 (m, 1H), 0.64 – 0.47 (m, 2H), 0.29 (q, $J = 4.7$ Hz, 2H). ^{13}C NMR (101 MHz, CDCl_3) δ 164.50, 162.05, 160.76, 156.36, 139.91, 128.86, 128.61, 127.48 (t, $J = 247.3$ Hz), 126.31, 90.39, 53.35 (t, $J = 32.2$ Hz), 51.68, 44.12, 43.95, 35.66, 33.94 (t, $J = 22.8$ Hz), 10.88, 3.50. HRMS [$\text{C}_{22}\text{H}_{27}\text{F}_2\text{N}_5\text{O} + \text{H}$] $^+$: 416.2256 calculated, 416.2260 found.



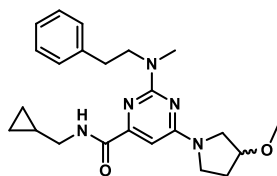
(±)-*N*-(Cyclopropylmethyl)-6-(3-hydroxypyrrolidin-1-yl)-2-(methyl(phenethyl)amino)pyrimidine-4-carboxamide (86). The title compound was prepared according to general procedure A using 2-chloropyrimidine **117y** (65 mg, 0.22 mmol, 1 eq), DiPEA (115 μL , 0.66 mmol, 3 eq) and *N*-methylphenethylamine (48 μL , 0.33 mmol, 1.5 eq). Total heating time: 4 h at 160 $^\circ\text{C}$ with μW irradiation. Column chromatography (70% \rightarrow 100% EtOAc/pentane) afforded the product (60 mg, 0.15 mmol, 68%). TLC: $R_f = 0.4$ (80% EtOAc/pentane). ^1H NMR (400 MHz, CDCl_3) δ 8.10 (t, $J = 5.2$ Hz, 1H), 7.32 – 7.26 (m, 2H), 7.25 – 7.17 (m, 3H), 6.50 (s, 1H), 4.58 (br s, 1H), 3.98 – 3.33 (m, 6H), 3.31 – 3.23 (m, 2H), 3.11 (s, 3H), 3.02 – 2.62 (m, 3H), 2.08 (br s, 2H), 1.10 – 0.98 (m, 1H), 0.63 – 0.45 (m, 2H), 0.27 (q, $J = 4.7$ Hz, 2H). ^{13}C NMR (101 MHz, CDCl_3) δ 165.08, 162.07, 160.78, 155.35, 140.10, 128.87, 128.54, 126.19, 91.26, 54.89, 51.73, 44.36, 44.10, 35.57, 33.91, 10.83, 3.48. HRMS [$\text{C}_{22}\text{H}_{29}\text{N}_5\text{O}_2 + \text{H}$] $^+$: 396.2394 calculated, 396.2400 found.



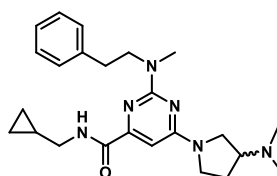
(*R*)-*N*-(Cyclopropylmethyl)-6-(3-hydroxypyrrolidin-1-yl)-2-(methyl(phenethyl)amino)pyrimidine-4-carboxamide (87). The title compound was prepared according to general procedure A using 2-chloropyrimidine **117z** (38 mg, 0.13 mmol, 1 eq), DiPEA (67 μL , 0.38 mmol, 3 eq) and *N*-methylphenethylamine (28 μL , 0.19 mmol, 1.5 eq). Total heating time: 4 h at 160 $^\circ\text{C}$ with μW irradiation. Column chromatography (80% \rightarrow 100% EtOAc/pentane) afforded the product (37 mg, 94 μmol , 72%). *ee*: >99% (as determined by chiral HPLC using 75:25 hexane/ethanol, Chiralcell OD). TLC: $R_f = 0.3$ (80% EtOAc/pentane). ^1H NMR (400 MHz, CDCl_3) δ 8.09 (br s, 1H), 7.33 – 7.27 (m, 2H), 7.26 – 7.17 (m, 3H), 6.52 (s, 1H), 4.59 (br s, 1H), 3.79 (dd, $J = 8.7, 5.8$ Hz, 2H), 3.74 – 3.37 (m, 4H), 3.33 – 3.22 (m, 2H), 3.12 (s, 3H), 2.96 – 2.82 (m, 2H), 2.70 – 2.21 (m, 1H), 2.09 (br s, 2H), 1.12 – 0.99 (m, 1H), 0.61 – 0.49 (m, 2H), 0.28 (q, $J = 4.7$ Hz, 2H). ^{13}C NMR (101 MHz, CDCl_3) δ 165.04, 162.12, 160.82, 155.49, 140.13, 128.90, 128.58, 126.22, 91.28, 70.52, 54.92, 51.75, 44.34, 44.12, 35.60, 33.93, 10.87, 3.50. HRMS [$\text{C}_{22}\text{H}_{29}\text{N}_5\text{O}_2 + \text{H}$] $^+$: 396.2394 calculated, 396.2394 found.



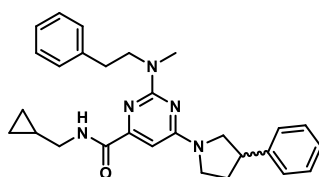
(*S*)-*N*-(Cyclopropylmethyl)-6-(3-hydroxypyrrolidin-1-yl)-2-(methyl(phenethyl)amino)pyrimidine-4-carboxamide (88). The title compound was prepared according to general procedure A using 2-chloropyrimidine **117aa** (36 mg, 0.12 mmol, 1 eq), DiPEA (63 μL , 0.36 mmol, 3 eq) and *N*-methylphenethylamine (27 μL , 0.18 mmol, 1.5 eq). Total heating time: 4 h at 160 $^\circ\text{C}$ with μW irradiation. Column chromatography (80% \rightarrow 100% EtOAc/pentane) afforded the product (36 mg, 91 μmol , 76%). *ee*: 97% (as determined by chiral HPLC using 75:25 hexane/ethanol, Chiralcell OD). TLC: $R_f = 0.3$ (80% EtOAc/pentane). ^1H NMR (400 MHz, CDCl_3) δ 8.10 (t, $J = 5.1$ Hz, 1H), 7.35 – 7.27 (m, 2H), 7.25 – 7.15 (m, 3H), 6.51 (s, 1H), 4.58 (br s, 1H), 3.82 – 3.74 (m, 2H), 3.74 – 3.35 (m, 4H), 3.32 – 3.22 (m, 2H), 3.12 (s, 3H), 2.94 – 2.84 (m, 2H), 2.80 – 2.48 (m, 1H), 2.08 (br s, 2H), 1.12 – 0.98 (m, 1H), 0.60 – 0.48 (m, 2H), 0.27 (q, $J = 4.7$ Hz, 2H). ^{13}C NMR (101 MHz, CDCl_3) δ 165.07, 162.07, 160.77, 155.36, 140.10, 128.88, 128.55, 126.20, 91.26, 70.88, 70.32, 54.89, 51.74, 44.35, 44.11, 35.58, 33.91, 10.83, 3.48. HRMS [$\text{C}_{22}\text{H}_{29}\text{N}_5\text{O}_2 + \text{H}$] $^+$: 396.2394 calculated, 396.2398 found.



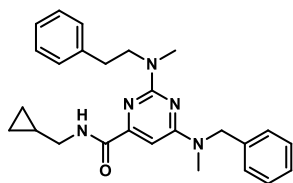
(±)-N-(Cyclopropylmethyl)-6-(3-methoxypyrrolidin-1-yl)-2-(methyl(phenethyl)amino)pyrimidine-4-carboxamide (89). A round-bottom flask was charged with alcohol **86** (35 mg, 88 μmol , 1 eq) in dry DMF (0.5 mL) and cooled to 0 °C. NaH (60% in mineral oil, 4 mg, 106 μmol , 1.2 eq) was added and the mixture was stirred for 15 min followed by addition of methyl iodide (6.0 μL , 97 μmol , 1.1 eq). The reaction was allowed to warm to rt while stirring overnight. The reaction was quenched with H₂O (20 mL) followed by extraction with DCM (3 x 20 mL), drying (Na₂SO₄), filtering and concentration under reduced pressure. The residue was purified by silica gel column chromatography (60 → 70% EtOAc/pentane) affording the product (16 mg, 39 μmol , 44%). TLC: R_f = 0.4 (60% EtOAc/pentane). ¹H NMR (400 MHz, CDCl₃) δ 8.07 (br s, 1H), 7.33 – 7.27 (m, 2H), 7.26 – 7.17 (m, 3H), 6.54 (s, 1H), 4.07 (br s, 1H), 3.88 – 3.72 (m, 3H), 3.72 – 3.45 (m, 3H), 3.37 (s, 3H), 3.33 – 3.23 (m, 2H), 3.13 (s, 3H), 2.98 – 2.84 (m, 2H), 2.29 – 1.96 (m, 2H), 1.14 – 0.99 (m, 1H), 0.62 – 0.48 (m, 2H), 0.29 (q, *J* = 4.7 Hz, 2H). ¹³C NMR (101 MHz, CDCl₃) δ 207.96, 164.96, 162.10, 160.86, 155.62, 140.16, 128.91, 128.57, 126.22, 91.25, 79.95, 79.15, 56.76, 51.75, 51.42, 44.42, 44.09, 35.62, 33.94, 30.45, 10.91, 3.50. HRMS [C₂₃H₃₁N₅O₂ + H]⁺: 410.2551 calculated, 410.2549 found.



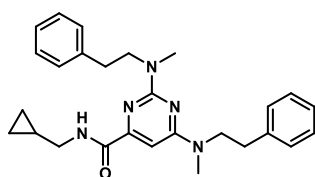
(±)-N-(Cyclopropylmethyl)-6-(3-(dimethylamino)pyrrolidin-1-yl)-2-(methyl(phenethyl)amino)pyrimidine-4-carboxamide (90). The title compound was prepared according to general procedure A using 2-chloropyrimidine **117ab** (50 mg, 0.15 mmol, 1 eq), DiPEA (78 μL , 0.60 mmol, 4 eq) and *N*-methylphenethylamine (33 μL , 0.23 mmol, 1.5 eq). Total heating time: 4 h at 160 °C with μW irradiation. Column chromatography (2.5% → 10% MeOH/DCM) afforded the product (3 mg, 7 μmol , 5%). TLC: R_f = 0.5 (5% MeOH/DCM). ¹H NMR (600 MHz, CDCl₃) δ 8.10 (br s, 1H), 7.31 – 7.27 (m, 2H), 7.24 – 7.18 (m, 3H), 6.69 (s, 1H), 3.98 (dd, *J* = 10.6, 7.2 Hz, 1H), 3.92 – 3.64 (m, 3H), 3.58 – 3.50 (m, 1H), 3.42 (br s, 1H), 3.35 – 3.25 (m, 2H), 2.99 (br s, 3H), 2.89 (t, *J* = 7.7 Hz, 2H), 2.41 (br s, 6H), 2.24 (br s, 1H), 2.06 – 1.89 (m, 1H), 1.80 – 1.51 (m, 1H), 1.12 – 1.02 (m, 1H), 0.59 – 0.49 (m, 2H), 0.34 – 0.24 (m, 2H). ¹³C NMR (151 MHz, CDCl₃) δ 164.89, 163.37, 159.54, 156.17, 128.99, 128.68, 126.44, 90.62, 65.56, 51.98, 45.61, 44.02, 33.80, 28.71, 11.00, 3.52. HRMS [C₂₄H₃₄N₆O + H]⁺: 423.2867 calculated, 423.2868 found.



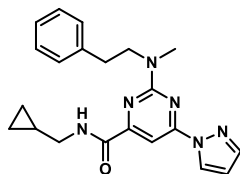
(±)-N-(Cyclopropylmethyl)-2-(methyl(phenethyl)amino)-6-(3-phenylpyrrolidin-1-yl)pyrimidine-4-carboxamide (91). The title compound was prepared according to general procedure C using dichloropyrimidine **116a** (40 mg, 0.16 mmol, 1 eq), DiPEA (43 μL , 0.24 mmol, 1.5 eq) and (±)-3-phenylpyrrolidine (24 μL , 0.16 mmol, 1.0 eq) in MeOH (1.6 mL), followed by concentration and addition of DiPEA (84 μL , 0.48 mmol, 3 eq), *N*-methylphenethylamine (35 μL , 0.24 mmol, 1.5 eq) and *n*-BuOH (0.75 mL). Total heating time: 4 h at 160 °C with μW irradiation. Column chromatography (70% → 90% EtOAc/pentane) afforded the product (35 mg, 91 μmol , 57%). TLC: R_f = 0.4 (30% EtOAc/pentane). ¹H NMR (400 MHz, CDCl₃) δ 8.08 (br s, 1H), 7.39 – 7.32 (m, 2H), 7.32 – 7.17 (m, 8H), 6.57 (s, 1H), 4.19 (br s, 1H), 3.94 (br s, 1H), 3.81 (br s, 2H), 3.74 – 3.38 (m, 3H), 3.30 (t, *J* = 6.4 Hz, 2H), 3.14 (s, 3H), 2.92 (br s, 2H), 2.42 (br s, 1H), 2.16 (br s, 1H), 1.14 – 1.00 (m, 1H), 0.62 – 0.46 (m, 2H), 0.29 (q, *J* = 4.9 Hz, 2H). ¹³C NMR (101 MHz, CDCl₃) δ 164.96, 161.90, 160.92, 155.72, 141.79, 140.15, 128.92, 128.80, 128.57, 127.19, 126.97, 126.23, 91.13, 52.89, 51.76, 46.36, 44.10, 43.39, 35.62, 33.98, 33.31, 10.93, 3.51. HRMS [C₂₈H₃₃N₅O + H]⁺: 456.2758 calculated, 456.2757 found.



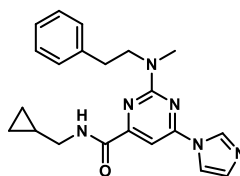
***N*-(Cyclopropylmethyl)-2-(methyl(phenethyl)amino)-6-(benzyl(methyl)amino)pyrimidine-4-carboxamide (92).** The title compound was prepared according to general procedure C using dichloropyrimidine **116a** (37 mg, 0.15 mmol, 1 eq), DiPEA (39 μ L, 0.23 mmol, 1.5 eq) and *N*-methylbenzylamine (19 μ L, 0.15 mmol, 1.0 eq) in MeOH (1.5 mL), followed by concentration and addition of DiPEA (78 μ L, 0.45 mmol, 3 eq), *N*-methylphenethylamine (33 μ L, 0.23 mmol, 1.5 eq) and *n*-BuOH (0.75 mL). Total heating time: 4 h at 160 $^{\circ}$ C with μ W irradiation. Purification by HPLC (C18 reverse phase, 43% to 49% CH₃CN/H₂O + 0.2% TFA) afforded the product (47 mg, 0.11 mmol, 73%). TLC: R_f = 0.6 (40% EtOAc/pentane). ¹H NMR (400 MHz, CDCl₃) δ 8.08 (br s, 1H), 7.36 – 7.28 (m, 2H), 7.28 – 7.03 (m, 8H), 6.75 (br s, 1H), 4.86 (br s, 2H), 3.77 (br s, 2H), 3.39 – 3.22 (m, 2H), 3.13 (s, 3H), 3.08 (br s, 2H), 2.86 (br s, 2H), 1.14 – 0.98 (m, 1H), 0.62 – 0.48 (m, 2H), 0.29 (q, J = 4.8 Hz, 2H). ¹³C NMR (101 MHz, CDCl₃) δ 164.88, 164.13, 160.83, 156.51, 139.96, 128.89, 128.74, 128.57, 127.24, 126.24, 90.07, 51.85, 44.14, 35.75, 33.95, 10.94, 3.52. HRMS [C₂₆H₃₁N₅O + H]⁺: 430.2601 calculated, 430.2604 found.



***N*-(Cyclopropylmethyl)-2,6-bis(methyl(phenethyl)amino)pyrimidine-4-carboxamide (93).** The title compound was prepared according to general procedure A using dichloropyrimidine **116a** (28 mg, 0.11 mmol, 1 eq), DiPEA (79 μ L, 0.46 mmol, 4 eq) and *N*-methylphenethylamine (41 μ L, 0.28 mmol, 2.5 eq). Total heating time: 4 h at 160 $^{\circ}$ C with μ W irradiation. Column chromatography (20% -> 40% EtOAc/pentane) afforded the product (30 mg, 68 μ mol, 62%). TLC: R_f = 0.6 (30% EtOAc/pentane). ¹H NMR (400 MHz, CDCl₃) δ 8.09 (t, J = 5.2 Hz, 1H), 7.32 – 7.24 (m, 4H), 7.24 – 7.12 (m, 6H), 6.68 (br s, 1H), 4.02 – 3.56 (m, 4H), 3.34 – 3.26 (m, 2H), 3.15 (s, 3H), 2.99 (br s, 3H), 2.96 – 2.87 (m, 4H), 1.15 – 1.01 (m, 1H), 0.60 – 0.48 (m, 2H), 0.29 (q, J = 4.8 Hz, 2H). ¹³C NMR (101 MHz, CDCl₃) δ 164.96, 163.42, 160.86, 156.14, 140.03, 128.97, 128.90, 128.68, 128.60, 126.43, 126.25, 90.24, 51.72, 44.09, 35.71, 34.01, 33.85, 10.93, 3.50. HRMS [C₂₇H₃₃N₅O + H]⁺: 444.2758 calculated, 444.2765 found.

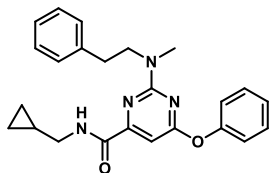


***N*-(Cyclopropylmethyl)-2-(methyl(phenethyl)amino)-6-(1H-pyrazol-1-yl)pyrimidine-4-carboxamide (94).** The title compound was prepared according to general procedure A using 2-chloropyrimidine **117ac** (28 mg, 0.10 mmol, 1 eq), DiPEA (52 μ L, 0.30 mmol, 3 eq) and *N*-methylphenethylamine (22 μ L, 0.15 mmol, 1.5 eq). Total heating time: 4 h at 160 $^{\circ}$ C with μ W irradiation. Column chromatography (20% -> 40% EtOAc/pentane) afforded the product (30 mg, 80 μ mol, 80%). TLC: R_f = 0.5 (30% EtOAc/pentane). ¹H NMR (400 MHz, CDCl₃) δ 8.51 (s, 1H), 7.98 – 7.81 (m, 2H), 7.81 – 7.73 (m, 1H), 7.33 – 7.27 (m, 2H), 7.26 – 7.18 (m, 3H), 6.56 – 6.39 (m, 1H), 3.97 – 3.83 (m, 2H), 3.33 (dd, J = 6.9, 6.0 Hz, 2H), 3.21 (s, 3H), 3.01 – 2.91 (m, 2H), 1.18 – 1.00 (m, 1H), 0.57 (q, J = 5.4 Hz, 2H), 0.30 (q, J = 4.8 Hz, 2H). ¹³C NMR (101 MHz, CDCl₃) δ 163.17, 160.57, 159.73, 159.48, 143.40, 139.40, 128.84, 128.69, 127.30, 126.52, 108.54, 94.69, 51.83, 44.24, 36.01, 33.79, 10.87, 3.52. HRMS [C₂₁H₂₄N₆O + H]⁺: 377.2084 calculated, 377.2088 found.

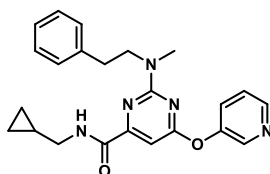


***N*-(Cyclopropylmethyl)-6-(1H-imidazol-1-yl)-2-(methyl(phenethyl)amino)pyrimidine-4-carboxamide (95).** The title compound was prepared according to general procedure A using 2-chloropyrimidine **117ad** (42 mg, 0.15 mmol, 1 eq), DiPEA (78 μ L, 0.45 mmol, 3 eq) and *N*-methylphenethylamine (33 μ L, 0.23 mmol, 1.5 eq). Total heating time: 4 h at 160 $^{\circ}$ C with μ W irradiation. Purification by preparative HPLC (C18 reverse phase, 35% to 45% CH₃CN/H₂O + 0.2% TFA, RT 8.87 min) afforded the product (27 mg, 72 μ mol, 48%). TLC: R_f = 0.5 (5% MeOH/DCM). ¹H NMR (400 MHz, CDCl₃) δ 8.46 (s, 1H), 7.99 – 7.72 (m, 1H), 7.68 (s, 1H), 7.33 – 7.27 (m, 3H), 7.25 – 7.17 (m, 4H), 4.00 – 3.81 (m, 2H), 3.38 – 3.29 (m, 2H), 3.22 (s, 3H), 3.02 – 2.90 (m, 2H), 1.16 – 1.03 (m,

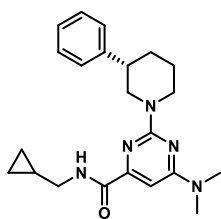
1H), 0.69 – 0.51 (m, 2H), 0.32 (q, $J = 4.9$ Hz, 2H). ^{13}C NMR (101 MHz, CDCl_3) δ 162.88, 160.89, 160.19, 157.03, 139.14, 135.37, 131.10, 128.82, 128.73, 126.61, 116.00, 93.80, 51.89, 44.36, 36.06, 33.78, 10.84, 3.56. HRMS $[\text{C}_{21}\text{H}_{24}\text{N}_6\text{O} + \text{H}]^+$: 377.2084 calculated, 377.2087 found.



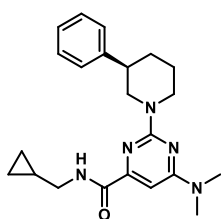
***N*-(Cyclopropylmethyl)-2-(methyl(phenethyl)amino)-6-phenoxy pyrimidine-4-carboxamide (96)**. The title compound was prepared according to general procedure A using 2-chloropyrimidine **117ae** (49 mg, 0.16 mmol, 1 eq), DiPEA (84 μL , 0.48 mmol, 3 eq) and *N*-methylphenethylamine (35 μL , 0.24 mmol, 1.5 eq). Total heating time: 4 h at 160 $^\circ\text{C}$ with μW irradiation. Column chromatography (5% \rightarrow 25% EtOAc/pentane) afforded the product (40 mg, 99 μmol , 62%). TLC: $R_f = 0.5$ (20% EtOAc/pentane). ^1H NMR (400 MHz, CDCl_3) δ 7.91 (br s, 1H), 7.46 – 7.36 (m, 2H), 7.35 – 7.05 (m, 7H), 7.04 – 6.68 (m, 2H), 4.00 – 3.39 (m, 2H), 3.30 (t, $J = 6.4$ Hz, 2H), 3.10 (br s, 3H), 2.97 – 2.53 (m, 2H), 1.13 – 1.01 (m, 1H), 0.56 (q, $J = 5.6$ Hz, 2H), 0.35 – 0.23 (m, 2H). ^{13}C NMR (101 MHz, CDCl_3) δ 171.62, 163.46, 160.96, 159.59, 152.85, 139.32, 129.64, 128.89, 128.50, 126.33, 125.47, 122.04, 51.85, 44.18, 35.78, 33.63, 10.88, 3.51. HRMS $[\text{C}_{24}\text{H}_{26}\text{N}_4\text{O}_2 + \text{H}]^+$: 403.2129 calculated, 403.2137 found.



***N*-(Cyclopropylmethyl)-2-(methyl(phenethyl)amino)-6-(pyridin-3-yloxy) pyrimidine-4-carboxamide (97)**. The title compound was prepared according to general procedure A using 2-chloropyrimidine **117af** (38 mg, 0.12 mmol, 1 eq), DiPEA (62 μL , 0.36 mmol, 3 eq) and *N*-methylphenethylamine (26 μL , 0.18 mmol, 1.5 eq). Total heating time: 4 h at 160 $^\circ\text{C}$ with μW irradiation. Column chromatography (60% \rightarrow 100% EtOAc/pentane) afforded the product (26 mg, 64 μmol , 53%). TLC: $R_f = 0.5$ (80% EtOAc/pentane). ^1H NMR (400 MHz, CDCl_3) δ 8.66 – 8.42 (m, 2H), 7.90 (br s, 1H), 7.65 – 7.44 (m, 1H), 7.41 – 7.32 (m, 1H), 7.31 – 7.12 (m, 4H), 7.07 – 6.71 (m, 2H), 3.82 (br s, 1H), 3.51 (br s, 1H), 3.38 – 3.26 (m, 2H), 3.13 (br s, 2H), 2.93 (br s, 2H), 2.65 (br s, 1H), 1.15 – 1.02 (m, 1H), 0.57 (q, $J = 5.1$ Hz, 2H), 0.30 (q, $J = 4.8$ Hz, 2H). ^{13}C NMR (101 MHz, CDCl_3) δ 170.88, 163.22, 160.69, 160.01, 149.45, 146.41, 144.26, 129.68, 128.80, 128.56, 126.44, 123.96, 51.74, 44.23, 35.78, 33.59, 10.88, 3.53. HRMS $[\text{C}_{23}\text{H}_{25}\text{N}_5\text{O}_2 + \text{H}]^+$: 404.2081 calculated, 404.2088 found.

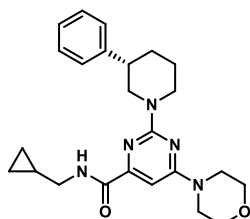


(*S*)-*N*-(Cyclopropylmethyl)-6-(dimethylamino)-2-(3-phenylpiperidin-1-yl)pyrimidine-4-carboxamide (98). The title compound was prepared according to general procedure A using 2-chloropyrimidine **117r** (25 mg, 0.10 mmol, 1 eq), DiPEA (52 μL , 0.30 mmol, 3 eq) and (*S*)-3-phenylpiperidine (21 mg, 0.13 mmol, 1.3 eq). Total heating time: 4 h at 160 $^\circ\text{C}$ with μW irradiation. Column chromatography (30% \rightarrow 50% EtOAc/pentane) afforded the product (28 mg, 74 μmol , 74%). *ee*: >99% (as determined by chiral HPLC using 70:30 hexane/isopropanol, Chiralcell OD). TLC: $R_f = 0.7$ (50% EtOAc/pentane). ^1H NMR (400 MHz, CDCl_3) δ 8.02 (br s, 1H), 7.43 – 7.16 (m, 5H), 6.70 (s, 1H), 4.84 (t, $J = 14.1$ Hz, 2H), 3.39 – 3.19 (m, 2H), 3.10 (s, 6H), 2.89 (t, $J = 12.1$ Hz, 2H), 2.77 (t, $J = 10.2$ Hz, 1H), 2.07 (d, $J = 13.1$ Hz, 1H), 1.88 – 1.60 (m, 3H), 1.14 – 0.98 (m, 1H), 0.63 – 0.44 (m, 2H), 0.36 – 0.20 (m, 2H). ^{13}C NMR (101 MHz, CDCl_3) δ 164.91, 164.18, 160.89, 156.13, 144.43, 128.61, 127.31, 126.58, 90.71, 51.38, 44.70, 44.02, 42.56, 37.30, 32.21, 25.58, 10.96, 3.51, 3.49. HRMS $[\text{C}_{22}\text{H}_{29}\text{N}_5\text{O} + \text{H}]^+$: 380.2445 calculated, 380.2452 found.

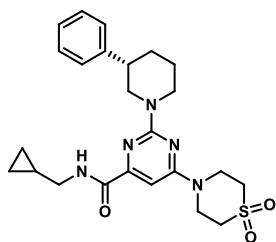


(*R*)-*N*-(Cyclopropylmethyl)-6-(dimethylamino)-2-(3-phenylpiperidin-1-yl)pyrimidine-4-carboxamide (99). The title compound was prepared according to general procedure A using 2-chloropyrimidine **117r** (25 mg, 0.10 mmol, 1 eq), DiPEA (52 μL , 0.30 mmol, 3 eq) and (*R*)-3-phenylpiperidine (21 mg, 0.13 mmol, 1.3 eq). Total heating time: 4 h at 160 $^\circ\text{C}$ with μW irradiation. Column chromatography (30% \rightarrow 50% EtOAc/pentane) afforded the product (32 mg, 84 μmol , 84%). *ee*: >97% (as determined by chiral HPLC using 70:30 hexane/isopropanol, Chiralcell OD). TLC: $R_f = 0.7$ (50%

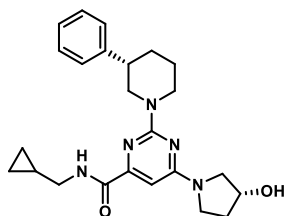
EtOAc/pentane). ^1H NMR (400 MHz, CDCl_3) δ 8.01 (t, $J = 5.4$ Hz, 1H), 7.39 – 7.28 (m, 4H), 7.28 – 7.21 (m, 1H), 6.70 (s, 1H), 4.95 – 4.74 (m, 2H), 3.40 – 3.18 (m, 2H), 3.10 (s, 6H), 2.96 – 2.83 (m, 2H), 2.83 – 2.70 (m, 1H), 2.07 (d, $J = 13.9$ Hz, 1H), 1.90 – 1.81 (m, 1H), 1.81 – 1.62 (m, 2H), 1.11 – 0.99 (m, 1H), 0.59 – 0.46 (m, 2H), 0.27 (q, $J = 4.7$ Hz, 2H). ^{13}C NMR (101 MHz, CDCl_3) δ 164.91, 164.18, 160.90, 156.12, 144.43, 128.61, 127.31, 126.58, 90.71, 51.38, 44.70, 44.02, 42.56, 37.30, 32.21, 25.58, 10.96, 3.51, 3.49. HRMS [$\text{C}_{22}\text{H}_{29}\text{N}_5\text{O} + \text{H}$] $^+$: 380.2445 calculated, 380.2452 found.



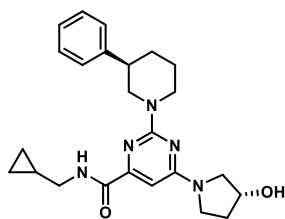
(S)-N-(Cyclopropylmethyl)-6-morpholino-2-(3-phenylpiperidin-1-yl)pyrimidine-4-carboxamide (100). The title compound was prepared according to general procedure A using 2-chloropyrimidine **28** (30 mg, 0.10 mmol, 1 eq), DiPEA (52 μL , 0.30 mmol, 3 eq) and (*S*)-3-phenylpiperidine (21 mg, 0.13 mmol, 1.3 eq). Total heating time: 4 h at 160 $^\circ\text{C}$ with μW irradiation. Column chromatography (40% \rightarrow 60% EtOAc/pentane) afforded the product (41 mg, 97 μmol , 97%). TLC: $R_f = 0.6$ (50% EtOAc/pentane). ^1H NMR (500 MHz, CDCl_3) δ 7.97 (br s, 1H), 7.40 – 7.32 (m, 2H), 7.32 – 7.21 (m, 3H), 6.73 (s, 1H), 4.90 – 4.70 (m, 2H), 3.83 – 3.70 (m, 4H), 3.69 – 3.56 (m, 4H), 3.36 – 3.19 (m, 2H), 2.97 – 2.83 (m, 2H), 2.76 (tt, $J = 11.5, 3.6$ Hz, 1H), 2.13 – 2.02 (m, 1H), 1.90 – 1.72 (m, 2H), 1.72 – 1.59 (m, 1H), 1.12 – 0.98 (m, 1H), 0.59 – 0.45 (m, 2H), 0.27 (q, $J = 4.7$ Hz, 2H). ^{13}C NMR (126 MHz, CDCl_3) δ 164.63, 164.11, 160.97, 156.96, 144.30, 128.66, 127.30, 126.67, 90.60, 66.73, 51.27, 44.71, 44.52, 44.06, 42.64, 32.28, 25.57, 10.94, 3.50, 3.48. HRMS [$\text{C}_{24}\text{H}_{31}\text{N}_5\text{O}_2 + \text{H}$] $^+$: 422.2551 calculated, 422.2549 found.



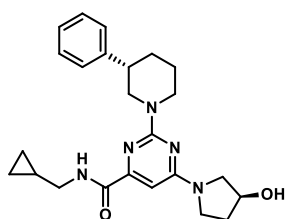
(S)-N-(Cyclopropylmethyl)-6-(1,1-dioxothiomorpholino)-2-(3-phenylpiperidin-1-yl)pyrimidine-4-carboxamide (101). The title compound was prepared according to general procedure A using 2-chloropyrimidine **117o** (4:1 mixture of regioisomers) (35 mg, 0.10 mmol, 1 eq), DiPEA (53 μL , 0.30 mmol, 3 eq) and (*S*)-3-phenylpiperidine (21 mg, 0.13 mmol, 1.3 eq). Total heating time: 4 h at 160 $^\circ\text{C}$ with μW irradiation. Purification by preparative HPLC (C18 reverse phase, 45% to 55% $\text{CH}_3\text{CN}/\text{H}_2\text{O} + 0.2\%$ TFA, RT 12.52 min) afforded the product (27 mg, 57 μmol , 57%). TLC: $R_f = 0.5$ (60% EtOAc/pentane). ^1H NMR (500 MHz, CDCl_3) δ 7.94 (br s, 1H), 7.43 – 7.32 (m, 2H), 7.32 – 7.27 (m, 3H), 6.83 (s, 1H), 4.78 (t, $J = 11.0$ Hz, 2H), 4.19 (br s, 4H), 3.38 – 3.19 (m, 2H), 3.12 – 2.99 (m, 4H), 2.94 (t, $J = 12.2$ Hz, 2H), 2.82 – 2.68 (m, 1H), 2.10 (dd, $J = 17.2, 4.5$ Hz, 1H), 1.88 (d, $J = 13.1$ Hz, 1H), 1.85 – 1.72 (m, 1H), 1.72 – 1.57 (m, 1H), 1.11 – 0.96 (m, 1H), 0.54 (q, $J = 5.3$ Hz, 2H), 0.28 (q, $J = 4.9$ Hz, 2H). ^{13}C NMR (126 MHz, CDCl_3) δ 164.07, 162.85, 160.95, 158.16, 143.95, 128.77, 127.24, 126.85, 90.31, 51.54, 51.28, 44.77, 44.14, 43.08, 42.71, 32.18, 25.50, 10.92, 3.52, 3.50. HRMS [$\text{C}_{24}\text{H}_{31}\text{N}_5\text{O}_3\text{S} + \text{H}$] $^+$: 470.2220 calculated, 470.2223 found.



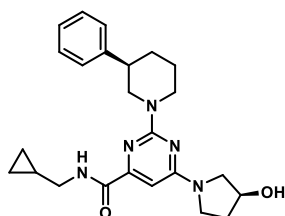
N-(Cyclopropylmethyl)-6-((R)-3-hydroxypyrrolidin-1-yl)-2-((S)-3-phenylpiperidin-1-yl)pyrimidine-4-carboxamide (102, LEI-401) The title compound was prepared according to general procedure A using 2-chloropyrimidine **117z** (24 mg, 81 μmol , 1 eq), DiPEA (42 μL , 0.24 mmol, 3 eq) and (*S*)-3-phenylpiperidine (17 mg, 0.11 mmol, 1.3 eq). Total heating time: 4 h at 160 $^\circ\text{C}$ with μW irradiation. Column chromatography (70% \rightarrow 90% EtOAc/pentane) afforded the product (23 mg, 55 μmol , 68%). TLC: $R_f = 0.4$ (80% EtOAc/pentane). ^1H NMR (400 MHz, CDCl_3) δ 8.02 (br s, 1H), 7.39 – 7.22 (m, 5H), 6.54 (s, 1H), 4.84 (t, $J = 14.0$ Hz, 2H), 4.57 (s, 1H), 3.86 – 3.37 (m, 4H), 3.37 – 3.17 (m, 2H), 2.87 (t, $J = 12.0$ Hz, 2H), 2.81 – 2.70 (m, 1H), 2.16 – 1.93 (m, 3H), 1.90 – 1.54 (m, 4H), 1.11 – 0.97 (m, 1H), 0.59 – 0.45 (m, 2H), 0.27 (q, $J = 4.7$ Hz, 2H). ^{13}C NMR (101 MHz, CDCl_3) δ 164.93, 162.20, 160.91, 155.71, 144.42, 128.64, 127.33, 126.60, 91.76, 54.96, 51.30, 44.67, 44.38, 44.07, 42.59, 32.24, 25.59, 10.93, 3.52. HRMS [$\text{C}_{24}\text{H}_{31}\text{N}_5\text{O}_2 + \text{H}$] $^+$: 422.2551 calculated, 422.2551 found.



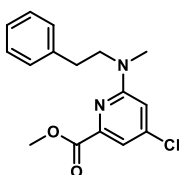
***N*-(Cyclopropylmethyl)-6-((*R*)-3-hydroxypyrrolidin-1-yl)-2-((*R*)-3-phenylpiperidin-1-yl)pyrimidine-4-carboxamide (103).** The title compound was prepared according to general procedure A using 2-chloropyrimidine **117z** (22 mg, 74 μ mol, 1 eq), DiPEA (39 μ L, 0.22 mmol, 3 eq) and (*R*)-3-phenylpiperidine (16 mg, 96 μ mol, 1.3 eq). Total heating time: 4 h at 160 $^{\circ}$ C with μ W irradiation. Column chromatography (70% \rightarrow 90% EtOAc/pentane) afforded the product (23 mg, 55 μ mol, 74%). TLC: R_f = 0.4 (80% EtOAc/pentane). ^1H NMR (400 MHz, CDCl_3) δ 8.03 (t, J = 5.7 Hz, 1H), 7.40 – 7.19 (m, 5H), 6.53 (s, 1H), 4.84 (t, J = 14.3 Hz, 2H), 4.57 (s, 1H), 3.90 – 3.37 (m, 4H), 3.37 – 3.17 (m, 2H), 2.94 – 2.81 (m, 2H), 2.81 – 2.69 (m, 1H), 2.56 (s, 1H), 2.07 (d, J = 12.7 Hz, 3H), 1.89 – 1.57 (m, 4H), 1.10 – 0.98 (m, 1H), 0.60 – 0.42 (m, 2H), 0.26 (q, J = 4.7 Hz, 2H). ^{13}C NMR (101 MHz, CDCl_3) δ 164.96, 162.19, 160.91, 155.67, 144.43, 128.62, 127.32, 126.59, 91.75, 70.36, 54.95, 51.36, 44.68, 44.38, 44.06, 42.54, 32.20, 25.60, 10.92, 3.51. HRMS [$\text{C}_{24}\text{H}_{31}\text{N}_5\text{O}_2 + \text{H}$] $^+$: 422.2551 calculated, 422.2552 found.



***N*-(Cyclopropylmethyl)-6-((*S*)-3-hydroxypyrrolidin-1-yl)-2-((*S*)-3-phenylpiperidin-1-yl)pyrimidine-4-carboxamide (104).** The title compound was prepared according to general procedure A using 2-chloropyrimidine **117aa** (37 mg, 0.12 mmol, 1 eq), DiPEA (65 μ L, 0.37 mmol, 3 eq) and (*S*)-3-phenylpiperidine (26 mg, 0.16 mmol, 1.3 eq). Total heating time: 4 h at 160 $^{\circ}$ C with μ W irradiation. Column chromatography (70% \rightarrow 100% EtOAc/pentane) afforded the product (26 mg, 62 μ mol, 52%). TLC: R_f = 0.4 (80% EtOAc/pentane). ^1H NMR (400 MHz, CDCl_3) δ 8.03 (br s, 1H), 7.40 – 7.20 (m, 5H), 6.53 (s, 1H), 4.84 (t, J = 14.3 Hz, 2H), 4.57 (s, 1H), 3.91 – 3.37 (m, 4H), 3.36 – 3.18 (m, 2H), 2.96 – 2.81 (m, 2H), 2.81 – 2.70 (m, 1H), 2.17 – 1.94 (m, 3H), 1.93 – 1.50 (m, 4H), 1.11 – 0.97 (m, 1H), 0.59 – 0.43 (m, 2H), 0.26 (q, J = 4.7 Hz, 2H). ^{13}C NMR (101 MHz, CDCl_3) δ 164.97, 162.17, 160.90, 155.63, 144.41, 128.62, 127.31, 126.58, 91.75, 71.02, 70.38, 54.95, 51.36, 44.68, 44.39, 44.05, 42.53, 32.19, 25.59, 10.91, 3.50. HRMS [$\text{C}_{24}\text{H}_{31}\text{N}_5\text{O}_2 + \text{H}$] $^+$: 422.2551 calculated, 422.2555 found.

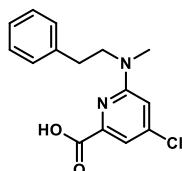


***N*-(Cyclopropylmethyl)-6-((*S*)-3-hydroxypyrrolidin-1-yl)-2-((*R*)-3-phenylpiperidin-1-yl)pyrimidine-4-carboxamide (105).** The title compound was prepared according to general procedure A using 2-chloropyrimidine **117aa** (32 mg, 0.11 mmol, 1 eq), DiPEA (56 μ L, 0.32 mmol, 3 eq) and (*R*)-3-phenylpiperidine (23 mg, 0.14 mmol, 1.3 eq). Total heating time: 4 h at 160 $^{\circ}$ C with μ W irradiation. Column chromatography (70% \rightarrow 100% EtOAc/pentane) afforded the product (26 mg, 56 μ mol, 51%). TLC: R_f = 0.4 (80% EtOAc/pentane). ^1H NMR (400 MHz, CDCl_3) δ 8.03 (t, J = 5.7 Hz, 1H), 7.40 – 7.19 (m, 5H), 6.53 (s, 1H), 4.84 (t, J = 14.3 Hz, 2H), 4.57 (s, 1H), 3.90 – 3.37 (m, 4H), 3.37 – 3.17 (m, 2H), 2.94 – 2.81 (m, 2H), 2.81 – 2.69 (m, 1H), 2.16 – 1.96 (m, 3H), 1.89 – 1.57 (m, 4H), 1.10 – 0.98 (m, 1H), 0.60 – 0.42 (m, 2H), 0.26 (q, J = 4.7 Hz, 2H). ^{13}C NMR (101 MHz, CDCl_3) δ 164.84, 162.10, 160.81, 155.58, 144.32, 128.52, 127.22, 126.48, 91.64, 70.84, 70.16, 54.84, 51.19, 44.55, 44.27, 43.95, 42.47, 32.13, 25.48, 10.82, 3.40. HRMS [$\text{C}_{24}\text{H}_{31}\text{N}_5\text{O}_2 + \text{H}$] $^+$: 422.2551 calculated, 422.2552 found.

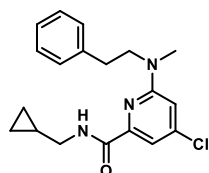


Methyl 4-chloro-6-(methyl(phenethyl)amino)picolinate (107). A round-bottom flask was charged with methyl 4,6-dichloropicolinate (**106**) (206 mg, 0.99 mmol, 1 eq), *N*-methylphenethylamine HBr salt (218 mg, 1.01 mmol, 1.02 eq), DiPEA (436 μ L, 2.5 mmol, 2.5 eq) and dry MeOH (2 mL). The solution was stirred at rt for 3 d and then refluxed for 24 h. The reaction mixture was concentrated under reduced pressure and the residue was purified by silica gel column chromatography (5% \rightarrow 35% EtOAc/pentane) affording the product (122 mg, 0.40 mmol, 40%). TLC: R_f = 0.2 (5% EtOAc/pentane). ^1H NMR

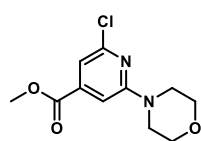
(400 MHz, CDCl₃) δ 7.35 – 7.26 (m, 3H), 7.23 (t, J = 7.3 Hz, 1H), 7.16 (d, J = 7.0 Hz, 2H), 6.56 (d, J = 2.3 Hz, 1H), 3.96 (s, 3H), 3.63 (t, J = 7.3 Hz, 2H), 2.93 – 2.81 (m, 5H). ¹³C NMR (101 MHz, CDCl₃) δ 165.68, 155.45, 152.41, 147.85, 138.19, 128.84, 128.80, 126.84, 107.83, 107.79, 53.84, 53.05, 38.50, 33.14. Regioselectivity was confirmed by ¹H, ¹³C-HMBC and ¹H-NOESY 2D NMR. HRMS [C₁₆H₁₇ClN₂O₂ + H]⁺: 305.1051 calculated, 305.1054 found.



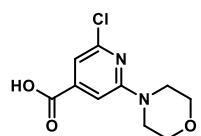
4-Chloro-6-(methyl(phenethyl)amino)picolinic acid (108). A round-bottom flask was charged with methyl ester **107** (122 mg, 0.4 mmol, 1 eq) and THF (2 mL). An aqueous 1.5 M NaOH solution (0.53 mL, 0.8 mmol, 2 eq) was added dropwise and the reaction was stirred for 1.5 h at rt. The mixture was cooled to 0 °C and acidified to pH 1 by dropwise addition of 37% w/w aq. HCl. The mixture was then extracted with DCM (3 x 5 mL), the combined organic layers washed with brine (1 x 15 mL), dried (MgSO₄), filtered and concentrated under reduced pressure to afford the product (104 mg, 0.36 mmol, 90%). TLC R_f = 0.1 (5% MeOH/DCM with 3 drops of AcOH). ¹H NMR (400 MHz, CDCl₃) δ 8.92 (br s, 1H), 7.37 – 7.20 (m, 4H), 7.20 – 7.12 (m, 2H), 6.57 (d, J = 2.4 Hz, 1H), 3.66 (t, J = 7.2 Hz, 2H), 2.96 – 2.81 (m, 5H). ¹³C NMR (101 MHz, CDCl₃) δ 164.25, 156.33, 150.90, 146.25, 138.01, 128.96, 128.86, 127.01, 108.27, 105.87, 54.04, 38.78, 33.21.



4-Chloro-N-(cyclopropylmethyl)-6-(methyl(phenethyl)amino)picolinamide (109). A round-bottom flask was charged with carboxylic acid **108** (104 mg, 0.36 mmol, 1 eq), HOBt (73 mg, 0.47 mmol, 1.3 eq), EDC hydrochloride (102 mg, 0.53 mmol, 1.5 eq) and dry DCM (1.8 mL). The suspension was stirred for 1 h at rt followed by the addition of cyclopropylmethanamine (37 μ L, 0.43 mmol, 1.2 eq). After stirring for 20 h the solvent was removed under reduced pressure and the residue was dissolved in EtOAc (10 mL) and washed with 1 M aq. HCl (1 x 10 mL), sat. aq. NaHCO₃ (1 x 10 mL) and brine (1 x 10 mL). The organic layer was dried (MgSO₄), filtered and concentrated under reduced pressure. The crude material was purified by silica gel column chromatography (isocratic, 30% EtOAc/pentane) affording the product (30 mg, 87 μ mol, 24%), R_f = 0.35 (30% EtOAc/pentane). ¹H NMR (400 MHz, CDCl₃) δ 7.99 (t, J = 5.9 Hz, 1H), 7.43 (d, J = 2.4 Hz, 1H), 7.35 – 7.26 (m, 2H), 7.28 – 7.18 (m, 1H), 7.20 – 7.15 (m, 2H), 6.50 (d, J = 2.4 Hz, 1H), 3.64 (t, J = 7.3 Hz, 2H), 3.30 (dd, J = 7.1, 5.9 Hz, 2H), 2.91 – 2.84 (m, 5H), 1.13 – 1.01 (m, 1H), 0.58 – 0.52 (m, 2H), 0.31 – 0.26 (m, 2H). ¹³C NMR (101 MHz, CDCl₃) δ 163.90, 155.94, 151.08, 150.38, 138.41, 128.93, 128.90, 126.86, 106.84, 104.87, 54.02, 44.51, 38.71, 33.25, 10.92, 3.76.

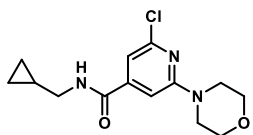


Methyl 2-chloro-6-morpholinoisonicotinate (111). A round-bottom flask was charged with methyl-2,6-dichloroisonicotinate (**110**) (0.41 g, 2.0 mmol, 1 eq), K₂CO₃ (0.55 g, 4.0 mmol, 2 eq) morpholine (0.26 mL, 3.0 mmol, 1.5 eq) and dry CH₃CN (10 mL). The mixture was heated to reflux. After 45 h the reaction was complete as judged by TLC and cooled to room temperature. The mixture was filtered and the filtrate concentrated under reduced pressure. The crude material was purified by silica gel column chromatography (10% -> 30% EtOAc/pentane) affording the product (0.32 g, 1.3 mmol, 65%). TLC: R_f = 0.6 (30% EtOAc/pentane). ¹H NMR (400 MHz, CDCl₃) δ 7.13 (d, J = 0.9 Hz, 1H), 7.07 (d, J = 1.0 Hz, 1H), 3.92 (s, 3H), 3.86 – 3.76 (m, 4H), 3.64 – 3.52 (m, 4H). ¹³C NMR (101 MHz, CDCl₃) δ 165.16, 159.40, 150.36, 141.33, 111.77, 104.69, 66.55, 52.83, 45.26. HRMS [C₁₁H₁₃ClN₂O₃ + H]⁺: 257.0688 calculated, 257.0690 found.

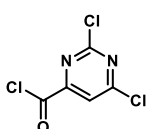


2-Chloro-6-morpholinoisonicotinic acid (112). A round-bottom flask was charged with methyl ester **111** (0.32 g, 1.3 mmol, 1 eq) and THF (5 mL). A 1 M aqueous solution of NaOH (2.5 mL, 2.5 mmol, 2 eq) was added dropwise. After stirring 20 minutes at room temperature the reaction mixture was acidified carefully with 37% w/w HCl to pH 1 and THF was removed under reduced pressure. The mixture was extracted with DCM (3 x 10 mL), the combined organic layers were washed with brine (1 x 15 mL), dried (MgSO₄), filtered and concentrated under reduced pressure affording the product (0.33 g, 1.3 mmol, 99%). TLC: R_f = 0.2

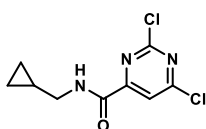
(30% EtOAc/pentane with 3 drops of AcOH). ^1H NMR (400 MHz, MeOD + CDCl_3) δ 7.12 (s, 1H), 7.09 (s, 1H), 3.78 (t, J = 4.9 Hz, 4H), 3.54 (t, J = 4.9 Hz, 4H). ^{13}C NMR (101 MHz, MeOD + CDCl_3) δ 167.10, 160.29, 150.79, 143.21, 112.56, 105.74, 67.18, 45.94. HRMS [$\text{C}_{10}\text{H}_{11}\text{ClN}_2\text{O}_3 + \text{H}$] $^+$: 243.0531 calculated, 243.0533 found.



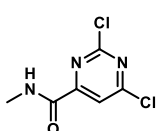
2-Chloro-*N*-(cyclopropylmethyl)-6-morpholinoisonicotinamide (113). A round-bottom flask was charged with carboxylic acid **112** (0.33 g, 1.3 mmol, 1 eq), EDC hydrochloride (0.30 g, 2.0 mmol, 1.5 eq) and HOBT (0.30 g, 2.0 mmol, 1.5 eq) and dry DCM (7 mL). The suspension was stirred for 1 h at room temperature followed by addition of cyclopropylmethanamine (0.14 mL, 1.6 mmol, 1.2 eq). After 20 h DCM was removed under reduced pressure and the residue was dissolved in EtOAc (15 mL) and sequentially washed with 1M HCl (aq) (2 x 15 mL), sat. aq. NaHCO_3 (2 x 15 mL) and brine (1 x 20 mL). The organic layer was dried (MgSO_4), filtered and concentrated under reduced pressure. The resulting crude material was purified by silica gel column chromatography (30% -> 60% EtOAc/pentane) affording the product (0.30 g, 1.0 mmol, 77%). TLC: R_f = 0.3 (40% EtOAc/pentane). ^1H NMR (400 MHz, CDCl_3) δ 6.91 (s, 1H), 6.81 (s, 1H), 6.45 – 6.31 (m, 1H), 3.84 – 3.73 (m, 4H), 3.66 – 3.51 (m, 4H), 3.28 (dd, J = 7.2, 5.4 Hz, 2H), 1.12 – 0.98 (m, 1H), 0.64 – 0.52 (m, 2H), 0.38 – 0.21 (m, 2H). ^{13}C NMR (101 MHz, CDCl_3) δ 165.28, 159.52, 150.25, 146.27, 109.10, 103.25, 66.61, 45.27, 45.25, 10.68, 3.73. HRMS [$\text{C}_{14}\text{H}_{18}\text{ClN}_3\text{O}_2 + \text{H}$] $^+$: 296.1160 calculated, 296.1158 found.



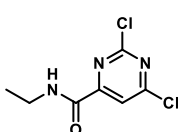
2,6-Dichloropyrimidine-4-carbonyl chloride (115). In a 500 mL round-bottom flask orotic acid (**114**) (15.6 g, 100 mmol, 1 equiv.) was dissolved in phosphorous oxychloride (46 mL, 500 mmol, 5 equiv.) and 10 drops of DMF were added. The mixture was heated to reflux and stirred for 19 h. *n*-Hexane (250 mL) was added and the mixture was stirred vigorously for 10 min and then transferred to a separatory funnel containing 100 mL H_2O . The flask was washed with 50 mL hexane. After shaking, the aqueous layer was removed and the organic layer was washed with brine (1 x 100 mL), dried (MgSO_4) and concentrated under reduced pressure to yield the product (12.8 g, 60.4 mmol, 60%). ^1H NMR (500 MHz, CDCl_3) δ 8.00 (s, 1H). ^{13}C NMR (126 MHz, CDCl_3) δ 167.17, 165.27, 161.56, 158.19, 119.70.



2,6-Dichloro-*N*-(cyclopropylmethyl)pyrimidine-4-carboxamide (116a). The title compound was prepared according to general procedure D using 2,6-dichloropyrimidine-4-carbonyl chloride **115** (0.63 mL, 5.0 mmol, 1 eq), Et_3N (0.91 mL, 6.5 mmol, 1.3 eq) and cyclopropylmethanamine (444 μL , 5.13 mmol, 1.025 eq). Column chromatography (5% -> 20% EtOAc/pentane) afforded the product (0.99 g, 4.0 mmol, 80%). TLC: R_f = 0.8 (20% EtOAc/pentane). ^1H NMR (400 MHz, CDCl_3) δ 8.11 (s, 1H), 7.96 (br s, 1H), 3.44 – 3.27 (m, 2H), 1.20 – 1.03 (m, 1H), 0.68 – 0.52 (m, 2H), 0.32 (q, J = 4.8 Hz, 2H). ^{13}C NMR (101 MHz, CDCl_3) δ 164.74, 160.44, 160.04, 159.77, 118.22, 44.72, 10.57, 3.67. HRMS [$\text{C}_9\text{H}_9\text{Cl}_2\text{N}_3\text{O} + \text{H}$] $^+$: 246.0195 calculated, 246.0196 found.

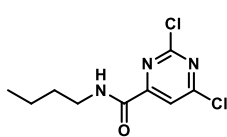


2,6-Dichloro-*N*-methylpyrimidine-4-carboxamide (116b). The title compound was prepared according to general procedure D using 2,6-dichloropyrimidine-4-carbonyl chloride **115** (0.63 mL, 5.0 mmol, 1 eq), Et_3N (1.6 mL, 11.5 mmol, 2.3 eq) and methylamine HCl salt (0.35 g, 5.13 mmol, 1.025 eq). Column chromatography (10% -> 30% EtOAc/pentane) afforded the product (0.97 g, 4.7 mmol, 94%). TLC: R_f = 0.3 (20% EtOAc/pentane). ^1H NMR (400 MHz, CDCl_3) δ 8.10 (s, 1H), 7.90 (br s, 1H), 3.08 (d, J = 5.1 Hz, 3H). ^{13}C NMR (101 MHz, CDCl_3) δ 164.84, 160.85, 160.25, 159.82, 118.11, 26.51. HRMS [$\text{C}_6\text{H}_5\text{Cl}_2\text{N}_3\text{O} + \text{H}$] $^+$: 205.9882 calculated, 205.9884 found.

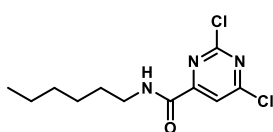


2,6-Dichloro-*N*-ethylpyrimidine-4-carboxamide (116c). The title compound was prepared according to general procedure D using 2,6-dichloropyrimidine-4-carbonyl chloride **115** (0.63 mL, 5.0 mmol, 1 eq), Et_3N (1.6 mL, 11.5 mmol, 2.3 eq) and ethylamine HCl salt (0.42 g, 5.13 mmol, 1.025 eq). Column chromatography (5% -> 20% EtOAc/pentane) afforded the product (0.88 g, 4.0 mmol, 80%). TLC: R_f = 0.6 (20% EtOAc/pentane). ^1H NMR

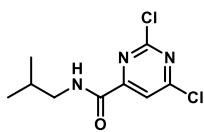
(400 MHz, CDCl₃) δ 8.10 (s, 1H), 7.83 (br s, 1H), 3.65 – 3.38 (m, 2H), 1.30 (t, *J* = 7.3 Hz, 3H). ¹³C NMR (101 MHz, CDCl₃) δ 164.84, 160.47, 160.06, 159.83, 118.18, 34.86, 14.63. HRMS [C₇H₇Cl₂N₃O + H]⁺: 220.0039 calculated, 220.0040 found.



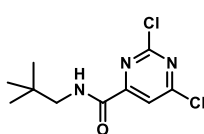
2,6-Dichloro-*N*-butylpyrimidine-4-carboxamide (116d). The title compound was prepared according to general procedure D using 2,6-dichloropyrimidine-4-carbonyl chloride **115** (0.25 mL, 2.0 mmol, 1 eq), Et₃N (0.36 mL, 2.60 mmol, 1.3 eq) and *n*-butylamine (0.20 mL, 2.05 mmol, 1.025 eq). Column chromatography (5% → 20% EtOAc/pentane) afforded the product (0.50 g, 2.0 mmol, 99%). TLC: R_f = 0.7 (20% EtOAc/pentane). ¹H NMR (400 MHz, CDCl₃) δ 8.10 (s, 1H), 7.85 (br s, 1H), 3.49 (q, *J* = 7.0 Hz, 2H), 1.74 – 1.56 (m, 2H), 1.53 – 1.35 (m, 2H), 0.97 (t, *J* = 7.4 Hz, 3H). ¹³C NMR (101 MHz, CDCl₃) δ 164.78, 160.46, 160.13, 159.78, 118.18, 39.64, 31.40, 20.09, 13.72. HRMS [C₉H₁₁Cl₂N₃O + H]⁺: 248.0352 calculated, 248.0354 found.



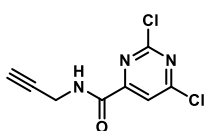
2,6-Dichloro-*N*-hexylpyrimidine-4-carboxamide (116e). The title compound was prepared according to general procedure D using 2,6-dichloropyrimidine-4-carbonyl chloride **115** (0.25 mL, 2.0 mmol, 1 eq), Et₃N (0.36 mL, 2.6 mmol, 1.3 eq) and *n*-hexylamine (0.27 mL, 2.05 mmol, 1.025 eq). Column chromatography (5% → 20% EtOAc/pentane) afforded the product (0.58 g, 2.0 mmol, 99%). TLC: R_f = 0.6 (10% EtOAc/pentane). ¹H NMR (400 MHz, CDCl₃) δ 8.10 (s, 1H), 7.89 (br s, 1H), 3.48 (q, *J* = 7.0 Hz, 2H), 1.66 (p, *J* = 7.8, 7.4 Hz, 2H), 1.46 – 1.23 (m, 6H), 0.98 – 0.83 (m, 3H). ¹³C NMR (101 MHz, CDCl₃) δ 164.71, 160.46, 160.06, 159.73, 118.14, 39.91, 31.38, 29.30, 26.55, 22.48, 13.96. HRMS [C₁₁H₁₅Cl₂N₃O + H]⁺: 276.0665 calculated, 276.0668 found.



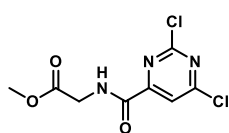
2,6-Dichloro-*N*-isobutylpyrimidine-4-carboxamide (116f). The title compound was prepared according to general procedure D using 2,6-dichloropyrimidine-4-carbonyl chloride **115** (0.25 mL, 2.0 mmol, 1 eq), Et₃N (0.36 mL, 2.60 mmol, 1.3 eq) and isobutylamine (0.20 mL, 2.05 mmol, 1.025 eq). Column chromatography (5% → 20% EtOAc/pentane) afforded the product (0.50 g, 2.0 mmol, 99%). TLC: R_f = 0.8 (20% EtOAc/pentane). ¹H NMR (400 MHz, CDCl₃) δ 8.11 (s, 1H), 7.94 (br s, 1H), 3.33 (t, *J* = 6.6 Hz, 2H), 2.07 – 1.87 (m, 1H), 1.00 (d, *J* = 6.8 Hz, 6H). ¹³C NMR (101 MHz, CDCl₃) δ 164.68, 160.41, 160.15, 159.70, 118.17, 47.10, 28.52, 20.07. HRMS [C₉H₁₁Cl₂N₃O + H]⁺: 248.0352 calculated, 248.0354 found.



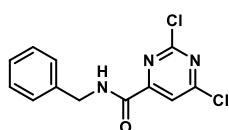
2,6-Dichloro-*N*-neopentylpyrimidine-4-carboxamide (116g). The title compound was prepared according to general procedure D using 2,6-dichloropyrimidine-4-carbonyl chloride **115** (0.25 mL, 2.0 mmol, 1 eq), Et₃N (0.36 mL, 2.6 mmol, 1.3 eq) and neopentylamine (0.24 mL, 2.05 mmol, 1.025 eq). Column chromatography (5% → 20% EtOAc/pentane) afforded the product (0.58 g, 2.0 mmol, 99%). TLC: R_f = 0.9 (20% EtOAc/pentane). ¹H NMR (400 MHz, CDCl₃) δ 8.11 (s, 1H), 7.91 (br s, 1H), 3.30 (d, *J* = 6.7 Hz, 2H), 1.01 (s, 9H). ¹³C NMR (101 MHz, CDCl₃) δ 164.69, 160.38, 160.22, 159.71, 118.24, 50.89, 32.35, 27.20. HRMS [C₁₀H₁₃Cl₂N₃O + H]⁺: 262.0508 calculated, 262.0510 found.



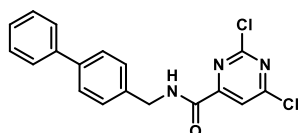
2,6-Dichloro-*N*-(prop-2-yn-1-yl)pyrimidine-4-carboxamide (116h). The title compound was prepared according to general procedure D using 2,6-dichloropyrimidine-4-carbonyl chloride **115** (0.25 mL, 2.0 mmol, 1 eq), Et₃N (0.36 mL, 2.60 mmol, 1.3 eq) and propargylamine (0.13 mL, 2.05 mmol, 1.025 eq). Column chromatography (5% → 20% EtOAc/pentane) afforded the product (0.44 g, 1.9 mmol, 95%). TLC: R_f = 0.6 (20% EtOAc/pentane). ¹H NMR (400 MHz, CDCl₃) δ 8.24 – 8.00 (m, 2H), 4.30 (dd, *J* = 5.7, 2.6 Hz, 2H), 2.36 (t, *J* = 2.6 Hz, 1H). ¹³C NMR (101 MHz, CDCl₃) δ 164.92, 160.08, 159.94, 159.63, 118.35, 78.30, 72.42, 29.52. HRMS [C₈H₅Cl₂N₃O + H]⁺: 229.9882 calculated, 229.9884 found.



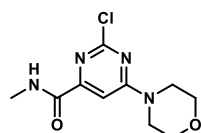
Methyl (2,6-dichloropyrimidine-4-carbonyl)glycinate (116i). The title compound was prepared according to general procedure D using 2,6-dichloropyrimidine-4-carbonyl chloride **115** (0.32 mL, 2.5 mmol, 1 eq), Et₃N (0.80 mL, 5.75 mmol, 2.3 eq) and glycine methylester HCl salt (0.32 g, 2.56 mmol, 1.025 eq). Column chromatography (5% → 20% EtOAc/pentane) afforded the product (0.51 g, 1.95 mmol, 78%). TLC: R_f = 0.5 (30% EtOAc/pentane). ¹H NMR (500 MHz, CDCl₃) δ 8.31 (br s, 1H), 8.09 (s, 1H), 4.28 (d, *J* = 5.8 Hz, 2H), 3.81 (s, 3H). ¹³C NMR (126 MHz, CDCl₃) δ 169.30, 164.89, 160.65, 160.02, 159.55, 118.31, 52.66, 41.35. HRMS [C₈H₇Cl₂N₃O₃ + H]⁺: 263.9937 calculated, 263.9939 found.



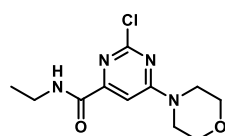
2,6-Dichloropyrimidine-N-benzyl-4-carboxamide (116j). The title compound was prepared according to general procedure D using 2,6-dichloropyrimidine-4-carbonyl chloride **115** (0.63 mL, 5.0 mmol, 1 eq), Et₃N (0.91 mL, 6.5 mmol, 1.3 eq) and benzylamine (0.56 mL, 5.13 mmol, 1.025 eq). Column chromatography (10% → 25% EtOAc/pentane) afforded the product (1.38 g, 4.9 mmol, 98%). TLC: R_f = 0.7 (20% EtOAc/pentane). ¹H NMR (400 MHz, CDCl₃) δ 8.18 (br s, 1H), 8.08 (s, 1H), 7.39 – 7.23 (m, 5H), 4.63 (d, *J* = 6.2 Hz, 2H). ¹³C NMR (101 MHz, CDCl₃) δ 164.81, 160.20, 160.17, 159.81, 137.00, 128.81, 127.90, 127.86, 118.35, 43.82. HRMS [C₁₂H₉Cl₂N₃O + H]⁺: 282.0195 calculated, 282.0197 found.



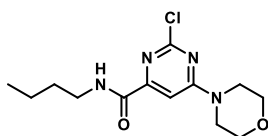
2,6-Dichloropyrimidine-N-([1,1'-biphenyl]-4-ylmethyl)-4-carboxamide (116k). The title compound was prepared according to general procedure D using 2,6-dichloropyrimidine-4-carbonyl chloride **115** (0.63 mL, 5.0 mmol, 1 eq), Et₃N (0.91 mL, 6.5 mmol, 1.3 eq) and 4-phenylbenzylamine (0.94 g, 5.13 mmol, 1.025 eq). Column chromatography (10% → 30% EtOAc/pentane) afforded the product (1.46 g, 4.1 mmol, 82%). TLC: R_f = 0.8 (20% EtOAc/pentane). ¹H NMR (400 MHz, CDCl₃) δ 8.16 (t, *J* = 5.7 Hz, 1H), 8.07 (s, 1H), 7.54 (d, *J* = 7.9 Hz, 4H), 7.46 – 7.29 (m, 5H), 4.65 (d, *J* = 6.2 Hz, 2H). ¹³C NMR (101 MHz, CDCl₃) δ 164.86, 160.26, 160.14, 159.86, 140.82, 140.40, 136.01, 128.84, 128.43, 127.52, 127.49, 127.03, 118.37, 43.57. HRMS [C₁₈H₁₃Cl₂N₃O + H]⁺: 358.0508 calculated, 358.0508 found.



2-Chloro-N-methyl-6-morpholinopyrimidine-4-carboxamide (117a). The title compound was prepared according to general procedure E using dichloropyrimidine **116b** (0.31 g, 1.5 mmol, 1 eq), DiPEA (0.39 mL, 2.3 mmol, 1.5 eq) and morpholine (0.14 mL, 1.6 mmol, 1.05 eq). Column chromatography (40% → 80% EtOAc/pentane) afforded the product as an 8.5:1 mixture of regioisomers (0.39 g, 1.5 mmol, 99%). TLC: R_f = 0.4 (100% EtOAc/pentane). Major regioisomer: ¹H NMR (400 MHz, CDCl₃) δ 7.93 – 7.77 (m, 1H), 7.26 (s, 1H), 3.83 – 3.61 (m, 8H), 3.00 (d, *J* = 5.2 Hz, 3H). ¹³C NMR (101 MHz, CDCl₃) δ 163.82, 162.92, 159.79, 157.70, 99.16, 66.34, 44.60, 44.38, 26.19. HRMS [C₁₀H₁₃ClN₄O₂ + H]⁺: 257.0800 calculated, 257.0800 found.

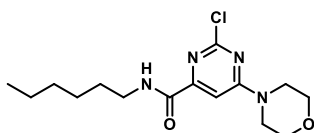


2-Chloro-N-ethyl-6-morpholinopyrimidine-4-carboxamide (117b). The title compound was prepared according to general procedure E using dichloropyrimidine **116c** (0.42 g, 1.9 mmol, 1 eq), DiPEA (0.49 mL, 2.8 mmol, 1.5 eq) and morpholine (0.17 mL, 2.0 mmol, 1.05 eq). Column chromatography (50% → 70% EtOAc/pentane) afforded the product (0.48 g, 1.8 mmol, 95%). TLC: R_f = 0.2 (50% EtOAc/pentane). ¹H NMR (400 MHz, CDCl₃) δ 7.82 (br s, 1H), 7.27 (s, 1H), 3.99 – 3.55 (m, 8H), 3.54 – 3.37 (m, 2H), 1.25 (t, *J* = 7.3 Hz, 3H). ¹³C NMR (101 MHz, CDCl₃) δ 163.86, 162.17, 159.85, 157.93, 99.27, 66.39, 44.63, 34.53, 14.71. HRMS [C₁₁H₁₅ClN₄O₂ + H]⁺: 271.0956 calculated, 271.0957 found.



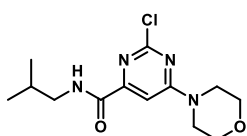
2-Chloro-*N*-butyl-6-morpholinopyrimidine-4-carboxamide (117c). The title compound was prepared according to general procedure E using dichloropyrimidine **116d** (193 mg, 0.78 mmol, 1 eq), DiPEA (203 μ L, 1.17 mmol, 1.5 eq) and morpholine (71 μ L, 0.82 mmol, 1.05 eq). Column chromatography (40% \rightarrow 60% EtOAc/pentane) afforded the product (212 mg, 0.71 mmol, 91%).

TLC: R_f = 0.4 (50% EtOAc/pentane). ^1H NMR (400 MHz, CDCl_3) δ 7.84 (br s, 1H), 7.27 (s, 1H), 3.91 – 3.61 (m, 8H), 3.43 (q, J = 7.1 Hz, 2H), 1.70 – 1.51 (m, 2H), 1.48 – 1.34 (m, 2H), 0.95 (t, J = 7.3 Hz, 3H). ^{13}C NMR (101 MHz, CDCl_3) δ 163.79, 162.19, 159.75, 157.88, 99.21, 66.31, 44.57, 39.29, 31.48, 20.07, 13.72. HRMS [$\text{C}_{13}\text{H}_{19}\text{ClN}_4\text{O}_2 + \text{H}$] $^+$: 299.1269 calculated, 299.1269 found.



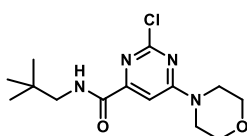
2-Chloro-*N*-hexyl-6-morpholinopyrimidine-4-carboxamide (117d). The title compound was prepared according to general procedure E using dichloropyrimidine **116e** (0.28 g, 1.02 mmol, 1 eq), DiPEA (0.27 mL, 1.54 mmol, 1.5 eq) and morpholine (94 μ L, 1.08 mmol, 1.05 eq). Column chromatography (40% \rightarrow 70% EtOAc/pentane) afforded the product (0.31 g, 0.95 mmol, 93%).

TLC: R_f = 0.5 (50% EtOAc/pentane). ^1H NMR (400 MHz, CDCl_3) δ 7.87 (t, J = 5.8 Hz, 1H), 7.28 (s, 1H), 4.01 – 3.53 (m, 8H), 3.42 (q, J = 6.9 Hz, 2H), 1.61 (p, J = 7.7, 7.3 Hz, 2H), 1.46 – 1.22 (m, 6H), 0.99 – 0.80 (m, 3H). ^{13}C NMR (101 MHz, CDCl_3) δ 163.71, 162.11, 159.68, 157.81, 99.17, 66.25, 44.55, 39.56, 31.37, 29.34, 26.53, 22.45, 13.97. HRMS [$\text{C}_{15}\text{H}_{23}\text{ClN}_4\text{O}_2 + \text{H}$] $^+$: 327.1582 calculated, 327.1582 found.



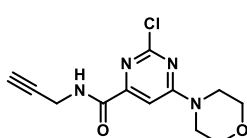
2-Chloro-*N*-isobutyl-6-morpholinopyrimidine-4-carboxamide (117e). The title compound was prepared according to general procedure E using dichloropyrimidine **116f** (0.28 g, 1.11 mmol, 1 eq), DiPEA (0.29 mL, 1.66 mmol, 1.5 eq) and morpholine (101 μ L, 1.16 mmol, 1.05 eq). Column chromatography (40% \rightarrow 60% EtOAc/pentane) afforded the product (0.33 g, 1.11 mmol, 99%).

TLC: R_f = 0.5 (50% EtOAc/pentane). ^1H NMR (400 MHz, CDCl_3) δ 7.91 (t, J = 5.8 Hz, 1H), 7.28 (s, 1H), 4.01 – 3.52 (m, 8H), 3.26 (t, J = 6.7 Hz, 2H), 2.00 – 1.81 (m, 1H), 0.97 (d, J = 6.7 Hz, 6H). ^{13}C NMR (101 MHz, CDCl_3) δ 163.75, 162.25, 159.71, 157.83, 99.23, 66.26, 46.82, 44.56, 28.58, 20.11. HRMS [$\text{C}_{13}\text{H}_{19}\text{ClN}_4\text{O}_2 + \text{H}$] $^+$: 299.1269 calculated, 299.1270 found.



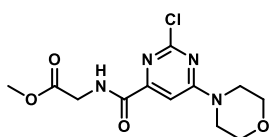
2-Chloro-6-morpholino-*N*-neopentylpyrimidine-4-carboxamide (117f). The title compound was prepared according to general procedure E using dichloropyrimidine **116g** (0.25 g, 0.96 mmol, 1 eq), DiPEA (0.25 mL, 1.44 mmol, 1.5 eq) and morpholine (88 μ L, 1.01 mmol, 1.05 eq). Column chromatography (30% \rightarrow 60% EtOAc/pentane) afforded the product (0.30 g, 0.96 mmol, 99%).

TLC: R_f = 0.5 (40% EtOAc/pentane). ^1H NMR (400 MHz, CDCl_3) δ 7.92 (br s, 1H), 7.28 (s, 1H), 3.96 – 3.50 (m, 8H), 3.24 (d, J = 6.7 Hz, 2H), 0.98 (s, 9H). ^{13}C NMR (101 MHz, CDCl_3) δ 163.77, 162.36, 159.74, 157.82, 99.30, 66.27, 50.64, 44.60, 32.34, 27.23. HRMS [$\text{C}_{14}\text{H}_{21}\text{ClN}_4\text{O}_2 + \text{H}$] $^+$: 313.1426 calculated, 313.1424 found.



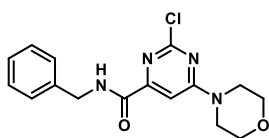
2-Chloro-6-morpholino-*N*-(prop-2-yn-1-yl)pyrimidine-4-carboxamide (117g). The title compound was prepared according to general procedure E using dichloropyrimidine **116h** (221 mg, 0.96 mmol, 1 eq), DiPEA (251 μ L, 1.44 mmol, 1.5 eq) and morpholine (88 μ L, 1.01 mmol, 1.05 eq). Column chromatography (40% \rightarrow 60% EtOAc/pentane) afforded the product (249 mg, 0.89 mmol, 93%).

TLC: R_f = 0.5 (50% EtOAc/pentane). ^1H NMR (400 MHz, CDCl_3) δ 8.00 (br s, 1H), 7.26 (s, 1H), 4.22 (dd, J = 5.7, 2.6 Hz, 2H), 3.88 – 3.59 (m, 8H), 2.29 (t, J = 2.6 Hz, 1H). ^{13}C NMR (101 MHz, CDCl_3) δ 163.84, 162.23, 160.04, 157.20, 99.53, 78.84, 72.05, 66.41, 29.32. HRMS [$\text{C}_{12}\text{H}_{13}\text{ClN}_4\text{O}_2 + \text{H}$] $^+$: 281.0800 calculated, 281.0800 found.



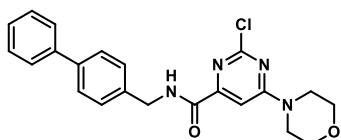
Methyl (2-chloro-6-morpholinopyrimidine-4-carbonyl)glycinate (117h). The title compound was prepared according to general procedure E using dichloropyrimidine **116i** (0.40 g, 1.50 mmol, 1 eq), DiPEA (0.39 mL, 2.25 mmol, 1.5 eq) and morpholine (137 μ L, 1.58 mmol, 1.05 eq). Column chromatography (60% -> 80% EtOAc/pentane) afforded the product (0.30 g, 0.95 mmol, 63%).

TLC: R_f = 0.5 (70% EtOAc/pentane). ^1H NMR (400 MHz, CDCl_3) δ 8.25 (t, J = 5.4 Hz, 1H), 7.25 (s, 1H), 4.22 (d, J = 5.9 Hz, 2H), 3.90 – 3.61 (m, 11H). ^{13}C NMR (101 MHz, CDCl_3) δ 169.59, 163.83, 162.85, 160.06, 157.09, 99.50, 66.39, 52.51, 44.69, 41.29. HRMS [$\text{C}_{12}\text{H}_{15}\text{ClN}_4\text{O}_4 + \text{H}$] $^+$: 315.0855 calculated, 315.0851 found.



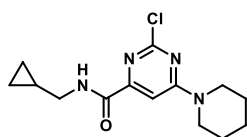
2-Chloro-N-benzyl-6-morpholinopyrimidine-4-carboxamide (117i) The title compound was prepared according to general procedure E using dichloropyrimidine **116j** (0.71 g, 2.50 mmol, 1 eq), DiPEA (0.65 mL, 3.75 mmol, 1.5 eq) and morpholine (0.23 mL, 2.63 mmol, 1.05 eq). Column chromatography (30% -> 60% EtOAc/pentane) afforded the product (0.68 g, 2.03 mmol, 81%).

TLC: R_f = 0.6 (60% EtOAc/pentane). ^1H NMR (400 MHz, CDCl_3) δ 8.18 (br s, 1H), 7.39 – 7.24 (m, 6H), 4.61 (d, J = 6.2 Hz, 2H), 3.90 – 3.54 (m, 8H). ^{13}C NMR (101 MHz, CDCl_3) δ 163.79, 162.37, 159.88, 157.63, 137.59, 128.77, 127.92, 127.67, 99.52, 66.37, 44.47, 43.60. HRMS [$\text{C}_{16}\text{H}_{17}\text{ClN}_4\text{O}_2 + \text{H}$] $^+$: 333.1113 calculated, 333.1112 found.



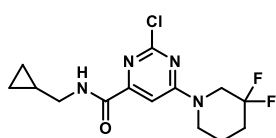
2-Chloro-N-([1,1'-biphenyl]-4-ylmethyl)-6-morpholinopyrimidine-4-carboxamide (117j). The title compound was prepared according to general procedure E using dichloropyrimidine **116k** (0.31 g, 1.0 mmol, 1 eq), DiPEA (0.26 mL, 1.5 mmol, 1.5 eq) and morpholine (91 μ L, 1.05 mmol, 1.05 eq). Column chromatography (20% -> 50% EtOAc/pentane) afforded the product (0.38 g, 0.94 mmol, 94%).

TLC: R_f = 0.4 (50% EtOAc/pentane). ^1H NMR (400 MHz, CDCl_3) δ 8.24 (t, J = 6.0 Hz, 1H), 7.61 – 7.52 (m, 4H), 7.47 – 7.31 (m, 5H), 7.28 (s, 1H), 4.64 (d, J = 6.2 Hz, 2H), 3.91 – 3.45 (m, 8H). ^{13}C NMR (101 MHz, CDCl_3) δ 163.79, 162.44, 159.91, 157.63, 140.62, 136.62, 128.86, 128.43, 127.48, 127.11, 99.53, 66.37, 44.65, 43.36. HRMS [$\text{C}_{22}\text{H}_{21}\text{ClN}_4\text{O}_2 + \text{H}$] $^+$: 409.1426 calculated, 409.1421 found.



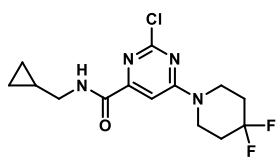
2-Chloro-N-(cyclopropylmethyl)-6-(piperidin-1-yl)pyrimidine-4-carboxamide (117k). The title compound was prepared according to general procedure E using dichloropyrimidine **116a** (0.26 g, 1.05 mmol, 1 eq), DiPEA (0.27 mL, 1.58 mmol, 1.5 eq) and piperidine (109 μ L, 1.10 mmol, 1.05 eq). Column chromatography (10% -> 40% EtOAc/pentane) afforded the product (0.29 g, 0.99 mmol, 94%).

TLC: R_f = 0.2 (20% EtOAc/pentane). ^1H NMR (400 MHz, CDCl_3) δ 7.95 (br s, 1H), 7.27 (s, 1H), 3.71 (br s, 4H), 3.29 (t, J = 6.5 Hz, 2H), 1.85 – 1.52 (m, 6H), 1.15 – 0.98 (m, 1H), 0.55 (q, J = 5.4 Hz, 2H), 0.28 (q, J = 4.8 Hz, 2H). ^{13}C NMR (101 MHz, CDCl_3) δ 163.12, 162.45, 159.77, 157.35, 99.29, 44.31, 25.55, 24.31, 10.61, 3.58. HRMS [$\text{C}_{14}\text{H}_{19}\text{ClN}_4\text{O} + \text{H}$] $^+$: 295.1320 calculated, 295.1321 found.

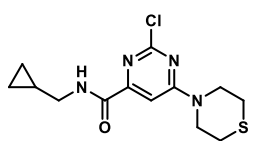


2-Chloro-N-(cyclopropylmethyl)-6-(3,3-difluoropiperidin-1-yl)pyrimidine-4-carboxamide (117l). The title compound was prepared according to general procedure E using dichloropyrimidine **116a** (0.10 g, 0.41 mmol, 1 eq), DiPEA (100 μ L, 0.57 mmol, 2.4 eq) and 3,3-difluoropiperidine HCl salt (68 mg, 0.43 mmol, 1.05 eq). Column chromatography (10% -> 40% EtOAc/pentane) afforded the product (88 mg, 0.26 mmol, 63%).

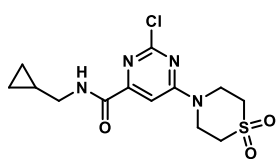
TLC: R_f = 0.4 (20% EtOAc/pentane). ^1H NMR (300 MHz, CDCl_3) δ 7.91 (br s, 1H), 7.35 (s, 1H), 3.99 (br s, 2H), 3.74 (br s, 2H), 3.29 (t, J = 6.5 Hz, 2H), 2.13 (tt, J = 13.3, 6.3 Hz, 2H), 2.02 – 1.74 (m, 2H), 1.17 – 0.95 (m, 1H), 0.67 – 0.44 (m, 2H), 0.28 (q, J = 5.1 Hz, 2H). ^{13}C NMR (75 MHz, CDCl_3) δ 164.08, 162.15, 159.87, 158.33, 119.17 (t, J = 244.8 Hz), 99.62, 44.54, 44.05, 32.63 (t, J = 23.5 Hz), 29.76, 21.70 (t, J = 4.5 Hz), 10.72, 3.71. HRMS [$\text{C}_{14}\text{H}_{17}\text{ClF}_2\text{N}_4\text{O} + \text{H}$] $^+$: 331.1132 calculated, 331.1127 found.



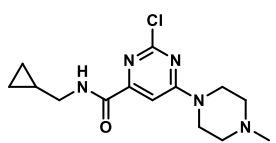
2-Chloro-*N*-(cyclopropylmethyl)-6-(4,4-difluoropiperidin-1-yl)pyrimidine-4-carboxamide (117m). The title compound was prepared according to general procedure E using dichloropyrimidine **116a** (0.12 g, 0.49 mmol, 1 eq), DiPEA (0.21 mL, 1.23 mmol, 2.5 eq) and 4,4-difluoropiperidine HCl salt (86 mg, 0.52 mmol, 1.05 eq). Column chromatography (5% → 25% EtOAc/pentane) afforded the product (90 mg, 0.27 mmol, 55%). TLC: $R_f = 0.4$ (15% EtOAc/pentane). $^1\text{H NMR}$ (300 MHz, CDCl_3) δ 7.91 (br s, 1H), 7.35 (s, 1H), 3.89 (br s, 4H), 3.38 – 3.20 (m, 2H), 2.06 (tt, $J = 13.2, 5.9$ Hz, 4H), 1.13 – 0.98 (m, 1H), 0.64 – 0.48 (m, 2H), 0.29 (q, $J = 4.8$ Hz, 2H). $^{13}\text{C NMR}$ (75 MHz, CDCl_3) δ 163.47, 162.18, 160.08, 158.40, 121.29 (t, $J = 242.4$ Hz), 99.44, 44.55, 41.49, 33.82 (t, $J = 23.7$ Hz), 10.72, 3.72. HRMS [$\text{C}_{14}\text{H}_{17}\text{ClF}_2\text{N}_4\text{O} + \text{H}$] $^+$: 331.1132 calculated, 331.1127 found.



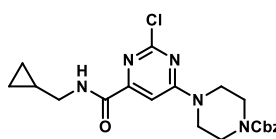
2-Chloro-*N*-(cyclopropylmethyl)-6-thiomorpholinopyrimidine-4-carboxamide (117n). The title compound was prepared according to general procedure E using dichloropyrimidine **116a** (0.12 g, 0.48 mmol, 1 eq), DiPEA (0.12 mL, 0.71 mmol, 1.5 eq) and thiomorpholine (51 μL , 0.50 mmol, 1.05 eq). Column chromatography (20% → 50% EtOAc/pentane) afforded the product (48 mg, 0.15 mmol, 31%). TLC: $R_f = 0.2$ (20% EtOAc/pentane). $^1\text{H NMR}$ (400 MHz, CDCl_3) δ 7.91 (br s, 1H), 7.28 (s, 1H), 4.07 (br s, 4H), 3.36 – 3.23 (m, 2H), 2.74 – 2.63 (m, 4H), 1.12 – 0.99 (m, 1H), 0.65 – 0.48 (m, 2H), 0.29 (q, $J = 4.8$ Hz, 2H). $^{13}\text{C NMR}$ (101 MHz, CDCl_3) δ 163.33, 162.30, 160.04, 158.07, 99.66, 44.55, 27.05, 10.73, 3.74. HRMS [$\text{C}_{13}\text{H}_{17}\text{ClN}_4\text{OS} + \text{H}$] $^+$: 313.0884 calculated, 313.0884 found.



2-Chloro-*N*-(cyclopropylmethyl)-6-(1,1-dioxidothiomorpholino)pyrimidine-4-carboxamide (117o). The title compound was prepared according to general procedure E using dichloropyrimidine **116a** (92 mg, 0.37 mmol, 1 eq), DiPEA (98 μL , 0.56 mmol, 1.5 eq) and thiomorpholine-1,1-dioxide (53 mg, 0.39 mmol, 1.05 eq). Column chromatography (60% → 70% EtOAc/pentane) afforded the product as a 4:1 mixture of regioisomers (69 mg, 0.20 mmol, 54%). TLC: $R_f = 0.5$ (60% EtOAc/pentane). Major regioisomer: $^1\text{H NMR}$ (500 MHz, $\text{CDCl}_3 + \text{MeOD}$) δ 7.41 (s, 1H), 4.26 (br s, 4H), 3.24 (d, $J = 7.1$ Hz, 2H), 3.18 – 3.12 (m, 4H), 1.10 – 0.98 (m, 1H), 0.59 – 0.49 (m, 2H), 0.32 – 0.21 (m, 2H). $^{13}\text{C NMR}$ (126 MHz, $\text{CDCl}_3 + \text{MeOD}$) δ 163.16, 162.11, 159.92, 158.47, 99.62, 51.14, 44.23, 42.86, 42.43, 10.18, 3.19. HRMS [$\text{C}_{13}\text{H}_{17}\text{ClN}_4\text{O}_3\text{S} + \text{H}$] $^+$: 345.0783 calculated, 345.0782 found.

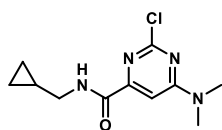


2-Chloro-*N*-(cyclopropylmethyl)-6-(4-methylpiperazin-1-yl)pyrimidine-4-carboxamide (117p). The title compound was prepared according to general procedure E using dichloropyrimidine **116a** (96 mg, 0.39 mmol, 1 eq), DiPEA (102 μL , 0.59 mmol, 1.5 eq) and 1-methylpiperazine (45 μL , 0.41 mmol, 1.05 eq). Column chromatography (5% → 10% MeOH/DCM) afforded the product (77 mg, 0.25 mmol, 64%). TLC: $R_f = 0.4$ (5% MeOH/DCM). $^1\text{H NMR}$ (500 MHz, CDCl_3) δ 7.99 – 7.84 (m, 1H), 7.28 (s, 1H), 3.96 – 3.58 (m, 4H), 3.35 – 3.24 (m, 2H), 2.54 – 2.44 (m, 4H), 2.34 (s, 3H), 1.12 – 0.99 (m, 1H), 0.64 – 0.50 (m, 2H), 0.28 (q, $J = 4.8$ Hz, 2H). $^{13}\text{C NMR}$ (126 MHz, CDCl_3) δ 163.61, 162.39, 159.88, 157.74, 99.52, 54.50, 46.06, 44.49, 43.44, 10.70, 3.71. HRMS [$\text{C}_{14}\text{H}_{20}\text{ClN}_5\text{O} + \text{H}$] $^+$: 310.1429 calculated, 310.1429 found.



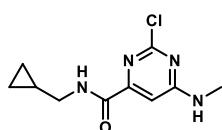
Benzyl-4-(2-chloro-6-((cyclopropylmethyl)carbamoyl)pyrimidin-4-yl)piperazine-1-carboxylate (117q). The title compound was prepared according to general procedure E using dichloropyrimidine **116a** (181 mg, 0.74 mmol, 1 eq), DiPEA (193 μL , 1.11 mmol, 1.5 eq) and 1-Cbz-piperazine (149 μL , 0.77 mmol, 1.05 eq). Column chromatography (30% → 60% EtOAc/pentane) afforded the product (290 mg, 0.67 mmol, 91%). TLC: $R_f = 0.5$ (50% EtOAc/pentane). $^1\text{H NMR}$ (400 MHz, CDCl_3) δ 7.92 (t, $J = 5.7$ Hz, 1H), 7.40 – 7.30 (m, 5H), 7.28 (s, 1H), 5.17 (s, 2H), 3.74 (br s, 4H), 3.65 – 3.55 (m, 4H), 3.34 – 3.22 (m, 2H), 1.12 – 0.98 (m, 1H), 0.63 – 0.46 (m, 2H), 0.36 – 0.19 (m, 2H). $^{13}\text{C NMR}$ (101 MHz, CDCl_3) δ

163.64, 162.10, 159.81, 158.01, 155.01, 136.26, 128.54, 128.20, 128.00, 99.44, 67.50, 44.40, 43.17, 10.63, 3.61.



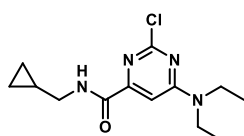
2-Chloro-*N*-(cyclopropylmethyl)-6-(dimethylamino)pyrimidine-4-carboxamide (117r).

The title compound was prepared according to general procedure E using dichloropyrimidine **116a** (0.25 g, 1.0 mmol, 1 eq), DiPEA (0.26 mL, 1.5 mmol, 1.5 eq) and dimethylamine (2 M in THF, 0.53 mL, 1.05 mmol, 1.05 eq). Column chromatography (40% → 60% EtOAc/pentane) afforded the product (225 mg, 0.88 mmol, 88%). TLC: $R_f = 0.5$ (50% EtOAc/pentane). ^1H NMR (400 MHz, CDCl_3) δ 7.97 (br s, 1H), 7.19 (s, 1H), 3.33 – 3.27 (m, 2H), 3.27 – 3.06 (m, 6H), 1.13 – 0.99 (m, 1H), 0.62 – 0.49 (m, 2H), 0.29 (q, $J = 4.8$ Hz, 2H). ^{13}C NMR (101 MHz, CDCl_3) δ 164.03, 162.29, 159.36, 156.93, 99.19, 44.26, 37.76, 37.29, 10.56, 3.53. HRMS [$\text{C}_{11}\text{H}_{15}\text{ClN}_4\text{O} + \text{H}$] $^+$: 255.1007 calculated, 255.1005 found.



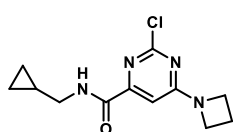
2-Chloro-*N*-(cyclopropylmethyl)-6-(methylamino)pyrimidine-4-carboxamide (117s).

The title compound was prepared according to general procedure E using dichloropyrimidine **116a** (123 mg, 0.50 mmol, 1 eq), DiPEA (218 μL , 1.25 mmol, 2.5 eq) and methylamine HCl salt (35 mg, 0.53 mmol, 1.05 eq). Column chromatography (50% → 70% EtOAc/pentane) afforded the product (77 mg, 0.32 mmol, 64%). TLC: $R_f = 0.4$ (60% EtOAc/pentane). ^1H NMR (500 MHz, CDCl_3) δ 7.93 (br s, 1H), 7.40 – 7.04 (m, 1H), 6.62 – 6.20 (m, 1H), 3.29 (br s, 2H), 3.04 (br s, 3H), 1.13 – 1.00 (m, 1H), 0.65 – 0.50 (m, 2H), 0.29 (q, $J = 4.9$ Hz, 2H). ^{13}C NMR (126 MHz, CDCl_3) δ 175.67, 166.23, 165.44, 162.63, 162.22, 160.34, 158.43, 155.80, 103.55, 98.02, 44.55, 29.81, 29.06, 28.22, 3.76. HRMS [$\text{C}_{10}\text{H}_{13}\text{ClN}_4\text{O} + \text{H}$] $^+$: 241.0851 calculated, 241.0849 found.



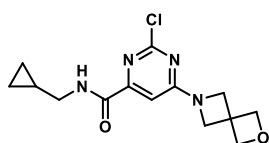
2-Chloro-*N*-(cyclopropylmethyl)-6-(diethylamino)pyrimidine-4-carboxamide (117t).

The title compound was prepared according to general procedure E using dichloropyrimidine **116a** (123 mg, 0.50 mmol, 1 eq), DiPEA (131 μL , 0.75 mmol, 1.5 eq) and diethylamine (55 μL , 0.53 mmol, 1.05 eq). Column chromatography (20% → 50% EtOAc/pentane) afforded the product (94 mg, 0.33 mmol, 66%). TLC: $R_f = 0.7$ (50% EtOAc/pentane). ^1H NMR (400 MHz, CDCl_3) δ 7.94 (br s, 1H), 7.16 (s, 1H), 3.77 – 3.37 (m, 4H), 3.34 – 3.24 (m, 2H), 1.22 (t, $J = 7.0$ Hz, 6H), 1.12 – 1.00 (m, 1H), 0.61 – 0.51 (m, 2H), 0.29 (q, $J = 4.8$ Hz, 2H). ^{13}C NMR (101 MHz, CDCl_3) δ 162.96, 162.57, 159.79, 157.11, 99.29, 44.41, 42.96, 42.73, 12.64, 10.69, 3.67. HRMS [$\text{C}_{13}\text{H}_{19}\text{ClN}_4\text{O} + \text{H}$] $^+$: 283.1320 calculated, 283.1319 found.



2-Chloro-*N*-(cyclopropylmethyl)-6-(azetidin-1-yl)pyrimidine-4-carboxamide (117u).

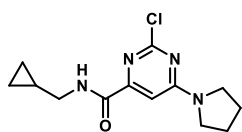
The title compound was prepared according to general procedure E using dichloropyrimidine **116a** (98 mg, 0.40 mmol, 1 eq), DiPEA (174 μL , 1.0 mmol, 2.5 eq) and azetidine HCl salt (39 mg, 0.42 mmol, 1.05 eq). Column chromatography (30% → 50% EtOAc/pentane) afforded the product (79 mg, 0.30 mmol, 75%). TLC: $R_f = 0.3$ (50% EtOAc/pentane). ^1H NMR (400 MHz, CDCl_3) δ 7.90 (br s, 1H), 6.88 (s, 1H), 4.44 – 4.07 (m, 4H), 3.28 (dd, $J = 7.0, 6.0$ Hz, 2H), 2.49 (p, $J = 7.6$ Hz, 2H), 1.14 – 0.99 (m, 1H), 0.62 – 0.51 (m, 2H), 0.28 (q, $J = 4.7$ Hz, 2H). ^{13}C NMR (101 MHz, CDCl_3) δ 163.91, 162.30, 159.95, 156.54, 98.54, 50.20, 44.44, 16.51, 10.69, 3.69. HRMS [$\text{C}_{12}\text{H}_{15}\text{ClN}_4\text{O} + \text{H}$] $^+$: 267.1007 calculated, 267.1005 found.



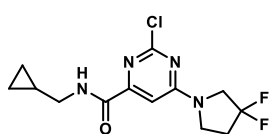
2-Chloro-*N*-(cyclopropylmethyl)-6-(2-oxa-6-azaspiro[3.3]heptan-6-yl)pyrimidine-4-carboxamide (117v).

The title compound was prepared according to general procedure E using dichloropyrimidine **116a** (98 mg, 0.40 mmol, 1 eq), DiPEA (174 μL , 1.0 mmol, 2.5 eq) and 2-oxa-6-azaspiro[3.3]heptane hemioxalate salt (61 mg, 0.42 mmol, 1.05 eq). Column chromatography (40% → 100% EtOAc/pentane) afforded the product (96 mg, 0.31 mmol, 78%). TLC: $R_f = 0.2$ (80% EtOAc/pentane). ^1H NMR (400 MHz, CDCl_3) δ 7.88 (br s, 1H), 6.92 (s, 1H), 4.86 (br s, 4H), 4.35 (s, 4H), 3.28 (dd, $J = 7.0, 6.0$ Hz,

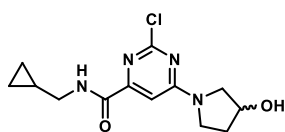
2H), 1.11 – 0.98 (m, 1H), 0.63 – 0.50 (m, 2H), 0.34 – 0.23 (m, 2H). ^{13}C NMR (101 MHz, CDCl_3) δ 164.01, 162.11, 160.06, 157.10, 98.96, 80.71, 59.73, 44.56, 39.16, 10.72, 3.76. HRMS [$\text{C}_{14}\text{H}_{17}\text{ClN}_4\text{O}_2 + \text{H}$] $^+$: 309.1113 calculated, 309.1110 found.



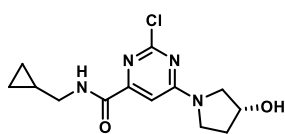
2-Chloro-*N*-(cyclopropylmethyl)-6-(pyrrolidin-1-yl)pyrimidine-4-carboxamide (117w). The title compound was prepared according to general procedure E using dichloropyrimidine **116a** (123 mg, 0.50 mmol, 1 eq), DiPEA (131 μL , 0.75 mmol, 1.5 eq) and pyrrolidine (43 μL , 0.53 mmol, 1.05 eq). Column chromatography (30% -> 60% EtOAc/pentane) afforded the product (150 mg, 0.40 mmol, 80%). TLC: R_f = 0.5 (40% EtOAc/pentane). ^1H NMR (400 MHz, CDCl_3) δ 7.93 (br s, 1H), 7.05 (s, 1H), 3.65 (t, J = 6.6 Hz, 2H), 3.46 (t, J = 6.7 Hz, 2H), 3.29 (t, J = 6.5 Hz, 2H), 2.09 (p, J = 6.3 Hz, 2H), 2.00 (p, J = 6.3 Hz, 2H), 1.13 – 0.99 (m, 1H), 0.56 (q, J = 5.2 Hz, 2H), 0.29 (q, J = 4.9 Hz, 2H). ^{13}C NMR (101 MHz, CDCl_3) δ 162.52, 161.97, 159.61, 156.52, 100.53, 47.23, 46.98, 44.43, 25.52, 24.82, 10.69, 3.69. HRMS [$\text{C}_{13}\text{H}_{17}\text{ClN}_4\text{O} + \text{H}$] $^+$: 281.1164 calculated, 281.1160 found.



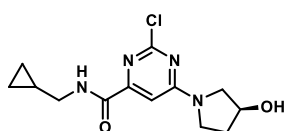
2-Chloro-*N*-(cyclopropylmethyl)-6-(3,3-difluoropyrrolidin-1-yl)pyrimidine-4-carboxamide (117x). The title compound was prepared according to general procedure E using dichloropyrimidine **116a** (98 mg, 0.40 mmol, 1 eq), DiPEA (174 μL , 1.0 mmol, 2.5 eq) and 3,3-difluoropyrrolidine HCl salt (60 mg, 0.42 mmol, 1.05 eq). Column chromatography (20% -> 40% EtOAc/pentane) afforded the product (108 mg, 0.34 mmol, 85%). TLC: R_f = 0.6 (40% EtOAc/pentane). ^1H NMR (500 MHz, CDCl_3) δ 7.90 (br s, 1H), 7.22 – 6.87 (m, 1H), 4.19 – 3.59 (m, 4H), 3.36 – 3.22 (m, 2H), 2.55 (br s, 2H), 1.14 – 0.97 (m, 1H), 0.63 – 0.50 (m, 2H), 0.37 – 0.18 (m, 2H). ^{13}C NMR (126 MHz, CDCl_3) δ 162.52, 162.11, 159.90, 157.70, 100.24, 99.83, 53.66 (t, J = 32.9 Hz), 44.62, 33.91, 3.78. HRMS [$\text{C}_{13}\text{H}_{15}\text{ClF}_2\text{N}_4\text{O} + \text{H}$] $^+$: 317.0975 calculated, 317.0974 found.



(±)-2-Chloro-*N*-(cyclopropylmethyl)-6-(3-hydroxypyrrolidin-1-yl)pyrimidine-4-carboxamide (117y). The title compound was prepared according to general procedure E using dichloropyrimidine **116a** (98 mg, 0.40 mmol, 1 eq), DiPEA (174 μL , 1.0 mmol, 2.5 eq) and (±)-3-hydroxypyrrolidine HCl salt (52 mg, 0.42 mmol, 1.05 eq). Column chromatography (70% -> 100% EtOAc/pentane) afforded the product (89 mg, 0.30 mmol, 75%). TLC: R_f = 0.2 (80% EtOAc/pentane). ^1H NMR (400 MHz, CDCl_3) δ 7.98 (t, J = 5.3 Hz, 1H), 7.08 – 6.89 (m, 1H), 4.73 – 4.55 (m, 1H), 3.87 – 3.45 (m, 4H), 3.33 – 3.20 (m, 2H), 2.25 – 2.07 (m, 2H), 1.12 – 0.98 (m, 1H), 0.63 – 0.50 (m, 2H), 0.29 (q, J = 4.9 Hz, 2H). ^{13}C NMR (101 MHz, CDCl_3) δ 162.63, 162.32, 162.16, 159.59, 156.38, 100.55, 100.49, 70.46, 69.78, 55.58, 55.35, 45.26, 45.02, 44.58, 33.87, 33.29, 10.62, 3.75. HRMS [$\text{C}_{13}\text{H}_{17}\text{ClN}_4\text{O}_2 + \text{H}$] $^+$: 297.1113 calculated, 297.1110 found.

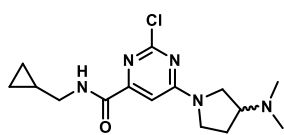


(*R*)-2-Chloro-*N*-(cyclopropylmethyl)-6-(3-hydroxypyrrolidin-1-yl)pyrimidine-4-carboxamide (117z). The title compound was prepared according to general procedure E using dichloropyrimidine **116a** (98 mg, 0.40 mmol, 1 eq), DiPEA (174 μL , 1.0 mmol, 2.5 eq) and (*R*)-3-hydroxypyrrolidine HCl salt (52 mg, 0.42 mmol, 1.05 eq). Column chromatography (70% -> 100% EtOAc/pentane) afforded the product (105 mg, 0.35 mmol, 88%). TLC: R_f = 0.2 (80% EtOAc/pentane). ^1H NMR (400 MHz, CDCl_3) δ 7.98 (t, J = 5.4 Hz, 1H), 7.08 – 6.91 (m, 1H), 4.74 – 4.54 (m, 1H), 3.90 – 3.39 (m, 5H), 3.34 – 3.20 (m, 2H), 2.24 – 2.07 (m, 2H), 1.13 – 0.98 (m, 1H), 0.63 – 0.48 (m, 2H), 0.36 – 0.17 (m, 2H). ^{13}C NMR (101 MHz, CDCl_3) δ 162.64, 162.34, 162.18, 159.73, 159.60, 156.40, 100.57, 100.52, 70.50, 69.81, 55.59, 55.36, 45.27, 45.03, 44.59, 33.87, 33.32, 10.63, 3.76. HRMS [$\text{C}_{13}\text{H}_{17}\text{ClN}_4\text{O}_2 + \text{H}$] $^+$: 297.1113 calculated, 297.1110 found.



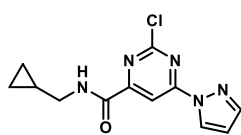
(*S*)-2-Chloro-*N*-(cyclopropylmethyl)-6-(3-hydroxypyrrolidin-1-yl)pyrimidine-4-carboxamide (117aa). The title compound was prepared according to general procedure E using dichloropyrimidine **116a** (98 mg, 0.40 mmol, 1 eq), DiPEA (174 μL , 1.0 mmol, 2.5 eq) and (*S*)-3-hydroxypyrrolidine HCl salt (52 mg, 0.42

mmol, 1.05 eq). Column chromatography (70% → 100% EtOAc/pentane) afforded the product (97 mg, 0.33 mmol, 83%). TLC: R_f = 0.2 (80% EtOAc/pentane). ^1H NMR (300 MHz, CDCl_3) δ 7.98 (t, J = 5.2 Hz, 1H), 7.11 – 6.86 (m, 1H), 4.81 – 4.47 (m, 1H), 3.93 – 3.35 (m, 5H), 3.33 – 3.21 (m, 2H), 2.25 – 2.06 (m, 2H), 1.16 – 0.96 (m, 1H), 0.57 (q, J = 5.5 Hz, 2H), 0.29 (q, J = 4.7 Hz, 2H). ^{13}C NMR (75 MHz, CDCl_3) δ 162.65, 162.34, 162.19, 159.73, 159.61, 156.41, 100.55, 100.51, 70.48, 69.79, 55.58, 55.35, 45.27, 45.03, 44.58, 33.87, 33.31, 10.62, 3.74. HRMS [$\text{C}_{13}\text{H}_{17}\text{ClN}_4\text{O}_2 + \text{H}$] $^+$: 297.1113 calculated, 297.1110 found.



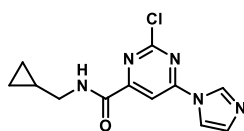
(±)-2-Chloro-*N*-(cyclopropylmethyl)-6-(3-(dimethylamino)pyrrolidin-1-yl)pyrimidine-4-carboxamide (117ab).

The title compound was prepared according to general procedure E using dichloropyrimidine **116a** (98 mg, 0.40 mmol, 1 eq), DIPEA (244 μL , 1.4 mmol, 3.5 eq) and (±)-3-(dimethylamino)pyrrolidine double HCl salt (79 mg, 0.42 mmol, 1.05 eq). Column chromatography (2.5% → 10% MeOH/DCM) afforded the product (50 mg, 0.15 mmol, 38%). TLC: R_f = 0.4 (5% MeOH/DCM). ^1H NMR (400 MHz, CDCl_3) δ 8.10 – 7.77 (m, 1H), 7.06 (s, 1H), 4.06 – 3.91 (m, 2H), 3.90 – 3.60 (m, 1H), 3.59 – 3.32 (m, 2H), 3.32 – 3.25 (m, 2H), 2.95 – 2.70 (m, 1H), 2.40 – 2.30 (m, 6H), 2.30 – 2.17 (m, 1H), 2.08 – 1.78 (m, 1H), 1.13 – 0.99 (m, 1H), 0.66 – 0.45 (m, 2H), 0.35 – 0.21 (m, 2H). ^{13}C NMR (101 MHz, CDCl_3) δ 171.69, 163.73, 162.56, 162.47, 162.15, 161.99, 159.76, 159.69, 159.50, 158.70, 158.27, 156.79, 106.57, 100.46, 100.22, 93.93, 65.41, 64.76, 53.71, 51.47, 51.33, 50.76, 46.42, 46.22, 45.79, 44.54, 44.51, 44.42, 44.28, 44.22, 44.02, 30.41, 29.81, 10.90, 10.85, 10.74, 3.76, 3.51, 3.47. HRMS [$\text{C}_{15}\text{H}_{22}\text{ClN}_5\text{O} + \text{H}$] $^+$: 324.1586 calculated, 324.1583 found.



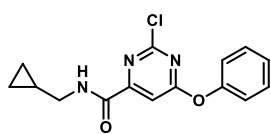
2-Chloro-*N*-(cyclopropylmethyl)-6-(1H-pyrazol-1-yl)pyrimidine-4-carboxamide (117ac).

The title compound was prepared according to general procedure F using dichloropyrimidine **116a** (123 mg, 0.50 mmol, 1 eq), K_2CO_3 (104 mg, 0.75 mmol, 1.5 eq) and pyrazole (36 mg, 0.53 mmol, 1.05 eq). Column chromatography (10% → 30% EtOAc/pentane) afforded the product (76 mg, 0.27 mmol, 54%). TLC: R_f = 0.8 (30% EtOAc/pentane). ^1H NMR (400 MHz, CDCl_3) δ 8.61 (s, 1H), 8.56 (d, J = 2.7 Hz, 1H), 7.92 (br s, 1H), 7.85 (d, J = 1.3 Hz, 1H), 6.55 (dd, J = 2.8, 1.6 Hz, 1H), 3.36 (dd, J = 7.1, 5.9 Hz, 2H), 1.19 – 1.00 (m, 1H), 0.71 – 0.49 (m, 2H), 0.32 (q, J = 4.7 Hz, 2H). ^{13}C NMR (101 MHz, CDCl_3) δ 161.28, 160.88, 160.48, 159.64, 145.18, 128.34, 110.22, 105.51, 44.73, 3.76. HRMS [$\text{C}_{12}\text{H}_{12}\text{ClN}_5\text{O} + \text{H}$] $^+$: 278.0803 calculated, 278.0802 found.



2-Chloro-*N*-(cyclopropylmethyl)-6-(1H-imidazol-1-yl)pyrimidine-4-carboxamide (117ad).

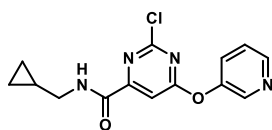
The title compound was prepared according to general procedure F using dichloropyrimidine **116a** (123 mg, 0.50 mmol, 1 eq), K_2CO_3 (104 mg, 0.75 mmol, 1.5 eq) and imidazole (36 mg, 0.53 mmol, 1.05 eq). Column chromatography (60% → 80% EtOAc/pentane) afforded the product as an inseparable mixture of regioisomers (2.5:1, 6-imidazolyl : 2-imidazolyl), that was used for the following step without further purification (100 mg, 0.36 mmol, 72%). TLC: R_f = 0.4 (5% MeOH/DCM). ^1H NMR (400 MHz, CDCl_3) δ 8.56 (s, 1H), 8.10 (s, 1H), 7.98 (br s, 1H), 7.77 (t, J = 1.4 Hz, 1H), 7.26 (s, 1H), 3.47 – 3.26 (m, 2H), 1.18 – 1.03 (m, 1H), 0.68 – 0.53 (m, 2H), 0.41 – 0.27 (m, 2H). ^{13}C NMR (101 MHz, CDCl_3) δ 161.93, 160.55, 159.94, 158.14, 135.73, 132.38, 116.02, 104.68, 44.84, 10.66, 3.76. HRMS [$\text{C}_{12}\text{H}_{12}\text{ClN}_5\text{O} + \text{H}$] $^+$: 278.0803 calculated, 278.0800 found.



2-Chloro-*N*-(cyclopropylmethyl)-6-phenoxy pyrimidine-4-carboxamide (117ae).

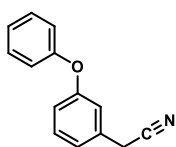
The title compound was prepared according to general procedure F using dichloropyrimidine **116a** (100 mg, 0.41 mmol, 1 eq), K_2CO_3 (86 mg, 0.62 mmol, 1.5 eq) and phenol (44 mg, 0.43 mmol, 1.05 eq). Column chromatography (5% → 30% EtOAc/pentane) afforded the product (100 mg, 0.33 mmol, 80%). TLC: R_f = 0.4 (20% EtOAc/pentane). ^1H NMR (300 MHz, CDCl_3) δ 7.90 (br s, 1H), 7.54 (s, 1H), 7.50 – 7.39 (m, 2H), 7.36 – 7.28 (m, 1H), 7.20 – 7.08 (m, 2H), 3.41 – 3.17 (m, 2H), 1.15 – 0.96 (m, 1H), 0.66 – 0.47 (m, 2H), 0.29 (q, J = 4.7 Hz, 2H). ^{13}C NMR (75 MHz,

CDCl_3) δ 172.25, 161.17, 161.02, 159.73, 151.84, 130.19, 126.62, 121.27, 104.58, 44.68, 10.70, 3.75. HRMS $[\text{C}_{15}\text{H}_{14}\text{ClN}_3\text{O}_2 + \text{H}]^+$: 304.0847 calculated, 304.0845 found.



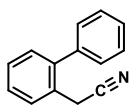
2-Chloro-*N*-(cyclopropylmethyl)-6-(pyridin-3-yloxy)pyrimidine-4-carboxamide (117af). The title compound was prepared according to general procedure F

using dichloropyrimidine **116a** (0.11 g, 0.45 mmol, 1 eq), K_2CO_3 (93 mg, 0.68 mmol, 1.5 eq) and pyridine-3-ol (45 mg, 0.47 mmol, 1.05 eq). Column chromatography (60% \rightarrow 100% EtOAc/pentane) afforded the product (70 mg, 0.23 mmol, 51%). TLC: R_f = 0.4 (80% EtOAc/pentane). ^1H NMR (300 MHz, CDCl_3) δ 8.56 (dd, J = 9.3, 3.2 Hz, 2H), 7.94 (br s, 1H), 7.69 (s, 1H), 7.63 – 7.50 (m, 1H), 7.43 (dd, J = 8.3, 4.7 Hz, 1H), 3.46 – 3.19 (m, 2H), 1.17 – 0.99 (m, 1H), 0.66 – 0.51 (m, 2H), 0.31 (q, J = 4.8 Hz, 2H). ^{13}C NMR (75 MHz, CDCl_3) δ 171.32, 161.44, 160.74, 159.43, 148.48, 147.52, 143.41, 129.09, 124.31, 105.26, 44.66, 10.66, 3.71. HRMS $[\text{C}_{14}\text{H}_{13}\text{ClN}_4\text{O}_2 + \text{H}]^+$: 305.0800 calculated, 305.0796 found.



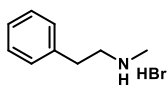
2-(3-Phenoxyphenyl)acetonitrile (119a). A round-bottom flask was charged with 1-(chloromethyl)-3-phenoxybenzene (**118a**) (0.37 mL, 2.0 mmol, 1 eq) in dioxane/EtOH/ H_2O (2:2:1, 6 mL) and KCN (0.26 g, 4.0 mmol, 2 eq). The reaction mixture was stirred overnight at reflux. The mixture was diluted with water and extracted with EtOAc (3x). The organic layer was washed with brine, dried (Na_2SO_4), filtered and concentrated under reduced

pressure. The crude material was purified by silica gel column chromatography (5% \rightarrow 7% EtOAc/pentane) to provide the product (0.35 g, 1.7 mmol, 85%). TLC: R_f = 0.6 (10% EtOAc/pentane). ^1H NMR (500 MHz, CDCl_3) δ 7.37 – 7.19 (m, 3H), 7.15 – 7.03 (m, 1H), 7.04 – 6.94 (m, 3H), 6.95 – 6.84 (m, 2H), 3.56 (s, 2H). ^{13}C NMR (126 MHz, CDCl_3) δ 157.73, 156.32, 131.81, 130.23, 129.71, 123.58, 122.34, 118.97, 117.96, 117.78, 117.51, 23.00.



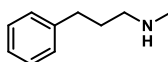
2-([1,1'-Biphenyl]-2-yl)acetonitrile (119b). A round-bottom flask was charged with 2-(bromomethyl)-1,1'-biphenyl (**118b**) (0.37 mL, 2.0 mmol, 1 eq), solvent mixture dioxane/EtOH/ H_2O (2:2:1, 6 mL) and KCN (0.26 g, 4.0 mmol, 2 eq). The reaction mixture was stirred overnight at reflux. The mixture was diluted with water and extracted with EtOAc (3x).

The organic layer was washed with brine, dried (Na_2SO_4), filtered and concentrated under reduced pressure. The crude material was purified by silica gel column chromatography (0.5% \rightarrow 5% EtOAc/pentane) to provide the product (0.40 g, 2.0 mmol, 99%). TLC: R_f = 0.6 (3% EtOAc/pentane). ^1H NMR (400 MHz, CDCl_3) δ 7.59 – 7.12 (m, 9H), 3.57 (s, 2H). ^{13}C NMR (101 MHz, CDCl_3) δ 141.72, 139.78, 130.35, 128.86, 128.84, 128.59, 128.12, 127.68, 118.23, 21.92.



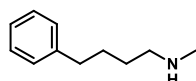
***N*-Methylphenethylamine HBr salt (121a).** A round-bottom flask was charged with methylamine (33 wt% in ethanol, 8.83 mL, 73.0 mmol, 10 eq) and cooled to 0 $^\circ\text{C}$. (2-bromoethyl)benzene (1.0 mL, 7.3 mmol, 1 eq) was added and the reaction was stirred and

allowed to warm up to room temperature. After 40 h the reaction showed complete conversion on TLC and the solvents were concentrated under reduced pressure. The product was obtained as a mixture with the di-substituted by product, *N*-methyl-*N*-phenethyl-2-phenylethan-1-amine (9:1) and used without further purification (1.4 g, 6.6 mmol, 90%). TLC: R_f = 0.35 (6% MeOH/DCM). ^1H NMR (400 MHz, MeOD) δ 7.52 – 6.99 (m, 5H), 3.42 – 3.10 (m, 2H), 3.10 – 2.85 (m, 2H), 2.67 (s, 3H). ^{13}C NMR (101 MHz, MeOD) δ 137.75, 129.86, 129.78, 128.10, 51.50, 33.92, 33.31.

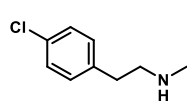


***N*-Methyl-3-phenylpropan-1-amine (121b).** *Carbamoylation:* The methyl carbamate was prepared according to general procedure G using 3-phenylpropan-1-amine (71 μL , 0.50 mmol, 1 eq), methylchloroformate (58 μL , 0.75 mmol, 1.5 eq) and DiPEA (174 μL , 1.0 mmol, 2 eq). Column chromatography (20% \rightarrow 50% EtOAc/pentane) afforded the product (91 mg, 0.47 mmol, 94%). TLC: R_f = 0.7 (50% EtOAc/pentane). ^1H NMR (400 MHz, CDCl_3) δ 7.33 – 7.22 (m, 2H), 7.22 – 7.13

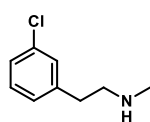
(m, 3H), 4.82 (br s, 1H), 3.65 (s, 3H), 3.26 – 3.07 (m, 2H), 2.69 – 2.57 (m, 2H), 1.82 (p, $J = 7.3$ Hz, 2H). ^{13}C NMR (101 MHz, CDCl_3) δ 157.18, 141.47, 128.49, 128.40, 126.02, 52.08, 40.68, 33.06, 31.68. HRMS [$\text{C}_{11}\text{H}_{15}\text{NO}_2 + \text{H}$] $^+$: 194.1176 calculated, 194.1175 found. *Carbamate reduction*: the title compound was prepared according to general procedure G using the methyl carbamate (91 mg, 0.47 mmol, 1 eq), LiAlH_4 (2 M THF solution, 0.75 mL, 1.54 mmol, 3.3 eq) and was used without further purification (39 mg, 0.13 mmol, 28%). TLC: $R_f = 0.1$ (5% MeOH/DCM). ^1H NMR (500 MHz, CDCl_3) δ 7.31 – 7.13 (m, 5H), 2.68 – 2.63 (m, 2H), 2.63 – 2.58 (m, 2H), 2.42 (s, 3H), 1.90 – 1.76 (m, 2H), 1.71 – 1.58 (m, 1H). HRMS [$\text{C}_{10}\text{H}_{15}\text{N} + \text{H}$] $^+$: 150.1277 calculated, 150.1278 found.



N-Methyl-4-phenylbutan-1-amine (121c). *Carbamoylation*: the methyl carbamate was prepared according to general procedure G using 4-phenylbutan-1-amine (79 μL , 0.50 mmol, 1 eq), methylchloroformate (58 μL , 0.75 mmol, 1.5 eq) and DiPEA (174 μL , 1.0 mmol, 2 eq). Column chromatography (10% -> 40% EtOAc/pentane) afforded the product (97 mg, 0.47 mmol, 94%). TLC: $R_f = 0.6$ (50% EtOAc/pentane). ^1H NMR (400 MHz, CDCl_3) δ 7.26 (t, $J = 7.5$ Hz, 2H), 7.17 (t, $J = 7.9$ Hz, 3H), 4.80 (br s, 1H), 3.64 (s, 3H), 3.29 – 3.00 (m, 2H), 2.61 (t, $J = 7.6$ Hz, 2H), 1.69 – 1.57 (m, 2H), 1.51 (p, $J = 6.9$ Hz, 2H). ^{13}C NMR (101 MHz, CDCl_3) δ 157.15, 142.15, 128.42, 128.37, 125.84, 52.01, 40.93, 35.54, 29.65, 28.55. HRMS [$\text{C}_{12}\text{H}_{17}\text{NO}_2 + \text{H}$] $^+$: 208.1332 calculated, 208.1333 found. *Carbamate reduction*: the title compound was prepared according to general procedure G using the methyl carbamate (97 mg, 0.47 mmol, 1 eq), LiAlH_4 (2 M THF solution, 0.38 mL, 0.75 mmol, 1.6 eq) and was used without further purification (64 mg, 0.39 mmol, 83%). TLC: $R_f = 0.1$ (5% MeOH/DCM). ^1H NMR (400 MHz, CDCl_3) δ 7.31 – 7.21 (m, 2H), 7.20 – 7.11 (m, 3H), 2.62 (t, $J = 7.6$ Hz, 2H), 2.59 – 2.54 (m, 2H), 2.40 (s, 3H), 1.77 – 1.57 (m, 3H), 1.57 – 1.46 (m, 2H). ^{13}C NMR (101 MHz, CDCl_3) δ 142.51, 128.45, 128.31, 125.73, 52.05, 36.57, 35.90, 29.61, 29.24. HRMS [$\text{C}_{11}\text{H}_{17}\text{N} + \text{H}$] $^+$: 164.1434 calculated, 164.1433 found.

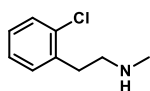


2-(4-Chlorophenyl)-N-methylethan-1-amine (121d). *Carbamoylation*: the methyl carbamate was prepared according to general procedure G using 2-(4-chlorophenyl)ethan-1-amine (70 μL , 0.50 mmol, 1 eq), methylchloroformate (58 μL , 0.75 mmol, 1.5 eq) and DiPEA (174 μL , 1.0 mmol, 2 eq). Column chromatography (10% -> 50% EtOAc/pentane) afforded the product (104 mg, 0.50 mmol, 99%). TLC: $R_f = 0.7$ (50% EtOAc/pentane). ^1H NMR (400 MHz, CDCl_3) δ 7.35 – 7.21 (m, 2H), 7.16 – 7.05 (m, 2H), 5.01 – 4.39 (m, 1H), 3.65 (s, 3H), 3.41 (q, $J = 6.7$ Hz, 2H), 2.78 (t, $J = 7.0$ Hz, 2H). ^{13}C NMR (101 MHz, CDCl_3) δ 157.04, 137.32, 132.39, 130.22, 128.80, 52.20, 42.17, 35.62. HRMS [$\text{C}_{10}\text{H}_{12}\text{ClNO}_2 + \text{H}$] $^+$: 214.0629 calculated, 214.0631 found. *Carbamate reduction*: the title compound was prepared according to general procedure G using the methyl carbamate (104 mg, 0.48 mmol, 1 eq), LiAlH_4 (2 M THF solution, 0.39 mL, 0.77 mmol, 1.6 eq). Column chromatography (isocratic, 5% MeOH/DCM + 0.5% Et_3N) afforded the product (36 mg, 0.21 mmol, 44%). TLC: $R_f = 0.1$ (2% MeOH/DCM with 3 drops of Et_3N). ^1H NMR (500 MHz, CDCl_3) δ 7.28 – 7.20 (m, 2H), 7.19 – 7.10 (m, 2H), 2.92 – 2.74 (m, 4H), 2.66 – 2.52 (m, 1H), 2.45 (s, 3H). ^{13}C NMR (126 MHz, CDCl_3) δ 138.30, 132.03, 130.14, 128.66, 52.87, 36.12, 35.26. HRMS [$\text{C}_9\text{H}_{12}\text{ClN} + \text{H}$] $^+$: 170.0731 calculated, 170.0732 found.



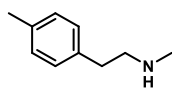
2-(3-Chlorophenyl)-N-methylethan-1-amine (121e). *Carbamoylation*: the methyl carbamate was prepared according to general procedure G using 2-(3-chlorophenyl)ethan-1-amine (70 μL , 0.40 mmol, 1 eq), methylchloroformate (58 μL , 0.75 mmol, 1.5 eq) and DiPEA (174 μL , 2.0 mmol, 2 eq). Column chromatography (20% -> 40% EtOAc/pentane) afforded the product (67 mg, 0.31 mmol, 78%). TLC: $R_f = 0.7$ (30% EtOAc/pentane). ^1H NMR (400 MHz, CDCl_3) δ 7.25 – 7.15 (m, 3H), 7.11 – 7.03 (m, 1H), 4.89 (br s, 1H), 3.65 (s, 3H), 3.41 (q, $J = 6.8$ Hz, 2H), 2.78 (t, $J = 7.1$ Hz, 2H). ^{13}C NMR (101 MHz, CDCl_3) δ 157.05, 140.94, 134.37, 129.90, 128.93, 127.04, 126.75, 52.15, 42.04, 35.90. HRMS [$\text{C}_{10}\text{H}_{12}\text{ClNO}_2 + \text{H}$] $^+$: 214.0629 calculated, 214.0630 found. *Carbamate reduction*: the title compound was prepared according to general procedure G using the methyl carbamate (67 mg, 0.31 mmol, 1 eq), LiAlH_4 (2 M THF solution, 0.250 mL, 0.50 mmol, 1.6 eq) and was used without further purification (33 mg,

0.14 mmol, 45%). $R_f = 0.15$ (6% MeOH/DCM). $^1\text{H NMR}$ (400 MHz, CDCl_3) δ 7.26 – 7.16 (m, 3H), 7.13 – 7.04 (m, 1H), 2.92 – 2.76 (m, 4H), 2.47 (s, 3H), 2.45 (br s, 1H). $^{13}\text{C NMR}$ (101 MHz, CDCl_3) δ 141.75, 134.40, 129.90, 128.92, 127.06, 126.63, 52.69, 36.06, 35.51. HRMS [$\text{C}_9\text{H}_{12}\text{ClN} + \text{H}$] $^+$: 170.0731 calculated, 170.0730 found.



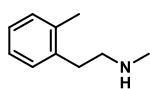
2-(2-Chlorophenyl)-N-methylethan-1-amine (121f). *Carbamoylation:* the methyl carbamate

was prepared according to general procedure G using 2-(2-chlorophenyl)ethan-1-amine (141 μL , 1.0 mmol, 1 eq), methylchloroformate (116 μL , 1.5 mmol, 1.5 eq) and DiPEA (0.35 mL, 2.0 mmol, 2 eq). Column chromatography (30% -> 50% EtOAc/pentane) afforded the product (183 mg, 0.85 mmol, 85%). TLC: $R_f = 0.7$ (50% EtOAc/pentane). $^1\text{H NMR}$ (400 MHz, CDCl_3) δ 7.39 – 7.30 (m, 1H), 7.25 – 7.12 (m, 3H), 4.94 (br s, 1H), 3.65 (s, 3H), 3.44 (q, $J = 6.7$ Hz, 2H), 2.95 (t, $J = 7.1$ Hz, 2H). $^{13}\text{C NMR}$ (101 MHz, CDCl_3) δ 157.10, 136.50, 134.17, 131.06, 129.65, 128.06, 126.97, 52.10, 40.67, 33.93. HRMS [$\text{C}_{10}\text{H}_{12}\text{ClNO}_2 + \text{H}$] $^+$: 214.0629 calculated, 214.0630 found ($\Delta = 0.14$ ppm). *Carbamate reduction:* the title compound was prepared according to general procedure G using the methyl carbamate (183 mg, 0.85 mmol, 1 eq), LiAlH_4 (2 M THF solution, 0.68 mL, 1.36 mmol, 1.6 eq) and was used without further purification (130 mg, 0.77 mmol, 91%). TLC: $R_f = 0.1$ (6% MeOH/DCM). $^1\text{H NMR}$ (400 MHz, CDCl_3) δ 7.38 – 7.26 (m, 1H), 7.26 – 7.08 (m, 3H), 3.02 – 2.73 (m, 4H), 2.50 – 2.26 (m, 4H). $^{13}\text{C NMR}$ (101 MHz, CDCl_3) δ 137.55, 134.08, 130.82, 129.58, 127.67, 126.81, 51.32, 36.18, 33.82. HRMS [$\text{C}_9\text{H}_{12}\text{ClN} + \text{H}$] $^+$: 170.0731 calculated, 170.0732 found.



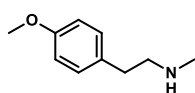
N-Methyl-2-(p-tolyl)ethan-1-amine (121g). *Carbamoylation:* the methyl carbamate was

prepared according to general procedure G using 2-(p-tolyl)ethan-1-amine (145 μL , 1.0 mmol, 1 eq), methylchloroformate (116 μL , 1.5 mmol, 1.5 eq) and DiPEA (0.35 mL, 2.0 mmol, 2 eq). Column chromatography (30% -> 50% EtOAc/pentane) afforded the product (198 mg, 1.0 mmol, 99%). TLC: $R_f = 0.7$ (50% EtOAc/pentane). $^1\text{H NMR}$ (400 MHz, CDCl_3) δ 7.18 – 6.91 (m, 4H), 5.02 (br s, 1H), 3.61 (s, 3H), 3.38 (q, $J = 6.8$ Hz, 2H), 2.74 (t, $J = 7.2$ Hz, 2H), 2.30 (s, 3H). $^{13}\text{C NMR}$ (101 MHz, CDCl_3) δ 157.00, 135.82, 135.66, 129.18, 128.55, 51.85, 42.26, 35.60, 20.91. HRMS [$\text{C}_{11}\text{H}_{15}\text{NO}_2 + \text{H}$] $^+$: 194.1176 calculated, 194.1176 found. *Carbamate reduction:* the title compound was prepared according to general procedure G using the methyl carbamate (198 mg, 1.0 mmol, 1 eq), LiAlH_4 (2 M THF solution, 0.80 mL, 1.0 mmol, 1.6 eq) and was used without further purification (130 mg, 0.87 mmol, 87%). TLC: $R_f = 0.2$ (5% MeOH/DCM). $^1\text{H NMR}$ (400 MHz, CDCl_3) δ 7.11 – 7.07 (m, 4H), 2.83 – 2.72 (m, 4H), 2.41 (s, 3H), 2.33 – 2.28 (m, 4H). $^{13}\text{C NMR}$ (101 MHz, CDCl_3) δ 136.87, 135.59, 129.17, 128.60, 80.66, 53.26, 36.28, 35.65, 21.02. HRMS [$\text{C}_{10}\text{H}_{15}\text{N} + \text{H}$] $^+$: 150.1277 calculated, 150.1277 found.



N-Methyl-2-(o-tolyl)ethan-1-amine (121h). *Carbamoylation:* the methyl carbamate was

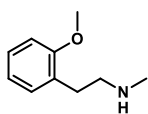
prepared according to general procedure G using 2-(o-tolyl)ethan-1-amine (70 μL , 0.50 mmol, 1 eq), methylchloroformate (58 μL , 0.75 mmol, 1.5 eq) and DiPEA (174 μL , 1.0 mmol, 2 eq). Column chromatography (30% -> 50% EtOAc/pentane) afforded the product (102 mg, 0.50 mmol, 99%). TLC: $R_f = 0.7$ (50% EtOAc/pentane). $^1\text{H NMR}$ (400 MHz, CDCl_3) δ 7.19 – 7.07 (m, 4H), 5.00 – 4.79 (m, 1H), 3.65 (s, 3H), 3.37 (q, $J = 6.9$ Hz, 2H), 2.81 (t, $J = 7.4$ Hz, 2H), 2.32 (s, 3H). $^{13}\text{C NMR}$ (101 MHz, CDCl_3) δ 157.12, 136.93, 136.37, 130.44, 129.34, 126.62, 126.11, 52.03, 41.16, 33.59, 19.29. HRMS [$\text{C}_{11}\text{H}_{15}\text{NO}_2 + \text{H}$] $^+$: 194.1176 calculated, 194.1176 found. *Carbamate reduction:* the title compound was prepared according to general procedure G using the methyl carbamate (102 mg, 0.50 mmol, 1 eq), LiAlH_4 (1 M THF solution, 0.85 mL, 0.85 mmol, 1.6 eq) and was used without further purification (74 mg, 0.50 mmol, 99%). TLC: $R_f = 0.1$ (6% MeOH/DCM). $^1\text{H NMR}$ (400 MHz, CDCl_3) δ 7.21 – 7.02 (m, 4H), 2.80 (s, 4H), 2.45 (s, 3H), 2.32 (s, 3H), 1.71 (br s, 1H). $^{13}\text{C NMR}$ (101 MHz, CDCl_3) δ 138.15, 136.21, 130.34, 129.25, 126.29, 126.01, 52.11, 36.44, 33.56, 19.42. HRMS [$\text{C}_{10}\text{H}_{15}\text{N} + \text{H}$] $^+$: 150.1277 calculated, 150.1277 found.



2-(4-Methoxyphenyl)-N-methylethan-1-amine (121i). *Carbamoylation:* the methyl

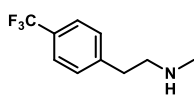
carbamate was prepared according to general procedure G using 2-(4-methoxyphenyl)ethan-1-amine (73 μL , 0.50 mmol, 1 eq), methylchloroformate (58 μL ,

0.75 mmol, 1.5 eq) and DiPEA (174 μ L, 1.0 mmol, 2 eq). Column chromatography (10% \rightarrow 40% EtOAc/pentane) afforded the product (108 mg, 0.50 mmol, 99%). TLC: R_f = 0.6 (50% EtOAc/pentane). ^1H NMR (400 MHz, CDCl_3) δ 7.09 (d, J = 8.5 Hz, 2H), 6.83 (d, 2H), 4.93 (br s, 1H), 3.77 (s, 3H), 3.63 (s, 3H), 3.38 (q, J = 6.8 Hz, 2H), 2.73 (t, J = 7.1 Hz, 2H). ^{13}C NMR (101 MHz, CDCl_3) δ 158.21, 157.04, 130.80, 129.69, 113.99, 55.21, 51.96, 42.42, 35.21. HRMS [$\text{C}_{11}\text{H}_{15}\text{NO}_3 + \text{H}$] $^+$: 210.1125 calculated, 210.1125 found. *Carbamate reduction*: the title compound was prepared according to general procedure G using the methyl carbamate (105 mg, 0.50 mmol, 1 eq), LiAlH_4 (2 M THF solution, 0.40 mL, 0.80 mmol, 1.6 eq) and was used without further purification (78 mg, 0.47 mmol, 94%). TLC: R_f = 0.1 (5% MeOH/DCM with 3 drops of Et_3N). ^1H NMR (400 MHz, CDCl_3) δ 7.17 – 7.05 (m, 2H), 6.87 – 6.77 (m, 2H), 3.77 (s, 3H), 2.87 – 2.65 (m, 4H), 2.49 – 2.19 (m, 4H). ^{13}C NMR (101 MHz, CDCl_3) δ 158.08, 132.00, 129.68, 113.96, 55.30, 53.37, 36.29, 35.18. HRMS [$\text{C}_{10}\text{H}_{15}\text{NO} + \text{H}$] $^+$: 166.1226 calculated, 166.1226 found.



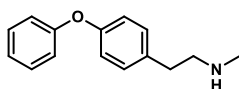
2-(2-Methoxyphenyl)-N-methylethan-1-amine (121j). *Carbamoylation*: the methyl carbamate was prepared according to general procedure G using 2-(2-methoxyphenyl)ethan-1-amine (145 μ L, 1.0 mmol, 1 eq), methylchloroformate (116 μ L, 1.5 mmol, 1.5 eq) and DiPEA (348 μ L, 2.0 mmol, 2 eq). Column chromatography (20% \rightarrow 40%

EtOAc/pentane) afforded the product (230 mg, 1.0 mmol, 99%). TLC: R_f = 0.5 (30% EtOAc/pentane). ^1H NMR (400 MHz, CDCl_3) δ 7.19 (td, J = 8.0, 1.7 Hz, 1H), 7.11 (d, J = 6.9 Hz, 1H), 6.94 – 6.78 (m, 2H), 5.19 – 4.71 (m, 1H), 3.79 (s, 3H), 3.61 (s, 3H), 3.39 (q, J = 6.6 Hz, 2H), 2.81 (t, J = 6.9 Hz, 2H). ^{13}C NMR (101 MHz, CDCl_3) δ 157.48, 157.04, 130.51, 127.75, 127.20, 120.51, 110.27, 55.14, 51.81, 41.08, 30.65. HRMS [$\text{C}_{11}\text{H}_{15}\text{NO}_3 + \text{H}$] $^+$: 210.1125 calculated, 210.1125 found. *Carbamate reduction*: the title compound was prepared according to general procedure G using the methyl carbamate (230 mg, 1.0 mmol, 1 eq), LiAlH_4 (1 M THF solution, 1.6 mL, 1.6 mmol, 1.6 eq) and was used without further purification (160 mg, 0.97 mmol, 97%). TLC: R_f = 0.3 (2% MeOH/DCM with 3 drops of Et_3N). ^1H NMR (400 MHz, CDCl_3) δ 7.24 – 7.07 (m, 2H), 6.95 – 6.74 (m, 2H), 3.80 (s, 3H), 2.90 – 2.70 (m, 4H), 2.43 (s, 3H), 1.26 (br s, 1H). ^{13}C NMR (101 MHz, CDCl_3) δ 157.59, 130.33, 128.44, 127.36, 120.39, 110.30, 55.20, 51.85, 36.37, 30.70. HRMS [$\text{C}_{10}\text{H}_{15}\text{NO} + \text{H}$] $^+$: 166.1226 calculated, 166.1225 found.



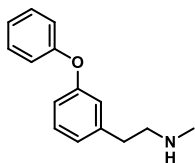
N-methyl-2-(4-(trifluoromethyl)phenyl)ethan-1-amine (121k). *Carbamoylation*: the methyl carbamate was prepared according to general procedure G using 2-(4-(trifluoromethyl)phenyl)ethan-1-amine (80 μ L, 0.50 mmol, 1 eq), methylchloroformate

(58 μ L, 0.75 mmol, 1.5 eq) and DiPEA (174 μ L, 1.0 mmol, 2 eq). Column chromatography (5% \rightarrow 40% EtOAc/pentane) afforded the product (113 mg, 0.45 mmol, 90%). TLC: R_f = 0.7 (50% EtOAc/pentane). ^1H NMR (400 MHz, CDCl_3) δ 7.56 (d, J = 8.0 Hz, 2H), 7.31 (d, J = 8.0 Hz, 2H), 4.89 – 4.64 (m, 1H), 3.66 (s, 3H), 3.45 (q, J = 6.7 Hz, 2H), 2.88 (t, J = 7.0 Hz, 2H). ^{13}C NMR (101 MHz, CDCl_3) δ 157.06, 143.06, 129.25, 128.82, 128.37, 125.62 (q, J = 3.8 Hz), 122.97, 52.25, 42.03, 36.14. HRMS [$\text{C}_{11}\text{H}_{12}\text{F}_3\text{NO}_2 + \text{H}$] $^+$: 248.0893 calculated, 248.0896 found. *Carbamate reduction*: the title compound was prepared according to general procedure G using the methyl carbamate (113 mg, 0.45 mmol, 1 eq), LiAlH_4 (2 M THF solution, 0.36 mL, 0.72 mmol, 1.6 eq). Column chromatography (isocratic, 5% MeOH/DCM + 0.5% Et_3N) afforded the product (40 mg, 0.20 mmol, 44%). TLC: R_f = 0.3 (2% MeOH/DCM with 3 drops of Et_3N). ^1H NMR (500 MHz, CDCl_3) δ 7.55 (d, J = 8.0 Hz, 2H), 7.34 (d, J = 7.9 Hz, 2H), 3.80 (br s, 1H), 2.99 – 2.91 (m, 4H), 2.51 (s, 3H). ^{13}C NMR (126 MHz, CDCl_3) δ 143.51, 129.13, 125.57 (q, J = 3.7 Hz), 125.41, 123.25, 52.36, 35.73, 35.29. HRMS [$\text{C}_{10}\text{H}_{12}\text{F}_3\text{N} + \text{H}$] $^+$: 204.0995 calculated, 204.0996 found.

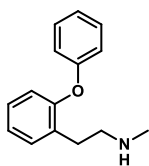


N-methyl-2-(4-phenoxyphenyl)ethan-1-amine (121l). *Carbamoylation*: the methyl carbamate was prepared according to general procedure G using 2-(4-phenoxyphenyl)ethan-1-amine TFA salt (211 mg, 0.64 mmol, 1 eq), methylchloroformate (74 μ L, 0.96 mmol, 1.5 eq) and DiPEA (245 μ L, 1.41 mmol, 2.2 eq). Column chromatography (10% \rightarrow 40% EtOAc/pentane) afforded the product (145 mg, 0.53 mmol, 83%). TLC: R_f = 0.8

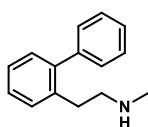
(100% EtOAc). ^1H NMR (400 MHz, CDCl_3) δ 7.40 – 7.27 (m, 2H), 7.22 – 7.04 (m, 3H), 7.03 – 6.89 (m, 4H), 4.96 – 4.65 (m, 1H), 3.65 (s, 3H), 3.51 – 3.29 (m, 2H), 2.77 (t, $J = 7.1$ Hz, 2H). ^{13}C NMR (101 MHz, CDCl_3) δ 157.36, 157.05, 155.85, 133.69, 130.06, 129.77, 123.20, 119.12, 118.76, 52.08, 42.36, 35.48. HRMS [$\text{C}_{16}\text{H}_{17}\text{NO}_3 + \text{H}$] $^+$: 272.1281 calculated, 272.1281 found. *Carbamate reduction*: the title compound was prepared according to general procedure G using the methyl carbamate (144 mg, 0.53 mmol, 1 eq), LiAlH_4 (2 M THF solution, 0.42 mL, 0.85 mmol, 1.6 eq). Column chromatography (isocratic, 5% MeOH/DCM + 0.5% Et_3N) afforded the product (65 mg, 0.29 mmol, 55%). TLC: $R_f = 0.1$ (5% MeOH/DCM with 3 drops of Et_3N). ^1H NMR (500 MHz, CDCl_3) δ 7.35 – 7.27 (m, 2H), 7.20 – 7.14 (m, 2H), 7.12 – 7.03 (m, 1H), 7.02 – 6.96 (m, 2H), 6.96 – 6.91 (m, 2H), 3.08 (br s, 1H), 2.92 – 2.80 (m, 4H), 2.48 (s, 3H). ^{13}C NMR (126 MHz, CDCl_3) δ 157.46, 155.65, 134.48, 130.01, 129.77, 123.15, 119.13, 118.73, 53.02, 36.00, 35.00. HRMS [$\text{C}_{15}\text{H}_{17}\text{NO} + \text{H}$] $^+$: 228.1383 calculated, 228.1385 found.



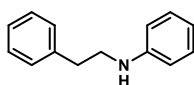
N-Methyl-2-(3-phenoxyphenyl)ethan-1-amine (121m). *Nitrile reduction*: A round-bottom flask was charged with nitrile **119a** (211 mg, 1.0 mmol, 1 eq), EtOH (5 mL) and 37% w/w aqueous HCl (0.16 mL, 2.0 mmol, 2 eq). N_2 was bubbled through the solution for 5 min and Pd/C (10% w/w, 52 mg, 50 μmol , 5 mol%) was added. The mixture was purged with N_2 and then with H_2 and was kept under H_2 atmosphere (balloon). After 50 h the reaction was complete as judged by TLC. The mixture was filtered over a Whatman filter, which was washed with EtOH and the filtrate was concentrated under reduced pressure. This afforded the primary amine (**120a**) as the HCl salt, which was used without further purification (246 mg, 0.98 mmol, 98%). TLC: $R_f = 0.05$ (6% MeOH/DCM). *Carbamoylation*: the methyl carbamate was prepared according to general procedure G using the primary amine **120a** (246 mg, 0.98 mmol, 1 eq), methylchloroformate (115 μL , 1.48 mmol, 1.5 eq) and DiPEA (517 μL , 3.0 mmol, 3 eq). Column chromatography (5% -> 40% EtOAc/pentane) afforded the product (176 mg, 0.65 mmol, 66%). TLC: $R_f = 0.3$ (10% EtOAc/pentane). *Carbamate reduction*: the title compound was prepared according to general procedure G using the methyl carbamate (170 mg, 0.62 mmol, 1 eq), LiAlH_4 (2 M THF solution, 0.52 mL, 1.04 mmol, 1.6 eq) and was used without further purification (125 mg, 0.55 mmol, 89%). TLC: $R_f = 0.1$ (6% MeOH/DCM). ^1H NMR (400 MHz, CDCl_3) δ 7.35 – 7.28 (m, 2H), 7.25 – 7.20 (m, 1H), 7.12 – 7.05 (m, 1H), 7.03 – 6.97 (m, 2H), 6.95 – 6.91 (m, 1H), 6.89 – 6.81 (m, 2H), 2.91 – 2.67 (m, 5H), 2.41 (s, 3H). ^{13}C NMR (101 MHz, CDCl_3) δ 157.45, 157.19, 142.10, 129.77, 129.74, 123.65, 123.26, 119.12, 118.94, 116.55, 52.94, 36.27, 35.99. HRMS [$\text{C}_{15}\text{H}_{17}\text{NO} + \text{H}$] $^+$: 228.1383 calculated, 228.1384 found.



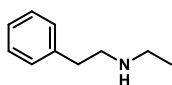
N-Methyl-2-(2-phenoxyphenyl)ethan-1-amine (121n). *Carbamoylation*: the methyl carbamate was prepared according to general procedure G using 2-(2-phenoxyphenyl)ethan-1-amine (99 μL , 0.50 mmol, 1 eq), methylchloroformate (58 μL , 0.75 mmol, 1.5 eq) and DiPEA (174 μL , 1.0 mmol, 2 eq). Column chromatography (20% -> 40% EtOAc/pentane) afforded the product (115 mg, 0.42 mmol, 84%). TLC: $R_f = 0.7$ (30% EtOAc/pentane). ^1H NMR (400 MHz, CDCl_3) δ 7.36 – 7.22 (m, 3H), 7.21 – 7.15 (m, 1H), 7.10 – 7.04 (m, 2H), 6.96 – 6.91 (m, 2H), 6.89 – 6.83 (m, 1H), 4.89 (br s, 1H), 3.62 (s, 3H), 3.44 (q, $J = 6.6$ Hz, 2H), 2.85 (t, $J = 6.9$ Hz, 2H). ^{13}C NMR (101 MHz, CDCl_3) δ 157.49, 157.08, 154.97, 131.27, 130.31, 129.85, 128.11, 123.97, 123.02, 119.26, 118.07, 52.05, 41.35, 30.73. HRMS [$\text{C}_{16}\text{H}_{17}\text{NO}_3 + \text{H}$] $^+$: 272.1281 calculated, 272.1281 found. *Carbamate reduction*: the title compound was prepared according to general procedure G using the methyl carbamate (115 mg, 0.42 mmol, 1 eq), LiAlH_4 (2 M THF solution, 0.34 mL, 0.67 mmol, 1.6 eq). Column chromatography (4% -> 7% MeOH/DCM + 0.5% Et_3N) afforded the product (72 mg, 0.32 mmol, 76%). TLC: $R_f = 0.3$ (4% MeOH/DCM with 3 drops of Et_3N). ^1H NMR (400 MHz, CDCl_3) δ 7.34 – 7.23 (m, 3H), 7.18 (td, $J = 7.8$, 1.7 Hz, 1H), 7.11 – 7.01 (m, 2H), 6.97 – 6.83 (m, 3H), 3.04 (br s, 1H), 2.87 (s, 4H), 2.42 (s, 3H). ^{13}C NMR (101 MHz, CDCl_3) δ 157.79, 154.81, 131.17, 131.12, 129.80, 127.88, 123.99, 122.82, 119.58, 117.88, 51.55, 35.80, 30.23. HRMS [$\text{C}_{15}\text{H}_{17}\text{NO} + \text{H}$] $^+$: 228.1383 calculated, 228.1383 found.



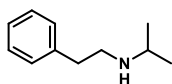
2-([1,1'-Biphenyl]-2-yl)-N-methylethan-1-amine (121o). *Nitrile reduction:* a round-bottom flask was charged with nitrile **119b** (195 mg, 1.0 mmol, 1 eq), EtOH (5 mL) and 37% w/w aqueous HCl (0.16 mL, 2.0 mmol, 2 eq). N₂ was bubbled through the solution for 5 min and Pd/C (10% w/w, 52 mg, 50 μmol, 5 mol%) was added. The mixture was purged with N₂ and then with H₂ and was kept under an H₂ atmosphere (balloon). After 3.5 days the reaction was complete as judged by TLC. The mixture was filtered over a Whatman filter and the filtrate was concentrated under reduced pressure to afford the primary amine (**120b**) as the HCl salt, which was used without further purification (235 mg, 1.0 mmol, 99%). TLC: R_f = 0.15 (6% MeOH/DCM). *Carbamoylation:* the methyl carbamate was prepared according to general procedure G using the amine HCl salt **120b** (235 mg, 1.0 mmol, 1 eq), methylchloroformate (116 μL, 1.5 mmol, 1.5 eq) and DiPEA (522 μL, 3.0 mmol, 3 eq). Column chromatography (10% → 40% EtOAc/pentane) afforded the product (210 mg, 0.82 mmol, 82%). TLC: R_f = 0.5 (20% EtOAc/pentane). ¹H NMR (400 MHz, CDCl₃) δ 7.48 – 7.16 (m, 9H), 4.86 – 4.47 (m, 1H), 3.56 (s, 3H), 3.28 – 3.08 (m, 2H), 2.79 (t, J = 7.2 Hz, 2H). ¹³C NMR (101 MHz, CDCl₃) δ 156.89, 142.40, 141.50, 136.16, 130.32, 129.68, 129.19, 128.26, 127.64, 127.05, 126.46, 51.98, 41.83, 33.26. HRMS [C₁₆H₁₇NO₂ + H]⁺: 256.1332 calculated, 256.1333 found. *Carbamate reduction:* the title compound was prepared according to general procedure G using the methyl carbamate (210 mg, 0.82 mmol, 1 eq), LiAlH₄ (2 M THF solution, 0.66 mL, 1.32 mmol, 1.6 eq) and was used without further purification (157 mg, 0.74 mmol, 90%). TLC: R_f = 0.3 (6% MeOH/DCM). ¹H NMR (400 MHz, CDCl₃) δ 7.42 – 7.36 (m, 2H), 7.35 – 7.19 (m, 7H), 2.83 – 2.73 (m, 2H), 2.70 – 2.58 (m, 2H), 2.26 (s, 3H), 2.11 (br s, 1H). ¹³C NMR (101 MHz, CDCl₃) δ 142.24, 141.70, 137.29, 130.25, 129.56, 129.22, 128.16, 127.50, 126.93, 126.13, 52.77, 36.06, 33.16. HRMS [C₁₅H₁₇N + H]⁺: 212.1434 calculated, 212.1434 found.



N-Phenethylamine (122). A round-bottom flask under N₂ atmosphere was charged with phenylboronic acid (0.49 g, 4.0 mmol, 2 eq), Cu(OAc)₂·H₂O (40 mg, 0.2 mmol, 0.1 eq), powdered 4 Å molecular sieves (1.5 g) and dry DCE (16 mL). The suspension was stirred for 5 minutes at room temperature followed by addition of 2-phenethylamine (0.25 mL, 2.0 mmol, 1 eq). The blue mixture was purged using a balloon of O₂ causing a color shift to purple and stirred under an O₂ atmosphere for 26 h. The mixture was then filtered through a plug of Celite and concentrated under reduced pressure. The residue was purified by silica gel column chromatography (2% → 8% EtOAc/pentane) affording the product (127 mg, 0.64 mmol, 32%). TLC: R_f = 0.6 (5% EtOAc/pentane). ¹H NMR (400 MHz, CDCl₃) δ 7.34 – 7.25 (m, 2H), 7.24 – 7.12 (m, 5H), 6.74 – 6.66 (m, 1H), 6.61 – 6.54 (m, 2H), 3.63 (br s, 1H), 3.36 (t, J = 7.1 Hz, 2H), 2.87 (t, J = 7.0 Hz, 2H). ¹³C NMR (101 MHz, CDCl₃) δ 148.06, 139.38, 129.35, 128.86, 128.67, 126.48, 117.50, 113.04, 45.08, 35.55. HRMS [C₁₄H₁₅N + H]⁺: 198.1277 calculated, 198.1275 found.

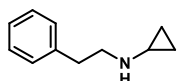


N-Ethyl-2-phenylethan-1-amine (123a). A round-bottom flask was charged with acetaldehyde (56 μL, 1.0 mmol, 1 eq), 2-phenethylamine (189 μL, 1.5 mmol, 1.5 eq) and dry DCM (10 mL). The solution was stirred at room temperature for 10 minutes and then NaBH(OAc)₃ (424 mg, 2 mmol, 2 eq) was added. After 16 h the reaction was complete as judged by TLC. The mixture was diluted with DCM (20 mL), washed with sat. aq. NaHCO₃ (1 x 30 mL), brine (1 x 30 mL), dried (MgSO₄), filtered and concentrated under reduced pressure. The residue was purified by silica gel column chromatography (5% → 7% MeOH/DCM with 0.5% Et₃N) affording the product (27 mg, 0.18 mmol, 18%). TLC: R_f = 0.3 (6% MeOH/DCM). ¹H NMR (400 MHz, CDCl₃) δ 7.34 – 7.24 (m, 2H), 7.24 – 7.16 (m, 3H), 2.96 – 2.77 (m, 4H), 2.68 (q, J = 7.1 Hz, 2H), 1.10 (t, J = 7.2 Hz, 3H). ¹³C NMR (101 MHz, CDCl₃) δ 140.14, 128.83, 128.59, 126.27, 51.11, 46.98, 44.09, 15.24. HRMS [C₁₀H₁₅N + H]⁺: 150.1277 calculated, 150.1277 found.



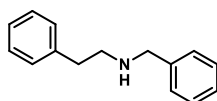
N-phenethylpropan-2-amine (123b). A round-bottom flask was charged with NaBH₄ (218 mg, 5.8 mmol, 1.9 eq) and dry DCM (5 mL). The solution was stirred in an ice bath for 3 minutes and glacial acetic acid (1 mL, 14.4 mmol, 5.8 eq) was added. The mixture was stirred for 1 h at 0 °C and 30 minutes at room temperature. Separately, a solution of 2-phenethylamine

(0.38 mL, 3.0 mmol, 1 eq) was prepared in dry DCM (2.5 mL) and acetone (198 μ L, 2.7 mmol, 0.9 eq). This solution was added dropwise to the NaBH(OAc)₃ mixture and was stirred at rt overnight. After 20 hours the reaction mixture was acidified to pH 2 with 0.1 M HCl (aq.) and washed with DCM (2 x 30 mL) to remove by-products. Then, the solution was basified with 1 M NaOH (aq.) until pH 10 and extracted with DCM (3 x 50 mL). The combined organic layers were dried (Na₂SO₄), filtered, concentrated under reduced pressure and the residue was purified by silica gel column chromatography (isocratic, 0.5% Et₃N/EtOAc) to provide the product (277 mg, 1.7 mmol, 57%). TLC: R_f = 0.3 (100% EtOAc with 3 drops of Et₃N). ¹H NMR (400 MHz, CDCl₃) δ 7.30 – 7.23 (m, 2H), 7.22 – 7.14 (m, 3H), 2.88 – 2.82 (m, 2H), 2.81 – 2.74 (m, 3H), 1.08 (br s, 1H), 1.03 (d, *J* = 6.4 Hz, 6H). ¹³C NMR (101 MHz, CDCl₃) δ 139.98, 128.52, 128.28, 125.95, 48.70, 48.38, 36.48, 22.80. HRMS [C₁₁H₁₇N + H]⁺: 164.1434 calculated, 164.1434 found.



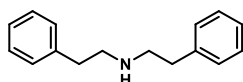
N-Phenethylcyclopropanamine (123c). A round-bottom flask was charged with phenylacetaldehyde (125 μ L, 1.0 mmol, 1 eq), cyclopropanamine (139 μ L, 2.0 mmol, 2 eq) and dry DCM (5 mL). The solution was stirred at room temperature for 10 minutes and

then NaHB(OAc)₃ (0.43 g, 2.0 mmol, 2 eq) and glacial AcOH (114 μ L, 2.0 mmol, 2 eq) were added. After 21 h the reaction mixture was diluted with DCM (10 mL), washed with sat. aq. NaHCO₃ (1 x 15 mL), brine (1 x 15 mL), dried (Na₂SO₄), filtered and concentrated under reduced pressure. The residue was purified by silica gel column chromatography (30% -> 50% EtOAc/pentane with 0.5% Et₃N) affording the product (85 mg, 0.53 mmol, 53%), R_f = 0.1 (6% MeOH/DCM). ¹H NMR (400 MHz, CDCl₃) δ 7.42 – 7.07 (m, 5H), 3.01 – 2.93 (m, 2H), 2.80 (t, *J* = 7.2 Hz, 2H), 2.26 – 2.02 (m, 2H), 0.47 – 0.40 (m, 2H), 0.37 – 0.31 (m, 2H). ¹³C NMR (101 MHz, CDCl₃) δ 140.23, 128.78, 128.54, 126.19, 50.84, 36.37, 30.24, 6.33. HRMS [C₁₁H₁₅N + H]⁺: 162.1277 calculated, 162.1277 found.



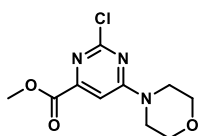
N-Benzyl-2-phenylethan-1-amine (123d). A round-bottom flask was charged with phenylacetaldehyde (125 μ L, 1.0 mmol, 1 eq), benzylamine (218 μ L, 2.0 mmol, 2 eq) and DCM (10 mL). The solution was stirred at room temperature for 3 minutes and then NaHB(OAc)₃ (0.42 g, 2.0 mmol, 2 eq) and glacial AcOH (114 μ L, 2 mmol, 2 eq)

were added. After 18 h the reaction mixture was diluted with DCM (20 mL), washed with sat. aq. NaHCO₃ (1 x 30 mL), brine (1 x 30 mL), dried (Na₂SO₄), filtered and concentrated under reduced pressure. The residue was purified by silica gel column chromatography with (4% -> 5% MeOH/DCM with 0.5% Et₃N) affording the product (125 mg, 0.59 mmol, 59%). TLC: R_f = 0.4 (5% MeOH/DCM with 3 drops of Et₃N). ¹H NMR (400 MHz, CDCl₃) δ 7.31 – 7.21 (m, 7H), 7.21 – 7.17 (m, 3H), 3.77 (s, 2H), 2.91 – 2.85 (m, 2H), 2.84 – 2.78 (m, 2H), 1.97 (br s, 1H). ¹³C NMR (101 MHz, CDCl₃) δ 140.21, 140.04, 128.77, 128.51, 128.44, 128.15, 126.98, 126.20, 53.88, 50.57, 36.36.

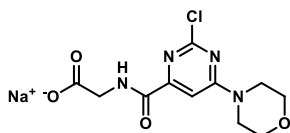


Diphenethylamine (123e). A round-bottom flask was charged with phenylacetaldehyde (125 μ L, 1.0 mmol, 1 eq), 2-phenethylamine (251 μ L, 2.0 mmol, 2 eq) and dry DCM (5 mL). The solution was stirred for 10 minutes and then

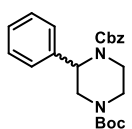
NaHB(OAc)₃ (0.43 g, 2.0 mmol, 2 eq) and glacial AcOH (114 μ L, 2.0 mmol, 2 eq) were added. After 19 h the reaction mixture was diluted with DCM (5 mL), washed with sat. aq. NaHCO₃ (1 x 10 mL), brine (1 x 10 mL), dried (Na₂SO₄), filtered and concentrated under reduced pressure. The residue was purified by silica gel column chromatography (isocratic, 5% MeOH/DCM with 0.5% Et₃N) affording the product (128 mg, 0.57 mmol, 57%). TLC: R_f = 0.3 (6% MeOH/DCM with 3 drops of Et₃N). ¹H NMR (400 MHz, CDCl₃) δ 7.73 – 6.67 (m, 10H), 3.05 – 2.61 (m, 8H), 1.96 (br s, 1H). ¹³C NMR (101 MHz, CDCl₃) δ 139.91, 128.67, 128.45, 126.12, 51.00, 36.25. HRMS [C₁₆H₁₉N + H]⁺: 226.1590 calculated, 226.1591 found.



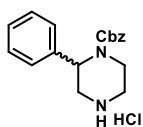
Methyl 2-chloro-6-morpholinopyrimidine-4-carboxylate (125). The title compound was prepared according to general procedure E using methyl 2,6-dichloropyrimidine-4-carboxylate (**124**) (0.62 g, 3.0 mmol, 1 eq), DiPEA (0.78 mL, 4.5 mmol, 1.5 eq) and morpholine (0.27 mL, 3.15 mmol, 1.05 eq). Column chromatography (40% → 60% EtOAc/pentane) afforded the product (0.69 g, 2.7 mmol, 90%). TLC: $R_f = 0.3$ (50% EtOAc/pentane). ^1H NMR (400 MHz, CDCl_3) δ 7.19 (s, 1H), 3.96 (s, 3H), 3.91 – 3.55 (m, 8H). ^{13}C NMR (101 MHz,) δ 163.80, 163.09, 160.65, 155.10, 101.89, 65.83, 52.84, 44.18. HRMS [$\text{C}_{10}\text{H}_{12}\text{ClN}_3\text{O}_3 + \text{H}$] $^+$: 258.0640 calculated, 258.0638 found.



Sodium (2-chloro-6-morpholinopyrimidine-4-carbonyl) glycinate (128). A round-bottom flask was charged with methyl ester **117h** (0.27 g, 0.85 mmol, 1 eq) in 5 mL THF/MeOH (4:1, v/v). A 1.5 M aqueous NaOH solution (0.57 mL, 0.85 mmol, 1 eq) was added together with 0.43 mL H_2O . The reaction was stirred overnight at rt after which the solvents were evaporated yielding the product which was used without further purification (0.27 g, 0.85 mmol, quant.). TLC: $R_f = 0.2$ (5% MeOH/DCM). ^1H NMR (400 MHz, MeOD) δ 7.30 (s, 1H), 3.95 – 3.86 (m, 2H), 3.81 – 3.65 (m, 8H). ^{13}C NMR (101 MHz, MeOD) δ 180.70, 159.60, 159.40, 158.60, 152.43, 99.06, 65.99, 43.24. HRMS [$\text{C}_{11}\text{H}_{13}\text{ClN}_4\text{O}_4 + \text{H}$] $^+$: 301.0698 calculated, 301.0696 found.



(±)-1-Benzyl 4-(tert-butyl) 2-phenylpiperazine-1,4-dicarboxylate (129). A round-bottom flask was charged with *tert*-butyl 3-phenylpiperazine-1-carboxylate (0.29 g, 1.1 mmol, 1 eq), NaHCO_3 (0.46 g, 5.5 mmol, 5 eq) in THF/ H_2O (8 mL, 1:1). The mixture was cooled to 0 °C and CbzCl (189 μL , 1.3 mmol, 1.2 eq) was added dropwise. The reaction mixture was allowed to warm to room temperature and stirred for 1.5 h. The mixture was extracted with EtOAc (3 x 20 mL), the combined organic layers were washed with brine (50 mL), dried (Na_2SO_4), filtered and concentrated under reduced pressure. The residue was purified by silica gel column chromatography (5% → 40% EtOAc/pentane) affording the product (0.40 g, 1.0 mmol, 91%). TLC: $R_f = 0.4$ (20% EtOAc/pentane). ^1H NMR (400 MHz, CDCl_3) δ 7.55 – 7.04 (m, 10H), 5.36 (br s, 1H), 5.27 – 5.12 (m, 2H), 4.50 (d, $J = 13.9$ Hz, 1H), 4.13 – 3.68 (m, 2H), 3.33 (dd, $J = 14.0, 4.3$ Hz, 1H), 3.19 – 2.79 (m, 2H), 1.42 (s, 9H). ^{13}C NMR (101 MHz, CDCl_3) δ 155.77, 154.43, 138.40, 136.48, 128.66, 128.61, 128.21, 128.00, 127.39, 126.88, 80.32, 67.64, 54.15, 46.04, 42.81, 39.80, 28.42. HRMS [$\text{C}_{23}\text{H}_{28}\text{N}_2\text{O}_4 + \text{Na}$] $^+$: 419.1941 calculated, 419.1934 found.

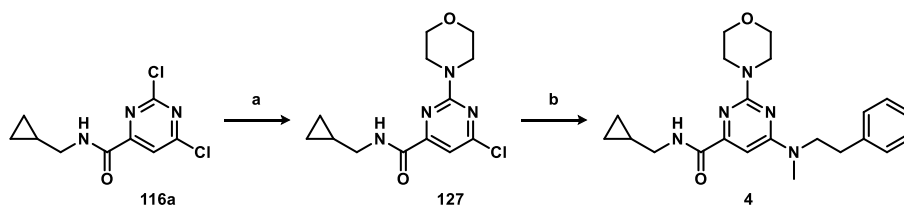


(±)-Benzyl 2-phenylpiperazine-1-carboxylate hydrochloride (130). A round-bottom flask was charged with Boc-protected amine **129** (103 mg, 0.26 mmol, 1 eq) and HCl (4 M solution in 1,4-dioxane, 1 mL, 4.0 mmol, 15.5 eq) and the reaction was stirred at rt. After 1 h the reaction was concentrated under reduced pressure to afford the product as the hydrochloride salt (87 mg, 0.26 mmol, 99%). TLC: $R_f = 0.3$ (50% EtOAc/pentane). ^1H NMR (400 MHz, CDCl_3) δ 10.24 (br s, 1H), 9.33 – 8.80 (m, 1H), 7.51 – 7.02 (m, 10H), 5.55 (br s, 1H), 5.29 – 4.95 (m, 2H), 4.22 (d, $J = 14.1$ Hz, 1H), 3.99 – 3.77 (m, 1H), 3.49 – 3.22 (m, 3H), 3.06 (br s, 1H). ^{13}C NMR (101 MHz, CDCl_3) δ 155.26, 135.78, 135.54, 129.31, 128.64, 128.42, 128.28, 128.11, 126.34, 68.19, 51.77, 44.38, 42.59, 36.98.

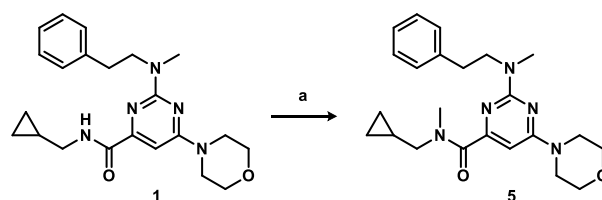
References

- Hussain, Z., Uyama, T., Tsuboi, K. & Ueda, N. Mammalian enzymes responsible for the biosynthesis of *N*-acylethanolamines. *Biochimica et Biophysica Acta (BBA) - Molecular and Cell Biology of Lipids* **1862**, 1546-1561 (2017).

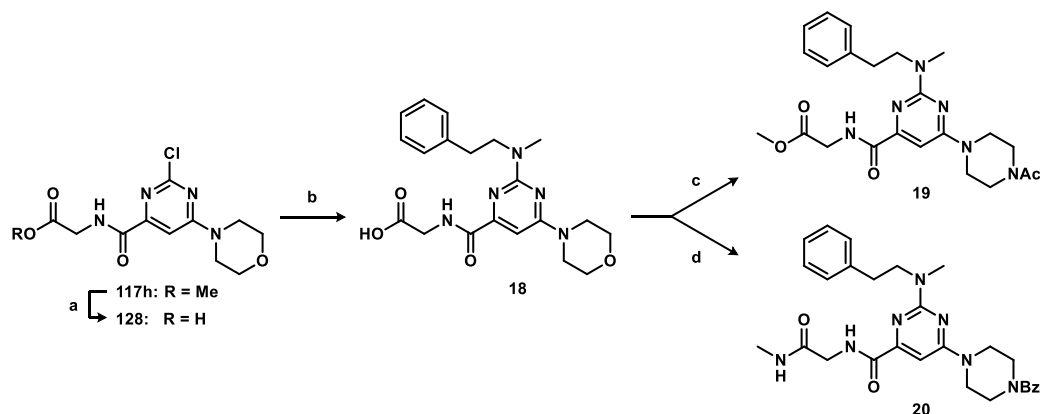
2. Okamoto, Y., Morishita, J., Tsuboi, K., Tonai, T. & Ueda, N. Molecular characterization of a phospholipase D generating anandamide and its congeners. *Journal of Biological Chemistry* **279**, 5298-5305 (2004).
3. Maccarrone, M. Metabolism of the endocannabinoid anandamide: open questions after 25 years. *Frontiers in Molecular Neuroscience* **10** (2017).
4. Leung, D., Saghatelian, A., Simon, G.M. & Cravatt, B.F. Inactivation of *N*-acyl phosphatidylethanolamine phospholipase D reveals multiple mechanisms for the biosynthesis of endocannabinoids. *Biochemistry* **45**, 4720-4726 (2006).
5. Simon, G.M. & Cravatt, B.F. Characterization of mice lacking candidate *N*-acyl ethanolamine biosynthetic enzymes provides evidence for multiple pathways that contribute to endocannabinoid production *in vivo*. *Molecular BioSystems* **6**, 1411-1418 (2010).
6. Tsuboi, K., Okamoto, Y., Ikematsu, N., Inoue, M., Shimizu, Y., Uyama, T., Wang, J., Deutsch, D.G., Burns, M.P., Ulloa, N.M., Tokumura, A. & Ueda, N. Enzymatic formation of *N*-acylethanolamines from *N*-acylethanolamine plasmalogen through *N*-acylphosphatidylethanolamine-hydrolyzing phospholipase D-dependent and -independent pathways. *Biochimica et Biophysica Acta (BBA) - Molecular and Cell Biology of Lipids* **1811**, 565-577 (2011).
7. Leishman, E., Mackie, K., Luquet, S. & Bradshaw, H.B. Lipidomics profile of a NAPE-PLD KO mouse provides evidence of a broader role of this enzyme in lipid metabolism in the brain. *Biochimica et Biophysica Acta (BBA) - Molecular and Cell Biology of Lipids* **1861**, 491-500 (2016).
8. Blankman, J.L. & Cravatt, B.F. Chemical probes of endocannabinoid metabolism. *Pharmacological Reviews* **65**, 849-871 (2013).
9. Petersen, G., Pedersen, A.H., Pickering, D.S., Begtrup, M. & Hansen, H.S. Effect of synthetic and natural phospholipids on *N*-acylphosphatidylethanolamine-hydrolyzing phospholipase D activity. *Chemistry and Physics of Lipids* **162**, 53-61 (2009).
10. Scott, S.A., Spencer, C.T., O'Reilly, M.C., Brown, K.A., Lavieri, R.R., Cho, C.-H., Jung, D.-I., Larock, R.C., Brown, H.A. & Lindsley, C.W. Discovery of desketoraloxifene analogues as inhibitors of mammalian, *Pseudomonas aeruginosa*, and NAPE phospholipase D enzymes. *ACS Chemical Biology* **10**, 421-432 (2015).
11. Castellani, B., Diamanti, E., Pizzirani, D., Tardia, P., Maccesi, M., Realini, N., Magotti, P., Garau, G., Bakkum, T., Rivara, S., Mor, M. & Piomelli, D. Synthesis and characterization of the first inhibitor of *N*-acylphosphatidylethanolamine phospholipase D (NAPE-PLD). *Chemical Communications* **53**, 12814-12817 (2017).
12. Bruno, N.C., Tudge, M.T. & Buchwald, S.L. Design and preparation of new palladium precatalysts for C–C and C–N cross-coupling reactions. *Chemical Science* **4**, 916-920 (2013).
13. Quach, T.D. & Batey, R.A. Ligand- and base-free copper(II)-catalyzed C–N bond formation: cross-coupling reactions of organoboron compounds with aliphatic amines and anilines. *Organic Letters* **5**, 4397-4400 (2003).
14. Talele, T.T. The “cyclopropyl fragment” is a versatile player that frequently appears in preclinical/clinical drug molecules. *Journal of Medicinal Chemistry* **59**, 8712-8756 (2016).
15. Lipinski, C.A., Lombardo, F., Dominy, B.W. & Feeney, P.J. Experimental and computational approaches to estimate solubility and permeability in drug discovery and development settings. *Adv. Drug Deliv. Rev.* **23**, 3-25 (1997).
16. Veber, D.F., Johnson, S.R., Cheng, H.-Y., Smith, B.R., Ward, K.W. & Kopple, K.D. Molecular properties that influence the oral bioavailability of drug candidates. *Journal of Medicinal Chemistry* **45**, 2615-2623 (2002).
17. Hitchcock, S.A. & Pennington, L.D. Structure–brain exposure relationships. *Journal of Medicinal Chemistry* **49**, 7559-7583 (2006).

Supplementary Information


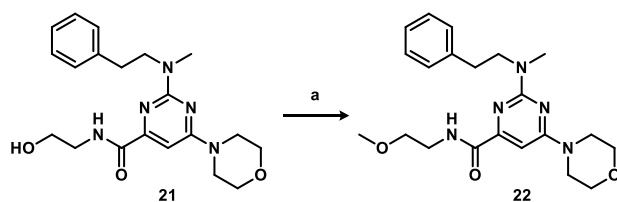
Supplementary Scheme 1. Synthesis of pyrimidine regioisomer **4**. Reagents and conditions: a) morpholine, DiPEA, MeOH, 0 °C, 5% (+ 89% regioisomer **28**); b) *N*-methylphenethylamine, DiPEA, MeOH, 70 °C, 71%.



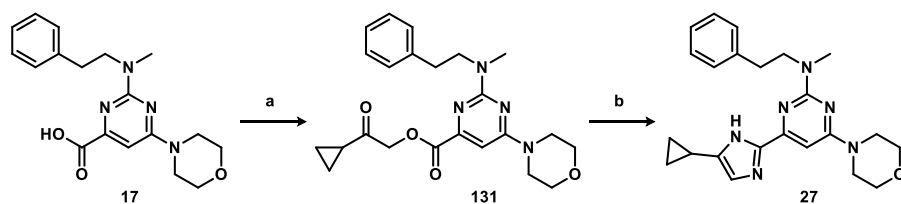
Supplementary Scheme 2. Synthesis of R₁ cyclopropylmethylamine analogue **5**. Reagents and conditions: a) NaH, MeI, DMF, 0 °C to rt, 44%.



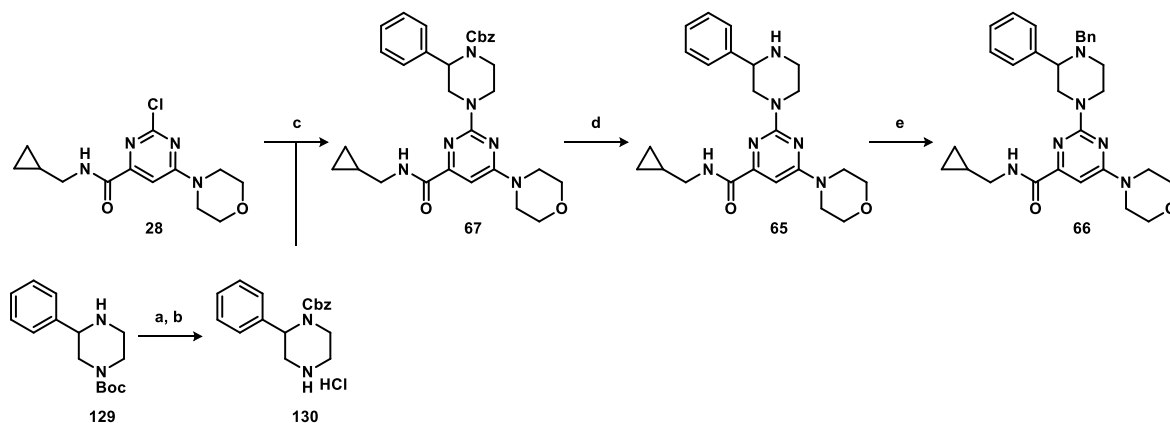
Supplementary Scheme 3. Synthesis of R₁ cyclopropylmethylamine analogues **18-20**. Reagents and conditions: a) NaOH, THF, MeOH, H₂O, rt, 99%; b) *N*-methylphenethylamine, DiPEA, *n*-BuOH, 120 °C, 20%; c) EDC·HCl, HOBT, MeOH, DCM, rt, 62%; d) MeNH₂·HCl, PyBOP, DiPEA, DMF, 50%.



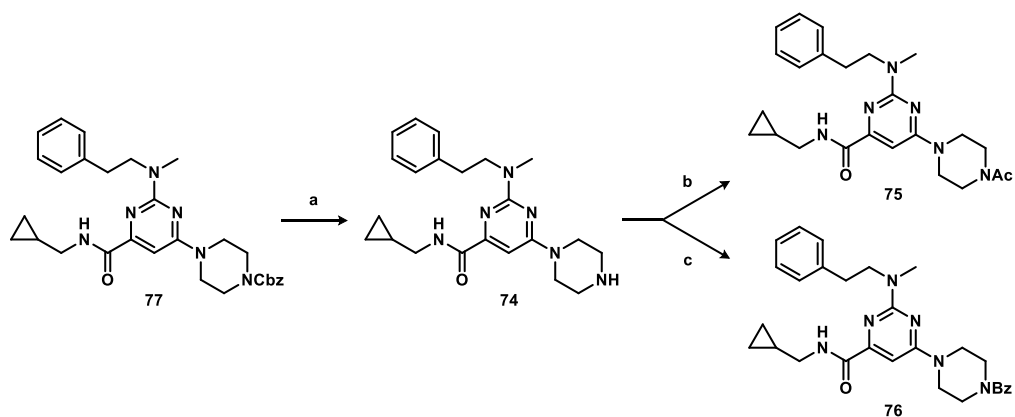
Supplementary Scheme 4. Synthesis of R₁ cyclopropylmethylamine analogue **22**. Reagents and conditions: a) NaOtBu, MeI, DMF, 0 °C to rt, 30%.



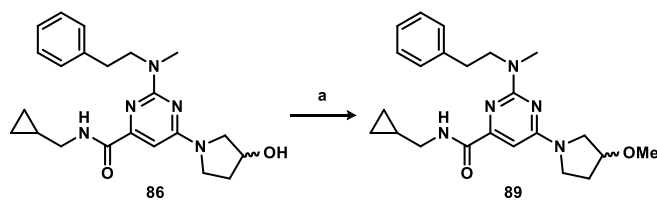
Supplementary Scheme 5. Synthesis of R₁ cyclopropylmethylamine analogue **27**. Reagents and conditions: a) 2-bromocyclopropylethanone, Cs₂CO₃, DMF, rt, 53%; b) NH₄OAc, xylene, 140 °C, 6%.



Supplementary Scheme 6. Synthesis of R₂ 3-phenylpiperazine analogues **65-67**. Reagents and conditions: a) CbzCl, NaHCO₃, THF, H₂O, 0 °C to rt, 91%; b) 4 M HCl, 1,4-dioxane, rt, 99%; c) **130**, DiPEA, *n*-BuOH, 120 °C, 99%; d) Pd/C, H₂, MeOH, rt, 90%; e) BnBr, DiPEA, CH₃CN, rt, 73%.



Supplementary Scheme 7. Synthesis of R₃ morpholine analogue **74-76**. Reagents and conditions: a) Pd/C, H₂, MeOH, AcOH, rt, 64%; b) Ac₂O, DiPEA, DCM, rt, 79%; c) BzCl, Et₃N, DCM, rt, 71%.



Supplementary Scheme 8. Synthesis of R₃ morpholine analogue **89**. Reagents and conditions: a) NaH, MeI, DMF, 0 °C to rt, 44%.

Chapter 4

Photoaffinity probes for NAPE-PLD confirm LEI-401 target engagement

4.1 Introduction

Proof of target engagement is an important checkpoint in drug discovery.¹ Confirmation of the physical interaction between the drug candidate and the protein of interest in a biological setting, preferably in cells or in live animals, in combination with the desired phenotypic effect, validates the proposed mode of action of the drug and its intended target.² This speeds up the clinical translation of drug development, as full target engagement with the absence of a therapeutic effect will dismiss a drug for the intended disease indication. In practice, establishing such a binding event *in vivo* is oftentimes a difficult task. The costly failure of clinical candidates in Phase II and Phase III clinical trials has been attributed to a lack of efficacy, which in certain cases was accompanied by the inability to show engagement of the intended targets.³

The emergence of the field of chemical biology in combination with the technical advancement of tandem mass spectrometry, has drastically improved and facilitated target engagement studies.⁴ In particular, activity based protein profiling (ABPP) and

photoaffinity labeling (PAL) are complementary techniques well suited to obtain ligand-protein binding information in cellular systems and living organisms.⁵ ABPP takes advantage of the catalytic nucleophile of an enzyme to form an irreversible bond with an electrophilic chemical probe containing a ligation handle, which enables affinity purification and protein identification. Using competition experiments this has allowed validation of target engagement of drug candidates in several classes of enzymes including, amongst others, proteases, serine hydrolases and glycosidases.⁵⁻⁹ In addition, the off-target landscape of a drug candidate within an enzyme family can be profiled using ABPP, providing important selectivity information.^{10,11} A critical requirement of ABPP is that targeted enzymes form a covalent bond with their substrates and the active-site catalytic nucleophile, which is not the case for enzyme classes such as metallohydrolases.¹² Consequently, photoaffinity labeling has come to the foreground, as it can be applied to the complete proteome, even including proteins that do not possess any enzymatic activity.¹³ This advantage has led to many new applications for PAL such as target identification of natural products^{14,15} and small molecules¹⁶, their protein binding site¹⁷, lipid-protein^{18,19} as well as protein-protein interactions²⁰.

Photoaffinity labeling utilizes a photoreactive group instead of an electrophile, that can be converted into a highly reactive intermediate with UV irradiation, thereby irreversibly inserting itself into side chain or backbone residues of the bound protein.¹² Analogous to ABPP, PAL probes contain an affinity group for optimal binding to the intended target and a ligation handle for click chemistry. The diazirine group has become a preferred photocrosslinker in recent years owing to its small size and its highly reactive, short-lived (~ 1 ns) singlet carbene intermediate which can insert into O-H, N-H and C-H bonds (Figure 1).²¹⁻²³ Furthermore, diazirines require low energy UV light (> 350 nm) for their photoactivation, minimizing damage to biological samples. Of note, labeling efficiencies of

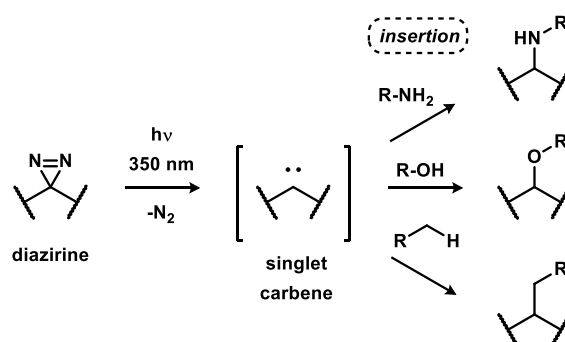


Figure 1. Photoactivation of diazirines with low-energy UV light generates a short-lived singlet carbene species that can insert into side chain or backbone residues of proteins.

small aliphatic diazirines with β -hydrogens are reduced compared to the bulkier trifluoromethylaryldiazirine, due to a competing 1,2-hydride shift side reaction which converts the carbene into an alkene.²⁴ The biological systems used for PAL at first predominantly consisted of purified proteins and lysates. Thanks to advances in bioorthogonal chemistry techniques (e.g. click chemistry), experiments have seen a shift towards intact cell settings.²⁵ Importantly, whole cells better imitate relevant physiological conditions, as factors such as protein localization, drug cellular permeability and biodistribution are taken into account, essential for establishing target engagement. A typical live cell PAL experiment is depicted in Figure 2. Cells are treated with a photoaffinity probe that will bind to its protein partners. A competitor, for example, a drug candidate on which the PAL probe is based, can be pre-incubated to reversibly compete out the probe from the binding site. Upon photoirradiation the photoprobe will covalently bind to the protein binding site, thereby making a snapshot of the cellular probe-target binding equilibrium. Lysis of the cells, followed by attachment of a fluorophore or biotin handle via click chemistry, allows identification of the targeted proteins and can demonstrate target engagement by the competing drug candidate. PAL probes have successfully been used to target a growing list of proteins, which include metalloproteases²⁶, kinases²⁷, γ -secretase²⁸, methyltransferases²⁹, GPCRs³⁰, and histone deacylases³¹. Currently, the required UV irradiation for activation of the photoreactive groups, limits the use of PAL in whole organisms as a result of the restricted tissue penetration of UV light. Recent studies in translucent zebrafish³² as well as intracranial photoactivation in mice using a fiber-optic cable³³, further increase the scope of PAL for *in vivo* use.

In this chapter, the development of photoaffinity probes for the enzyme *N*-acylphosphatidylethanolamine phospholipase D (NAPE-PLD) is described. NAPE-PLD

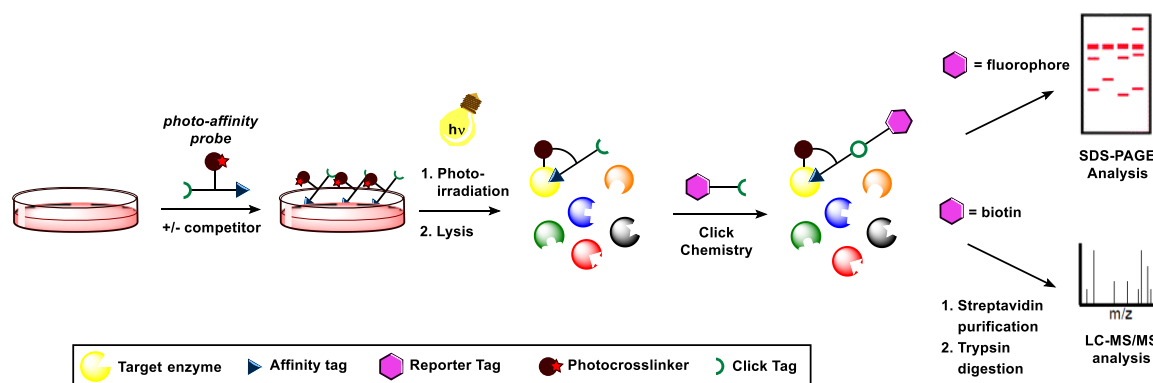


Figure 2. General work-flow of a live cell photoaffinity labeling experiment.

catalyzes the production of a family of signaling lipids called *N*-acylethanolamines (NAEs) from their NAPE precursors.³⁴ NAPE-PLD has a metallo- β -lactamase fold and contains two zinc ions in its active site that coordinate a water molecule which hydrolyzes the phosphodiester bond of NAPE.³⁵ To confirm cellular target engagement of *in vitro* active NAPE-PLD inhibitors, a photoaffinity labeling assay was realized. For the design of the PAL probes two strategies were investigated: stabilized analogues of the natural substrate NAPE and photoactivatable probes based on the pyrimidine-6-carboxamide NAPE-PLD inhibitor series described in Chapter 3. Unfortunately, the NAPE-based probes were ineffective in labeling NAPE-PLD, whereas the pyrimidine-based probes **50** and **51** were able to visualize NAPE-PLD *in situ* in transfected HEK293T cells overexpressing this enzyme. Using these pyrimidine-based probes, cellular binding of **LEI-401** with NAPE-PLD was confirmed, thereby providing evidence for its target engagement.

4.2 Results

4.2.1 Design and synthesis of NAPE-based photoprobes.

The design of the photoprobes was inspired by a previous report of a racemic phosphoramidate NAPE mimic, which had reasonable inhibitory activity for NAPE-PLD ($IC_{50} = \sim 10 \mu\text{M}$).³⁶ Incorporation of this phosphoramidate group in combination with a photoreactive aliphatic diazirine group and an alkyne fatty acid, gave photoprobe **1** (Figure 3). A short *N*-pentyl photocrosslinking acyl chain was chosen due to synthetic accessibility from levulinic acid, while retaining affinity for NAPE-PLD.³⁷ Different phosphodiester bioisosteres containing one or two sulfur atoms, that can potentially coordinate to the active site zinc ions, were incorporated into the design for probes **2-5**, to investigate their influence on the NAPE-PLD inhibitory activity. The photocrosslinker and click tag were placed on the *N*-acyl fatty acid to circumvent phospholipase-mediated loss of labeling signal by hydrolysis of the ester group. In addition, the fatty acids of the phosphatidylethanolamine were selected based on their predominant natural occurrence.³⁸ Lastly, the influence of the diazirine position on the labeling efficiency of NAPE-PLD was investigated with probes **4**, **6** and **7**.

The synthesis of probe **1** is shown in Scheme 1. Generation of 15-hexadecynoic acid (**12**) was achieved in four steps starting from 15-hydroxypentadecanoic acid (**8**). First, the carboxylic was esterified followed by oxidation of the alcohol to the aldehyde with pyridinium chlorochromate (PCC). Next, the alkyne was installed using the Ohira-Bestmann reagent³⁹ and the ester was hydrolyzed, affording fatty acid **12**. Utilizing a

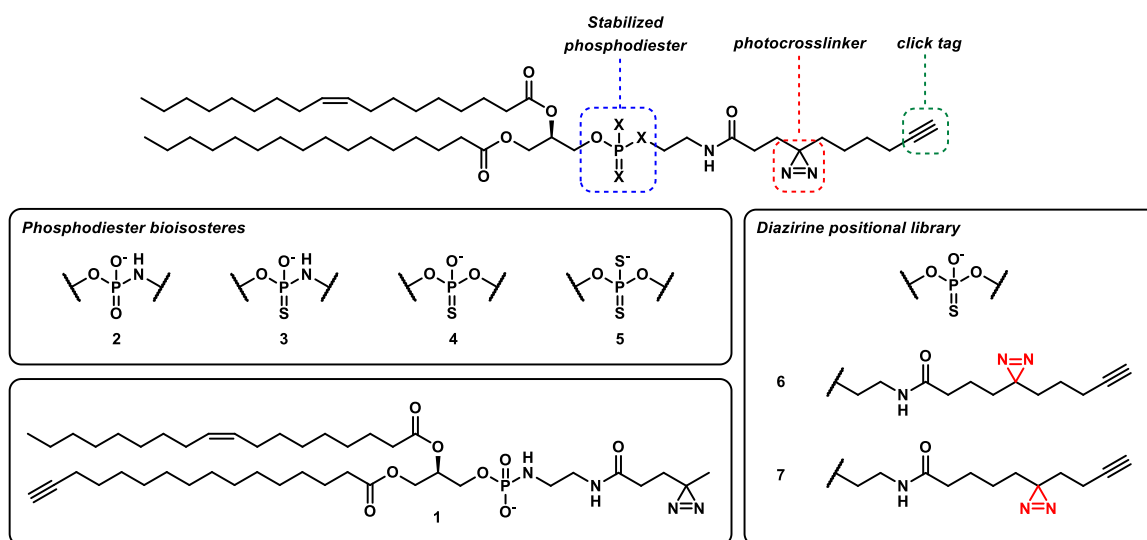
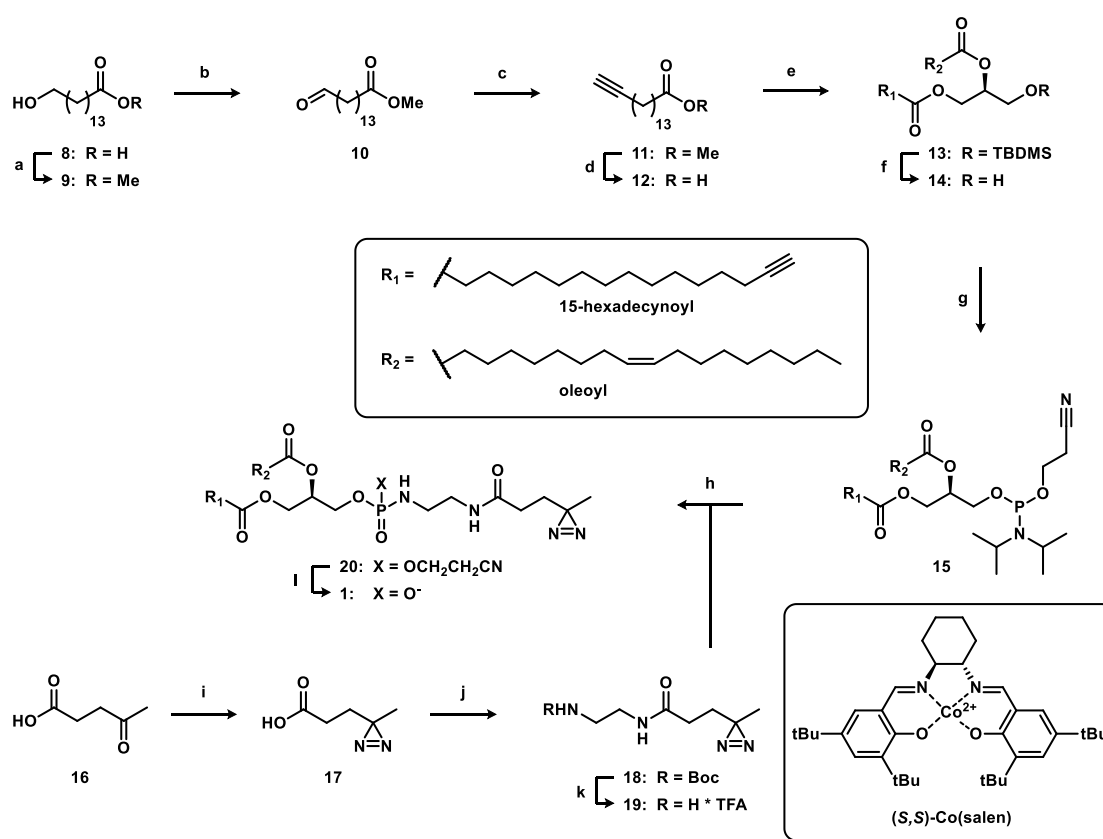


Figure 3. Design of NAPE-based photoaffinity probes **1-7**, incorporating a stabilized phosphodiester, a photoreactive diazirine and an alkyne ligation handle.

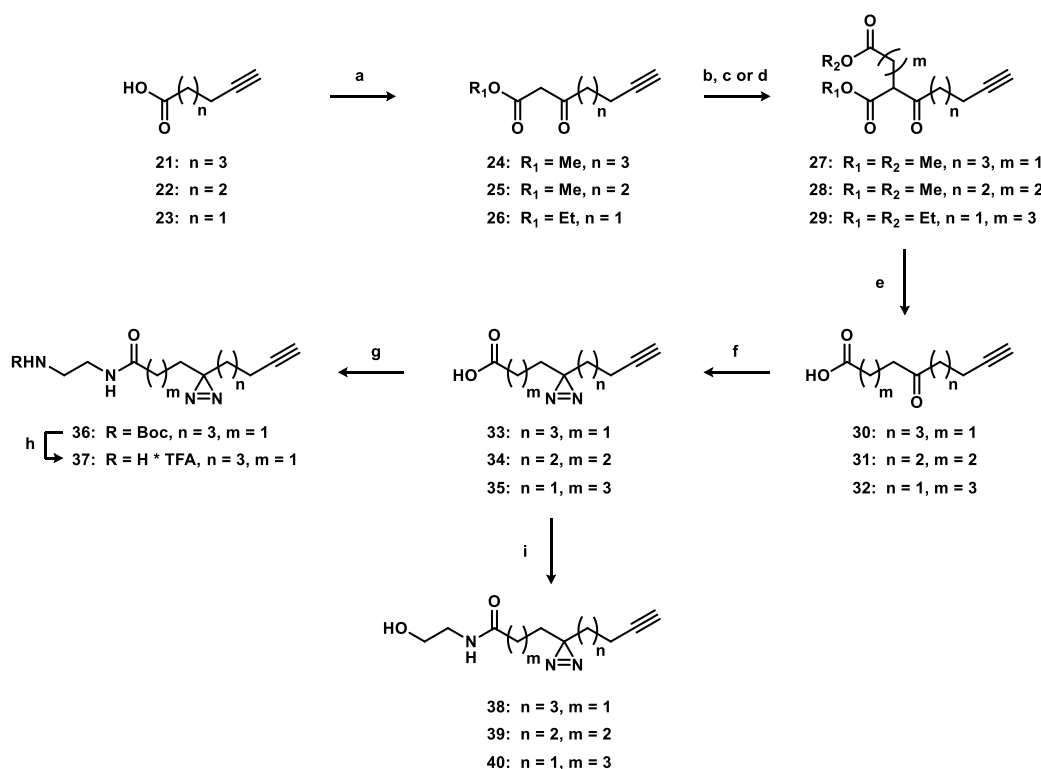
two-step one-pot sequence described by Minnaard and co-workers⁴⁰, **12** was treated with TBDMS-protected (*R*)-glycidol to give regioselective opening of the epoxide with (*S,S*)-Co(salen) as a catalyst. Esterification of the secondary alcohol with oleic acid delivered the mixed 1,2-diacylglycerol **13**. Mild deprotection of the TBDMS group to afford **14** was achieved with Et₃N·3HF in high yield, with no rearrangement to the 1,3-diacylglycerol observed. Phosphoramidite **15** was generated using standard phosphor coupling conditions. Next, amine **19** was synthesized in three steps, starting from levulinic acid (**16**), which was converted to the diazirine **17** using a three-step one pot procedure.⁴¹ This involved treatment with ammonia in methanol followed by hydroxylamine-*O*-sulfonic acid to form the diaziridine and subsequent oxidation with iodine and triethylamine to form diazirine **17**. Subsequent amide coupling with Boc-ethylenediamine and Boc deprotection afforded **19**. To form the desired phosphoramidate bond an Atherton-Todd coupling was envisioned. Phosphoramidite **15** was converted to the *H*-phosphonate after which treatment with tetrachloromethane, triethylamine and amine **19** gave phosphoramidate **20**. Deprotection of the cyanoethyl group afforded the final product **1**.

To circumvent NAPE-PLD- or phospholipase-mediated hydrolysis of the photoprobe, resulting in release of the alkyne from the photocrosslinker, bifunctional fatty acids were incorporated as the *N*-acyl group. Three different ω -alkyne diazirine fatty acids (**33-35**) were prepared to probe the optimal site of the photocrosslinker (Scheme 2). A modular synthesis was developed using commercially available ω -alkyne fatty acids **21-23**, which were converted to β -ketoesters **24-26** via coupling with Meldrum's acid followed by reflux

in methanol or ethanol. Alkylation with methyl bromoacetate for **24** or ethyl 4-bromobutanoate for **26** afforded diesters **27** or **29**, respectively. Diester **28** was generated via Michael addition of methyl acrylate and β -ketoester **25**. Subsequent hydrolysis and decarboxylation afforded the γ -ketoacids **30-32**. Using a similar three-step one-pot procedure as for levulinic acid, ketoacids **30-32** were transformed to diazirines **33-35**. **33** was coupled with Boc-ethylenediamine and deprotected to form amine **37**. Alternatively, carboxylic acids **30-32** were condensed with ethanolamine to generate ethanolamides **38-40**.

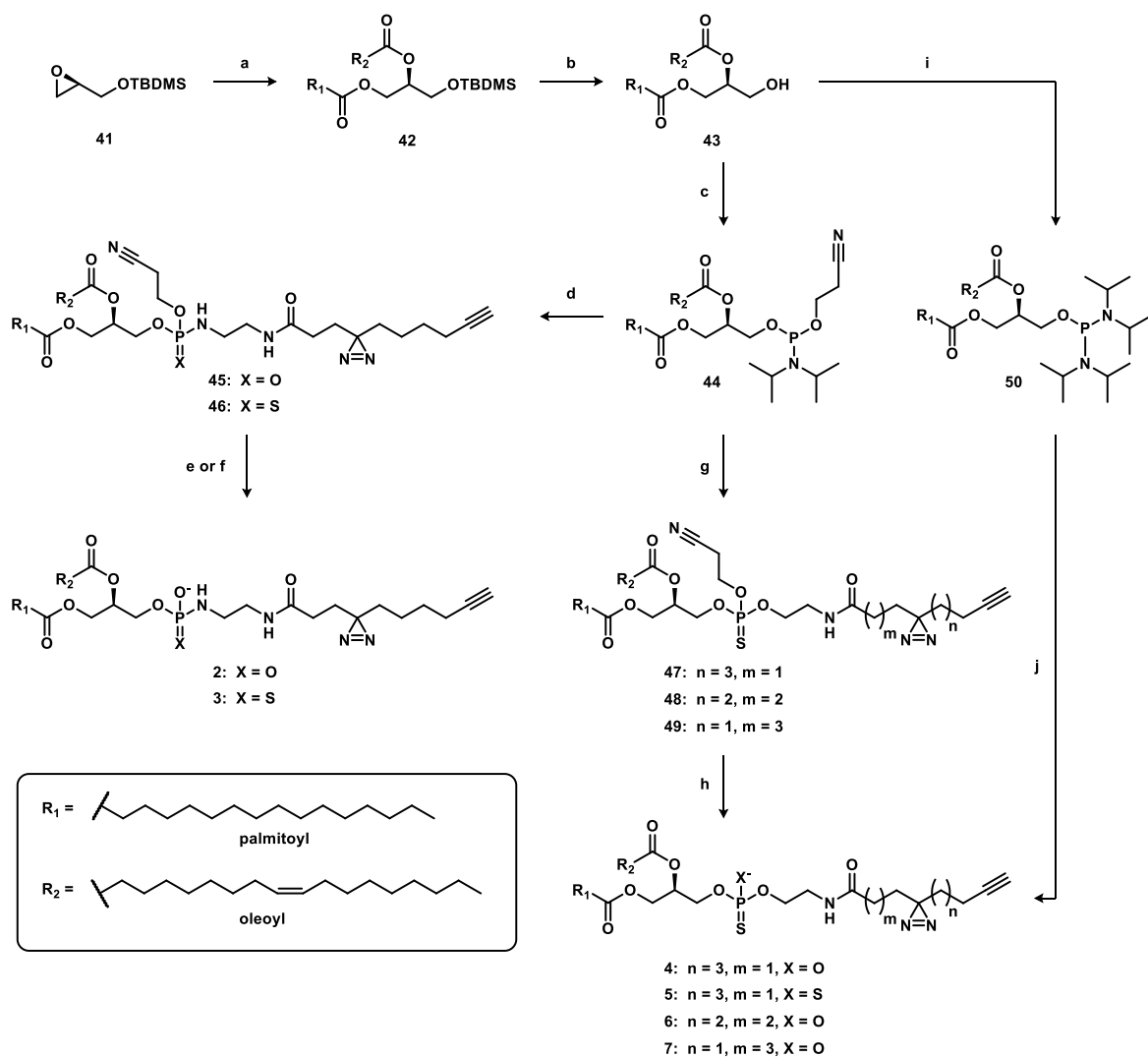


Scheme 1. Synthesis of photoprobe **1**. Reagents and conditions: a) AcCl, MeOH, 83%; b) PCC, DCM, 74%; c) dimethyl (1-diazo-2-oxopropyl)phosphonate (Ohira-Bestmann reagent), K_2CO_3 , MeOH, 0 °C to rt, 40%; d) NaOH, THF, H_2O , 99%; e) *i.* (*R*)-*tert*-butyldimethyl(oxiran-2-ylmethoxy)silane, (*S,S*)-Co(salen), DiPEA, O_2 ; *ii.* oleic acid, DIC, DMAP, heptane, 0 °C to rt, 35%; f) $Et_3N \cdot 3HF$, THF, CH_3CN , 93%; g) 2-cyanoethyl *N,N*-diisopropylchlorophosphoramidite, DiPEA, DCM, 98%; h) *i.* 1*H*-tetrazole, CH_3CN , H_2O ; *ii.* **19**, CCl_4 , Et_3N , CH_3CN , 55%; i) *i.* 7 M NH_3 in MeOH, 0 °C; *ii.* $NH_2O(SO_3H)$, 0 °C to rt; *iii.* I_2 , Et_3N , MeOH, 0 °C to rt, 47%; j) *i.* *N*-hydroxysuccinimide, EDC·HCl, Et_3N , DCM, *ii.* *N*-Boc-ethylenediamine, 71%; k) TFA, DCM, 99%, l) DBU, DCM, 41%.



Scheme 2. Synthesis of bifunctional fatty acids **33-35**. Reagents and conditions: a) *i.* Meldrum's acid, DIC, DMAP, DCM; *ii.* MeOH or EtOH, reflux, **24**: 74%, **25**: 52%, **26**: 58%; b) for **27**: **24**, methyl bromoacetate, NaOMe, MeOH, 66%; c) for **28**: **25**, methyl acrylate, K_2CO_3 , DCM/DMF, 53% d) for **29**: **26**, ethyl 4-bromobutanoate, NaOEt, EtOH, 38%; e) *i.* NaOH, THF, H_2O ; *ii.* HCl, 0 °C to 55 °C, **30**: 99%, **31**: 84%; **32**: 82%; f) *i.* 7 M NH_3 in MeOH, 0 °C; *ii.* $\text{NH}_2\text{O}(\text{SO}_3\text{H})$, 0 °C to rt; *iii.* I_2 , Et_3N , MeOH, 0 °C to rt, **33**: 51%, **34**: 55%; **35**: 38%; g) *N*-Boc-ethylenediamine, EDC·HCl, HOBT, DCM, 97%; h) TFA, DCM, 99%; i) ethanolamine, EDC·HCl, HOBT, DCM, **38**: 78%, **39**: 76%, **40**: 69%.

Next, *sn*-1-palmitoyl-*sn*-2-oleoylglycerol **43** was prepared in three steps using an analogous route as for **14** (Scheme 3). Installation of the phosphoramidite with standard P^{III} chemistry afforded key intermediate **44**. Using a similar Atherton-Todd procedure as for probe **1**, phosphoramidite **44** was converted to the *H*-phosphonate and coupled with amine **37** to generate phosphoramidate **45**. Deprotection with DBU gave photoprobe **2**. As the phosphoramidate moiety is known to be labile under acidic conditions, synthesis of a more stable thiophosphoramidate was explored.⁴² A solution of hydrogen sulfide in THF was used to generate the *H*-thiophosphonate from **44**, that was converted to the desired thiophosphoramidate **46** with amine **37** using Atherton-Todd conditions. Deprotection of the cyanoethyl group with *tert*-butylamine to scavenge the liberated acrylonitrile, that could potentially react with the nucleophilic sulfur, afforded thiophosphoramidate **3** as a mixture of two diastereomers.



Scheme 3. Synthesis of photoprobes **2-7**. Reagents and conditions: a) *i.* palmitic acid, (*S,S*)-Co(salen), DiPEA, O_2 ; *ii.* oleic acid, DIC, DMAP, heptane, $0^\circ C$ to rt, 64%; b) $Et_3N \cdot 3HF$, THF, CH_3CN , 99%; c) 2-cyanoethyl-*N,N*-diisopropylchlorophosphoramidite, DiPEA, DCM, 93%; d) *i.* for **45**: H_2O , 1*H*-tetrazole, CH_3CN ; for **46**: H_2S , 1*H*-tetrazole, CH_3CN ; *ii.* **37**, CCl_4 , Et_3N , CH_3CN/DCM , $0^\circ C$ to rt, **45**: 80%, **46**: 31%; e) for **2**: **45**, DBU, DCM, 24%; f) for **3**: **46**, *t*- $BuNH_2$, DCM, 99%; g) *i.* **38**, **39** or **40**, 1*H*-tetrazole, DCM; *ii.* S_8 , **47**: 59%, **48**: 42% **49**: 35%; h) *t*- $BuNH_2$, DCM, **4**: 81%, **6**: 21%, **7**: 25%; i) bis(diisopropylamino)chlorophosphine, DiPEA, DCM, 76%; j) for **5**: *i.* **38**, diisopropylammonium tetrazolide, DCM; *ii.* H_2S , 1*H*-tetrazole; *iii.* Et_3N , S_8 , 7%.

Stabilized mono- and dithiophosphates were investigated as hydrolysis-resistant phosphodiester isosteres.⁴³⁻⁴⁶ In addition, a potential favorable zinc-sulfur interaction was envisioned to increase enzyme affinity. Using phosphoramidite **44**, coupling with ethanolamides **38-40** and subsequent sulfurization with elemental sulfur gave protected monothiophosphates **47-49**. *tert*-Butylamine mediated deprotection afforded

thiophosphates **4**, **6** and **7** as a mixture of two diastereomers. For the dithiophosphate probe **5** an alternative route was investigated. Diacylglycerol **43** was transformed to phosphordiamidite **50**. To allow successful incorporation of both sulfur atoms, a three-step one-pot sequence was developed. This involved coupling of diamidite **50** with ethanolamide **38** using diisopropylammonium tetrazolid⁴⁷, affording the monosubstituted phosphoramidite. Of note, all attempts to couple with 1*H*-tetrazole resulted in disubstitution. Subsequently, the *in situ* generated monosubstituted phosphoramidite was converted to the *H*-thiophosphonate using hydrogen sulfide and finally sulfurized to obtain the desired dithiophosphate **5**.

4.2.2 Biological evaluation of NAPE-based photoprobes

The inhibitory activities of photoprobes **1-7** were assessed in the previously developed NAPE-PLD fluorescent substrate assay (Chapter 2). All compounds showed inhibitory activity for NAPE-PLD with poor to modest potencies (Figure 4A-B). In particular, the thiophosphoramidate **3** and dithiophosphate **5** showed reasonable activity with a K_i below 10 μM . Next, the photoaffinity labeling properties of the photoprobes were evaluated in human embryonic kidney (HEK293T) cells. The probes (20 μM) were incubated with the cells for 30 minutes, irradiated with 350 nm UV light for 10 minutes, lysed, clicked with a Cy5-N₃ fluorophore and resolved by sodium dodecyl sulfate polyacrylamide gel electrophoresis (SDS-PAGE). Visualization by in-gel fluorescence scanning showed a UV-dependent protein labeling pattern (Figure 5). From this gel it was apparent that the thiophosphoramidate probe **3** was most effective in photocrosslinking various proteins. In

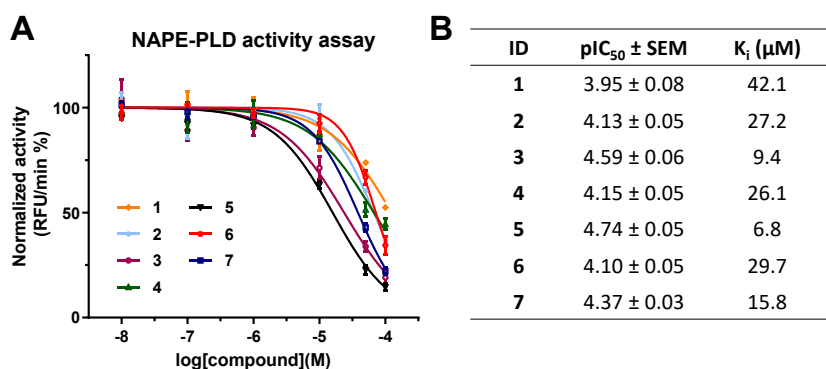


Figure 4. NAPE-PLD inhibitory activities of NAPE-like photoprobes **1-7**. **A**) Dose response curves. **B**) pIC₅₀ and K_i values. Data represent mean values ± SEM (N = 2, n = 2).

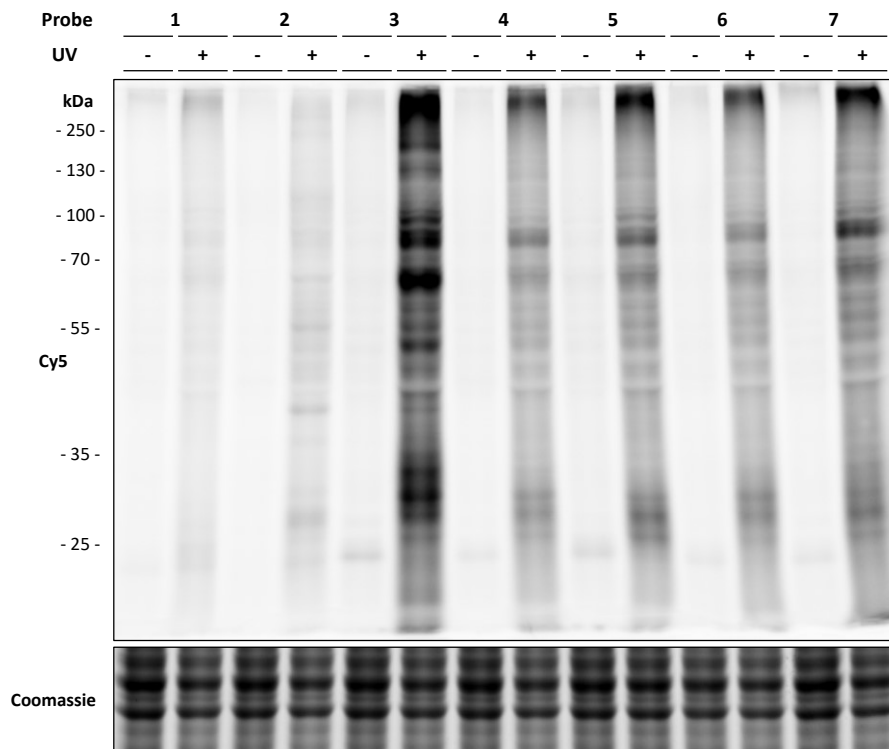


Figure 5. Photoaffinity labeling of NAPE-based photoprobes **1-7** (20 μ M) shows UV-dependent labeling of proteins in live HEK293T cells. Coomassie was used as a protein loading control.

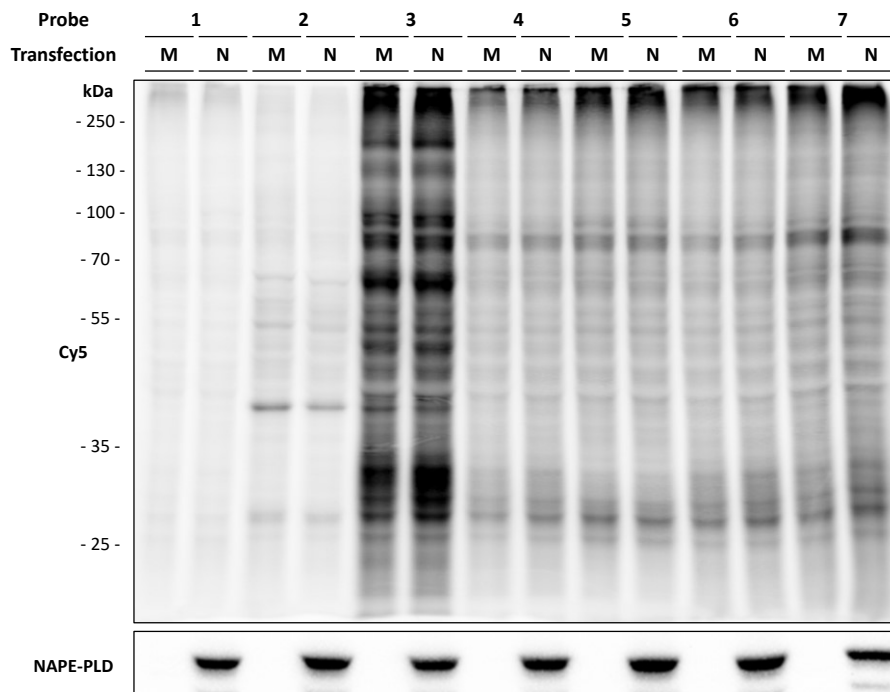
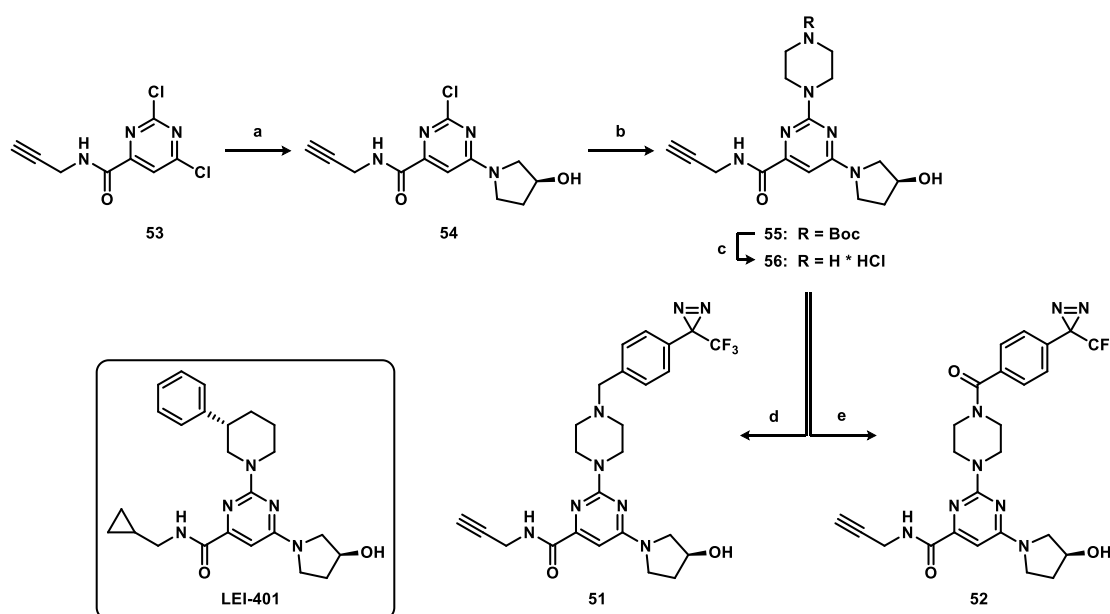


Figure 6. Live cell photoaffinity labeling of mock (M) and hNAPE-PLD (N) transfected HEK293T cells with NAPE-based photoprobes **1-7**. No labeling of NAPE-PLD was apparent at the expected height of 46 kDa (upper panel). Overexpression of hNAPE-PLD is confirmed in the western blot (lower panel).

contrast, probes **1** and **2** showed far less protein labeling, possibly due to their more labile phosphoramidate group or hydrolysis of the alkyne-containing acyl moiety.⁴² The different mono- and dithiophosphate probes **4-7** exhibited similar labeling intensities and protein patterns. Furthermore, the position of the diazirine (probes **4**, **6** and **7**) did not appear to influence the labeling profile. To establish whether the photoprobes could visualize NAPE-PLD, HEK293T cells were overexpressed with human NAPE-PLD. 48 hours after transient transfection with a mock or hNAPE-PLD-FLAG containing pcDNA3.1 plasmid, the cells were treated with the different probes (20 μ M) for 30 minutes. No band was visible at the expected height of hNAPE-PLD (46 kDa) for any of the photoprobes (Figure 6), indicating that these compounds were not capable of labeling NAPE-PLD.



Scheme 4. Synthesis of photoprobes **51** and **52**. Reagents and conditions: a) (*S*)-3-hydroxypyrrolidine-HCl, DiPEA, MeOH, 0 °C, 83%; b) *N*-Boc-piperazine, DiPEA, *n*-BuOH, 100 °C, 90%; c) 4 M HCl, 1,4-dioxane, quant.; d) 4-(3-(trifluoromethyl)-3*H*-diazirin-3-yl)benzyl bromide, DiPEA, CH₃CN, 32%; e) 4-(3-(trifluoromethyl)-3*H*-diazirin-3-yl)benzoic acid, PyBOP, DiPEA, DMF, 0 °C to rt, 18%.

4.2.3 Synthesis of LEI-401-based photoprobes

LEI-401 pyrimidine-6-carboxamide derivatives were explored as PAL probes, since this inhibitor series was developed to have optimal inhibitory activity towards NAPE-PLD and favorable physicochemical properties. Using the structure activity relationship map described in Chapter 3, photoprobes **51** and **52** were designed (Scheme 4). The

3-phenylpiperidine was substituted for a (trifluoromethyl-diazirine)benzyl- or benzoyl-piperazine as a photoreactive group. Replacement of the cyclopropylmethyl moiety for a propargyl group allowed introduction of reporter groups using click chemistry. Synthesis of probes **51** and **52** started with regioselective substitution of the dichloropyrimidine **53** (synthesis described in Chapter 3) with (*S*)-3-hydroxypyrrolidine to afford chloropyrimidine **54**. Nucleophilic aromatic substitution with *N*-Boc-piperazine followed by Boc deprotection furnished **56**. This compound was alkylated with 4-(3-(trifluoromethyl)-3*H*-diazirin-3-yl)benzyl bromide or condensed with 4-(3-(trifluoromethyl)-3*H*-diazirin-3-yl)benzoic acid, affording probes **51** and **52**, respectively.

4.2.4 Biological evaluation photoprobe **51** and **52**.

The inhibitory activities of photoprobes **51** and **52** for hNAPE-PLD were measured in the PED6 assay, affording comparable submicromolar K_i values (Figure 7A-B). Both probes showed a more than 30-fold increase in activity compared to the most potent NAPE-based photoactivatable probe **5**. In addition, due to their reduced lipophilicity, compounds **51** and **52** exhibit similar or greater lipophilic efficiencies (LipE) than **LEI-401** (Figure 7B).

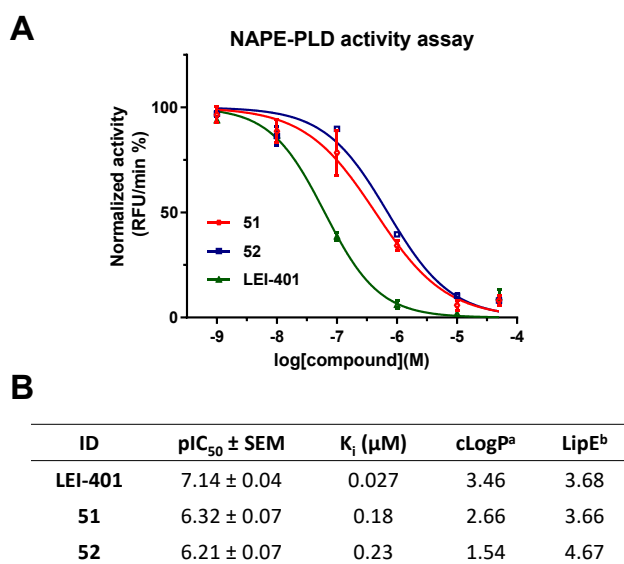


Figure 7. hNAPE-PLD inhibitory activities of pyrimidine-based photoprobes **51** and **52**. **A**) Dose response curves. **B**) pIC₅₀, K_i values and physicochemical parameters. Data represent mean values ± SEM (N = 2, n = 2). ^a cLogP was calculated using Chemdraw 15; ^b Lipophilic efficiency (LipE) = pIC₅₀ – cLogP.

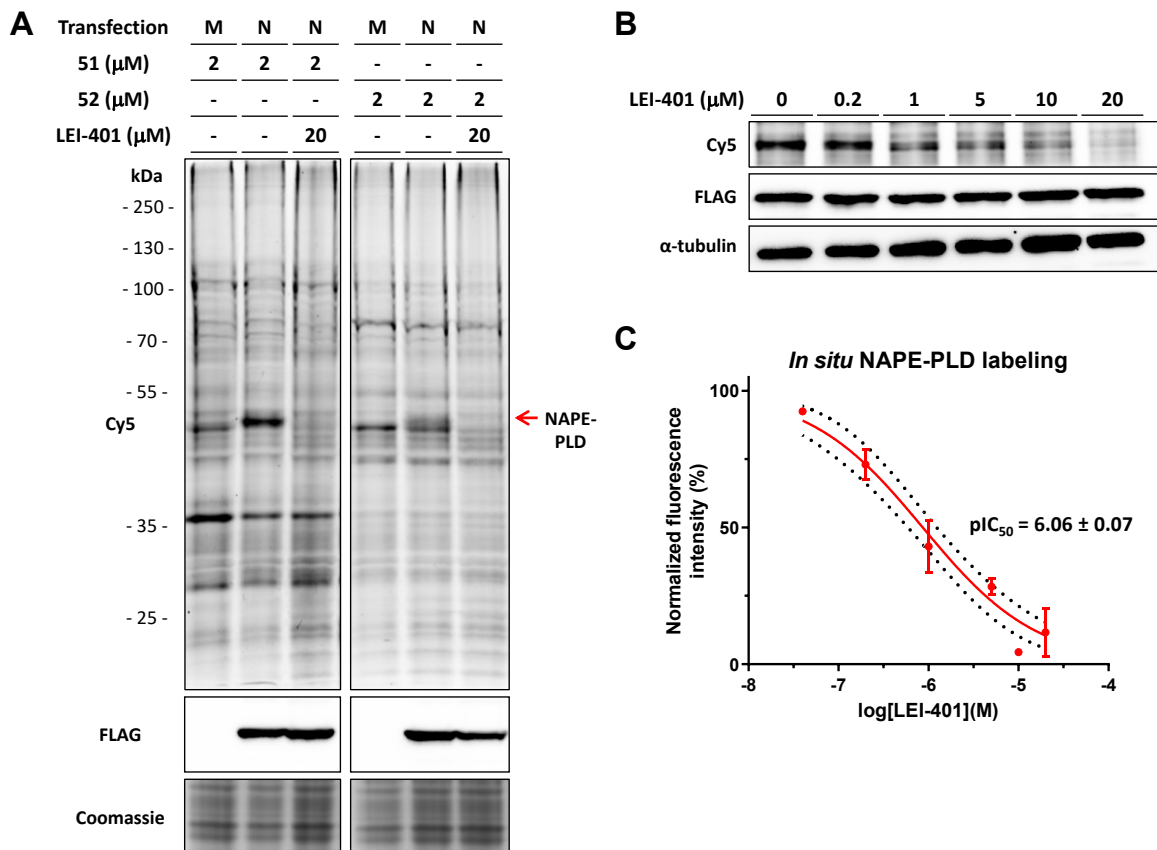


Figure 8. Photoprobes **51** and **52** enable visualization of NAPE-PLD in overexpressing HEK293T cells. **A**) Live cell photoaffinity labeling showing *in situ* fluorescent labeling of hNAPE-PLD-FLAG (N) at ~46 kDa in HEK293T cells but not in mock (M) transfected cells with probe **51** and **52** (2 μM) and displacement with **LEI-401** (20 μM) (upper panels). Anti-FLAG western blot displays expression of hNAPE-PLD-FLAG (lower panels). **B**) Representative gel of dose-dependent competition of probe **51** (2 μM) with **LEI-401**. **C**) Dose-response curve of **LEI-401** ($\text{pIC}_{50} = 6.06 \pm 0.07$, dotted lines show 95% confidence interval). Data represent mean values \pm SEM for 3 biological replicates.

Probes **51** and **52** were also evaluated whether they could visualize NAPE-PLD in cells using the same experimental protocol as for the substrate-based probes. A fluorescent band at the expected molecular weight (MW) of ~46 kDa was apparent in the hNAPE-PLD transfected cells, but not in the control cells, for both probes. The fluorescent band overlapped with the FLAG-tag signal on western blot (Figure 8A, left and middle lanes). These results indicate that hNAPE-PLD can be successfully labeled by the inhibitor-based photoaffinity probes. Importantly, the intensity of the fluorescent band was reduced when co-incubated with **LEI-401** (20 μM), thereby confirming that **LEI-401** engaged with NAPE-PLD in living cells (Figure 8A, right lanes). Of note, a fluorescent band was observed at the same MW in the mock lanes that also could be competed out by **LEI-401**, which

may possibly indicate the presence of endogenous NAPE-PLD. Next, concentration response experiments were performed with probe **51**, as the labeling of this compound was more intense than **52**. **LEI-401** displayed a dose-dependent reduction of NAPE-PLD labeling, which was quantified as a cellular IC_{50} of $0.86 \mu\text{M}$ (95% confidence interval (CI): $0.60 - 1.2 \mu\text{M}$) (Figure 8B-C).

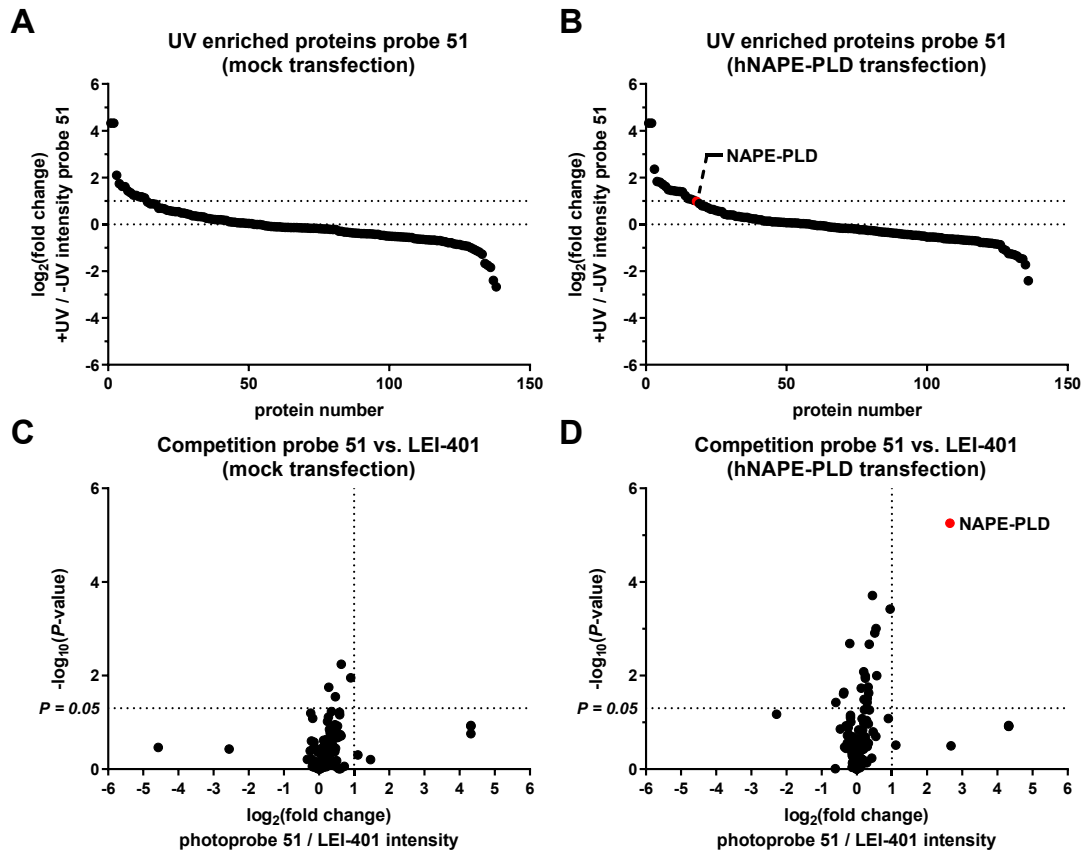


Figure 9. A-B) Waterfall plots showing UV enriched proteins of photoprobe **51** (2 μM) in HEK293T with mock or hNAPE-PLD-FLAG transfection. C-D) Volcano plots displaying competed protein targets for photoprobe **51** (2 μM) vs. **LEI-401** (20 μM) in mock (C) or hNAPE-PLD-FLAG (D) transfected HEK293T cells (3 biological replicates per condition). Cut-off values for protein target validation: unique peptides ≥ 2 ; UV enrichment: $\log_2(\text{fold change}) > 1$ (+UV/-UV **51** intensity); for competition: $\log_2(\text{fold change}) > 1$ (**51** intensity/**LEI-401** intensity). Statistically significant targets: $P < 0.05$ using Student's t -test (unpaired, two-tailed) and Benjamini-Hochberg correction with a false discovery rate (FDR) of 10%.

Table 1. Protein targets of photoprobe **51** in mock and hNAPE-PLD-FLAG transfected HEK293T cells.

| Name | Gene | MW (kDa) | Accession | Peptides | | log ₂ (ratio) | | | | P-value | | | |
|---|-----------------------|-----------|---------------|----------|----------|--------------------------|----------------|-------------|----------------|-------------|----------------|------------------|------------------|
| | | | | | | mock | | NAPE-PLD | | mock | | NAPE-PLD | |
| | | | | Total | Unique | +UV/ -UV | 51/ LEI-401 | +UV/ -UV | 51/ LEI-401 | +UV/ -UV | 51/ LEI-401 | +UV/ -UV | 51/ LEI-401 |
| <i>N</i>-acylphosphatidyl-ethanolamine phospholipase D | <i>NAPEPLD</i> | 46 | Q6IQ20 | 8 | 6 | - | - | 0.99 | 2.65 | - | - | >0.001 | >0.001 |
| Epoxide hydrolase 1 | <i>EPHX1</i> | 53 | P07099 | 16 | 10 | 1.25 | 0.90 | 1.62 | 0.95 | 0.0023 | 0.0112 | >0.001 | >0.001 |
| Ras-related protein Rab-10 | <i>RAB10</i> | 23 | P61026 | 5 | 2 | 1.18 | 0.16 | 1.71 | 0.36 | 0.0056 | 0.2808 | 0.0032 | 0.0542 |
| Probable serine carboxypeptidase | <i>CPVL</i> | 54 | Q9H3G5 | 5 | 5 | 1.74 | 0.24 | 1.80 | 0.33 | >0.001 | 0.0956 | 0.0016 | 0.1077 |
| Lamin-B1 | <i>LMNB1</i> | 67 | P20700 | 14 | 13 | 2.10 | 0.18 | 2.36 | 0.06 | 0.0012 | 0.3413 | >0.001 | 0.6149 |
| Lamin-B2 | <i>LMNB2</i> | 70 | Q03252 | 8 | 6 | 4.32 | 0.13 | 4.32 | -0.01 | >0.001 | 0.4515 | >0.001 | 0.9016 |

Cut-off values for protein target validation: unique peptides ≥ 2 , UV enrichment: $\log_2(\text{fold change}) \geq 1$ (UV+ / UV- **51** intensity), for competition: $\log_2(\text{fold change}) \geq 1$ (**51** intensity / **LEI-401** intensity). Statistically significant targets: $P < 0.05$ using Student's *t*-test (unpaired, two-tailed) and Benjamini-Hochberg correction with FDR of 10%.

To unequivocally establish the identity of the labeled band and determine the selectivity of **LEI-401**, label-free chemical proteomics experiments were performed.¹¹ Cell lysates prepared from mock or hNAPE-PLD-HEK293T cells incubated and UV-irradiated with probe **51** (2 μ M), were clicked with a biotin-N₃, which allowed for an enrichment of the probe-labeled proteins using avidin agarose beads, followed by trypsin digestion and protein identification by mass spectrometry. Proteomic analysis revealed that probe **51** interacted with 136 to 138 proteins (Figure 9A-B). NAPE-PLD was significantly enriched by probe **51** in a UV-dependent manner, exclusively in the hNAPE-PLD transfected cells (Figure 9B), and its labeling was prevented by co-incubation with **LEI-401** (20 μ M) (Figure 9D). Besides NAPE-PLD, five endogenous protein targets were confirmed for probe **51** in both mock and NAPE-PLD overexpressing cells (Table 1). **LEI-401** did not compete with probe **51** for any of these proteins, indicating that **LEI-401** selectively engages with NAPE-PLD over the other targets of **51** in HEK293T cells (Figure 9C-D).

4.3 Discussion

In this chapter, two strategies were explored for the development of NAPE-PLD PAL probes. Seven synthetically challenging NAPE-based photoprobes were produced, incorporating various phosphodiester bioisosteres. Probes **1-7** did not exhibit high affinity for NAPE-PLD and, as a result, were unable to visualize NAPE-PLD in live cell gel experiments. The second design was based on the potent NAPE-PLD inhibitor **LEI-401**, which yielded photoactivatable probes **51** and **52**. These probes exhibited several advantages compared to the NAPE-based compounds, including increased inhibitory activity for NAPE-PLD, a more efficient photocrosslinking group and improved physicochemical parameters thereby enhancing solubility and cell-permeability. In particular, probe **51** showed efficient photolabeling of NAPE-PLD in live overexpressing HEK293T cells, which could be competed out by co-incubation with **LEI-401**. Chemical proteomics was used to confirm the identity of NAPE-PLD, thereby providing evidence that **LEI-401** binds with its intended target in a cellular system.

Visualization of endogenous NAPE-PLD is highly valuable to study its biological role in cells. Although a band was apparent in the mock transfected HEK293T cells for both probes **51** and **52** which could be competed out by **LEI-401**, no endogenous NAPE-PLD was observed in the proteomics experiments for these samples. Also in mouse neuroblastoma Neuro2A cells which express NAPE-PLD, probes **51** and **52** were not able to label NAPE-PLD (data not shown). Possible explanations include low efficiency of photocrosslinking, inherent to photoaffinity labeling, as well as technical limitations with regard to

measuring low abundant NAPE-PLD peptides. Discrepancies between the efficiency of the click reaction with Cy5-N₃ or biotin-N₃ have to be taken into account as well. Further optimizations to enable endogenous NAPE-PLD labeling could consist of increasing the NAPE-PLD affinity of the probes or adjusting the position of the photocrosslinker. Alternatively, increasing endogenous NAPE-PLD expression could be used to obtain effective labeling, although so far, no such agents have been identified.

To conclude, the development of photoaffinity probe **51** and **52** enabled the detection of NAPE-PLD in living cells and its target engagement by **LEI-401**. Photoprobes **51** and **52** in combination with **LEI-401** therefore expand the currently available toolbox for studying NAPE-PLD and anandamide biology in cellular models.

Acknowledgements

Rob Bosman, Branca van Veen and Jasper van de Sande are kindly acknowledged for contributing to the compound synthesis and biochemical testing. Bobby Florea and Alexander Bakker are kindly acknowledged for performing proteomics measurements.

4.4 Experimental Section

A. Biological procedures

NAPE-PLD surrogate substrate activity assay

The NAPE-PLD activity assay was performed as described in Chapter 2.

Cloning of plasmid DNA

Full length human cDNA of human NAPE-PLD (obtained from Natsuo Ueda³⁴) was cloned into mammalian expression vector pcDNA3.1, containing a C-terminal FLAG-tag and genes for ampicillin and neomycin resistance. All plasmids were grown in XL-10 Z-competent cells and prepped (Maxi Prep, Qiagen). Constructs were verified by Sanger sequencing (Macrogen).

Cell culture

HEK293T cells (ATCC) were cultured at 37 °C and 7% CO₂ in DMEM (Sigma Aldrich, D6546) with GlutaMax (2 mM), penicillin (100 µg/ml), streptomycin (100 µg/ml) and 10% fetal calf serum. Cells were passaged twice a week to appropriate confluence by thorough pipetting.

Gel-based photoaffinity labeling

500,000 HEK293T cells per well were seeded in a 12-well plate 1 day before transfection. On the day of transfection the medium was refreshed with 0.375 mL medium per well. Transfection was performed with polyethyleneimine (PEI, 3 µg per well) and human NAPE-PLD or Mock pcDNA3.1Neo plasmids (1 µg per well). PEI and plasmids were combined in serum-free medium (0.125 mL per well) and incubated for 15 min at rt, then added to each well. After 24 h the medium was refreshed. 48 hours after transfection the

medium was removed and cells were washed with warm PBS (1x). This was followed by treatment with the photoprobes **1-7** (1000x in DMSO, final concentration: 20 μ M) or photoprobes **51-52** (1000x in DMSO, final concentration: 2 μ M) together with vehicle or competitor (600x in DMSO) in medium + serum (0.30 mL per well) for 30 min at 37 °C. The medium was aspirated and the cells were covered with PBS (0.15 mL per well), followed by 350 nm UV irradiation using a Caprobox™ at 4 °C for 10 min. The cells were harvested into 1.5 mL epps with cold PBS and centrifuged for 10 min at 2000 rpm at 4 °C. The PBS was removed and the cells were flash frozen with liquid N₂ (cells can optionally be stored at -80 °C). The cells were lysed with lysis buffer (30 μ L, 20 mM HEPES pH 7.2, 0.25 M sucrose, 1 mM MgCl₂, benzonase 25 U/mL) followed by pipetting up and down and incubating for 30 min on ice. Protein concentrations were measured using a Bradford assay (Bio-Rad), and cell lysates were diluted to 2 μ g/ μ L with lysis buffer. 18 μ g cell lysate (9 μ L) was then clicked with Cy5-N₃ (for molecular structure see Figure S2) using a click mix (1 μ L per sample, final concentrations: 1 mM CuSO₄, 6 mM sodium ascorbate, 0.2 mM tris(3-hydroxypropyltriazolylmethyl)-amine (THPTA), 2 μ M Cy5-N₃) for 1 h at rt (Note: it is important to separately prepare the click mix first with CuSO₄ and sodium ascorbate, until a yellow color change is observed). Samples were denatured with 4x Laemmli buffer (3.33 μ L, stock concentration: 240 mM Tris-HCl pH 6.8, 8% w/v SDS, 40% v/v glycerol, 5% v/v β -mercaptoethanol, 0.04% v/v bromophenol blue) and incubated for 30 min at rt. The samples were resolved by SDS-PAGE (10% acrylamide gel) at 180 V for 75 min, after which the gels were imaged at Cy3 and Cy5 channels (605/50 and 695/55 filters, respectively) on a ChemiDoc™ Imaging System (Bio-Rad). Fluorescence is normalized to Coomassie or α -tubulin by western blot using ImageLab software (Bio-Rad). IC₅₀ curves were generated using Graphpad Prism v6.

Western blot

Proteins were transferred from the resolved SDS-PAGE gel to a 0.2 μ m PVDF membrane using a Trans-Blot® Turbo (Bio-Rad). The membranes were washed with TBS (50 mM Tris-HCl pH 7.5, 150 mM NaCl) and blocked with 5% milk in TBST (50 mM Tris-HCl pH 7.5, 150 mM NaCl, 0.05% Tween 20) 1 h at rt or overnight at 4 °C. Primary antibodies against NAPE-PLD (Abcam, ab95397, 1:200, in TBST), FLAG-tagged proteins (Sigma Aldrich, F3165, 1:5000 in 5% milk in TBST) or α -tubulin (Genetex, GTX76511, 1:5000 in 5% milk in TBST) were incubated 1 h at rt or overnight at 4 °C. Membranes were washed with TBST and incubated with secondary antibodies: for NAPE-PLD, goat-anti-rabbit-HRP (Santa Cruz, sc-2030, 1:2000 in 5% milk in TBST); for FLAG-tagged proteins, goat-anti-mouse-HRP (Santa Cruz, sc-2005, 1:5000 in 5% milk in TBST); for α -tubulin, goat-anti-rat (Santa Cruz, sc-2032, 1:5000 in 5% milk in TBST). All secondary antibodies were incubated or 1 h at rt. Membranes were washed with TBST and TBS. The blot was developed in the dark using a luminol solution (10 mL, 1.4 mM luminol in Tris-HCl pH 7.5), ECL enhancer (100 μ L, 6.7 mM *para*-hydroxycoumaric acid in DMSO) and H₂O₂ (3 μ L, 30% w/w in H₂O). Chemiluminescence was visualized using a ChemiDoc™ Imaging System (Bio-Rad). Band intensity is normalized to α -tubulin using ImageLab software (Bio-Rad).

Chemical proteomics-based photoaffinity labeling

$2 \cdot 10^6$ HEK293T cells per well were seeded in a 6-well plate 1 day before transfection. On the day of transfection the medium was removed and refreshed with 1.125 mL fresh medium per well. Transfection was performed with polyethyleneimine (PEI, 9 μ g per well) and human NAPE-PLD or Mock pcDNA3.1Neo plasmids (3 μ g per well). PEI and plasmids were combined in serum-free medium (0.375 mL per well) and incubated for 15 min at rt, then added to each well. After 24 h the medium was refreshed. 48 hours after transfection the medium was removed and cells were washed with warm PBS (1x). This was followed by treatment with photoprobe **51** (1000x in DMSO, final concentration: 2 μ M) together with vehicle or competitor (1000x in DMSO, final concentration: 20 μ M) in medium + serum (1 mL per well) for 30 min at 37 °C. The medium was aspirated and the cells were covered with PBS (0.5 mL per well), followed by 350 nm UV irradiation using a Caprobox™ at 4 °C for 10 min. The cells were harvested into 1.5 mL epps with cold PBS and centrifuged for 10 min at 2000 rpm at 4 °C. The PBS was removed and the cells were flash frozen with

liquid N₂ (cells can optionally be stored at -80 °C). The cells were lysed with lysis buffer (30 µL, 20 mM HEPES pH 7.2, 0.25 M sucrose, 1 mM MgCl₂, benzonase 25 U/mL) followed by pipetting up and down and incubating for 30 min on ice. Protein concentrations were measured using a Bradford assay (Bio-Rad), and cell lysates were diluted to 1 µg/µL with lysis buffer.

From here the label-free chemical proteomics protocol was followed as previously described.¹¹ 270 µg cell lysate (270 µL) was clicked with biotin-N₃ (Sigma Aldrich, 762024) using a click mix (30 µL per sample, final concentrations: 1 mM CuSO₄, 6 mM sodium ascorbate, 0.2 mM tris(3-hydroxypropyltriazolylmethyl)amine (THPTA), 4 µM biotin-N₃) for 1 h at rt (Note: it is important to separately prepare the click mix first with CuSO₄ and sodium ascorbate, until a yellow color change is observed). Proteins were precipitated using chloroform (166 µL), methanol (666 µL) and MilliQ (366 µL). Samples were centrifuged for 10 min at 1500 g and the solvents were carefully removed. Methanol (600 µL) was added and the proteins were resuspended using a probe sonicator (30% amplitude, 10 s). After centrifugation (5 min, 18,400 g) the supernatant was removed and the samples were resuspended again in urea buffer (250 µL, 6 M urea, 250 mM NH₄HCO₃) by pipetting up and down. DTT (2.5 µL, final concentration 10 mM) was added and the samples were incubated at 65 °C with shaking (600 rpm) for 15 min. After cooling to rt, iodoacetamide (20 µL, final concentration 40 mM) was added and incubated in the dark at 20 °C with shaking (600 rpm) for 30 min. Next, SDS (70 µL, 10%) was added and incubated at 65 °C with shaking (600 rpm) for 5 min. For 18 samples, 1.8 mL of avidin agarose beads (Thermo Scientific, 20219) were divided over three 15 mL tubes and washed with PBS (3 x 10 mL). The beads in each tube were resuspended in PBS (6 mL) and divided over 18 tubes (1 mL each). To each tube was added the denatured sample and PBS (2 mL) and the tubes were rotated with an overhead shaker at rt for 3 h. After centrifugation (2 min, 2,500 g) and removal of the supernatant, the beads were consecutively washed with 0.5% SDS in PBS (w/v, 6 mL) and PBS (3 x 6 mL), each time centrifuging (2 min, 2,500 g). The beads were transferred to a 1.5 mL low binding epp (Sarstedt, 72.706.600) with on-bead digestion buffer (250 µL, 100 mM Tris pH 8.0, 100 mM NaCl, 1 mM CaCl₂, 2% v/v acetonitrile) and to each sample was added 1 µL trypsin solution (0.5 µg/µL trypsin (Promega, V5111), 0.1 mM HCl). Proteins were digested at 37 °C with shaking (950 rpm) overnight. Formic acid (12.5 µL) was added to each sample and the beads were filtered off using a biospin column (Bio-Rad, 7326204), the flow-through was collected in a 2 mL epp. Samples were purified using StageTips⁴⁸. Each StageTip was conditioned with MeOH (50 µL, centrifugation: 2 min, 300 g), followed by StageTip solution B (50 µL, 80% v/v acetonitrile, 0.5% v/v formic acid in MilliQ, centrifugation: 2 min, 300 g) and StageTip solution A (50 µL, 0.5% v/v formic acid in MilliQ, centrifugation: 2 min, 300 g). Next, the samples were loaded, centrifuged (2 min, 600 g) and the peptides on the StageTip were washed with StageTip solution A (100 µL, centrifugation: 2 min, 600 g). The StageTips were transferred to a new 1.5 mL low binding epp and the peptides were eluted with StageTip solution B (100 µL, centrifugation: 2 min, 600 g). The solvents were evaporated to dryness in a SpeedVac concentrator at 45 °C for 3 h. Samples were reconstituted in LC-MS solution (50 µL, 3% v/v acetonitrile, 0.1% v/v formic acid, 1 µM yeast enolase peptide digest (Waters, 186002325) in MilliQ).

The peptides were measured as described previously for the NanoACQUITY UPLC System coupled to SYNAPT G2-Si high definition mass spectrometer.¹¹ A trap-elute protocol, where 5 µL of the digest is loaded on a trap column (C18 100 Å, 5 µM, 180 µM x 20 mm, Waters) followed by elution and separation on the analytical column (HSS-T3 C18 1.8 µM, 75 µM x 250 mm, Waters). The sample is brought onto this column at a flow rate of 10 µL/min with 99.5% solvent A for 2 min before switching to the analytical column. Peptide separation is achieved using a multistep concave gradient based on gradients previously described.⁴⁹ The column is re-equilibrated to initial conditions after washing with 90% solvent B. The rear seals of the pump are flushed every 30 min with 10% (v/v) acetonitrile. [Glu1]-fibrinopeptide B (GluFib) is used as a lock mass compound. The auxiliary pump of the LC system is used to deliver this peptide to the reference sprayer (0.2 µL/min). A UDMSe method is set up as previously described.⁴⁹ Briefly, the mass range is set from 50 to 2,000 Da with a scan time of 0.6 seconds in positive, resolution mode. The collision energy is set to 4 V in the trap cell for low-energy MS mode. For the elevated energy scan, the transfer cell collision energy is ramped using

drift-time specific collision energies. The lock mass is sampled every 30 seconds. For raw data processing, PLGS (v3.0.3) was used. The MS^E identification workflow was performed with the parameters summarized in Table S1 to search the human proteome from Uniprot (uniprot-homo-sapiens-trypsin-reviewed-2016_08_29.fasta). Protein quantification was performed using ISOQuant (v1.5). The parameter settings used are summarized in Table S2.

Table S1. The PLGS parameter settings used

| Parameter | Value |
|---------------------------|--|
| Lock mass m/z | 785.8426 |
| Low energy threshold | 150 counts |
| Elevated energy threshold | 30 counts |
| Digest reagent | trypsin |
| Max missed cleavages | 2 |
| Modifications | Fixed carbamidomethyl C, variable oxidation M |
| FDR less than | 1% |
| Fragments/peptide | 2 |
| Fragments/protein | 5 |
| Peptides/protein | 1 |

Table S2. ISOQuant parameter settings used

| Parameter | Value |
|--|---|
| isoquant.pluginQueue.name | design project and run ISOQuant analysis |
| process.peptide.deplete.PEP_FRAG_2 | false |
| process.peptide.deplete.CURATED_0 | false |
| process.peptide.statistics.doSequenceSearch | false |
| process.emrt.minIntensity | 1000 |
| process.emrt.minMass | 500 |
| process.emrt.rt.alignment.match.maxDeltaMass.ppm | 10 |
| process.emrt.rt.alignment.match.maxDeltaDriftTime | 2 |
| process.emrt.rt.alignment.normalizeReferenceTime | false |
| process.emrt.rt.alignment.maxProcesses | 24 |
| process.emrt.rt.alignment.referenceRun.selectionMethod | AUTO |
| process.emrt.clustering.preclustering.orderSequence | MTMTMT |
| process.emrt.clustering.preclustering.maxDistance.mass.ppm | 6.06E-6 |
| process.emrt.clustering.preclustering.maxDistance.time.min | 0.202 |
| process.emrt.clustering.preclustering.maxDistance.drift | 2.02 |
| process.emrt.clustering.distance.unit.mass.ppm | 6.0E-6 |
| process.emrt.clustering.distance.unit.time.min | 0.2 |
| process.emrt.clustering.distance.unit.drift.bin | 2 |
| process.emrt.clustering.dbscan.minNeighborCount | 1 |

| | |
|--|------------|
| process.identification.peptide.minReplicationRate | 2 |
| process.identification.peptide.minScore | 5.5 |
| process.identification.peptide.minOverallMaxScore | 5.5 |
| process.identification.peptide.minSequenceLength | 6 |
| process.identification.peptide.acceptType.PEP_FRAG_1 | true |
| process.identification.peptide.acceptType.IN_SOURCE | false |
| process.identification.peptide.acceptType.MISSING_CLEAVAGE | false |
| process.identification.peptide.acceptType.NEUTRAL_LOSS_H2O | false |
| process.identification.peptide.acceptType.NEUTRAL_LOSS_NH3 | false |
| process.identification.peptide.acceptType.PEP_FRAG_2 | true |
| process.identification.peptide.acceptType.DDA | true |
| process.identification.peptide.acceptType.VAR_MOD | true |
| process.identification.peptide.acceptType.PTM | true |
| process.annotation.peptide.maxSequencesPerEMRTCluster | 1 |
| process.annotation.protein.resolveHomology | true |
| process.annotation.peptide.maxFDR | 0.01 |
| process.annotation.useSharedPeptides | all |
| process.normalization.lowess.bandwidth | 0.3 |
| process.normalization.orderSequence | XPIR |
| process.normalization.minIntensity | 3000 |
| process.quantification.peptide.minMaxScorePerCluster | 5.5 |
| process.quantification.peptide.acceptType.IN_SOURCE | false |
| process.quantification.peptide.acceptType.MISSING_CLEAVAGE | false |
| process.quantification.peptide.acceptType.NEUTRAL_LOSS_H2O | false |
| process.quantification.peptide.acceptType.NEUTRAL_LOSS_NH3 | false |
| process.quantification.peptide.acceptType.PEP_FRAG_1 | true |
| process.quantification.peptide.acceptType.PEP_FRAG_2 | false |
| process.quantification.peptide.acceptType.VAR_MOD | false |
| process.quantification.peptide.acceptType.PTM | false |
| process.quantification.peptide.acceptType.DDA | true |
| process.quantification.topx.degree | 3 |
| process.quantification.topx.allowDifferentPeptides | true |
| process.quantification.minPeptidesPerProtein | 2 |
| process.quantification.absolute.standard.entry | ENO1_YEAST |
| process.quantification.absolute.standard.fmol | 50 |
| process.quantification.topx.allowDifferentPeptides | true |
| process.quantification.absolute.standard.entry | ENO1_YEAST |
| process.quantification.absolute.standard.fmol | 50 |
| process.quantification.maxProteinFDR | 0.01 |

Data analysis

Protein targets of photoprobe **51** were selected based on the following cut-offs: 1) ≥ 2 -fold enrichment for UV-treated vs. non-UV-treated samples; 2) unique peptides ≥ 2 ; 3) testing for significance using Student's *t*-test (unpaired, two-tailed), $P < 0.05$ is considered significant; 4) Benjamini–Hochberg correction with a false discovery rate (FDR) of 10%.

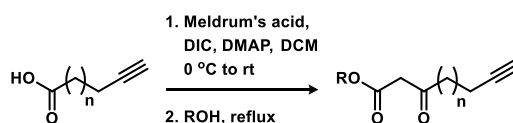
B. Synthetic procedures

General

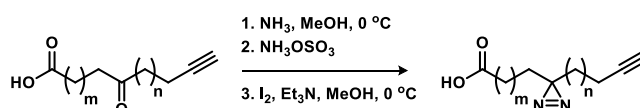
All chemicals (Sigma-Aldrich, Fluka, Acros, Merck, Combi-Blocks, Fluorochem, TCI) were used as received. All solvents used for reactions were of analytical grade. THF, Et₂O, DMF, CH₃CN and DCM were dried over activated 4 Å molecular sieves, MeOH over 3 Å molecular sieves. Flash chromatography was performed on silica gel (Screening Devices BV, 40–63 μm, 60 Å). The eluent EtOAc was of technical grade and distilled before use. Reactions were monitored by thin layer chromatography (TLC) analysis using Merck aluminium sheets (Silica gel 60, F₂₅₄). Compounds were visualized by UV-absorption (254 nm) and spraying for general compounds: KMnO₄ (20 g/L) and K₂CO₃ (10 g/L) in water, or for amines: ninhydrin (0.75 g/L) and acetic acid (12.5 mL/L) in ethanol, followed by charring at ~150 °C. ¹H, ¹³C and ³¹P NMR experiments were recorded on a Bruker AV-300 (300/75 MHz), Bruker AV-400 (400/101/162 MHz), Bruker DMX-400 (400/101/162 MHz), Bruker AV-500 (500/126/202 MHz) and Bruker AV-600 (600/151 MHz). Chemical shifts are given in ppm (δ) relative to tetramethylsilane or CDCl₃ as internal standards. Multiplicity: s = singlet, br s = broad singlet, d = doublet, dd = doublet of doublet, t = triplet, q = quartet, p = pentet, m = multiplet. Coupling constants (*J*) are given in Hz. LC-MS measurements were performed on a Thermo Finnigan LCQ Advantage MAX ion-trap mass spectrometer (ESI⁺) coupled to a Surveyor HPLC system (Thermo Finnigan) equipped with a standard C18 (Gemini, 4.6 mm D x 50 mm L, 5 μm particle size, Phenomenex) analytical column and buffers A: H₂O, B: CH₃CN, C: 0.1% aq. TFA. High resolution mass spectra were recorded on a LTQ Orbitrap (Thermo Finnigan) mass spectrometer or a Synapt G2-Si high definition mass spectrometer (Waters) equipped with an electrospray ion source in positive mode (source voltage 3.5 kV, sheath gas flow 10 mL min⁻¹, capillary temperature 250 °C) with resolution *R* = 60000 at *m/z* 400 (mass range *m/z* = 150–2000) and dioctylphthalate (*m/z* = 391.28428) as a lock mass. Preparative HPLC was performed on a Waters Acquity Ultra Performance LC with a C18 column (Gemini, 150 x 21.2 mm, Phenomenex). All final compounds were determined to be > 95% pure by integrating UV intensity recorded via HPLC.

Important experimental note

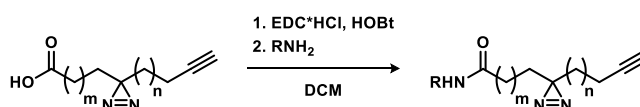
Trace metal chelation: the phosphothioate and phosphordithioate moieties are known to chelate trace metals. High purity grade silica gel (Sigma-Aldrich, Davisil Grade 633) should be used for the purification of these compounds. The silica gel can be regenerated after use by flushing with MeOH (4 CV) and Et₂O (2 CV), followed by drying in a vacuum stove at 100 °C. In the case of metal chelation, strong peak broadening was observed by ³¹P-NMR. This could be reversed by dissolving the compound in 10% MeOH in CHCl₃, adding an excess of EDTA-disodium in MilliQ and stirring for 30 min. The ³¹P-NMR peak intensity could be recovered, after which the aqueous layer was separated, the organic layer was washed with MilliQ and the solvents were concentrated under reduced pressure.

General procedure A

A round bottom flask was charged with the fatty acid (1 eq) and dry DCM (0.5 M) and cooled to 0 °C. Meldrum's acid (1.1 eq) and DMAP (1.2 – 1.3 eq) were added. This was followed by dropwise addition of a DIC solution (1.2 – 1.3 eq) in DCM (2 M) over 30 min, giving a yellow solution. The reaction was warmed to rt and stirred for 3 h. The mixture was diluted with DCM and washed with 1 M aq. KHSO₄ (2x), brine (1x), dried (Na₂SO₄), filtered and concentrated under reduced pressure. The crude product was dissolved in MeOH (0.2 M) and refluxed overnight. The solvents were evaporated and the crude residue was purified using silica gel column chromatography, affording the β-ketoester.

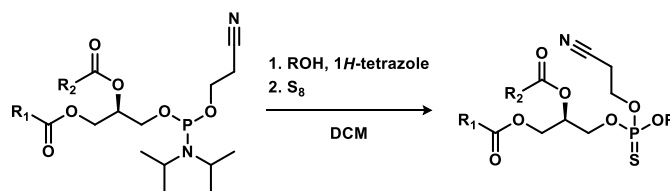
General procedure B

A round bottom flask was charged with ketoacid (1 eq) and dry MeOH (0.7 M) and cooled to 0 °C. Ammonia (7 M in MeOH, 21 eq) was added and the reaction was stirred for 4.5 h at 0 °C. Next, hydroxylamine-O-sulfonic acid (1.4 eq) was added and the mixture was stirred warming up to rt overnight. With a Pasteur pipette air was bubbled through the suspension for 1 h, followed by filtration of the formed (NH₄)₂SO₄ precipitate, washing with MeOH and concentration under reduced pressure. The crude residue was dissolved in dry MeOH (0.7 M), cooled to 0 °C and the flask was covered with aluminium foil. Et₃N (1.5 eq) was added, followed by dropwise addition of a saturated solution of iodine in MeOH until the dark color persists. The reaction was quenched with 1 M aq. Na₂S₂O₃ and diluted with EtOAc. The organic layer was washed with 1 M aq. HCl (1x) and the aqueous layer was extracted again with EtOAc (1x). The combined organic layers were washed with brine (1x), dried (Na₂SO₄), filtered and concentrated under reduced pressure. The crude residue was purified using silica gel column chromatography, affording the diazirine product.

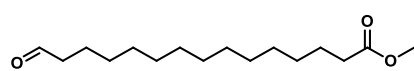
General procedure C

A round bottom flask covered with aluminium foil was charged with diazirine carboxylic acid (1 eq), EDC·HCl (1.5 eq), HOBt (1.5 eq) and dry DCM (0.2 M) and stirred for 1 h. Next, the amine (2 – 7 eq) was added and the reaction was stirred overnight. The mixture was concentrated under reduced pressure, dissolved in EtOAc and sequentially washed with 1 M aq. HCl (2x), sat. aq. NaHCO₃ (2x) and brine (1x). Each aqueous layer was back-extracted with EtOAc (1x) and the combined organic layers were dried (MgSO₄), filtered and concentrated under reduced pressure. The crude residue was purified using silica gel column chromatography, affording the amide product.

General procedure D

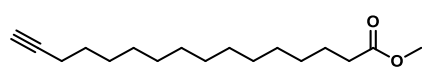


A round bottom flask was charged with phosphoramidite (1 eq), ethanolamide (1.1 eq), 1*H*-tetrazole (2 eq) and dry DCM (0.2 M) and stirred for 75 min. Sulfur (S₈, 20 eq) was added and the mixture was stirred overnight. The solvents were evaporated under reduced pressure and the crude residue was purified using silica gel column chromatography, affording the thiophosphotriester product.

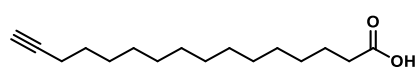
NAPE-based photoprobes 1-7

Methyl 15-oxopentadecanoate (10). *Esterification:* A round bottom flask was charged with 15-hydroxypentadecanoic acid **8** (1.0 g, 4.0 mmol, 1 eq) and MeOH (10 mL) and was cooled with a water bath.

Acetylchloride (1.4 mL, 20 mmol, 5 eq) was added carefully and the reaction was stirred for 3.5 h. The solvents were evaporated and coevaporated with toluene (1x). The mixture was dissolved in DCM (40 mL) and washed with sat. aq. NaHCO₃ (1 x 40 mL), brine (1 x 40 mL), dried (Na₂SO₄), filtered and concentrated under reduced pressure, affording the methyl ester **9** (0.91 g, 3.3 mmol, 83%). *Oxidation:* A round bottom flask was charged with methyl ester **9** (0.91 g, 3.3 mmol, 83%) and DCM (16 mL). Pyridinium chlorochromate (1.2 g, 5.6 mmol, 1.7 eq) and Celite (1.2 g, 20 mmol, 6 eq) were added and the reaction was stirred for 2 h. The reaction was diluted with Et₂O (50 mL) and the mixture was filtered over a plug of Celite and washed extensively with Et₂O. The solvents were evaporated under reduced pressure and the crude residue was purified by column chromatography (1% → 20% EtOAc in pentane) affording the aldehyde **10** (0.66 g, 2.5 mmol, 74%), which was in accordance with reported NMR data.⁵⁰ ¹H NMR (400 MHz, CDCl₃) δ 9.93 – 9.59 (m, 1H), 3.66 (s, 3H), 2.51 – 2.36 (m, 2H), 2.30 (t, *J* = 7.5 Hz, 2H), 1.71 – 1.54 (m, 4H), 1.37 – 1.20 (m, 18H). ¹³C NMR (101 MHz, CDCl₃) δ 202.80, 174.24, 51.38, 43.89, 34.06, 29.58, 29.55, 29.42, 29.35, 29.25, 29.15, 29.14, 24.94, 22.07.

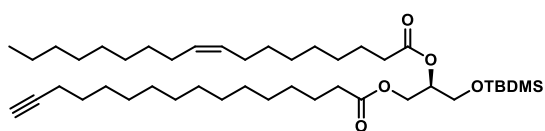


Methyl hexadec-15-ynoate (11). A round bottom flask was charged with the aldehyde **10** (0.66 g, 2.5 mmol, 1 eq) and MeOH (12 mL) and cooled to 0 °C. Ohira-Bestmann reagent (0.88 mL, 3.7 mmol, 1.5 eq) and K₂CO₃ (0.68 g, 4.9 mmol, 2 eq) were added and the mixture was stirred for 30 min at 0 °C and warmed to rt overnight. The reaction was quenched with sat. aq. NH₄Cl (10 mL) and extracted with Et₂O (4 x 50 mL). The combined organic layers were washed with brine (1 x 150 mL), dried (MgSO₄), filtered and concentrated under reduced pressure. The crude residue was purified by column chromatography (1% → 3% EtOAc in pentane) affording the alkyne **11** (0.26 g, 0.98 mmol, 40%). ¹H NMR (400 MHz, CDCl₃) δ 3.66 (s, 3H), 2.30 (t, *J* = 7.6 Hz, 2H), 2.17 (td, *J* = 7.1, 2.6 Hz, 2H), 1.94 (t, *J* = 2.7 Hz, 1H), 1.62 (p, *J* = 7.3 Hz, 2H), 1.57 – 1.46 (m, 2H), 1.44 – 1.35 (m, 2H), 1.35 – 1.15 (m, 16H). ¹³C NMR (101 MHz, CDCl₃) δ 174.22, 84.66, 68.11, 51.39, 34.10, 29.64, 29.62, 29.61, 29.54, 29.48, 29.30, 29.18, 29.15, 28.79, 28.53, 24.98, 18.41. HRMS [C₁₇H₃₀O₂ + H]⁺: 267.2319 calculated, 267.2319 found.



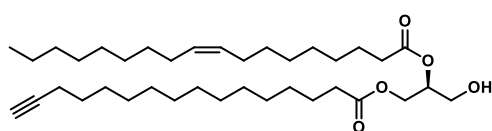
Hexadec-15-ynoic acid (12). A round bottom flask was charged with alkyne methyl ester **11** (0.26 g, 0.98 mmol, 1 eq), THF (3 mL) and 1.5 M NaOH (aq, 3 mL, 4.5 mmol, 4.5 eq). The reaction was stirred vigorously overnight after which 1 M HCl (30 mL). The aqueous layer was extracted with EtOAc (50 mL) and the organic layer was washed with brine (1 x 50 mL), dried (Na₂SO₄), filtered and concentrated under reduced pressure affording the carboxylic acid **12** (0.25 g, 0.98 mmol, quant), which was used for the next

step without further purification. ^1H NMR (400 MHz, CDCl_3) δ 10.44 (br s, 1H), 2.34 (t, J = 7.5 Hz, 2H), 2.18 (td, J = 7.1, 2.6 Hz, 2H), 1.94 (t, J = 2.6 Hz, 1H), 1.63 (p, J = 7.4 Hz, 2H), 1.52 (p, J = 7.0 Hz, 2H), 1.45 – 1.36 (m, 2H), 1.35 – 1.23 (m, 16H). ^{13}C NMR (101 MHz, CDCl_3) δ 180.20, 84.83, 68.15, 34.20, 29.69, 29.67, 29.66, 29.59, 29.52, 29.34, 29.20, 29.16, 28.85, 28.59, 24.78, 18.48. HRMS [$\text{C}_{16}\text{H}_{28}\text{O}_2 + \text{H}$] $^+$: 253.2162 calculated, 253.2164 found.



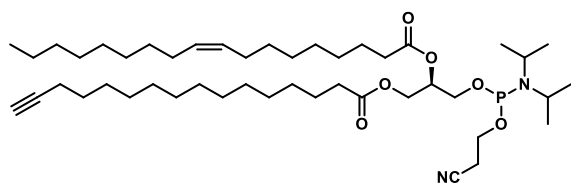
(R)-1-((tert-Butyltrimethylsilyloxy)-3-(hexadec-15-ynoyloxy)propan-2-yl oleate (13). A 10 mL round bottom flask was charged with **12** (100 mg, 0.40 mmol, 1 eq) and (*S,S*)-(+)-*N,N'*-bis(3,5-di-*tert*-butylsalicylidene)-

1,2-cyclohexane-diaminocobalt(II) (2.4 mg, 4 μmol , 1 mol%) in Et_2O (1 mL) and stirred under an O_2 atmosphere (balloon). After 15 min the solvent was evaporated and DiPEA (70 μL , 0.40 mmol, 1 eq) and *tert*-butyltrimethylsilyl (*R*)-(-)-glycidyl ether (87 μL , 0.40 mmol, 1 eq) were added. The reaction mixture was stirred overnight under an O_2 atmosphere, after which the solvents were concentrated under reduced pressure. The crude residue was purified by column chromatography (5 \rightarrow 25% EtOAc/pentane), affording the *sn*-1-monoacylglycerol (100 mg, 0.23 mmol, 57%). The product was dissolved in heptane (1 mL) and cooled to 0 $^\circ\text{C}$ under an argon atmosphere. Next, oleic acid (215 μL , 0.68 mmol, 3 eq), DMAP (3 mg, 0.03 mmol, 10 mol%) and DIC (43 μL , 0.28 mmol, 1.2 eq) were added. After 30 min the reaction was warmed to rt and stirred overnight. The solvents were concentrated under reduced pressure and the crude residue was purified by column chromatography (2.5% \rightarrow 5% EtOAc in pentane) affording the mixed diacylglycerol **13** (98 mg, 0.14 mmol, 60%). ^1H NMR (400 MHz, CDCl_3) δ 5.43 – 5.26 (m, 2H), 5.12 – 5.03 (m, 1H), 4.34 (dd, J = 11.8, 3.7 Hz, 1H), 4.16 (dd, J = 11.8, 6.3 Hz, 1H), 3.78 – 3.64 (m, 2H), 2.30 (td, J = 7.6, 2.2 Hz, 4H), 2.18 (td, J = 7.1, 2.6 Hz, 2H), 2.01 (q, J = 6.4 Hz, 4H), 1.93 (t, J = 2.6 Hz, 1H), 1.66 – 1.57 (m, 4H), 1.57 – 1.47 (m, 2H), 1.41 – 1.36 (m, 2H), 1.36 – 1.21 (m, 36H), 0.92 – 0.85 (m, 12H), 0.05 (s, 6H). ^{13}C NMR (101 MHz, CDCl_3) δ 173.56, 173.19, 130.11, 129.82, 84.87, 71.79, 68.16, 62.56, 61.57, 34.46, 34.28, 32.04, 29.89, 29.84, 29.73, 29.64, 29.60, 29.45, 29.42, 29.33, 29.25, 29.21, 28.89, 28.62, 27.34, 27.30, 25.88, 25.06, 25.04, 22.82, 18.52, 18.33, 14.25, -5.34, -5.38. HRMS [$\text{C}_{43}\text{H}_{80}\text{O}_5\text{Si} + \text{H}$] $^+$: 705.5848 calculated, 705.5852 found. $[\alpha]_D = +7.2$ (c = 0.92 in CHCl_3).



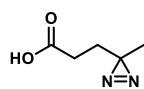
(S)-1-(Hexadec-15-ynoyloxy)-3-hydroxypropan-2-yl oleate (14). A round bottom flask was charged with protected diacylglycerol **13** (45 mg, 64 μmol , 1 eq) and a mixture of THF/ CH_3CN (1:1, 1 mL). $\text{Et}_3\text{N}\cdot 3\text{HF}$ (125 μL , 0.76 mmol, 12 eq)

was added and the reaction was stirred overnight. The mixture was cooled to 0 $^\circ\text{C}$ and quenched with sat. aq. NaHCO_3 (10 mL). The aqueous phase was extracted with DCM (3 x 20 mL) and the combined organic layers were washed with brine (1 x 50 mL), dried (Na_2SO_4), filtered and concentrated under reduced pressure. The crude residue was purified by column chromatography (10% \rightarrow 30% EtOAc in pentane) affording the diacylglycerol **14** (35 mg, 59 μmol , 93%). ^1H NMR (400 MHz, CDCl_3) δ 5.42 – 5.27 (m, 2H), 5.08 (p, J = 5.0 Hz, 1H), 4.32 (dd, J = 11.9, 4.5 Hz, 1H), 4.23 (dd, J = 11.9, 5.7 Hz, 1H), 3.73 (d, J = 5.0 Hz, 2H), 2.40 – 2.28 (m, 4H), 2.18 (td, J = 7.1, 2.6 Hz, 2H), 2.01 (q, J = 6.2 Hz, 4H), 1.94 (t, J = 2.6 Hz, 1H), 1.68 – 1.57 (m, 4H), 1.57 – 1.47 (m, 2H), 1.42 – 1.20 (m, 39H), 0.88 (t, J = 6.8 Hz, 3H). ^{13}C NMR (101 MHz, CDCl_3) δ 173.92, 173.54, 130.16, 129.82, 84.94, 72.25, 68.17, 62.15, 61.68, 34.42, 34.24, 32.04, 29.90, 29.84, 29.73, 29.66, 29.64, 29.60, 29.46, 29.40, 29.32, 29.25, 29.20, 28.90, 28.64, 27.36, 27.31, 25.06, 25.02, 22.82, 18.54, 14.25. HRMS [$\text{C}_{37}\text{H}_{66}\text{O}_5 + \text{H}$] $^+$: 591.4983 calculated, 591.4982 found. $[\alpha]_D = -2.3$ (c = 0.7 in CHCl_3).

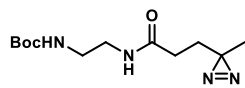


(2R)-1-(((2-Cyanoethoxy)(diisopropylamino)phosphan-yl)oxy)-3-(hexadec-15-ynoyloxy)propan-2-yl oleate (15). A round bottom flask was charged with **14** (32 mg, 54 μmol , 1 eq), DiPEA (38 μL , 0.22 mmol, 4 eq) and dry DCM (1 mL). 2-Cyanoethyl *N,N*-diisopropylchloro-

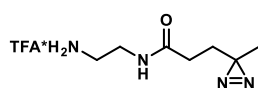
phosphoramidite (24 μL , 0.11 mmol, 2 eq) was added. The reaction mixture was stirred for 30 min then quenched with sat. aq. NaHCO_3 in ice (20 mL). EtOAc (20 mL) was added and the organic layer was separated, washed with H_2O (2 x 20 mL) and brine (1 x 20 mL), dried (Na_2SO_4), filtered and concentrated under reduced pressure. The crude residue was purified by column chromatography (pre-treat silica gel with 90:5:5 pentane/EtOAc/ Et_3N , elute 90:5:5 pentane/EtOAc/ Et_3N), affording the phosphoramidite **15** (42 mg, 53 μmol , 98%). ^1H NMR (400 MHz, CDCl_3) δ 5.41 – 5.27 (m, 2H), 5.24 – 5.13 (m, 1H), 4.40 – 4.30 (m, 1H), 4.17 (td, J = 11.5, 6.3 Hz, 1H), 3.90 – 3.74 (m, 3H), 3.74 – 3.66 (m, 1H), 3.66 – 3.52 (m, 2H), 2.63 (t, J = 6.4 Hz, 2H), 2.38 – 2.25 (m, 4H), 2.18 (td, J = 7.1, 2.6 Hz, 2H), 2.08 – 1.96 (m, 4H), 1.93 (t, J = 2.6 Hz, 1H), 1.67 – 1.57 (m, 4H), 1.56 – 1.47 (m, 2H), 1.42 – 1.21 (m, 38H), 1.21 – 1.09 (m, 12H), 0.88 (t, J = 6.8 Hz, 3H). ^{13}C NMR (101 MHz, CDCl_3) δ 173.49, 173.07, 130.13, 129.82, 117.64, 84.91, 70.84, 70.80, 70.76, 70.73, 68.16, 62.51, 62.50, 61.94, 61.78, 61.63, 58.73, 58.64, 58.54, 58.46, 43.37, 43.36, 43.25, 43.23, 34.43, 34.25, 32.03, 29.90, 29.85, 29.83, 29.74, 29.65, 29.64, 29.60, 29.45, 29.42, 29.34, 29.27, 29.24, 29.22, 28.89, 28.63, 27.35, 27.31, 25.04, 25.02, 24.75, 24.68, 22.81, 20.53, 20.46, 18.53, 14.24. ^{31}P NMR (162 MHz, CDCl_3) δ 149.92, 149.77.



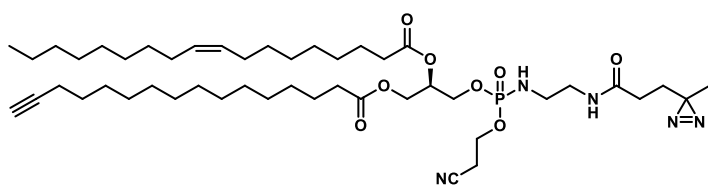
3-(3-Methyl-3H-diazirin-3-yl)propanoic acid (17). The title compound was prepared according to general procedure B using levulinic acid **16** (1.0 mL, 10 mmol, 1 eq), ammonia (7 M in MeOH, 10 mL, 70 mmol, 7 eq), hydroxylamine-*O*-sulfonic acid (1.3 g, 12 mmol, 1.15 eq) and Et_3N (2.1 mL, 15 mmol, 1.5 eq), affording the product **17** (0.60 g, 4.7 mmol, 47%), which was in accordance with reported NMR data.⁵¹ ^1H NMR (400 MHz, CDCl_3) δ 10.87 (br s, 1H), 2.31 – 2.23 (m, 2H), 1.80 – 1.65 (m, 2H), 1.05 (s, 3H). ^{13}C NMR (101 MHz, CDCl_3) δ 178.71, 29.31, 28.53, 25.07, 19.59.



tert-Butyl (2-(3-(3-methyl-3H-diazirin-3-yl)propanamido)ethyl)carbamate (18). A round bottom flask was charged with carboxylic acid **12** (81 mg, 0.63 mmol, 1 eq) and DCM (3 mL). EDC·HCl (182 mg, 0.95 mmol, 1.5 eq) and HOSu (109 mg, 0.95 mmol, 1.5 eq) were added and the mixture was stirred for 3 h. DiPEA (0.33 mL, 1.9 mmol, 3 eq) and *N*-Boc-ethylenediamine (0.11 mL, 0.69 mmol, 1.1 eq) were added and the reaction was stirred overnight. The mixture was diluted with EtOAc (50 mL) and washed with 0.1 M HCl (2 x 50 mL), sat. aq. NaHCO_3 (1 x 50 mL), brine (1 x 50 mL), dried (Na_2SO_4), filtered and concentrated under reduced pressure. The crude residue was purified by column chromatography (20% → 80% EtOAc in pentane), affording the amide **18** (0.12 g, 0.45 mmol, 71%). ^1H NMR (400 MHz, CDCl_3) δ 6.55 – 6.35 (m, 1H), 5.16 – 5.05 (m, 1H), 3.40 – 3.32 (m, 2H), 3.32 – 3.22 (m, 2H), 2.12 – 1.93 (m, 2H), 1.75 (t, J = 7.7 Hz, 2H), 1.44 (s, 9H), 1.03 (s, 3H). ^{13}C NMR (101 MHz, CDCl_3) δ 172.15, 79.83, 40.94, 40.24, 30.73, 30.13, 25.56, 19.97. HRMS [$\text{C}_{12}\text{H}_{22}\text{N}_4\text{O}_3 + \text{H}$]⁺: 271.1765 calculated, 271.1762 found.

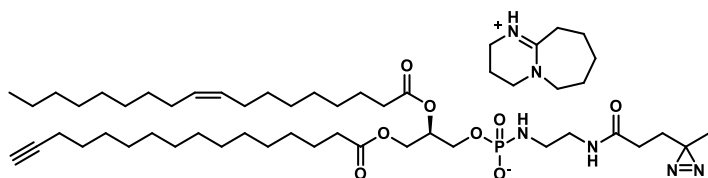


***N*-(2-Aminoethyl)-3-(3-methyl-3H-diazirin-3-yl)propanamide TFA salt (19).** A round bottom flask was charged with Boc-protected amine **18** (115 mg, 0.43 mmol, 1 eq) and a mixture of TFA/DCM (1:1, 4 mL). The reaction was stirred for 1 h after which the solvents were evaporated under reduced pressure. The residue was coevaporated with toluene (3x) affording the product as the TFA salt **19** (122 mg, 0.43 mmol, quant), which was used without further purification.



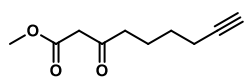
(2R)-1-(((2-Cyanoethoxy)((2-(3-(3-methyl-3H-diazirin-3-yl)propanamido)-ethyl)-amino)-phosphoryl)-oxy)-3-(hexadec-15-ynoyloxy)propan-2-yl oleate (20**).** *H*-phosphonate formation: A round bottom flask was charged with

phosphoramidite **15** (24 mg, 30 μ mol, 1 eq), 1*H*-tetrazole (4 mg, 56 μ mol, 2 eq) and CH₃CN (1 mL). The mixture was stirred for 10 min, after which H₂O was added (100 μ L) and then further stirred for 25 min. The reaction was diluted with DCM (20 mL) and washed with brine (1 x 20 mL), dried (MgSO₄), filtered and concentrated under reduced pressure, affording the *H*-phosphonate intermediate (22 mg, 31 μ mol, quant). *Phosphoramidate synthesis*: A round bottom flask was charged with TFA salt **19** (20 mg, 70 μ mol, 2.2 eq), CCl₄ (12 μ L, 124 μ mol, 4 eq), Et₃N (43 μ L, 0.31 mmol, 10 eq) and CH₃CN (0.5 mL). The *H*-phosphonate (22 mg, 31 μ mol, 1 eq) was taken up in DCM (1.2 mL) and added to the mixture via syringe. The reaction was stirred for 2.5 h after which the solvents were evaporated under reduced pressure. The crude residue was purified by column chromatography (2% -> 6% MeOH in DCM), affording the phosphoramidate **20** (15 mg, 17 μ mol, 55%). ¹H NMR (600 MHz, CDCl₃) δ 6.49 – 6.26 (m, 1H), 5.39 – 5.31 (m, 2H), 5.30 – 5.23 (m, 1H), 4.34 (ddd, *J* = 11.8, 7.6, 4.1 Hz, 1H), 4.28 – 3.97 (m, 5H), 3.59 – 3.46 (m, 1H), 3.42 – 3.28 (m, 2H), 3.18 – 3.03 (m, 2H), 2.77 (t, *J* = 6.0 Hz, 2H), 2.38 – 2.28 (m, 4H), 2.18 (td, *J* = 7.2, 2.6 Hz, 2H), 2.06 – 1.97 (m, 6H), 1.94 (t, *J* = 2.6 Hz, 1H), 1.80 (t, *J* = 7.6 Hz, 2H), 1.66 – 1.57 (m, 4H), 1.55 – 1.49 (m, 2H), 1.42 – 1.37 (m, 2H), 1.37 – 1.20 (m, 36H), 1.04 (s, 3H), 0.88 (t, *J* = 7.0 Hz, 3H). ¹³C NMR (151 MHz, CDCl₃) δ 173.59, 173.57, 173.26, 173.19, 172.26, 172.25, 130.17, 129.79, 117.04, 84.95, 69.65, 69.62, 69.60, 69.58, 68.18, 64.85, 64.82, 64.73, 64.70, 61.89, 61.81, 61.19, 61.15, 41.20, 41.17, 41.02, 40.99, 40.96, 34.31, 34.15, 32.04, 30.62, 29.90, 29.87, 29.86, 29.76, 29.74, 29.74, 29.66, 29.64, 29.62, 29.46, 29.42, 29.35, 29.28, 29.26, 29.25, 29.20, 28.90, 28.62, 27.36, 27.31, 25.78, 24.98, 24.97, 22.82, 20.10, 19.97, 19.93, 18.53, 14.27. ³¹P NMR (162 MHz, CDCl₃) δ 9.55, 9.43. HRMS [C₄₇H₈₂N₅O₈P + H]⁺: 876.5974 calculated, 876.5982 found.

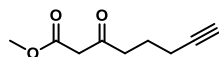


(R)-3-(hexadec-15-ynoyloxy)-2-(oleoyloxy)-propyl (2-(3-(3-methyl-3H-diazirin-3-yl)propanamido)-ethyl)-phosphoramidate DBU-H⁺ salt (1**).** A round bottom flask was charged with protected phosphoramidate **20** (13 mg,

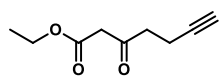
15 μ mol, 1 eq), 1,8-diazabicyclo[5.4.0]undec-7-ene (2.5 μ L, 17 μ mol, 1.1 eq) and DCM (0.5 mL). The mixture was stirred for 2 h after which the solvents were evaporated under reduced pressure and the residue was coevaporated with toluene (2x). The crude residue was purified by column chromatography (10% -> 20% MeOH in DCM), affording the phosphoramidate as the DBU salt **1** (6 mg, 6.2 μ mol, 41%). ¹H NMR (600 MHz, CDCl₃ + MeOD) δ 5.35 – 5.27 (m, 2H), 5.22 – 5.16 (m, 1H), 4.39 (dd, *J* = 12.0, 3.0 Hz, 1H), 4.16 (dd, *J* = 12.0, 6.9 Hz, 1H), 3.94 – 3.83 (m, 2H), 3.61 – 3.56 (m, 2H), 3.54 (t, *J* = 5.9 Hz, 2H), 3.35 (t, *J* = 5.8 Hz, 2H), 3.21 (t, *J* = 5.8 Hz, 2H), 2.98 – 2.90 (m, 2H), 2.70 – 2.63 (m, 2H), 2.36 – 2.25 (m, 4H), 2.14 (td, *J* = 7.1, 2.6 Hz, 2H), 2.08 – 2.03 (m, 4H), 2.03 – 1.95 (m, 5H), 1.83 – 1.78 (m, 2H), 1.78 – 1.70 (m, 4H), 1.70 – 1.64 (m, 2H), 1.63 – 1.53 (m, 4H), 1.48 (p, *J* = 7.1 Hz, 2H), 1.41 – 1.35 (m, 2H), 1.34 – 1.19 (m, 36H), 1.00 (s, 3H), 0.86 (t, *J* = 7.0 Hz, 3H). ¹³C NMR (151 MHz, CDCl₃ + MeOD) δ 174.56, 174.18, 173.80, 166.81, 130.47, 130.20, 84.99, 78.37, 78.16, 77.94, 71.37, 71.31, 68.66, 63.36, 63.23, 63.20, 55.08, 42.27, 41.13, 38.78, 34.77, 34.61, 33.28, 32.46, 30.94, 30.88, 30.28, 30.16, 30.14, 30.06, 30.05, 29.86, 29.82, 29.80, 29.69, 29.68, 29.65, 29.39, 29.27, 29.08, 27.70, 27.69, 27.02, 25.88, 25.47, 25.43, 24.39, 23.19, 19.88, 19.79, 18.75, 14.33. ³¹P NMR (162 MHz, CDCl₃ + MeOD) δ 6.86. HRMS [C₄₄H₇₉N₄O₈P + H]⁺: 823.5708 calculated, 823.5702 found.



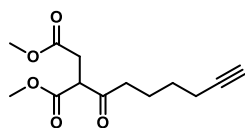
Methyl 3-oxonon-8-ynoate (24). The title compound was prepared according to general procedure A using 6-heptynoic acid **21** (1.1 mL, 8.9 mmol, 1 eq), Meldrum's acid (1.6 g, 11 mmol, 1.1 eq), DMAP (1.5 g, 12 mmol, 1.3 eq) and DIC (1.8 mL, 12 mmol, 1.3 eq). Column chromatography (10% → 20% EtOAc in pentane) afforded the product **24** (1.2 g, 6.7 mmol, 74%). ¹H NMR (400 MHz, CDCl₃) δ 3.74 (s, 3H), 3.46 (s, 2H), 2.58 (t, *J* = 7.3 Hz, 2H), 2.21 (td, *J* = 7.0, 2.7 Hz, 2H), 1.97 (t, *J* = 2.6 Hz, 1H), 1.77 – 1.67 (m, 2H), 1.60 – 1.50 (m, 2H). ¹³C NMR (101 MHz, CDCl₃) δ 202.35, 167.65, 83.91, 68.74, 52.36, 49.00, 42.37, 27.63, 22.46, 18.20. HRMS [C₁₀H₁₄O₃ + H]⁺: 183.1016 calculated, 183.1016 found.



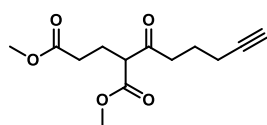
Methyl 3-oxooct-7-ynoate (25). The title compound was prepared according to general procedure A using 5-hexynoic acid **22** (2.2 mL, 20 mmol, 1 eq), Meldrum's acid (3.2 g, 22 mmol, 1.1 eq), DMAP (2.9 g, 24 mmol, 1.2 eq) and DIC (3.7 mL, 24 mmol, 1.2 eq). Column chromatography (5% → 10% EtOAc in pentane) afforded the product **25** (1.8 g, 10.4 mmol, 52%). ¹H NMR (300 MHz, CDCl₃) δ 3.74 (s, 3H), 3.50 (s, 2H), 2.71 (t, *J* = 7.2 Hz, 2H), 2.24 (td, *J* = 6.9, 2.7 Hz, 2H), 2.02 (t, *J* = 2.7 Hz, 1H), 1.81 (p, *J* = 7.0 Hz, 2H). ¹³C NMR (75 MHz, CDCl₃) δ 202.00, 167.43, 83.20, 69.21, 52.17, 48.91, 41.19, 21.82, 17.37. HRMS [C₉H₁₂O₃ + H]⁺: 169.0859 calculated, 169.0859 found.



Ethyl 3-oxohept-6-ynoate (26). The title compound was prepared according to general procedure A using 4-pentynoic acid **23** (2.0 g, 20 mmol, 1 eq), Meldrum's acid (3.2 g, 22 mmol, 1.1 eq), DMAP (2.9 g, 24 mmol, 1.2 eq) and DIC (3.7 mL, 24 mmol, 1.2 eq). Column chromatography (5% → 10% EtOAc in pentane) afforded the product **26** (2.0 g, 11.5 mmol, 58%). ¹H NMR (300 MHz, CDCl₃) δ 4.27 – 4.12 (m, 2H), 3.48 (s, 2H), 2.89 – 2.73 (m, 2H), 2.48 (td, *J* = 7.2, 2.6 Hz, 2H), 2.01 – 1.94 (m, 1H), 1.34 – 1.23 (m, 3H). ¹³C NMR (75 MHz, CDCl₃) δ 200.64, 166.94, 82.57, 69.04, 61.51, 49.21, 41.61, 14.11, 12.82. HRMS [C₉H₁₂O₃ + H]⁺: 169.0859 calculated, 169.0859 found.

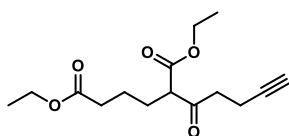


Dimethyl 2-(hept-6-ynoyl)succinate (27). A round bottom flask was charged with β-ketoester **24** (1.2 g, 6.7 mmol, 1 eq) and NaOMe (0.47 g, 8.6 mmol, 1.3 eq) and dry MeOH (30 mL) and stirred for 30 min. Next, methyl bromoacetate (0.82 mL, 8.7 mmol, 1.3 eq) was added and the reaction mixture was stirred at reflux temperature for 3.5 h. The solvents were removed under reduced pressure and the crude residue was dissolved in EtOAc. The organic layer was washed with water (1 x 120 mL) and brine (1 x 120 mL), dried (MgSO₄), filtered and concentrated under reduced pressure. The crude residue was purified by column chromatography (10% → 20% EtOAc in pentane) affording the product **27** (1.1 g, 4.4 mmol, 66%) and recovered starting material (0.23 g, 2.0 mmol, 19%). ¹H NMR (400 MHz, CDCl₃) δ 3.99 (dd, *J* = 8.4, 6.1 Hz, 1H), 3.75 (s, 3H), 3.68 (s, 3H), 3.00 (dd, *J* = 17.6, 8.5 Hz, 1H), 2.84 (dd, *J* = 17.5, 6.1 Hz, 1H), 2.80 – 2.60 (m, 2H), 2.20 (td, *J* = 7.0, 2.6 Hz, 2H), 1.96 (t, *J* = 2.6 Hz, 1H), 1.78 – 1.68 (m, 2H), 1.59 – 1.48 (m, 2H). ¹³C NMR (101 MHz, CDCl₃) δ 203.53, 171.81, 168.88, 84.00, 68.66, 53.74, 52.78, 52.07, 42.19, 32.20, 27.64, 22.46, 18.23. HRMS [C₁₃H₁₈O₅ + H]⁺: 255.1227 calculated, 255.1226 found.

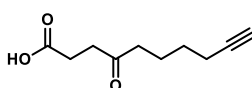


Dimethyl 2-(hex-5-ynoyl)pentanedioate (28). A round bottom flask was charged with β-ketoester **25** (1.7 g, 10 mmol, 1 eq), K₂CO₃ (1.4 g, 10 mmol, 1 eq), methyl acrylate (0.93 mL, 10 mmol, 1 eq) and DCM (50 mL). The mixture was stirred for 20 h at rt, followed by addition of methyl acrylate (0.47 mL, 5.1 mmol, 0.5 eq) and stirring for 4 h at rt, then for 16 h at reflux. DMF (20 mL) was added and the reaction was refluxed for 4 h, after which starting material was consumed as judged by TLC analysis. H₂O was added (50 mL) and the mixture was extracted with Et₂O (3 x 50 mL). The combined organic layers were washed with water (2 x 100 mL), brine (1 x 100 mL), dried (MgSO₄), filtered and concentrated under reduced pressure. The crude residue was purified by column chromatography (5% → 30% EtOAc in pentane) affording the product **28** (1.4 g, 5.5 mmol, 53%). ¹H NMR (300 MHz, CDCl₃) δ 3.74 (s, 3H), 3.70 – 3.58 (m, 4H), 2.90 – 2.58 (m, 2H), 2.41 – 2.30 (m, 2H), 2.22 (td, *J* = 6.9, 2.7 Hz, 2H), 2.18 – 2.08 (m, 2H), 2.05 (t, *J* = 2.6 Hz, 1H), 1.79 (p, *J* = 7.0 Hz, 2H).

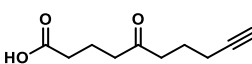
^{13}C NMR (75 MHz, CDCl_3) δ 203.70, 172.65, 169.29, 82.99, 69.04, 56.94, 52.08, 51.24, 40.15, 30.81, 22.64, 21.67, 17.09. HRMS [$\text{C}_{13}\text{H}_{18}\text{O}_5 + \text{H}$] $^+$: 255.1227 calculated, 255.1224 found.



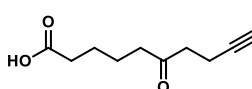
Diethyl 2-(pent-4-ynoyl)hexanedioate (29). A round bottom flask was charged with β -ketoester **26** (1.9 g, 11.4 mmol, 1 eq), NaOEt (0.86 g, 12.6 mmol, 1.1 eq), NaI (0.16 g, 1.1 mmol, 0.1 eq) and dry EtOH (11 mL) and stirred for 30 min. Next, a solution of ethyl 4-bromobutanoate (2.3 mL, 16.1 mmol, 1.4 eq) in EtOH (16 mL) was added dropwise and the reaction mixture was stirred at reflux overnight. Additional NaOEt (2.7 M in EtOH, 2.6 mL, 6.9 mmol, 0.6 eq) was added and the reaction was stirred for 0.5 h. The solvents were removed under reduced pressure and the crude residue was dissolved in 0.5 M HCl (aq, 75 mL) and extracted with Et_2O (3 x 60 mL). The combined organic layers were washed with H_2O (2 x 180 mL), dried (MgSO_4), filtered and concentrated under reduced pressure. The crude residue was purified by column chromatography (5% \rightarrow 20% EtOAc in pentane) affording the product **29** (1.2 g, 4.3 mmol, 38%) and recovered starting material (0.38 g, 2.3 mmol, 20%). ^1H NMR (300 MHz, CDCl_3) δ 4.26 – 4.07 (m, 4H), 3.48 (t, $J = 7.3$ Hz, 1H), 2.94 – 2.66 (m, 2H), 2.46 (td, $J = 7.3$, 2.6 Hz, 2H), 2.33 (t, $J = 7.3$ Hz, 2H), 1.97 (t, $J = 2.7$ Hz, 1H), 1.95 – 1.83 (m, 2H), 1.68 – 1.54 (m, 2H), 1.27 (q, $J = 7.2$ Hz, 6H). ^{13}C NMR (75 MHz, CDCl_3) δ 202.73, 172.94, 169.23, 82.65, 68.94, 61.54, 60.38, 58.61, 40.59, 33.84, 27.36, 22.66, 14.23, 14.11, 12.86. HRMS [$\text{C}_{15}\text{H}_{22}\text{O}_5 + \text{H}$] $^+$: 283.1540 calculated, 283.1535 found.



4-Oxodec-9-ynoic acid (30). A round bottom flask was charged with ketodiester **27** (1.7 g, 6.9 mmol, 1 eq), THF (40 mL) and 1 M NaOH (aq, 40 mL, 40 mmol, 5.8 eq) and the reaction was stirred vigorously overnight. The mixture was cooled to 0 $^\circ\text{C}$ and 3 M HCl (aq, 60 mL) was added carefully. The reaction was stirred at rt for 2 h and at 55 $^\circ\text{C}$ for 1 h. The mixture was extracted with EtOAc (3 x 100 mL) and the combined organic layers were washed with brine (1 x 200 mL), dried (MgSO_4), filtered and concentrated under reduced pressure. The crude residue was purified by column chromatography (40% \rightarrow 60% EtOAc in pentane + 0.5% AcOH) affording the ketoacid **30** (1.3 g, 6.9 mmol, quant). ^1H NMR (400 MHz, $\text{CDCl}_3 + \text{MeOD}$) δ 2.74 (t, $J = 6.4$ Hz, 2H), 2.58 (t, $J = 6.4$ Hz, 2H), 2.51 (t, $J = 7.3$ Hz, 2H), 2.20 (td, $J = 6.8$, 2.2 Hz, 2H), 2.05 – 1.96 (m, 1H), 1.71 (p, $J = 7.3$ Hz, 2H), 1.53 (p, $J = 7.1$ Hz, 2H). ^{13}C NMR (101 MHz, $\text{CDCl}_3 + \text{MeOD}$) δ 209.70, 175.20, 83.76, 68.47, 41.85, 36.83, 27.59, 27.52, 22.54, 17.91. HRMS [$\text{C}_{10}\text{H}_{14}\text{O}_3 + \text{H}$] $^+$: 183.1016 calculated, 183.1016 found.

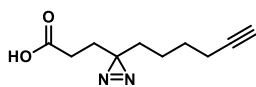


5-Oxodec-9-ynoic acid (31). A round bottom flask was charged with ketodiester **28** (1.4 g, 5.4 mmol, 1 eq), THF (32 mL) and 1 M NaOH (aq, 32 mL, 32 mmol, 5.8 eq) and the reaction was stirred vigorously for 2 h. The mixture was cooled to 0 $^\circ\text{C}$ and 3 M HCl (aq, 47 mL) was added carefully, followed by stirring at 55 $^\circ\text{C}$ overnight. The mixture was extracted with EtOAc (3 x 80 mL) and the combined organic layers were washed with brine (1 x 160 mL), dried (MgSO_4), filtered and concentrated under reduced pressure. The crude residue was purified by column chromatography (40% \rightarrow 60% EtOAc in pentane + 0.5% AcOH) affording the ketoacid **31** (0.83 g, 4.6 mmol, 84%). ^1H NMR (300 MHz, CDCl_3) δ 11.36 (br s, 1H), 2.57 (q, $J = 7.5$ Hz, 4H), 2.40 (t, $J = 6.9$ Hz, 2H), 2.22 (t, $J = 6.6$ Hz, 2H), 2.08 – 1.99 (m, 1H), 1.95 – 1.81 (m, 2H), 1.81 – 1.69 (m, 2H). ^{13}C NMR (75 MHz, CDCl_3) δ 209.75, 178.61, 83.23, 69.03, 41.09, 40.74, 32.60, 21.89, 18.22, 17.33. HRMS [$\text{C}_{10}\text{H}_{14}\text{O}_3 + \text{H}$] $^+$: 183.1016 calculated, 183.1015 found.

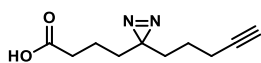


6-Oxodec-9-ynoic acid (32). A round bottom flask was charged with ketodiester **29** (1.2 g, 4.2 mmol, 1 eq), THF (25 mL) and 1 M NaOH (aq, 25 mL, 25 mmol, 5.8 eq) and the reaction was stirred vigorously for 2 h. The mixture was cooled to 0 $^\circ\text{C}$ and 3 M HCl (aq, 47 mL) was added carefully, followed by stirring at 55 $^\circ\text{C}$ overnight. The mixture was extracted with EtOAc (3 x 60 mL) and the combined organic layers were washed with brine (1 x 120 mL), dried (MgSO_4), filtered and concentrated under reduced pressure. The crude residue was purified by column chromatography (40% \rightarrow 60% EtOAc in pentane + 0.5% AcOH) affording the ketoacid **32** (0.63 g, 3.4 mmol,

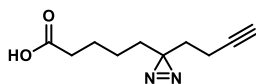
82%). ^1H NMR (300 MHz, CDCl_3) δ 11.47 (s, 1H), 2.68 (t, J = 7.1 Hz, 2H), 2.55 – 2.30 (m, 6H), 2.02 – 1.94 (m, 1H), 1.75 – 1.55 (m, 4H). ^{13}C NMR (75 MHz, CDCl_3) δ 208.39, 179.53, 82.97, 68.76, 42.12, 41.10, 33.64, 23.93, 22.80, 12.82. HRMS [$\text{C}_{10}\text{H}_{14}\text{O}_3 + \text{H}$] $^+$: 183.1016 calculated, 183.1015 found.



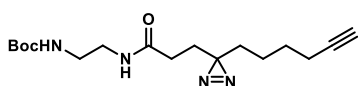
3-(3-(Hex-5-yn-1-yl)-3H-diazirin-3-yl)propanoic acid (33). The title compound was prepared according to general procedure B using ketoacid **30** (1.3 g, 6.9 mmol, 1 eq), ammonia (7 M in MeOH, 13 mL, 91 mmol, 21 eq), hydroxylamine-*O*-sulfonic acid (1.1 g, 9.8 mmol, 1.4 eq) and Et_3N (1.5 mL, 10.5 mmol, 1.5 eq). Column chromatography (10% → 40% EtOAc in pentane + 0.5% AcOH) afforded the product **33** (0.69 g, 3.5 mmol, 51%). ^1H NMR (400 MHz, CDCl_3) δ 10.89 (br s, 1H), 2.21 – 2.12 (m, 4H), 1.96 (t, J = 2.6 Hz, 1H), 1.75 (t, J = 7.7 Hz, 2H), 1.53 – 1.40 (m, 4H), 1.28 – 1.18 (m, 2H). ^{13}C NMR (101 MHz, CDCl_3) δ 178.85, 83.94, 68.78, 32.28, 28.42, 27.96, 27.93, 27.85, 22.96, 18.22. HRMS [$\text{C}_{10}\text{H}_{14}\text{N}_2\text{O}_2 + \text{H}$] $^+$: 195.1128 calculated, 195.1128 found.



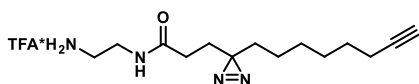
4-(3-(Pent-4-yn-1-yl)-3H-diazirin-3-yl)butanoic acid (34). The title compound was prepared according to general procedure B using ketoacid **31** (0.83 g, 4.6 mmol, 1 eq), ammonia (7 M in MeOH, 13.7 mL, 96 mmol, 21 eq), hydroxylamine-*O*-sulfonic acid (0.73 g, 6.4 mmol, 1.4 eq) and Et_3N (0.95 mL, 6.8 mmol, 1.5 eq). Column chromatography (10% → 40% EtOAc in pentane + 0.5% AcOH) afforded the product **34** (0.49 g, 2.5 mmol, 55%). ^1H NMR (300 MHz, CDCl_3) δ 11.50 (br s, 1H), 2.38 – 2.27 (m, 2H), 2.16 (td, J = 6.9, 2.6 Hz, 2H), 1.97 (t, J = 2.6 Hz, 1H), 1.57 – 1.49 (m, 2H), 1.49 – 1.40 (m, 4H), 1.39 – 1.29 (m, 2H). ^{13}C NMR (75 MHz, CDCl_3) δ 179.64, 83.31, 69.11, 33.26, 32.13, 31.53, 28.00, 22.67, 18.96, 17.89. HRMS [$\text{C}_{10}\text{H}_{14}\text{N}_2\text{O}_2 + \text{H}$] $^+$: 195.1128 calculated, 195.1128 found.



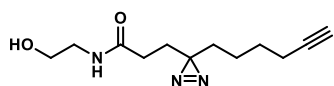
5-(3-(But-3-yn-1-yl)-3H-diazirin-3-yl)pentanoic acid (35). The title compound was prepared according to general procedure B using ketoacid **32** (0.62 g, 3.4 mmol, 1 eq), ammonia (7 M in MeOH, 10.2 mL, 71 mmol, 21 eq), hydroxylamine-*O*-sulfonic acid (0.54 g, 4.8 mmol, 1.4 eq) and Et_3N (0.71 mL, 5.1 mmol, 1.5 eq). Column chromatography (10% → 40% EtOAc in pentane + 0.5% AcOH) afforded the product **35** (0.25 g, 1.3 mmol, 38%) and recovered starting material (0.16 g, 0.89 mmol, 26%). ^1H NMR (300 MHz, CDCl_3) δ 10.91 (br s, 1H), 2.33 (t, J = 7.4 Hz, 2H), 2.09 – 1.94 (m, 3H), 1.61 (ddd, J = 15.5, 8.6, 4.9 Hz, 4H), 1.53 – 1.41 (m, 2H), 1.30 – 1.05 (m, 2H). ^{13}C NMR (75 MHz, CDCl_3) δ 179.61, 69.26, 33.81, 32.50, 32.39, 28.17, 24.22, 23.44, 13.44. HRMS [$\text{C}_{10}\text{H}_{14}\text{N}_2\text{O}_2 + \text{H}$] $^+$: 195.1128 calculated, 195.1127 found.



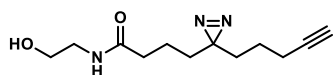
tert-Butyl (2-(3-(3-(hex-5-yn-1-yl)-3H-diazirin-3-yl)propanamido)ethyl)carbamate (36). The title compound was prepared according to general procedure C using carboxylic acid **33** (80 mg, 0.41 mmol, 1 eq), EDC·HCl (118 mg, 0.62 mmol, 1.5 eq), HOBT (84 mg, 0.62 mmol, 1.5 eq) and *N*-Boc-ethylenediamine (129 μL , 0.82 mmol, 2 eq). Column chromatography (50% → 100% EtOAc in pentane) afforded the product Boc protected amide **36** (134 mg, 0.40 mmol, 97%). ^1H NMR (400 MHz, CDCl_3) δ 6.71 – 6.47 (m, 1H), 5.30 – 5.17 (m, 1H), 3.33 (q, J = 5.3 Hz, 2H), 3.30 – 3.18 (m, 2H), 2.15 (td, J = 7.0, 2.4 Hz, 2H), 1.98 – 1.88 (m, 3H), 1.78 (t, J = 7.6 Hz, 2H), 1.51 – 1.40 (m, 13H), 1.28 – 1.19 (m, 2H). ^{13}C NMR (101 MHz, CDCl_3) δ 172.12, 157.01, 83.94, 79.67, 68.73, 40.71, 40.18, 32.42, 30.43, 28.58, 28.41, 28.33, 27.84, 22.94, 18.20. HRMS [$\text{C}_{17}\text{H}_{28}\text{N}_4\text{O}_3 + \text{H}$] $^+$: 337.2234 calculated, 337.2230 found.



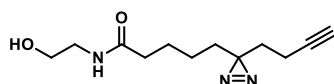
***N*-(2-Aminoethyl)-3-(3-(oct-7-yn-1-yl)-3H-diazirin-3-yl)propanamide TFA salt (37).** A round bottom flask was charged with Boc-protected amine **36** (133 mg, 0.40 mmol, 1 eq) and a mixture of TFA/DCM (1:1, 3 mL). The reaction was stirred for 1.5 h after which the solvents were evaporated under reduced pressure. The residue was coevaporated with toluene (3x) affording the product as the TFA salt **37** (140 mg, 0.40 mmol, quant), which was used without further purification.



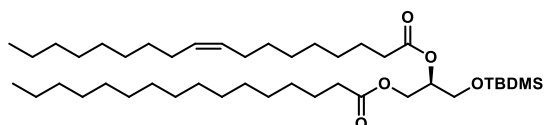
3-(3-(Hex-5-yn-1-yl)-3H-diazirin-3-yl)-N-(2-hydroxyethyl)propanamide (38). The title compound was prepared according to general procedure C using carboxylic acid **33** (224 mg, 1.2 mmol, 1 eq), EDC-HCl (332 mg, 1.7 mmol, 1.5 eq), HOBT (234 mg, 1.7 mmol, 1.5 eq) and 2-aminoethanol (349 μ L, 5.8 mmol, 5 eq). Column chromatography (0% \rightarrow 4% MeOH in EtOAc) afforded the amide product **38** (215 mg, 0.91 mmol, 78%). ^1H NMR (400 MHz, CDCl_3) δ 6.63 (s, 1H), 3.70 (t, J = 5.1 Hz, 2H), 3.60 (s, 1H), 3.38 (q, J = 5.2 Hz, 2H), 2.16 (td, J = 7.0, 2.6 Hz, 2H), 2.03 – 1.90 (m, 3H), 1.80 (t, J = 7.7 Hz, 2H), 1.53 – 1.37 (m, 4H), 1.28 – 1.15 (m, 2H). ^{13}C NMR (101 MHz, CDCl_3) δ 172.70, 114.72, 83.97, 68.77, 61.64, 42.35, 32.36, 30.39, 28.54, 28.40, 27.78, 22.91, 18.16. HRMS [$\text{C}_{12}\text{H}_{19}\text{N}_3\text{O}_2 + \text{H}$] $^+$: 238.1550 calculated, 238.1552 found.



N-(2-Hydroxyethyl)-4-(3-(pent-4-yn-1-yl)-3H-diazirin-3-yl)butanamide (39). The title compound was prepared according to general procedure C using carboxylic acid **34** (148 mg, 0.76 mmol, 1 eq), EDC-HCl (219 mg, 1.1 mmol, 1.5 eq), HOBT (154 mg, 1.1 mmol, 1.5 eq) and 2-aminoethanol (320 μ L, 5.3 mmol, 7 eq). Column chromatography (0% \rightarrow 4% MeOH in EtOAc) afforded the amide product **39** (137 mg, 0.58 mmol, 76%). ^1H NMR (400 MHz, CDCl_3) δ 6.83 – 6.68 (m, 1H), 3.96 (br s, 1H), 3.67 (t, J = 5.1 Hz, 2H), 3.37 (q, J = 5.3 Hz, 2H), 2.21 – 2.12 (m, 4H), 2.00 (t, J = 2.6 Hz, 1H), 1.55 – 1.48 (m, 2H), 1.48 – 1.39 (m, 4H), 1.37 – 1.27 (m, 2H). ^{13}C NMR (101 MHz, CDCl_3) δ 173.55, 83.31, 69.13, 61.55, 42.22, 35.45, 32.12, 31.45, 28.13, 22.61, 19.97, 17.82. HRMS [$\text{C}_{12}\text{H}_{19}\text{N}_3\text{O}_2 + \text{H}$] $^+$: 238.1550 calculated, 238.1552 found.

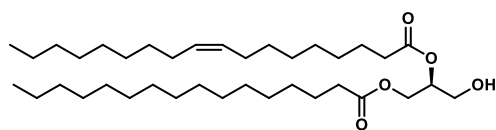


5-(3-(But-3-yn-1-yl)-3H-diazirin-3-yl)-N-(2-hydroxyethyl)pentanamide (40). The title compound was prepared according to general procedure C using carboxylic acid **35** (100 mg, 0.51 mmol, 1 eq), EDC-HCl (148 mg, 0.77 mmol, 1.5 eq), HOBT (104 mg, 0.77 mmol, 1.5 eq) and 2-aminoethanol (220 μ L, 3.6 mmol, 7 eq). Column chromatography (0% \rightarrow 4% MeOH in EtOAc) afforded the amide product **40** (84 mg, 0.35 mmol, 69%). ^1H NMR (400 MHz, CDCl_3) δ 6.55 – 6.47 (m, 1H), 3.73 – 3.66 (m, 2H), 3.58 (br s, 1H), 3.39 (q, J = 5.3 Hz, 2H), 2.17 (t, J = 7.5 Hz, 2H), 2.04 – 1.96 (m, 3H), 1.66 – 1.53 (m, 4H), 1.51 – 1.44 (m, 2H), 1.17 – 1.05 (m, 2H). ^{13}C NMR (101 MHz, CDCl_3) δ 174.04, 82.84, 69.27, 61.91, 42.36, 36.20, 32.33, 32.27, 28.18, 25.13, 23.47, 13.33. HRMS [$\text{C}_{12}\text{H}_{19}\text{N}_3\text{O}_2 + \text{H}$] $^+$: 238.1550 calculated, 238.1552 found.



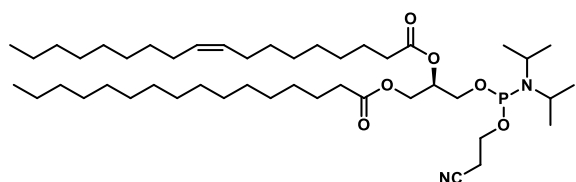
(R)-1-((tert-Butyldimethylsilyl)oxy)-3-(palmitoyloxy)propan-2-yl oleate (42). A 10 mL round bottom flask was charged with palmitic acid (1.0 g, 4.0 mmol, 1 eq) and (*S,S*)-(+)-*N,N'*-bis(3,5-di-*tert*-butylsalicylidene)-1,2-cyclohexane-diaminocobalt(II) (24 mg, 0.04 mmol, 1 mol%) in Et_2O (2 mL) and stirred under an O_2 atmosphere (balloon). After 75 min the solvent was evaporated and DiPEA (0.70 mL, 4.0 mmol, 1 eq) and *tert*-butyldimethylsilyl (*R*)-(-)-glycidyl ether **41** (0.87 mL, 4.0 mmol, 1 eq) were added. The reaction mixture was stirred overnight under an O_2 atmosphere, after which the solvents were concentrated under reduced pressure. The mixture was dissolved in heptane (8 mL) and cooled to 0 $^\circ\text{C}$ under an argon atmosphere. Next, oleic acid (1.5 mL, 4.7 mmol, 1.2 eq), DMAP (49 mg, 0.40 mmol, 10 mol%) and DIC (0.74 mL, 4.8 mmol, 1.2 eq) were added. After 30 min the reaction was warmed to rt and stirred overnight. The solvents were concentrated under reduced pressure and the crude residue was purified by column chromatography (0.5% \rightarrow 3% EtOAc in pentane) affording the diacylglycerol **42** (1.9 g, 2.6 mmol, 64%). ^1H NMR (400 MHz, CDCl_3) δ 5.36 – 5.24 (m, 2H), 5.08 – 4.98 (m, 1H), 4.31 (dd, J = 11.8, 3.7 Hz, 1H), 4.12 (dd, J = 11.8, 6.3 Hz, 1H), 3.71 – 3.65 (m, 2H), 2.26 (td, J = 7.5, 2.6 Hz, 4H), 1.97 (q, J = 6.4 Hz, 4H), 1.63 – 1.53 (m, 4H), 1.24 (d, J = 17.6 Hz, 44H), 0.88 – 0.81 (m, 15H), 0.02 (s, 6H). ^{13}C NMR (101 MHz, CDCl_3) δ 173.30, 172.95, 129.99, 129.71, 71.75, 62.45, 61.54, 34.36, 34.19, 32.02, 32.00, 29.84, 29.79, 29.75, 29.72, 29.62, 29.57, 29.46, 29.41, 29.38, 29.27, 29.21, 29.18, 29.15, 27.28, 27.23, 25.80, 24.99, 22.76,

18.23, 14.16, -5.45, -5.49. HRMS [C₄₃H₈₄O₅Si + H]⁺: 709.6161 calculated, 709.6163 found. [α]_D = +7.7 (c = 3.0 in CHCl₃).



(S)-1-((tert-Butyldimethylsilyloxy)-3-(palmitoyloxy)propan-2-yl oleate (43). A round bottom flask was charged with protected diacylglycerol **42** (1.9 g, 2.6 mmol, 1 eq) and a mixture of THF/CH₃CN (1:1, 20 mL). Et₃N·3HF (4.2 mL, 26 mmol, 10 eq) was added and the

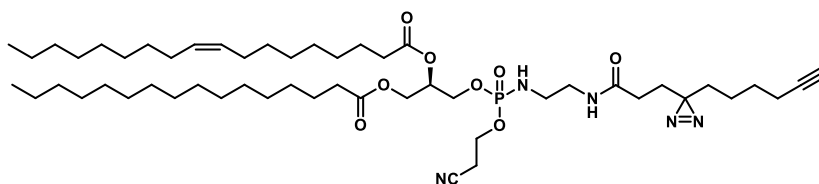
reaction was stirred overnight. The mixture was cooled to 0 °C and quenched with sat. aq. NaHCO₃ (120 mL). The aqueous phase was extracted with DCM (3 x 100 mL) and the combined organic layers were washed with brine (1 x 150 mL), dried (Na₂SO₄), filtered and concentrated under reduced pressure. The crude residue was purified by column chromatography (10% → 30% EtOAc in pentane) affording the diacylglycerol **43** (1.5 g, 2.6 mmol, 99%). ¹H NMR (400 MHz, CDCl₃) δ 5.42 – 5.25 (m, 2H), 5.09 (p, *J* = 5.1 Hz, 1H), 4.33 (dd, *J* = 11.9, 4.3 Hz, 1H), 4.22 (dd, *J* = 11.9, 5.9 Hz, 1H), 3.72 (d, *J* = 5.1 Hz, 2H), 2.60 (br s, 1H), 2.39 – 2.25 (m, 4H), 2.01 (q, *J* = 6.5 Hz, 4H), 1.72 – 1.53 (m, 4H), 1.39 – 1.19 (m, 44H), 0.88 (t, *J* = 6.8 Hz, 6H). ¹³C NMR (101 MHz, CDCl₃) δ 173.83, 173.48, 130.05, 129.73, 72.16, 62.22, 61.43, 34.36, 34.34, 34.17, 32.01, 31.99, 29.84, 29.79, 29.75, 29.71, 29.61, 29.57, 29.45, 29.41, 29.36, 29.27, 29.20, 29.18, 29.15, 27.29, 27.24, 25.01, 24.99, 24.96, 22.77, 14.18. HRMS [C₃₇H₇₀O₅ + H]⁺: 595.5296 calculated, 595.5297 found. [α]_D = -1.7 (c = 1.2 in CHCl₃)



(2R)-1-(((2-Cyanoethoxy)(diisopropylamino)-phosphanyl)oxy)-3-(palmitoyloxy)propan-2-yl oleate (44). A round bottom flask was charged with **43** (163 mg, 0.27 mmol, 1 eq), DiPEA (191 μL, 1.1 mmol, 4 eq) and dry DCM (3 mL). 2-Cyanoethyl *N,N*-diisopropylchlorophosphoramidite (90 μL, 0.41

mmol, 1.5 eq) was added. The reaction mixture was stirred for 45 min then quenched with sat. aq. NaHCO₃ in ice (30 mL). EtOAc (30 mL) was added and the organic layer was separated, washed with H₂O (1 x 30 mL) and brine (1 x 30 mL), dried (Na₂SO₄), filtered and concentrated under reduced pressure. Column chromatography (pre-treat silica gel with 90:5:5 pentane/EtOAc/Et₃N, elute 93:5:2 pentane/EtOAc/Et₃N) afforded the phosphoramidite **44** (200 mg, 0.25 mmol, 260 mg, 93%). ¹H NMR (400 MHz, CDCl₃) δ 5.41 – 5.27 (m, 2H), 5.26 – 5.12 (m, 1H), 4.42 – 4.27 (m, 1H), 4.17 (td, *J* = 11.6, 6.3 Hz, 1H), 3.92 – 3.74 (m, 3H), 3.74 – 3.65 (m, 1H), 3.65 – 3.52 (m, 2H), 2.63 (t, *J* = 6.4 Hz, 2H), 2.38 – 2.26 (m, 4H), 2.10 – 1.91 (m, 4H), 1.67 – 1.56 (m, 4H), 1.38 – 1.22 (m, 44H), 1.20 – 1.16 (m, 12H), 0.88 (t, *J* = 6.8 Hz, 6H). ¹³C NMR (101 MHz, CDCl₃) δ 173.44, 173.03, 130.08, 129.78, 117.61, 70.80, 70.76, 70.72, 70.69, 62.47, 62.45, 61.89, 61.74, 61.58, 58.70, 58.61, 58.51, 58.42, 43.32, 43.31, 43.20, 43.19, 34.42, 34.40, 34.22, 32.03, 32.01, 29.87, 29.81, 29.77, 29.74, 29.63, 29.59, 29.47, 29.43, 29.40, 29.31, 29.24, 29.19, 27.32, 27.28, 25.00, 24.72, 24.65, 22.80, 20.49, 20.43, 14.22. ³¹P NMR (162 MHz, CDCl₃) δ 149.49, 149.35.

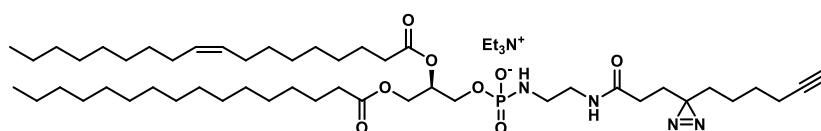
(2R)-1-(((2-Cyanoethoxy)((2-(3-(3-(hex-5-yn-1-yl)-3H-diazirin-3-yl)propanamido)ethyl)amino)phosphoryl)oxy)-3-(palmitoyloxy)propan-2-yl oleate (45).



***H*-phosphonate formation:** A round bottom flask was charged with phosphoramidite **44** (86 mg, 0.11 mmol, 1 eq), 1*H*-tetrazole (16 mg, 0.22 mmol, 2 eq) and CH₃CN (2 mL). The mixture was stirred for 10 min, after which H₂O was added (200 μL) and then further stirred for 30 min. The reaction was diluted with DCM (25

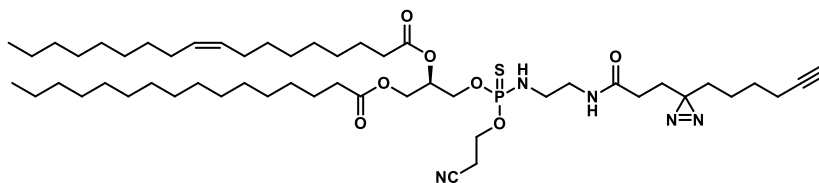
mL) and washed with brine (1 x 25 mL), dried (MgSO₄), filtered and concentrated under reduced pressure, affording the *H*-phosphonate intermediate (76 mg, 0.11 mmol, quant). *Phosphoramidate synthesis*: A round bottom flask was charged with TFA salt **37** (57 mg, 0.16 mmol, 1.5 eq) and CH₃CN (0.5 mL) and cooled to 0 °C. CCl₄ (64 μL, 0.66 mmol, 5 eq) and Et₃N (153 μL, 1.1 mmol, 10 eq) were added and the *H*-phosphonate (76 mg, 0.11 mmol, 1 eq) was taken up in DCM (1 mL) and added to the mixture via syringe. After 5 min the reaction mixture was warmed to rt and stirred for 1.5 h. The solvents were evaporated under reduced pressure and coevaporated with toluene (1x). The crude residue was purified by column chromatography (2.5% -> 7.5% MeOH in DCM), affording the phosphoramidate **45** (81 mg, 86 μmol, 80%). ¹H NMR (400 MHz, CDCl₃) δ 6.65 – 6.48 (m, 1H), 5.40 – 5.31 (m, 2H), 5.29 – 5.23 (m, 1H), 4.35 (dd, *J* = 12.0, 3.9 Hz, 1H), 4.23 – 4.08 (m, 5H), 3.88 – 3.75 (m, 1H), 3.41 – 3.27 (m, 2H), 3.15 – 2.98 (m, 2H), 2.78 (t, *J* = 6.0 Hz, 2H), 2.33 (q, *J* = 7.9 Hz, 4H), 2.15 (td, *J* = 7.0, 2.6 Hz, 2H), 2.05 – 1.98 (m, 4H), 1.95 (t, *J* = 2.7 Hz, 1H), 1.94 – 1.87 (m, 2H), 1.86 – 1.78 (m, 2H), 1.66 – 1.58 (m, 4H), 1.52 – 1.44 (m, 2H), 1.44 – 1.38 (m, 2H), 1.37 – 1.20 (m, 46H), 0.88 (t, *J* = 6.7 Hz, 6H). ¹³C NMR (101 MHz, CDCl₃) δ 173.49, 173.47, 173.08, 172.11, 130.10, 129.73, 116.99, 69.64, 69.61, 69.57, 69.54, 68.74, 64.74, 64.69, 64.65, 64.60, 61.89, 61.83, 61.15, 61.10, 41.14, 40.88, 34.25, 34.10, 32.58, 32.00, 30.34, 29.84, 29.78, 29.74, 29.60, 29.59, 29.44, 29.39, 29.30, 29.22, 29.19, 29.15, 28.57, 28.34, 27.90, 27.30, 27.26, 24.93, 23.01, 22.76, 19.91, 19.84, 18.25, 14.20. ³¹P NMR (162 MHz, CDCl₃) δ 9.47, 9.38. HRMS [C₅₂H₉₂N₅O₈P + H]⁺: 946.6756 calculated, 946.6759 found.

(*R*)-2-(Oleoyloxy)-3-(palmitoyloxy)propyl(2-(3-(3-(hex-5-yn-1-yl)-3*H*-diazirin-3-yl)propanamido)ethyl) phosphoramidate triethylammonium salt (2**).**



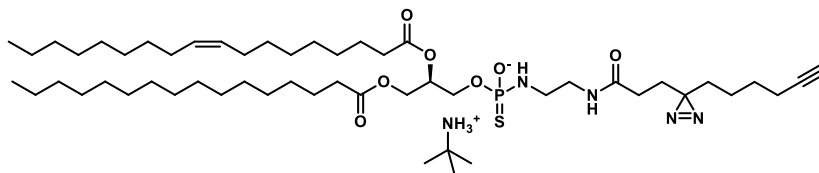
A round bottom flask was charged with protected phosphoramidate **45** (40 mg, 42 μmol, 1 eq), 1,8-diazabicyclo[5.4.0]undec-7-ene (8.6 μL, 57 μmol, 1.3 eq) and DCM (1 mL). The mixture was stirred for 2 h after which the solvents were evaporated under reduced pressure and the residue was coevaporated with toluene (2x). The crude residue was purified by column chromatography (pre-treat the silica gel with 85:5:10 DCM/MeOH/Et₃N, elute with 5% -> 10% MeOH in DCM), affording the phosphoramidate as the triethylammonium salt with Et₃N·HCl contamination. The product was taken up in 10% MeOH in CHCl₃, washed with MilliQ (3x) and concentrated under reduced pressure to give the phosphoramidate triethylammonium salt **2** (10 mg, 10 μmol, 24%). ¹H NMR (500 MHz, CDCl₃ + MeOD) δ 5.36 – 5.25 (m, *J* = 5.5 Hz, 2H), 5.21 – 5.13 (m, 1H), 4.34 (dd, *J* = 12.0, 3.0 Hz, 2H), 4.11 (dd, *J* = 12.0, 7.1 Hz, 2H), 3.90 – 3.77 (m, *J* = 5.9 Hz, 2H), 3.20 (t, *J* = 6.2 Hz, 2H), 3.12 (q, *J* = 7.3 Hz, 6H), 2.87 (dt, *J* = 12.0, 6.1 Hz, 2H), 2.31 – 2.24 (m, 4H), 2.11 (td, *J* = 7.0, 2.6 Hz, 2H), 2.02 – 1.93 (m, 6H), 1.74 – 1.68 (m, 2H), 1.60 – 1.54 (m, 4H), 1.47 – 1.41 (m, 2H), 1.41 – 1.36 (m, 2H), 1.33 (t, *J* = 7.3 Hz, 9H), 1.24 (d, *J* = 24.7 Hz, 44H), 0.84 (t, *J* = 6.9 Hz, 6H). ¹³C NMR (126 MHz, CDCl₃ + MeOD) δ 174.34, 173.96, 173.53, 130.32, 129.93, 84.09, 70.93, 70.86, 68.96, 63.05, 46.72, 41.58, 40.85, 34.52, 34.38, 32.46, 32.23, 30.54, 30.05, 30.00, 29.98, 29.96, 29.85, 29.82, 29.67, 29.62, 29.57, 29.46, 29.45, 29.40, 29.04, 28.58, 28.13, 27.49, 27.46, 25.17, 23.19, 22.97, 18.37, 14.25, 8.82. ³¹P NMR (202 MHz, CDCl₃ + MeOD) δ 5.37. HRMS [C₄₉H₈₉N₄O₈P + H]⁺: 893.6491 calculated, 893.6491 found.

(2R)-1-(((2-Cyanoethoxy)((2-(3-(3-(hex-5-yn-1-yl)-3H-diazirin-3-yl)propanamido)ethyl)amino)phosphorothioyl)oxy)-3-(palmitoyloxy)propan-2-yl oleate (46).



H-thiophosphonate formation: A round bottom flask was charged with phosphoramidite **44** (72 mg, 91 μmol , 1 eq), 1*H*-tetrazole (13 mg, 0.18 mmol, 2 eq) and dry CH_3CN (2 mL). The mixture was stirred for 10 min, after which H_2S (0.8 M in THF, 1.1 mL, 0.91 mmol, 10 eq) was added and then further stirred for 1 h. Argon was bubbled through the reaction mixture and the flow of H_2S was quenched by bleach. The reaction was quenched with sat. aq. NaHCO_3 (25 mL) and the aqueous layer was extracted with DCM (2 x 25 mL). The combined organic layers were washed with brine (1 x 25 mL), dried (MgSO_4), filtered and concentrated under reduced pressure, affording the product as a mixture of *H*-thiophosphonate and *H*-phosphonate (1 : 0.4, 67 mg in total). *Thiophosphoramidate synthesis*: A round bottom flask was charged with TFA salt **37** (53 mg, 0.15 mmol, 1.6 eq) and CH_3CN (0.5 mL) and cooled to 0 $^\circ\text{C}$. CCl_4 (45 μL , 0.47 mmol, 5 eq) and Et_3N (129 μL , 0.93 mmol, 10 eq) were added and the *H*-thiophosphonate/*H*-phosphonate mixture (67 mg) was taken up in DCM (1 mL) and added to the mixture via syringe. After 5 min the reaction mixture was warmed to rt and stirred for 2 h. The solvents were evaporated under reduced pressure and coevaporated with toluene (1x). The crude residue was purified by column chromatography (2% \rightarrow 4% MeOH in DCM), affording the thiophosphoramidate **46** (20 mg, 21 μmol , 31%). ^1H NMR (500 MHz, CDCl_3) δ 6.13 (t, J = 5.3 Hz, 1H), 5.40 – 5.30 (m, 2H), 5.31 – 5.23 (m, 1H), 4.38 – 4.29 (m, 1H), 4.25 – 4.14 (m, 4H), 4.14 – 4.05 (m, 1H), 3.71 – 3.61 (m, 1H), 3.41 – 3.27 (m, 2H), 3.23 – 3.11 (m, 2H), 2.77 (t, J = 6.0 Hz, 2H), 2.34 (q, J = 7.8 Hz, 4H), 2.16 (td, J = 7.0, 2.6 Hz, 2H), 2.07 – 1.97 (m, 4H), 1.97 – 1.90 (m, 3H), 1.83 (t, J = 7.1 Hz, 2H), 1.67 – 1.56 (m, 4H), 1.51 – 1.44 (m, 2H), 1.44 – 1.38 (m, 2H), 1.38 – 1.19 (m, 46H), 0.88 (t, J = 6.9 Hz, 6H). ^{13}C NMR (126 MHz, CDCl_3) δ 173.63, 173.61, 173.28, 173.20, 172.24, 130.17, 129.80, 117.19, 84.09, 77.41, 77.16, 76.91, 69.63, 69.56, 68.77, 65.20, 65.16, 65.00, 64.96, 61.97, 61.89, 61.50, 61.47, 41.67, 40.85, 40.81, 34.35, 34.20, 32.64, 32.06, 30.44, 29.90, 29.84, 29.80, 29.66, 29.64, 29.50, 29.46, 29.35, 29.28, 29.20, 28.61, 28.39, 28.37, 27.96, 27.36, 27.31, 24.99, 23.07, 22.83, 19.73, 19.67, 18.32, 14.27. ^{31}P NMR (202 MHz, CDCl_3) δ 74.40, 74.16. HRMS [$\text{C}_{52}\text{H}_{92}\text{N}_5\text{O}_7\text{PS} + \text{H}$] $^+$: 962.6528 calculated, 962.6531 found.

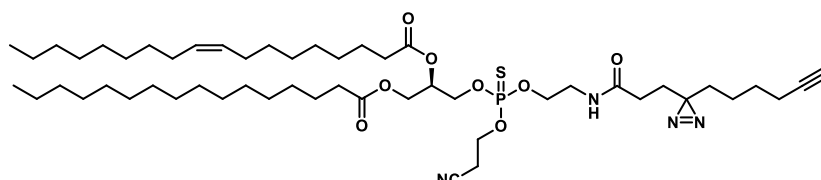
***O*-((*R*)-2-(Oleoyloxy)-3-(palmitoyloxy)propyl)(2-(3-(3-(hex-5-yn-1-yl)-3H-diazirin-3-yl)propanamido)ethyl)phosphoramidothioate *tert*-butylammonium salt (**3**).**



A round bottom flask was charged with protected thiophosphoramidate **46** (19 mg, 20 μmol , 1 eq) was dissolved in dry DCM (0.75 mL). *tert*-Butylamine (0.75 mL, 7.1 mmol, 350 eq) was added and the reaction mixture was stirred for 5 hours, after which the solvents were evaporated, affording the thiophosphoramidate as the pure *tert*-butylammonium salt **3** (20 mg, 20 μmol , quant). ^1H NMR (500 MHz, $\text{CDCl}_3 + \text{MeOD}$) δ 5.41 – 5.30 (m, 2H), 5.30 – 5.19 (m, 1H), 4.23 – 4.15 (m, 1H), 4.06 – 3.98 (m, 1H), 3.98 – 3.88 (m, 1H), 3.31 – 3.17 (m, 2H), 3.10 – 2.97 (m, 2H), 2.38 – 2.28 (m, 4H), 2.16 (td, J = 7.0, 2.6 Hz, 2H), 2.07 – 1.95 (m, 7H), 1.80 – 1.71 (m, 2H), 1.67 – 1.55 (m, 4H), 1.53 – 1.45 (m, 2H), 1.45 – 1.40 (m, 2H), 1.39 (s, 9H), 1.29 (d, J = 24.0 Hz, 44H), 1.24 – 1.18 (m, 2H), 0.88 (q, J = 6.1, 5.5 Hz, 6H). *1H* from (*sn*-1 CH_2) underneath

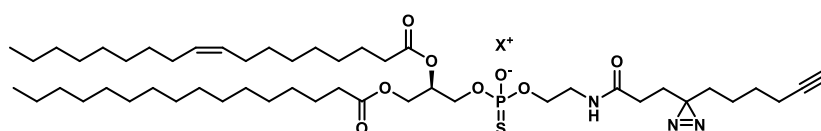
H₂O solvent. ¹³C NMR (126 MHz, CDCl₃ + MeOD) δ 174.41, 174.01, 173.95, 173.20, 130.27, 129.97, 100.35, 84.13, 71.01, 70.94, 70.89, 70.82, 68.92, 63.53, 63.50, 63.45, 63.18, 51.83, 49.51, 49.34, 49.17, 49.00, 48.83, 48.66, 48.49, 41.78, 41.77, 41.75, 41.74, 40.81, 40.79, 34.58, 34.42, 32.45, 32.22, 32.20, 30.53, 30.04, 30.03, 29.98, 29.96, 29.94, 29.80, 29.65, 29.61, 29.59, 29.54, 29.44, 29.42, 29.38, 29.09, 28.59, 28.14, 27.66, 27.48, 27.45, 25.19, 25.16, 23.19, 22.96, 18.36, 14.24. ³¹P NMR (202 MHz, CDCl₃ + MeOD) δ 60.66, 60.55. HRMS [C₄₉H₈₉N₄O₇PS + H]⁺: 909.6262 calculated, 909.6276 found.

(2R)-1-(((2-Cyanoethoxy)(2-(3-(3-(hex-5-yn-1-yl)-3H-diazirin-3-yl)propanamido)ethoxy)phosphorothioyl)oxy)-3-(palmitoyloxy)propan-2-yl oleate (47).



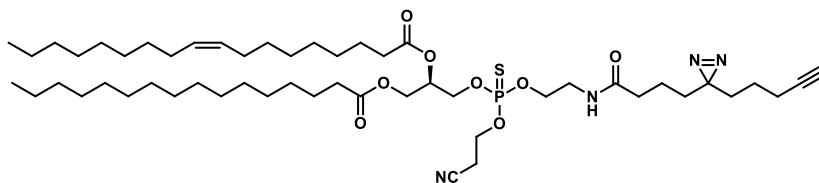
The title compound was prepared according to General Procedure D using phosphoramidite **44** (66 mg, 83 μmol, 1 eq), ethanolamide **38** (22 mg, 91 μmol, 1.1 eq), 1*H*-tetrazole (12 mg, 166 μmol, 2 eq) and sulfur (S₈, 50 mg, 1.6 mmol, 19 eq). Column chromatography (0% → 2% MeOH in DCM) afforded the thiophosphotriester product **47** (47 mg, 49 μmol, 59%). ¹H NMR (400 MHz, CDCl₃) δ 6.44 – 6.16 (m, 1H), 5.40 – 5.30 (m, 2H), 5.29 – 5.22 (m, 1H), 4.36 – 4.09 (m, 8H), 3.57 – 3.49 (m, 2H), 2.77 (td, *J* = 6.1, 3.0 Hz, 2H), 2.34 (q, *J* = 7.5 Hz, 4H), 2.15 (td, *J* = 7.0, 2.6 Hz, 2H), 2.09 – 1.89 (m, 7H), 1.83 – 1.77 (m, 2H), 1.67 – 1.56 (m, 4H), 1.52 – 1.44 (m, 2H), 1.44 – 1.38 (m, 2H), 1.37 – 1.23 (m, 46H), 0.88 (t, *J* = 6.8 Hz, 6H). ¹³C NMR (101 MHz, CDCl₃) δ 173.56, 173.51, 173.24, 173.10, 171.97, 130.15, 129.78, 116.76, 116.72, 84.07, 69.46, 69.38, 69.30, 68.72, 67.95, 67.90, 67.86, 67.80, 66.49, 66.44, 66.39, 66.35, 62.72, 62.68, 62.64, 61.83, 61.75, 53.56, 39.69, 39.67, 39.62, 39.60, 34.31, 34.29, 34.16, 32.54, 32.04, 30.30, 29.88, 29.81, 29.64, 29.61, 29.48, 29.43, 29.41, 29.32, 29.25, 29.17, 28.54, 28.43, 27.96, 27.34, 27.29, 24.96, 23.06, 22.80, 19.70, 19.63, 18.30, 14.24. ³¹P NMR (162 MHz, CDCl₃) δ 69.26. HRMS [C₅₂H₉₁N₄O₈PS + H]⁺: 963.6368 calculated, 963.6375 found.

***O*-(2-(3-(3-(Hex-5-yn-1-yl)-3H-diazirin-3-yl)propanamido)ethyl)-*O*-((*R*)-2-(oleoyloxy)-3-(palmitoyloxy)propyl) phosphorothioate (4).**



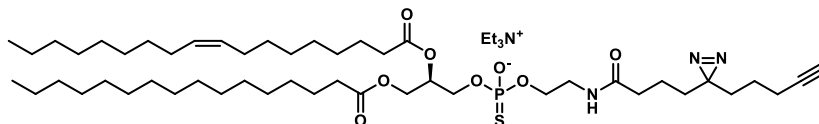
A round bottom flask was charged with thiophosphotriester **48** (47 mg, 49 μmol, 1 eq) was dissolved in dry DCM (0.5 mL). *tert*-Butylamine (0.5 mL, 4.8 mmol, 100 eq) was added and the reaction mixture was stirred for 3 hours, after which the solvents were evaporated. The crude residue was purified by column chromatography with high-purity grade silica gel (1% → 10% MeOH in DCM), affording the thiophosphodiester **4** as a salt with undefined cation (36 mg, 40 μmol, 81%, based on the free anion). ¹H NMR (500 MHz, CDCl₃ + MeOD) δ 5.36 – 5.25 (m, 2H), 5.24 – 5.17 (m, 1H), 4.37 – 4.31 (m, 1H), 4.17 – 4.10 (m, 1H), 4.08 – 3.89 (m, 4H), 3.45 – 3.34 (m, 2H), 2.29 (q, *J* = 7.2 Hz, 4H), 2.12 (td, *J* = 7.0, 2.7 Hz, 2H), 2.03 – 1.92 (m, 7H), 1.74 – 1.68 (m, 2H), 1.63 – 1.53 (m, 4H), 1.48 – 1.41 (m, 2H), 1.41 – 1.36 (m, 2H), 1.33 – 1.17 (m, 46H), 0.92 – 0.77 (m, 6H). ¹³C NMR (126 MHz, CDCl₃ + MeOD) δ 174.39, 173.98, 173.95, 173.49, 130.33, 130.00, 84.12, 70.68, 70.65, 70.61, 70.58, 69.04, 64.74, 64.70, 64.66, 64.54, 64.51, 64.45, 64.40, 62.97, 40.42, 40.37, 34.59, 34.46, 32.50, 32.28, 32.26, 30.55, 30.10, 30.05, 30.03, 30.01, 29.87, 29.72, 29.68, 29.65, 29.61, 29.51, 29.50, 29.45, 29.12, 28.58, 28.20, 27.54, 27.51, 25.25, 25.23, 23.26, 23.02, 18.42, 14.28. ³¹P NMR (162 MHz, CDCl₃ + MeOD) δ 54.95. HRMS [C₄₉H₈₇N₃O₈PS + H]⁺: 910.6103 calculated, 910.6106 found.

(2R)-1-(((2-(5-(3-(But-3-yn-1-yl)-3H-diazirin-3-yl)pentanamido)ethoxy)(2-cyanoethoxy)phosphorothioyl)oxy)-3-(palmitoyloxy)propan-2-yl oleate (48**).**

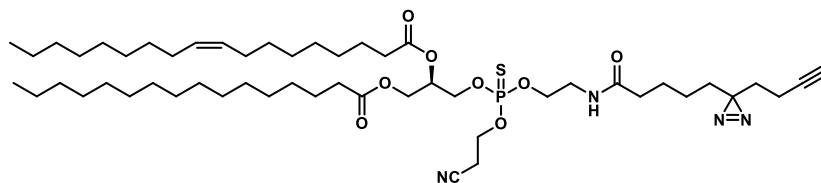


The title compound was prepared according to General Procedure D using phosphoramidite **44** (69 mg, 86 μmol , 1 eq), ethanamide **39** (21 mg, 88 μmol , 1 eq), 1*H*-tetrazole (0.45 M in CH_3CN , 0.39 mL, 0.18 mmol, 2 eq) and sulfur (S_8 , 50 mg, 1.6 mmol, 18 eq). Column chromatography (0% \rightarrow 2% MeOH in DCM) afforded the thiophosphotriester product **48** (35 mg, 37 μmol , 42%). ^1H NMR (500 MHz, CDCl_3) δ 6.38 – 6.20 (m, 1H), 5.39 – 5.30 (m, 2H), 5.30 – 5.23 (m, 1H), 4.38 – 4.09 (m, 8H), 3.59 – 3.48 (m, 2H), 2.82 – 2.73 (m, 2H), 2.38 – 2.30 (m, 4H), 2.21 – 2.13 (m, 4H), 2.06 – 1.97 (m, 4H), 1.95 (t, $J = 2.6$ Hz, 1H), 1.67 – 1.56 (m, 4H), 1.54 – 1.48 (m, 2H), 1.44 – 1.37 (m, 2H), 1.36 – 1.22 (m, 48H), 0.88 (t, $J = 6.9$ Hz, 6H). ^{13}C NMR (126 MHz, CDCl_3) δ 173.52, 173.47, 173.18, 173.06, 172.68, 172.66, 130.14, 129.76, 116.75, 116.72, 83.47, 69.41, 69.35, 69.28, 69.11, 68.01, 67.97, 67.91, 67.87, 66.46, 66.44, 66.40, 66.36, 62.71, 62.68, 62.64, 61.80, 61.73, 39.57, 39.55, 39.51, 39.49, 35.54, 35.53, 34.29, 34.27, 34.15, 32.45, 32.42, 32.04, 32.02, 31.61, 29.87, 29.82, 29.78, 29.75, 29.64, 29.61, 29.48, 29.44, 29.41, 29.33, 29.24, 29.17, 28.27, 27.33, 27.29, 24.95, 22.81, 20.07, 20.05, 19.70, 19.64, 18.03, 14.25. ^{31}P NMR (162 MHz, CDCl_3) δ 69.31. HRMS [$\text{C}_{52}\text{H}_{91}\text{N}_4\text{O}_8\text{PS} + \text{H}$] $^+$: 963.6368 calculated, 963.6383 found.

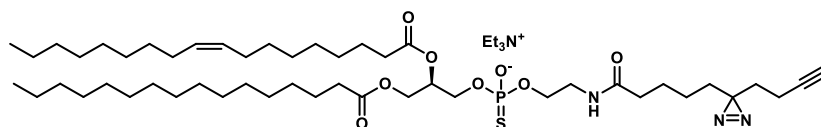
***O*-((*R*)-2-(Oleoyloxy)-3-(palmitoyloxy)propyl)-*O*-(2-(4-(3-(pent-4-yn-1-yl)-3*H*-diazirin-3-yl)butan-amido)ethyl) phosphorothioate triethylammonium salt (**6**).**



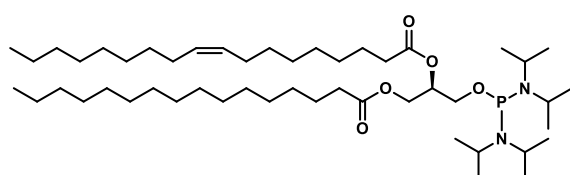
A round bottom flask was charged with thiophosphotriester **48** (35 mg, 37 μmol , 1 eq) and dry DCM (1.5 mL). *tert*-Butylamine (0.5 mL, 4.8 mmol, 130 eq) was added and the reaction mixture was stirred for 3.5 hours, after which the solvent was evaporated. Column chromatography with high-purity grade silica gel (5% MeOH in DCM + 0.5% Et_3N) gave the desired product on ^1H -NMR and ^{13}C -NMR but not on ^{31}P -NMR, suggesting that metals cations were chelating the thiophosphate. The product was dissolved in a 1:1 mixture of MilliQ and 10% MeOH in CHCl_3 (2 mL) and EDTA- Na_2 (56 mg, 0.17 mmol, 4.6 eq) was added. After stirring for 30 min a clear peak was observed again by ^{31}P -NMR. The mixture was washed with MilliQ (2 x 20 mL) and the combined aqueous layers were back-extracted with 10% MeOH in CHCl_3 . The combined organic layers were concentrated under reduced pressure and purified by column chromatography with high-purity grade silica gel (5% MeOH in DCM + 0.5% Et_3N), affording the thiophosphodiester product as the triethylammonium salt **6** (7.6 μmol , 7.7 mg, 21%). ^1H NMR (500 MHz, $\text{CDCl}_3 + \text{MeOD}$) δ 5.35 – 5.26 (m, 2H), 5.26 – 5.19 (m, 1H), 4.37 (dd, $J = 12.0, 3.3$ Hz, 1H), 4.18 – 4.12 (m, 1H), 4.10 – 3.91 (m, 4H), 3.43 – 3.37 (m, 2H), 3.14 (q, $J = 7.3$ Hz, 6H), 2.29 (q, $J = 7.3$ Hz, 4H), 2.17 – 2.09 (m, 4H), 2.04 – 1.90 (m, 5H), 1.62 – 1.54 (m, 4H), 1.52 – 1.45 (m, 2H), 1.45 – 1.35 (m, 4H), 1.34 – 1.20 (m, 55H), 0.88 – 0.81 (m, 6H). ^{13}C NMR (126 MHz, $\text{CDCl}_3 + \text{MeOD}$) δ 174.40, 174.19, 173.96, 130.37, 130.09, 83.63, 70.80, 70.72, 69.41, 65.01, 64.96, 64.96, 64.92, 64.62, 64.58, 64.50, 63.05, 46.73, 40.53, 40.48, 35.78, 34.66, 34.53, 32.81, 32.34, 32.32, 31.96, 30.16, 30.10, 30.06, 29.92, 29.76, 29.72, 29.70, 29.65, 29.55, 29.50, 28.49, 27.59, 27.57, 25.30, 23.16, 23.06, 20.50, 18.19, 14.28, 8.88. ^{31}P NMR (202 MHz, MeOD) δ 59.73, 59.70. HRMS [$\text{C}_{49}\text{H}_{87}\text{N}_3\text{O}_8\text{PS} + \text{H}$] $^+$: 910.6103 calculated, 910.6105 found.

(2R)-1-(((2-Cyanoethoxy)(2-(4-(3-(pent-4-yn-1-yl)-3H-diazirin-3-yl)butanamido)ethoxy)phosphorothioyl)oxy)-3-(palmitoyloxy)propan-2-yl oleate (49).

The title compound was prepared according to General Procedure D using phosphoramidite **44** (72 mg, 91 μmol , 1.05 eq), ethanolamide **40** (21 mg, 86 μmol , 1 eq), 1*H*-tetrazole (0.45 M in CH_3CN , 0.39 mL, 0.18 mmol, 2 eq) and sulfur (S_8 , 50 mg, 1.6 mmol, 17 eq). Column chromatography (0% \rightarrow 2% MeOH in DCM) afforded the thiophosphotriester product **49** (29 mg, 30 μmol , 35%). ^1H NMR (500 MHz, CDCl_3) δ 6.35 – 6.18 (m, 1H), 5.40 – 5.31 (m, 2H), 5.30 – 5.23 (m, 1H), 4.37 – 4.11 (m, 8H), 3.60 – 3.48 (m, 2H), 2.77 (td, J = 6.0, 3.4 Hz, 2H), 2.38 – 2.30 (m, 4H), 2.18 (td, J = 7.5, 4.1 Hz, 2H), 2.06 – 1.95 (m, 7H), 1.67 – 1.55 (m, 8H), 1.49 – 1.43 (m, 2H), 1.36 – 1.21 (m, 44H), 1.16 – 1.08 (m, 2H), 0.88 (t, J = 6.9 Hz, 6H). ^{13}C NMR (126 MHz, CDCl_3) δ 173.51, 173.47, 173.17, 173.12, 173.10, 173.06, 130.15, 129.77, 116.76, 116.73, 82.91, 69.41, 69.35, 69.29, 69.21, 68.06, 68.01, 67.96, 67.91, 66.45, 66.41, 66.36, 62.71, 62.68, 62.64, 61.80, 61.73, 39.58, 39.55, 39.52, 39.49, 36.14, 36.11, 34.30, 34.28, 34.15, 32.49, 32.40, 32.04, 32.02, 29.88, 29.82, 29.78, 29.76, 29.64, 29.61, 29.48, 29.44, 29.41, 29.33, 29.25, 29.17, 28.24, 27.34, 27.29, 25.13, 25.11, 24.95, 23.59, 22.81, 19.71, 19.65, 14.25, 13.44. ^{31}P NMR (202 MHz, CDCl_3) δ 69.46, 69.44. HRMS [$\text{C}_{52}\text{H}_{91}\text{N}_4\text{O}_8\text{PS} + \text{H}$] $^+$: 963.6368 calculated, 963.6387 found.

***O*-(2-(5-(3-(But-3-yn-1-yl)-3H-diazirin-3-yl)pentanamido)ethyl)-*O*-((*R*)-2-(oleoyloxy)-3-(palmitoyloxy)propyl) phosphorothioate triethylammonium salt (7).**

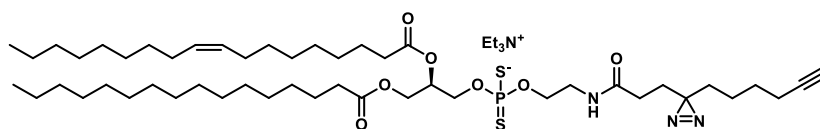
A round bottom flask was charged with thiophosphotriester **49** (29 mg, 30 μmol , 1 eq) and dry DCM (1.5 mL). *tert*-Butylamine (0.5 mL, 4.8 mmol, 160 eq) was added and the reaction mixture was stirred for 3.5 hours, after which the solvent was evaporated. Column chromatography with high-purity grade silica gel (5% MeOH in DCM + 0.5% Et_3N) afforded the thiophosphodiester product as the triethylamine salt **7** (8 mg, 7 μmol , 25%). ^1H NMR (500 MHz, $\text{CDCl}_3 + \text{MeOD}$) δ 5.36 – 5.26 (m, 2H), 5.25 – 5.19 (m, 1H), 4.37 (dd, J = 12.0, 3.3 Hz, 1H), 4.15 (ddd, J = 12.0, 6.7, 1.7 Hz, 1H), 4.09 – 3.94 (m, 4H), 3.43 – 3.37 (m, 2H), 3.13 (q, J = 7.3 Hz, 6H), 2.29 (q, J = 6.9 Hz, 4H), 2.16 – 2.11 (m, 2H), 2.04 (t, J = 2.7 Hz, 1H), 2.01 – 1.92 (m, 6H), 1.63 – 1.50 (m, 8H), 1.46 – 1.39 (m, 2H), 1.33 – 1.21 (m, 53H), 1.13 – 1.06 (m, 2H), 0.87 – 0.81 (m, 6H). ^{13}C NMR (126 MHz, $\text{CDCl}_3 + \text{MeOD}$) δ 174.60, 174.35, 173.90, 130.35, 130.07, 83.08, 70.78, 70.71, 69.52, 64.92, 64.84, 64.55, 64.50, 64.47, 64.42, 63.05, 46.61, 40.54, 40.49, 36.26, 34.64, 34.50, 32.75, 32.69, 32.30, 32.29, 30.13, 30.07, 30.03, 29.89, 29.73, 29.69, 29.62, 29.52, 29.47, 28.46, 27.56, 27.54, 25.61, 25.28, 25.27, 23.85, 23.03, 14.26, 13.54, 8.85. ^{31}P NMR (202 MHz, $\text{CDCl}_3 + \text{MeOD}$) δ 58.38, 58.36. HRMS [$\text{C}_{49}\text{H}_{87}\text{N}_3\text{O}_8\text{PS} + \text{H}$] $^+$: 910.61025 calculated, 910.61084 found.



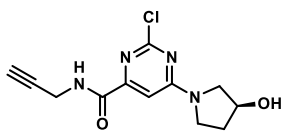
(*R*)-1-((Bis(diisopropylamino)phosphanyl)oxy)-3-(palmitoyloxy)propan-2-yl oleate (50). A round bottom flask was charged with **43** (0.28 g, 0.47 mmol, 1 eq), DiPEA (0.27 mL, 1.9 mmol, 4 eq) and dry DCM (2 mL). Bis(diisopropylamino)-chlorophosphine (0.16

g, 0.62 mmol, 1.3 eq) was added. The reaction mixture was stirred for 2 h and then quenched with sat. aq. NaHCO₃ in ice (50 mL). EtOAc (100 mL) was added and the organic layer was separated, washed with H₂O (2 x 100 mL) and brine (1 x 100 mL), dried (Na₂SO₄), filtered and concentrated under reduced pressure. The crude residue was purified by column chromatography (pre-treat silica with 5% Et₃N in pentane, elute with 2% Et₃N in pentane) affording the phosphordiamidite **50** (0.30 g, 0.36 mmol, 76%). ¹H NMR (400 MHz, CDCl₃) δ 5.40 – 5.28 (m, 2H), 5.18 (p, *J* = 5.0 Hz, 1H), 4.36 (dd, *J* = 11.8, 3.7 Hz, 1H), 4.19 (dd, *J* = 11.7, 6.4 Hz, 1H), 3.66 (t, *J* = 5.7 Hz, 2H), 3.60 – 3.41 (m, 4H), 2.29 (td, *J* = 7.5, 3.4 Hz, 4H), 2.10 – 1.94 (m, 4H), 1.66 – 1.56 (m, 4H), 1.37 – 1.20 (m, 44H), 1.20 – 1.12 (m, 24H), 0.88 (t, *J* = 6.7 Hz, 6H). ¹³C NMR (101 MHz, CDCl₃) δ 173.50, 173.11, 130.09, 129.82, 71.34, 71.24, 62.93, 62.73, 62.51, 44.67, 44.56, 44.44, 34.49, 34.28, 32.07, 32.05, 29.91, 29.86, 29.84, 29.80, 29.77, 29.67, 29.62, 29.51, 29.46, 29.43, 29.35, 29.28, 29.27, 29.24, 27.35, 27.31, 25.04, 24.76, 24.73, 24.68, 24.65, 23.99, 23.93, 23.87, 22.83, 14.24. ³¹P NMR (162 MHz, CDCl₃) δ 125.07.

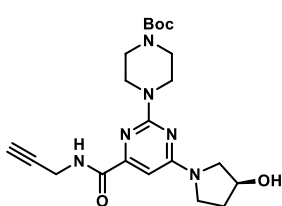
(R)-O-(2-(3-(3-(Hex-5-yn-1-yl)-3H-diazirin-3-yl)propanamido)ethyl)-O-(2-(oleoyloxy)-3-(palmitoyloxy)propyl) phosphorodithioate triethylammonium salt (5).



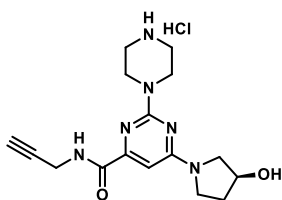
A round bottom flask was charged with diisopropylammonium tetrazolide (12 mg, 71 μmol, 0.55 eq), ethanolamide **38** (31 mg, 0.13 mmol, 1 eq) and dry DCM (1 mL). Phosphordiamidite **50** was taken up in dry DCM (1 mL) and added to the mixture via syringe. The reaction was stirred for 2 h, after which H₂S (0.8 M in THF, 1.6 mL, 1.3 mmol, 10 eq) and 1*H*-tetrazole (0.45 M in CH₃CN, 0.57 mL, 0.26 mmol, 2 eq) were added. After stirring for 1 h, argon was bubbled through the reaction mixture and the flow of H₂S was quenched by bleach. Et₃N (0.11 mL, 0.78 mmol, 6 eq) and sulfur (S₈, 21 mg, 0.65 mmol, 5 eq) were added and the reaction mixture was stirred overnight. The solvents were evaporated under reduced pressure and the crude residue was purified by column chromatography (97:1:2 → 94:4:2 DCM/MeOH/AcOH), affording the desired product on ¹H-NMR and ¹³C-NMR but not on ³¹P-NMR, suggesting that metals cations were chelating the dithiophosphate. The product was dissolved in a 1:1 mixture of MilliQ and 10% MeOH in CHCl₃ (2 mL) and EDTA-Na₂ (192 mg, 0.52 mmol, 4 eq) was added. After stirring for 30 min a clear peak was observed again by ³¹P-NMR. The mixture was washed with MilliQ (2 x 20 mL) and the combined aqueous layers were back-extracted with 10% MeOH in CHCl₃. The combined organic layers were concentrated under reduced pressure and purified by column chromatography with high-purity grade silica gel (1% → 4% MeOH in DCM + 0.5% Et₃N), affording the dithiophosphodiester product as the triethylammonium salt **5** (9.1 μmol, 9.3 mg, 7%). ¹H NMR (500 MHz, CDCl₃ + MeOD) δ 5.36 – 5.27 (m, 2H), 5.27 – 5.21 (m, 1H), 4.38 – 4.35 (m, 1H), 4.17 (dd, *J* = 12.0, 6.6 Hz, 1H), 4.09 (dd, *J* = 9.2, 5.3 Hz, 2H), 4.03 (dt, *J* = 9.8, 5.0 Hz, 2H), 3.46 – 3.39 (m, 2H), 3.21 (q, *J* = 7.3 Hz, 6H), 2.33 – 2.24 (m, 4H), 2.11 (td, *J* = 7.0, 2.6 Hz, 2H), 2.03 – 1.89 (m, 7H), 1.73 – 1.65 (m, 2H), 1.62 – 1.53 (m, 4H), 1.47 – 1.41 (m, 2H), 1.41 – 1.37 (m, 2H), 1.35 (t, *J* = 7.3 Hz, 9H), 1.31 – 1.18 (m, 46H), 0.84 (t, *J* = 6.8 Hz, 6H). ¹³C NMR (126 MHz, CDCl₃ + MeOD) δ 174.35, 173.92, 173.07, 130.27, 130.02, 84.16, 70.67, 70.59, 68.95, 64.84, 64.78, 63.98, 63.93, 63.13, 62.60, 46.92, 40.29, 40.24, 34.60, 34.46, 32.43, 32.24, 32.22, 30.60, 30.06, 30.05, 30.01, 29.98, 29.97, 29.83, 29.68, 29.63, 29.61, 29.56, 29.47, 29.45, 29.41, 29.26, 28.59, 28.17, 27.50, 27.48, 25.21, 23.23, 22.98, 18.39, 14.25, 8.93. ³¹P NMR (202 MHz, CDCl₃ + MeOD) δ 114.99. HRMS [C₄₉H₈₈N₃O₇PS₂ + H]⁺: 926.5874 calculated, 926.5878 found.

LEI-401-based photoprobes 51-52

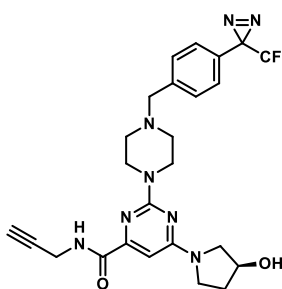
(S)-2-Chloro-6-(3-hydroxypyrrolidin-1-yl)-N-(prop-2-yn-1-yl)pyrimidine-4-carboxamide (54). A round bottom flask was charged with dichloropyrimidine **53** (described in Chapter 3, 138 mg, 0.60 mmol, 1 eq) and MeOH (3 mL) and cooled to 0 °C. DiPEA (261 μ L, 1.5 mmol, 2.5 eq) and (S)-3-hydroxypyrrolidine HCl salt (78 mg, 0.63 mmol, 1.05 eq) were added and the reaction was stirred for 1.5 hours after which the solvents were evaporated. The residue was purified by silica gel column chromatography (80% -> 100% EtOAc/pentane) affording the product **54** (139 mg, 0.50 mmol, 83%). TLC: R_f = 0.2 (90% EtOAc/pentane). ^1H NMR (400 MHz, CDCl_3) δ 8.13 (t, J = 5.6 Hz, 1H), 7.06 – 6.89 (m, 1H), 4.73 – 4.57 (m, 1H), 4.29 – 4.15 (m, 2H), 3.88 – 3.19 (m, 5H), 2.33 (t, J = 2.5 Hz, 1H), 2.23 – 2.07 (m, 2H). ^{13}C NMR (101 MHz, CDCl_3) δ 162.58, 162.16, 162.01, 159.71, 159.59, 155.59, 100.70, 100.64, 78.74, 72.13, 70.43, 69.73, 55.57, 55.28, 45.29, 45.03, 33.79, 33.26, 29.28. HRMS [$\text{C}_{12}\text{H}_{13}\text{ClN}_4\text{O}_2 + \text{H}$] $^+$: 281.0800 calculated, 281.0796 found.



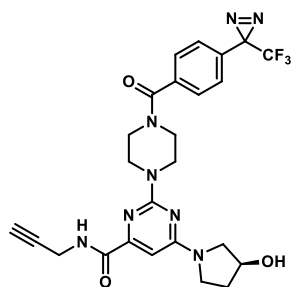
tert-Butyl (S)-4-(4-(3-hydroxypyrrolidin-1-yl)-6-(prop-2-yn-1-ylcarbamoyl)pyrimidin-2-yl)piperazine-1 carboxylate (55). A round bottom flask was charged with 2-chloropyrimidine **54** (117 mg, 0.42 mmol, 1 eq), DiPEA (218 μ L, 1.25 mmol, 3 eq), 1-Boc-piperazine (110 mg, 0.59 mmol, 1.4 eq) and *n*-BuOH (2 mL). The reaction was stirred at 100 °C for 48 h, after which the solvents were evaporated. The residue was purified by silica gel column chromatography (80% -> 100% EtOAc/pentane) affording the product **55** (163 mg, 0.38 mmol, 90%). TLC: R_f = 0.3 (90% EtOAc/pentane). ^1H NMR (400 MHz, CDCl_3) δ 8.10 (t, J = 5.4 Hz, 1H), 6.63 – 6.27 (m, 1H), 4.56 (s, 1H), 4.20 (dd, J = 5.5, 2.2 Hz, 2H), 3.88 – 3.69 (m, 5H), 3.69 – 3.51 (m, 3H), 3.51 – 3.35 (m, 5H), 2.31 (t, J = 2.4 Hz, 1H), 2.19 – 1.95 (m, 2H), 1.49 (s, 9H). ^{13}C NMR (101 MHz, CDCl_3) δ 164.62, 161.73, 160.68, 154.88, 154.51, 92.43, 79.97, 79.37, 71.64, 70.56, 69.81, 54.74, 44.36, 43.67, 34.00, 33.16, 28.99, 28.42. HRMS [$\text{C}_{21}\text{H}_{30}\text{N}_6\text{O}_4 + \text{H}$] $^+$: 431.2401 calculated, 431.2397 found.



(S)-6-(3-Hydroxypyrrolidin-1-yl)-2-(piperazin-1-yl)-N-(prop-2-yn-1-yl)pyrimidine-4-carboxamide (56). A round bottom flask was charged with Boc-piperazine **55** (160 mg, 0.37 mmol, 1 eq) and 4 M HCl in dioxane (2 mL, 8 mmol, 21 eq). After stirring for 2 h at rt the solvents were evaporated under reduced pressure affording the HCl salt **56**, which was used for the next step without further purification (135 mg, 0.37 mmol, quant.)



(S)-6-(3-Hydroxypyrrolidin-1-yl)-N-(prop-2-yn-1-yl)-2-(4-(4-(3-(trifluoromethyl)-3H-diazirin-3-yl)benzyl)piperazin-1-yl)pyrimidine-4-carboxamide (51). A round bottom flask was charged with amine HCl salt **56** (26 mg, 45 μ mol, 1 eq) in dry CH_3CN (1 mL). This was followed by addition of DiPEA (37 μ L, 0.21 mmol, 3 eq) and 4-[3-(trifluoromethyl)-3H-diazirin-3-yl]benzyl bromide (14 μ L, 85 μ mol, 1.2 eq). The reaction was stirred in the dark for 3 h at rt after which the solvents were evaporated under reduced pressure. The residue was purified by silica gel column chromatography (2.5 -> 7.5% MeOH/DCM) affording the product **51** (12 mg, 23 μ mol, 32%). TLC: R_f = 0.4 (5% MeOH/DCM). ^1H NMR (500 MHz, CDCl_3) δ 7.99 (t, J = 5.5 Hz, 1H), 7.40 (d, J = 8.2 Hz, 2H), 7.16 (d, J = 8.0 Hz, 2H), 6.54 (s, 1H), 4.58 (br s, 1H), 4.20 (dd, J = 5.6, 2.5 Hz, 2H), 3.80 (br s, 4H), 3.62 (br s, 2H), 3.56 (s, 2H), 3.43 (s, 1H), 2.58 – 2.34 (m, 4H), 2.25 (t, J = 2.5 Hz, 1H), 2.08 (br s, 2H), 1.71 (br s, 2H). ^{13}C NMR (126 MHz, CDCl_3) δ 122.28 (q, J = 274.7, 273.4 Hz). ^{13}C NMR (126 MHz, CDCl_3) δ 164.73, 162.05, 160.92, 154.93, 140.07, 129.66, 128.09, 126.55, 122.28 (q, J = 274.4 Hz), 92.22, 79.56, 71.65, 70.36, 62.62, 54.92, 53.17, 44.36, 43.91, 34.25, 29.15, 28.51 (q, J = 40.4 Hz). HRMS [$\text{C}_{25}\text{H}_{27}\text{F}_3\text{N}_8\text{O}_2 + \text{H}$] $^+$: 529.2282 calculated, 529.2296 found.



(S)-6-(3-Hydroxypyrrolidin-1-yl)-N-(prop-2-yn-1-yl)-2-(4-(4-(3-(trifluoromethyl)-3H-diazirin-3-yl)benzoyl)piperazin-1-yl)pyrimidine-4-carboxamide (52). A round bottom flask was charged with amine HCl salt **56** (30 mg, 82 μ mol, 1 eq) in dry DMF (1 mL) at 0 °C. This was followed by addition of DiPEA (57 μ L, 0.33 mmol, 4 eq), 4-[3-(trifluoromethyl)-3H-diazirin-3-yl]benzoic acid (19 mg, 82 μ mol, 1.2 eq) and PyBOP (47 mg, 90 μ mol, 1.1 eq). The reaction was stirred in the dark overnight warming up to rt after which the solvents were evaporated under reduced pressure and the residue was coevaporated with toluene. The residue was purified by silica gel column chromatography (2.5 -> 7.5% MeOH/DCM) affording the product **52** (8 mg, 15 μ mol, 18%). TLC: R_f = 0.5 (100% EtOAc). ^1H NMR (500 MHz, MeOD) δ 7.58 (d, J = 8.5 Hz, 2H), 7.38 (d, J = 8.1 Hz, 2H), 6.60 – 6.40 (m, 1H), 4.59 – 4.41 (m, 1H), 4.18 – 4.07 (m, 2H), 3.97 (br s, 2H), 3.83 (br s, 4H), 3.76 – 3.49 (m, 4H), 3.49 – 3.34 (m, 2H), 2.58 (t, J = 2.5 Hz, 1H), 2.22 – 1.91 (m, 2H). ^{13}C NMR (126 MHz, MeOD) δ 171.27, 166.81, 163.30, 162.25, 156.47, 138.57, 131.69, 128.99, 127.98, 123.47 (q, J = 273.7 Hz), 93.19, 80.63, 79.48, 71.91, 70.77, 55.53, 45.34, 44.64, 43.49, 34.73, 34.02, 29.44 (d, J = 40.5 Hz), 29.43. HRMS [$\text{C}_{25}\text{H}_{25}\text{F}_3\text{N}_8\text{O}_3 + \text{H}$] $^+$: 543.2075 calculated, 543.2085 found.

References

- Durham, T.B. & Wiley, M.R. Target engagement measures in preclinical drug discovery: theory, methods, and case studies, in *Translating Molecules into Medicines: Cross-Functional Integration at the Drug Discovery-Development Interface*. (eds. S.N. Bhattachar, J.S. Morrison, D.R. Mudra & D.M. Bender) 41-80 (Springer International Publishing, Cham; 2017).
- Simon, G.M., Niphakis, M.J. & Cravatt, B.F. Determining target engagement in living systems. *Nature Chemical Biology* **9**, 200 (2013).
- Cummings, J. Lessons learned from Alzheimer disease: clinical trials with negative outcomes. *Clinical and Translational Science* **11**, 147-152 (2018).
- McClure, R.A. & Williams, J.D. Impact of mass spectrometry-based technologies and strategies on chemoproteomics as a tool for drug discovery. *ACS Medicinal Chemistry Letters* **9**, 785-791 (2018).
- Niphakis, M.J. & Cravatt, B.F. Enzyme inhibitor discovery by activity-based protein profiling. *Annual Review of Biochemistry* **83**, 341-377 (2014).
- Willems, L.I., Overkleeft, H.S. & van Kasteren, S.I. Current developments in activity-based protein profiling. *Bioconjugate Chemistry* **25**, 1181-1191 (2014).
- Baggelaar, M.P., Chameau, P.J.P., Kantae, V., Hummel, J., Hsu, K.L., Janssen, F., van der Wel, T., Soethoudt, M., Deng, H., den Dulk, H., Allara, M., Florea, B.I., Di Marzo, V., Wadman, W.J., Kruse, C.G., Overkleeft, H.S., Hankemeier, T., Werkman, T.R., Cravatt, B.F. & van der Stelt, M. Highly selective, reversible inhibitor identified by comparative chemoproteomics modulates diacylglycerol lipase activity in neurons. *J. Am. Chem. Soc.* **137**, 8851-8857 (2015).
- Baggelaar, M.P., Janssen, F.J., van Esbroeck, A.C.M., den Dulk, H., Allara, M., Hoogendoorn, S., McGuire, R., Florea, B.I., Meeuwenoord, N., van den Elst, H., van der Marel, G.A., Brouwer, J., Di Marzo, V., Overkleeft, H.S. & van der Stelt, M. Development of an activity-based probe and *in silico* design reveal highly selective inhibitors for diacylglycerol lipase-alpha in brain. *Angew. Chem.-Int. Edit.* **52**, 12081-12085 (2013).
- Ogasawara, D., Deng, H., Viader, A., Baggelaar, M.P., Breman, A., den Dulk, H., van den Nieuwendijk, A.M.C.H., Soethoudt, M., van der Wel, T., Zhou, J., Overkleeft, H.S., Sanchez-Alavez, M., Mori, S., Nguyen, W., Conti, B., Liu, X., Chen, Y., Liu, Q.-s., Cravatt, B.F. & van der Stelt, M. Rapid and profound

- rewiring of brain lipid signaling networks by acute diacylglycerol lipase inhibition. *Proceedings of the National Academy of Sciences* **113**, 26 (2016).
10. van Esbroeck, A.C.M., Janssen, A.P.A., Cognetta, A.B., Ogasawara, D., Shpak, G., van der Kroeg, M., Kantae, V., Baggelaar, M.P., de Vrij, F.M.S., Deng, H., Allara, M., Fezza, F., Lin, Z., van der Wel, T., Soethoudt, M., Mock, E.D., den Dulk, H., Baak, I.L., Florea, B.I., Hendriks, G., de Petrocellis, L., Overkleeft, H.S., Hankemeier, T., De Zeeuw, C.I., Di Marzo, V., Maccarrone, M., Cravatt, B.F., Kushner, S.A. & van der Stelt, M. Activity-based protein profiling reveals off-target proteins of the FAAH inhibitor BIA 10-2474. *Science* **356**, 1084-1087 (2017).
 11. van Rooden, E.J., Florea, B.I., Deng, H., Baggelaar, M.P., van Esbroeck, A.C.M., Zhou, J., Overkleeft, H.S. & van der Stelt, M. Mapping *in vivo* target interaction profiles of covalent inhibitors using chemical proteomics with label-free quantification. *Nature Protocols* **13**, 752 (2018).
 12. Geurink, P.P., Prely, L.M., van der Marel, G.A., Bischoff, R. & Overkleeft, H.S. Photoaffinity labeling in activity-based protein profiling. *Top. Curr. Chem.* **324**, 85-113 (2012).
 13. Lapinsky, D.J. & Johnson, D.S. Recent developments and applications of clickable photoprobes in medicinal chemistry and chemical biology. *Future Medicinal Chemistry* **7**, 2143-2171 (2015).
 14. Pan, S., Zhang, H., Wang, C., Yao, S.C.L. & Yao, S.Q. Target identification of natural products and bioactive compounds using affinity-based probes. *Natural Product Reports* **33**, 612-620 (2016).
 15. Wright, M.H. & Sieber, S.A. Chemical proteomics approaches for identifying the cellular targets of natural products. *Natural Product Reports* **33**, 681-708 (2016).
 16. Flaxman, H.A. & Woo, C.M. Mapping the small molecule interactome by mass spectrometry. *Biochemistry* **57**, 186-193 (2018).
 17. Smith, E. & Collins, I. Photoaffinity labeling in target- and binding-site identification. *Future Medicinal Chemistry* **7**, 159-183 (2015).
 18. Xia, Y. & Peng, L. Photoactivatable lipid probes for studying biomembranes by photoaffinity labeling. *Chemical Reviews* **113**, 7880-7929 (2013).
 19. Haberkant, P. & Holthuis, J.C.M. Fat & fabulous: Bifunctional lipids in the spotlight. *Biochimica et Biophysica Acta (BBA) - Molecular and Cell Biology of Lipids* (2014).
 20. Murale, D.P., Hong, S.C., Haque, M.M. & Lee, J.-S. Photo-affinity labeling (PAL) in chemical proteomics: a handy tool to investigate protein-protein interactions (PPIs). *Proteome Science* **15**, 14 (2017).
 21. Das, J. Aliphatic diazirines as photoaffinity probes for proteins: recent developments. *Chemical Reviews* **111**, 4405-4417 (2011).
 22. Dubinsky, L., Krom, B.P. & Meijler, M.M. Diazirine based photoaffinity labeling. *Bioorganic & Medicinal Chemistry* **20**, 554-570 (2012).
 23. Ge, S.-S., Chen, B., Wu, Y.-Y., Long, Q.-S., Zhao, Y.-L., Wang, P.-Y. & Yang, S. Current advances of carbene-mediated photoaffinity labeling in medicinal chemistry. *RSC Advances* **8**, 29428-29454 (2018).
 24. Nickon, A. New perspectives on carbene rearrangements: migratory aptitudes, bystander assistance, and geminal efficiency. *Accounts of Chemical Research* **26**, 84-89 (1993).
 25. Tanaka, Y., Bond, M.R. & Kohler, J.J. Photocrosslinkers illuminate interactions in living cells. *Molecular BioSystems* **4**, 473-480 (2008).
 26. Saghatelian, A., Jessani, N., Joseph, A., Humphrey, M. & Cravatt, B.F. Activity-based probes for the proteomic profiling of metalloproteases. *Proceedings of the National Academy of Sciences of the United States of America* **101**, 10000-10005 (2004).
 27. Shi, H., Cheng, X., Sze, S.K. & Yao, S.Q. Proteome profiling reveals potential cellular targets of staurosporine using a clickable cell-permeable probe. *Chemical Communications* **47**, 11306-11308 (2011).
 28. Crump, C.J., Murrey, H.E., Ballard, T.E., am Ende, C.W., Wu, X., Gertsik, N., Johnson, D.S. & Li, Y.-M. Development of sulfonamide photoaffinity inhibitors for probing cellular γ -secretase. *ACS Chemical Neuroscience* **7**, 1166-1173 (2016).

29. Horning, B.D., Suciu, R.M., Ghadiri, D.A., Ulanovskaya, O.A., Matthews, M.L., Lum, K.M., Backus, K.M., Brown, S.J., Rosen, H. & Cravatt, B.F. Chemical proteomic profiling of human methyltransferases. *J. Am. Chem. Soc.* **138**, 13335-13343 (2016).
30. Soethoudt, M., Stolze, S.C., Westphal, M.V., van Stralen, L., Martella, A., van Rooden, E.J., Guba, W., Varga, Z.V., Deng, H., van Kasteren, S.I., Grether, U., Ijzerman, A.P., Pacher, P., Carreira, E.M., Overkleeft, H.S., Ioan-Facsinay, A., Heitman, L.H. & van der Stelt, M. Selective photoaffinity probe that enables assessment of cannabinoid CB₂ receptor expression and ligand engagement in human cells. *J. Am. Chem. Soc.* **140**, 6067-6075 (2018).
31. Xie, Y., Ge, J., Lei, H., Peng, B., Zhang, H., Wang, D., Pan, S., Chen, G., Chen, L., Wang, Y., Hao, Q., Yao, S.Q. & Sun, H. Fluorescent probes for single-step detection and proteomic profiling of histone deacetylases. *J. Am. Chem. Soc.* **138**, 15596-15604 (2016).
32. Keow, J.Y., Pond, E.D., Cisar, J.S., Cravatt, B.F. & Crawford, B.D. Activity-based labeling of matrix metalloproteinases in living vertebrate embryos. *PLoS ONE* **7**, e43434 (2012).
33. Chicca, A., Nicolussi, S., Bartholomäus, R., Blunder, M., Aparisi Rey, A., Petrucci, V., Reynoso-Moreno, I.d.C., Viveros-Paredes, J.M., Dalghi Gens, M., Lutz, B., Schiöth, H.B., Soeberdt, M., Abels, C., Charles, R.-P., Altmann, K.-H. & Gertsch, J. Chemical probes to potently and selectively inhibit endocannabinoid cellular reuptake. *Proceedings of the National Academy of Sciences* **114**, E5006-E5015 (2017).
34. Okamoto, Y., Morishita, J., Tsuboi, K., Tonai, T. & Ueda, N. Molecular characterization of a phospholipase D generating anandamide and its congeners. *Journal of Biological Chemistry* **279**, 5298-5305 (2004).
35. Magotti, P., Bauer, I., Igarashi, M., Babagoli, M., Marotta, R., Piomelli, D. & Garau, G. Structure of human *N*-acylphosphatidylethanolamine-hydrolyzing phospholipase D: regulation of fatty acid ethanolamide biosynthesis by bile acids. *Structure* **23**, 598-604 (2015).
36. Petersen, G., Pedersen, A.H., Pickering, D.S., Begtrup, M. & Hansen, H.S. Effect of synthetic and natural phospholipids on *N*-acylphosphatidylethanolamine-hydrolyzing phospholipase D activity. *Chemistry and Physics of Lipids* **162**, 53-61 (2009).
37. Wang, J., Okamoto, Y., Morishita, J., Tsuboi, K., Miyatake, A. & Ueda, N. Functional analysis of the purified anandamide-generating phospholipase D as a member of the metallo- β -lactamase family. *Journal of Biological Chemistry* **281**, 12325-12335 (2006).
38. Astarita, G., Ahmed, F. & Piomelli, D. Identification of biosynthetic precursors for the endocannabinoid anandamide in the rat brain. *Journal of Lipid Research* **49**, 48-57 (2008).
39. Müller, S., Liepold, B., Roth, G.J. & Bestmann, H.J. An improved one-pot procedure for the synthesis of alkynes from aldehydes. *Synlett* **1996**, 521-522 (1996).
40. Fodran, P. & Minnaard, A.J. Catalytic synthesis of enantiopure mixed diacylglycerols - synthesis of a major *M. tuberculosis* phospholipid and platelet activating factor. *Organic & Biomolecular Chemistry* **11**, 6919-6928 (2013).
41. Bond, M.R., Zhang, H., Vu, P.D. & Kohler, J.J. Photocrosslinking of glycoconjugates using metabolically incorporated diazirine-containing sugars. *Nature Protocols* **4**, 1044 (2009).
42. Pongracz, K. & Gryaznov, S. Oligonucleotide N3'→P5' thiophosphoramidates: synthesis and properties. *Tetrahedron Letters* **40**, 7661-7664 (1999).
43. Franklin, C.L., Li, H. & Martin, S.F. Design, synthesis, and evaluation of water-soluble phospholipid analogues as inhibitors of phospholipase C from *Bacillus cereus*. *The Journal of Organic Chemistry* **68**, 7298-7307 (2003).
44. Prestwich, G.D., Xu, Y., Qian, L., Gajewiak, J. & Jiang, G. New metabolically stabilized analogues of lysophosphatidic acid: agonists, antagonists and enzyme inhibitors. *Biochemical Society Transactions* **33**, 1357-1361 (2005).
45. Yang, X. & Mierzejewski, E. Synthesis of nucleoside and oligonucleoside dithiophosphates. *New Journal of Chemistry* **34**, 805-819 (2010).

46. Guga, P. & Koziółkiewicz, M. Phosphorothioate nucleotides and oligonucleotides – recent progress in synthesis and application. *Chemistry & Biodiversity* **8**, 1642-1681 (2011).
47. Barone, A.D., Tang, J.Y. & Caruthers, M.H. In situ activation of bis-dialkylaminophosphines--a new method for synthesizing deoxyoligonucleotides on polymer supports. *Nucleic acids research* **12**, 4051-4061 (1984).
48. Rappsilber, J., Mann, M. & Ishihama, Y. Protocol for micro-purification, enrichment, pre-fractionation and storage of peptides for proteomics using StageTips. *Nature Protocols* **2**, 1896 (2007).
49. Distler, U., Kuharev, J., Navarro, P. & Tenzer, S. Label-free quantification in ion mobility-enhanced data-independent acquisition proteomics. *Nature Protocols* **11**, 795 (2016).
50. Rawling, T., Duke, C.C., Cui, P.H. & Murray, M. Facile and stereoselective synthesis of (Z)-15-octadecenoic acid and (Z)-16-nonadecenoic acid: monounsaturated omega-3 fatty acids. *Lipids* **45**, 159-165 (2010).
51. Ahad, A.M., Jensen, S.M. & Jewett, J.C. A traceless Staudinger reagent to deliver diazirines. *Organic Letters* **15**, 5060-5063 (2013).

Chapter 5

LEI-401 is an *in vivo* active NAPE-PLD inhibitor that reduces brain anandamide levels and pain behavior

5.1 Introduction

In recent years lipids have come to the foreground as signaling mediators in the central nervous system (CNS).¹⁻⁴ While classical neurotransmitters are stored in synaptic vesicles and released upon fusion with the plasma membrane of neurons, due to their lipophilic nature, lipids readily diffuse through membranes and are not stored in vesicles. It is, therefore, generally accepted that signaling lipids are produced 'on demand' and are rapidly metabolized to terminate their biological action.⁵ In particular, the endocannabinoid anandamide (*N*-arachidonylethanolamine, AEA) has emerged as a key lipid that regulates neurotransmission via its interaction with the cannabinoid CB₁ receptor and ion channels, such as the *N*-methyl-D-aspartate (NMDA) receptor⁶, T-type Ca²⁺ channels⁷, the acid-sensitive background K⁺ channel (TASK-1)⁸ and transient receptor potential vanilloid type 1 (TRPV1)⁹. Genetic deletion or pharmacological inhibition of the anandamide degrading enzyme, fatty acid amide hydrolase (FAAH), has revealed that elevated anandamide levels modulate various physiological processes such as pain¹⁰,

anxiety¹¹, appetite¹² and inflammation¹³. The physiological effects resulting from perturbation of anandamide biosynthesis in living systems are, however, poorly studied, partly because of a lack of pharmacological tools that can modulate the enzymes involved in anandamide production.¹⁴

N-acylphosphatidylethanolamine phospholipase D (NAPE-PLD) is generally considered the major anandamide biosynthetic enzyme.^{15,16} Biochemical and structural studies have demonstrated that NAPE-PLD is a membrane-associated, constitutively active zinc hydrolase with a metallo- β -lactamase fold.¹⁷ The enzyme generates a family of bioactive lipids, termed *N*-acylethanolamines (NAEs), including *N*-palmitoylethanolamine (PEA), *N*-oleoylethanolamine (OEA) and anandamide, by hydrolysis of the phosphodiester bond between the phosphoglyceride and the *N*-acylethanolamine in *N*-acylphosphatidylethanolamines (NAPEs).¹⁵ Knockout (KO) studies have shown that the conversion of NAPEs to NAEs bearing both saturated and polyunsaturated fatty acyl groups were reduced by 5-fold in brain lysates from mice that genetically lack *Napepld*.¹⁸ In accordance, depleted levels of saturated and mono-unsaturated NAEs were observed in the brain of NAPE-PLD KO mice.¹⁸⁻²⁰ Surprisingly, anandamide levels were not reduced in all transgenic models, which led to the discovery of alternative biosynthetic pathways for anandamide.^{16,18,21-23} However, compensatory pathways render these long-term, constitutive genetic mouse models poorly suited for studying the rapid and dynamic formation of anandamide and its biological role. Thus, a great need exists for pharmacological tools that can help to clarify the function of NAPE-PLD in 'on demand' production of anandamide. Unfortunately, potent CNS-active inhibitors are currently not available. Previously described NAPE-PLD inhibitors lack the potency, selectivity and/or physicochemical properties to function as *in situ* and/or *in vivo* active NAPE-PLD inhibitors.²⁴⁻²⁶

In this chapter, **LEI-401** (Figure 1), which was identified in Chapter 3 as a nanomolar potent NAPE-PLD inhibitor, is profiled in cellular and animal models. **LEI-401** reduced a broad range of NAEs including anandamide in neuronal cells, but not in NAPE-PLD KO cells, thereby confirming 'on-target' activity. Mice administered an intraperitoneal (i.p.) injection of **LEI-401** showed a dose-dependent reduction of anandamide in the brain at 2 hours. Behavioral profiling of **LEI-401**-treated mice showed hypomotility,

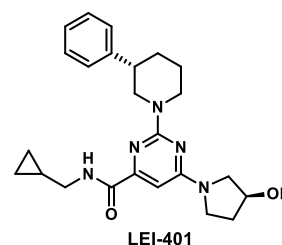


Figure 1. Structure of NAPE-PLD inhibitor **LEI-401**.

hypothermia and antinociception in the hot plate test. Taken together, **LEI-401** demonstrates the crucial role of NAPE-PLD as an anandamide-producing enzyme in the CNS, and points to a role for NAPE-PLD in the acute and dynamic regulation of neurophysiological pain behavior. **LEI-401** opens new opportunities to study anandamide and NAE signaling *in vivo*.

5.2 Results

5.2.1 Profiling the selectivity of LEI-401 for the endocannabinoid system (ECS).

LEI-401 was selected from a NAPE-PLD inhibitor library of pyrimidine-6-carboxamides for further biological profiling due to its optimal potency and physicochemical parameters (described in Chapter 3). First, the activity profile of **LEI-401** for the receptors and metabolic enzymes of the endocannabinoid system was assessed. No inhibitory activities were measured at 10 μ M for the cannabinoid receptors type 1 and 2 (CB₁/CB₂) (Table 1) as well as for the enzymes involved in anandamide biosynthesis and degradation, respectively, phospholipase A₂ group IV E (PLA2G4E) and FAAH (Table 2). In addition, **LEI-401** did not inhibit enzymes involved in the biosynthesis and degradation of the other endocannabinoid 2-arachidonoylglycerol (2-AG), including diacylglycerol lipases (DAGL α or DAGL β), monoacylglycerol lipase (MAGL) and α,β -hydrolase domain 6 (ABHD6) (Table 2).

Table 1. **LEI-401** did not significantly inhibit the CB₁ and CB₂ receptors.

| Radioligand displacement at 10 μ M LEI-401 (% \pm SD) | |
|---|------------|
| hCB1 | hCB2 |
| 36 \pm 2 | 47 \pm 9 |
| > 50% is considered a target | |

Table 2. **LEI-401** showed no inhibitory activity for metabolic enzymes of the ECS. Activities were measured using surrogate or natural substrate assays for DAGL α/β and MAGL, or activity-based protein profiling for PLA2G4E, FAAH and ABHD6.

| Remaining enzyme activity at 10 μ M LEI-401 (% \pm SD) | | | | | | |
|---|----------------|---------------|-------------|-------------|--------------|-------------|
| hDAGL α | mDAGL α | mDAGL β | hMAGL | hPLA2G4E | mFAAH | mABHD6 |
| 81 \pm 7 | 76 \pm 21 | 96 \pm 23 | 64 \pm 15 | 89 \pm 14 | 107 \pm 14 | 101 \pm 2 |
| < 50% is considered a target | | | | | | |

5.2.2 LEI-401 lowers anandamide levels in WT Neuro-2a, but not in NAPE-PLD KO cells.

Having established that **LEI-401** is a cell-permeable inhibitor that engages with NAPE-PLD (described in Chapter 4), and is selective over the receptors and metabolic enzymes of the ECS, we then investigated whether **LEI-401** inhibited endogenous NAPE-PLD in living cells. To this end, the mouse Neuro-2a neuroblastoma cell line was selected, because it expressed endogenous NAPE-PLD as determined by quantitative PCR (qPCR) (*Napepld*: $C_q \pm SD = 24.22 \pm 0.088$, *Hprt* (housekeeping gene): $C_q \pm SD = 19.48 \pm 0.047$) and western blot

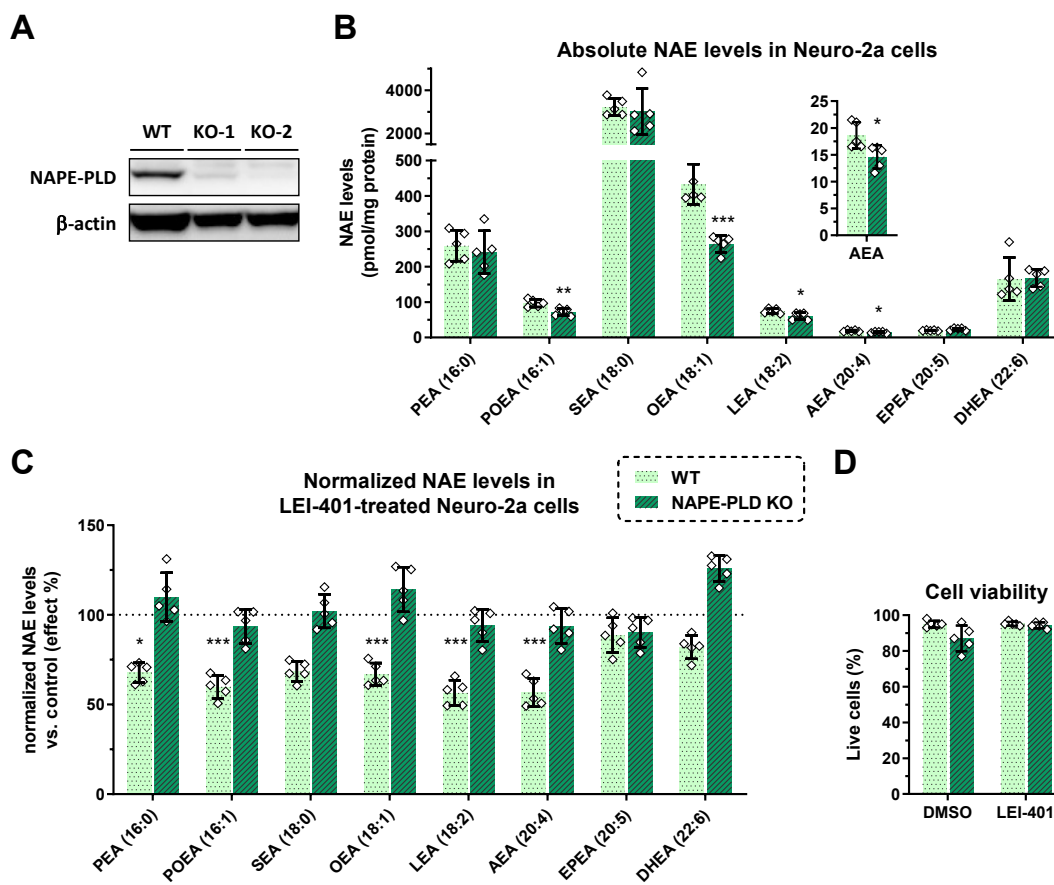


Figure 2. **LEI-401** reduces *N*-acyl ethanolamine (NAE) levels in wild-type (WT) Neuro-2a cells, but not in NAPE-PLD KO cells. **A**) Western blot showing NAPE-PLD protein expression in WT cells, but not in NAPE-PLD knockout cell line KO-2. **B**) Absolute NAE levels of WT and NAPE-PLD KO cells. **C**) Relative NAE levels of WT and NAPE-PLD KO cells treated with **LEI-401** (10 μ M, 2 h), represented as effect %. Data were normalized against WT or NAPE-PLD KO cells treated with vehicle (DMSO). Absolute values for all NAEs are depicted in Supplementary Figure 1. **D**) **LEI-401** (10 μ M, 2 h) showed no effect on the viability of Neuro-2a WT and NAPE-PLD KO cells. Live cells were identified based on Trypan blue exclusion. Data represent mean values \pm SD for 5 biological replicates. *, $P < 0.05$, **, $P < 0.01$, ***, $P < 0.001$ by one-way ANOVA.

using NAPE-PLD antibodies (Figure 2A). Targeted lipidomics on lipid extracts of Neuro-2a cells allowed the quantification of eight different NAEs by liquid chromatography-mass spectrometry (LC-MS) (Figure 2B). As an appropriate negative control, a NAPE-PLD KO cell line was generated using CRISPR-Cas9. Due to single cell heterogeneity of the Neuro-2a cell line, two KO populations were prepared by three sequential rounds of transfections with Cas9 and two different single guide RNAs (sgRNA), which targeted exon 2 (KO-1) or exon 3 (KO-2). The cell line KO-2 showed most efficient ablation of NAPE-PLD protein expression as demonstrated by western blot analysis (Figure 2A). Next, wild-type (WT) and KO cells were incubated with **LEI-401** (10 μ M) for 2 h. A significant 2-fold reduction of anandamide was apparent in the WT cells but not in the NAPE-PLD KO cells, indicating that the **LEI-401**-induced reduction in anandamide levels depended on expression of NAPE-PLD in Neuro-2a cells (Figure 2C). **LEI-401**-treated cells did not show any sign of reduced cell viability (Figure 2D). Notably, the smaller but significant decrease of anandamide (~25%) in NAPE-PLD KO cells compared to WT may indicate the occurrence of compensatory mechanisms in the NAPE-PLD KO cells, as also observed by others in *Napepld*-deficient mice (Supplementary Figure 1A).¹⁸ Furthermore, other saturated, mono- and (ω -6)-polyunsaturated NAEs showed a similar 2-fold decrease in WT cells upon **LEI-401** treatment, but not in NAPE-PLD KO cells (Figure 2C, Supplementary Figure 1B-F). (ω -3)-Polyunsaturated EPEA and DHEA did not respond to **LEI-401** treatment (Figure 2C, Supplementary Figure 2G-H). Our data are in line with previously reported biochemical substrate studies using purified recombinant NAPE-PLD and indicate that endogenously expressed NAPE-PLD is responsible for biosynthesis of saturated, mono- and (ω -6)-polyunsaturated NAEs in Neuro-2a cells. The lack of effect on (ω -3)-polyunsaturated NAEs may suggest that these signaling lipids are produced via another pathway. Of note, recently it was found that dietary (ω -3)-polyunsaturated fatty acids augment brain NAE levels in mice via a pathway independent of NAPE-PLD.²⁷

LEI-401 also reduced 2-AG and related monoacylglycerols (MAGs) 2-lineoylglycerol (2-LG) and 2-oleoylglycerol (2-OG) in both WT and NAPE-PLD KO cells, indicating a NAPE-PLD-independent mechanism of action (Supplementary Figure 1I-K). Although no evidence was found for direct inhibition of the MAG biosynthetic enzymes DAGL α/β by **LEI-401** (Table 2), possible modulation of the DAGL α/β activity or expression levels via an alternative pathway cannot be ruled out at this point. The elevation of arachidonic acid (AA) in the KO cells compared to WT suggests that NAPE-PLD ablation may have an inflammatory effect (Supplementary Figure 1L), although this AA increase was not observed upon 24 h treatment with or without **LEI-401** (data not shown).

5.2.3 LEI-401 shows high CNS penetration and reduces brain anandamide levels *in vivo*.

Before testing whether **LEI-401** possesses *in vivo* efficacy, its absorption, distribution, metabolism and excretion (ADME) profile was determined. **LEI-401** demonstrated favorable physicochemical properties for oral bioavailability and brain penetration (MW = 422 Da; LogD = 3.3 and topological polar surface area (tPSA) = 80.5 Å²). **LEI-401** had low aqueous solubility (1.7 µg/mL) and permeates well through membranes (PAMPA P_{eff} = 0.37 cm/µs). Clearance in human and mouse microsomes (10 and 42 µL/min/mg protein, respectively) as well as in hepatocytes (6.9 and 28.8 µl/min/10⁶ cells, respectively) was moderate, except for the low human microsomal clearance. **LEI-401** exhibited high human and mouse protein binding (> 99.8 %). Of note, it did not interact with either human or mouse PGP-transporter (efflux ratios: 1.7 and 1.8, respectively).

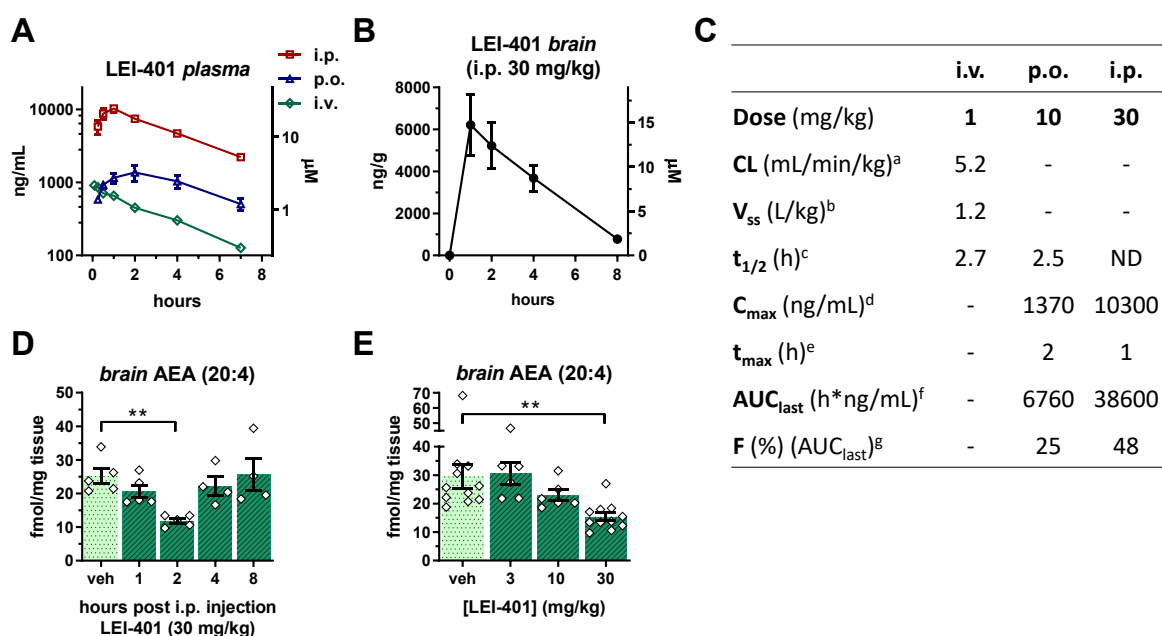


Figure 3. **LEI-401** pharmacokinetic (PK) profile, showing high CNS penetration and dose-dependent reduction of anandamide in mouse brain. **A)** *In vivo* PK of **LEI-401** in plasma of C57BL/6J mice via intraperitoneal (i.p., 30 mg/kg), oral (p.o., 10 mg/kg) or intravenous (i.v., 1 mg/kg) administration. **B)** Brain PK profile of **LEI-401** in C57BL/6J mice after i.p. administration (30 mg/kg). For **A-B)**: data represent mean values ± SEM for 3-5 biological replicates per group. **C)** PK parameters of **LEI-401** in C57BL/6J mice after i.p., p.o. or i.v. administration. ^a CL = clearance. ^b V_{ss} = volume of distribution at steady state. ^c t_{1/2} = half-life. ^d C_{max} = maximum plasma drug concentration. ^e t_{max} = time to reach C_{max}. ^f AUC_{last} = area under plasma concentration-time curve from t₀ → t_{last}. ^g F = bioavailability. **D)** Time-dependent effect of **LEI-401** on brain AEA. C57BL/6J mice i.p. injected with **LEI-401** (30 mg/kg). **E)** Dose-dependent effect of **LEI-401** on brain AEA at 2 h after i.p. administration. For **D-E)**: data represent mean values ± SEM for 5-11 biological replicates. **, P < 0.01, by one-way ANOVA.

Pharmacokinetic analysis for **LEI-401** in male C57BL/6J mice revealed a low clearance (CL = 5.2 mL/min/kg) and moderate volume of distribution (V_{ss} = 1.2 L/kg), resulting in a half-life of 2.7 h (Figure 3A,C). The low *in vivo* clearance was not expected based on the *in vitro* clearance, but can be explained by the tight protein binding. Bioavailability after oral administration (F_{po}) reached 25% and a more favorable bioavailability was achieved via intraperitoneal (i.p.) injection (F_{ip} = 48%). In both cases good plasma exposures (AUC) were obtained. The brain to plasma ratio was 0.7 at C_{max} (2 h post injection). This led to an excellent brain exposure (> 10 μ M) after 30 mg/kg i.p. administration (Figure 3B), which corresponds to approximately 70-fold the mouse NAPE-PLD K_i -value (0.18 μ M), and should be sufficient to modulate NAPE-PLD activity in mouse brain.

In view of the encouraging PK properties and brain exposure, **LEI-401** or vehicle was administered to male C57BL/6J mice (30 mg/kg, i.p., single dose) and the mice were sacrificed after 1, 2, 4 or 8 hours to determine whether NAE levels were reduced. To this end, brain NAE levels were analyzed by LC-MS. **LEI-401** induced a significant and time-dependent reduction for anandamide (P = 0.0051), which was maximal at 2 h and returned to vehicle level by 4 h (Figure 3D). A similar trend, though not significant, was observed for OEA and DHEA (Supplementary Figure 2A,B). In contrast to long-term ablation of NAPE-PLD as seen in knockout mice¹⁸, these data indicate that acute NAPE-PLD inhibition primarily affects anandamide levels in mouse brain. Next, mice were treated with various doses of **LEI-401** (3, 10 and 30 mg/kg or vehicle, i.p., single dose) and brain lipids were analyzed at 2 h. A dose-dependent reduction of anandamide was observed with a 2-fold decrease apparent at the highest dose (30 mg/kg) (Figure 3E). Other NAE lipid species did not achieve significant reductions at the highest dose (Supplementary Figure 3A-C). Notably, 2-AG was also dose-dependently decreased compared to vehicle-treated animals (Supplementary Figure 3D). Together, these data establish that acute NAPE-PLD inhibition reduces brain anandamide levels and indicate that **LEI-401** can be used to target NAPE-PLD in living animals to investigate the biological role of NAPE-PLD.

5.2.4 LEI-401 produces analgesic effects *in vivo*.

To assess the effect of acute anandamide reduction in the brain, an explorative *in vivo* behavioral profiling study was undertaken in which locomotion, antinociception, body temperature and catalepsy were measured. **LEI-401** treatment (30 mg/kg, i.p., single dose) in male C57BL/6J mice significantly reduced locomotor activity (P = 0.039) and decreased body temperature (P = 0.0005) at 2 h, while showing no signs of catalepsy in the bar test (Figure 4A-C). An antinociceptive response was observed in the hot plate test of thermal pain sensation, showing elevated latencies (P = 0.0087), albeit less pronounced

than a positive control (CP-55,940, a CB₁/CB₂ receptor agonist) (Figure 4D). No antinociception was apparent in the tail-immersion test (Figure 4E). To rule out that **LEI-401** or its metabolites produced these behavioral effects via the CB₁ receptor, the same set of experiments were repeated in CB₁ receptor KO mice. Again, **LEI-401** induced locomotion depression, hypothermia and antinociception in the hot plate assay (Figure 5A-E), indicative of a CB₁ receptor-independent mechanism.

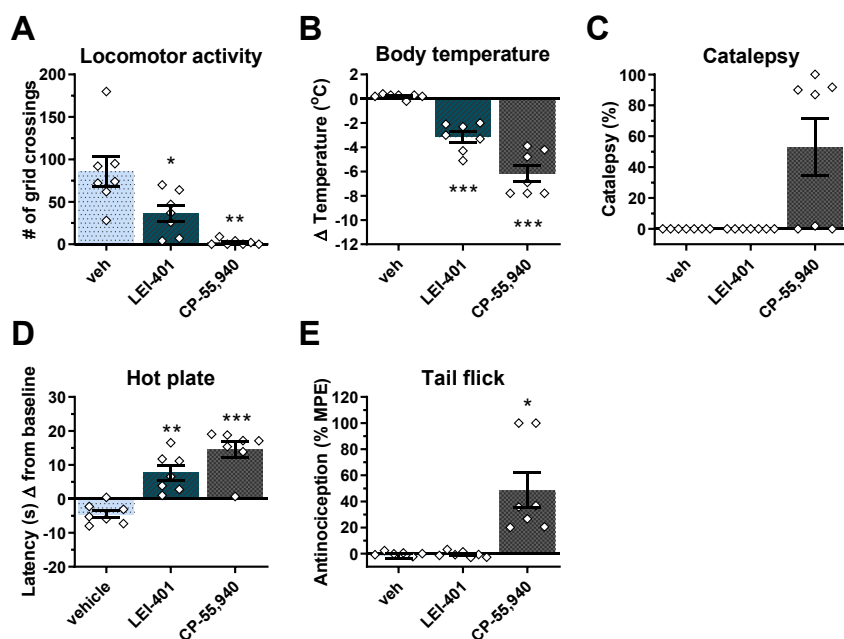


Figure 4. *In vivo* behavioral effects of **LEI-401** in the tetrad test in C57BL/6J mice. **LEI-401** (30 mg/kg, i.p., single dose) produced locomotor depression (A) and hypothermia (B), but no catalepsy (C). Elevated latencies in the hot plate test of thermal pain were observed (D), but no antinociception in the tail flick assay (E) (% MPE = maximum possible effect %). The CB₁/CB₂ receptor agonist CP-55940 was used as a positive control. Data represent mean values ± SEM for 7-11 biological replicates. *, $P < 0.05$, **, $P < 0.01$, ***, $P < 0.001$ by one-way ANOVA.

5.2.5 LEI-401 reverses LPS-induced allodynia.

The analgesic effect of **LEI-401** observed in the hot plate test, encouraged further investigation into its antinociceptive potential. Therefore, **LEI-401** was tested in a model of inflammatory pain of lipopolysaccharide (LPS)-induced mechanical allodynia in mice. Intraplantar LPS injection (2.5 μg) in the hind paw produced significant allodynic responses compared to vehicle (Figure 6A). **LEI-401** treatment (30 mg/kg, i.p, single dose) 22 h after LPS injection fully reversed LPS-induced allodynia for 2 to 4 h after

administration ($P = 0.0027$ and 0.0061 , respectively), consistent with its PK profile (Figure 3A,B).

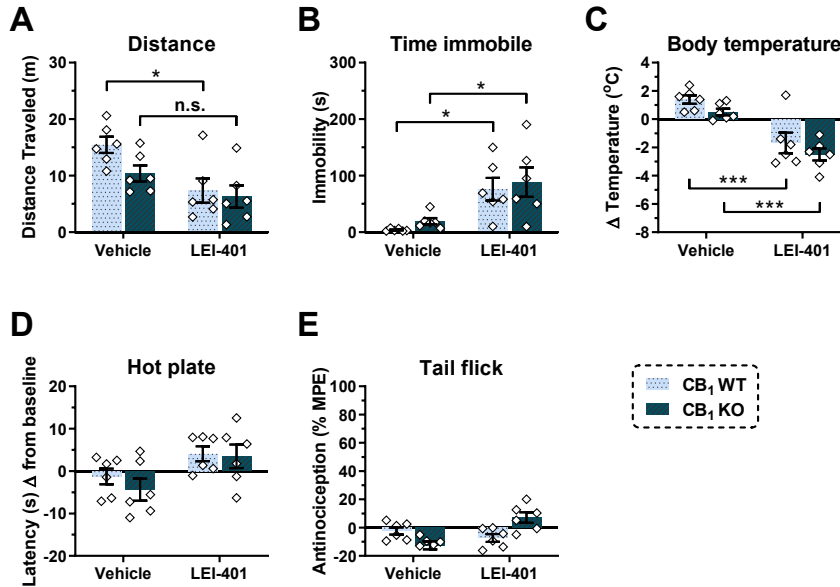


Figure 5. LEI-401-induced behavioral effects were sustained in CB₁ KO mice. LEI-401 (30 mg/kg, i.p., single dose) induced hypomotility (A,B), hypothermia (C) and antinociception in the hot plate assay (D) but not in the tail flick test (E). No catalepsy was observed (data not shown). Data represent mean values \pm SEM for 6 biological replicates. *, $P < 0.05$, ***, $P < 0.001$ by two-way ANOVA.

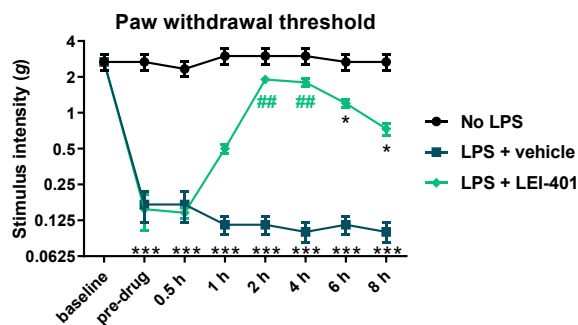


Figure 6. LEI-401 showed antinociception in a mouse model of inflammatory pain. Von Frey nociceptive testing in C57BL/6J mice displayed complete reversal of LPS-induced allodynic pain for 2 to 4 h after LEI-401 administration (30 mg/kg, i.p., single dose). Data represent mean values \pm SEM for 6-8 biological replicates. *, $P < 0.05$, ***, $P < 0.001$ compared to 'No LPS' treatment; ##, $P < 0.01$ compared to 'LPS + vehicle' by two-way ANOVA.

5.3 Discussion

Anandamide regulates synaptic plasticity in the brain and modulates various physiological and behavioral functions. Inhibitors of its degradation have shed light on its role in pain, energy balance, locomotion and emotional states, such as anxiety. However, assessing the biological consequences of reducing anandamide levels represents an increased challenge because of a lack of selective, CNS-active inhibitors that block *in vivo* anandamide production. In addition, the development of NAPE-PLD KO mice revealed the presence of alternative, compensatory biosynthetic pathways in the brain, which questioned the biological role of NAPE-PLD in anandamide production.¹⁶ Here, we have addressed these important questions by developing the first centrally active NAPE-PLD inhibitor **LEI-401**.

Acute NAPE-PLD inhibition by **LEI-401** in mouse neuronal Neuro-2a cells decreased saturated, mono- and (ω -6)-polyunsaturated NAEs (including anandamide), while leaving (ω -3)-polyunsaturated NAEs unperturbed. This effect was not present in Neuro-2a cells lacking NAPE-PLD, showing the specificity of **LEI-401**. Of note, acute NAPE-PLD inhibition resulted in lower anandamide levels than observed in the NAPE-PLD KO cells, thereby indicating that long-term inactivation of NAPE-PLD in cells also may lead to activation of compensatory pathways (Supplementary Figure 1A). Administration of **LEI-401** to WT mice resulted in a time- and dose-dependent decrease in anandamide content in the brain and influenced nociceptive behavior. These findings provide strong experimental evidence for the biological action of NAPE-PLD in anandamide production in the CNS, support the 'on demand' model of anandamide biosynthesis and reveal a role of NAPE-PLD in complex neurophysiological behavior.

While NAPE-PLD does not show any substrate specificity in biochemical and cellular studies, our findings indicate that primarily anandamide levels are acutely reduced in brains of freely moving mice. The factors that regulate the specific turnover of anandamide over other NAEs remain unknown, but previous studies have shown that anandamide levels are strongly influenced by FAAH activity, the metabolic enzyme of anandamide.²⁸ The tonic flux of anandamide in the brain undoubtedly depends on the relative contribution of NAPE-PLD and FAAH activity; especially in brain regions where the two enzymes are co-expressed, such as the hippocampus and frontal cortex.²⁹ In addition, the specific activity and localization of phospholipase and acyltransferases (PLAAT1-5)³⁰ and the Ca²⁺-dependent N-acyltransferase (PLA2G4E)³¹, enzymes that produce the substrates of NAPE-PLD, represent other determinants in the biosynthesis of NAEs. Lastly, it is possible that the *in vivo* substrate specificity and activity of NAPE-PLD could be controlled by its protein-protein interactions, post-translational modifications (> 10

potential sites for PTMs have been detected (<https://www.phosphosite.org>) and/or endogenous allosteric modulators. For example, bile acids and polyamines significantly increased NAPE-PLD activity *in vitro*.^{17,32,33} Regardless of the precise mechanism that specifically controls anandamide production, our data highlight the importance of NAPE-PLD in the biosynthesis of anandamide in the brain.

LEI-401 elicited hypothermia, hypomotility and antinociception in the hot plate test. This neurophysiological behavior was maintained in CB₁ receptor KO mice, indicating that CB₁ receptor signaling is not involved in the actions of **LEI-401** or its metabolites. This finding contrasts to pharmacological inhibition or deletion of FAAH, in which anandamide elevation produces CB₁ receptor-dependent antinociceptive effects, as evidenced by blockade of the CB₁ receptor with the antagonist rimonabant.^{28,34,35} In addition, similar to inhibitors of FAAH³⁶, **LEI-401** evoked analgesia in a model of inflammatory pain. While the exact molecular mechanism underpinning the neurophysiological behavior of acute NAPE-PLD inhibition is yet unknown, it is interesting to note that anandamide interacts with various other proteins in the CNS, including nuclear receptors (PPAR) and ion channels (e.g. TASK-1, T-type Ca²⁺ channels, NMDA and TRPV1).⁹ Furthermore, NAPE-PLD is expressed in nociceptive sensory neurons and thalamus.^{37,38} Thus, our data suggest that NAPE-PLD may set an endogenous tone that plays a role in the neural circuitries mediating nociceptive behavior.^{38,39} Alternatively, we cannot exclude the possibility that the substrates and other products of NAPE-PLD – NAPEs and phosphatidic acids, respectively – act as signaling molecules in their own right and/or alter (plasma)membrane properties, thereby exerting biological effects.^{26,40} It will be critical to evaluate the **LEI-401**-induced effects in NAPE-PLD KO mice, to confirm an on-target mechanism of action. Nevertheless, our data indicate that **LEI-401** produces useful analgesic effects *in vivo* that will be the focus of future research.

Finally, our studies suggest that **LEI-401** and the developed NAPE-PLD photoaffinity probes (Chapter 4) constitute a valuable toolbox to study various aspects of NAPE-PLD and anandamide biology both in animal and cellular models. Although **LEI-401** was shown to be selective in a chemical proteomics setting (Chapter 4) and did not inhibit DAGL α and DAGL β , the enzymes responsible for the production of the other endocannabinoid 2-AG, it depleted 2-AG, 2-LG and 2-OG content in Neuro-2a cells in a NAPE-PLD-independent manner. Furthermore, **LEI-401** dose-dependently reduced brain 2-AG levels in mice. These observations indicate that **LEI-401** or its metabolites may have off-target activities and highlight the need of combining chemical probes with genetic models to study on-target and off-target interactions of pharmacological agents. Second generation NAPE-PLD inhibitors will benefit from the identification of the off-targets. From a translational

perspective, it will be interesting to study NAPE-PLD inhibitors in various animal models of human disease, such as metabolic syndrome⁴¹, type II diabetes⁴², neurodegeneration^{43,44}, anxiety⁴⁵, inflammatory and neuropathic pain³⁸, stress-related disorders⁴⁶, chronic liver disease⁴⁷ and cancer⁴⁸. The NAPE-PLD inhibitor reported in this study provides the first opportunity to study the central role of NAPE-PLD in anandamide biosynthesis in the brain of living animals in an acute and dynamic manner, thereby revealing the function of this enzyme in acute nociceptive behavior. It is envisioned that **LEI-401** may help to validate NAPE-PLD as a therapeutic target and serve as a starting point for the discovery of future drug candidates.

Acknowledgements

Annelot van Esbroeck is kindly acknowledged for generating the NAPE-PLD KO cell lines. Andrea Martella, Marjolein Soethoudt, Ming Jiang, Tom van der Wel, Timo Wendel and Anthe Janssen are acknowledged for performing biochemical assays. Vasudev Kantae, Xinyu Di and Thomas Hankemeier are kindly thanked for determining cellular lipid levels. The ADME profile and *in vivo* PK of **LEI-401** was measured at Hoffman-La Roche under supervision of Matthias Wittwer and Uwe Grether, for which they are kindly acknowledged. Resat Cinar, Zoltan Varga, Janos Paloczi, Joshua Park, Pal Pacher, Mohammed Mustafa, Giulia Donvito and Aron Lichtman are kindly thanked for profiling **LEI-401** *in vivo* and performing lipidomics and behavioral experiments.

5.4 Experimental section

A. Biological procedures

Cell culture

Neuro-2a cells (ATCC) were cultured at 37 °C and 7% CO₂ in DMEM (Sigma Aldrich, D6546) with GlutaMax (2 mM), penicillin (100 µg/ml), streptomycin (100 µg/ml) and 10% New Born Calf serum. Cells were passaged twice a week to appropriate confluence by thorough pipetting.

Cell lysate preparation

Neuro-2a cells were harvested by removal of culture medium and addition of cold PBS. Cells were pipetted loose, transferred to 50 mL tubes, centrifuged (10 min, 200 g, 4 °C) and the supernatant was removed. The cell pellets were flash frozen in liquid N₂ and stored at -80 °C. Whole cell lysates were prepared by addition of lysis buffer: 20 mM HEPES, 2 mM DTT, 0.25 M sucrose, 1 mM MgCl₂, 2.5 U/mL benzonase. Cells were homogenized by thorough pipetting and incubated for 30 minutes on ice. Protein concentrations were determined using a Bradford assay (Bio-Rad) and samples were stored at -80 °C.

qPCR

RNA isolation and cDNA synthesis: Total RNA from Neuro-2a cells was extracted using Trizol reagent (ThermoFisher Scientific). Once isolated, RNA concentration and purity was determined by Nanodrop (Denovix Inc.). Subsequently cDNA synthesis was carried out with Maxima H minus first strand cDNA synthesis kit (ThermoFisher Scientific) according to the manufacturer's instructions.

qPCR analysis: 10 ng of input cDNA was analyzed using SybrGreen qPCR master mix (Biotool) in combination with CFX96 optical thermal cycler (Bio-Rad). Data analysis was performed using CFX Manager software (Bio-Rad). The housekeeping gene hypoxanthine guanine phosphoribosyl transferase (*Hprt*) was used as a control. Data are expressed in quantitation cycles (C_q) and standard deviation of three technical replicates.

Table S1. Primer sequences of *Napepld* and *Hprt* used for qPCR.

| Gene | Forward (5'-3') | Reverse (5'-3') | Accession number |
|----------------|-----------------------|----------------------|------------------|
| <i>Napepld</i> | AGCGCCAAGCTATCAGTATCC | ACGTCCTCTAGTCTGTAATC | NM_178728 |
| <i>Hprt</i> | TTGACACTGGTAAACAATGC | GCCTGTATCCAACACTTCG | NM_013556 |

Western blot

Cell lysates were denatured with 4x Laemmli buffer (stock concentrations: 240 mM Tris-HCl pH 6.8, 8% w/v SDS, 40% v/v glycerol, 5% v/v β -mercaptoethanol, 0.04% v/v bromophenol blue, 30 min, rt) and 10-20 μ g per sample was resolved on a 10% acrylamide SDS-PAGE gel (180 V, 75 min). Proteins were transferred from the gel to a 0.2 μ m PVDF membrane using a Trans-Blot[®] Turbo (Bio-Rad). The membranes were washed with TBS (50 mM Tris-HCl pH 7.5, 150 mM NaCl) and blocked with 5% milk in TBST (50 mM Tris-HCl pH 7.5, 150 mM NaCl, 0.05% Tween 20) 1 h at rt or overnight at 4 °C. Primary antibodies against NAPE-PLD (Abcam, ab95397, 1:200, in TBST) and β -actin (Abcam, ab8226, 1:5000 in 5% milk in TBST) were incubated 1 h at rt or overnight at 4 °C. Membranes were washed with TBST and incubated with secondary antibodies: for NAPE-PLD, goat-anti-rabbit-HRP (Santa Cruz, sc-2030, 1:2000 in 5% milk in TBST); for β -actin, goat-anti-mouse-HRP (Santa Cruz, sc-2005, 1:5000 in 5% milk in TBST). All secondary antibodies were incubated 1 h at rt or overnight at 4 °C. Membranes were washed with TBST and TBS. The blot was developed in the dark using a luminol solution (10 mL, 1.4 mM luminol in Tris-HCl pH 8.8), ECL enhancer (100 μ L, 6.7 mM *para*-hydroxycoumaric acid in DMSO) and H₂O₂ (3 μ L, 30% w/w in H₂O). Chemiluminescence was visualized using a ChemiDoc[™] Imaging System (Bio-Rad). Band intensity was normalized to β -actin using ImageLab software (Bio-Rad).

CB₁ and CB₂ receptor radioligand displacement assay

The hCB₁ and hCB₂ receptor radioligand displacement assays were performed as described in Chapter 2.

Natural substrate-based fluorescence assay DAGL α

The human or mouse DAGL α activity assay was performed as described in Chapter 2.

Surrogate substrate-based fluorescence assay DAGL β

The hDAGL β activity assay was performed as described in Chapter 2.

Natural substrate-based fluorescence assay MAGL

The hMAGL activity assay was performed as described in Chapter 2.

Activity-based protein profiling for FAAH, ABHD6, ABHD12 and PLA2G4E activity

Gel-based activity-based protein profiling (ABPP) was performed as described in Chapter 2.

Generation of Neuro-2a NAPE-PLD KO populations

sgRNA selection: two sgRNA's, located in exon 2 and 3 with high efficiency and specificity as predicted by CHOPCHOP v2 online web tool (<http://chopchop.cbu.uib.no>)⁴⁹ were selected. Guides were cloned into the BbsI restriction site of plasmid px330-U6-Chimeric_BB-CBh-hSpCas9 (gift from Feng Zhang, Addgene plasmid #42230) as previously described.^{50,51} The sgRNA targeting exon 3 yielded higher knockout efficiency as determined by western blot and in the T7E1-assays. This population was used for further experiments.

Sequential transfection: Neuro-2a cells were transfected sequentially (3 times within the course of 10 days) to yield populations with a high knockout efficiency. Cells were seeded at day 0, day 3 and day 6 and transfected at day 1, day 4, and day 7. Samples for T7E1 assays were harvested at day 2, day 5, day 11 and after several weeks of culturing the cells. One day prior to the first transfection, Neuro-2a cells were seeded to a 6 wells plate to reach 80-90% confluence at the time of transfection. Prior to transfection, culture medium was aspirated and 2 mL of fresh medium was added. A 5:1 (m/m) mixture of polyethyleneimine (PEI) (17.5 µg/well) and plasmid DNA (3.5 µg/well) was prepared in serum free culture medium (250 µL each) and incubated (15 min, rt). Transfection was performed by dropwise addition of the PEI/DNA mixture to the cells. 24 h post-transfection the culture medium was refreshed, a small amount of cells was harvested for analysis by T7E1 assay and ABPP while the remainder was kept in culture under standard conditions for following transfections. After three transfection rounds, the cells were cultured according to standard protocol.

T7E1 assay: genomic DNA was obtained by mixing 50 µL QuickExtract™ (Epicentre) with cell pellet (~10% of a well, from a 6 well plate). The samples were incubated at 65 °C for 6 min, mixed by vortexing and then incubated at 98 °C for 2 min. Genomic DNA extracts were diluted in sterile water and directly used in PCR reactions. Genomic PCR reactions were performed on 2.5-5 µL isolated genomic DNA extract using Phusion High-Fidelity DNA Polymerase (Thermo Fisher) in Phusion HF buffer in a final volume of 20 µL, for primers see Table S2.

For the T7E1 assay, genomic PCR products were denatured and reannealed in a thermocycler using the following program: 5 min at 95 °C, 95 to 85 °C using a ramp rate of -2 °C/s, 85 to 25 °C using a ramp rate of -0.2 °C/s. To annealed PCR product (8.5 µL) was added NEB2 buffer (1 µL) and T7 endonuclease I (5 U, 0.5 µL; New England Biolabs), followed by incubation at 37 °C for 30 min. Digested PCR products were analyzed using agarose gel electrophoresis with ethidium bromide staining. Agarose gels were analyzed using ImageLab Software (Bio-Rad) and CRISPR gene editing efficiency was expressed as percentage T7E cleavage (volume integral of digested bands / volume integral all bands * 100 %).

Table S2. Primer sequences for sgRNA and T7E1 assay.

| sgRNA Target | Primer sequence* |
|---------------------------------------|---|
| <i>Napepld</i> – Exon 2 (KO-1) | Top: <u>CACCGATAGCTTGGCGCTGGAGAC</u> |
| | Bottom: <u>AAACGTCTCCAGCGCCAAGCTATC</u> |
| | Forward: ccgaggtaccataCTTAAAATCCTGTTTTGCAGCC |
| | Reverse: caacaccggtatcGTGGTCATAGGACCCATTTGTT |
| <i>Napepld</i> – Exon 3 (KO-2) | Top: <u>CACCAGTTCGCTTATTGTACACGG</u> |
| | Bottom: <u>AAACCCGTGTACAATAAGCGAACT</u> |
| | Forward: ccgaggtaccataAGGTACACGCTGTGTAAGAGCA |
| | Reverse: caacaccggtatcAAGGACCAAACCTTTTTTCCAAT |

* The *Napepld*-specific sequence is underlined.

B. Targeted lipidomics in Neuro-2a cells

The targeted lipidomics experiments are based on previously reported methods with small alterations.⁵²

Sample preparation

$2 \cdot 10^6$ Neuro-2a cells (grown at 37 °C, 7% CO₂) were seeded 1 day before treatment in 6 cm dishes. Before treatment, cells were washed twice with warm PBS and then treated with vehicle or compound (10 μM, 0.1% DMSO) in 3 mL medium without serum (2 h at 37 °C, n = 5 per condition). Washing with cold PBS (1x) followed by harvesting in 1.5 mL Eppendorf tubes and centrifugation (10 min, 1500 rpm). PBS was removed and the cell pellets were flash frozen with liquid nitrogen and stored at -80 °C. Live cell count with trypan blue was performed after compound treatment to test for cell viability. 10% of each cell sample (collected during harvesting) was used to determine the protein concentration using a Bradford assay (Bio-Rad) for normalization after lipid measurements.

Lipid extraction

Lipids extraction was performed on ice. In brief, cell pellets with $2 \cdot 10^6$ cells were transferred to 1.5 mL Eppendorf tubes, spiked with 10 μL each of deuterium labeled internal standard mix for endocannabinoids (*N*-arachidonylethanolamine (AEA)-d8, *N*-docosahexaenylethanolamine (DHEA)-d4, 2-arachidonoylglycerol (2-AG)-d8, *N*-stearoylethanolamine (SEA)-d3, *N*-palmitoylethanolamine (PEA)-d4, *N*-linoleoylethanolamine (LEA)-d3 and *N*-oleoylethanolamine (OEA)-d4), and negative polar lipids (fatty acid (FA)17:0-d33), followed by the addition of ammonium acetate buffer (100 μL, 0.1 M, pH 4). After extraction with methyl *tert*-butyl ether (MTBE, 1 mL), the tubes were thoroughly mixed for 4 min using a bullet blender at medium speed (Next Advance Inc., Averill park, NY, USA), followed by a centrifugation step (5,000 *g*, 12 min, 4 °C). Then 925 μL of the upper MTBE layer was transferred into clean 1.5 mL Eppendorf tubes. Samples were dried in a speed-vac followed by reconstitution in acetonitrile/water (50 μL, 90 : 10, v/v). The samples were centrifuged (14,000 *g*, 3 min, 4 °C) and transferred into LC-MS vials. Each sample was injected on two different lipidomics platforms: endocannabinoids (5 μL) and negative polar lipids (8 μL).

LC-MS/MS analysis for endocannabinoids

A targeted analysis of endocannabinoids and related NAEs (*N*-acylethanolamines) was measured using an Acquity UPLC I class binary solvent manager pump (Waters, Milford, USA) in conjugation with AB SCIEX 6500 quadrupole ion trap (QTRAP) (AB Sciex, Massachusetts, USA). Separation was performed with an Acquity HSS T3 column (1.2 x 100 mm, 1.8 μm) maintained at 40 °C. The aqueous mobile phase A consisted of 2 mM ammonium formate and 10 mM formic acid, and the organic mobile phase B was acetonitrile. The flow rate was set to 0.4 ml/min; initial gradient conditions were 55% B held for 2 min and linearly ramped to 100% B over 6 minutes and held for 2 min; after 10 s the system returned to initial conditions and held 2 min before next injection. Electrospray ionization-MS was operated in positive mode for measurement of endocannabinoids and NAEs, and a selective Multiple Reaction Mode (sMRM) was used for quantification.

LC-MS/MS analysis for negative polar lipids

This method is measured on an Acquity UPLC binary solvent manager 8 pump (Waters) coupled to an Agilent 6530 electrospray ionization quadrupole time-of-flight (ESI-Q-TOF, Agilent, Jose, CA, USA) high resolution mass spectrometer using reference mass correction. The chromatographic separation was achieved on an Acquity HSS T3 column (1.2 x 100 mm, 1.8 μm) maintained at 40 °C for both methods. The negative apolar lipids that constitute free fatty acids were separated with a flow of 0.4 mL/min over 15 min gradient. In negative mode, the aqueous mobile phase A consisted of 5:95 (v/v) acetonitrile:H₂O with 10 mM ammonium formate, and the organic mobile phase B consisted of 99% (v/v) methanol with 10 mM ammonium formate.

Statistical analysis

Absolute values of lipid levels were corrected using the measured protein concentrations. Data were tested for significance with GraphPad v6 using one-way ANOVA with Tukey correction for multiple comparisons. *P*-values < 0.05 were considered significant.

C. *In vitro* absorption, distribution, metabolism and excretion (ADME) profile of LEI-401.

Kinetic aqueous solubility (LYSA = LYophilization Solubility Assay)

The solubility of **LEI-401** in phosphate buffer at pH 6.5 from an evaporated 10 mM DMSO compound stock solution was measured. Two aliquots of the test compound were dried and dissolved in phosphate buffer at pH 6.5. The solutions were then filtered and diluted (3 different dilution levels for each compound) before RapidFire MS analysis was performed. Each test compound was quantified using a 6-point calibration curve prepared with the same DMSO starting solution.

Passive membrane permeability (PAMPA)

PAMPA (Parallel Artificial Membrane Permeability Assay) is a method which determines the permeability of substances from a donor compartment, through a lipid-infused artificial membrane into an acceptor compartment. Read-out is a permeation coefficient P_{eff} drug as well as test compound concentrations in donor, membrane and acceptor compartments. The assay was performed as described elsewhere.⁵³

Microsomal clearance

The microsomal clearance assay was performed as previously described.⁵⁴ Pooled commercially available microsome preparations from male mouse microsomes (C57BL/6J, Lot 4339006) were purchased from Corning Incorporated (Woburn, USA)). For human, ultra-pooled liver microsomes (150 mixed gender donors, BD UltraPool HLM 150, Lot 38289) were purchased to account for the biological variance *in vivo* from human liver tissues. For the microsome incubations (incubation buffer 0.1 M phosphate buffer pH 7.4), 96-deep well plates were applied, which were incubated at 37 °C on a TECAN (Tecan Group Ltd, Switzerland) equipped with Te-Shake shakers and a warming device (Tecan Group Ltd, Switzerland). The NADPH regenerating system consisted of 30 mM glucose-6-phosphate disodium salt hydrate; 10 mM NADP; 30 mM $\text{MgCl}_2 \times 6 \text{H}_2\text{O}$ and 5 $\mu\text{g}/\mu\text{L}$ glucose-6-phosphate dehydrogenase (Roche Diagnostics) in 0.1 M potassium phosphate buffer pH 7.4. Incubations of **LEI-401** at 1 μM in microsome incubations of 0.5 $\mu\text{g}/\mu\text{L}$ plus cofactor NADPH were performed in 96-well plates at 37 °C. After 1, 3, 6, 9, 15, 25, 35 and 45 minutes 40 μL incubation solutions were transferred and quenched with 3:1 (v/v) acetonitrile containing internal standards. Samples were then cooled and centrifuged before analysis by LC-MS/MS. Log peak area ratios (test compound peak area / internal standard peak area) were plotted against incubation time using a linear fit. The calculated slope was used to determine the intrinsic clearance: CL_{int} ($\mu\text{L}/\text{min}/\text{mg}$ protein) = -slope (min^{-1}) * 1000 / [protein concentration ($\mu\text{g}/\mu\text{L}$)].

Hepatocyte clearance

The hepatocyte clearance assay was performed as previously described.⁵⁵ For animals, hepatocyte suspension cultures were either freshly prepared by liver perfusion studies or prepared from cryopreserved hepatocyte batches (pooled C57BL6 mouse hepatocytes were purchased from BioreclamationIVT (NY, USA)). For human, commercially available, pooled (5-20 donors), cryopreserved human hepatocytes from non-transplantable liver tissues were used. For the suspension cultures, Nunc U96 PP-0.5 mL (Nunc Natural, 267245) plates were used, which were incubated in a Thermo Forma incubator from Fischer Scientific (Wohlen, Switzerland) equipped with shakers from Variomag® Teleshake shakers (Sterico, Wangen, Switzerland) for maintaining cell dispersion. The cell culture medium was William's media supplemented with Glutamine, antibiotics, insulin, dexamethasone and 10% FCS. Incubations of a test compound at 1 μM

test concentration in suspension cultures of $1 \cdot 10^6$ cells/mL ($\sim 1 \mu\text{g}/\mu\text{L}$ protein concentration) were performed in 96-well plates and shaken at 900 rpm for up to 2 hours in a 5% CO_2 atmosphere at 37°C . After 3, 6, 10, 20, 40, 60 and 120 minutes 100 μL cell suspension in each well is quenched with 200 μL methanol containing an internal standard. Samples are then cooled and centrifuged before analysis by LC-MS/MS. Log peak area ratios (test compound peak area / internal standard peak area) or concentrations were plotted against incubation time with a linear fit. The slope of the fit was used to calculate the intrinsic clearance: $\text{CL}_{\text{int}} (\mu\text{L}/\text{min}/1 \cdot 10^6 \text{ cells}) = -\text{slope} (\text{min}^{-1}) * 1000 / [1 \cdot 10^6 \text{ cells}]$.

Plasma protein binding

The plasma protein binding assay was performed as previously described.^{56,57} Pooled and frozen plasma from human (HMPLEDTA, Lot BRH1060627) and mouse (MSEPLEDTA3-C57, Lot MSE196204) were obtained from BioreclamationIVT (NY, USA). The Teflon equilibrium dialysis plate (96-well, 150 μL , half-cell capacity) and cellulose membranes (12–14 kDa molecular weight cut-off) were purchased from HT-Dialysis (Gales Ferry, Connecticut). Both biological matrix and phosphate buffer pH were adjusted to 7.4 on the day of the experiment. The determination of unbound compound was performed using a 96-well format equilibrium dialysis device with a molecular weight cut-off membrane of 12 to 14 kDa. The equilibrium dialysis device itself was made of Teflon to minimize non-specific binding of the test substance. Compounds were tested in cassettes of 2-5 with an initial total concentration of 1000 nM, one of the cassette compounds being the positive control diazepam. Equal volumes of matrix samples containing substances and blank dialysis buffer (Soerensen buffer at pH 7.4) were loaded into the opposite compartments of each well. The dialysis block was sealed and kept for 5 hours at a temperature of 37°C and 5% CO_2 environment in an incubator. After this time, equilibrium has been reached for the majority of small molecule compounds with a molecular weight of <600 . The seal was then removed and matrix and buffer from each dialysis was prepared for analysis by LC-MS/MS. All protein binding determinations were performed in triplicates. The integrity of membranes was tested in the HTDialysis device by determining the unbound fraction values for the positive control diazepam in each well. At equilibrium, the unbound drug concentration in the biological matrix compartment of the equilibrium dialysis apparatus was the same as the concentration of the compound in the buffer compartment. Thus, the percent unbound fraction (f_u) was calculated by determining the compound concentrations in the buffer and matrix compartments after dialysis as follows: $\%f_u = 100 * \text{buffer concentration after dialysis} / \text{matrix concentration after dialysis}$. The device recovery was checked by measuring the compound concentrations in the matrix before dialysis and calculating the percent recovery (mass balance). The recovery must be within 80% to 120% for data acceptance.

LogD-assay

For the determination of the octanol/water distribution coefficient (logD), the Carrier-Mediated Distribution System (CAMDIS)-assay was used as described elsewhere.⁵⁸

P-glycoprotein active efflux assay

P-glycoprotein (permeability-glycoprotein, abbreviated as 'P-gp' also known as multidrug resistance protein 1 (MDR1)) is the most studied and best characterized drug transporter. The P-gp assay evaluates the ability of test compounds to serve as a P-gp substrate. The assay was performed as described elsewhere.⁵⁹

D. *In vivo* pharmacokinetics of LEI-401.

Subjects

Male C57BL/6J mice (Jackson Laboratory, Bar Harbor, Maine, USA) served as subjects for the *in vivo* pharmacokinetic and brain lipid analysis of **LEI-401**. Animal protocols were approved by the Institutional Animal Care and Use Committee at National Institute on Alcohol Abuse and Alcoholism, National Institute of

Health and Bundesamt für Lebensmittelsicherheit und Veterinärwesen (BLV) der Schweizerischen Eidgenossenschaft.

Pharmacokinetic analysis of LEI-401 (mouse plasma)

Test compounds were formulated according to respective protocols either by dissolution (i.v.) or in a glass potter until homogeneity was achieved (p.o. and i.p.). Formulations were injected i.v. using a 30G needle in the lateral tail vein mice yielding a 1 mg/kg-dose. For p.o. applications, animals were gavaged (yielding a 10 mg/kg dose) and for i.p. applications the compounds were injected into the abdomen (yielding a 30 mg/kg dose). At the following time points blood was drawn into EDTA: 0.083, 0.25, 0.5, 1, 2, 4, 7, 24 h (for p.o. and i.p. the first time point was omitted). Three animals each were used for the i.v. and p.o. arm and 6 animals were used in the i.p. arm. Animals were distributed randomly over the time course and at each time point, a volume of 100 μ L of blood was taken. Quantitative plasma measurement of the compound was performed by LC-MS/MS analysis. Pharmacokinetic analysis was performed using Phoenix WinNonlin 6.4 software using a non-compartmental approach consistent with the route of administration. For assessment of the exposure C_{max} , T_{max} , AUC and bioavailability were determined from the plasma concentration profiles. Parameters (CL , V_{ss} , $t_{1/2}$) were estimated using nominal sampling times relative to the start of each administration.

Pharmacokinetic analysis of LEI-401 (mouse brain)

Mice were injected with **LEI-401** (30 mg/kg, i.p., single dose) dissolved in sterile DMSO (D2650 Sigma, MO, USA) and mixed with Tween-80 and distilled H₂O at a ratio of 1:1:8. Mice were sacrificed after 1, 2, 4 and 8 h. Brain samples were rapidly collected, washed in ice cold saline, blotted dry, frozen in liquid N₂ and stored at -80 °C until further analysis. Brain levels of **LEI-401** were quantified by LC-MS/MS using an Agilent 6410 triple quadrupole mass spectrometer (Agilent Technologies, USA) coupled with an Agilent 1200 LC system (Agilent Technologies, Germany). Chromatographic and mass spectrometer conditions were set as described previously.⁶⁰ Chromatographic separation was obtained using 2.5 μ l samples injected onto a Zorbax SB-C18 rapid resolution HT column (2.1 mm \times 50 mm, 1.8 Micron, Agilent). The mass spectrometer was set for electrospray ionization in positive ion mode. The source parameters were as follows: capillary voltage, 4000 V; gas temperature, 350 °C; drying gas, 10 liters/min; nitrogen was used as the nebulizing gas with a pressure of 40 psig. Collision-induced dissociation (CID) energy was performed by using nitrogen. Levels of **LEI-401** were analyzed by multiple reactions monitoring (MRM). Mass spectrometric conditions were optimized for **LEI-401** with injection of synthetic standard by using MassHunter Workstation Optimizer software (Agilent Technologies, USA). The molecular ion and fragments for **LEI-401** measured were as follows: m/z 422.26 \rightarrow 70.1 and 422.26 \rightarrow 137 (CID-energy: 56 V and 40 V, respectively). The amounts of **LEI-401** in the samples were determined against standard curves. Values are expressed as ng/g in wet brain tissue weight.

Lipid measurements in mouse brain

Levels of NAEs, 2-AG and arachidonic acid were measured by stable isotope dilution liquid chromatography/tandem mass spectrometry (LC-MS/MS) as described previously.⁶¹

Statistical analysis

Data were tested for significance with GraphPad v6 using one-way ANOVA with Dunnett's correction for multiple comparisons. *P*-values < 0.05 were considered significant.

E. *In vivo* behavioral assays.

Subjects

Male C57BL/6J mice (Jackson Laboratory, Bar Harbor, Maine, USA) and male and female CB₁ KO and WT mice (VCU transgenic core, Richmond, Virginia, USA) served as subjects for *in vivo* nociceptive testing. The animal protocols were approved by the Institutional Animal Care and Use Committee at Virginia Commonwealth University in accordance with the National Institutes of Health Guide for the Care and Use of Laboratory Animals.⁶² All studies involving animals are reported in accordance with the ARRIVE guidelines for reporting experiments involving animals.⁶³

Drugs

LEI-401 was synthesized as described in Chapter 3 and the Drug Supply Program at the National Institute on Drug Abuse (Bethesda, MD) provided CP-55,940. LEI-401 and CP-55,940 were dissolved in respective vehicles consisting of a ratio 1:1:8 ratio of DMSO, Tween 80 and distilled H₂O, and a 1:1:18 ratio of ethanol, emulphor-620 (Rhodia, Cranbury, NJ) and saline (0.9% NaCl). All injections were administered via the i.p. route of administration in a volume of 0.01 ml/g of body mass.

Hot plate nociceptive testing

Mice were placed on a 52 °C surface of the hot plate (IITC Life Science Inc., Woodland Hills, CA) and the latency to display jumping behavior or licking or shaking of a hind paw was scored during a 30 s observation period. The experimenter used a stopwatch to score latencies to the nearest 0.01 s and was blinded to injection condition. Each mouse was given a pre-injection hot plate test and a second hot plate test 120 min after LEI-401 (30 mg/kg) administration or 30 min after CP-55,940 (10 mg/kg) administration.

Statistical analysis: nociceptive behavior was expressed as post-injection hot plate latency minus pre-injection latency and are reported as the mean ± SEM difference scores in seconds. ANOVA was used to test LEI-401 and CP-55,940 vs. vehicle in C57BL/6J mice and Dunnett's test was used for post hoc analysis. Two-way ANOVA was used to evaluate LEI-401 vs. vehicle in CB₁ KO vs. WT mice. Differences were considered significant at $P < 0.05$.

Evaluation of LEI-401 in body temperature, locomotor behavior, catalepsy and tail immersion assays.

LEI-401 was tested for hypothermia, locomotor depression, catalepsy and antinociception in the tail flick assay as described elsewhere.⁶⁴

Evaluation of LEI-401 in LPS mouse model of inflammatory pain

The LPS-induced allodynia assay was performed as previously described.⁶⁴ Mice were given an injection of 2.5 µg of LPS from *Escherichia coli* (026:B6, Sigma), in 20 µL of physiological sterile saline (Hospira Inc., Lake Forest, IL, USA) into the plantar surface of the right hind paw. As previously reported, this dose of LPS elicits mechanical allodynia without producing measurable increases in paw thickness.⁶⁵ Mice were returned to their home cages after the LPS injection. 22 hours following LPS administration, each mouse was given an intraperitoneal (i.p.) injection of LEI-401 (30 mg/kg) or vehicle and tested for mechanical allodynia at 0.5, 1, 2, 4, 6 and 8 h post injection.

Behavioral assessment of mechanical allodynia

Baseline responses to light mechanical touch were assessed using von Frey filaments following habituation to the testing environment. In brief, mice were acclimated to the testing conditions in which they were given a daily 15 min habituation session for 2 days. They were placed under an inverted wire mesh basket, which allowed unrestricted air flow, that was on top of a wire mesh screen, with spaces 0.5 mm apart. During acclimation and testing, each mouse was unrestrained and singly housed. The von Frey test utilizes a series of calibrated monofilaments, (2.83–4.31 log stimulus intensity; North Coast Medical, Morgan Hills, CA,

USA) applied randomly to the left and right plantar surfaces of the hind paw for 3 touches, 1/2 seconds apart. Lifting, licking, or shaking the paw was considered a response.

References

1. Piomelli, D. The molecular logic of endocannabinoid signalling. *Nature Reviews Neuroscience* **4**, 873 (2003).
2. Hannun, Y.A. & Obeid, L.M. Principles of bioactive lipid signalling: lessons from sphingolipids. *Nature Reviews Molecular Cell Biology* **9**, 139 (2008).
3. Kano, M., Ohno-Shosaku, T., Hashimotodani, Y., Uchigashima, M. & Watanabe, M. Endocannabinoid-mediated control of synaptic transmission. *Physiological Reviews* **89**, 309-380 (2009).
4. Rouzer, C.A. & Marnett, L.J. Endocannabinoid oxygenation by cyclooxygenases, lipoxygenases, and cytochromes P450: cross-talk between the eicosanoid and endocannabinoid signaling pathways. *Chemical Reviews* **111**, 5899-5921 (2011).
5. Alger, B.E. & Kim, J. Supply and demand for endocannabinoids. *Trends in Neurosciences* **34**, 304-315 (2011).
6. Hampson, A.J., Bornheim, L.M., Scanziani, M., Yost, C.S., Gray, A.T., Hansen, B.M., Leonoudakis, D.J. & Bickler, P.E. Dual effects of anandamide on NMDA receptor-mediated responses and neurotransmission. *Journal of Neurochemistry* **70**, 671-676 (1998).
7. Chemin, J., Monteil, A., Perez-Reyes, E., Nargeot, J. & Lory, P. Direct inhibition of T-type calcium channels by the endogenous cannabinoid anandamide. *The EMBO Journal* **20**, 7033-7040 (2001).
8. Maingret, F., Patel, A.J., Lazdunski, M. & Honoré, E. The endocannabinoid anandamide is a direct and selective blocker of the background K⁺ channel TASK-1. *The EMBO Journal* **20**, 47-54 (2001).
9. van der Stelt, M., Trevisani, M., Vellani, V., De Petrocellis, L., Schiano Moriello, A., Campi, B., McNaughton, P., Geppetti, P. & Di Marzo, V. Anandamide acts as an intracellular messenger amplifying Ca²⁺ influx via TRPV1 channels. *The EMBO Journal* **24**, 3026-3037 (2005).
10. Piomelli, D. & Sasso, O. Peripheral gating of pain signals by endogenous lipid mediators. *Nature Neuroscience* **17**, 164 (2014).
11. Lutz, B., Marsicano, G., Maldonado, R. & Hillard, C.J. The endocannabinoid system in guarding against fear, anxiety and stress. *Nature Reviews Neuroscience* **16**, 705 (2015).
12. Witkamp, R.F. The role of fatty acids and their endocannabinoid-like derivatives in the molecular regulation of appetite. *Molecular Aspects of Medicine* (2018).
13. Turcotte, C., Chouinard, F., Lefebvre Julie, S. & Flamand, N. Regulation of inflammation by cannabinoids, the endocannabinoids 2-arachidonoyl-glycerol and arachidonoyl-ethanolamide, and their metabolites. *Journal of Leukocyte Biology* **97**, 1049-1070 (2015).
14. Maccarrone, M. Metabolism of the endocannabinoid anandamide: open questions after 25 years. *Frontiers in Molecular Neuroscience* **10** (2017).
15. Okamoto, Y., Morishita, J., Tsuboi, K., Tonai, T. & Ueda, N. Molecular characterization of a phospholipase D generating anandamide and its congeners. *Journal of Biological Chemistry* **279**, 5298-5305 (2004).
16. Hussain, Z., Uyama, T., Tsuboi, K. & Ueda, N. Mammalian enzymes responsible for the biosynthesis of N-acylethanolamines. *Biochimica et Biophysica Acta (BBA) - Molecular and Cell Biology of Lipids* **1862**, 1546-1561 (2017).
17. Magotti, P., Bauer, I., Igarashi, M., Babagoli, M., Marotta, R., Piomelli, D. & Garau, G. Structure of human N-acylphosphatidylethanolamine-hydrolyzing phospholipase D: regulation of fatty acid ethanolamide biosynthesis by bile acids. *Structure* **23**, 598-604 (2015).

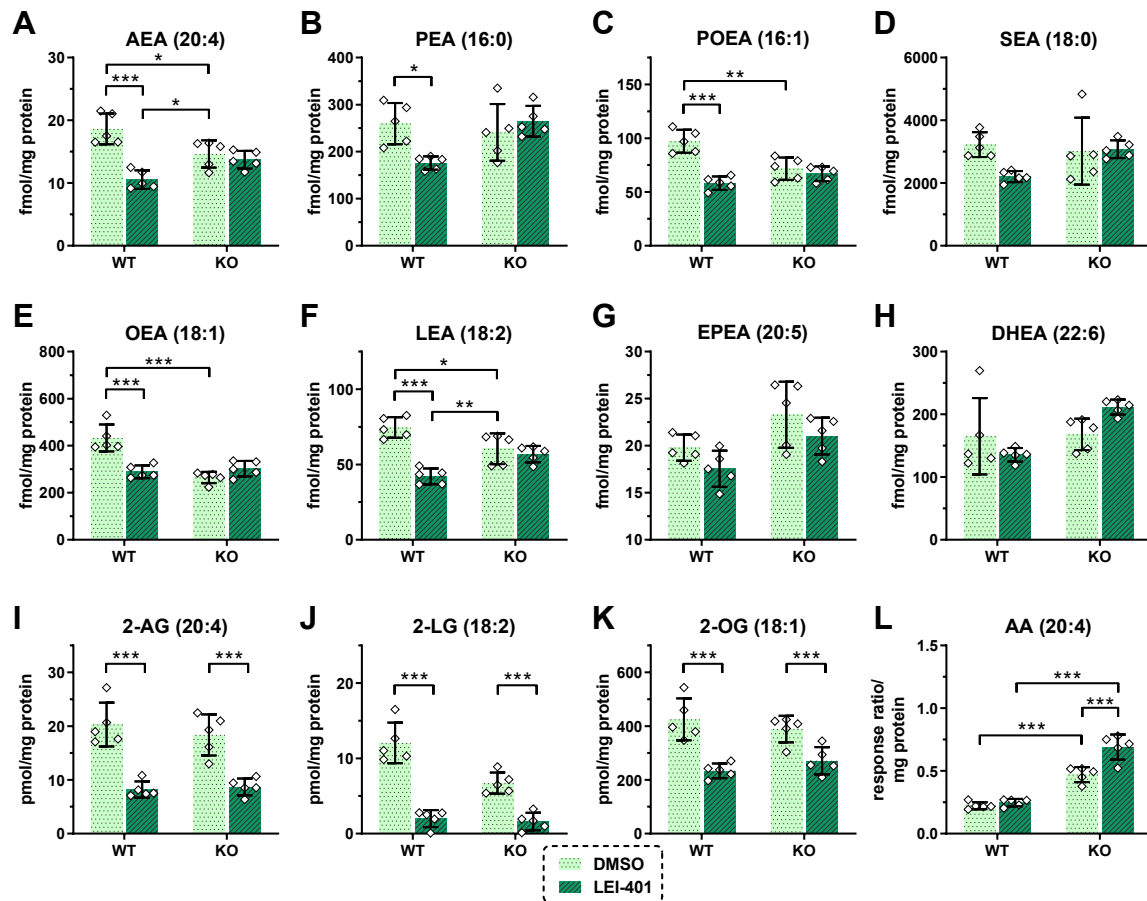
18. Leung, D., Saghatelian, A., Simon, G.M. & Cravatt, B.F. Inactivation of *N*-acyl phosphatidylethanolamine phospholipase D reveals multiple mechanisms for the biosynthesis of endocannabinoids. *Biochemistry* **45**, 4720-4726 (2006).
19. Tsuboi, K., Okamoto, Y., Ikematsu, N., Inoue, M., Shimizu, Y., Uyama, T., Wang, J., Deutsch, D.G., Burns, M.P., Ulloa, N.M., Tokumura, A. & Ueda, N. Enzymatic formation of *N*-acylethanolamines from *N*-acylethanolamine plasmalogen through *N*-acylphosphatidylethanolamine-hydrolyzing phospholipase D-dependent and -independent pathways. *Biochimica et Biophysica Acta (BBA) - Molecular and Cell Biology of Lipids* **1811**, 565-577 (2011).
20. Leishman, E., Mackie, K., Luquet, S. & Bradshaw, H.B. Lipidomics profile of a NAPE-PLD KO mouse provides evidence of a broader role of this enzyme in lipid metabolism in the brain. *Biochimica et Biophysica Acta (BBA) - Molecular and Cell Biology of Lipids* **1861**, 491-500 (2016).
21. Blankman, J.L. & Cravatt, B.F. Chemical probes of endocannabinoid metabolism. *Pharmacological Reviews* **65**, 849-871 (2013).
22. Simon, G.M. & Cravatt, B.F. Characterization of mice lacking candidate *N*-acyl ethanolamine biosynthetic enzymes provides evidence for multiple pathways that contribute to endocannabinoid production in vivo. *Molecular BioSystems* **6**, 1411-1418 (2010).
23. Simon, G.M. & Cravatt, B.F. Endocannabinoid biosynthesis proceeding through glycerophospho-*N*-acyl ethanolamine and a role for α/β -hydrolase 4 in this pathway. *Journal of Biological Chemistry* **281**, 26465-26472 (2006).
24. Petersen, G., Pedersen, A.H., Pickering, D.S., Begtrup, M. & Hansen, H.S. Effect of synthetic and natural phospholipids on *N*-acylphosphatidylethanolamine-hydrolyzing phospholipase D activity. *Chemistry and Physics of Lipids* **162**, 53-61 (2009).
25. Scott, S.A., Spencer, C.T., O'Reilly, M.C., Brown, K.A., Lavieri, R.R., Cho, C.-H., Jung, D.-I., Larock, R.C., Brown, H.A. & Lindsley, C.W. Discovery of desketoraloxifene analogues as inhibitors of mammalian, *Pseudomonas aeruginosa*, and NAPE phospholipase D enzymes. *ACS Chemical Biology* **10**, 421-432 (2015).
26. Castellani, B., Diamanti, E., Pizzirani, D., Tardia, P., Maccesi, M., Realini, N., Magotti, P., Garau, G., Bakkum, T., Rivara, S., Mor, M. & Piomelli, D. Synthesis and characterization of the first inhibitor of *N*-acylphosphatidylethanolamine phospholipase D (NAPE-PLD). *Chemical Communications* **53**, 12814-12817 (2017).
27. Lin, L., Metherel, A.H., Kitson, A.P., Alashmali, S.M., Hopperton, K.E., Trépanier, M.-O., Jones, P.J. & Bazinet, R.P. Dietary fatty acids augment tissue levels of *n*-acylethanolamines in *N*-acylphosphatidylethanolamine phospholipase D (NAPE-PLD) knockout mice. *The Journal of Nutritional Biochemistry* **62**, 134-142 (2018).
28. Cravatt, B.F., Demarest, K., Patricelli, M.P., Bracey, M.H., Giang, D.K., Martin, B.R. & Lichtman, A.H. Supersensitivity to anandamide and enhanced endogenous cannabinoid signaling in mice lacking fatty acid amide hydrolase. *Proceedings of the National Academy of Sciences* **98**, 9371-9376 (2001).
29. Egertová, M., Simon, G.M., Cravatt, B.F. & Elphick, M.R. Localization of *N*-acyl phosphatidylethanolamine phospholipase D (NAPE-PLD) expression in mouse brain: a new perspective on *N*-acylethanolamines as neural signaling molecules. *Journal of Comparative Neurology* **506**, 604-615 (2008).
30. Uyama, T., Tsuboi, K. & Ueda, N. An involvement of phospholipase A/acyltransferase family proteins in peroxisome regulation and plasmalogen metabolism. *FEBS Letters* **591**, 2745-2760 (2017).
31. Ogura, Y., Parsons, W.H., Kamat, S.S. & Cravatt, B.F. A calcium-dependent acyltransferase that produces *N*-acyl phosphatidylethanolamines. *Nature Chemical Biology* **12**, 669 (2016).
32. Margheritis, E., Castellani, B., Magotti, P., Peruzzi, S., Romeo, E., Natali, F., Mostarda, S., Gioiello, A., Piomelli, D. & Garau, G. Bile acid recognition by NAPE-PLD. *ACS Chemical Biology* **11**, 2908-2914 (2016).
33. Liu, Q., Tonai, T. & Ueda, N. Activation of *N*-acylethanolamine-releasing phospholipase D by polyamines. *Chemistry and Physics of Lipids* **115**, 77-84 (2002).

34. Kathuria, S., Gaetani, S., Fegley, D., Valiño, F., Duranti, A., Tontini, A., Mor, M., Tarzia, G., Rana, G.L., Calignano, A., Giustino, A., Tattoli, M., Palmery, M., Cuomo, V. & Piomelli, D. Modulation of anxiety through blockade of anandamide hydrolysis. *Nature Medicine* **9**, 76 (2002).
35. Long, J.Z., Nomura, D.K., Vann, R.E., Walentiny, D.M., Booker, L., Jin, X., Burston, J.J., Sim-Selley, L.J., Lichtman, A.H., Wiley, J.L. & Cravatt, B.F. Dual blockade of FAAH and MAGL identifies behavioral processes regulated by endocannabinoid crosstalk in vivo. *Proceedings of the National Academy of Sciences* **106**, 20270 (2009).
36. Lamont, B., G, K.S., A, A.R., L, B.J., Z, L.J., Cyrine, E., L, B.D., F, C.B. & H, L.A. The fatty acid amide hydrolase (FAAH) inhibitor PF-3845 acts in the nervous system to reverse LPS-induced tactile allodynia in mice. *British Journal of Pharmacology* **165**, 2485-2496 (2012).
37. Morishita, J., Okamoto, Y., Tsuboi, K., Ueno, M., Sakamoto, H., Maekawa, N. & Ueda, N. Regional distribution and age-dependent expression of *N*-acylphosphatidylethanolamine-hydrolyzing phospholipase D in rat brain. *Journal of Neurochemistry* **94**, 753-762 (2005).
38. Sousa-Valente, J., Varga, A., Torres-Perez, J.V., Jenes, A., Wahba, J., Mackie, K., Cravatt, B., Ueda, N., Tsuboi, K., Santha, P., Jancso, G., Tailor, H., Avelino, A. & Nagy, I. Inflammation of peripheral tissues and injury to peripheral nerves induce differing effects in the expression of the calcium-sensitive *N*-arachidonylethanolamine-synthesizing enzyme and related molecules in rat primary sensory neurons. *Journal of Comparative Neurology* **525**, 1778-1796 (2017).
39. Gauldie, S.D., McQueen, D.S., Pertwee, R. & Chessell, I.P. Anandamide activates peripheral nociceptors in normal and arthritic rat knee joints. *British Journal of Pharmacology* **132**, 617-621 (2001).
40. Wellner, N., Diep, T.A., Janfelt, C. & Hansen, H.S. *N*-Acylation of phosphatidylethanolamine and its biological functions in mammals. *Biochimica et Biophysica Acta (BBA) - Molecular and Cell Biology of Lipids* **1831**, 652-662 (2013).
41. Geurts, L., Everard, A., Van Hul, M., Essaghir, A., Duparc, T., Matamoros, S., Plovier, H., Castel, J., Denis, R.G.P., Bergiers, M., Druart, C., Alhouayek, M., Delzenne, N.M., Muccioli, G.G., Demoulin, J.-B., Luquet, S. & Cani, P.D. Adipose tissue NAPE-PLD controls fat mass development by altering the browning process and gut microbiota. *Nature Communications* **6**, 6495 (2015).
42. Jourdan, T., Godlewski, G., Cinar, R., Bertola, A., Szanda, G., Liu, J., Tam, J., Han, T., Mukhopadhyay, B., Skarulis, M.C., Ju, C., Aouadi, M., Czech, M.P. & Kunos, G. Activation of the Nlrp3 inflammasome in infiltrating macrophages by endocannabinoids mediates beta cell loss in type 2 diabetes. *Nature Medicine* **19**, 1132 (2013).
43. Hansen, H.H., Ikonomidou, C., Bittigau, P., Hansen, S.H. & Hansen, H.S. Accumulation of the anandamide precursor and other *N*-acylethanolamine phospholipids in infant rat models of in vivo necrotic and apoptotic neuronal death. *Journal of Neurochemistry* **76**, 39-46 (2001).
44. Janfelt, C., Wellner, N., Leger, P.-L., Kokesch-Himmelreich, J., Hansen, S.H., Charriaut-Marlangue, C. & Hansen, H.S. Visualization by mass spectrometry of 2-dimensional changes in rat brain lipids, including *N*-acylphosphatidylethanolamines, during neonatal brain ischemia. *The FASEB Journal* **26**, 2667-2673 (2012).
45. Dincheva, I., Drysdale, A.T., Hartley, C.A., Johnson, D.C., Jing, D., King, E.C., Ra, S., Gray, J.M., Yang, R., DeGruccio, A.M., Huang, C., Cravatt, B.F., Glatt, C.E., Hill, M.N., Casey, B.J. & Lee, F.S. FAAH genetic variation enhances fronto-amygdala function in mouse and human. *Nature Communications* **6**, 6395 (2015).
46. Bowles, N.P., Karatsoreos, I.N., Li, X., Vemuri, V.K., Wood, J.-A., Li, Z., Tamashiro, K.L.K., Schwartz, G.J., Makriyannis, A.M., Kunos, G., Hillard, C.J., McEwen, B.S. & Hill, M.N. A peripheral endocannabinoid mechanism contributes to glucocorticoid-mediated metabolic syndrome. *Proceedings of the National Academy of Sciences* **112**, 285-290 (2015).
47. Caraceni, P., Viola, A., Piscitelli, F., Giannone, F., Berzigotti, A., Cescon, M., Domenicali, M., Petrosino, S., Giampalma, E., Riili, A., Grazi, G., Golfieri, R., Zoli, M., Bernardi, M. & Di Marzo, V. Circulating and

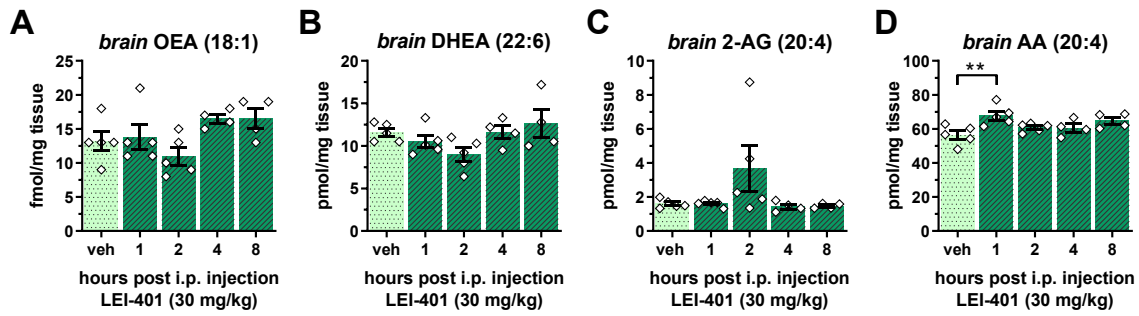
- hepatic endocannabinoids and endocannabinoid-related molecules in patients with cirrhosis. *Liver International* **30**, 816-825 (2010).
48. Mukhopadhyay, B., Schuebel, K., Mukhopadhyay, P., Cinar, R., Godlewski, G., Xiong, K., Mackie, K., Lizak, M., Yuan, Q., Goldman, D. & Kunos, G. Cannabinoid receptor 1 promotes hepatocellular carcinoma initiation and progression through multiple mechanisms. *Hepatology* **61**, 1615-1626 (2015).
 49. Labun, K., Montague, T.G., Gagnon, J.A., Thyme, S.B. & Valen, E. CHOPCHOP v2: a web tool for the next generation of CRISPR genome engineering. *Nucleic Acids Research* **44**, W272-W276 (2016).
 50. Cong, L., Ran, F.A., Cox, D., Lin, S., Barretto, R., Habib, N., Hsu, P.D., Wu, X., Jiang, W., Marraffini, L.A. & Zhang, F. Multiplex genome engineering using CRISPR/Cas systems. *Science* **339**, 819-823 (2013).
 51. Ran, F.A., Hsu, P.D., Wright, J., Agarwala, V., Scott, D.A. & Zhang, F. Genome engineering using the CRISPR-Cas9 system. *Nature Protocols* **8**, 2281 (2013).
 52. van Esbroeck, A.C.M., Janssen, A.P.A., Cognetta, A.B., Ogasawara, D., Shpak, G., van der Kroeg, M., Kantae, V., Baggelaar, M.P., de Vrij, F.M.S., Deng, H., Allarà, M., Fezza, F., Lin, Z., van der Wel, T., Soethoudt, M., Mock, E.D., den Dulk, H., Baak, I.L., Florea, B.I., Hendriks, G., De Petrocellis, L., Overkleeft, H.S., Hankemeier, T., De Zeeuw, C.I., Di Marzo, V., Maccarrone, M., Cravatt, B.F., Kushner, S.A. & van der Stelt, M. Activity-based protein profiling reveals off-target proteins of the FAAH inhibitor BIA 10-2474. *Science* **356**, 1084-1087 (2017).
 53. Kansy, M., Senner, F. & Gubernator, K. Physicochemical high throughput screening: parallel artificial membrane permeation assay in the description of passive absorption processes. *Journal of Medicinal Chemistry* **41**, 1007-1010 (1998).
 54. Di, L., Keefer, C., Scott, D.O., Strelevitz, T.J., Chang, G., Bi, Y.-A., Lai, Y., Duckworth, J., Fenner, K., Troutman, M.D. & Obach, R.S. Mechanistic insights from comparing intrinsic clearance values between human liver microsomes and hepatocytes to guide drug design. *European Journal of Medicinal Chemistry* **57**, 441-448 (2012).
 55. LeCluyse, E.L., Witek, R.P., Andersen, M.E. & Powers, M.J. Organotypic liver culture models: meeting current challenges in toxicity testing. *Critical Reviews in Toxicology* **42**, 501-548 (2012).
 56. Banker, M.J., Clark, T.H. & Williams, J.A. Development and validation of a 96-well equilibrium dialysis apparatus for measuring plasma protein binding. *Journal of Pharmaceutical Sciences* **92**, 967-974 (2003).
 57. Zamek-Gliszczynski, M.J., Ruterbories, K.J., Ajamie, R.T., Wickremsinhe, E.R., Pothuri, L., Rao, M.V.S., Basavanakatti, V.N., Pinjari, J., Ramanathan, V.K. & Chaudhary, A.K. Validation of 96-well equilibrium dialysis with non-radiolabeled drug for definitive measurement of protein binding and application to clinical development of highly-bound drugs. *Journal of Pharmaceutical Sciences* **100**, 2498-2507 (2011).
 58. Wagner, B., Fischer, H., Kansy, M., Seelig, A. & Assmus, F. Carrier Mediated Distribution System (CAMDIS): A new approach for the measurement of octanol/water distribution coefficients. *European Journal of Pharmaceutical Sciences* **68**, 68-77 (2015).
 59. Poirier, A., Cascais, A.-C., Bader, U., Portmann, R., Brun, M.-E., Walter, I., Hillebrecht, A., Ullah, M. & Funk, C. Calibration of in vitro multidrug resistance protein 1 substrate and inhibition assays as a basis to support the prediction of clinically relevant interactions in vivo. *Drug Metabolism and Disposition* **42**, 1411-1422 (2014).
 60. Cinar, R., Iyer, M.R., Liu, Z., Cao, Z., Jourdan, T., Erdelyi, K., Godlewski, G., Szanda, G., Liu, J., Park, J.K., Mukhopadhyay, B., Rosenberg, A.Z., Liow, J.-S., Lorenz, R.G., Pacher, P., Innis, R.B. & Kunos, G. Hybrid inhibitor of peripheral cannabinoid-1 receptors and inducible nitric oxide synthase mitigates liver fibrosis. *JCI Insight* **1** (2016).
 61. Mukhopadhyay, B., Cinar, R., Yin, S., Liu, J., Tam, J., Godlewski, G., Harvey-White, J., Mordi, I., Cravatt, B.F., Lotersztajn, S., Gao, B., Yuan, Q., Schuebel, K., Goldman, D. & Kunos, G. Hyperactivation of anandamide synthesis and regulation of cell-cycle progression via cannabinoid type 1 (CB₁) receptors in the regenerating liver. *Proceedings of the National Academy of Sciences* **108**, 6323-6328 (2011).

62. Council, N.R. *Guide for the care and use of laboratory animals: eighth edition*. (The National Academies Press, Washington, DC; 2011).
63. Kilkeny, C., Browne, W., Cuthill, I.C., Emerson, M. & Altman, D.G. Animal research: Reporting in vivo experiments: The ARRIVE guidelines. *British Journal of Pharmacology* **160**, 1577-1579 (2010).
64. Wilkerson, J.L., Donvito, G., Grim, T.W., Abdullah, R.A., Ogasawara, D., Cravatt, B.F. & Lichtman, A.H. Investigation of diacylglycerol lipase alpha inhibition in the mouse lipopolysaccharide inflammatory pain model. *Journal of Pharmacology and Experimental Therapeutics* **363**, 394-401 (2017).
65. Booker, L., Kinsey, S.G., Abdullah, R.A., Blankman, J.L., Long, J.Z., Ezzili, C., Boger, D.L., Cravatt, B.F. & Lichtman, A.H. The fatty acid amide hydrolase (FAAH) inhibitor PF-3845 acts in the nervous system to reverse LPS-induced tactile allodynia in mice. *British Journal of Pharmacology* **165**, 2485-2496 (2012).

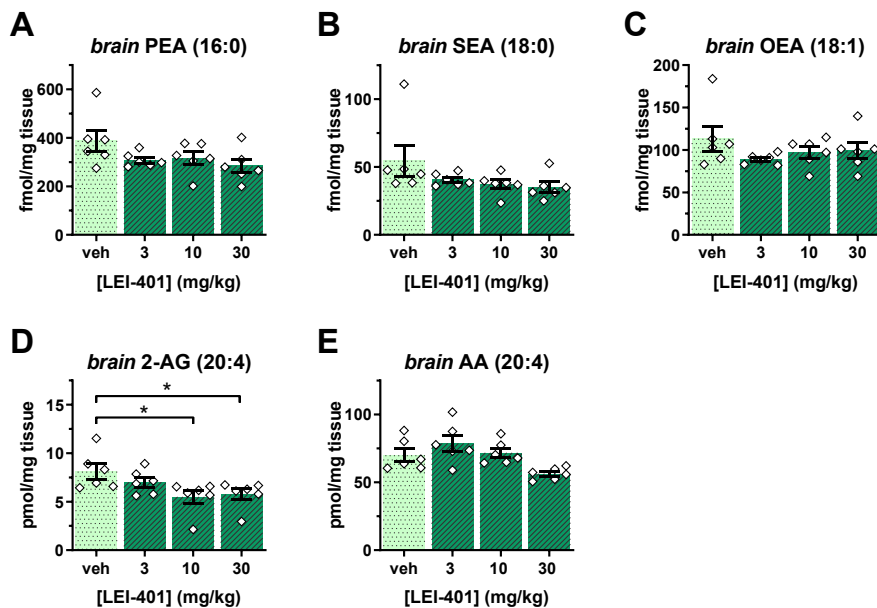
Supplementary Information



Supplementary Figure 1. Absolute lipid levels of NAEs, monoacylglycerols (MAGs) and arachidonic acid (AA) in Neuro-2a wild-type (WT) and NAPE-PLD knockout (KO) cells treated with **LEI-401** (10 μ M) for 2 h. **A)** Anandamide (AEA, 20:4- ω -6), **B)** *N*-palmitoylethanolamine (PEA, 16:0), **C)** *N*-palmitoleoylethanolamine (POEA, 16:1- ω -9), **D)** *N*-stearoylethanolamine (SEA, 18:0), **E)** *N*-oleoylethanolamine (OEA, 18:1- ω -9), **F)** *N*-linoleoylethanolamine (LEA, 18:2- ω -6), **G)** *N*-eicosapentaenoylethanolamine (EPEA, 20:5- ω -3), **H)** *N*-docosahexaenoylethanolamine (DHEA, 22:6- ω -3), **I)** 2-arachidonoylglycerol (2-AG, 20:4- ω -6), **J)** 2-linoleoylglycerol (2-LG, 18:2- ω -6), **K)** 2-oleoylglycerol (2-OG, 18:1- ω -9) and **L)** arachidonic acid (AA, 20:4- ω -6). Data represent mean values \pm SD for 5 biological replicates. *, $P < 0.05$, **, $P < 0.01$, ***, $P < 0.001$ by one-way ANOVA.



Supplementary Figure 2. *In vivo* treatment of **LEI-401** (30 mg/kg, i.p., single dose) showed time-dependent effects on brain NAEs and other bioactive lipids in C57BL/6J mice. **A)** OEA, **B)** DHEA, **C)** 2-AG, **D)** AA. Data represent mean values \pm SEM for 5-6 biological replicates. **, $P < 0.01$ by one-way ANOVA.



Supplementary Figure 3. *In vivo* treatment of **LEI-401** revealed dose-dependent effects on brain NAEs and other bioactive lipids in C57BL/6J mice 2 h after i.p. administration. **A)** PEA, **B)** SEA, **C)** OEA, **D)** 2-AG and **E)** AA. Data represent mean values \pm SEM for 5-6 biological replicates. *, $P < 0.05$, **, $P < 0.01$ by one-way ANOVA.

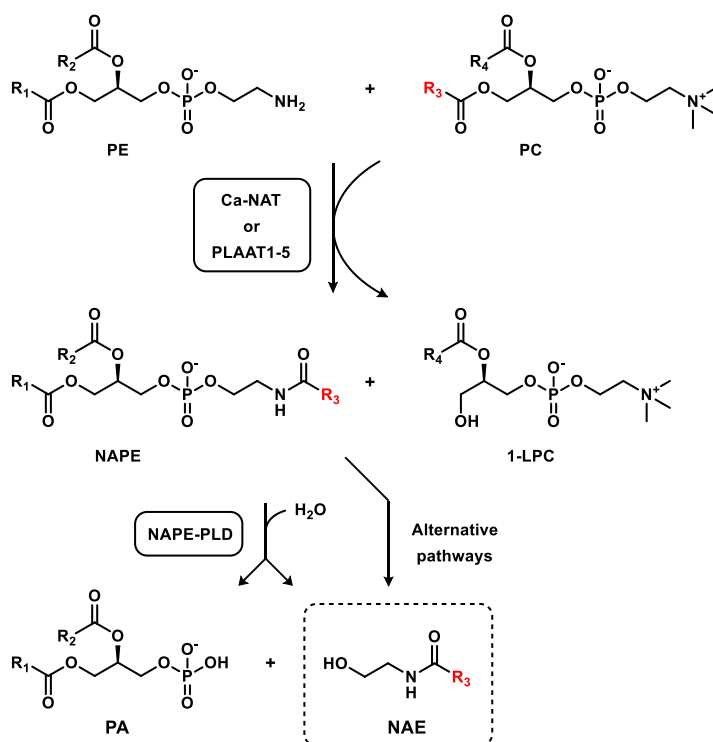
Chapter 6

Discovery and optimization of α -ketoamide inhibitors for the *N*-acyltransferase PLAAT2

6.1 Introduction

The subfamily of phospholipase A and acyltransferases (PLAAT) consists of five members that are part of the lecithin retinol acyltransferase (LRAT) protein family.^{1,2} The LRAT protein family itself is part of the NlpC/P60 superfamily of thiol hydrolases. They share a conserved catalytic motif of six amino acids (NCEHFV) containing a cysteine residue that acts as the active site nucleophile.³ Though initially described as tumor suppressors named HRASLS1-5 (Harvey Rat Sarcoma viral oncogene Like Suppressor 1-5), it was shown that PLAAT1-5 are in fact enzymes involved in phospholipid metabolism.⁴⁻⁹ The PLAAT family members exhibit differing levels of *N*- and *O*-acyltransferase or phospholipase A_{1/2} activity *in vitro*, which may lead to the production of *N*-acylphosphatidylethanolamines (NAPEs) and lyso-phosphatidylcholine (LPC), phosphatidylcholine (PC) and LPC or fatty acids.¹⁰ NAPEs are an underexplored class of triacylated phospholipids that function as precursor for the *N*-acylethanolamines (NAEs), an important family of signaling molecules that includes the endocannabinoid anandamide.¹¹ The canonical enzyme responsible for

NAPE biosynthesis in the brain is a Ca^{2+} -dependent *N*-acyltransferase (Ca-NAT), recently identified as PLA2G4E (Scheme 1).¹² The NAPEs are in turn converted to the NAEs in one step by NAPE- phospholipase D, although other multistep pathways have also been reported.¹³ In contrast, the PLAAT family members operate via a calcium-independent mechanism, providing a new pathway through which NAEs are biosynthesized.¹⁰



Scheme 1. Biosynthesis of *N*-acylethanolamines (NAEs). The *sn*-1-acyl of phosphatidylcholine (PC) is transferred to the amine of phosphatidylethanolamine (PE) by the acyltransferase activity of PLA2G4E or PLAAT1-5 forming *N*-acyl-PE (NAPE) and 1-lyso-PC (1-LPC). NAPE-PLD hydrolyzes the phosphodiester bond of NAPE to form NAE and phosphatidic acid (PA). R₁, R₂ and R₃ denote saturated, mono- or polyunsaturated fatty acids.

Ueda and co-workers reported that PLAAT2 in particular displays high *N*-acyltransferase activity.¹⁰ HEK293 cells stably overexpressing PLAAT2 exhibited a remarkable increase in NAPE and NAE content. The enzyme showed a preference for the transfer of the *sn*-1 acyl group over the *sn*-2 acyl from phosphatidylcholine (PC) to the amine of phosphatidylethanolamine (PE) (Scheme 1). Utilizing a Cys-His-His catalytic triad, the enzymatic mechanism involves the formation of a thioester followed by nucleophilic attack of the amine acceptor, which generates the NAPE product and releases the catalytic cysteine. Expression of PLAAT2 was found to be high in the liver, kidney, small

intestine, colon, testis and trachea.^{7,14} NAEs have well-established signaling roles in the gastrointestinal system.¹⁵ For instance, *N*-oleoylethanolamide (OEA) was found to act as a satiety factor via activation of peroxisome proliferator-activated receptor (PPAR)- α .¹⁶ This raises the possibility that PLAAT2 is involved in NAE biosynthesis in the gut. To validate the role of PLAAT2 in NAE signaling, pharmacological inhibitors would be valuable tools to confirm its *N*-acyltransferase activity. However, so far no inhibitors have been described for PLAAT2.

In this chapter, the discovery and optimization of a library of α -ketoamide PLAAT2 inhibitors is described. A previously reported activity-based protein profiling (ABPP) assay¹⁷ for PLAAT2 was used to screen a focused library of lipase inhibitors for activity. This furnished hit compound **1**, which was modified through structure-activity relationship (SAR) analysis to deliver nanomolar potent inhibitor **LEI-301**. **LEI-301** showed similar potency for the other members of the PLAAT family and was selective over the proteins of the endocannabinoid system. NAE levels including anandamide were found to be highly increased in U2OS cells overexpressing PLAAT2. Importantly, **LEI-301** could partially reverse the NAE elevation in PLAAT2 transfected cells, but not in control cells. These findings suggest that PLAAT2 is involved in NAE biosynthesis and provide **LEI-301** as a new pharmacological tool to investigate its role in biological systems.

6.2 Results

6.2.1 Screening for PLAAT2 inhibitors using competitive ABPP.

A focused library of lipase inhibitors was screened for PLAAT2 inhibition using gel-based competitive ABPP.¹⁷ Cytosol fractions of HEK293T cells overexpressing PLAAT2 were treated with inhibitors at 10 μM , followed by incubation with the broad-spectrum lipase probe MB064¹⁸ (Figure 1A). The proteins were resolved by sodium dodecyl sulfate polyacrylamide gel electrophoresis (SDS-PAGE), which allowed visualization of PLAAT2 activity by in-gel fluorescence scanning. A leftover protein activity of $\leq 50\%$ was considered to be a hit, upon which an IC_{50} curve was generated using a dose-response ABPP experiment (Figure 1B). Data are reported in Table 1 as $\text{pIC}_{50} \pm \text{SEM}$ ($n = 3$). α -Ketoamides **1** and **2** were identified as submicromolar hits (for both: $\text{pIC}_{50} = 6.2 \pm 0.1$). A structure-activity relationship emerged from the structurally similar keto- and hydroxyamides (**3-22**) present in this library. The position of the ketone relative to the amide was essential for binding (compare α -ketoamides **1** and **2** with β -ketoamides **5-8**). Furthermore, the phenethylamine of **1** was preferred over benzylamine (**10**) and ethylamine (**11**). *N*-methylation resulted in complete loss of activity (**12**), which suggested that the N-H is potentially involved in hydrogen bond formation. Similarly, secondary amides **13-22** did not show any activity.

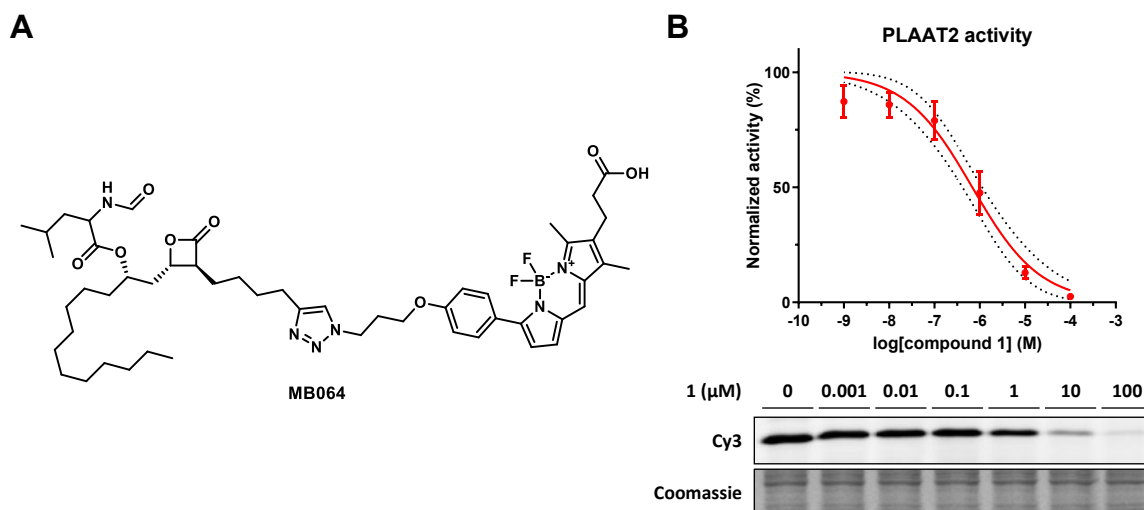
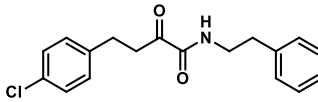
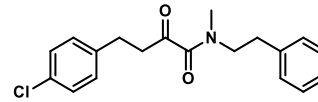
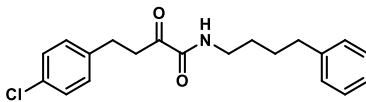
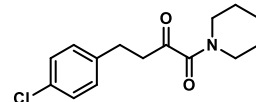
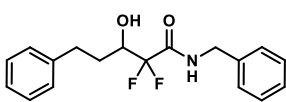
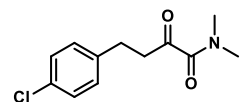
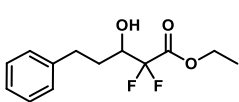
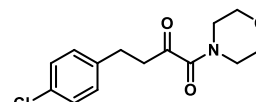
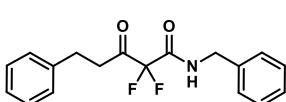
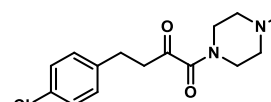
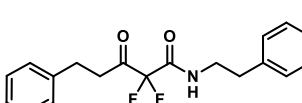
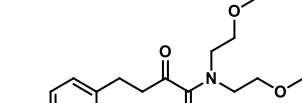
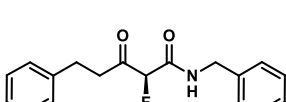
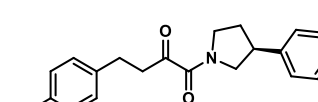
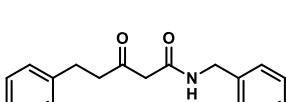
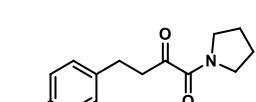
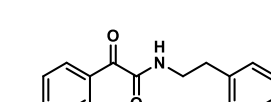
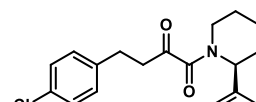
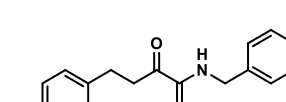
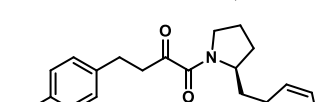
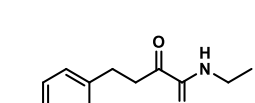
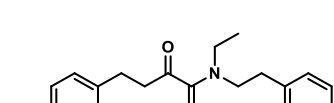


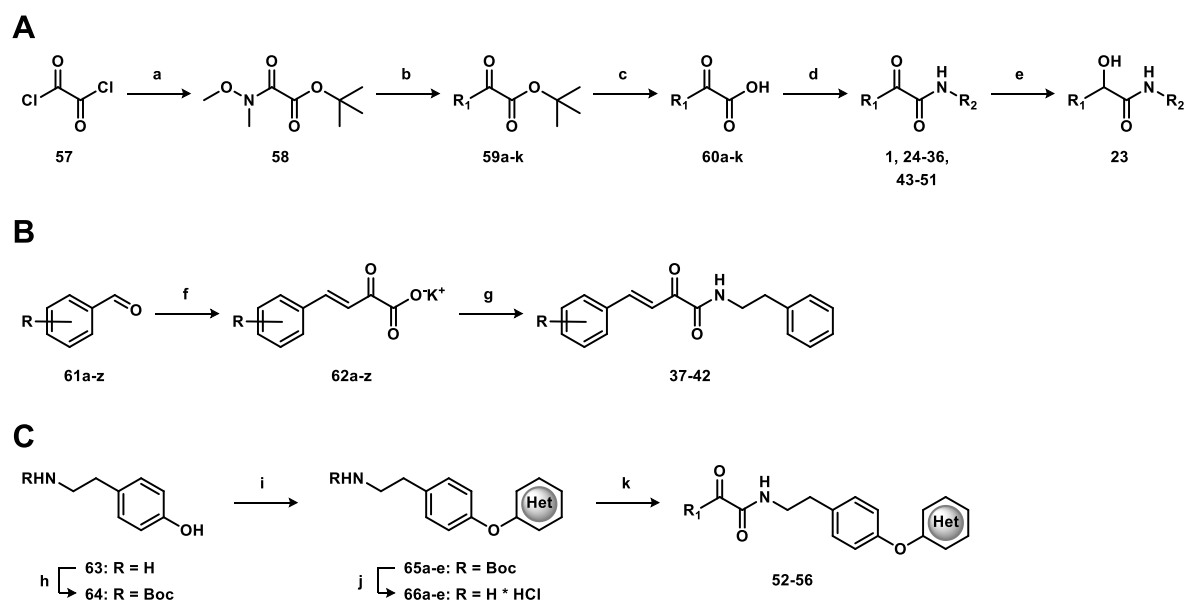
Figure 1. A) Structure of broad-spectrum lipase probe MB064. B) Representative gel and IC_{50} curve of a competitive ABPP experiment. Labeling of PLAAT2 by MB064 and dose-dependent inhibition by **1** ($\text{pIC}_{50} = 6.2 \pm 0.1$, dotted lines show 95% confidence interval). Data represent mean values \pm SEM ($n = 3$). Coomassie staining was used as a protein loading control.

Table 1. PLAAT2 activity of the lipase inhibitor library (1-22).

| ID | Structure | pIC_{50} \pm SEM | ID | Structure | pIC_{50} \pm SEM |
|----|---|--------------------------------|----|--|--------------------------------|
| 1 |  | 6.2 \pm 0.1 | 12 |  | < 5 |
| 2 |  | 6.2 \pm 0.1 | 13 |  | < 5 |
| 3 |  | < 5 | 14 |  | < 5 |
| 4 |  | < 5 | 15 |  | < 5 |
| 5 |  | < 5 | 16 |  | < 5 |
| 6 |  | < 5 | 17 |  | < 5 |
| 7 |  | < 5 | 18 |  | < 5 |
| 8 |  | < 5 | 19 |  | < 5 |
| 9 |  | < 5 | 20 |  | < 5 |
| 10 |  | 5.6 \pm 0.1 | 21 |  | < 5 |
| 11 |  | 5.6 \pm 0.1 | 22 |  | < 5 |

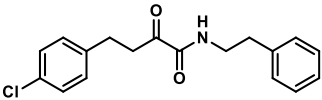
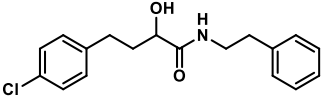
6.2.2 Evaluation of an α -ketoamide inhibitor library delivers nanomolar hit LEI-301.

α -Ketoamide **1** exhibited optimal PLAAT2 activity in this library, therefore this compound was resynthesized utilizing a general route depicted in Scheme 1A. Oxalyl chloride (**57**) was reacted with *tert*-butanol and *N,O*-dimethylhydroxylamine·HCl giving Weinreb amide **58**. Treatment with an *in situ* formed Grignard reagent from 4-chlorophenethyl bromide followed by *tert*-butyl deprotection gave ketoacid **59a**. Finally, amide coupling using HCTU afforded α -ketoamide **1**. After retesting in the ABPP assay, compound **1** was confirmed as an active hit ($pIC_{50} = 6.2 \pm 0.1$, $n = 3$) (Table 2). It was envisioned that the electrophilic ketone of **1** could bind with the PLAAT2 active site cysteine through a reversible covalent mechanism forming a hemithioacetal adduct, similar to other reported α -ketoamide inhibitors.¹⁹ To test this hypothesis, α -hydroxyamide **23** was prepared by reduction of **1** using sodium borohydride (Scheme 1A) and tested, showing no activity at 10 μ M (Table 2).



Scheme 1. General synthetic routes for **A**) α -ketoamide **1** analogues, **B**) β,γ -unsaturated α -ketoamides and **C**) *O*-heteroaryl phenethylamine derivatives. Reagents and conditions: a) *i.* *t*-BuOH, THF, 0 °C; *ii.* *N,O*-dimethylhydroxylamine·HCl, Et₃N, 0 °C, 75%; b) *i.* Mg, alkylbromide, Et₂O, reflux; *ii.* Weinreb amide, -78 °C, 21% – 83%; c) TFA, DCM, rt, 99%; d) HATU or HCTU, DiPEA, amine, DMF, rt, 22% – 80%; e) NaBH₄, THF, rt, 72%. f) pyruvic acid, KOH, MeOH, 0 °C to rt; g) *i.* oxalyl chloride, DCM, 0 °C to rt; *ii.* phenethylamine, DCM, 0 °C to rt, 14% – 35% over two steps. h) Boc₂O, NaHCO₃, THF, H₂O, rt, 85%; i) heteroaryl halide, K₂CO₃, DMSO or DMF, rt or 85 °C, 63% - 92%; j) HCl, dioxane, rt, 99%; k) EDC·HCl, HOBt, ketoacid, NMM, DCM, 0 °C to rt, 15% – 30%.

Table 2. Structure and PLAAT2 activity of α -ketoamide **1** and α -hydroxyamide **23**.

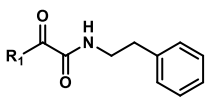
| ID | Structure | pIC ₅₀ ± SEM |
|-----------|---|-------------------------|
| 1 |  | 6.2 ± 0.1 |
| 23 |  | < 5 |

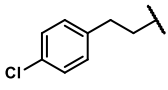
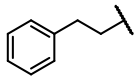
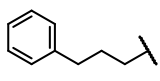
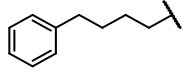
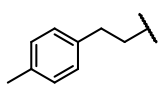
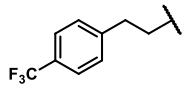
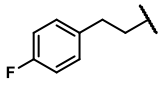
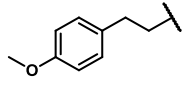
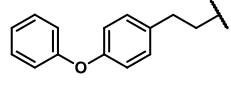
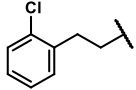
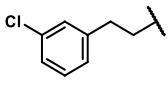
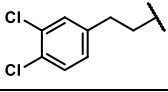
To improve the potency of **1**, R₁-ketone and R₂-phenethylamine analogues were systematically synthesized (compounds **24-56**). R₁-derivatives **24-36** and R₂-analogues **44-52** were synthesized via the general route (Scheme 1A). β,γ -Unsaturated α -ketoamides (**37-43**) were prepared using a two-step procedure (Scheme 1B): condensation of a benzaldehyde (**61a-z**) with pyruvic acid, which afforded the β,γ -unsaturated α -ketoacid as the potassium salt (**62a-z**), followed by acid chloride formation and coupling with phenethylamine. *O*-Arylated 4-hydroxyphenethylamine derivatives **53-57** were synthesized via Scheme 1C. Tyramine (**63**) was Boc-protected, followed by nucleophilic aromatic substitution (S_NAr) with a heteroaryl halide. Boc deprotection and subsequent amide coupling provided the α -ketoamides **52-56**.

First, the effect of various substitutions on the R₁-group of **1** was evaluated with derivatives **24-36** (Table 3). Removal of the chloride was detrimental for the activity (**24**). The length of the alkyl chain was investigated (**24-27**), showing that propyl derivative **25** was optimal, which had similar potency as **1**, but lower lipophilicity (cLogP). The 4-chloro on the phenyl ring seemed to be optimal (**29-33**). Electron-donating groups such as 4-methyl (**29**) and 4-methoxy (**32**) substituents decreased potency as well as a lipophilic electron withdrawing group (*e.g.* 4-trifluoromethyl, **30**). Small (4-fluoro, **31**) and large (4-phenoxy, **33**) substituents lowered the activity. Furthermore, substitution of the 4-chloro to the *ortho* or *meta* position, did not result in improved potency (compounds **34-36**). This indicated the presence of a small lipophilic pocket restricted in size, which is occupied by the 4-chlorophenyl group.

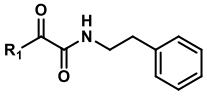
Next, β,γ -unsaturated α -ketoamides **37-42** were evaluated to test whether conformational restriction of the alkyl linker would lead to a gain in activity (Table 4). Although unsaturation was tolerated in the alkyl chain (compare compounds **1** and **37**), no activity improvement was observed for these derivatives. Overall, this indicates that the R₁ group is positioned towards a shallow pocket.

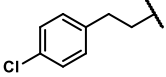
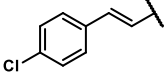
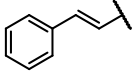
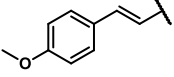
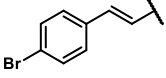
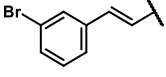
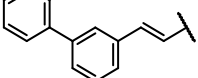
Table 3. Structure-activity relationship analysis of α -ketoamide analogues **24-36**.



| ID | R ₁ : | pIC ₅₀ ± SEM | cLogP ^a |
|----|---|-------------------------|--------------------|
| 1 |  | 6.2 ± 0.1 | 4.37 |
| 24 |  | < 5 | 3.66 |
| 25 |  | 6.3 ± 0.1 | 4.04 |
| 26 |  | 5.5 ± 0.1 | 4.57 |
| 27 |  | < 5 | 3.04 |
| 28 |  | < 5 | 1.56 |
| 29 |  | 5.3 ± 0.1 | 4.16 |
| 30 |  | 5.7 ± 0.1 | 4.54 |
| 31 |  | 5.1 ± 0.1 | 3.80 |
| 32 |  | 5.5 ± 0.1 | 3.58 |
| 33 |  | 5.4 ± 0.1 | 5.76 |
| 34 |  | 5.9 ± 0.1 | 4.37 |
| 35 |  | 5.6 ± 0.1 | 4.37 |
| 36 |  | 5.7 ± 0.2 | 4.97 |

^a cLogP was calculated using Chemdraw 15.

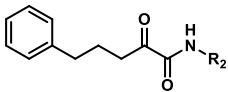
Table 4. Structure-activity relationship analysis of α -ketoamide analogues **37-43**.


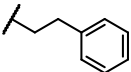
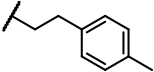
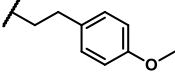
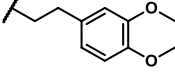
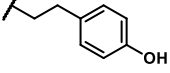
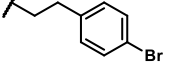
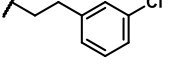
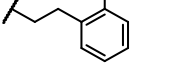
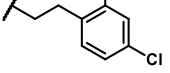
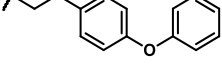
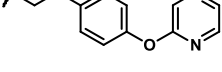
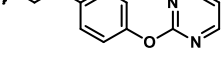
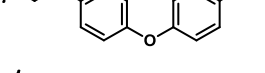
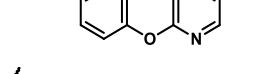
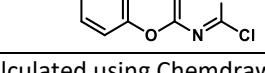
| ID | R ₁ : | pIC ₅₀ ± SEM | cLogP ^a |
|-----------|---|-------------------------|--------------------|
| 1 |  | 6.2 ± 0.1 | 4.37 |
| 37 |  | 5.8 ± 0.1 | 4.37 |
| 38 |  | 5.1 ± 0.1 | 3.66 |
| 39 |  | 5.8 ± 0.1 | 3.58 |
| 40 |  | 5.3 ± 0.1 | 4.52 |
| 41 |  | < 5 | 4.52 |
| 42 |  | 5.6 ± 0.1 | 5.55 |

^a cLogP was calculated using Chemdraw 15.

Focus was shifted towards the optimization of the phenethylamine moiety. Analogues **43-56** incorporating substituted phenethylamines, were prepared in combination with the optimal 2-oxo-5-phenylpentanoyl motif of compound **25** (Table 5). Substitutions on the *para* position were unfavorable for methyl (**43**), methoxy (**44**) and hydroxyl (**46**). The *meta* and *ortho* positions (**48**, **49**) also did not afford an improvement in potency. Increasing the lipophilicity gave a 2-fold increase in activity for 4-bromo analog **47**, while further expansion with a 4-phenoxy moiety (**51**) improved the potency 10-fold compared to **25**. Addition of the phenoxy group raised the cLogP of **51** with two log units to 6.14, therefore more polar heteroaryl rings were introduced to lower the lipophilicity (**52-56**). After testing for activity, a decrease in potency was observed for all these inhibitors compared to **51**. Therefore, being the most potent inhibitor of PLAAT2, **51** (termed **LEI-301**) was selected for further characterization.

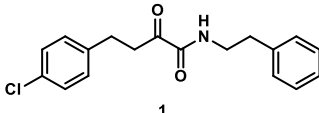
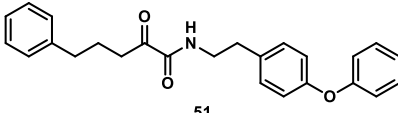
Table 5. Structure-activity relationship analysis of phenethylamine analogues **43-56**.



| ID | R ₂ : | pIC ₅₀ ± SEM | cLogP ^a |
|-----------------|---|-------------------------|--------------------|
| 3 |  | 6.3 ± 0.1 | 4.04 |
| 43 |  | 5.7 ± 0.1 | 4.54 |
| 44 |  | 5.8 ± 0.1 | 3.96 |
| 45 |  | 5.3 ± 0.1 | 3.70 |
| 46 |  | 5.9 ± 0.1 | 3.37 |
| 47 |  | 6.6 ± 0.1 | 4.90 |
| 48 |  | 6.1 ± 0.1 | 4.75 |
| 49 |  | 5.2 ± 0.1 | 4.75 |
| 50 |  | 5.9 ± 0.1 | 5.47 |
| 51 (LEI-301) |  | 7.3 ± 0.1 | 6.14 |
| 52 |  | 6.3 ± 0.1 | 3.68 |
| 53 |  | 5.7 ± 0.1 | 3.68 |
| 54 |  | 6.7 ± 0.1 | 5.67 |
| 55 |  | 6.8 ± 0.1 | 5.67 |
| 56 |  | 6.2 ± 0.1 | 4.44 |

^a cLogP was calculated using Chemdraw 15.

Table 6. PLAAT2 activity data and physicochemical parameters of **1** and **LEI-301**.

| Compound | pIC ₅₀ ± SEM | cLogP ^a | LipE ^b | MW ^c (Da) | tPSA ^a (Å ²) | HBD ^d | HBA ^e | RB ^f |
|--|-------------------------|--------------------|-------------------|-------------------------|--|------------------|------------------|-----------------|
|  1 | 6.2 ± 0.1 | 4.4 | 1.8 | 316 | 46.2 | 1 | 2 | 8 |
|  51 (LEI-301) | 7.3 ± 0.1 | 6.1 | 1.2 | 387 | 55.4 | 1 | 3 | 11 |

^a cLogP and topological polar surface area (tPSA) were calculated using Chemdraw 15; ^b Lipophilic efficiency (LipE) = pIC₅₀ – cLogP; ^c MW: molecular weight; ^d HBD: H-bond donors; ^e HBA: H-bond acceptors; ^f RB: rotatable bonds.

A summary of the activity data and physicochemical parameters of **1** and **LEI-301** is shown in Table 6. **LEI-301** is a nanomolar potent PLAAT2 inhibitor (IC₅₀ = 50 nM), displaying a 13-fold increase in activity compared to **1**. Due to a 50-fold increase in lipophilicity, the lipophilic efficiency (LipE) is too low to regard **LEI-301** as a suitable candidate for *in vivo* experiments. Nevertheless, **LEI-301** shows favorable physicochemical parameters such as low molecular weight (MW < 500), topological polar surface area (tPSA < 90 Å²), hydrogen bond donors (HBD < 5) and acceptors (HBA < 10). This highlights **LEI-301** as a promising starting point to obtain *in vivo* active PLAAT2 inhibitors.

6.2.3 *In silico* modeling of α -ketoamides inhibitors.

To explain the binding mode of the α -ketoamides inhibitors in PLAAT2, **LEI-301** and **1** were docked in a PLAAT2 crystal structure (PDB: 4DPZ).²⁰ Residues 39-52 and 105-111 were absent from this structure, therefore a homology model was prepared using the closely related PLAAT3 crystal structure (PDB: 4DOT)²⁰ from which the shape of the loop for residues 105-111 could be adopted. A second loop comprising residues 39-52 was modeled based on sequence, since it is not present in both crystal structures.

It has been proposed that the electrophilic ketone of α -ketoamides could engage with the active site cysteine through a reversible covalent mechanism¹⁹, therefore **LEI-301** and **1** were covalently docked to Cys113 in the enzyme (Figure 2). Both compounds revealed a hydrogen bonding network between the oxy-anion and amide carbonyl with His23 and the Trp24 backbone amide N-H, while the backbone carbonyl of Leu108 formed a H-bond

with the amide of the inhibitors. Hydrophobic interactions were apparent for the R₁-ketone substituent of **LEI-301** and **1** with the Leu108 sidechain. The modelled loop of residue 39-52 enclosed the R₁-phenyl ring, thereby providing an explanation why expansion on this side of the molecule was unfavored. Introduction of the 4-phenoxy group in **LEI-301** enabled an additional π - π stacking interaction with Tyr21. This offered a possible reason for the observed activity increase of **LEI-301**.

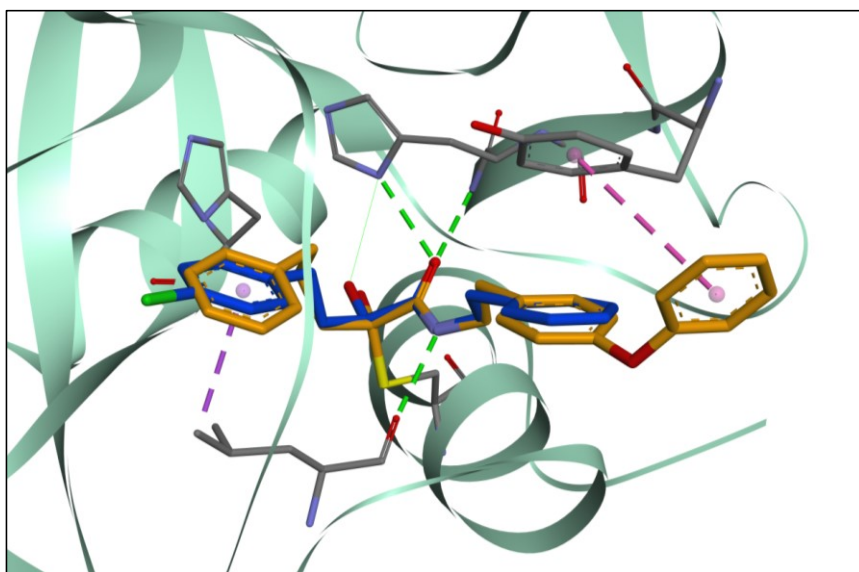


Figure 2. Compounds **1** (blue) and **LEI-301** (orange) in complex with PLAAT2, covalently bound to Cys113. Green dotted lines represent a hydrogen bond, pink and purple represent π -interactions.

6.2.4 Off-target profile of **LEI-301** for the PLAAT family and endocannabinoid system.

The activity of **LEI-301** for the other members of the PLAAT family was assessed via ABPP with **MB064** using cytosolic fractions of HEK293T cells overexpressing the corresponding PLAAT enzymes. **LEI-301** was found to be equally potent towards PLAAT4 and PLAAT5, but less active for PLAAT3 (Table 7). Unfortunately, PLAAT1 could not be expressed and could therefore not be tested. Next, the activity of **LEI-301** for the receptors and metabolic enzymes of the endocannabinoid system (ECS) was determined. No inhibitory activity was observed at 10 μ M for the cannabinoid receptors type 1 and 2 (CB₁/CB₂) (Table 7). The enzymes involved in NAE biosynthesis (PLA2G4E, NAPE-PLD) and degradation (FAAH) were also not inhibited at this concentration (Table 8). Enzymes involved in the metabolism of the other endocannabinoid 2-arachidonoylglycerol (2-AG), such as diacylglycerol lipase α and β (DAGL- α / β), monoacylglycerol lipase (MAGL) and α , β -hydrolase domain containing 6 (ABHD6) were not inhibited.

Table 7. LEI-301 is equally potent for PLAAT4 and PLAAT5, but less active towards PLAAT3.

| pIC ₅₀ ± SEM (n = 3) | | |
|---------------------------------|-----------|-----------|
| PLAAT3 | PLAAT4 | PLAAT5 |
| 6.6 ± 0.1 | 7.3 ± 0.2 | 7.4 ± 0.1 |

Table 8. LEI-301 shows no significant inhibitory activity for the cannabinoid receptors.

| Radioligand displacement at 10 μ M LEI-301 (% ± SD; N = 2, n = 2) | |
|--|------------------|
| hCB ₁ | hCB ₂ |
| 49 ± 8 | 32 ± 4 |
| > 50% is considered a target | |

Table 9. LEI-301 shows no inhibitory activity for metabolic enzymes of the ECS.

| Remaining enzyme activity at 10 μ M LEI-301 (% ± SD; n = 3) | | | | | | |
|---|----------|----------------|---------------|----------|---------|--------|
| hNAPE-PLD | hPLA2G4E | mDAGL α | mDAGL β | hMAGL | mFAAH | mABHD6 |
| 92 ± 8 | 95 ± 5 | 97 ± 10 | 83 ± 1 | 105 ± 19 | 108 ± 4 | 92 ± 5 |

Activities were obtained from surrogate (hNAPE-PLD, mDAGL β) or natural (hMAGL) substrate assays. hPLA2G4E, mDAGL α/β , mFAAH and mABHD6 were determined by gel-based ABPP. < 50% is considered a target.

6.2.5 Targeted lipidomics shows that LEI-301 inhibits PLAAT2 in overexpressing cells.

Having established that **LEI-301** is a potent inhibitor of PLAAT2 and selective over the other enzymes of the ECS, it was investigated whether **LEI-301** can decrease anandamide levels in living cells. Human U2OS osteosarcoma cells were transiently transfected with a pcDNA3.1 plasmid containing *PLAAT2* or an empty (mock) vector. To ensure that the NAPEs generated by PLAAT2 could be converted to NAEs, the expression of NAPE-PLD in this cell line was confirmed by quantitative PCR (qPCR) (*NAPEPLD*: C_q ± SEM = 27.30 ± 0.050, *RPS18* (housekeeping gene): C_q ± SEM = 17.76 ± 0.011). Targeted lipidomics on the lipid extracts of the transfected cells allowed the quantification of eight different NAEs and ten fatty acids (FFAs) by liquid chromatography-mass spectrometry (LC-MS). A striking increase of 9- to 99-fold for all NAE species was observed for the PLAAT2 overexpressing cells compared to control, including anandamide (AEA, fold change ± SD = 54 ± 20, *P* = 0.0016) (Table 10, Figure 3A-B). This is in contrast to a previous report, where only a small elevation of anandamide levels was detected.¹⁰ Notably, PLAAT2 transfection did not

produce significant elevations of fatty acid species, except for arachidonic acid (fold change \pm SD = 1.81 ± 0.45 , $P = 0.040$) while a decrease was measured for γ -linolenic (18:3- ω 6) and α -linoleic acid (18:2- ω 3) (Figure 3A, Supplementary Table 1). Next, **LEI-301** was incubated at 10 μ M for 4 hours with the PLAAT2-transfected or control cells. A significant 2-fold reduction of anandamide was apparent in the PLAAT2 cells, which was absent in the control samples (Figure 3B and E). Other mono- and polyunsaturated NAE also showed significant reductions upon treatment with **LEI-301** in the PLAAT2 overexpressing cells but not in the mock cells (Figure 3E). Of note, the saturated *N*-palmitoylethanolamine (PEA) and *N*-stearoylethanolamine (SEA) did not reach statistical significance ($P = 0.085$ and $P = 0.25$). Furthermore, **LEI-301** reduced arachidonic acid levels, but not significantly ($P = 0.06$) (Figure 3E). No changes were observed for 2-AG (Figure 3D).

Table 10. PLAAT2 overexpression greatly increases NAE levels in U2OS cells. Data represent mean values \pm SD for 4 biological replicates. P -values were determined by one-way ANOVA.

| NAE | Absolute NAE levels (pmol/ 10^6 cells \pm SD) | | Fold change \pm SD PLAAT2 vs. mock | P -value |
|-------------|---|------------------|---|------------|
| | mock | PLAAT2 | | |
| PEA (16:0) | 0.196 \pm 0.05 | 18.62 \pm 5.97 | 95 \pm 30 | 0.0008 |
| POEA (16:1) | 0.031 \pm 0.01 | 2.247 \pm 0.78 | 73 \pm 25 | 0.0013 |
| SEA (18:0) | 0.516 \pm 0.12 | 47.39 \pm 13.1 | 92 \pm 25 | 0.0004 |
| OEA (18:1) | 0.190 \pm 0.05 | 18.83 \pm 5.02 | 99 \pm 26 | 0.0003 |
| LEA (18:2) | 0.047 \pm 0.01 | 1.569 \pm 0.50 | 33 \pm 10 | 0.0009 |
| AEA (20:4) | 0.040 \pm 0.01 | 2.194 \pm 0.79 | 54 \pm 20 | 0.0016 |
| EPEA (20:5) | 0.010 \pm 0.01 | 0.555 \pm 0.15 | 53 \pm 14 | 0.0004 |
| DHEA (22:6) | 0.032 \pm 0.01 | 0.286 \pm 0.11 | 8.9 \pm 3.4 | 0.0034 |

Abbreviations: PEA = *N*-palmitoylethanolamine, POEA = *N*-palmitoleoylethanolamine, SEA = *N*-stearoylethanolamine, OEA = *N*-oleoylethanolamine, LEA = *N*-linoleoylethanolamine, AEA = *N*-arachidonoylethanolamine, EPEA = *N*-eicosapentaenoylethanolamine, DHEA = *N*-docosahexaenoylethanolamine.

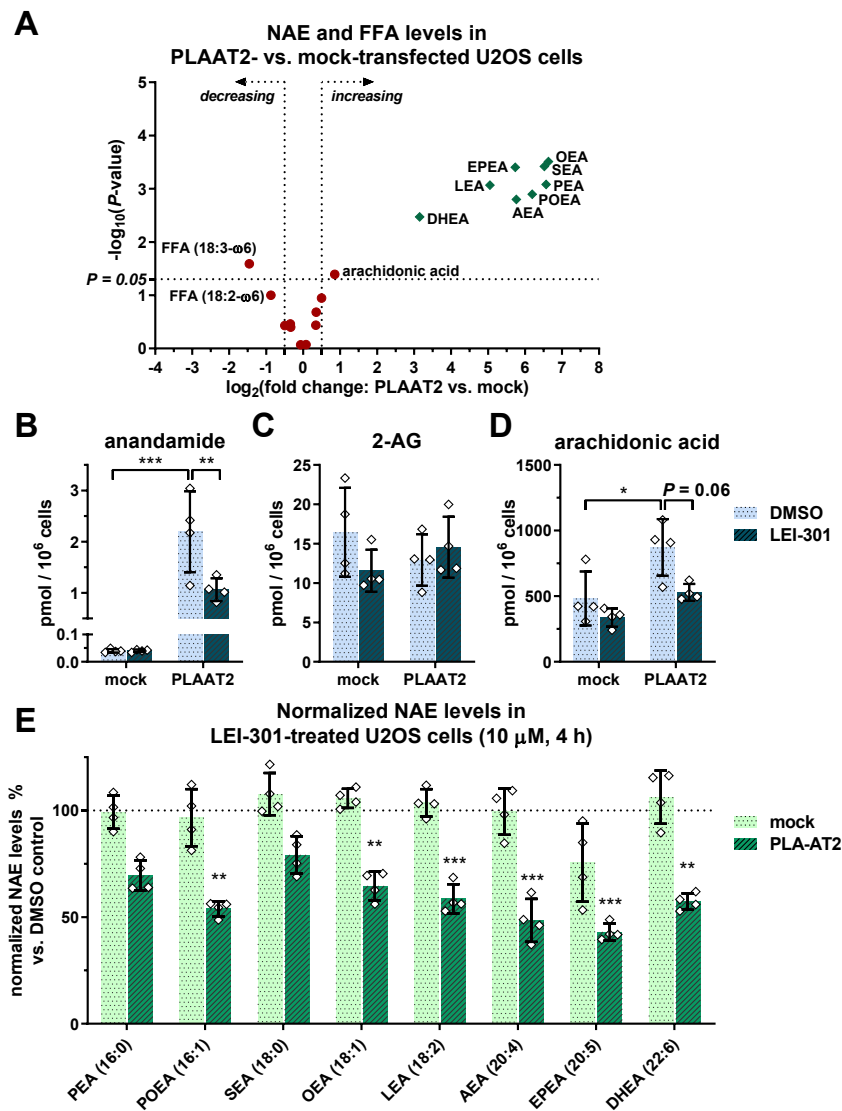


Figure 3. U2OS cells transiently transfected with PLAAT2 exhibit highly increased NAE levels and **LEI-301** can inhibit NAE formation. **A**) Volcano plot depicting the $\log_2(\text{fold change})$ vs. $-\log_{10}(P\text{-value})$ of NAEs (green diamonds) and free fatty acids (FFAs, red circles) in PLAAT2 vs. mock overexpressing cells. **B-D**) Absolute levels of **(B)** anandamide (AEA), **(C)** 2-AG and **(D)** arachidonic acid in mock- or PLAAT2-transfected cells treated with vehicle (DMSO) or **LEI-301** (10 μ M, 4 h). **E**) Normalized NAE levels of mock- and PLAAT2-transfected cells treated with **LEI-301** (10 μ M, 4 h) represented as effect %. Data were normalized against PLAAT2 or mock cells treated with vehicle (DMSO). Data represent mean values \pm SD for 4 biological replicates. *, $P < 0.05$, **, $P < 0.01$, ***, $P < 0.001$ by one-way ANOVA.

6.3 Conclusion

In this chapter the discovery and optimization of an α -ketoamide PLAAT2 inhibitor library is described. A map displaying an overview of the SAR is presented in Figure 4. Extension of the ketone alkyl chain to three methylenes and removal of the chloride on the left phenyl group gave a similar potency with reduced lipophilicity. The phenethylamine was expanded with a *para*-phenoxy moiety affording the nanomolar potent inhibitor **LEI-301**, having a 13-fold higher activity for PLAAT2 compared to the initial hit. Attempts to decrease the high lipophilicity of **LEI-301** while retaining the activity, were not yet successful. Covalent docking in the PLAAT2 crystal structure provided a possible binding mode of **LEI-301** and a potential explanation for the observed potency increase. Subsequent selectivity profiling revealed that **LEI-301** is also a potent inhibitor for PLAAT3, PLAAT4 and PLAAT5. Further inhibitor optimization is desired to obtain selectivity over the other PLAAT family members. No off-targets were found for proteins of the endocannabinoid system.

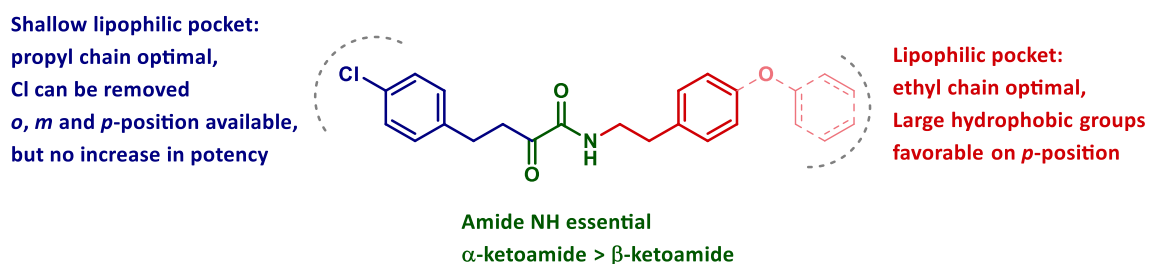


Figure 4. Structure activity map for the PLAAT2 α -ketoamide inhibitor library.

Overexpression of PLAAT2 in U2OS cells gave a dramatic increase of all measured NAE species, while no significant elevations of fatty acids were observed, except for arachidonic acid. These findings provide more evidence that PLAAT2 can produce NAEs and confirms that this enzyme can function as an *N*-acyltransferase. Furthermore, treatment of overexpressing PLAAT2 cells with **LEI-301** decreased NAE levels, including a 2-fold reduction for the endocannabinoid anandamide, which was absent in the control cells. This validates **LEI-301** as a promising tool compound to study PLAAT2 function in biological systems.

Acknowledgements

Karol Al Ayed, Tim Ofman, Yvonne Tran, Nicky de Koster, Martin Li and Laura Mulder are kindly acknowledged for contributing to the compound synthesis and biochemical testing. Juan Zhou is kindly thanked for performing ABPP and lipidomics experiments. qPCR, cannabinoid receptor and enzyme assays were performed by Floor Stevens, Andrea Martella, Florian Mohr, Ming Jiang, Tom van der Wel and Timo Wendel, for which they are kindly acknowledged. Vasudev Kantae, Xinyu Di and Thomas Hankemeier are kindly thanked for determining cellular lipid levels. Lindsey Burggraaff and Gerard van Westen are kindly acknowledged for modeling **LEI-301** in the PLAAT2 crystal structure.

6.4 Experimental section

A. Biological procedures

Plasmids

Full-length human cDNA of PLAAT1-5 (obtained from Natsuo Ueda⁶) was cloned into mammalian expression vector pcDNA3.1 with a C-terminal FLAG-tag and containing genes for ampicillin and neomycin resistance. Plasmids were isolated from transformed XL-10 Z-competent cells (Maxi Prep kit: Qiagen) and sequenced at the Leiden Genome Technology Center. Sequences were analyzed and verified (CLC Main Workbench).

Cell culture

HEK293T and U2OS cells (ATCC) were cultured at 37 °C and 7% CO₂ in DMEM (Sigma Aldrich, D6546) with GlutaMax (2 mM), penicillin (100 µg/ml, Duchefa), streptomycin (100 µg/ml, Duchefa) and 10% (v/v) newborn calf serum (Thermo Fisher). Medium was refreshed every 2-3 days and cells were passaged twice a week at 80-90% confluence. Cells were passaged twice a week to appropriate confluence by thorough pipetting (HEK293T) or trypsinization (U2OS).

Transient transfection

10⁷ HEK293T cells were seeded in 15 cm petri dishes one day before transfection. Two hours before transfection the medium was refreshed with 13 mL medium. Transfection was performed with polyethylenimine (PEI, 60 µg per dish) in a ratio of 3:1 with plasmid DNA (20 µg per dish). PEI and plasmid DNA were incubated in serum-free medium (2 mL per dish) at rt for 15 min, followed by dropwise addition to the cells. Transfection with the empty pcDNA3.1 vector was used to generate control (mock) samples. The medium was refreshed after 24 hours and cells were harvested after 48 or 72 hours in cold PBS. Cells were pelleted by centrifugation (5 min, 1,000 g) and the pellet was washed with PBS. The supernatant was removed and cell pellets were flash frozen in liquid N₂ and stored at -80 °C.

Cell lysate preparation

Cell pellets were thawed on ice, and resuspended in cold lysis buffer (50 mM Tris-HCl pH 8, 2 mM DTT, 1 mM MgCl₂, 2.5 U/mL benzonase) and incubated on ice for 30 minutes. The cytosolic fraction (supernatant) was separated from the membranes by ultra-centrifugation (100,000 g, 45 min, 4 °C, Beckman Coulter, Ti 70.1 rotor). The pellet (membrane fraction) was resuspended in cold storage buffer (50 mM Tris-HCl pH 8, 2 mM DTT) and homogenized by thorough pipetting and passage through an insulin needle (29G). Protein concentrations were determined by a Quick Start™ Bradford protein assay (Bio-Rad) or Qubit™ protein assay (Invitrogen). Samples were flash frozen in liquid N₂ and stored at -80 °C.

Mouse brain lysate preparation

Mouse brain membrane or cytosol fractions were prepared as described in Chapter 2.

Activity-based protein profiling on PLAAT2-5 transfected HEK293T cell lysate.

Gel-based activity based protein profiling (ABPP) was performed with minor changes as described previously.¹⁸ For ABPP assays on HEK293T cells overexpressing PLAAT2, the cytosol proteome (0.25 µg/µL, 20 µL) was pre-incubated with vehicle (DMSO) or inhibitor (0.5 µL in DMSO, 30 min, rt) followed by incubation with MB064 (final concentration: 250 nM, 20 min, rt). For PLAAT3, PLAAT4 and PLAAT5 the protocols differed for the protein concentrations (0.5 µg/µL, 1 µg/µL and 1 µg/µL, respectively) and MB064 concentration (250 nM, 500 nM and 500 nM, respectively). Final concentrations for the inhibitors are indicated in the main text and figure legends. For the dose-response experiments only cytosol proteome was used. Proteins were denatured with 4x Laemmli buffer (5 µL, stock concentration: 240 mM Tris pH 6.8, 8% (w/v) SDS, 40% (v/v) glycerol, 5% (v/v) β-mercaptoethanol, 0.04% (v/v) bromophenol blue). 10 µl sample per reaction was resolved on a 10% acrylamide SDS-PAGE gel (180 V, 70 min). Gels were scanned using Cy3 and Cy5 multichannel settings (605/50 and 695/55 filters, respectively) on a ChemiDoc™ Imaging System (Bio-Rad). Fluorescence was normalized to Coomassie staining and quantified with Image Lab (Bio-Rad). Experiments were performed in triplicate. Dose-response IC₅₀ curves were generated with Graphpad Prism 6.

qPCR

RNA isolation and cDNA synthesis: Total RNA from U2OS cells was extracted using a NucleoSpin® RNA kit (Macherey-Nagel) according to the manufacturer's instructions. Subsequently, cDNA synthesis was carried out with a SuperScript™ First-Strand Synthesis System (Invitrogen) according to the manufacturer's instructions.

qPCR analysis: 2.5 ng of input cDNA was analyzed using SybrGreen qPCR master mix (Thermo-Fisher) in combination with CFX96 optical thermal cycler (Bio-Rad). Data analysis was performed using CFX Manager software (Bio-Rad). The housekeeping gene 40S ribosomal protein S18 (*RPS18*) was used as a control. Data are expressed in quantitation cycles (C_q) ± SEM of three technical replicates.

Table S1. Primer sequences of *Napepld* and *Hprt* used for qPCR.

| Gene | Forward (5'-3') | Reverse (5'-3') | Accession number |
|----------------|----------------------|------------------------|------------------|
| <i>NAPEPLD</i> | CTTAGCTCTCGTGCTTCACC | CGCATCTATTGGAGGGAGTTCA | NM_001122838.1 |
| <i>RPS18</i> | TAGCCTTGCCATCACTGCC | TCACACGTTCCACCTCATCC | NM_022551.3 |

CB₂ receptor radioligand displacement assay

The CB₂ receptor radioligand displacement assay was performed as described in Chapter 2.

hNAPE-PLD surrogate substrate activity assay

The hNAPE-PLD activity assay was performed as described in Chapter 2.

Natural substrate-based fluorescence assay hMAGL

The hMAGL activity assay was performed as described in Chapter 2.

Activity-based protein profiling for determining mDAGLα, mFAAH, mABHD6 and hPLA2G4E activities

Gel-based activity-based protein profiling (ABPP) was performed as described in Chapter 2.

B. Targeted lipidomics in U2OS cells

The targeted lipidomics experiments are based on previously reported methods with small alterations.²¹

Sample preparation

$2 \cdot 10^6$ U2OS cells (grown at 37 °C, 7% CO₂) were seeded 1 day before transfection in 6 cm dishes. After 24 h, PLAAT2 plasmid DNA (2.7 μ g/dish) and polyethylenimine (PEI, 1 μ g/ μ L) were incubated in serum-free culture medium (15 min, rt), and then added dropwise to the cells. After 24 h, medium was aspirated and cells were washed once with serum-free medium. New serum-free medium was added with **LEI-301** (final concentration: 10 μ M, 0.1% DMSO) or DMSO as a control. After incubating for 4 hours (37 °C, 7% CO₂) the medium was removed and the cells were washed with cold PBS (3x). The cells were harvested in 1.5 mL Eppendorf tubes by trypsinization, followed by centrifugation (10 min, 1,500 rpm). PBS was removed and the cell pellets were flash frozen with liquid N₂ and stored at -80 °C. Live cell count with trypan blue was performed after compound treatment to test for cell viability and for sample normalization after lipid measurements.

Lipid extraction

Lipids extraction was performed on ice. In brief, cell pellets with $2 \cdot 10^6$ cells were transferred to 1.5 mL Eppendorf tubes, spiked with 10 μ L each of deuterium labeled internal standard mix for endocannabinoids (*N*-arachidonylethanolamine (AEA)-d8, *N*-docosahexaenylethanolamine (DHEA)-d4, 2-arachidonoylglycerol (2-AG)-d8, *N*-stearoylethanolamine (SEA)-d3, *N*-palmitoylethanolamine (PEA)-d4, *N*-linoleoylethanolamine (LEA)-d3 and *N*-oleoylethanolamine (OEA)-d4), and negative polar lipids (fatty acid (FA)17:0-d33), followed by the addition of ammonium acetate buffer (100 μ L, 0.1 M, pH 4). After extraction with methyl *tert*-butyl ether (MTBE, 1 mL), the tubes were thoroughly mixed for 4 min using a bullet blender at medium speed (Next Advance Inc., Averill park, NY, USA), followed by a centrifugation step (5,000 *g*, 12 min, 4 °C). Then 925 μ L of the upper MTBE layer was transferred into clean 1.5 mL Eppendorf tubes. Samples were dried in a speed-vac followed by reconstitution in acetonitrile/water (50 μ L, 90 : 10, v/v). The samples were centrifuged (14,000 *g*, 3 min, 4 °C) before transferring into LC-MS vials. Each sample was injected on two different lipidomics platforms: endocannabinoids (5 μ L) and negative polar lipids (8 μ L).

LC-MS/MS analysis for endocannabinoids

A targeted analysis of endocannabinoids and related NAEs (*N*-acylethanolamines) was measured using an Acquity UPLC I class binary solvent manager pump (Waters, Milford, USA) in conjugation with AB SCIEX 6500 quadrupole ion trap (QTRAP) (AB Sciex, Massachusetts, USA). Separation was performed with an Acquity HSS T3 column (1.2 x 100 mm, 1.8 μ m) maintained at 40 °C. The aqueous mobile phase A consisted of 2 mM ammonium formate and 10 mM formic acid, and the organic mobile phase B was acetonitrile. The flow rate was set to 0.4 ml/min; initial gradient conditions were 55% B held for 2 min and linearly ramped to 100% B over 6 minutes and held for 2 min; after 10 s the system returned to initial conditions and held 2 min before next injection. Electrospray ionization-MS was operated in positive mode for measurement of endocannabinoids and NAEs, and a selective Multiple Reaction Mode (sMRM) was used for quantification.

LC-MS/MS analysis for negative polar lipids

This method is measured on an Acquity UPLC binary solvent manager 8 pump (Waters) coupled to an Agilent 6530 electrospray ionization quadrupole time-of-flight (ESI-Q-TOF, Agilent, Jose, CA, USA) high resolution mass spectrometer using reference mass correction. The chromatographic separation was achieved on an Acquity HSS T3 column (1.2 x 100 mm, 1.8 μ m) maintained at 40 °C. The negative apolar lipids that constitute free fatty acids were separated with a flow of 0.4 mL/min over 15 min gradient. In negative mode, the aqueous mobile phase A consisted of 5:95 (v/v) acetonitrile:H₂O with 10 mM ammonium formate, and the organic mobile phase B consisted of 99% (v/v) methanol with 10 mM ammonium formate.

Statistical analysis

Absolute values of lipid levels were corrected using the measured live cell count numbers. Data were tested for significance with GraphPad v6 using one-way ANOVA with Tukey correction for multiple comparisons. *P*-values < 0.05 were considered significant.

C. Computational Chemistry

Ligand preparation

Molecular structures of **LEI-301** and **1** were drawn with specified chirality and prepared for docking using Ligprep from Schrödinger.²² Default Ligprep settings were applied: states of heteroatoms were generated using Epik at a pH 7 ± 2.²³ No tautomers were created by the program, which resulted in one standardized structure per ligand.

Protein preparation

The x-ray structure of PLAAT2 was extracted from the PDB (PDB ID: 4DPZ).²⁰ The apo protein structure was prepared for docking with the Protein Preparation tool from the Schrödinger 2017-4 suite. Waters were removed and default protein preparation settings were applied: explicit hydrogens were added and states of heteroatoms were generated using Epik at a pH 7 ± 2, resulting in a protonated state of binding pocket His23. Missing side chains and loops were added using Prime²⁴: loop 39-53 based on sequence and loop 105-111 based on the structure of PLAAT3 (PDB ID: 4DOT).²⁰

Docking

The PLAAT2 binding pocket was induced using the binding pose from **1** in PLAAT3 as previously reported and molecular dynamic simulations (10 ns).^{17,25} Both **LEI-301** and **1** were docked with induced-fit, followed by covalent docking to Cys113. Compounds were docked using the Schrödinger 2017-4 suite²⁵ with SP precision. The poses with the lowest docking scores were manually examined and one pose per ligand was selected. Selection was based on docking score, frequency of recurring poses, and interactions made between the ligand and the protein.

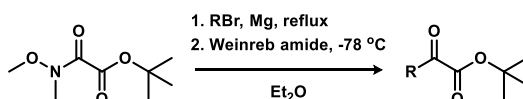
D. Synthetic procedures

General

All chemicals (Sigma-Aldrich, Fluka, Acros, Merck) were used as received. All solvents used for reactions were of analytical grade. THF, Et₂O, DMF, CH₃CN and DCM were dried over activated 4 Å molecular sieves, MeOH over 3 Å molecular sieves. Flash chromatography was performed on silica gel (Screening Devices BV, 40-63 μm, 60 Å). The eluent EtOAc was of technical grade and distilled before use. Reactions were monitored by thin layer chromatography (TLC) analysis using Merck aluminium sheets (Silica gel 60, F₂₅₄). Compounds were visualized by UV-absorption (254 nm) and spraying for general compounds: KMnO₄ (20 g/L) and K₂CO₃ (10 g/L) in water, or for amines: ninhydrin (0.75 g/L) and acetic acid (12.5 mL/L) in ethanol, followed by charring at ~150 °C. ¹H and ¹³C NMR experiments were recorded on a Bruker AV-300 (300/75 MHz), Bruker AV-400 (400/100 MHz) or Bruker DMX-400 (400/101 MHz). Chemical shifts are given in ppm (δ) relative to tetramethylsilane or CDCl₃ as internal standards. Multiplicity: s = singlet, br s = broad singlet, d = doublet, dd = doublet of doublet, t = triplet, q = quartet, p = pentet, m = multiplet. Coupling constants (*J*) are given in Hz. LC-MS measurements were performed on a Thermo Finnigan LCQ Advantage MAX ion-trap mass spectrometer (ESI⁺) coupled to a Surveyor HPLC system (Thermo Finnigan) equipped with a standard C18 (Gemini, 4.6 mmD x 50 mmL, 5 μm particle size, Phenomenex) analytical column and buffers A: H₂O, B: CH₃CN, C: 0.1% aq. TFA. High resolution mass spectra were recorded on a LTQ Orbitrap (Thermo Finnigan)

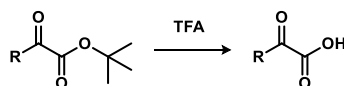
mass spectrometer or a Synapt G2-Si high definition mass spectrometer (Waters) equipped with an electrospray ion source in positive mode (source voltage 3.5 kV, sheath gas flow 10 mL min⁻¹, capillary temperature 250 °C) with resolution $R = 60000$ at m/z 400 (mass range $m/z = 150-2000$) and dioctylphthalate ($m/z = 391.28428$) as a lock mass. Preparative HPLC was performed on a Waters Acquity Ultra Performance LC with a C18 column (Gemini, 150 x 21.2 mm, Phenomenex). All final compounds were determined to be >95% pure by integrating UV intensity recorded via HPLC.

General procedure A



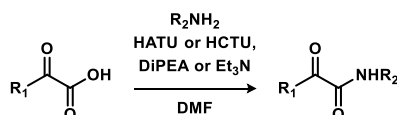
Magnesium turnings were activated by stirring in a 3 M solution of HCl for 5 min. The magnesium was then washed with water and acetone and dried under reduced pressure. A round-bottom flask connected to a reflux condenser was flame dried before addition of activated magnesium turnings (2 eq) under an argon atmosphere. Dry Et₂O (2 mL) and a small piece of iodine were added followed by dropwise addition of a solution of alkyl bromide (1 - 1.5 eq) in dry Et₂O (1 M). The reaction was initiated with a heat gun and refluxed for 1 h. In a separate flask, a solution of the Weinreb amide **58** (1 eq) in dry Et₂O (1 M) was prepared and cooled to -78 °C. The Grignard solution was taken up by syringe and added dropwise to the Weinreb amide solution. After stirring for 2 h at -78 °C the reaction was quenched with sat. aq. NH₄Cl and extracted with Et₂O (2x). The combined organic layers were dried (MgSO₄), filtered and concentrated under reduced pressure. The crude residue was purified using silica gel column chromatography (EtOAc/pentane) affording the α -ketoester.

General procedure B



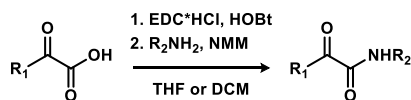
A round bottom flask was charged with α -ketoester (1 eq), DCM (0.3 M) and TFA (5-10 eq) and stirred for 1-24 h at rt. The reaction mixture was concentrated under reduced pressure after TLC analysis showed complete consumption of the starting material, followed by coevaporation with toluene (3x). The obtained α -ketoacid was used in the next step without further purification.

General procedure C



A round bottom flask was charged with α -ketoacid (1 eq) and DMF (0.2 M). HATU or HCTU (1-1.2 eq), DiPEA (1-2 eq) or Et₃N (1-2 eq), and amine (1-1.1 eq) were added and the mixture was stirred for 2-24 h at rt. Water was added and the mixture was extracted with DCM (2x). The combined organic layers were washed with 1 M HCl, sat. aq. NaHCO₃, brine, dried (MgSO₄), filtered and concentrated under reduced pressure. The crude residue was purified by silica gel column chromatography (EtOAc/pentane) affording the α -ketoamide.

General procedure D



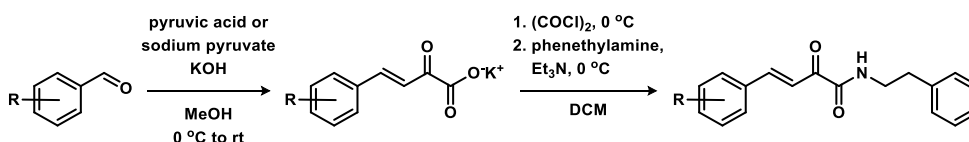
A round bottom flask was charged with α -ketoacid (1 eq) and THF or DCM (0.2 M) at 0 °C. EDC·HCl (1-1.5 eq) and HOBT (1-1.5 eq) were added and the mixture was stirred for 30 min, followed by addition of NMM (optional, 4 eq) and the amine (1.2 eq). The mixture was stirred for 1-4 days warming to rt. Work-up involved addition of sat. aq. NaHCO₃ and extraction with EtOAc (2 x 25 mL). The combined organic layers were washed with brine (1x), dried (MgSO₄), filtered and concentrated under reduced pressure. The crude residue was purified by silica gel column chromatography (EtOAc/pentane) or preparative HPLC affording the α -ketoamide.

General procedure E

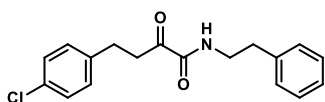


A microwave vial was charged with *N*-Boc-tyramine **64** (1 eq), heteroaryl halide (1 eq), K₂CO₃ (2 eq) in DMSO or DMF (0.2 – 1 M) and capped. The mixture was stirred for 24 - 42 h at 85 °C in an oil bath until TLC showed complete conversion. The mixture was diluted with H₂O and extracted with EtOAc (3x). The combined organic layers were washed with brine (1x), dried (MgSO₄), filtered and concentrated under reduced pressure. The crude residue was purified by silica gel column chromatography (EtOAc/pentane) affording the product.

General procedure F

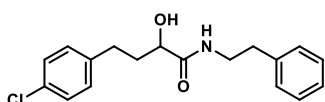


A round bottom flask was charged with pyruvic acid or sodium pyruvate (1 eq), aldehyde (1 eq) and MeOH (1 M) and cooled to 0 °C. A solution of KOH (2 M, 1.5 eq) in MeOH was added dropwise while keeping the temperature below 25 °C. The reaction was stirred at rt overnight, forming a yellow precipitate. The reaction mixture was filtered, the precipitate was washed with cold MeOH (2x), Et₂O (2x) and dried affording the α -ketoacid as the potassium salt. A new round bottom flask was charged with the potassium salt and DCM (0.5 M) and the suspension was sonicated for 20 min. This was followed by cooling to 0 °C and addition of oxalyl chloride (2 eq). After consumption of the potassium salt, the reaction mixture was concentrated under reduced pressure and coevaporated with toluene (2x). The α -ketoacid chloride was then dissolved in DCM (0.5 M) and cooled to 0 °C, followed by addition of phenethylamine (1 eq) and Et₃N (2 eq). The reaction was stirred for 2 h. Work-up involved addition of H₂O and extraction with EtOAc. The organic layer was then washed with 1 M HCl (2x), sat. aq. NaHCO₃ (2x) and brine (1x), dried (MgSO₄), filtered and concentrated under reduced pressure. The crude residue was purified by silica gel column chromatography (EtOAc/pentane) affording the α -ketoamide.

**4-(4-Chlorophenyl)-2-oxo-N-phenethylbutanamide (1).** *t*-Butyl deprotection

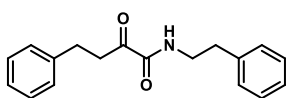
59a: the α -ketoacid was prepared according to general procedure B using α -ketoester **59a** (0.85 g, 3.2 mmol, 1 eq) and TFA (2.5 mL, 32 mmol, 10 eq) affording the α -ketoacid **60a** (0.68 g, 3.2 mmol, quant.). *Amide coupling:* the

title compound was prepared according to general procedure C using the α -ketoacid **60a** (0.68 g, 3.2 mmol, 1 eq), phenethylamine (0.15 mL, 1.2 mmol, 1.1 eq), HATU (1.2 g, 3.2 mmol, 1 eq) and DiPEA (0.61 mL, 3.5 mmol, 1.1 eq) in DMF, affording the product (0.70 g, 2.2 mmol, 70%). $^1\text{H NMR}$ (300 MHz, CDCl_3) δ 7.54 – 6.79 (m, 10H), 3.52 (q, $J = 6.9$ Hz, 2H), 3.21 (t, $J = 7.4$ Hz, 2H), 2.91 – 2.73 (m, 4H). $^{13}\text{C NMR}$ (75 MHz, CDCl_3) δ 197.80, 159.82, 138.78, 138.13, 131.88, 129.71, 128.67, 128.60, 128.51, 126.67, 40.44, 38.06, 35.28, 28.35. HRMS [$\text{C}_{18}\text{H}_{18}\text{NClO}_2 + \text{H}$] $^+$: 316.1099 calculated, 316.1099 found.

**4-(4-Chlorophenyl)-2-hydroxy-N-phenethylbutanamide (23).** A round

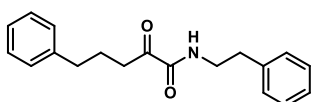
bottom flask was charged with α -ketoamide **1** (70 mg, 0.22 mmol, 1 eq) and THF (1 mL). NaBH_4 (12 mg, 0.33 mmol, 1.5 eq) was added and the mixture was stirred for 15 min. The reaction was quenched with water (10 mL) and

extracted with EtOAc (1 x 10 mL). The organic layer was washed with 1 M aq. HCl (2 x 10 mL), brine (1 x 10 mL), dried (MgSO_4), filtered and concentrated under reduced pressure. Purification by silica gel column chromatography afforded the product (50 mg, 0.16 mmol, 72%). $^1\text{H NMR}$ (400 MHz, CDCl_3) δ 7.34 – 7.25 (m, 2H), 7.25 – 7.14 (m, 5H), 7.08 (d, $J = 8.4$ Hz, 2H), 6.61 (t, $J = 5.4$ Hz, 1H), 4.03 (dd, $J = 7.9, 3.7$ Hz, 1H), 3.66 – 3.40 (m, 2H), 3.24 (br s, 1H), 2.80 (t, $J = 7.0$ Hz, 2H), 2.65 (t, $J = 7.9$ Hz, 2H), 2.11 – 1.97 (m, 1H), 1.90 – 1.80 (m, 1H). $^{13}\text{C NMR}$ (101 MHz, CDCl_3) δ 173.79, 139.74, 138.63, 131.87, 129.93, 128.81, 128.78, 128.65, 126.74, 71.33, 40.33, 36.38, 35.76, 30.57. HRMS [$\text{C}_{18}\text{H}_{20}\text{NClO}_2 + \text{H}$] $^+$: 318.1255 calculated, 318.1252 found.

**2-Oxo-N-phenethyl-4-phenylbutanamide (24).** *t*-Butyl deprotection

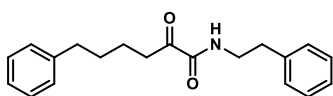
59b: the α -ketoacid was prepared according to general procedure B using α -ketoester **59b** (0.50 g, 2.1 mmol, 1 eq) and TFA (0.80 mL, 32 mmol, 5 eq) affording the α -ketoacid **60b** (0.40 g, 2.1 mmol, quant.). *Amide coupling:* the title compound

was prepared according to general procedure C using the α -ketoacid **60b** (0.20 g, 1.2 mmol, 1 eq), phenethylamine (0.15 mL, 1.2 mmol, 1.1 eq), HCTU (0.48 g, 1.15 mmol, 1 eq) and DiPEA (0.22 mL, 1.3 mmol, 1.1 eq) in DMF, affording the product (80 mg, 0.28 mmol, 24%). $^1\text{H NMR}$ (300 MHz, CDCl_3) δ 7.40 – 7.07 (m, 10H), 7.07 – 6.88 (m, 1H), 3.55 (q, $J = 6.9$ Hz, 2H), 3.26 (t, $J = 7.5$ Hz, 2H), 2.92 (t, $J = 7.5$ Hz, 2H), 2.83 (t, $J = 7.1$ Hz, 2H). $^{13}\text{C NMR}$ (75 MHz, CDCl_3) δ 198.25, 160.05, 140.46, 138.27, 128.85, 128.77, 128.60, 128.46, 126.85, 126.36, 40.58, 38.40, 35.51, 29.22. HRMS [$\text{C}_{18}\text{H}_{19}\text{NO}_2 + \text{H}$] $^+$: 282.1489 calculated, 282.1487 found.

**2-Oxo-N-phenethyl-5-phenylpentanamide (25).** The title compound was

prepared according to general procedure C using the α -ketoacid **60c** (0.12 g, 0.63 mmol, 1 eq), phenethylamine (86 μL , 0.69 mmol, 1.1 eq), HCTU (0.26 g, 0.63 mmol, 1 eq) and DiPEA (0.12 mL, 0.70 mmol, 1.1 eq) in DCM, affording

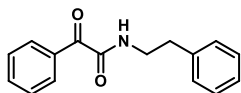
the product (70 mg, 0.24 mmol, 38%). $^1\text{H NMR}$ (400 MHz, CDCl_3) δ 7.34 – 7.20 (m, 5H), 7.20 – 7.13 (m, 5H), 6.98 (br s, 1H), 3.53 (q, $J = 7.0$ Hz, 2H), 2.92 (t, $J = 7.3$ Hz, 2H), 2.83 (t, $J = 7.1$ Hz, 2H), 2.64 (t, $J = 7.6$ Hz, 2H), 1.92 (p, $J = 7.4$ Hz, 2H). $^{13}\text{C NMR}$ (101 MHz, CDCl_3) δ 198.97, 160.15, 141.42, 138.30, 128.83, 128.75, 128.57, 128.51, 126.83, 126.12, 40.56, 36.20, 35.52, 35.12, 24.92. HRMS [$\text{C}_{19}\text{H}_{21}\text{NO}_2 + \text{H}$] $^+$: 296.1645 calculated, 296.1646 found.

**2-Oxo-N-phenethyl-6-phenylhexanamide (26).** *t*-Butyl deprotection

59d: the α -ketoacid was prepared according to general procedure B using α -ketoester **59d** (0.33 g, 1.3 mmol, 1 eq) and TFA (1.9 mL, 25 mmol, 19 eq) affording the α -ketoacid **60d** (0.26 g, 1.3 mmol, quant.). *Amide coupling:*

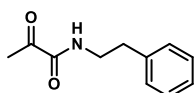
the title compound was prepared according to general procedure C using the α -ketoacid **60d** (0.26 g, 1.3 mmol, 1 eq), phenethylamine (0.22 mL, 1.72 mmol, 1.3 eq), HATU (0.59 g, 1.56 mmol, 1.2 eq) and DiPEA

(0.30 mL, 1.72 mmol, 1.3 eq), affording the product (0.34 g, 1.11 mmol, 71%). ^1H NMR (300 MHz, CDCl_3) δ 7.43 – 7.08 (m, 10H), 7.09 – 6.89 (m, 1H), 3.52 (q, J = 6.9 Hz, 2H), 3.01 – 2.86 (m, 2H), 2.81 (t, J = 7.1 Hz, 2H), 2.61 (t, J = 7.0 Hz, 2H), 1.62 (p, J = 3.5 Hz, 4H). ^{13}C NMR (75 MHz, CDCl_3) δ 198.99, 160.11, 142.05, 138.25, 128.74, 128.68, 128.40, 128.34, 126.73, 125.81, 40.50, 36.55, 35.62, 35.42, 30.79, 22.81. HRMS [$\text{C}_{20}\text{H}_{23}\text{NO}_2 + \text{H}$] $^+$: 310.1802 calculated, 310.1801 found.



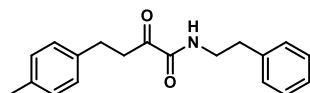
2-Oxo-N-phenethyl-2-phenylacetamide (27). *t*-Butyl deprotection **59e**: the α -ketoacid was prepared according to general procedure B using α -ketoester **59e** (0.68 g, 3.3 mmol, 1 eq) and TFA (2.4 mL, 32 mmol, 10 eq) affording the α -ketoacid **60e** (0.58 g, 3.2 mmol, quant.).

Amide coupling: the title compound was prepared according to general procedure C using the α -ketoacid **60e** (0.25 g, 1.7 mmol, 1 eq), phenethylamine (0.23 mL, 1.8 mmol, 1.1 eq), HCTU (0.69 g, 1.7 mmol, 1 eq) and DIPEA (0.32 mL, 1.8 mmol, 1.1 eq) in DCM, affording the product (0.22 g, 0.86 mmol, 52%). ^1H NMR (400 MHz, CDCl_3) δ 8.33 – 8.19 (m, 2H), 7.62 – 7.52 (m, 1H), 7.47 – 7.38 (m, 2H), 7.34 – 7.26 (m, 2H), 7.26 – 7.14 (m, 4H), 3.62 (q, J = 7.0 Hz, 2H), 2.88 (t, J = 7.2 Hz, 2H). ^{13}C NMR (101 MHz, CDCl_3) δ 187.86, 161.98, 138.36, 134.36, 133.30, 131.11, 128.75, 128.72, 128.47, 126.68, 40.60, 35.46. HRMS [$\text{C}_{16}\text{H}_{15}\text{NO}_2 + \text{H}$] $^+$: 254.1176 calculated, 254.1175 found.



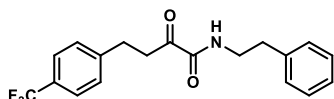
2-Oxo-N-phenethylpropanamide (28). A round bottom flask was charged with pyruvic acid (0.79 mL, 12 mmol, 1 eq) and cooled to 0 °C. Thionyl chloride (0.93 mL, 13 mmol, 1.1 eq) was added and the mixture was stirred for 3 h at rt. The reaction mixture was concentrated under reduced pressure and coevaporated with toluene (3x). The acid chloride was dissolved in DCM (50 mL) and cooled to 0 °C. Phenethylamine (1.5 mL, 12 mmol, 1 eq) and Et_3N (1.8 mL, 13 mmol, 1.1 eq) were added and the reaction was stirred for 2 h. Work-up involved addition of H_2O and extraction with EtOAc. The organic layer was then washed with 1 M HCl (2x), sat. aq. NaHCO_3 (2x) and brine (1x), dried (MgSO_4), filtered and concentrated under reduced pressure. The crude residue was purified by silica gel column chromatography (EtOAc/pentane) affording the product (100 mg, 0.52 mmol, 4%).

^1H NMR (300 MHz, CDCl_3) δ 7.43 – 7.15 (m, 5H), 7.13 – 6.82 (m, 1H), 3.57 (q, J = 7.0 Hz, 2H), 2.87 (t, J = 7.1 Hz, 2H), 2.47 (s, 3H). ^{13}C NMR (101 MHz, CDCl_3) δ 197.16, 160.18, 138.27, 128.88, 128.78, 126.87, 40.65, 35.54, 24.58. HRMS [$\text{C}_{11}\text{H}_{13}\text{NO}_2 + \text{H}$] $^+$: 192.1019 calculated, 192.1019 found.



2-Oxo-N-phenethyl-4-(*p*-tolyl)butanamide (29). *t*-Butyl deprotection **59f**: the α -ketoacid was prepared according to general procedure B using α -ketoester **59f** (0.54 g, 2.2 mmol, 1 eq) and TFA (1.6 mL, 22 mmol, 10 eq) affording the α -ketoacid **60f** (0.42 g, 2.2 mmol, quant.).

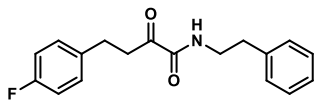
Amide coupling: the title compound was prepared according to general procedure C using the α -ketoacid **60f** (0.42 g, 2.2 mmol, 1 eq), phenethylamine (0.30 mL, 2.4 mmol, 1.1 eq), HATU (0.83 g, 2.2 mmol, 1 eq) and DIPEA (0.42 mL, 2.4 mmol, 1.1 eq) in DCM, affording the product (0.48 g, 1.6 mmol, 74%). ^1H NMR (300 MHz, CDCl_3) δ 7.32 – 7.23 (m, 2H), 7.23 – 7.18 (m, 1H), 7.18 – 7.11 (m, 2H), 7.11 – 6.97 (m, 5H), 3.51 (q, J = 6.9 Hz, 2H), 3.21 (t, J = 7.5 Hz, 2H), 2.97 – 2.69 (m, 4H), 2.28 (s, 3H). ^{13}C NMR (75 MHz, CDCl_3) δ 198.18, 159.96, 138.21, 137.24, 135.61, 129.12, 128.66, 128.62, 128.18, 126.64, 40.44, 38.37, 35.33, 28.64, 20.97. HRMS [$\text{C}_{19}\text{H}_{21}\text{NO}_2 + \text{H}$] $^+$: 296.1645 calculated, 296.1643 found.



2-Oxo-N-phenethyl-4-(4-(trifluoromethyl)phenyl)butanamide (30). *t*-Butyl deprotection **59g**: the α -ketoacid was prepared according to general procedure B using α -ketoester **59g** (0.25 g, 0.83 mmol, 1 eq) and TFA (0.62 mL, 8.3 mmol, 10 eq) affording the α -ketoacid **60g** (0.20 g, 0.83 mmol, quant.).

Amide coupling: The title compound was prepared according to general procedure C using the α -ketoacid **60g** (0.20 g, 0.80 mmol, 1 eq), phenethylamine (0.11 mL, 0.88 mmol, 1.1 eq), HATU (0.38 g, 0.80 mmol, 1 eq) and DIPEA (0.15 mL, 0.80 mmol, 1.1 eq) in DMF. Column chromatography (20% -> 60% EtOAc in pentane) afforded the product (0.22 g, 0.64 mmol, 80%). ^1H NMR (400 MHz, CDCl_3) δ 7.57 (d, J = 8.1 Hz, 2H),

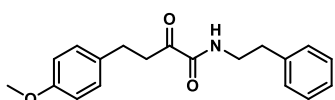
7.39 – 7.31 (m, 4H), 7.31 – 7.25 (m, 1H), 7.25 – 7.19 (m, 2H), 7.12 – 7.00 (m, 1H), 3.60 (q, $J = 7.0$ Hz, 2H), 3.32 (t, $J = 7.4$ Hz, 2H), 3.01 (t, $J = 7.4$ Hz, 2H), 2.88 (t, $J = 7.1$ Hz, 2H). ^{13}C NMR (101 MHz, CDCl_3) δ 197.70, 159.88, 144.56 (q, $J = 1.3$ Hz), 138.19, 128.78, 128.70, 128.48, 126.80, 125.46 (q, $J = 3.8$ Hz), 124.31 (q, $J = 271.8$ Hz), 40.55, 37.89, 35.39, 28.89. HRMS [$\text{C}_{19}\text{H}_{18}\text{F}_3\text{NO}_2 + \text{H}$] $^+$: 350.1362 calculated, 350.1362 found.



4-(4-Fluorophenyl)-2-oxo-*N*-phenethylbutanamide (31). *t*-Butyl deprotection

59h: the α -ketoacid was prepared according to general procedure B using α -ketoester **59h** (0.15 g, 0.59 mmol, 1 eq) and TFA (0.44 mL, 5.9 mmol, 10 eq) affording the α -ketoacid **60h** (0.12 g, 0.59 mmol, quant.). *Amide coupling:*

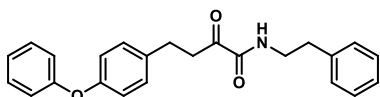
the title compound was prepared according to general procedure C using the α -ketoacid **60h** (0.12 g, 0.63 mmol, 1 eq), phenethylamine (80 μL , 0.63 mmol, 1 eq), HCTU (0.26 g, 0.63 mmol, 1 eq) and DiPEA (0.12 mL, 0.69 mmol, 1.1 eq) in DMF, affording the product (0.12 g, 0.39 mmol, 62%). ^1H NMR (300 MHz, CDCl_3) δ 7.35 – 7.21 (m, 3H), 7.21 – 7.08 (m, 4H), 7.08 – 6.99 (m, 1H), 6.99 – 6.88 (m, 2H), 3.54 (q, $J = 6.9$ Hz, 2H), 3.22 (t, $J = 7.4$ Hz, 2H), 2.99 – 2.64 (m, 4H). ^{13}C NMR (75 MHz, CDCl_3) δ 198.05, 163.13, 159.97, 138.22, 136.05 (d, $J = 3.2$ Hz), 129.85 (d, $J = 7.9$ Hz), 128.77 (d, $J = 6.8$ Hz), 126.82, 115.32 (d, $J = 21.2$ Hz), 40.55, 38.44, 35.44, 28.39. HRMS [$\text{C}_{18}\text{H}_{18}\text{FNO}_2 + \text{H}$] $^+$: 300.1394 calculated, 300.1393 found.



4-(4-Methoxyphenyl)-2-oxo-*N*-phenethylbutanamide (32). A round

bottom flask was charged with unsaturated α -ketoamide **39** (0.10 g, 0.32 mmol, 1 eq) and MeOH (1 mL) and flushed with N_2 . Pd/C (10 wt. %, 10 mg, 9.4 μmol , 3 mol%) was added and the flask was purged again with N_2 ,

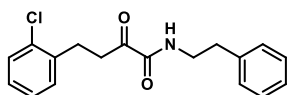
followed by H_2 and the reaction was stirred overnight under a H_2 atmosphere (balloon). The reaction was filtered over Celite, which was washed with MeOH and the filtrate was concentrated under reduced pressure. The crude residue was purified by silica gel column chromatography (EtOAc/pentane) affording the product (50 mg, 0.16 mmol, 50%). ^1H NMR (400 MHz, CDCl_3) δ 7.36 – 7.27 (m, 2H), 7.27 – 7.21 (m, 1H), 7.18 (d, $J = 7.0$ Hz, 2H), 7.11 (d, $J = 8.6$ Hz, 2H), 7.05 – 6.90 (m, 1H), 6.88 – 6.71 (m, 2H), 3.77 (s, 3H), 3.55 (q, $J = 7.0$ Hz, 2H), 3.22 (t, $J = 7.5$ Hz, 2H), 2.95 – 2.73 (m, 4H). ^{13}C NMR (101 MHz, CDCl_3) δ 198.37, 160.05, 158.13, 138.26, 132.48, 129.41, 128.86, 128.77, 126.85, 113.99, 55.35, 40.57, 38.67, 35.51, 28.38. HRMS [$\text{C}_{19}\text{H}_{21}\text{NO}_3 + \text{H}$] $^+$: 312.1594 calculated, 312.1593 found.



2-Oxo-*N*-phenethyl-4-(4-phenoxyphenyl)butanamide (33). A round

bottom flask was charged with unsaturated α -ketoamide **67** (0.12 g, 0.33 mmol, 1 eq) and MeOH (1 mL) and flushed with N_2 . Pd/C (10 wt. %, 10 mg, 9.4 μmol , 3 mol%) was added and the flask was purged again

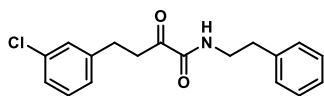
with N_2 , followed by H_2 and the reaction was stirred overnight under a H_2 atmosphere (balloon). The reaction was filtered over Celite, which was washed with MeOH and the filtrate was concentrated under reduced pressure. The ketone was overreduced to the alcohol according to NMR analysis, therefore it was reoxidized. A round bottom flask was charged with the alcohol, Dess-Martin periodinane (0.21 g, 0.49 mmol, 1.5 eq) and DCM (5 mL) and stirred at rt. Work-up involved addition of H_2O and extraction with EtOAc. The organic layer was washed with 1 M HCl (2x), sat. aq. NaHCO_3 (2x) and brine (1x), dried (MgSO_4), filtered and concentrated under reduced pressure. The crude residue was purified by silica gel column chromatography (EtOAc/pentane) affording the product (80 mg, 0.23 mmol, 65%). ^1H NMR (400 MHz, CDCl_3) δ 7.36 – 7.27 (m, 4H), 7.27 – 7.20 (m, 1H), 7.20 – 7.11 (m, 4H), 7.11 – 7.04 (m, 1H), 7.04 – 6.95 (m, 3H), 6.95 – 6.88 (m, 2H), 3.55 (q, $J = 7.0$ Hz, 2H), 3.25 (t, $J = 7.5$ Hz, 2H), 2.90 (t, $J = 7.5$ Hz, 2H), 2.84 (t, $J = 7.1$ Hz, 2H). ^{13}C NMR (101 MHz, CDCl_3) δ 198.20, 160.01, 157.51, 155.62, 138.23, 135.36, 129.79, 129.71, 128.85, 128.76, 126.85, 123.16, 119.14, 118.74, 40.58, 38.55, 35.49, 28.49. HRMS [$\text{C}_{24}\text{H}_{23}\text{NO}_3 + \text{H}$] $^+$: 374.1751 calculated, 374.1748 found.



4-(2-Chlorophenyl)-2-oxo-N-phenethylbutanamide (34). *t*-Butyl deprotection

59i: the α -ketoacid was prepared according to general procedure B using α -ketoester **59i** (0.23 g, 0.87 mmol, 1 eq) and TFA (0.94 mL, 13 mmol, 15 eq) affording the α -ketoacid **60i** (0.18 g, 0.87 mmol, quant.).

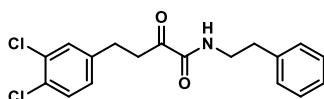
Amide coupling: the title compound was prepared according to general procedure C using the α -ketoacid **60i** (0.18 g, 0.87 mmol, 1 eq), phenethylamine (0.12 mL, 0.95 mmol, 1.1 eq), HATU (0.33 g, 0.87 mmol, 1 eq) and DiPEA (0.16 mL, 0.95 mmol, 1.1 eq) in DCM, affording the product (0.13 g, 0.42 mmol, 48%). ^1H NMR (300 MHz, CDCl_3) δ 7.50 – 7.08 (m, 9H), 7.08 – 6.89 (m, 1H), 3.55 (q, J = 6.9 Hz, 2H), 3.27 (t, J = 7.5 Hz, 2H), 3.01 (t, J = 7.4 Hz, 2H), 2.84 (t, J = 7.1 Hz, 2H). ^{13}C NMR (75 MHz, CDCl_3) δ 197.96, 159.93, 138.24, 138.01, 134.04, 130.52, 129.65, 128.82, 128.74, 127.92, 126.96, 126.82, 40.56, 36.78, 35.48, 27.23. HRMS [$\text{C}_{18}\text{H}_{18}\text{ClNO}_2 + \text{H}$] $^+$: 316.1099 calculated, 316.1100 found.



4-(3-Chlorophenyl)-2-oxo-N-phenethylbutanamide (35). *t*-Butyl deprotection

59j: the α -ketoacid was prepared according to general procedure B using α -ketoester **59j** (0.55 g, 2.0 mmol, 1 eq) and TFA (2 mL, 26 mmol, 13 eq) affording the α -ketoacid **60j** (0.47 g, 2.0 mmol, quant.).

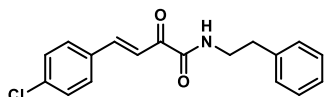
Amide coupling: The title compound was prepared according to general procedure C using the α -ketoacid **60j** (0.47 g, 2.0 mmol, 1 eq), phenethylamine (0.31 mL, 2.4 mmol, 1.2 eq), HATU (0.84 mg, 2.2 mmol, 1.1 eq) and DiPEA (0.42 mL, 2.4 mmol, 1.2 eq), affording the product (0.37 g, 1.2 mmol, 53%). ^1H NMR (300 MHz, CDCl_3) δ 7.73 – 6.73 (m, 10H), 3.58 (q, J = 6.9 Hz, 2H), 3.28 (t, J = 7.4 Hz, 2H), 3.07 – 2.74 (m, 4H). ^{13}C NMR (75 MHz, CDCl_3) δ 197.71, 159.83, 142.40, 138.16, 134.13, 129.72, 128.69, 128.62, 128.53, 126.69, 126.55, 126.42, 40.47, 37.95, 35.32, 28.65. HRMS [$\text{C}_{18}\text{H}_{18}\text{ClNO}_2 + \text{H}$] $^+$: 316.1099 calculated, 316.1098 found.



4-(3,4-Dichlorophenyl)-2-oxo-N-phenethylbutanamide (36). *t*-Butyl deprotection

59k: the α -ketoacid was prepared according to general procedure B using α -ketoester **59k** (90 mg, 0.30 mmol, 1 eq) and TFA (0.25 mL, 32 mmol, 10 eq) affording the α -ketoacid **60k** (74 mg, 0.30 mmol, quant.).

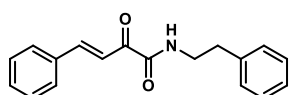
Amide coupling: the title compound was prepared according to general procedure C using α -ketoacid **60k** (66 mg, 0.27 mmol, 1 eq), phenethylamine (36 μL , 0.29 mmol, 1.1 eq), HATU (110 mg, 0.29 mmol, 1.1 eq) and DiPEA (92 μL , 0.53 mmol, 2 eq) in DCM, affording the product (42 mg, 0.12 mmol, 44%). ^1H NMR (400 MHz, CDCl_3) δ 7.41 – 7.32 (m, 4H), 7.32 – 7.26 (m, 1H), 7.22 (d, J = 7.0 Hz, 2H), 7.07 (dd, J = 8.2, 2.0 Hz, 1H), 7.05 – 6.97 (m, 1H), 3.60 (q, J = 7.0 Hz, 2H), 3.28 (t, J = 7.4 Hz, 2H), 3.03 – 2.79 (m, 4H). ^{13}C NMR (101 MHz, CDCl_3) δ 197.63, 159.85, 140.68, 138.17, 132.46, 130.53, 130.50, 130.39, 128.88, 128.76, 127.98, 126.90, 40.61, 37.94, 35.49, 28.29. HRMS [$\text{C}_{18}\text{H}_{17}\text{Cl}_2\text{NO}_2 + \text{H}$] $^+$: 350.0709 calculated, 350.0708 found.



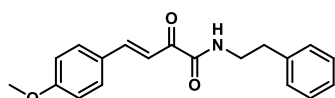
(E)-4-(4-Chlorophenyl)-2-oxo-N-phenethylbut-3-enamide (37). α -Ketoacid

formation: the α -ketoacid salt was prepared according to general procedure F using pyruvic acid (1.7 mL, 18 mmol, 1 eq), 4-chlorobenzaldehyde (2.2 mL, 19 mmol, 1 eq), KOH (2.1 g, 38 mmol, 2 eq) in MeOH affording potassium 4-

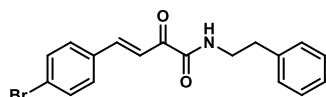
(4-chlorophenyl)-2-oxobut-3-enoate **62a** (2.0 g, 8.0 mmol, 42%). *Amide coupling*: the title compound was prepared according to general procedure F using potassium salt **62a** (2.0 g, 8.0 mmol, 1 eq), oxalyl chloride (1.4 mL, 16 mmol, 2 eq), phenethylamine (1.1 mL, 8.8 mmol, 1.1 eq) and Et_3N (2.2 mL, 16 mmol, 2 eq) in DCM, affording the product (0.30 g, 0.96 mmol, 12%). ^1H NMR (300 MHz, CDCl_3) δ 7.86 (d, J = 16.2 Hz, 1H), 7.73 (d, J = 16.1 Hz, 1H), 7.59 (d, J = 8.5 Hz, 2H), 7.43 – 7.36 (m, 2H), 7.36 – 7.28 (m, 2H), 7.28 – 7.17 (m, 4H), 3.63 (q, J = 7.0 Hz, 2H), 2.89 (t, J = 7.1 Hz, 2H). ^{13}C NMR (75 MHz, CDCl_3) δ 185.32, 161.24, 146.51, 138.34, 137.61, 132.94, 130.37, 129.48, 128.87, 128.81, 126.86, 119.09, 40.77, 35.58. HRMS [$\text{C}_{18}\text{H}_{16}\text{ClNO}_2 + \text{H}$] $^+$: 314.0942 calculated, 314.0939 found.



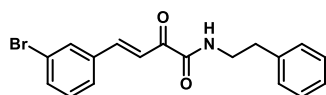
(E)-2-Oxo-*N*-phenethyl-4-phenylbut-3-enamide (38). *α -Ketoacid formation:* the α -ketoacid salt was prepared according to general procedure F using pyruvic acid (0.79 mL, 11 mmol, 1 eq), benzaldehyde (1.2 g, 11 mmol, 1 eq), KOH (0.98 g, 17 mmol, 1.5 eq) in MeOH affording potassium 2-oxo-4-phenylbut-3-enoate **62b** (0.85 g, 3.9 mmol, 36%). *Amide coupling:* the title compound was prepared according to general procedure C using potassium salt **62b** (0.20 g, 0.93 mmol, 1 eq), phenethylamine (0.12 mL, 0.93 mmol, 1 eq), HCTU (0.39 g, 0.93 mmol, 1 eq) and DiPEA (0.32 mL, 1.86 mmol, 2 eq) in DMF (5 mL) affording the product (70 mg, 0.25 mmol, 27%). ^1H NMR (300 MHz, CDCl_3) δ 7.93 (d, J = 16.2 Hz, 1H), 7.77 (d, J = 16.1 Hz, 1H), 7.71 – 7.62 (m, 2H), 7.49 – 7.37 (m, 3H), 7.36 – 7.16 (m, 6H), 3.63 (q, J = 7.0 Hz, 2H), 2.89 (t, J = 7.1 Hz, 2H). ^{13}C NMR (75 MHz, CDCl_3) δ 185.49, 161.38, 148.12, 138.40, 134.48, 131.60, 129.28, 129.15, 128.85, 128.82, 126.83, 118.67, 40.76, 35.61. HRMS [$\text{C}_{18}\text{H}_{17}\text{NO}_2 + \text{H}$] $^+$: 280.1332 calculated, 280.1331 found.



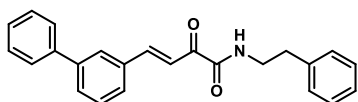
(E)-4-(4-Methoxyphenyl)-2-oxo-*N*-phenethylbut-3-enamide (39). *α -Ketoacid formation:* the α -ketoacid salt was prepared according to general procedure F using sodium pyruvate (3.0 g, 27 mmol, 1 eq), 4-methoxybenzaldehyde (3.3 mL, 27 mmol, 1 eq), KOH (2.3 g, 41 mmol, 1.5 eq) in MeOH affording potassium 4-(4-methoxyphenyl)-2-oxobut-3-enoate **62c** (6.5 g, 27 mmol, 98%). *Amide coupling:* the title compound was prepared according to general procedure F using potassium salt **62c** (1.0 g, 4.1 mmol, 1 eq), oxalyl chloride (0.87 mL, 8.2 mmol, 2 eq), phenethylamine (0.52 mL, 4.1 mmol, 1 eq) and Et_3N (1.1 mL, 8.2 mmol, 2 eq) in DCM, affording the product (1.2 g, 3.8 mmol, 93%). ^1H NMR (400 MHz, CDCl_3) δ 7.89 (d, J = 16.0 Hz, 1H), 7.68 – 7.57 (m, 3H), 7.37 – 7.27 (m, 3H), 7.26 – 7.18 (m, 3H), 6.95 – 6.88 (m, 2H), 3.83 (s, 3H), 3.61 (q, J = 7.0 Hz, 2H), 2.88 (t, J = 7.2 Hz, 2H). ^{13}C NMR (101 MHz, CDCl_3) δ 185.15, 162.54, 161.66, 147.93, 138.44, 131.23, 128.76, 127.27, 126.72, 116.20, 114.59, 55.50, 40.69, 35.56. HRMS [$\text{C}_{19}\text{H}_{19}\text{NO}_3 + \text{H}$] $^+$: 310.1438 calculated, 310.1435 found.



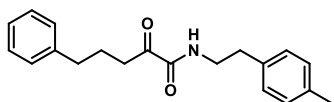
(E)-4-(4-Bromophenyl)-2-oxo-*N*-phenethylbut-3-enamide (40). *α -Ketoacid formation:* the α -ketoacid salt was prepared according to general procedure F using pyruvic acid (1.4 mL, 16 mmol, 1 eq), 4-bromobenzaldehyde (1.6 mL, 16 mmol, 1 eq), KOH (1.8 g, 32 mmol, 2 eq) in MeOH affording potassium 4-(4-bromophenyl)-2-oxobut-3-enoate **62d** (2.0 g, 6.8 mmol, 42%). *Amide coupling:* the title compound was prepared according to general procedure F using potassium salt **62d** (2.0 g, 6.8 mmol, 1 eq), oxalyl chloride (1.2 mL, 14 mmol, 2 eq), phenethylamine (0.94 mL, 7.5 mmol, 1.1 eq) and Et_3N (1.90 mL, 14 mmol, 2 eq) in DCM, affording the product (0.84 g, 2.3 mmol, 34%). ^1H NMR (300 MHz, CDCl_3) δ 7.84 (d, J = 16.2 Hz, 1H), 7.74 (d, J = 16.1 Hz, 1H), 7.64 – 7.42 (m, 4H), 7.38 – 7.15 (m, 6H), 3.62 (q, J = 7.0 Hz, 2H), 2.89 (t, J = 7.1 Hz, 2H). ^{13}C NMR (75 MHz, CDCl_3) δ 185.37, 161.22, 146.55, 138.35, 133.37, 132.45, 130.52, 128.87, 128.81, 126.86, 126.08, 119.23, 40.77, 35.60. HRMS [$\text{C}_{18}\text{H}_{16}\text{BrNO}_2 + \text{H}$] $^+$: 358.0437 calculated, 358.0437 found.



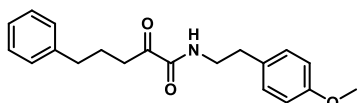
(E)-4-(3-Bromophenyl)-2-oxo-*N*-phenethylbut-3-enamide (41). *α -Ketoacid formation:* the α -ketoacid salt was prepared according to general procedure F using sodium pyruvate (1.0 g, 11 mmol, 1 eq), 3-bromobenzaldehyde (1.3 mL, 11 mmol, 1 eq), KOH (0.96 g, 17 mmol, 1.5 eq) in MeOH affording potassium 4-(3-bromophenyl)-2-oxobut-3-enoate **62e** (0.40 g, 1.4 mmol, 12%). *Amide coupling:* the title compound was prepared according to general procedure F using potassium salt **62e** (0.40 g, 1.4 mmol, 1 eq), oxalyl chloride (0.24 mL, 2.7 mmol, 2 eq), phenethylamine (0.19 mL, 1.5 mmol, 1.1 eq) and Et_3N (0.38 mL, 2.7 mmol, 2 eq) in DCM, affording the product (0.31 g, 0.87 mmol, 62%). ^1H NMR (400 MHz, CDCl_3) δ 7.86 – 7.78 (m, 2H), 7.74 (d, J = 16.2 Hz, 1H), 7.62 – 7.51 (m, 2H), 7.37 – 7.28 (m, 3H), 7.28 – 7.19 (m, 4H), 3.63 (q, J = 7.0 Hz, 2H), 2.89 (t, J = 7.1 Hz, 2H). ^{13}C NMR (101 MHz, CDCl_3) δ 185.33, 161.12, 146.13, 138.34, 136.52, 134.25, 131.84, 130.63, 128.88, 128.82, 127.72, 126.88, 123.27, 119.96, 40.78, 35.59. HRMS [$\text{C}_{18}\text{H}_{16}\text{BrNO}_2 + \text{H}$] $^+$: 358.0437 calculated, 358.0437 found.



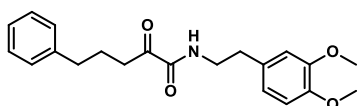
(E)-4-([1,1'-Biphenyl]-3-yl)-2-oxo-N-phenethylbut-3-enamide (42). A round bottom flask was charged with aryl bromide **41** (0.20 g, 0.56 mmol, 1 eq) and toluene/EtOH (4:1, 3 mL) and degassed for 20 min with sonication. Pd(PPh₃)₄ (13 mg, 0.01 mmol, 2 mol%), phenylboronic acid (0.10 g, 0.84 mmol, 1.5 eq) and K₂CO₃ (0.46 g, 3.4 mmol, 6 eq) were added and the reaction was stirred for 16 h at 80 °C. The reaction mixture was filtered over a pad of Celite and concentrated under reduced pressure. The crude residue was purified by silica gel column chromatography (EtOAc/pentane) affording the product (0.15 g, 0.42 mmol, 75%). ¹H NMR (300 MHz, CDCl₃) δ 8.03 (d, *J* = 16.2 Hz, 1H), 7.94 – 7.78 (m, 2H), 7.73 – 7.18 (m, 14H), 3.67 (q, *J* = 6.9 Hz, 2H), 2.93 (t, *J* = 7.1 Hz, 2H). ¹³C NMR (75 MHz, CDCl₃) δ 185.46, 161.38, 148.00, 142.21, 140.23, 138.39, 134.95, 130.35, 129.57, 129.02, 128.85, 128.81, 128.04, 127.94, 127.91, 127.24, 126.82, 118.96, 40.76, 35.59. HRMS [C₂₄H₂₁NO₂ + H]⁺: 356.1645 calculated, 356.1641 found.



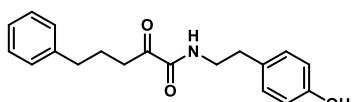
N-(4-Methylphenethyl)-2-oxo-5-phenylpentanamide (43). The title compound was prepared according to general procedure D using α-ketoacid **60c** (57 mg, 0.29 mmol, 1 eq), 2-(*p*-tolyl)ethan-1-amine (47 μL, 0.32 mmol, 1.1 eq), EDC·HCl (85 mg, 0.44 mmol, 1.5 eq), HOBT (60 mg, 0.44 mmol, 1.5 eq) in DCM. Column chromatography (2.5% → 20% EtOAc in pentane) afforded the product (18 mg, 58 μmol, 20%). ¹H NMR (400 MHz, CDCl₃) δ 7.39 – 7.22 (m, 3H), 7.22 – 7.14 (m, 3H), 7.12 (d, *J* = 7.9 Hz, 2H), 7.07 (d, *J* = 8.0 Hz, 2H), 7.01 – 6.86 (m, 1H), 3.52 (q, *J* = 7.0 Hz, 2H), 2.93 (t, *J* = 7.3 Hz, 2H), 2.80 (t, *J* = 7.1 Hz, 2H), 2.65 (t, *J* = 7.6 Hz, 2H), 2.32 (s, 3H), 1.93 (p, *J* = 7.5 Hz, 2H). ¹³C NMR (75 MHz, CDCl₃) δ 199.02, 160.11, 141.47, 136.44, 135.16, 129.56, 128.65, 128.61, 128.56, 126.21, 126.16, 40.68, 36.24, 35.13, 24.94, 21.18. HRMS [C₂₀H₂₃NO₂ + H]⁺: 310.1802 calculated, 310.1803 found.



N-(4-Methoxyphenethyl)-2-oxo-5-phenylpentanamide (44). The title compound was prepared according to general procedure D using α-ketoacid **60c** (89 mg, 0.46 mmol, 1 eq), 2-(4-methoxyphenyl)ethan-1-amine (75 μL, 0.51 mmol, 1.1 eq), EDC·HCl (0.13 g, 0.69 mmol, 1.5 eq), HOBT (94 mg, 0.69 mmol, 1.5 eq) in DCM. Column chromatography (2.5% → 40% EtOAc in pentane) afforded the product (13 mg, 40 μmol, 9%). ¹H NMR (300 MHz, CDCl₃) δ 7.32 – 7.24 (m, 2H), 7.23 – 7.14 (m, 3H), 7.10 (d, *J* = 8.6 Hz, 2H), 7.04 – 6.90 (m, 1H), 6.85 (d, *J* = 8.6 Hz, 2H), 3.79 (s, 3H), 3.50 (q, *J* = 6.9 Hz, 2H), 2.94 (t, *J* = 7.3 Hz, 2H), 2.78 (t, *J* = 7.1 Hz, 2H), 2.65 (t, *J* = 7.6 Hz, 2H), 1.93 (p, *J* = 7.5 Hz, 2H). ¹³C NMR (75 MHz, CDCl₃) δ 199.03, 160.10, 158.52, 141.45, 130.25, 129.75, 128.60, 128.54, 126.15, 114.27, 55.39, 40.77, 36.23, 35.14, 34.65, 24.94. HRMS [C₂₀H₂₃NO₃ + H]⁺: 326.1751 calculated, 326.1752 found.

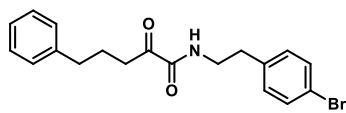


N-(3,4-Dimethoxyphenethyl)-2-oxo-5-phenylpentanamide (45). The title compound was prepared according to general procedure D using α-ketoacid **60c** (57 mg, 0.30 mmol, 1 eq), 2-(3,4-dimethoxyphenyl)ethan-1-amine (56 μL, 0.33 mmol, 1.1 eq), EDC·HCl (86 mg, 0.45 mmol, 1.5 eq), HOBT (61 mg, 0.45 mmol, 1.5 eq) in DCM. Column chromatography (2.5% → 40% EtOAc in pentane) afforded the product (6 mg, 17 μmol, 6%). ¹H NMR (400 MHz, CDCl₃) δ 7.31 – 7.26 (m, 2H), 7.22 – 7.11 (m, 3H), 7.03 – 6.91 (m, 1H), 6.81 (d, *J* = 8.1 Hz, 1H), 6.77 – 6.66 (m, 2H), 3.87 (s, 3H), 3.86 (s, 3H), 3.52 (q, *J* = 7.0 Hz, 2H), 2.94 (t, *J* = 7.3 Hz, 2H), 2.78 (t, *J* = 7.1 Hz, 2H), 2.65 (t, *J* = 7.6 Hz, 2H), 1.93 (p, *J* = 7.5 Hz, 2H). ¹³C NMR (75 MHz, CDCl₃) δ 199.04, 160.13, 149.01, 147.96, 141.44, 130.77, 128.56, 126.17, 120.73, 111.86, 111.53, 56.02, 40.69, 36.25, 35.16, 24.95. HRMS [C₂₁H₂₅NO₄ + H]⁺: 356.1856 calculated, 356.1858 found.

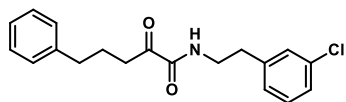


N-(4-Hydroxyphenethyl)-2-oxo-5-phenylpentanamide (46). The title compound was prepared according to general procedure D using α-ketoacid **60c** (98 mg, 0.51 mmol, 1 eq), 4-(2-aminoethyl)phenol (77 mg, 0.56 mmol, 1.1 eq), EDC·HCl (0.15 g, 0.77 mmol, 1.5 eq), HOBT (0.10 g, 0.77 mmol, 1.5 eq) in DCM. Column chromatography (10% → 60% EtOAc in pentane) afforded the product

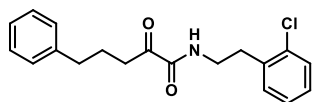
(18 mg, 58 μ mol, 20%). ^1H NMR (400 MHz, CDCl_3) δ 7.32 – 7.23 (m, 2H), 7.23 – 7.12 (m, 3H), 7.04 (d, J = 8.5 Hz, 2H), 7.01 – 6.90 (m, 1H), 6.83 – 6.72 (m, 2H), 5.26 (br s, 1H), 3.50 (q, J = 7.0 Hz, 2H), 2.93 (t, J = 7.3 Hz, 2H), 2.76 (t, J = 7.1 Hz, 2H), 2.64 (t, J = 7.6 Hz, 2H), 1.93 (p, J = 7.5 Hz, 2H). ^{13}C NMR (75 MHz, CDCl_3) δ 198.97, 160.18, 154.71, 141.43, 130.14, 129.92, 128.61, 128.55, 126.16, 115.75, 40.84, 36.27, 35.13, 34.65, 24.95. HRMS [$\text{C}_{19}\text{H}_{21}\text{NO}_3 + \text{H}$] $^+$: 312.1594 calculated, 312.1595 found.



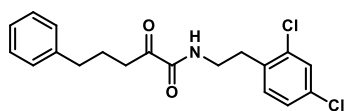
***N*-(4-Bromophenethyl)-2-oxo-5-phenylpentanamide (47).** The title compound was prepared according to general procedure D using α -ketoacid **60c** (0.96 g, 5.0 mmol, 1 eq), 2-(4-bromophenyl)ethan-1-amine (0.85 mL, 5.5 mmol, 1.1 eq), EDC·HCl (1.5 g, 7.5 mmol, 1.5 eq), HOBT (1.2 g, 7.5 mmol, 1.5 eq) and Et_3N (1.4 mL, 10 mmol, 2.0 eq) in DCM. Column chromatography (2.5% \rightarrow 20% EtOAc in pentane) afforded the product (0.28 g, 0.74 mmol, 15%). ^1H NMR (400 MHz, CDCl_3) δ 7.41 (d, J = 7.6 Hz, 2H), 7.32 – 7.22 (m, 2H), 7.22 – 7.12 (m, 3H), 7.04 (d, J = 7.8 Hz, 2H), 7.02 – 6.95 (m, 1H), 3.50 (q, J = 6.8 Hz, 2H), 2.92 (t, J = 7.2 Hz, 2H), 2.78 (t, J = 7.1 Hz, 2H), 2.64 (t, J = 7.5 Hz, 2H), 1.92 (p, J = 7.3 Hz, 2H). ^{13}C NMR (101 MHz, CDCl_3) δ 198.86, 160.13, 141.35, 137.23, 131.87, 130.47, 128.55, 128.51, 126.12, 120.68, 40.31, 36.18, 35.07, 34.91, 24.87. HRMS [$\text{C}_{19}\text{H}_{20}\text{NBrO}_2 + \text{H}$] $^+$: 374.0750 calculated, 374.0751 found.



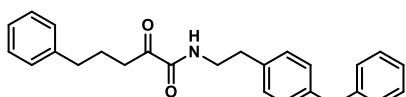
***N*-(3-Chlorophenethyl)-2-oxo-5-phenylpentanamide (48).** The title compound was prepared according to general procedure D using α -ketoacid **60c** (72 mg, 0.37 mmol, 1 eq), 2-(3-chlorophenyl)ethan-1-amine (57 μ L, 0.41 mmol, 1.1 eq), EDC·HCl (0.11 g, 0.56 mmol, 1.5 eq), HOBT (86 mg, 0.56 mmol, 1.5 eq) in DCM. Column chromatography (2.5% \rightarrow 40% EtOAc in pentane) afforded the product (29 mg, 87 μ mol, 24%). ^1H NMR (400 MHz, CDCl_3) δ 7.33 – 7.13 (m, 8H), 7.11 – 7.02 (m, 1H), 7.02 – 6.90 (m, 1H), 3.53 (q, J = 6.8 Hz, 2H), 2.93 (t, J = 7.3 Hz, 2H), 2.82 (t, J = 7.2 Hz, 2H), 2.65 (t, J = 7.6 Hz, 2H), 1.94 (p, J = 7.5 Hz, 2H). ^{13}C NMR (101 MHz, CDCl_3) δ 198.91, 165.51, 140.31, 130.11, 128.94, 128.61, 128.56, 127.12, 126.97, 126.17, 40.35, 36.23, 35.24, 35.15, 24.95. HRMS [$\text{C}_{19}\text{H}_{20}\text{ClNO}_2 + \text{H}$] $^+$: 330.1255 calculated, 330.1256 found.



***N*-(2-Chlorophenethyl)-2-oxo-5-phenylpentanamide (49).** The title compound was prepared according to general procedure D using α -ketoacid **60c** (81 mg, 0.42 mmol, 1 eq), 2-(2-chlorophenyl)ethan-1-amine (66 μ L, 0.47 mmol, 1.1 eq), EDC·HCl (0.12 g, 0.64 mmol, 1.5 eq) and HOBT (86 mg, 0.64 mmol, 1.5 eq) in DCM. Column chromatography (2.5% \rightarrow 20% EtOAc in pentane) afforded the product (11 mg, 32 μ mol, 8%). ^1H NMR (400 MHz, CDCl_3) δ 7.41 – 7.32 (m, 1H), 7.32 – 7.26 (m, 2H), 7.24 – 7.08 (m, 6H), 7.07 – 6.91 (m, 1H), 3.57 (q, J = 6.9 Hz, 2H), 2.99 (t, J = 7.1 Hz, 2H), 2.93 (t, J = 7.3 Hz, 2H), 2.65 (t, J = 7.6 Hz, 2H), 1.93 (p, J = 7.4 Hz, 2H). ^{13}C NMR (75 MHz, CDCl_3) δ 198.96, 160.23, 141.45, 136.03, 134.27, 131.00, 129.90, 128.63, 128.56, 128.45, 127.23, 126.17, 39.08, 36.23, 35.15, 33.30, 24.96. HRMS [$\text{C}_{19}\text{H}_{20}\text{ClNO}_2 + \text{H}$] $^+$: 330.1255 calculated, 330.1256 found.

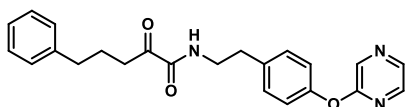


***N*-(2,4-Dichlorophenethyl)-2-oxo-5-phenylpentanamide (50).** The title compound was prepared according to general procedure D using α -ketoacid **60c** (95 mg, 0.49 mmol, 1 eq), 2-(2,4-dichlorophenyl)ethan-1-amine (89 μ L, 0.54 mmol, 1.1 eq), EDC·HCl (0.14 g, 0.74 mmol, 1.5 eq) and HOBT (0.10 g, 0.74 mmol, 1.5 eq) in DCM. Column chromatography (2.5% \rightarrow 40% EtOAc in pentane) afforded the product (14 mg, 38 μ mol, 8%). ^1H NMR (400 MHz, CDCl_3) δ 7.38 (s, 1H), 7.32 – 7.26 (m, 2H), 7.23 – 7.15 (m, 4H), 7.15 – 7.10 (m, 1H), 7.07 – 6.87 (m, 1H), 3.54 (q, J = 6.8 Hz, 2H), 2.94 (q, J = 7.5 Hz, 4H), 2.65 (t, J = 7.6 Hz, 2H), 1.94 (p, J = 7.4 Hz, 2H). ^{13}C NMR (101 MHz, CDCl_3) δ 198.87, 160.25, 141.40, 134.92, 134.63, 133.46, 131.72, 129.68, 128.61, 128.56, 127.50, 126.18, 38.91, 36.21, 35.13, 32.79, 24.93. HRMS [$\text{C}_{19}\text{H}_{19}\text{Cl}_2\text{NO}_2 + \text{H}$] $^+$: 364.0866 calculated, 364.0867 found.



2-Oxo-N-(4-phenoxyphenethyl)-5-phenylpentanamide (51, LEI-301). The title compound was prepared according to general procedure D using α -ketoacid **60c** (0.19 g, 1.0 mmol, 1 eq), 2-(4-phenoxyphenyl)ethan-1-amine TFA salt (0.36 g, 1.1 mmol, 1.1 eq),

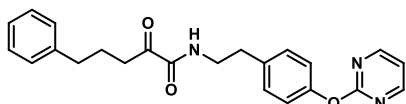
EDC-HCl (0.29 g, 1.5 mmol, 1.5 eq), HOBT (0.23 g, 1.5 mmol, 1.5 eq) and Et₃N (0.28 mL, 2.0 mmol, 2.0 eq) in DCM. Column chromatography (2.5% → 20% EtOAc in pentane) afforded the product (32 mg, 86 μ mol, 9%). ¹H NMR (400 MHz, CDCl₃) δ 7.36 – 7.24 (m, 4H), 7.22 – 7.06 (m, 6H), 7.04 – 6.91 (m, 5H), 3.53 (q, J = 6.7 Hz, 2H), 2.94 (t, J = 7.2 Hz, 2H), 2.81 (t, J = 7.1 Hz, 2H), 2.65 (t, J = 7.5 Hz, 2H), 1.94 (p, J = 7.4 Hz, 2H). ¹³C NMR (101 MHz, CDCl₃) δ 199.01, 160.14, 157.33, 156.18, 141.42, 133.07, 130.04, 129.86, 128.60, 128.55, 126.16, 123.36, 119.24, 118.95, 40.68, 36.23, 35.13, 34.82, 24.93. HRMS [C₂₅H₂₅NO₃ + H]⁺: 388.1907 calculated, 388.1909 found.



2-Oxo-5-phenyl-N-(4-(pyrazin-2-yloxy)phenethyl)pentanamide (52).

Boc-deprotection 65a: a round bottom flask was charged with Boc-protected amine **65a** (0.32 g, 1.0 mmol, 1 eq) and HCl (4 M in dioxane, 4.5 mL, 18 mmol, 18 eq). After stirring for 1 h the mixture

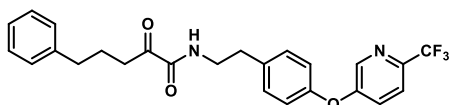
was concentrated under reduced pressure and coevaporated with toluene (3x), which afforded the deprotected amine **66a** as the HCl salt (0.25 g, 1.0 mmol, quant.). *Amide coupling:* the title compound was prepared according to general procedure D using α -ketoacid **60c** (38 mg, 0.20 mmol, 1 eq), EDC-HCl (46 mg, 0.24 mmol, 1.2 eq), HOBT (32 mg, 0.24 mmol, 1.2 eq), NMM (87 μ L, 0.80 mmol, 4 eq) and the amine HCl salt **66a** (60 mg, 0.24 mmol, 1.2 eq). Column chromatography (30% → 70% EtOAc in pentane) afforded the product (23 mg, 59 μ mol, 30%). ¹H NMR (400 MHz, CDCl₃) δ 8.43 (d, J = 1.3 Hz, 1H), 8.26 (d, J = 2.7 Hz, 1H), 8.10 (dd, J = 2.7, 1.4 Hz, 1H), 7.33 – 7.22 (m, 4H), 7.22 – 7.15 (m, 3H), 7.14 – 7.08 (m, 2H), 7.07 – 6.98 (m, 1H), 3.57 (q, J = 7.0 Hz, 2H), 2.95 (t, J = 7.3 Hz, 2H), 2.87 (t, J = 7.2 Hz, 2H), 2.66 (t, J = 7.6 Hz, 2H), 1.94 (p, J = 7.4 Hz, 2H). ¹³C NMR (101 MHz, CDCl₃) δ 198.97, 160.17, 151.83, 141.42, 141.17, 138.62, 136.08, 135.48, 130.17, 128.60, 128.54, 126.16, 121.66, 40.54, 36.23, 35.13, 35.01, 24.92. HRMS [C₂₃H₂₃N₃O₃ + H]⁺: 390.1812 calculated, 390.1823 found.



2-Oxo-5-phenyl-N-(4-(pyrimidin-2-yloxy)phenethyl)pentanamide (53).

Boc-deprotection 65b: a round bottom flask was charged with Boc-protected amine **65b** (0.30 g, 0.94 mmol, 1 eq) and HCl (4 M in dioxane, 4.5 mL, 18 mmol, 19 eq). After stirring for 1 h the mixture

was concentrated under reduced pressure and coevaporated with toluene (3x), which afforded the deprotected amine **66b** as the HCl salt (0.24 g, 0.94 mmol, quant.). *Amide coupling:* the title compound was prepared according to general procedure D using α -ketoacid **60c** (38 mg, 0.20 mmol, 1 eq), EDC-HCl (46 mg, 0.24 mmol, 1.2 eq), HOBT (32 mg, 0.24 mmol, 1.2 eq), NMM (87 μ L, 0.80 mmol, 4 eq) and the amine HCl salt **66b** (76 mg, 0.24 mmol, 1.2 eq). Purification by preparative HPLC (C18 reverse phase, 45% to 55% ACN/H₂O + 0.2% TFA, RT 10.86 min) afforded the product (12 mg, 31 μ mol, 15%). ¹H NMR (400 MHz, CDCl₃) δ 8.56 (d, J = 4.8 Hz, 2H), 7.33 – 7.22 (m, 4H), 7.22 – 7.12 (m, 5H), 7.04 (t, J = 4.8 Hz, 2H), 3.57 (q, J = 6.9 Hz, 2H), 2.95 (t, J = 7.3 Hz, 2H), 2.87 (t, J = 7.2 Hz, 2H), 2.66 (t, J = 7.6 Hz, 2H), 1.95 (p, J = 7.4 Hz, 2H). ¹³C NMR (101 MHz, CDCl₃) δ 198.96, 165.46, 160.19, 159.86, 151.70, 141.43, 135.50, 130.02, 128.61, 128.54, 126.15, 122.03, 116.32, 40.54, 36.24, 35.13, 35.04, 24.92. HRMS [C₂₃H₂₃N₃O₃ + H]⁺: 390.1812 calculated, 390.1824 found.

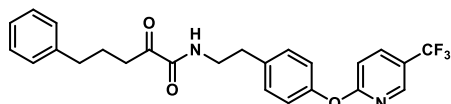


2-Oxo-5-phenyl-N-(4-((6-(trifluoromethyl)pyridin-3-yl)oxy)phenethyl)pentanamide (54).

Boc-deprotection 65c: a round bottom flask was charged with Boc-protected amine **65c** (0.18 g, 0.48 mmol, 1 eq) and HCl (4 M in dioxane, 3 mL, 12 mmol, 25

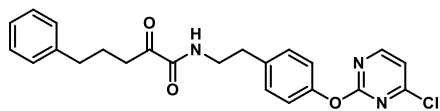
eq). After stirring for 1 h the mixture was concentrated under reduced pressure and coevaporated with toluene (3x), which afforded the deprotected amine **66c** as the HCl salt (0.15 g, 0.48 mmol, quant.). *Amide coupling:* the title compound was prepared according to general procedure D using α -ketoacid **60c** (38 mg,

0.20 mmol, 1 eq), EDC·HCl (46 mg, 0.24 mmol, 1.2 eq), HOBt (32 mg, 0.24 mmol, 1.2 eq), NMM (87 μ L, 0.80 mmol, 4 eq) and the amine HCl salt **66c** (68 mg, 0.24 mmol, 1.2 eq). Purification by preparative HPLC (C18 reverse phase, 65% to 75% ACN/H₂O + 0.2% TFA, RT 8.55 min) afforded the product (21 mg, 46 μ mol, 23%). ¹H NMR (400 MHz, CDCl₃) δ 8.46 (d, *J* = 2.7 Hz, 1H), 7.62 (d, *J* = 8.6 Hz, 1H), 7.34 – 7.22 (m, 5H), 7.21 – 7.15 (m, 3H), 7.07 – 6.95 (m, 3H), 3.56 (q, *J* = 6.9 Hz, 2H), 2.95 (t, *J* = 7.3 Hz, 2H), 2.87 (t, *J* = 7.2 Hz, 2H), 2.69 – 2.62 (m, 2H), 1.94 (p, *J* = 7.5 Hz, 2H). ¹³C NMR (101 MHz, CDCl₃) δ 198.97, 160.15, 156.50, 153.74, 142.12 (q, *J* = 35.1 Hz), 141.38, 140.89, 135.45, 130.69, 128.60, 128.56, 126.18, 124.53, 124.08 (q, *J* = 209.2 Hz), 121.63 (q, *J* = 2.7 Hz), 120.28, 40.55, 36.23, 35.12, 34.92, 24.93. HRMS [C₂₅H₂₃F₃N₂O₃ + H]⁺: 457.1734 calculated, 457.1743 found.



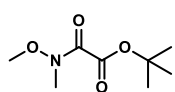
2-Oxo-5-phenyl-*N*-(4-((5-(trifluoromethyl)pyridin-2-yl)oxy)phenethyl)pentanamide (55). *Boc-deprotection 65d*: a round bottom flask was charged with Boc-protected amine **65d** (0.19 g, 0.50 mmol, 1 eq) and HCl (4 M in dioxane, 4.5 mL, 18 mmol, 36

eq). After stirring for 1 h the mixture was concentrated under reduced pressure and coevaporated with toluene (3x), which afforded the deprotected amine **66d** as the HCl salt (0.16 g, 0.50 mmol, quant.). *Amide coupling*: the title compound was prepared according to general procedure D using α -ketoacid **60c** (38 mg, 0.20 mmol, 1 eq), EDC·HCl (46 mg, 0.24 mmol, 1.2 eq), HOBt (32 mg, 0.24 mmol, 1.2 eq), NMM (87 μ L, 0.80 mmol, 4 eq) and the amine HCl salt **66d** (76 mg, 0.24 mmol, 1.2 eq). Purification by preparative HPLC (C18 reverse phase, 55% to 65% ACN/H₂O + 0.2% TFA, RT 8.74 min) afforded the product (26 mg, 57 μ mol, 28%). ¹H NMR (400 MHz, CDCl₃) δ 8.51 – 8.37 (m, 1H), 7.90 (dd, *J* = 8.7, 2.3 Hz, 1H), 7.32 – 7.22 (m, 4H), 7.22 – 7.15 (m, 3H), 7.13 – 7.07 (m, 2H), 7.07 – 6.98 (m, 2H), 3.57 (q, *J* = 7.0 Hz, 2H), 2.95 (t, *J* = 7.3 Hz, 2H), 2.87 (t, *J* = 7.2 Hz, 2H), 2.74 – 2.59 (m, 2H), 1.94 (p, *J* = 7.5 Hz, 2H). ¹³C NMR (101 MHz, CDCl₃) δ 198.97, 165.88, 160.18, 151.99, 145.56 (q, *J* = 4.3 Hz), 141.41, 136.85 (q, *J* = 3.2 Hz), 135.52, 130.17, 128.60, 128.55, 126.16, 123.79 (q, *J* = 271.4 Hz), 121.86, 121.49, 111.52, 40.54, 36.24, 35.13, 35.01, 24.93. HRMS [C₂₅H₂₃F₃N₂O₃ + H]⁺: 457.1734 calculated, 457.1746 found.



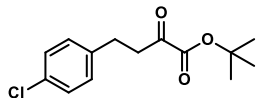
***N*-(4-((4-Chloropyrimidin-2-yl)oxy)phenethyl)-2-oxo-5-phenylpentanamide (56).** *Boc-deprotection 65e*: a round bottom flask was charged with Boc-protected amine **65e** (0.18 g, 0.50 mmol, 1 eq) and HCl (4 M in dioxane, 3 mL, 12 mmol, 24 eq). After stirring

for 1 h the mixture was concentrated under reduced pressure and coevaporated with toluene (3x), which afforded the deprotected amine **66e** as the HCl salt (0.14 g, 0.50 mmol, quant.). *Amide coupling*: the title compound was prepared according to general procedure D using α -ketoacid **60c** (38 mg, 0.20 mmol, 1 eq), EDC·HCl (46 mg, 0.24 mmol, 1.2 eq), HOBt (32 mg, 0.24 mmol, 1.2 eq), NMM (87 μ L, 0.80 mmol, 4 eq) and the amine HCl salt **66e** (60 mg, 0.24 mmol, 1.2 eq). Purification by preparative HPLC (C18 reverse phase, 50% to 60% ACN/H₂O + 0.2% TFA, RT 10.44 min) afforded the product (20 mg, 47 μ mol, 24%). ¹H NMR (400 MHz, CDCl₃) δ 8.43 (d, *J* = 5.7 Hz, 1H), 7.32 – 7.22 (m, 4H), 7.22 – 7.14 (m, 3H), 7.14 – 7.07 (m, 2H), 7.04 (t, *J* = 5.7 Hz, 1H), 6.78 (d, *J* = 5.7 Hz, 1H), 3.57 (q, *J* = 6.9 Hz, 2H), 2.95 (t, *J* = 7.3 Hz, 2H), 2.88 (t, *J* = 7.2 Hz, 2H), 2.70 – 2.60 (m, 2H), 1.94 (p, *J* = 7.5 Hz, 2H). ¹³C NMR (101 MHz, CDCl₃) δ 198.95, 170.46, 160.74, 160.38, 160.18, 150.64, 141.39, 136.40, 130.27, 128.59, 128.54, 126.16, 121.62, 106.77, 40.51, 36.23, 35.12, 35.01, 24.92. HRMS [C₂₃H₂₂ClN₃O₃ + Na]⁺: 446.1242 calculated, 446.1274 found.

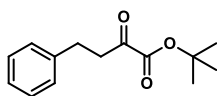


***tert*-Butyl 2-(methoxyamino)-2-oxoacetate (58).** A round bottom flask was charged with oxalyl chloride (13.5 ml, 158 mmol, 1 eq) in dry THF (200 mL) under an inert atmosphere and was cooled to 0 °C. *tert*-Butanol (14.7 ml, 154 mmol, 0.975 eq.) was added in one batch and the mixture was stirred for 1 h at 0 °C. *N,O*-dimethylhydroxylamine hydrochloride (15.4 g, 158 mmol, 1 eq) was added to the reaction mixture followed by Et₃N (66 mL, 472 mmol, 3 eq). The reaction mixture was stirred for 2 h at 0 °C, followed by quenching with H₂O (200 mL). The aqueous layer was extracted with EtOAc (2 x 200 mL). The combined organic layers were washed with sat. aq. NaHCO₃ (2 x 200

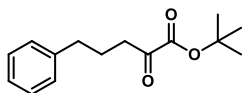
mL), brine (1 x 200 mL), dried (MgSO₄), filtered and concentrated under reduced pressure. The crude residue was purified using silica gel column chromatography (0% → 20% EtOAc in pentane) affording the product (22.3 g, 117 mmol, 75%). ¹H NMR (300 MHz, CDCl₃) δ 3.76 (s, 3H), 3.20 (s, 3H), 1.56 (s, 9H). ¹³C NMR (75 MHz, CDCl₃) δ 161.98, 161.63, 83.89, 61.82, 30.88, 27.62.



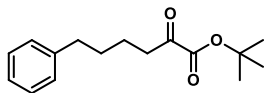
tert-Butyl 4-(4-chlorophenyl)-2-oxobutanoate (59a). The title compound was prepared according to general procedure A using magnesium (0.42 gram, 18.3 mmol, 2.0 eq), 1-(2-bromoethyl)-4-chlorobenzene (1.3 mL, 9.1 mmol, 1 eq) and Weinreb amide **58** (1.7 gram, 9.1 mmol, 1.0 eq), affording the product (0.85 g, 3.2 mmol, 35%). ¹H NMR (300 MHz, CDCl₃) δ 7.24 (d, *J* = 8.4 Hz, 2H), 7.14 (d, *J* = 8.4 Hz, 2H), 3.10 (t, *J* = 7.3 Hz, 2H), 2.90 (t, *J* = 7.4 Hz, 2H), 1.53 (s, 9H). ¹³C NMR (75 MHz, CDCl₃) δ 194.31, 160.25, 138.78, 132.05, 129.84, 128.63, 84.12, 40.57, 28.42, 27.78.



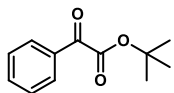
tert-Butyl 2-oxo-4-phenylbutanoate (59b). The title compound was prepared according to general procedure A using magnesium (72 mg, 3.0 mmol, 0.7 eq), (2-bromoethyl)benzene (0.58 mL, 4.2 mmol, 1 eq) and Weinreb amide **58** (0.80 g, 4.2 mmol, 1 eq), affording the product (0.22 g, 0.95 mmol, 22%). ¹H NMR (400 MHz, CDCl₃) δ 7.33 – 7.25 (m, 2H), 7.25 – 7.09 (m, 3H), 3.15 – 3.06 (m, 2H), 2.93 (t, *J* = 7.5 Hz, 2H), 1.53 (s, 9H). ¹³C NMR (101 MHz, CDCl₃) δ 194.74, 160.47, 140.38, 128.65, 128.49, 126.40, 84.11, 40.92, 29.20, 27.88.



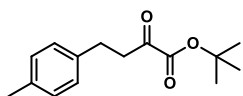
tert-Butyl 2-oxo-5-phenylpentanoate (59c). The title compound was prepared according to general procedure A using magnesium (2.3 g, 94 mmol, 2.0 eq), (3-bromopropyl)benzene (11 mL, 71 mmol, 1.5 eq) and Weinreb amide **58** (8.9 g, 47 mmol, 1.0 eq). Column chromatography (0% → 10% EtOAc in pentane) afforded the product (7.4 g, 30 mmol, 64%). ¹H NMR (300 MHz, CDCl₃) δ 7.34 – 7.21 (m, 2H), 7.16 (t, *J* = 7.1 Hz, 3H), 2.76 (t, *J* = 7.3 Hz, 2H), 2.63 (t, *J* = 7.6 Hz, 2H), 1.92 (p, *J* = 7.4 Hz, 2H), 1.51 (s, 9H). ¹³C NMR (75 MHz, CDCl₃) δ 195.22, 160.57, 141.16, 128.34, 125.95, 83.65, 38.21, 34.75, 27.66, 24.56.



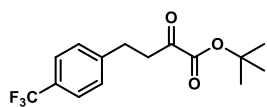
tert-Butyl 4-(2-chlorophenyl)-2-oxobutanoate (59d). The title compound was prepared according to general procedure A using magnesium (0.17 g, 7.0 mmol, 2 eq), (4-bromobutyl)benzene (0.62 mL, 3.5 mmol, 1 eq) and Weinreb amide **58** (0.67 g, 3.5 mmol, 1 eq), affording the product (0.33 g, 1.3 mmol, 36%). ¹H NMR (400 MHz, CDCl₃) δ 7.29 – 7.20 (m, 2H), 7.20 – 7.10 (m, 3H), 2.83 – 2.70 (m, 2H), 2.66 – 2.55 (m, 2H), 1.71 – 1.57 (m, 4H), 1.51 (s, 9H). ¹³C NMR (101 MHz, CDCl₃) δ 195.46, 160.77, 141.94, 128.36, 128.31, 125.79, 83.76, 38.89, 35.59, 30.69, 27.77, 22.64.



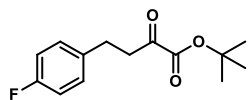
tert-Butyl 2-oxo-2-phenylacetate (59e). The title compound was prepared according to general procedure A using magnesium (0.21 g, 8.5 mmol, 2 eq), bromobenzene (0.43 mL, 4.2 mmol, 1 eq) and Weinreb amide **58** (0.80 g, 4.2 mmol, 1 eq), affording the product (0.73 g, 3.5 mmol, 83%). ¹H NMR (400 MHz, MeOD) δ 7.97 – 7.87 (m, 2H), 7.58 (t, *J* = 7.4 Hz, 1H), 7.46 (t, *J* = 7.7 Hz, 2H), 1.55 (s, 9H). ¹³C NMR (101 MHz, MeOD) δ 187.86, 164.89, 135.68, 133.15, 130.42, 129.84, 85.53, 85.32, 28.22.



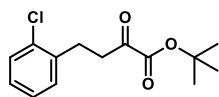
tert-Butyl 2-oxo-4-(p-tolyl)butanoate (59f). The title compound was prepared according to general procedure A using magnesium (0.24 g, 10 mmol, 2 eq), 1-(2-bromoethyl)-4-methylbenzene (0.77 mL, 5.0 mmol, 1 eq) and Weinreb amide **58** (0.95 g, 5.0 mmol, 1 eq), affording the product (0.54 g, 2.2 mmol, 44%). ¹H NMR (400 MHz, CDCl₃) δ 7.09 – 7.03 (m, 4H), 3.10 – 3.01 (m, 2H), 2.86 (t, *J* = 7.5 Hz, 2H), 2.28 (s, 3H), 1.50 (s, 9H). ¹³C NMR (101 MHz, CDCl₃) δ 194.42, 160.24, 137.09, 135.51, 129.06, 128.13, 83.59, 40.81, 28.54, 27.58.



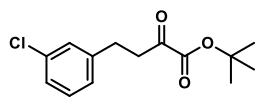
tert-Butyl 2-oxo-4-(4-(trifluoromethyl)phenyl)butanoate (59g). The title compound was prepared according to general procedure A using magnesium (0.18 g, 7.9 mmol, 2 eq), 1-(2-bromoethyl)-4-(trifluoromethyl)benzene (0.67 mL, 4.0 mmol, 1 eq) and Weinreb amide **58** (0.75 g, 4.0 mmol, 1 eq), affording the product (0.21 g, 0.83 mmol, 21%). ^1H NMR (300 MHz, CDCl_3) δ 7.53 (d, J = 8.1 Hz, 2H), 7.33 (d, J = 8.0 Hz, 2H), 3.25 – 3.09 (m, 2H), 2.99 (t, J = 7.3 Hz, 2H), 1.53 (s, 9H). ^{13}C NMR (75 MHz, CDCl_3) δ 194.12, 160.18, 144.54 (q, J = 1.1 Hz), 128.86, 128.67 (q, J = 36.7 Hz), 125.45 (q, J = 3.8 Hz), 124.30 (q, J = 272.0 Hz), 84.21, 40.27, 28.83, 27.70.



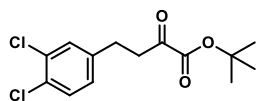
tert-Butyl 4-(4-fluorophenyl)-2-oxobutanoate (59h). The title compound was prepared according to general procedure A using magnesium (0.24 g, 10.6 mmol, 2 eq), 1-(2-bromoethyl)-4-fluorobenzene (0.72 mL, 5.3 mmol, 1 eq) and Weinreb amide **59** (1.1 g, 5.3 mmol, 1 eq), affording the product (0.28 g, 1.1 mmol, 21%). ^1H NMR (400 MHz, CDCl_3) δ 7.23 – 7.07 (m, 2H), 7.04 – 6.88 (m, 2H), 3.09 (t, J = 7.5 Hz, 2H), 2.91 (t, J = 7.4 Hz, 2H), 1.53 (s, 9H). ^{13}C NMR (101 MHz, CDCl_3) δ 194.55, 162.77, 160.37 (d, J = 5.3 Hz), 136.00 (d, J = 3.2 Hz), 129.93 (d, J = 7.8 Hz), 115.37 (d, J = 21.2 Hz), 84.18, 40.90, 28.37, 27.85.



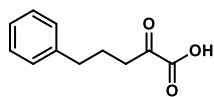
tert-Butyl 4-(2-chlorophenyl)-2-oxobutanoate (59i). The title compound was prepared according to general procedure A using magnesium (0.22 g, 9.1 mmol, 2 eq), 1-(2-bromoethyl)-2-chlorobenzene (0.69 mL, 4.6 mmol, 1 eq) and Weinreb amide **58** (0.86 g, 4.6 mmol, 1 eq), affording the product (0.34 g, 1.3 mmol, 28%). ^1H NMR (400 MHz, CDCl_3) δ 7.32 (dd, J = 7.4, 1.8 Hz, 1H), 7.25 (dd, J = 7.2, 2.1 Hz, 1H), 7.20 – 7.10 (m, 2H), 3.21 – 3.07 (m, 2H), 3.08 – 2.97 (m, 2H), 1.52 (s, 9H). ^{13}C NMR (101 MHz, CDCl_3) δ 194.24, 160.12, 137.77, 133.79, 130.64, 129.48, 127.86, 126.93, 83.90, 38.87, 27.68, 27.14.



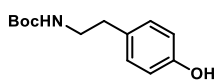
tert-Butyl 4-(3-chlorophenyl)-2-oxobutanoate (59j). The title compound was prepared according to general procedure A using magnesium (0.22 g, 9.1 mmol, 2 eq), 1-(2-bromoethyl)-3-chlorobenzene (0.67 mL, 4.6 mmol, 1 eq) and Weinreb amide **58** (0.86 g, 4.6 mmol, 1 eq), affording the product (0.51 g, 1.9 mmol, 42%). ^1H NMR (400 MHz, CDCl_3) δ 7.24 – 7.11 (m, 3H), 7.11 – 7.03 (m, 1H), 3.10 (t, J = 7.5 Hz, 2H), 2.89 (t, J = 7.5 Hz, 2H), 1.52 (s, 9H). ^{13}C NMR (101 MHz, CDCl_3) δ 194.02, 160.08, 142.29, 134.06, 129.73, 128.45, 126.61, 126.38, 83.92, 40.29, 28.59, 27.64.



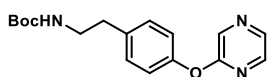
tert-Butyl 4-(3,4-dichlorophenyl)-2-oxobutanoate (59k). The title compound was prepared according to general procedure A using magnesium (34 mg, 1.4 mmol, 1.2 eq), 4-(2-bromoethyl)-1,2-dichlorobenzene (0.30 g, 1.2 mmol, 1 eq) and Weinreb amide **58** (0.27 g, 1.4 mmol, 1.2 eq), affording the product (90 mg, 0.30 mmol, 25%). ^1H NMR (400 MHz, CDCl_3) δ 7.43 – 7.22 (m, 2H), 7.05 (dd, J = 8.2, 1.6 Hz, 1H), 3.10 (t, J = 7.4 Hz, 2H), 2.89 (t, J = 7.4 Hz, 2H), 1.54 (s, 9H). ^{13}C NMR (101 MHz, CDCl_3) δ 194.04, 160.22, 140.61, 132.46, 130.65, 130.53, 130.52, 128.06, 84.36, 40.28, 28.23, 27.86.



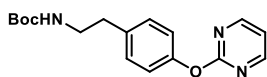
2-Oxo-5-phenylpentanoic acid (60c). The title compound was prepared according to general procedure B using α -ketoester **59c** (7.4 g, 30 mmol, 1 eq) and TFA (23 mL, 300 mmol, 10 eq) affording the product (5.8 g, 30 mmol, quant.). ^1H NMR (400 MHz, CDCl_3) δ 7.33 – 7.12 (m, 5H), 2.91 (t, J = 7.2 Hz, 2H), 2.66 (t, J = 7.5 Hz, 2H), 1.98 (p, J = 7.4 Hz, 2H). ^{13}C NMR (101 MHz, CDCl_3) δ 195.53, 160.50, 140.94, 128.63, 128.56, 126.32, 37.15, 34.86, 24.66. HRMS [$\text{C}_{11}\text{H}_{12}\text{O}_3 + \text{H}$] $^+$: 193.0859 calculated, 193.0859 found.



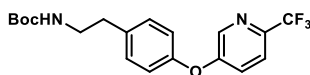
***N*-Boc-tyramine (64).** A round bottom flask was charged with tyramine (5.0 gram, 36 mmol, 1.0 eq), and dissolved in THF (160 mL). Boc_2O (8.1 gram, 37 mmol, 1.0 eq) and a solution of NaHCO_3 (3.4 gram, 40 mmol, 1.1 eq) in water (80 mL) was added and the reaction was stirred vigorously overnight. The mixture was then extracted with Et_2O (3 x 50 mL) and the combined organic layers were sequentially washed with 0.1 M HCl (1 x 100 mL), water (1 x 100 mL) and brine (1 x 100 mL), dried over MgSO_4 , filtered and concentrated under reduced pressure. Purification by silica gel column chromatography (10% \rightarrow 40% EtOAc in pentane) afforded (9.1 g, 31 mmol, 85%). ^1H NMR (400 MHz, CDCl_3) δ 7.65 (br s, 1H), 6.98 (d, J = 7.8 Hz, 2H), 6.80 (d, J = 8.0 Hz, 2H), 4.92 – 4.47 (m, 1H), 3.46 – 3.17 (m, 2H), 2.77 – 2.56 (m, 2H), 1.44 (s, 9H). ^{13}C NMR (101 MHz, CDCl_3) δ 156.53, 155.06, 130.01, 129.81, 115.61, 79.87, 42.14, 35.22, 28.48. HRMS [$\text{C}_{13}\text{H}_{19}\text{NO}_3 + \text{Na}$] $^+$: 260.1257 calculated, 260.1253 found.



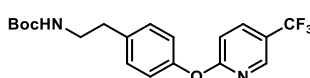
***tert*-Butyl (4-(pyrazin-2-yloxy)phenethyl)carbamate (65a).** The title compound was prepared according to general procedure E using *N*-Boc-tyramine **64** (0.48 g, 2.0 mmol, 1 eq), 2-chloropyrazine (0.18 mL, 2.0 mmol, 1 eq) and K_2CO_3 (0.55 g, 4.0 mmol, 2 eq) in DMSO (2 mL). Column chromatography (20% \rightarrow 60% EtOAc/pentane) afforded the product (0.50 g, 1.6 mmol, 79%). ^1H NMR (300 MHz, CDCl_3) δ 8.40 (s, 1H), 8.23 (s, 1H), 8.08 (s, 1H), 7.25 (d, J = 8.0 Hz, 2H), 7.10 (d, J = 8.0 Hz, 2H), 5.14 – 4.70 (m, 1H), 3.58 – 3.20 (m, 2H), 2.82 (t, J = 6.8 Hz, 2H), 1.44 (s, 9H). ^{13}C NMR (75 MHz, CDCl_3) δ 160.04, 155.80, 151.32, 140.91, 138.28, 136.15, 135.74, 130.02, 121.16, 78.97, 41.62, 35.53, 28.31. HRMS [$\text{C}_{17}\text{H}_{21}\text{N}_3\text{O}_3 + \text{Na}$] $^+$: 338.1475 calculated, 338.1469 found.



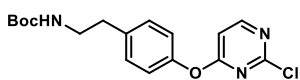
***tert*-Butyl (4-(pyrimidin-2-yloxy)phenethyl)carbamate (65b).** The title compound was prepared according to general procedure E using *N*-Boc-tyramine **64** (0.48 g, 2 mmol, 1 eq), 2-chloro-pyrimidine (0.23 g, 2 mmol, 1 eq) and K_2CO_3 (0.55 g, 4 mmol, 2 eq) in DMSO (2 mL). Column chromatography (40% \rightarrow 70% EtOAc/pentane) afforded the product (0.52 g, 1.7 mmol, 83%). ^1H NMR (300 MHz, CDCl_3) δ 8.56 (d, J = 4.8 Hz, 2H), 7.31 – 7.19 (m, 2H), 7.14 (d, J = 8.4 Hz, 2H), 7.04 (t, J = 4.8 Hz, 1H), 4.84 – 4.29 (m, 1H), 3.40 (q, J = 6.3 Hz, 2H), 2.82 (t, J = 6.9 Hz, 2H), 1.44 (s, 9H). ^{13}C NMR (75 MHz, CDCl_3) δ 165.60, 159.82, 155.95, 151.48, 136.25, 130.10, 121.77, 116.23, 79.26, 41.74, 35.75, 28.51. HRMS [$\text{C}_{17}\text{H}_{21}\text{N}_3\text{O}_3 + \text{H}$] $^+$: 316.1656 calculated, 316.1653 found.



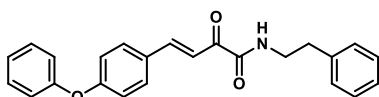
***tert*-Butyl (4-((6-(trifluoromethyl)pyridin-3-yl)oxy)phenethyl) carbamate (65c).** The title compound was prepared according to general procedure E using *N*-Boc-tyramine **64** (0.25 g, 1.05 mmol, 1.05 eq), 2-trifluoromethyl-5-fluoropyridine (0.12 mL, 1 mmol, 1 eq) and K_2CO_3 (0.21 g, 1.5 mmol, 1.5 eq) in DMF (5 mL). Column chromatography (10% \rightarrow 40% EtOAc/pentane) afforded the product (0.28 g, 0.73 mmol, 73%). ^1H NMR (300 MHz, CDCl_3) δ 8.46 (d, J = 2.6 Hz, 1H), 7.61 (d, J = 8.7 Hz, 1H), 7.45 – 7.15 (m, 3H), 7.02 (d, J = 8.5 Hz, 2H), 4.89 – 4.35 (m, 1H), 3.39 (q, J = 6.6 Hz, 2H), 2.82 (t, J = 7.1 Hz, 2H), 1.44 (s, 9H). ^{13}C NMR (75 MHz, CDCl_3) δ 156.60, 155.96, 153.40, 140.77, 136.36, 130.76, 124.35, 121.54, 120.10, 79.38, 41.89, 35.75, 28.48. HRMS [$\text{C}_{19}\text{H}_{21}\text{F}_3\text{N}_2\text{O}_3 + \text{H}$] $^+$: 383.1577 calculated, 383.1576 found.



***tert*-Butyl(4-((5-(trifluoromethyl)pyridin-2-yl)oxy)phenethyl) carbamate (65d).** The title compound was prepared according to general procedure E using *N*-Boc-tyramine **64** (0.24 g, 1.0 mmol, 1 eq), 2-chloro-5-(trifluoromethyl)pyridine (0.18 g, 1.0 mmol, 1 eq) and K_2CO_3 (0.28 g, 2.0 mmol, 2 eq). Column chromatography (20% \rightarrow 60% EtOAc/pentane) afforded the product (0.35 g, 0.92 mmol, 92%). ^1H NMR (300 MHz, CDCl_3) δ 8.44 (s, 1H), 8.03 – 7.76 (m, 1H), 7.26 (d, J = 7.7 Hz, 2H), 7.09 (d, J = 8.2 Hz, 2H), 7.01 (d, J = 8.6 Hz, 1H), 4.80 – 4.21 (m, 1H), 3.40 (q, J = 6.0 Hz, 2H), 2.82 (t, J = 6.9 Hz, 2H), 1.45 (s, 9H). ^{13}C NMR (75 MHz, CDCl_3) δ 165.95, 155.99, 151.80, 145.56, 136.77, 136.36, 130.28, 121.63, 111.48, 41.85, 35.81, 28.54. HRMS [$\text{C}_{19}\text{H}_{21}\text{F}_3\text{N}_2\text{O}_3 + \text{H}$] $^+$: 383.1577 calculated, 383.1575 found.



tert-Butyl (4-((2-chloropyrimidin-4-yl)oxy)phenethyl)carbamate (65e). The title compound was prepared according to general procedure E using *N*-Boc-tyramine **64** (0.25 g, 1.05 mmol, 1.05 eq), 2,4-dichloropyrimidine (0.15 g, 1 mmol, 1 eq) and K_2CO_3 (0.21 g, 1.5 mmol, 1.5 eq) in DMF (5 mL). The reaction was stirred for 19 h at rt. Column chromatography (20% \rightarrow 80% EtOAc/pentane) afforded the product (0.22 g, 0.63 mmol, 63%). 1H NMR (300 MHz, $CDCl_3$) δ 8.42 (d, J = 5.7 Hz, 1H), 7.26 (d, J = 8.5 Hz, 2H), 7.13 – 7.03 (m, 2H), 6.78 (d, J = 5.7 Hz, 1H), 4.93 – 4.42 (m, 1H), 3.40 (q, J = 6.5 Hz, 2H), 2.83 (t, J = 7.0 Hz, 2H), 1.44 (s, 9H). ^{13}C NMR (75 MHz, $CDCl_3$) δ 170.49, 160.66, 160.31, 155.91, 150.36, 137.23, 130.32, 121.30, 106.64, 79.32, 41.77, 35.77, 28.47. HRMS [$C_{17}H_{20}ClN_3O_3 + Na$] $^+$: 372.1085 calculated, 372.1080 found.



(E)-2-Oxo-N-phenethyl-4-(4-phenoxyphenyl)but-3-enamide (67). *α -Ketoacid formation:* the α -ketoacid salt was prepared according to general procedure F using sodium pyruvate (0.44 g, 5.1 mmol, 1 eq), 4-phenoxybenzaldehyde (1.0 g, 5.1 mmol, 1 eq), KOH (0.42 g, 7.6 mmol, 1.5 eq) in MeOH affording potassium 4-(4-phenoxyphenyl)-2-oxobut-3-enoate **62f** (0.51 g, 1.9 mmol, 38%). *Amide coupling:* the title compound was prepared according to general procedure C using potassium salt **62f** (0.20 g, 0.93 mmol, 1 eq), phenethylamine (0.26 mL, 2.1 mmol, 1.1 eq), HCTU (0.87 g, 2.1 mmol, 1.1 eq) and DiPEA (0.66 mL, 3.8 mmol, 2 eq) in DMF affording the product (0.31 g, 0.82 mmol, 88%). 1H NMR (300 MHz, $CDCl_3$) δ 7.93 (d, J = 15.9 Hz, 1H), 7.82 – 7.53 (m, 3H), 7.50 – 7.16 (m, 9H), 7.16 – 6.91 (m, 4H), 3.76 – 3.48 (m, 2H), 2.91 (t, J = 6.8 Hz, 2H). ^{13}C NMR (75 MHz, $CDCl_3$) δ 185.23, 161.51, 160.85, 149.08, 147.45, 138.41, 131.18, 130.11, 129.07, 128.81, 126.78, 124.56, 120.11, 118.27, 117.19, 40.73, 35.59.

References

1. Ueda, N., Tsuboi, K. & Uyama, T. Metabolism of endocannabinoids and related *N*-acylethanolamines: canonical and alternative pathways. *The FEBS Journal* **280**, 1874-1894 (2013).
2. Mardian, E.B., Bradley, R.M. & Duncan, R.E. The HRASLS (PLA/AT) subfamily of enzymes. *Journal of Biomedical Science* **22**, 99 (2015).
3. Kiser, P.D., Golczak, M. & Palczewski, K. Chemistry of the retinoid (visual) cycle. *Chemical Reviews* **114**, 194-232 (2014).
4. Jin, X.-H., Okamoto, Y., Morishita, J., Tsuboi, K., Tonai, T. & Ueda, N. Discovery and characterization of a Ca^{2+} -independent phosphatidylethanolamine *N*-acyltransferase generating the anandamide precursor and its congeners. *Journal of Biological Chemistry* **282**, 3614-3623 (2007).
5. Duncan, R.E., Sarkadi-Nagy, E., Jaworski, K., Ahmadian, M. & Sul, H.S. Identification and functional characterization of adipose-specific phospholipase A2 (AdPLA). *Journal of Biological Chemistry* **283**, 25428-25436 (2008).
6. Jin, X.-H., Uyama, T., Wang, J., Okamoto, Y., Tonai, T. & Ueda, N. cDNA cloning and characterization of human and mouse Ca^{2+} -independent phosphatidylethanolamine *N*-acyltransferases. *Biochimica et Biophysica Acta (BBA) - Molecular and Cell Biology of Lipids* **1791**, 32-38 (2009).
7. Uyama, T., Jin, X.-H., Tsuboi, K., Tonai, T. & Ueda, N. Characterization of the human tumor suppressors TIG3 and HRASLS2 as phospholipid-metabolizing enzymes. *Biochimica et Biophysica Acta (BBA) - Molecular and Cell Biology of Lipids* **1791**, 1114-1124 (2009).
8. Uyama, T., Morishita, J., Jin, X.-H., Okamoto, Y., Tsuboi, K. & Ueda, N. The tumor suppressor gene H-Rev107 functions as a novel Ca^{2+} -independent cytosolic phospholipase A1/2 of the thiol hydrolase type. *Journal of Lipid Research* **50**, 685-693 (2009).

9. Shinohara, N., Uyama, T., Jin, X.-H., Tsuboi, K., Tonai, T., Houchi, H. & Ueda, N. Enzymological analysis of the tumor suppressor A-C1 reveals a novel group of phospholipid-metabolizing enzymes. *Journal of Lipid Research* **52**, 1927-1935 (2011).
10. Uyama, T., Ikematsu, N., Inoue, M., Shinohara, N., Jin, X.-H., Tsuboi, K., Tonai, T., Tokumura, A. & Ueda, N. Generation of *N*-acylphosphatidylethanolamine by members of the phospholipase A/acyltransferase (PLA/AT) family. *Journal of Biological Chemistry* **287**, 31905-31919 (2012).
11. Wellner, N., Diep, T.A., Janfelt, C. & Hansen, H.S. *N*-acylation of phosphatidylethanolamine and its biological functions in mammals. *Biochimica et Biophysica Acta (BBA) - Molecular and Cell Biology of Lipids* **1831**, 652-662 (2013).
12. Ogura, Y., Parsons, W.H., Kamat, S.S. & Cravatt, B.F. A calcium-dependent acyltransferase that produces *N*-acyl phosphatidylethanolamines. *Nature Chemical Biology* **12**, 669 (2016).
13. Hussain, Z., Uyama, T., Tsuboi, K. & Ueda, N. Mammalian enzymes responsible for the biosynthesis of *N*-acylethanolamines. *Biochimica et Biophysica Acta (BBA) - Molecular and Cell Biology of Lipids* **1862**, 1546-1561 (2017).
14. Shyu, R.-Y., Hsieh, Y.-C., Tsai, F.-M., Wu, C.-C. & Jiang, S.-Y. Cloning and functional characterization of the HRASLS2 gene. *Amino Acids* **35**, 129-137 (2008).
15. Hansen, H.S. & Vana, V. Non-endocannabinoid *N*-acylethanolamines and 2-monoacylglycerols in the intestine. *British Journal of Pharmacology* (2018).
16. Fu, J., Gaetani, S., Oveisi, F., Lo Verme, J., Serrano, A., Rodríguez de Fonseca, F., Rosengarth, A., Luecke, H., Di Giacomo, B., Tarzia, G. & Piomelli, D. Oleoylethanolamide regulates feeding and body weight through activation of the nuclear receptor PPAR- α . *Nature* **425**, 90 (2003).
17. Zhou, J., Mock, E.D., Martella, A., Kantae, V., Di, X., Burggraaff, L., Baggelaar, M.P., Al-Ayed, K., Bakker, A., Florea, B.I., Grimm, S.H., den Dulk, H., Li, C.T., Mulder, L., Overkleeft, H.S., Hankemeier, T., van Westen, G.J.P. & van der Stelt, M. Activity-based protein profiling identifies α -ketoamides as inhibitors for phospholipase A₂ group XVI. *ACS Chemical Biology* **14**, 164-169 (2019).
18. Baggelaar, M.P., Janssen, F.J., van Esbroeck, A.C.M., den Dulk, H., Allara, M., Hoogendoorn, S., McGuire, R., Florea, B.I., Meeuwenoord, N., van den Elst, H., van der Marel, G.A., Brouwer, J., Di Marzo, V., Overkleeft, H.S. & van der Stelt, M. Development of an activity-based probe and in silico design reveal highly selective inhibitors for diacylglycerol lipase- α in brain. *Angew. Chem.-Int. Edit.* **52**, 12081-12085 (2013).
19. De Risi, C., Pollini, G.P. & Zanirato, V. Recent developments in general methodologies for the synthesis of α -ketoamides. *Chemical Reviews* **116**, 3241-3305 (2016).
20. Golczak, M., Kiser, P.D., Sears, A.E., Lodowski, D.T., Blaner, W.S. & Palczewski, K. Structural basis for the acyltransferase activity of lecithin:retinol acyltransferase-like proteins. *Journal of Biological Chemistry* **287**, 23790-23807 (2012).
21. van Esbroeck, A.C.M., Janssen, A.P.A., Cognetta, A.B., Ogasawara, D., Shpak, G., van der Kroeg, M., Kantae, V., Baggelaar, M.P., de Vrij, F.M.S., Deng, H., Allarà, M., Fezza, F., Lin, Z., van der Wel, T., Soethoudt, M., Mock, E.D., den Dulk, H., Baak, I.L., Florea, B.I., Hendriks, G., De Petrocellis, L., Overkleeft, H.S., Hankemeier, T., De Zeeuw, C.I., Di Marzo, V., Maccarrone, M., Cravatt, B.F., Kushner, S.A. & van der Stelt, M. Activity-based protein profiling reveals off-target proteins of the FAAH inhibitor BIA 10-2474. *Science* **356**, 1084-1087 (2017).
22. Schrödinger Release 2017-4, LigPrep, Schrödinger, LLC, New York, NY, 2017.
23. Schrödinger Release 2017-4, Epik, Schrödinger, LLC, New York, NY, 2017.
24. Schrödinger Small-Molecule Drug Discovery Suite 2017-4, Schrödinger, LLC, New York, NY, 2017.
25. Schrödinger Release 2017-4: Desmond Molecular Dynamics System, D. E. Shaw Research, New York, NY, 2017. Maestro-Desmond Interoperability Tools, Schrödinger, New York, NY, 2017.

Supplementary Information

Supplementary Table 1. PLAAT2 overexpression does not significantly increase fatty acid levels in U2OS cells, except for arachidonic acid. Data represent mean values \pm SD for 4 biological replicates. *P*-values were determined by one-way ANOVA.

| Fatty acid | Fold change \pm SD PLAAT2 vs. mock | <i>P</i> -value |
|---|---|-----------------|
| palmitic acid (16:0) | 1.28 \pm 0.24 | 0.208 |
| stearic acid (18:0) | 1.41 \pm 0.23 | 0.113 |
| oleic acid (18:1- ω 9) | 1.05 \pm 0.32 | 0.847 |
| α -linoleic acid (18:2- ω 6) | 0.55 \pm 0.18 | 0.100 |
| α -linolenic acid (18:3- ω 3) | 0.71 \pm 0.28 | 0.370 |
| γ -linolenic acid (18:3- ω 6) | 0.36 \pm 0.13 | 0.026 |
| mead acid (20:3- ω 9) | 0.79 \pm 0.26 | 0.399 |
| arachidonic acid (20:4- ω 6) | 1.81 \pm 0.45 | 0.040 |
| FFA (20:3- ω 6-&- ω 3) | 0.79 \pm 0.22 | 0.345 |
| eicosapentaenoic acid (20:5- ω 3) | 1.27 \pm 0.42 | 0.366 |
| docosapentaenoic acid (22:5- ω 3) | 0.95 \pm 0.31 | 0.856 |

Chapter 7

Summary and future prospects

In this thesis, the discovery and optimization is described of chemical tools to study the *N*-acylethanolamine (NAE) biosynthetic pathway. In particular, two enzymes – *N*-acylphosphatidylethanolamine phospholipase D (NAPE-PLD) and phospholipase A and acyltransferase 2 (PLAAT2) – were targeted, which produce NAEs or their NAPE precursors, respectively. To identify inhibitors for these enzymes, high-throughput screening (HTS) or focused-library screening approaches were applied. Using structure-activity relationship (SAR) studies, initial hits were optimized to potent inhibitors, possessing cellular and/or *in vivo* efficacy. On-target confirmation was achieved by employing photoaffinity labeling (PAL) or activity-based protein profiling (ABPP). Cellular and/or *in vivo* activity of the described inhibitors was confirmed with targeted lipidomics experiments. Finally, the herein described NAPE-PLD inhibitor **LEI-401** demonstrated analgesic effects in mice that could be of therapeutic value and will be the focus of ongoing research.

In **Chapter 1**, an overview is provided of the metabolism and bioactivities of NAEs. NAEs are a family of lipid signaling molecules that includes *N*-palmitoylethanolamine

(PEA), *N*-oleoylethanolamine (OEA), *N*-arachidonylethanolamine (anandamide or AEA) and *N*-docosahexaenylethanolamine (DHEA). The NAEs exert their signaling role through activation of several receptors in the brain as well as in the periphery. Over the past three decades a growing list of G protein-coupled receptors (GPCRs), ion channels and nuclear receptors were found to be targeted by specific NAEs. Most famously, anandamide was discovered in 1992 as the first endogenous agonist for the cannabinoid CB₁ receptor, and was therefore coined an endogenous cannabinoid or endocannabinoid.¹ Continuing studies have shown that anandamide is also an agonist for the CB₂ receptor and transient receptor potential vanilloid receptor 1 (TRPV1) and, as a result, AEA is considered an endovanilloid as well.² Many biological activities have been attributed to anandamide, which include pain reduction³, appetite stimulation⁴, regulation of fertility⁵, neuroprotection⁶, memory consolidation⁷ and anti-depressive⁸ and anti-anxiety⁹ functions.

Furthermore, **Chapter 1** discusses the therapeutic opportunities of modulating the endogenous NAE tone including AEA, with a specific focus on depleting NAE levels. NAEs and their metabolic enzymes were found to be aberrantly regulated and associated with disease severity in obesity¹⁰, metabolic syndrome¹¹, hepatic¹² and blood¹³ cancers and liver cirrhosis¹⁴. Pharmacological inhibition of CB₁ and other NAE receptors has shown efficacy for these conditions in clinical or pre-clinical studies. Unfortunately, antagonism of brain CB₁ receptors triggered adverse psychiatric side effects, leading to the market withdrawal of the obesity drug rimonabant. Peripheral CB₁ receptor blockade is currently being investigated as a new therapeutic option.¹⁵ Alternatively, targeting the biosynthetic enzymes of NAEs may be a viable strategy for treatment of these pathological conditions. A potential advantage of depleting NAE signaling could be that this leads to partial antagonism, since most NAE receptors have other endogenous lipid agonists, thereby providing a fine-tuned therapeutic effect. So far, no inhibitors are available that allow reduction of NAE levels in cellular or animal models, making this an underexplored area of research. New pharmacological tools that block NAE biosynthetic enzymes are therefore needed to enable the study of NAE signaling in health and disease models.

7.1 Development of *in vivo* active NAPE-PLD inhibitors

Whereas the degradation of anandamide by the enzyme fatty acid amide hydrolase (FAAH) has been well studied by genetic and pharmacological means, the exact conditions that govern AEA biosynthesis are not completely clear.¹⁶ The zinc hydrolase NAPE-PLD is considered to be the main enzyme that produces NAEs including AEA. However, mouse

NAPE-PLD knock-out (KO) models have shown varying degrees of anandamide reduction, with only two out of three studies reporting decreased brain AEA levels.¹⁷⁻¹⁹ Compensatory mechanisms or other NAE biosynthetic pathways have therefore been suggested to take over the role of NAPE-PLD.¹⁷ To study anandamide signaling in closer detail, pharmacological tools are necessary that allow acute inhibition of its biosynthesis. At present, no such tools are available for NAPE-PLD to modulate its activity in cells or whole animals.

In **Chapter 2**, new chemotypes that inhibit NAPE-PLD were sought by screening a large compound collection using high-throughput screening (HTS). A fluorescence-based NAPE-PLD activity assay was optimized to be HTS-compatible. The assay utilizes the fluorescence-quenched substrate PED6, which is hydrolyzed at the phosphodiester bond by NAPE-PLD. This releases the fluorophore from the quencher, providing a fluorescence increase proportional to the enzymatic activity. In the HTS campaign, a library of ~350,000 compounds was screened at 10 μM (single point measurement) in a 1536-well format. After hit validation, dose-response experiments and two deselection assays, which filtered for zinc chelators and quenchers, five hit compounds were identified. Owing to its favorable submicromolar potency, physicochemical properties and synthetic accessibility, pyrimidine-4-carboxamide **1** (Figure 1) was resynthesized and its activity confirmed in the PED6 assay. Off-target profiling for the receptors and enzymes of the endocannabinoid system (ECS) showed that **1** is selective for NAPE-PLD *in vitro*. Thus, compound **1** constituted a new scaffold with potential for further optimization to obtain *in vivo* active NAPE-PLD inhibitors.

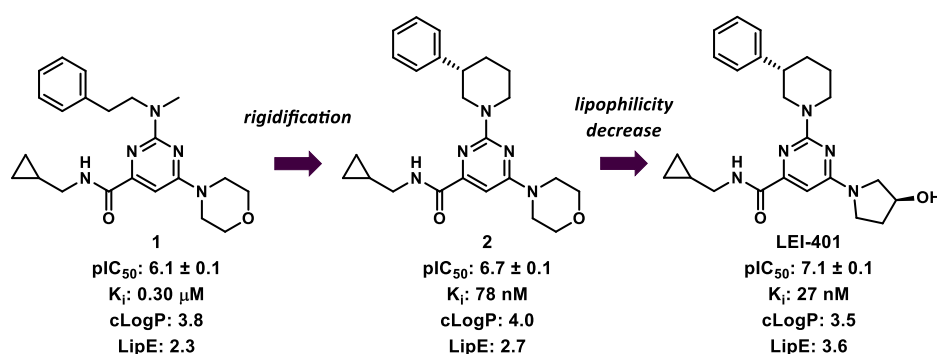


Figure 1. Strategy employed to optimize hit compound **1** to potent NAPE-PLD inhibitor **LEI-401**. cLogP was calculated using Chemdraw 15. Lipophilic efficiency (LipE) = pIC₅₀ - cLogP.

A structure-activity relationship (SAR) study was performed in **Chapter 3** to improve the potency of hit compound **1** for NAPE-PLD. Synthesis and activity testing of 104 analogues of **1** resulted in the identification of **LEI-401**, a nanomolar potent NAPE-PLD inhibitor. Conformational restriction of the *N*-methylphenethylamine of **1** to an (*S*)-3-phenylpiperidine increased the potency by 4-fold (compound **2**, Figure 1). Modification of the morpholine of **1** for an (*S*)-3-hydroxypyrrolidine further improved the inhibitory activity by 3-fold and simultaneously reduced the lipophilicity. **LEI-401** possessed favorable physicochemical (drug-like) properties such as lipophilic efficiency (LipE) and topological polar surface area (tPSA), making it suitable for cellular and *in vivo* studies.

In **Chapter 4**, target engagement of **LEI-401** was investigated to verify its binding interaction with NAPE-PLD in live cells. A photoaffinity labeling (PAL) approach was chosen, which is an established technique to identify protein-drug interactions for metallo-hydrolases.²⁰ Here, a photoaffinity probe covalently binds its intended target upon UV-irradiation, allowing protein identification by gel- or chemical proteomics-based methods. The probe-protein labeling can be displaced with a competitor, which provides proof of target engagement. Two strategies were investigated for the development of NAPE-PLD photoprobes. The first strategy involved synthesis of NAPE substrate mimics, incorporating a diazirine photocrosslinker, a stabilized phosphodiester bioisostere and an alkyne ligation handle. Biological evaluation revealed that these probes had low affinity for NAPE-PLD in an *in vitro* activity assay and were not able to label NAPE-PLD in human embryonic kidney (HEK293T) cells transiently transfected with this enzyme. A second strategy took advantage of the NAPE-PLD inhibitor library (as described in Chapter 3) to guide the design of pyrimidine-4-carboxamide-based photoaffinity probes. Photoprobe **3** displayed submicromolar potency for NAPE-PLD and could efficiently label this enzyme in overexpressing HEK293T cells (Figure 3). Gel- and chemical proteomics-based competition experiments provided evidence of NAPE-PLD target engagement by **LEI-401** in live cells.

In **Chapter 5**, **LEI-401** was profiled in cellular and animal models. First, it was determined that **LEI-401** is selective for NAPE-PLD over the receptors and enzymes in the ECS. Targeted lipidomics measurements in mouse neuronal cells revealed that **LEI-401** reduces NAE levels in wild-type (WT), but not in NAPE-PLD KO cells. Encouraged by this result, **LEI-401** was tested in C57BL/6J mice, where it showed favorable pharmacokinetic (PK) properties. Two hours after a single intraperitoneal dose (30 mg/kg), **LEI-401** displayed high brain and plasma levels. A time- and dose-dependent reduction of brain anandamide levels was observed, matching the **LEI-401** PK profile. This indicated that **LEI-401** is an *in vivo* active, brain penetrant NAPE-PLD inhibitor and emphasized the role of NAPE-PLD in brain AEA production. To assess the pharmacological effect of acute brain

anandamide reduction, **LEI-401** was profiled in several behavioral assays. This revealed that **LEI-401** elicited antinociceptive, hypomotile and hypothermic effects in C57BL/6J mice, which were not mediated by the CB₁ receptor. Furthermore, in a mouse model of inflammatory pain, **LEI-401** was able to fully reverse lipopolysaccharide (LPS)-induced allodynia. Collectively, these data show that **LEI-401** possesses analgesic properties that could be of therapeutic use. Future studies with **LEI-401** in NAPE-PLD KO mice are necessary to establish whether these behavioral effects are NAPE-PLD dependent.

7.1.1 Towards improved *in vivo* active NAPE-PLD inhibitors.

In **Chapters 4** and **5**, **LEI-401** displayed cellular target engagement, high brain penetration and *in vivo* efficacy. While **LEI-401** will be tested in various disease models in mice as a 1st-generation centrally active NAPE-PLD inhibitor, its high dosing (30 mg/kg) may give rise to off-target interactions and toxicity issues, especially after repeated administration. Further optimization of the inhibitor scaffold is therefore required. This can be accomplished by improving drug properties such as potency, selectivity, solubility and metabolic stability. Ideally, a drug candidate possesses single digit nanomolar potency, a LipE greater than 5 and a half-life ($t_{1/2}$) of 12 h by oral dosing.^{21,22} For **LEI-401** these parameters are: $K_{i,NAPE-PLD}$ = 27 nM (human), 180 nM (mouse); LipE = 3.68 (human), 2.89 (mouse); $t_{1/2}$ = 2.7 h.

In Figure 2, an overview is given of potential strategies to improve the **LEI-401** inhibitor structure. The SAR-analysis described in **Chapter 3** showed that the *ortho* position on the phenyl ring was suitable for modification. Bulky biphenyl and diphenyl ether derivatives displayed inhibitory activities equivalent to the unsubstituted phenyl of **1**. This suggests that polar groups such as nitrile and methoxy or small heterocycles can be accommodated at this position, improving the solubility and LipE. Incorporation of a *para*-fluoro substituent on the phenyl ring can increase the metabolic stability by reducing compound degradation in the liver.²³ Additional sites that can be explored are the 2-, 4- and 6-position on the piperidine ring, as well as the 2-, 4- and 5-position of the pyrrolidine, where additional space was found in the SAR. However, it has to be taken into account that for optimal brain exposure the tPSA should not exceed 90 Å², limiting the possible polar modifications. Optimization of the core scaffold can be explored with annulated bicyclic rings. Finally, generating a co-crystal structure of **LEI-401** in the reported NAPE-PLD crystal structure will shed light on its binding mode and aid future inhibitor development.

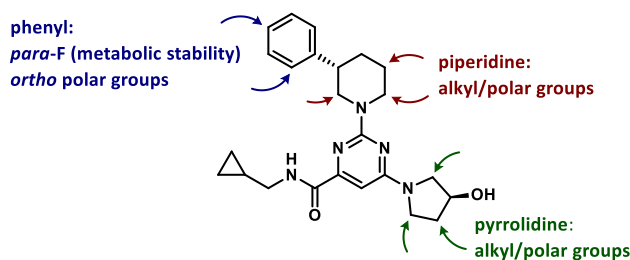


Figure 2. Possible strategies to improve the potency and pharmacokinetic profile of **LEI-401**.

Besides targeting NAPE-PLD in the brain, specifically inhibiting NAPE-PLD in the periphery could be of therapeutic use as well. For example, modulating peripheral levels of OEA and AEA may be beneficial in pathological conditions such as leukemia¹³ and obesity¹¹. An often employed strategy for developing peripherally restricted inhibitors is by increasing the tPSA, which should be between 90 and 120 Å² to minimize brain exposure, while still allowing passive plasma membrane diffusion.²⁴ This may be accomplished by introducing polar substituents (e.g. H-bond donors and/or acceptors) on the **LEI-401** structure as depicted in Figure 2.

7.1.2 Photoaffinity labeling of endogenous NAPE-PLD and looking for **LEI-401** off-targets.

In **Chapter 4**, photoprobe **3** was effective to show target binding of **LEI-401** with NAPE-PLD in HEK293T cells overexpressing this enzyme. Efforts to label endogenous NAPE-PLD in different cell lines (HEK293T, Neuro-2a, RAW264.7) were unsuccessful so far. In mock-transfected HEK293T cells, a fluorescent band was visible at the estimated height of NAPE-PLD (**Chapter 4**, **Figure 8A-B**) and could be competed out by **LEI-401**. However, in subsequent label-free proteomics experiments no NAPE-PLD peptides were detected. To boost the detection sensitivity in a pulldown experiment, different strategies can be employed. Firstly, increasing the potency of the photoprobe can improve photocrosslinking efficiency. This can be achieved by generating new photoprobes that closely mimic the potent inhibitor **LEI-401**, for example compound **4** (**Figure 3**). Compound **5** could exploit a lipophilic binding pocket that was discovered during the SAR-analysis (**Chapter 3**), that allowed incorporation of the large *N*-methylphenethylamine group. Alternatively, the efficiency of the azide-alkyne click reaction may be improved. In **Chapter 3**, it was found that the alkyne resides in a small hydrophobic pocket, suggesting that it may be buried in the protein structure. Therefore, positioning the alkyne handle in more available positions (e.g. compounds **6** and **7**) could make the click reaction more efficient and improve protein detection.

Apart from labeling NAPE-PLD, the photoaffinity probes developed in **Chapter 4** can aid in the discovery of **LEI-401** off-targets. In Chapter 5, **LEI-401** reduced 2-AG and other monoacylglycerol (MAG) levels in both WT and NAPE-PLD KO Neuro-2a cells. In the brains of C57BL/6J mice, **LEI-401** also significantly decreased 2-AG levels in a dose-dependent manner, which is known to cause anti-inflammatory effects.²⁵ It is possible that the **LEI-401**-induced AEA depletion in the brain generated a crosstalk with 2-AG metabolism. Similar interconnected endocannabinoid changes in the brains of mice have been reported for FAAH and diacylglycerol lipase- α (DAGL α) inhibitors, the enzymes that hydrolyze AEA or produce 2-AG, respectively.^{25,26} Alternatively, **LEI-401** could exert cellular and *in vivo* effects through one or more yet unknown protein targets. Photoaffinity labeling coupled with chemical proteomics is an established method for protein target identification of small molecules and natural products.^{27,28} In recent years, technological advances have also enabled determination of the site of protein photocrosslinking.²⁹ To pinpoint the binding site, most often cleavable linkers are used, which facilitate enrichment of probe-labeled peptides.³⁰ Screening various cell lines using the PAL protocol described in Chapter 4, *e.g.* cell lines involved in the inflammatory response, is thus a suitable approach to find additional targets of **LEI-401**.

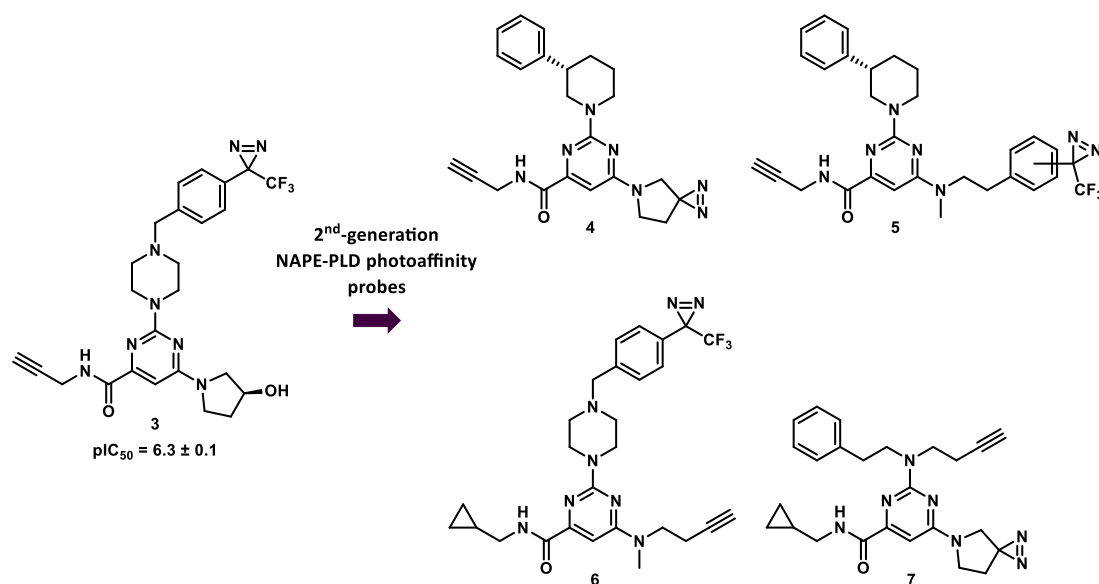


Figure 3. Structures of NAPE-PLD photoprobes **3** and suggested 2nd-generation NAPE-PLD PAL probes **4-7**.

7.2 Development of Ca²⁺-independent NAPE biosynthesis inhibitors

It is generally assumed that the rate-limiting step in NAE biosynthesis is the formation of NAPEs catalyzed by *N*-acyltransferase (NAT) activity.^{31,32} Besides the canonical Ca²⁺-dependent NAPE-producing pathway, in recent years, new Ca²⁺-independent enzymes have been identified.¹⁶ In particular, PLAAT2 was reported to have high *N*-acyltransferase activity *in vitro*.³³ So far, no pharmacological tools have been reported that allow interrogation of cellular PLAAT2 activity. In **Chapter 6**, a recently reported ABPP assay³⁴ was used to screen a focused library of lipase inhibitors for PLAAT2 activity. Compound **8** was identified as the most potent hit of several α -ketoamide inhibitors that were effective against PLAAT2 (Figure 4). SAR-analysis of the α -ketoamide scaffold culminated in optimized inhibitor **LEI-301**, which had a 13-fold increase in potency compared to **8**. **LEI-301** exhibited similar inhibitory activities for the other members of the PLAAT family, but was selective over the receptors and enzymes of the ECS. Human osteosarcoma (U2OS) cells transiently transfected with PLAAT2 showed a remarkable increase in NAE content, which was significantly reduced when treated with **LEI-301**. In control cells, NAE levels were not affected by **LEI-301** treatment, indicating that the compound inhibited PLAAT2 in live cells. The work described in this chapter confirms that PLAAT2 can contribute to NAE biosynthesis. Furthermore, α -ketoamides are presented as a novel class of inhibitors that enable the study of NAE and NAPE signaling in cellular systems.

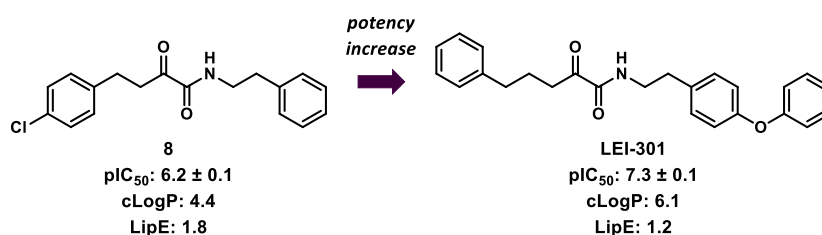


Figure 4. Structures and physicochemical parameters of α -ketoamide screening hit **8** and optimized PLAAT2 inhibitor **LEI-301**. $cLogP$ was calculated using Chemdraw 15. Lipophilic efficiency (LipE) = pIC_{50} - $cLogP$.

7.2.1 Towards selective and *in vivo* active PLAAT2 inhibitors.

LEI-301 was identified in **Chapter 6** as a potent inhibitor of PLAAT2 inhibitor with cellular activity. However, due to its high lipophilicity and low LipE, **LEI-301** is not suitable for *in vivo* use. Modification of the α -ketoamide scaffold is therefore required to improve these

properties. Possible sites that merit further optimization are highlighted in Figure 5. SAR-analysis and molecular docking experiments revealed that introduction of a *para*-phenoxy substituent on the phenethylamine group gave a boost in potency due to π - π stacking with a tyrosine side chain. By placing the phenoxy group on the *ortho* or *meta* positions, the optimal site for the π -interaction can be probed. Also, different heterocyclic or biphenyl motifs should be explored. Recently, a patent describing α -ketoamide inhibitors for PLAAT3 showed that heteroatoms and alkyl groups can be incorporated across the alkyl chain (for example compound **9**, Figure 5).³⁵ Because of the similar potency of **LEI-301** for PLAAT3 and PLAAT2 and the high homology between these two enzymes (69%), **LEI-301** could also benefit from heteroatom and alkyl modifications on the alkyl chain, thereby decreasing the lipophilicity. Replacing the phenyl group on the ketone side for a CF_3 could improve the solubility, while the activating effect on the ketone compensates for the loss of the aromatic interaction. Finally, the reported crystal structures for PLAAT2 and PLAAT3 may guide the development of family member-selective inhibitors, using molecular docking or co-crystal structures.^{36,37}

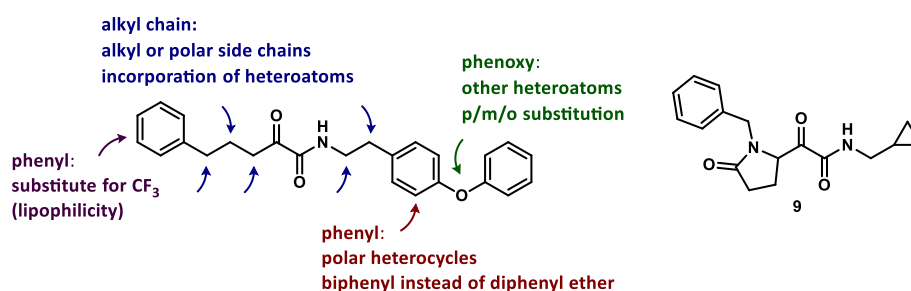


Figure 5. Left: possible strategies to improve the potency and physicochemical properties of **LEI-301**. Right: structure of reported PLAAT3 inhibitor **9**.

7.2.2 Novel covalent α -ketoamide inhibitors and ABPs for the PLAAT family.

The fluorescent activity-based probe (ABP) MB064 has enabled visualization of PLAAT family members in lysates of transiently transfected cells, as well as endogenous PLAAT3 activity in brown and white adipose tissue.³⁴ So far, efforts to confirm target engagement of the PLAAT enzymes by chemical proteomics using the corresponding biotin probe MB108³⁸ (Figure 6A) have been unsuccessful. A possible explanation could be the thioester linkage that is formed between the active site cysteine of the PLAAT members and the β -lactone of the ABP. Thioesters may be susceptible to hydrolysis or transthioesterification with DTT during the pulldown protocol.³⁹ Therefore, when MB108

is used in chemical proteomics experiments with the aim of identifying PLAAT enzymes, strictly non-reducing conditions should be employed. Alternatively, the design of new ABPs that produce a stable covalent linkage with the PLAAT enzymes could be investigated. For example, ABPs for cathepsin and caspase cysteine proteases have used the phenoxyethylketone (PEK) motif as electrophilic trap, which generates a stable thioether bond.⁴⁰⁻⁴² Incorporation in the α -ketoamide scaffold yields PMK **10**, which could represent a possible broad-spectrum ABP for PLAAT enzymes (Figure 6B). A proposed synthesis of probe **10** is depicted in Scheme 1. Alkylation of Boc-protected tyramine **11** with propargyl bromide affords **12**. Boc deprotection and amide coupling with β -chlorolactic acid gives **14**. Subsequent DMP oxidation generates chloromethylketone **15**, which can be converted to the PMK **10** using 2,3,5,6-tetrafluorophenol and potassium fluoride.⁴⁰

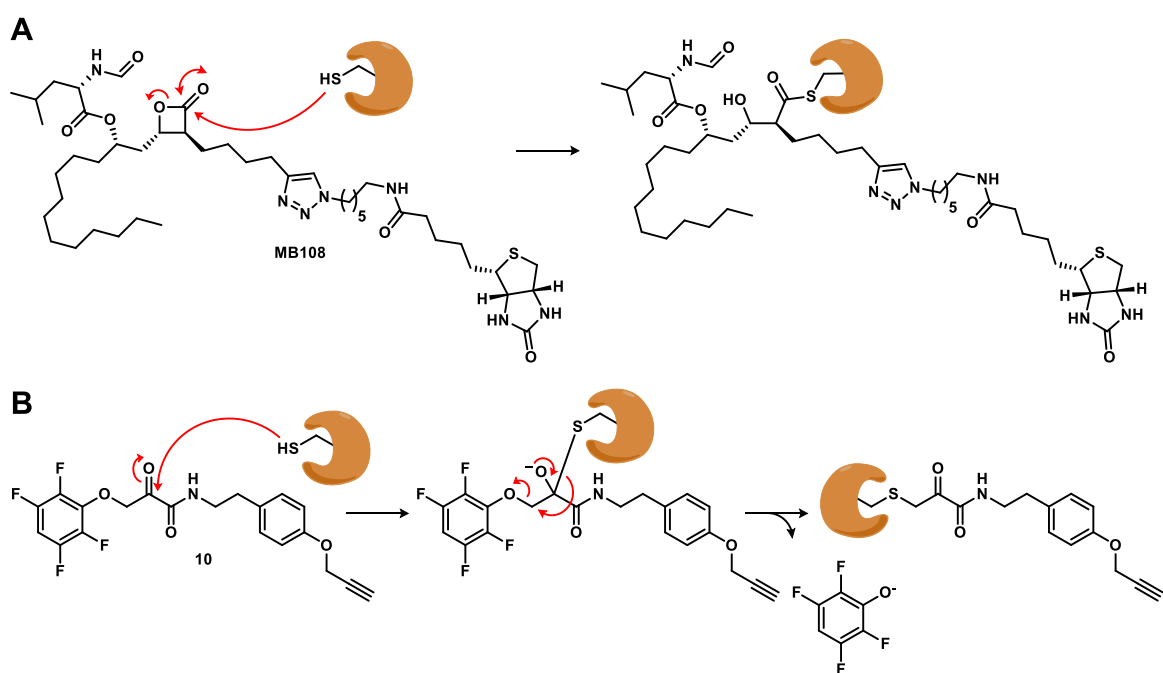
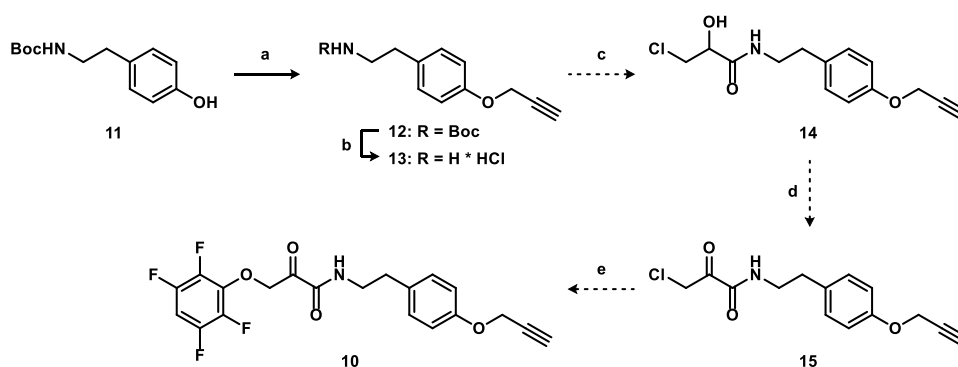


Figure 6. **A)** Proposed mechanism of activity-based probe (ABP) MB108 with PLAAT enzymes, which produces a labile thioester. **B)** Suggested structure of a phenoxyethylketone ABP **10** that targets the PLAAT family and forms a stable thioether bond.

An ABP that is specific for the PLAAT family will help to reveal the endogenous activities of the family members in different tissues. This is specifically relevant for PLAAT2 of which the physiological role is yet unknown. High expression levels of PLAAT2 were found in organs of the human digestive system, including liver, kidney, small intestine and

colon.^{43,44} PLAAT2 could therefore contribute to NAE biosynthesis in the gut, where anandamide and OEA are involved in food intake and satiety.^{45,46} The described inhibitors and ABPs will enable further investigation of these questions.



Scheme 1. Synthetic route towards putative activity-based probe **10** for the PLAAT family. Reagents and conditions: a) propargyl bromide, K_2CO_3 , DMF, rt, 92%; b) HCl, dioxane, rt, 99%; c) β -chlorolactic acid, HATU, DiPEA, DMF; d) Dess-Martin periodinane, DCM; e) 2,3,5,6-tetrafluorophenol, KF, DMF.

7.3 Identification of NAPE protein targets using photoaffinity labeling.

In **Chapter 1**, NAPes are highlighted as an underexplored class of phospholipids in human physiology. NAPes are primarily considered to be precursors for NAEs.¹⁶ In recent years, multiple studies have suggested that NAPes have a bioactive role themselves.^{47,48} NAPes have a reported membrane-stabilizing role and possess fusogenic properties.⁴⁹⁻⁵² In mammals, NAPE levels are highly elevated during cellular injury in several tissues, such as brain and heart, presumably due to an influx of Ca^{2+} -ions.⁵³⁻⁵⁹ Also in plants, NAPes accumulate under cellular stress.^{60,61} NAPes are implicated in neuroprotection, anti-inflammation and satiety.^{47,48} However, the molecular mechanisms through which NAPes exert their biological functions are unclear.

A photoaffinity labeling approach was applied to search for protein targets that can explain the putative bioactivities of NAPes. To this end, NAPE-like photoprobes **16-22** (Figure 7A, synthesis described in Chapter 4) were used to identify covalently bound targets by chemical proteomics. As a model system, the mouse Neuro-2a neuroblastoma cell line was selected, to detect binding partners of NAPes in the brain. The photolabeling efficiencies of probes **16-22** in this cell line were assessed in a gel-based photoaffinity labeling experiment. 750.000 cells were incubated with the different photoprobes

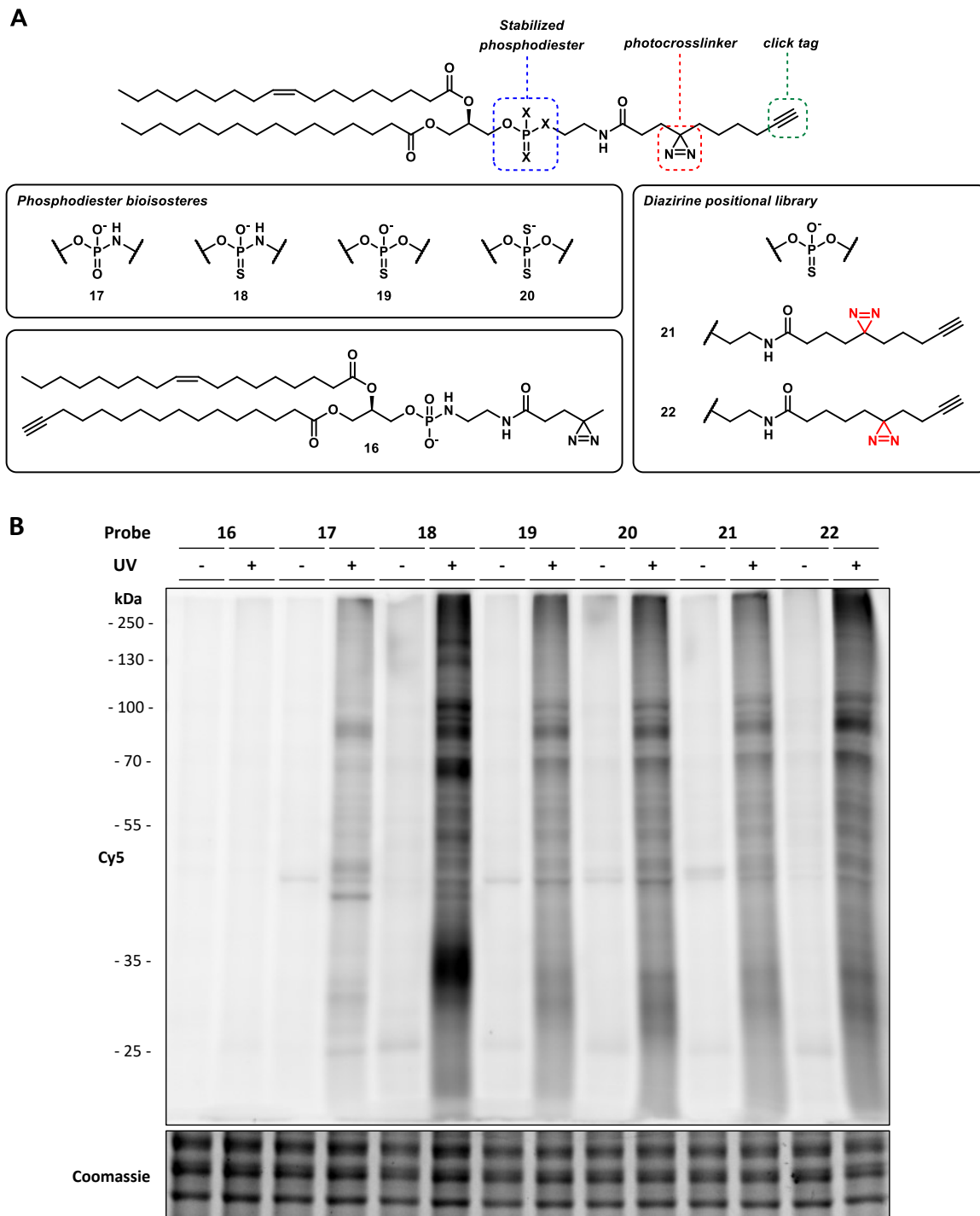


Figure 7. **A)** Structures of NAPE-based PAL probes **16-22**, which incorporate a stabilized phosphodiester mimic, a photoreactive diazirine and an alkyne ligation handle (synthesis described in Chapter 4). **B)** Photoaffinity labeling of NAPE-like photoprobes **16-22** (20 μ M, 30 min) showing UV-dependent labeling of proteins in live Neuro-2a cells.

(20 μ M, 30 min) and irradiated with 350 nm UV light for 10 min or kept in the dark as a control. The cells were lysed, clicked with Cy5-N₃ and the proteins were resolved by

sodium dodecyl sulfate polyacrylamide gel electrophoresis (SDS-PAGE). UV-dependent labeling of various proteins was apparent for all probes except for **16**, possibly due to instability of the phosphoramidate moiety (Figure 7B).⁶² Thiophosphoramidate probe **18** displayed the highest labeling intensity of all the probes and was therefore selected for further characterization.

To identify the labeled proteins by probe **18** a chemical proteomics experiment was performed (similar workflow as in Chapter 4, Figure 2). Ten million cells were treated with probe **18** (20 μ M, 30 min, $n = 3$ per condition) and were either UV irradiated (350 nm, 10 min) or kept in the dark. The cells were lysed and separated in membrane and cytosol fractions by ultracentrifugation to increase the peptide detection sensitivity. The lysates were clicked with biotin- N_3 and the probe-targeted proteins were enriched with avidin agarose beads, followed by on-bead trypsin digestion. The tryptic peptides were treated with deuterated (heavy) or hydrogen (light) isotopically labeled formaldehyde to allow quantification by reductive dimethylation using MaxQuant software (Figure 8).^{63,64} By combining heavy labeled and light labeled peptide fragments with or without UV-irradiation in equal parts (1:1), ratios were obtained of the UV-dependent labeling of the protein target (+UV/-UV intensity) or reproducibility of the experiment (+UV/+UV intensity). Cut-offs for protein target identification were: 1) at least 2 unique peptides, 2) a heavy/light ratio x between $0.5 \leq x \leq 2$ for +UV/+UV intensity, 3) a heavy/light ratio $x \geq 2$ for +UV/-UV intensity and testing for significance ($P < 0.05$) using Student's t -test (unpaired, two-tailed) with Benjamini-Hochberg correction (false discovery rate (FDR) 25%).

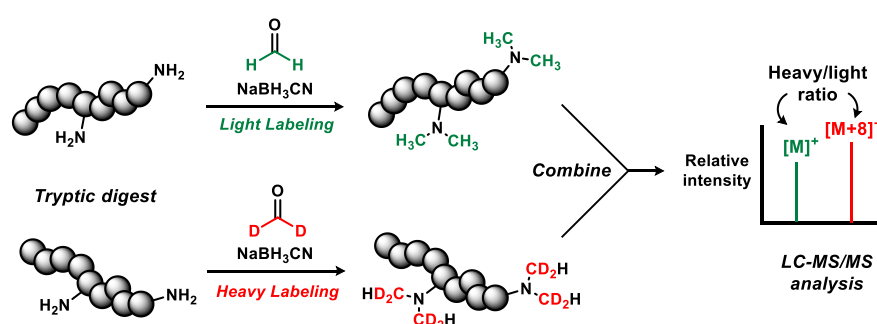


Figure 8. Dimethyl labeling using deuterium (heavy) and hydrogen (light) isotopically labeled formaldehyde allows quantification of peptide fragments.

A total of 162 proteins were identified in this experiment, which gave 17 UV-enriched protein targets (Figure 9A). Of these, four proteins were considered significant: cathepsin D (Ctsd), prosaposin (Psap), Ras-related C3 botulinum toxin substrate 1 (Rac1) and Myb-

binding protein 1a (Mybbp1a or p160) (Figure 9B, Table 1). Cathepsin D was previously reported to be a putative target of aliphatic diazirine photocrosslinkers in human A549 and HeLa cell lines and was therefore not further pursued.⁶⁵ A literature search for Psap revealed that it is a precursor for a family of non-enzymatic lipid binding proteins called sphingolipid activator proteins or saposins A-D.⁶⁶ Saposins A-D reside in the lysosome where they facilitate the breakdown of sphingolipids and gangliosides by different hydrolases. Of note, proteolysis of prosaposin to the individual saposins can be performed by cathepsin D in the lysosome.⁶⁷ To elucidate which form of prosaposin was labeled by probe **18** – the precursor protein or the individual saposins A-D – a closer look was taken at the identified peptides. An overview of the mouse prosaposin amino acid sequence and the labeled peptides (in bold) are displayed in Figure 10. Saposins A-D were each covered with at least one peptide. From this data it could not be established which Psap form was labeled, therefore a second pulldown experiment was performed to reproduce the results and expand the peptide coverage. Again, prosaposin was UV-enriched in this experiment (ratio +UV/-UV intensity = 7.25) and one peptide (ANEDVCQDCMK) was identified that was both part of the precursor protein and saposin B (Figure 10, bold). This may indicate that intact prosaposin is targeted by probe **18**. To confirm labeling of probe **18** to prosaposin, a pcDNA3.1 vector was generated containing prosaposin cDNA with a C-terminal FLAG-tag. Unfortunately, Psap overexpression in transfected Neuro-2a or HEK293T cells could not be confirmed by western blot.

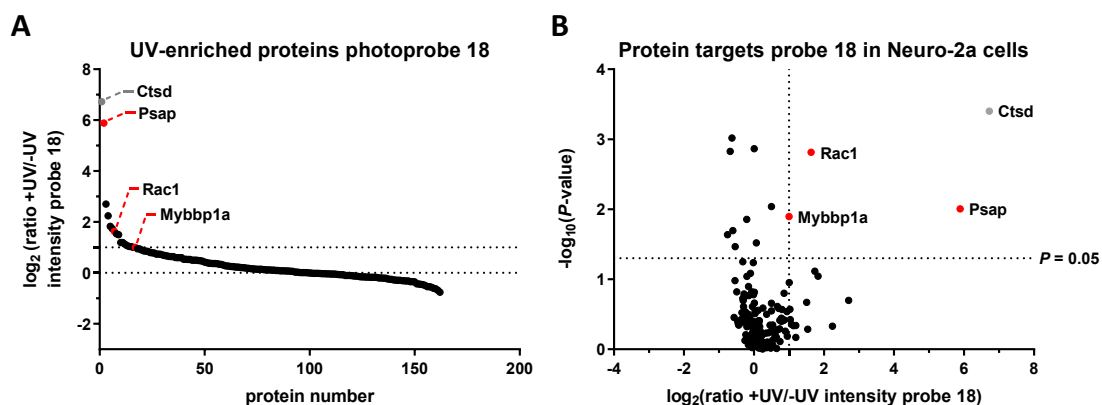


Figure 9. A) Waterfall plot showing UV enriched proteins of photoprobe **18** (20 μ M) in Neuro-2a cells. B) Volcano plot displaying significant protein targets for probe **18** (20 μ M). Red circles depict high confidence and grey circles low confidence targets. Data represent 3 biological replicates per condition. Cut-off values for protein target validation: unique peptides ≥ 2 , ratio +UV (*heavy*)/+UV (*light*) probe **18** intensity $0.5 \leq x \leq 2$, ratio +UV (*heavy*)/-UV (*light*) probe **18** intensity $x \geq 2$. Statistically significant targets: $P < 0.05$ using Student's *t*-test (unpaired, two-tailed) and Benjamini-Hochberg correction with FDR of 25%.

Table 1. Protein targets of photoprobe **18** in Neuro-2a cells.

| Name | Gene | MW (kDa) | Accession | Peptides | | Ratio | | P-value +UV/-UV Intensity | Function | Localization |
|--|----------------|----------|-----------|----------|--------|-------------------|-------------------|---------------------------|---|-------------------------|
| | | | | Total | Unique | +UV/+UV intensity | +UV/-UV intensity | | | |
| Cathepsin D | <i>Ctsd</i> | 45 | P18242 | 8 | 8 | 1.22 | 106 | 0.0003 | Protease; cleaves prosaposin to saposins A-D ⁶⁷ | Lysosome |
| Prosaposin | <i>Psap</i> | 58 | Q61207 | 9 | 9 | 1.21 | 59.2 | 0.0098 | Neurotrophic factor ⁶⁸ ; saposins A-D are lipid binding proteins that activate sphingolipid hydrolases ⁶⁶ | Cell membrane, lysosome |
| Ras-related C3 botulinum toxin substrate 1 | <i>Rac1</i> | 21 | P63001 | 6 | 5 | 0.96 | 3.10 | 0.0015 | GTPase ⁶⁹ | Cell membrane |
| Myb-binding protein 1a (p160) | <i>Mybbp1a</i> | 152 | Q7TPV4 | 9 | 9 | 0.99 | 2.00 | 0.0127 | Tumor suppressor ^{70,71} | Nucleus, cytosol |

Cut-off values for protein target validation: unique peptides ≥ 2 , ratio +UV (*heavy*)/+UV (*light*) probe **18** intensity $0.5 \leq x \leq 2$, ratio +UV (*heavy*)/-UV (*light*) probe **18** intensity $x \geq 2$. Statistically significant targets: $P < 0.05$ using Student's *t*-test (unpaired, two-tailed) and Benjamini-Hochberg correction with FDR of 25%.

| | | | |
|-----|--|-----|-------|
| 1 | MYALALFASLLATALTSPVQDPKTCSSGSAVLCRDVKTAVDCGAVKHCQQ | 50 | |
| 51 | MVWSKPTAK <u>SLPCDICK - TVVTEAGNLLKDNATQEEILHYLEKTCEWIHDS</u> | 100 | Sap A |
| 101 | <u>SLSASCK - EVVDSYLPVILDMIKGEMSNPGEVCSALNLCQSLQ</u> EYLAEQNQ | 151 | |
| 151 | KQLESNKIPEVDMARVVAPFMSNIPLLLYPQDHPRSQPQPK <u>ANEDVCQDC</u> | 200 | |
| 201 | <u>MK - LVSDVQTAVKTNSSFIQGFVDHVKEDCDRLGPGVSDICKNYVDQYSEV</u> | 250 | Sap B |
| 251 | <u>CVQMLMHMQDQPKEICVLAGFCNEVKRVPMKTLVPATETIKNILPALEM</u> | 300 | |
| 301 | MDPYEQNLVQAHN <u>VILCQTCQFVMNKFSELIVNNATEELLVKGLSNACAL</u> | 350 | Sap C |
| 351 | <u>LPDPARTKCQEVVGTFFGPSLLDIFIHEVNPSSLCGVIGLCAARPELVEAL</u> | 400 | |
| 401 | EQPAPAIVSALLKEPTPPKQPAQPKQSALPAHVPPQK <u>NGGFCEVCKKLVL</u> | 450 | |
| 451 | <u>YLEHNLEKNSTKEEILAALEKGSFLPDYQKQCDDFVAEYEP L L L E I L V</u> | 500 | Sap D |
| 501 | <u>EVMDPGFVCSKIGVCP SAY</u> KLLLGTEKCVWGPSYWCQNMETAARCNVDH | 550 | |
| 551 | CKRHVWN | | |

Figure 10. Amino acid sequence of full-length mouse prosaposin, showing the individual sequences of saposins A-D and the covered peptides (underlined) from two chemical proteomics experiments.

To summarize, four potential binding partners of NAPEs were identified using photoaffinity labeling. Considerable evidence suggests that the NAPE-prosaposin interaction could be an interesting topic for future studies in relation to neurodegeneration. Firstly, anionic phospholipids have been reported to stimulate the catalytic activity of saposin-mediated sphingolipid hydrolysis.⁷² Furthermore, saposin B is involved in the breakdown of a class of sphingolipids called gangliosides. During brain ischemia and similar to NAPEs, certain gangliosides were found to be elevated in and confined to areas that show severe cell death.⁷³⁻⁷⁵ The impact of anionic NAPE accumulation on sphingolipid metabolism is however not yet known. Secondly, prosaposin itself has been identified as a secreted and membrane-associated neurotrophic factor and a high-affinity ligand for the orphan G protein-coupled receptors GPR37 and GPR37L1.^{76,77} Psap levels are also highly elevated in brain ischemia and prosaposin spinal cord infusion was found to be neuroprotective in a gerbil model of ischemia.^{68,78,79} NAPEs could interfere with the trafficking of prosaposin from the ER to the lysosome where it undergoes proteolysis, thereby increasing the amount of secreted Psap and depleting the lysosomal pool of saposins A-D.⁷⁹

Of the other protein targets, Rac1 also merits closer examination. Rac1 is a small guanosine triphosphatase (GTPase) in the Rho family of GTPases that regulates the rearrangement of the actin cytoskeleton and promotes phagocytosis.⁶⁹ During phagosome formation, Rac1 localizes to anionic phospholipids in the plasma membrane via its polybasic domain.⁸⁰ *N*-palmitoyl-PE (NPPE)-enriched liposomes decreased phagocytosis in mouse J774A.1 macrophages by inhibiting Rac1 activity, thereby terminating inflammation.⁸¹ Furthermore, in a mouse model of brain ischemia, genetic deletion of *Rac1* showed to be neuroprotective.⁸² Thus, Rac1 constitutes an interesting target to study with regard to the anti-inflammatory and/or neuroprotective effects of NAPEs.

7.4 Closing remarks

Selective and *in vivo* active inhibitors are essential for the elucidation of biological signaling networks and for the development of new drugs. The work described in this thesis provides new inhibitors (**LEI-301** and **LEI-401**), chemical tools and assays to study the NAE-producing enzymes NAPE-PLD and PLAAT2. Genetic KO models have not been able to fully illuminate the complexity of NAE biosynthesis, possibly due to long-term compensatory effects. By blocking these enzymes in an acute fashion, the contributory role of NAPE-PLD and PLAAT2 with regard to NAE formation can be assessed across specific cells and tissues. In addition, **LEI-301** and **LEI-401** are suitable starting points to investigate the biological consequences of depleting the NAE tone, which may be useful in pathological conditions such as obesity, metabolic syndrome, chronic liver disease and cancer.

Acknowledgements

Bobby Florea, Peter van Veelen and Arnoud de Ru are kindly acknowledged for performing proteomics measurements.

7.4 Experimental section

Cell culture

Neuro-2a cells (ATCC) were cultured at 37 °C and 7% CO₂ in DMEM (Sigma Aldrich, D6546) with GlutaMax, penicillin (100 µg/ml), streptomycin (100 µg/ml) and 10% fetal calf serum. Cells were passaged twice a week to appropriate confluence by thorough pipetting.

Gel-based photoaffinity labeling

Neuro-2a cells were seeded in a 12-well plate (750,000 cells per well) 1 day before treatment. The cells were treated with the photoprobes **16-22** (500x in DMSO, final concentration: 20 μ M) in medium + serum (0.30 mL per well) for 30 min at 37 °C. The medium was aspirated and the cells were covered with PBS (0.15 mL per well), followed by UV irradiation using a Caprobox™ (10 min, 350 nm, 4 °C) or kept in the dark as a control. The cells were harvested into 1.5 mL epps with cold PBS and centrifuged (10 min, 2000 rpm, 4 °C). The PBS was removed and the cells were flash frozen with liquid N₂ (cells pellets can be stored at -80 °C). The cells were lysed with lysis buffer (30 μ L, 20 mM HEPES pH 7.2, 0.25 M sucrose, 1 mM MgCl₂, benzonase 25 U/mL) followed by pipetting up and down and incubating for 30 min on ice. Protein concentrations were measured using a Bradford assay (Bio-Rad), and cell lysates were diluted to 2 μ g/ μ L with lysis buffer. 18 μ g cell lysate (9 μ L) was then clicked with Cy5-N₃ using a click mix (1 μ L per sample, final concentrations: 1 mM CuSO₄, 6 mM sodium ascorbate, 0.2 mM tris(3-hydroxypropyltriazolylmethyl)-amine (THPTA), 2 μ M Cy5-N₃) for 1 h at rt (Note: it is important to separately prepare the click mix first with CuSO₄ and sodium ascorbate, until a yellow color change is observed). Samples were denatured with 4x Laemmli buffer (3.33 μ L, stock concentration: 240 mM Tris-HCl pH 6.8, 8% w/v SDS, 40% v/v glycerol, 5% v/v β -mercaptoethanol, 0.04% v/v bromophenol blue) and incubated for 30 min at rt. The samples were resolved by SDS-PAGE (10% acrylamide gel) at 180 V for 75 min, after which the gels were imaged at Cy3 and Cy5 channels (605/50 and 695/55 filters, respectively) on a ChemiDoc™ Imaging System (Bio-Rad). Gels were stained with Coomassie as a loading control.

Chemical proteomics-based photoaffinity labeling

10⁷ Neuro-2a cells were seeded in a 10 cm dish 1 day before treatment, three replicates per group. Cells were treated with photoprobe **18** (500x in DMSO, final concentration: 20 μ M) in medium + serum (4 mL per dish) for 30 min at 37 °C. The medium was aspirated and the cells were covered with PBS (1.5 mL per dish), followed by UV irradiation using a Caprobox™ (10 min, 350 nm, 4 °C) or kept in the dark as a control. The cells were harvested into 15 mL tubes with cold PBS and centrifuged (10 min, 2000 rpm, 4 °C). The supernatant was removed and the cells were washed with PBS (1 x 10 mL) and centrifuged (10 min, 2000 rpm, 4 °C). The PBS was removed and the cell pellets were flash frozen with liquid N₂ (cell pellets can be stored at -80 °C for later use). The cells were lysed with lysis buffer (200 μ L, 20 mM HEPES pH 7.2, 0.25 M sucrose, 1 mM MgCl₂, benzonase 25 U/mL) followed by probe sonication (10% amplitude, 4 x 2.5 s) and incubation for 30 min on ice. The lysates were centrifuged (90 min, 30,000 g, 4 °C) giving the cytosol fraction (supernatant). The membrane fraction (pellet) was resuspended in storage buffer (250 μ L, 20 mM HEPES pH 7.2) and homogenized by probe sonication (10% amplitude, 4 x 2.5 s). Protein concentrations were determined using a Bradford assay (Bio-Rad) and cell lysates were diluted to 2 μ g/ μ L with lysis buffer.

From here the quantitative chemical proteomics protocol using dimethyl labeling was followed as previously described with small alterations.⁸³ 225 μ L cytosol or membrane lysate (450 μ g) was clicked with biotin-N₃ (Sigma Aldrich, 762024) using a click mix (25 μ L per sample, final concentrations: 1 mM CuSO₄, 6 mM sodium ascorbate, 0.2 mM tris(3-hydroxypropyltriazolylmethyl)amine (THPTA), 100 μ M biotin-N₃) for 1 h at rt (Note: it is important to separately prepare the click mix first with CuSO₄ and sodium ascorbate, until a yellow color change is observed). Proteins were precipitated using chloroform (166 μ L), methanol (666 μ L) and MilliQ (416 μ L). Samples were centrifuged (10 min, 1,500 g) and the solvents were carefully removed. Methanol (600 μ L) was added and the proteins were resuspended using a probe sonicator (30% amplitude, 10 s). After centrifugation (5 min, 18,400 g) the supernatant was removed and the samples were resuspended in urea buffer (500 μ L, 6 M urea, 250 mM NH₄HCO₃) by pipetting up and down. 1 M DTT (5 μ L, final concentration 10 mM) was added and the samples were incubated with shaking (15 min, 600 rpm, 65 °C). After cooling to rt, 0.5 M iodoacetamide (40 μ L, final concentration 40 mM) was added and incubated in the dark with shaking (30 min, 600 rpm, 20 °C). Next, 10% SDS (140 μ L, final concentration 2%) was added and incubated with shaking (5 min, 600 rpm, 65 °C). For 18 samples, 1.8 mL of avidin agarose beads (Sigma-

Aldrich, A9207) was divided over three 15 mL tubes and washed with PBS (3 x 10 mL). The beads in each tube were resuspended in PBS (6 mL) and divided over 18 tubes (1 mL each). To each tube was added the denatured sample and PBS (4.5 mL) and the tubes were rotated with an overhead shaker at rt for 2 h. After centrifugation (2 min, 2,500 g) and removal of the supernatant, the beads were consecutively washed with 0.5% SDS in PBS (w/v, 6 mL) and PBS (3 x 6 mL), each time centrifuging (2 min, 2,500 g). The beads were transferred to a 1.5 mL low binding epp (Sarstedt, 72.706.600) with on-bead digestion buffer (200 μ L, 100 mM Tris pH 8.0, 100 mM NaCl, 1 mM CaCl₂, 2% v/v acetonitrile) and to each sample was added 1 μ L trypsin solution (0.5 μ g/ μ L trypsin (Promega, V5111), 0.1 mM HCl). Proteins were digested with vigorous shaking overnight (950 rpm, 37 °C). Formic acid (10 μ L) was added to each sample and the beads were filtered off by centrifugation (2.5 min, 600 g) using a biospin column (Bio-Rad, 7326204), the flow-through was collected in a 2 mL epp.

Tryptic digests were desalted and treated with heavy or light isotopically labeled formaldehyde using StageTips.⁸⁴ The samples were treated according to the following steps:

| Step | Treatment | Centrifugation* |
|-------------------|---|-----------------|
| Conditioning 1 | Methanol (50 μ L) | 2 min, 600 g |
| Conditioning 2 | StageTip solution B (50 μ L) | 2 min, 600 g |
| Conditioning 3 | StageTip solution A (50 μ L) | 2 min, 600 g |
| Loading | Load samples on StageTips | 2.5 min, 800 g |
| Washing | StageTip solution A (100 μ L) | 2.5 min, 800 g |
| Dimethyl labeling | Heavy or light reagent mix (5 x 20 μ L) | 5.0 min, 400 g |
| Washing | StageTip solution A (100 μ L) | 2.5 min, 800 g |
| Transfer | Transfer StageTip to new 1.5 mL low binding epp | |
| Elution | StageTip solution B (100 μ L) | 2.5 min, 800 g |

* Indication speed.

StageTip solution A: 80% v/v acetonitrile, 0.5% v/v formic acid in MilliQ.

StageTip solution B: 0.5% v/v formic acid in MilliQ.

Heavy reagent mix: 50 mM phosphate buffer pH 7.5, 2% v/v CD₂O, 30 mM NaBH₃CN.

Light reagent mix: 50 mM phosphate buffer pH 7.5, 2% v/v CH₂O, 30 mM NaBH₃CN.

The solvents were evaporated to dryness in a SpeedVac concentrator (3 h, 45 °C). Samples were reconstituted in LC-MS solution (50 μ L, 3% v/v acetonitrile, 0.1% v/v formic acid in MilliQ). Samples were combined in a 1:1 ratio, affording 4 sample groups:

- Heavy (+UV) + light (+UV) labeled membrane fraction (quality control)
- Heavy (+UV) + light (+UV) labeled cytosol fraction (quality control)
- Heavy (+UV) + light (-UV) labeled membrane fraction (UV-enrichment)
- Heavy (+UV) + light (-UV) labeled cytosol fraction (UV-enrichment)

Tryptic peptides were analyzed on a Surveyor nanoLC system (Thermo) hyphenated to a LTQ-Orbitrap mass spectrometer (ThermoFisher). Briefly, emitter, trap and analytical column (C18, 120 Å) were purchased from Nanoseparations (Nieuwkoop, The Netherlands) and mobile phases (A: 0.1% formic acid/H₂O, B: 0.1% formic acid/ACN) were made with ULC/MS grade solvents (Biosolve). General mass spectrometric conditions were: electrospray voltage of 1.8-2.5 kV, no sheath and auxiliary gas flow, capillary voltage 40 V, tube lens voltage 155 V and ion transfer tube temperature 150 °C. Polydimethylcyclosiloxane (m/z = 445.12002) and dioctyl phthalate ions (m/z = 391.28429) from the milieu were used as lock mass. Some 10 μ L of the samples was pressure loaded on the trap column for 5 min with a 10 μ L/min flow and separated with a gradient of

35 min 5%-30% B, 15 min 30%-60% B, 5 min A at a flow of 300 $\mu\text{L}/\text{min}$ split to 250 nL/min by the LTQ divert valve. Full MS scans (300-2000 m/z) acquired at high mass resolution (60,000 at 400 m/z, maximum injection time 1000 ms, AGC 106) in the Orbitrap was followed by three MS/MS fragmentations in the LTQ linear ion trap (AGC 5 x 10³, maximum injection time 120 ms) from the three most abundant ions. MS/MS settings were: collision gas pressure 1.3 mT, normalized collision energy 35%, ion selection threshold of 750 counts, activation $q = 0.25$ and activation time 30 ms. Ions of $z < 2$ or unassigned were not analyzed and fragmented precursor ions were measured twice within 10 s and were dynamically excluded for 60 s.

Data analysis was performed using Maxquant with acetylation (protein N-terminus) and oxidation (M) as variable modifications. The false discovery rate was set at 1% and the peptides were screened against mouse proteome (Uniprot). Proteins were designated as probe **18** targets according to the following cut-offs: unique peptides ≥ 2 , ratio +UV (*heavy*)/+UV (*light*) probe **18** intensity $0.5 \leq x \leq 2$, ratio +UV (*heavy*)/-UV (*light*) probe **18** intensity $x \geq 2$. Statistic testing: $P < 0.05$ using Student's *t*-test (unpaired, two-tailed) and Benjamini-Hochberg correction with FDR of 25%.

References

1. Devane, W., Hanus, L., Breuer, A., Pertwee, R., Stevenson, L., Griffin, G., Gibson, D., Mandelbaum, A., Etinger, A. & Mechoulam, R. Isolation and structure of a brain constituent that binds to the cannabinoid receptor. *Science* **258**, 1946-1949 (1992).
2. Stelt, M.v.d. & Marzo, V.D. Endovanilloids. *European Journal of Biochemistry* **271**, 1827-1834 (2004).
3. Cravatt, B.F., Demarest, K., Patricelli, M.P., Bracey, M.H., Giang, D.K., Martin, B.R. & Lichtman, A.H. Supersensitivity to anandamide and enhanced endogenous cannabinoid signaling in mice lacking fatty acid amide hydrolase. *Proceedings of the National Academy of Sciences* **98**, 9371-9376 (2001).
4. Williams, C.M. & Kirkham, T.C. Anandamide induces overeating: mediation by central cannabinoid (CB₁) receptors. *Psychopharmacology* **143**, 315-317 (1999).
5. Wang, H., Xie, H., Guo, Y., Zhang, H., Takahashi, T., Kingsley, P.J., Marnett, L.J., Das, S.K., Cravatt, B.F. & Dey, S.K. Fatty acid amide hydrolase deficiency limits early pregnancy events. *The Journal of Clinical Investigation* **116**, 2122-2131 (2006).
6. Eljaschewitsch, E., Witting, A., Mawrin, C., Lee, T., Schmidt, P.M., Wolf, S., Hoertnagl, H., Raine, C.S., Schneider-Stock, R., Nitsch, R. & Ullrich, O. The endocannabinoid anandamide protects neurons during CNS inflammation by induction of MKP-1 in microglial cells. *Neuron* **49**, 67-79 (2006).
7. Morena, M., Roozendaal, B., Trezza, V., Ratano, P., Peloso, A., Hauer, D., Atsak, P., Trabace, L., Cuomo, V., McGaugh, J.L., Schelling, G. & Campolongo, P. Endogenous cannabinoid release within prefrontal- limbic pathways affects memory consolidation of emotional training. *Proceedings of the National Academy of Sciences* **111**, 18333-18338 (2014).
8. Gobbi, G., Bambico, F.R., Mangieri, R., Bortolato, M., Campolongo, P., Solinas, M., Cassano, T., Morgese, M.G., Debonnel, G., Duranti, A., Tontini, A., Tarzia, G., Mor, M., Trezza, V., Goldberg, S.R., Cuomo, V. & Piomelli, D. Antidepressant-like activity and modulation of brain monoaminergic transmission by blockade of anandamide hydrolysis. *Proceedings of the National Academy of Sciences* **102**, 18620-18625 (2005).
9. Kathuria, S., Gaetani, S., Fegley, D., Valiño, F., Duranti, A., Tontini, A., Mor, M., Tarzia, G., Rana, G.L., Calignano, A., Giustino, A., Tattoli, M., Palmery, M., Cuomo, V. & Piomelli, D. Modulation of anxiety through blockade of anandamide hydrolysis. *Nature Medicine* **9**, 76 (2002).
10. Fanelli, F., Mezzullo, M., Repaci, A., Belluomo, I., Ibarra Gasparini, D., Di Dalmazi, G., Mastroberto, M., Vicennati, V., Gambineri, A., Morselli-Labate, A.M., Pasquali, R. & Pagotto, U. Profiling plasma N-acylethanolamine levels and their ratios as a biomarker of obesity and dysmetabolism. *Molecular Metabolism* **14**, 82-94 (2018).

11. Bowles, N.P., Karatsoreos, I.N., Li, X., Vemuri, V.K., Wood, J.-A., Li, Z., Tamashiro, K.L.K., Schwartz, G.J., Makriyannis, A.M., Kunos, G., Hillard, C.J., McEwen, B.S. & Hill, M.N. A peripheral endocannabinoid mechanism contributes to glucocorticoid-mediated metabolic syndrome. *Proceedings of the National Academy of Sciences* **112**, 285-290 (2015).
12. Mukhopadhyay, B., Schuebel, K., Mukhopadhyay, P., Cinar, R., Godlewski, G., Xiong, K., Mackie, K., Lizak, M., Yuan, Q., Goldman, D. & Kunos, G. Cannabinoid receptor 1 promotes hepatocellular carcinoma initiation and progression through multiple mechanisms. *Hepatology* **61**, 1615-1626 (2015).
13. Masoodi, M., Lee, E., Eiden, M., Bahlo, A., Shi, Y., Ceddia, R.B., Baccei, C., Prasit, P. & Spaner, D.E. A role for oleoylethanolamide in chronic lymphocytic leukemia. *Leukemia* **28**, 1381 (2014).
14. Caraceni, P., Viola, A., Piscitelli, F., Giannone, F., Berzigotti, A., Cescon, M., Domenicali, M., Petrosino, S., Giampalma, E., Riili, A., Grazi, G., Golfieri, R., Zoli, M., Bernardi, M. & Di Marzo, V. Circulating and hepatic endocannabinoids and endocannabinoid-related molecules in patients with cirrhosis. *Liver International* **30**, 816-825 (2010).
15. Tam, J., Hinden, L., Drori, A., Udi, S., Azar, S. & Baraghithy, S. The therapeutic potential of targeting the peripheral endocannabinoid/CB₁ receptor system. *European Journal of Internal Medicine* **49**, 23-29 (2018).
16. Hussain, Z., Uyama, T., Tsuboi, K. & Ueda, N. Mammalian enzymes responsible for the biosynthesis of *N*-acylethanolamines. *Biochimica et Biophysica Acta (BBA) - Molecular and Cell Biology of Lipids* **1862**, 1546-1561 (2017).
17. Leung, D., Saghatelian, A., Simon, G.M. & Cravatt, B.F. Inactivation of *N*-acyl phosphatidylethanolamine phospholipase D reveals multiple mechanisms for the biosynthesis of endocannabinoids. *Biochemistry* **45**, 4720-4726 (2006).
18. Tsuboi, K., Okamoto, Y., Ikematsu, N., Inoue, M., Shimizu, Y., Uyama, T., Wang, J., Deutsch, D.G., Burns, M.P., Ulloa, N.M., Tokumura, A. & Ueda, N. Enzymatic formation of *N*-acylethanolamines from *N*-acylethanolamine plasmalogen through *N*-acylphosphatidylethanolamine-hydrolyzing phospholipase D-dependent and -independent pathways. *Biochimica et Biophysica Acta (BBA) - Molecular and Cell Biology of Lipids* **1811**, 565-577 (2011).
19. Leishman, E., Mackie, K., Luquet, S. & Bradshaw, H.B. Lipidomics profile of a NAPE-PLD KO mouse provides evidence of a broader role of this enzyme in lipid metabolism in the brain. *Biochimica et Biophysica Acta (BBA) - Molecular and Cell Biology of Lipids* **1861**, 491-500 (2016).
20. Lapinsky, D.J. & Johnson, D.S. Recent developments and applications of clickable photoprobes in medicinal chemistry and chemical biology. *Future Medicinal Chemistry* **7**, 2143-2171 (2015).
21. Smith, D.A., Beaumont, K., Maurer, T.S. & Di, L. Relevance of half-life in drug design. *Journal of Medicinal Chemistry* **61**, 4273-4282 (2018).
22. Hopkins, A.L., Keserü, G.M., Leeson, P.D., Rees, D.C. & Reynolds, C.H. The role of ligand efficiency metrics in drug discovery. *Nature Reviews Drug Discovery* **13**, 105 (2014).
23. Meanwell, N.A. Fluorine and fluorinated motifs in the design and application of bioisosteres for drug design. *Journal of Medicinal Chemistry* **61**, 5822-5880 (2018).
24. Bagal, S.K. & Bungay, P.J. Minimizing drug exposure in the CNS while maintaining good oral absorption. *ACS Medicinal Chemistry Letters* **3**, 948-950 (2012).
25. Ogasawara, D., Deng, H., Viader, A., Baggelaar, M.P., Breman, A., den Dulk, H., van den Nieuwendijk, A.M.C.H., Soethoudt, M., van der Wel, T., Zhou, J., Overkleeft, H.S., Sanchez-Alavez, M., Mori, S., Nguyen, W., Conti, B., Liu, X., Chen, Y., Liu, Q.-s., Cravatt, B.F. & van der Stelt, M. Rapid and profound rewiring of brain lipid signaling networks by acute diacylglycerol lipase inhibition. *Proceedings of the National Academy of Sciences* **113**, 26 (2016).
26. Maccarrone, M., Rossi, S., Bari, M., De Chiara, V., Fezza, F., Musella, A., Gasperi, V., Prosperetti, C., Bernardi, G., Finazzi-Agrò, A., Cravatt, B.F. & Centonze, D. Anandamide inhibits metabolism and physiological actions of 2-arachidonoylglycerol in the striatum. *Nature Neuroscience* **11**, 152 (2008).

27. Wright, M.H. & Sieber, S.A. Chemical proteomics approaches for identifying the cellular targets of natural products. *Natural Product Reports* **33**, 681-708 (2016).
28. Flaxman, H.A. & Woo, C.M. Mapping the small molecule interactome by mass spectrometry. *Biochemistry* **57**, 186-193 (2018).
29. Smith, E. & Collins, I. Photoaffinity labeling in target- and binding-site identification. *Future Medicinal Chemistry* **7**, 159-183 (2015).
30. Yang, Y., Fonović, M. & Verhelst, S.H.L. Cleavable linkers in chemical proteomics applications, in *Activity-Based Proteomics: Methods and Protocols*. (eds. H.S. Overkleeft & B.I. Florea) 185-203 (Springer New York, New York, NY; 2017).
31. van der Stelt, M., Hansen, H.H., Veldhuis, W.B., Bär, P.R., Nicolay, K., Veldink, G.A., Vliegthart, J.F.G. & Hansen, H.S. Biosynthesis of endocannabinoids and their modes of action in neurodegenerative diseases. *Neurotoxicity Research* **5**, 183-199 (2003).
32. Wang, J. & Ueda, N. Biology of endocannabinoid synthesis system. *Prostaglandins & Other Lipid Mediators* **89**, 112-119 (2009).
33. Uyama, T., Ikematsu, N., Inoue, M., Shinohara, N., Jin, X.-H., Tsuboi, K., Tonai, T., Tokumura, A. & Ueda, N. Generation of *N*-acylphosphatidylethanolamine by members of the phospholipase A/acyltransferase (PLA/AT) family. *Journal of Biological Chemistry* **287**, 31905-31919 (2012).
34. Zhou, J., Mock, E.D., Martella, A., Kantae, V., Di, X., Burggraaff, L., Baggelaar, M.P., Al-Ayed, K., Bakker, A., Florea, B.I., Grimm, S.H., den Dulk, H., Li, C.T., Mulder, L., Overkleeft, H.S., Hankemeier, T., van Westen, G.J.P. & van der Stelt, M. Activity-based protein profiling identifies α -ketoamides as inhibitors for phospholipase A₂ group XVI. *ACS Chemical Biology* **14**, 164-169 (2019).
35. Fischl, W., Whittaker, M., Yarnold, C.J., Pons, J.-F., Kerry, M.A., Amouzegh, P.L., Morao, I., Ingram, P.N. & Chudyk, E.I., Vol. WO2018050631A1.
36. Golczak, M., Kiser, P.D., Sears, A.E., Lodowski, D.T., Blaner, W.S. & Palczewski, K. Structural basis for the acyltransferase activity of lecithin:retinol acyltransferase-like proteins. *J Biol Chem* **287**, 23790-23807 (2012).
37. Pang, X.-Y., Cao, J., Addington, L., Lovell, S., Battaile, K.P., Zhang, N., Rao, J.L.U.M., Dennis, E.A. & Moise, A.R. Structure/function relationships of adipose phospholipase A₂ containing a Cys-His-His catalytic triad. *Journal of Biological Chemistry* **287**, 35260-35274 (2012).
38. Baggelaar, M.P., Janssen, F.J., van Esbroeck, A.C.M., den Dulk, H., Allara, M., Hoogendoorn, S., McGuire, R., Florea, B.I., Meeuwenoord, N., van den Elst, H., van der Marel, G.A., Brouwer, J., Di Marzo, V., Overkleeft, H.S. & van der Stelt, M. Development of an activity-based probe and in silico design reveal highly selective inhibitors for diacylglycerol lipase-alpha in brain. *Angew. Chem.-Int. Edit.* **52**, 12081-12085 (2013).
39. Mulder, M.P.C., Witting, K., Berlin, I., Pruneda, J.N., Wu, K.-P., Chang, J.-G., Merckx, R., Bialas, J., Groettrup, M., Vertegaal, A.C.O., Schulman, B.A., Komander, D., Neefjes, J., El Oualid, F. & Ova, H. A cascading activity-based probe sequentially targets E1-E2-E3 ubiquitin enzymes. *Nature Chemical Biology* **12**, 523 (2016).
40. Verdoes, M., Oresic Bender, K., Segal, E., van der Linden, W.A., Syed, S., Withana, N.P., Sanman, L.E. & Bogyo, M. Improved quenched fluorescent probe for imaging of cysteine cathepsin activity. *Journal of the American Chemical Society* **135**, 14726-14730 (2013).
41. Sanman, L.E. & Bogyo, M. Activity-based profiling of proteases. *Annual Review of Biochemistry* **83**, 249-273 (2014).
42. Leyva, M.J., DeGiacomo, F., Kaltenbach, L.S., Holcomb, J., Zhang, N., Gafni, J., Park, H., Lo, D.C., Salvesen, G.S., Ellerby, L.M. & Ellman, J.A. Identification and evaluation of small molecule pan-caspase inhibitors in Huntington's disease models. *Chemistry & Biology* **17**, 1189-1200 (2010).
43. Shyu, R.-Y., Hsieh, Y.-C., Tsai, F.-M., Wu, C.-C. & Jiang, S.-Y. Cloning and functional characterization of the HRASLS2 gene. *Amino Acids* **35**, 129-137 (2008).

44. Uyama, T., Jin, X.-H., Tsuboi, K., Tonai, T. & Ueda, N. Characterization of the human tumor suppressors TIG3 and HRASLS2 as phospholipid-metabolizing enzymes. *Biochimica et Biophysica Acta (BBA) - Molecular and Cell Biology of Lipids* **1791**, 1114-1124 (2009).
45. Piomelli, D. A fatty gut feeling. *Trends in Endocrinology & Metabolism* **24**, 332-341 (2013).
46. van Eenige, R., van der Stelt, M., Rensen, P.C.N. & Kooijman, S. Regulation of adipose tissue metabolism by the endocannabinoid system. *Trends in Endocrinology & Metabolism* **29**, 326-337 (2018).
47. Coulon, D., Faure, L., Salmon, M., Wattelet, V. & Bessoule, J.-J. Occurrence, biosynthesis and functions of *N*-acylphosphatidylethanolamines (NAPE): Not just precursors of *N*-acylethanolamines (NAE). *Biochimie* **94**, 75-85 (2012).
48. Wellner, N., Diep, T.A., Janfelt, C. & Hansen, H.S. *N*-Acylation of phosphatidylethanolamine and its biological functions in mammals. *Biochimica et Biophysica Acta (BBA) - Molecular and Cell Biology of Lipids* **1831**, 652-662 (2013).
49. Domingo, J.C., Mora, M. & Africa de Madariaga, M. Role of headgroup structure in the phase behaviour of *N*-acylethanolamine phospholipids: hydrogen-bonding ability and headgroup size. *Chemistry and Physics of Lipids* **69**, 229-240 (1994).
50. Swamy, M.J., Tarafdar, P.K. & Kamlekar, R.K. Structure, phase behaviour and membrane interactions of *N*-acylethanolamines and *N*-acylphosphatidylethanolamines. *Chemistry and Physics of Lipids* **163**, 266-279 (2010).
51. Shangguan, T., Pak, C.C., Ali, S., Janoff, A.S. & Meers, P. Cation-dependent fusogenicity of an *N*-acyl phosphatidylethanolamine. *Biochimica et Biophysica Acta (BBA) - Biomembranes* **1368**, 171-183 (1998).
52. Mora, M., Mir, F., de Madariaga, M.A. & Sagrista, M.L. Aggregation and fusion of vesicles composed of *N*-palmitoyl derivatives of membrane phospholipids. *Lipids* **35**, 513-524 (2000).
53. Epps, D.E., Natarajan, V., Schmid, P.C. & Schmid, H.H.O. Accumulation of *N*-acylethanolamine glycerophospholipids in infarcted myocardium. *Biochimica et Biophysica Acta (BBA) - Lipids and Lipid Metabolism* **618**, 420-430 (1980).
54. Natarajan, V., Schmid, P.C. & Schmid, H.H.O. *N*-Acylethanolamine phospholipid metabolism in normal and ischemic rat brain. *Biochimica et Biophysica Acta (BBA) - Lipids and Lipid Metabolism* **878**, 32-41 (1986).
55. Moesgaard, B., Petersen, G., Jaroszewski, J.W. & Hansen, H.S. Age dependent accumulation of *N*-acylethanolamine phospholipids in ischemic rat brain: a ³¹P NMR and enzyme activity study. *Journal of Lipid Research* **41**, 985-990 (2000).
56. Hansen, H.H., Ikonomidou, C., Bittigau, P., Hansen, S.H. & Hansen, H.S. Accumulation of the anandamide precursor and other *N*-acylethanolamine phospholipids in infant rat models of *in vivo* necrotic and apoptotic neuronal death. *Journal of Neurochemistry* **76**, 39-46 (2001).
57. Moesgaard, B., Hansen, H.H., Hansen, S.L., Hansen, S.H., Petersen, G. & Hansen, H.S. Brain levels of *N*-acylethanolamine phospholipids in mice during pentylenetetrazol-induced seizure. *Lipids* **38**, 387-390 (2003).
58. Janfelt, C., Wellner, N., Leger, P.-L., Kokesch-Himmelreich, J., Hansen, S.H., Charriaut-Marlangue, C. & Hansen, H.S. Visualization by mass spectrometry of 2-dimensional changes in rat brain lipids, including *N*-acylphosphatidylethanolamines, during neonatal brain ischemia. *The FASEB Journal* **26**, 2667-2673 (2012).
59. Basit, A., Pontis, S., Piomelli, D. & Armirotti, A. Ion mobility mass spectrometry enhances low-abundance species detection in untargeted lipidomics. *Metabolomics* **12**, 50 (2016).
60. Rawlyer, A.J. & Braendle, R.A. *N*-Acylphosphatidylethanolamine accumulation in potato cells upon energy shortage caused by anoxia or respiratory inhibitors. *Plant Physiology* **127**, 240-251 (2001).

61. Zhang, C. & Tian, S. Peach fruit acquired tolerance to low temperature stress by accumulation of linolenic acid and *N*-acylphosphatidylethanolamine in plasma membrane. *Food Chemistry* **120**, 864-872 (2010).
62. Pongracz, K. & Gryaznov, S. Oligonucleotide N3'→P5' thiophosphoramidates: synthesis and properties. *Tetrahedron Letters* **40**, 7661-7664 (1999).
63. Hsu, J.-L., Huang, S.-Y., Chow, N.-H. & Chen, S.-H. Stable-isotope dimethyl labeling for quantitative proteomics. *Analytical Chemistry* **75**, 6843-6852 (2003).
64. Cox, J. & Mann, M. MaxQuant enables high peptide identification rates, individualized p.p.b.-range mass accuracies and proteome-wide protein quantification. *Nature Biotechnology* **26**, 1367 (2008).
65. Kleiner, P., Heydenreuter, W., Stahl, M., Korotkov, V.S. & Sieber, S.A. A whole proteome inventory of background photocrosslinker binding. *Angewandte Chemie International Edition* **56**, 1396-1401 (2017).
66. Kolter, T. & Sandhoff, K. Lysosomal degradation of membrane lipids. *FEBS Letters* **584**, 1700-1712 (2010).
67. Hiraiwa, M., Martin, B.M., Kishimoto, Y., Conner, G.E., Tsuji, S. & O'Brien, J.S. Lysosomal proteolysis of prosaposin, the precursor of saposins (sphingolipid activator proteins): its mechanism and inhibition by ganglioside. *Archives of Biochemistry and Biophysics* **341**, 17-24 (1997).
68. Meyer, R.C., Giddens, M.M., Coleman, B.M. & Hall, R.A. The protective role of prosaposin and its receptors in the nervous system. *Brain Research* **1585**, 1-12 (2014).
69. Payapilly, A. & Malliri, A. Compartmentalisation of RAC1 signalling. *Current Opinion in Cell Biology* **54**, 50-56 (2018).
70. Mori, S., Bernardi, R., Laurent, A., Resnati, M., Crippa, A., Gabrieli, A., Keough, R., Gonda, T.J. & Blasi, F. Myb-binding protein 1a (MYBBP1A) is essential for early embryonic development, controls cell cycle and mitosis, and acts as a tumor suppressor. *PLOS ONE* **7**, e39723 (2012).
71. Akaogi, K., Ono, W., Hayashi, Y., Kishimoto, H. & Yanagisawa, J. MYBBP1A suppresses breast cancer tumorigenesis by enhancing the p53 dependent anoikis. *BMC Cancer* **13**, 65 (2013).
72. Abdul-Hammed, M., Breiden, B., Schwarzmann, G. & Sandhoff, K. Lipids regulate the hydrolysis of membrane bound glucosylceramide by lysosomal β -glucocerebrosidase. *Journal of Lipid Research* **58**, 563-577 (2017).
73. Trindade, V.M.T., Daniotti, J.L., Raimondi, L., Chazan, R., Netto, C.A. & Maccioni, H.J.F. Effects of neonatal hypoxia/ischemia on ganglioside expression in the rat hippocampus. *Neurochemical Research* **26**, 591-597 (2001).
74. Whitehead, S.N., Chan, K.H.N., Gangaraju, S., Slinn, J., Li, J. & Hou, S.T. Imaging mass spectrometry detection of gangliosides species in the mouse brain following transient focal cerebral ischemia and long-term recovery. *PLOS ONE* **6**, e20808 (2011).
75. Luptakova, D., Baciak, L., Pluhacek, T., Skriba, A., Sediva, B., Havlicek, V. & Juranek, I. Membrane depolarization and aberrant lipid distributions in the neonatal rat brain following hypoxic-ischaemic insult. *Scientific Reports* **8**, 6952 (2018).
76. O'Brien, J.S., Carson, G.S., Seo, H.C., Hiraiwa, M. & Kishimoto, Y. Identification of prosaposin as a neurotrophic factor. *Proceedings of the National Academy of Sciences* **91**, 9593-9596 (1994).
77. Meyer, R.C., Giddens, M.M., Schaefer, S.A. & Hall, R.A. GPR37 and GPR37L1 are receptors for the neuroprotective and glioprotective factors prosaptide and prosaposin. *Proceedings of the National Academy of Sciences* **110**, 9529-9534 (2013).
78. Sano, A., Matsuda, S., Wen, T.C., Kotani, Y., Kondoh, K., Ueno, S., Kakimoto, Y., Yoshimura, H. & Sakanaka, M. Protection by prosaposin against ischemia-induced learning disability and neuronal loss. *Biochemical and Biophysical Research Communications* **204**, 994-1000 (1994).
79. Costain, W.J., Haqqani, A.S., Rasquinha, I., Giguere, M.-S., Slinn, J., Zurakowski, B. & Stanimirovic, D.B. Proteomic analysis of synaptosomal protein expression reveals that cerebral ischemia alters lysosomal Psap processing. *Proteomics* **10**, 3272-3291 (2010).

80. Magalhaes, M.A.O. & Glogauer, M. Pivotal advance: phospholipids determine net membrane surface charge resulting in differential localization of active Rac1 and Rac2. *Journal of Leukocyte Biology* **87**, 545-555 (2010).
81. Ichiki, M., Sugimoto, N., Ueda, N., Okamoto, Y., Takuwa, Y., Nakanishi, Y. & Shiratsuchi, A. Inhibitory effect of *N*-palmitoylphosphatidylethanolamine on macrophage phagocytosis through inhibition of Rac1 and Cdc42. *The Journal of Biochemistry* **145**, 43-50 (2008).
82. Karabiyik, C., Fernandes, R., Figueiredo, F.R., Socodato, R., Brakebusch, C., Lambertsen, K.L., Relvas, J.B. & Santos, S.D. Neuronal Rho GTPase Rac1 elimination confers neuroprotection in a mouse model of permanent ischemic stroke. *Brain Pathology* **28**, 569-580 (2018).
83. Baggelaar, M.P., Chameau, P.J.P., Kantae, V., Hummel, J., Hsu, K.L., Janssen, F., van der Wel, T., Soethoudt, M., Deng, H., den Dulk, H., Allara, M., Florea, B.I., Di Marzo, V., Wadman, W.J., Kruse, C.G., Overkleeft, H.S., Hankemeier, T., Werkman, T.R., Cravatt, B.F. & van der Stelt, M. Highly selective, reversible inhibitor identified by comparative chemoproteomics modulates diacylglycerol lipase activity in neurons. *Journal of the American Chemical Society* **137**, 8851-8857 (2015).
84. Rappsilber, J., Mann, M. & Ishihama, Y. Protocol for micro-purification, enrichment, pre-fractionation and storage of peptides for proteomics using StageTips. *Nature Protocols* **2**, 1896 (2007).

Samenvatting

Nieuw moleculair gereedschap voor het bestuderen van de biosynthese van *N*-acylethanolamines

Dit proefschrift beschrijft de ontdekking en optimalisatie van moleculair gereedschap om de biosynthese van *N*-acylethanolamines (NAEs) beter in kaart te brengen. Twee relevante enzymen zijn hiervoor bestudeerd, te weten *N*-acylfosfatidylethanolamine fosfolipase D (NAPE-PLD) en fosfolipase A en acyltransferase 2 (PLAAT2), respectievelijk betrokken bij de productie van NAEs of hun directe precursors, de NAPEs. Om nieuwe remmers te identificeren, zogeheten *hits*, zijn verschillende screeningsmethodes toegepast zoals *high-throughput screening* (HTS) en screenings van specifieke molecuulbibliotheken. Door middel van structuur-activiteitrelaties zijn deze initiële *hits* geoptimaliseerd tot potente enzymremmers, die werkzaam zijn in cellulaire en/of diermodellen. Het vaststellen van remmer-enzym interactie, ook wel *target engagement* genoemd, is bevestigd met fotoaffiniteitlabeling (PAL) of activiteit-gebaseerde eiwit profilering (ABPP). Verder is met behulp van *lipidomics* cellulaire en/of *in vivo* activiteit aangetoond van de beschreven remmers. Tot slot liet de hier beschreven NAPE-PLD remmer **LEI-401** pijnstillende effecten zien in meerdere muismodellen, dat mogelijk van therapeutische waarde is en verder zal worden bestudeerd in toekomstig onderzoek.

Hoofdstuk 1 geeft een overzicht van de aanmaak en afbraak van NAEs en hun biologische functies. De NAEs zijn een familie van signaallipiden waartoe onder andere *N*-palmitoylethanolamine (PEA), *N*-oleoylethanolamine (OEA), *N*-arachidonoylethanolamine (AEA, anandamide) en *N*-docosahexaenoylethanolamine (DHEA) behoren. De verschillende NAEs activeren specifieke receptoren zowel in het brein als in de periferie, zoals G-eiwit gekoppelde receptoren (GPCRs), ionkanalen en kernreceptoren. Het meest bekende voorbeeld is anandamide, in 1992 ontdekt als endogene agonist van de cannabis CB₁ receptor en om deze reden gemunt als endocannabinoïde.¹ Vervolgonderzoek liet zien dat anandamide ook de CB₂ receptor en de *transient receptor potential receptor 1* (TRPV1, capsaïcine receptor) kan activeren. Om deze reden wordt anandamide ook tot de endovanilloïden gerekend.² Een scala aan biologische functies zijn aan anandamide gekoppeld, zoals pijnstilling³, stimulering van de

eetlust⁴, de regulatie van vruchtbaarheid⁵, neurobescherming⁶, geheugenconsolidatie en extinctie⁷, evenals antidepressieve⁸ en angstreducerende⁹ werkingen.

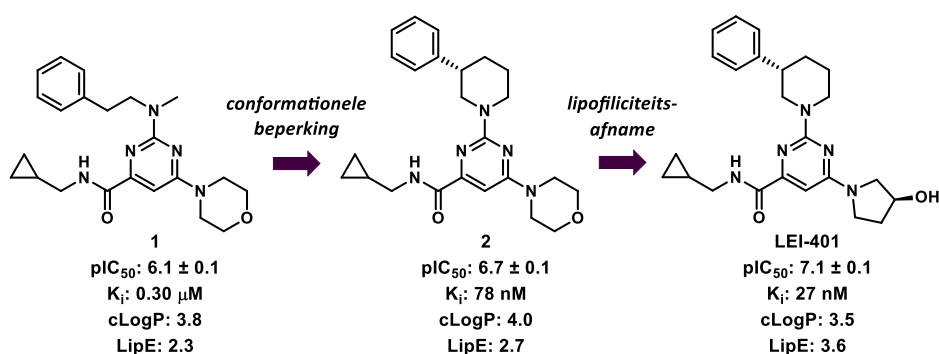
Tevens wordt in **Hoofdstuk 1** behandeld wat de therapeutische mogelijkheden zijn van het aanpassen van endogene NAE-niveaus, inclusief anandamide, met bijzondere aandacht voor het *verlagen* van NAEs. Bij meerdere ziektes zijn NAEs en hun metabole enzymen verstoord. Deze verstoringen zijn gerelateerd aan de ernst van het ziektebeeld, onder andere bij obesitas¹⁰, metabool syndroom¹¹, lever-¹² en bloedkanker¹³ en levercirrose¹⁴. Klinisch en preklinisch onderzoek heeft aangetoond dat farmacologische remming van de CB₁ receptor of andere NAE-receptoren effectief kan zijn bij de behandeling van deze aandoeningen. Helaas bleek dat de inhibitie van de CB₁ receptor in de hersenen ernstige psychologische bijeffecten kan geven en om die reden is het obesitasmedicijn rimonabant van de markt gehaald. Momenteel wordt remming van de CB₁ receptor enkel in de periferie onderzocht als nieuwe therapeutische strategie.¹⁵ Inhibitie van de biosynthetische enzymen van NAEs kan een geschikt alternatief zijn om deze ziektes te behandelen. Een bijkomend voordeel hiervan is partiële remming van de desbetreffende receptor, aangezien de NAE-receptoren ook andere endogene liganden hebben die hun signaalfunctie blijven vervullen. Dit kan leiden tot een betere afstemming van het gewenste effect en vergroting van de therapeutische breedte. Tot dusver zijn er geen farmacologische middelen om NAE-niveaus te verlagen in cel- of diermodellen waardoor dit onderzoek nog in de kinderschoenen staat. Nieuwe remmers voor de biosynthetische enzymen van NAEs zijn dus nodig om de signaleringsfuncties van NAEs te kunnen bestuderen in modellen van ziekte en gezondheid.

Ontwikkeling van *in vivo* actieve NAPE-PLD remmers

De afbraak van anandamide door het enzym vetzuuramide hydrolase (FAAH) is uitvoerig onderzocht met behulp van genetische en farmacologische modellen. Daarentegen is het tot op heden onduidelijk hoe de biosynthese van anandamide is gereguleerd.¹⁶ NAPE-PLD, een zink hydrolase, wordt beschouwd als het enzym dat hoofdverantwoordelijk is voor de productie van NAEs waaronder anandamide. Verschillende NAPE-PLD *knockout* muismodellen lieten echter een spreiding zien in de mate van anandamideverlaging in de hersenen, met slechts een significant resultaat in twee van drie uitgekomen studies.¹⁷⁻¹⁹ Als verklaring zijn compensatiemechanismen voorgesteld die gedurende de ontwikkeling kunnen optreden.¹⁷ Bovendien zijn alternatieve biosyntheseroutes van NAEs ontdekt die mogelijk kunnen compenseren voor het gemis van NAPE-PLD.¹⁶ Om anandamide beter te bestuderen zijn daarom farmacologische gereedschappen noodzakelijk waarmee de

biosynthese van anandamide acuut kan worden geblokkeerd. Tot nu toe zijn voor NAPE-PLD dergelijke gereedschappen niet beschikbaar.

In **Hoofdstuk 2** is gestart met de zoektocht naar nieuwe chemotypes die NAPE-PLD kunnen remmen door middel van *high-throughput screening* (HTS). Hiervoor is een op fluorescentie gebaseerde NAPE-PLD activiteits-*assay* gebruikt, die geoptimaliseerd is om een dergelijke HTS uit te kunnen voeren. In deze *assay* wordt het substraat PED6 gebruikt, dat door NAPE-PLD kan worden gehydrolyseerd zodat een fluorofoor vrijkomt. De toename in fluorescentie kan worden gemeten en is proportioneel met de enzymatische activiteit van NAPE-PLD. De HTS-campagne startte met het screenen van een bibliotheek van ~350,000 stoffen bij een concentratie van 10 μM . Nadat de initiële *hits* waren bevestigd, zijn er dosis-respons experimenten en twee deselectie-*assays* uitgevoerd, waarbij is gefilterd op zink chelatoren en fluorescentie *quenchers* (uitdoovers). Dit resulteerde in vijf *hit*moleculen. Uit deze verbindingen is pyrimidine-4-carboxamide **1** (Figuur 1) gekozen om te worden hergesynthetiseerd, vanwege zijn gunstige potentie, goede fysicochemische eigenschappen, en relatief eenvoudige synthese. Stof **1** kon worden bevestigd als NAPE-PLD remmer met submicromolaire activiteit. Verder was **1**, wat betreft het endocannabinoïde systeem (ECS), selectief voor NAPE-PLD *in vitro*, aangezien geen *off-target* activiteit voor deze receptoren en enzymen werd gevonden. Verbinding **1** kan dus als nieuw beginpunt worden beschouwd om *in vivo* actieve NAPE-PLD remmers te ontwikkelen.



Figuur 1. De gebruikte strategie om *hit* verbinding **1** te optimaliseren naar NAPE-PLD remmer **LEI-401** met verbetering van potentie en lipofiliciteit. cLogP is berekend met Chemdraw 15. Lipofiele efficiëntie (LipE) = $\text{pIC}_{50} - \text{cLogP}$.

De optimalisatie van stof **1** is beschreven in **Hoofdstuk 3**. Hierin wordt een studie naar de structuur-activiteitsrelatie van **1** behandeld om de potentie en lipofiliciteit te

verbeteren. Verbinding **LEI-401** is geïdentificeerd nadat 104 analogen van **1** waren gesynthetiseerd. Deze optimale verbinding remt NAPE-PLD bij nanomolaire concentraties. Conformationele beperking van de *N*-methylfenethylamine van **1** naar een (*S*)-3-fenylpiperidine zorgde voor een viervoudige toename van de activiteit (verbinding **2**, Figuur 1). De vervanging van de morfoline van **1** met een (*S*)-3-hydroxypyrrolidine (**LEI-401**) verhoogde de potentie verder en verminderde tegelijk de lipofiliciteit. **LEI-401** bezit gunstige fysicochemische eigenschappen zoals een redelijke lipofiele efficiëntie (LipE) en laag topologisch polair oppervlak (tPSA) en is hierdoor geschikt om cellulaire en *in vivo* studies uit te voeren.

In **Hoofdstuk 4** is onderzocht of **LEI-401** een bindingsinteractie aangaat met NAPE-PLD in levende cellen, het zogeheten *target engagement*. Hiervoor is een strategie gekozen op basis van fotoaffiniteitlabeling (PAL), dat een veelgebruikte techniek is om eiwit-molecuul interacties aan te tonen, bijvoorbeeld bij metallohydrolases.²⁰ Bij PAL bindt een fotoaffiniteitprobe covalent aan het desbetreffende eiwit nadat deze is beschenen met uv-licht. Vervolgens kan met behulp van gel of *chemical proteomics* methodes het eiwit worden gevisualiseerd en geïdentificeerd. Met een remmer kan in een competitie-experiment de probe-eiwit labeling worden verdrongen, dat het bewijs levert van *target engagement*. Twee ontwerpen van fotoaffiniteitprobes zijn uitgewerkt. Het eerste ontwerp bestond uit *mimics* van het endogene substraat van NAPE-PLD, de NAPes. Bij deze verbindingen werd een diazine *photocrosslinker*, een gestabiliseerde fosfordiester bioisosteer en een alkyn 'haakje' voor klikchemie ingebouwd. Deze moleculen hadden lage affiniteit voor NAPE-PLD in de *in vitro* activiteits-assay en konden NAPE-PLD niet visualiseren in humane embryonale niercellen (HEK293T) waarin dit eiwit tot overexpressie was gebracht. Een tweede ontwerp ging uit van de bibliotheek van NAPE-PLD remmers beschreven in Hoofdstuk 3, om hiermee een fotoaffiniteitprobe te maken met een pyrimidine-4-carboxamide *scaffold*. Probe **3** had een submicromolaire potentie voor NAPE-PLD en liet efficiënte labeling van dit eiwit zien in getransfecteerde HEK293T cellen. Door middel van competitie-experimenten op gel en via *chemical proteomics* kon *target engagement* van **LEI-401** met NAPE-PLD worden vastgesteld in levende cellen.

Hoofdstuk 5 beschrijft de verdere profilering van **LEI-401** in cel- en diermodellen. Eerst werd de selectiviteit van **LEI-401** bepaald voor de receptoren en enzymen van het ECS, waaruit bleek dat **LEI-401** een selectieve NAPE-PLD remmer is. Lipidenmetingen in neuronale cellen van muizen toonden aan dat **LEI-401** NAE-niveaus kan verlagen in wildtype cellen, maar niet in NAPE-PLD *knockout* cellen. Vanwege dit positieve resultaat is **LEI-401** getest in C57BL/6J muizen. Hieruit bleek dat deze stof een gunstig farmacokinetisch (PK) profiel bezit. Twee uur na toediening van een enkele

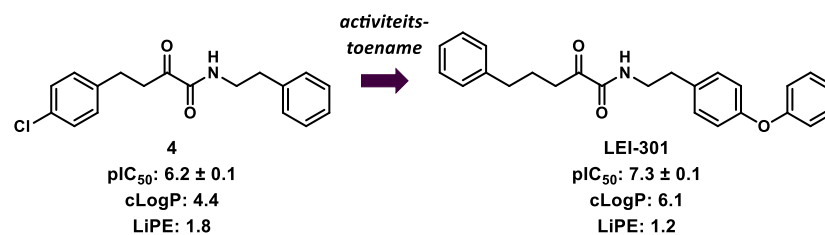
intraperitoneale dosis (30 mg/kg) werden hoge niveaus van **LEI-401** gemeten in het bloedplasma en de hersenen. Bovendien werd een tijd- en dosisafhankelijke verlaging van anandamide gemeten, in overeenstemming met het PK-profiel. Dit duidt er op dat **LEI-401** een *in vivo* actieve NAPE-PLD remmer is die de bloed-hersenbarrière gemakkelijk passeert. Daarnaast onderstreept het de rol van NAPE-PLD bij de biosynthese van anandamide in de hersenen. Om de farmacologische effecten van acute anandamideverlaging in de hersenen te bepalen, werd **LEI-401** getest in verschillende gedragsassays. Hieruit bleek dat **LEI-401** een pijnverlagende werking heeft in C57BL/6J muizen. Hiernaast zorgt **LEI-401** ook voor vermindering van beweging en verlaging van de lichaamstemperatuur. Deze effecten waren niet gemedieerd door de CB₁ receptor. Tot slot werd in een muismodel van inflammatoire pijn vastgesteld dat **LEI-401** allodynie, opgewekt door lipopolysaccharide (LPS), volledig kan omkeren. Tezamen tonen deze experimenten aan dat **LEI-401** analgetische eigenschappen bezit die van therapeutisch nut kunnen zijn. Vervolgstudies zijn noodzakelijk waarbij **LEI-401** wordt toegediend aan NAPE-PLD *knockout* muizen om vast te stellen of deze gedragseffecten afhankelijk zijn van NAPE-PLD.

Ontwikkeling van remmers van de calcium-onafhankelijke NAPE-biosynthese

De productie van NAPes door een *N*-acyltransferase (NAT) activiteit wordt algemeen beschouwd als de snelheidsbepalende stap van de NAE-biosynthese.^{21,22} In de afgelopen jaren zijn, naast de canonieke Ca²⁺-afhankelijke route voor de vorming van NAPes, ook nieuwe calcium-onafhankelijke enzymen ontdekt.¹⁶ Met name het eiwit PLAAT2 heeft *in vitro* hoge *N*-acyltransferase activiteit volgens eerdere studies.²³ Tot op heden zijn er geen farmacologische gereedschappen beschikbaar om PLAAT2-activiteit in cellen te moduleren. In **Hoofdstuk 6** is gebruik gemaakt van een recent beschreven ABPP-*assay*²⁴ om een kleine bibliotheek van lipaseremmers te testen op inhibitie van PLAAT2. Verbinding **4** is hierbij geïdentificeerd als de meeste potente stof van een serie α -ketoamide remmers (Figuur 2).

Analyse van de structuur-activiteitrelatie van het α -ketoamide *scaffold* resulteerde in de geoptimaliseerde remmer **LEI-301**, waarmee een dertienvoudige toename in potentie was bereikt vergeleken met stof **4**. **LEI-301** toonde vergelijkbare activiteit voor de andere eiwitten in de PLAAT familie, maar remde de receptoren en overige enzymen van het ECS niet. Vervolgens zijn lipidenmetingen uitgevoerd met humane osteosarcoma (U2OS) cellen getransfecteerd met PLAAT2. Dit zorgde voor een zeer grote toename van de

NAE-niveaus. Behandeling met **LEI-301** gaf een significante verlaging van de meeste NAEs, specifiek in de PLAAT2 overexpressiecellen maar niet in de controlecellen. Hiermee is aangetoond dat **LEI-301** cellulair PLAAT2 kan remmen en dat PLAAT2 zelf een belangrijke bijdrage kan leveren aan de biosynthese van NAEs. Daarbij zijn de α -ketoamides een nieuwe klasse van remmers die, in celmodellen, verder onderzoek mogelijk maken naar de signaalfuncties van NAEs en NAEs.



Figuur 2. Moleculaire structuren en fysicochemische parameters van α -ketoamide **4** en geoptimaliseerde PLAAT2 remmer **LEI-301**. cLogP is berekend met Chemdraw 15. Lipofiele efficiëntie (LipE) = $\text{pIC}_{50} - \text{cLogP}$.

Slotwoord

Selectieve en *in vivo* actieve remmers zijn essentiële benodigdheden voor het ophelderen van biologische signaleringsnetwerken en de ontwikkeling van nieuwe medicijnen. In dit proefschrift worden nieuwe remmers (**LEI-301** en **LEI-401**), fotoaffiniteitprobes en assays beschreven om de enzymen NAPE-PLD en PLAAT2 te bestuderen, die beide betrokken zijn bij de productie van NAEs. Tot nu toe hebben genetische *knockout*-modellen niet volledig de complexiteit van de NAE-biosynthese kunnen verduidelijken, mogelijk door compensatie-effecten die kunnen optreden op de lange termijn. Acute blokkade van deze enzymen met de hierin beschreven farmacologische remmers kan de bijdrage van NAPE-PLD en PLAAT2 aan de vorming van NAEs beter in kaart brengen in specifieke cellen en weefsels. Daarnaast zijn **LEI-301** en **LEI-401** geschikte gereedschappen om de biologische consequenties van NAE-verlaging te onderzoeken. Deze verlaging zou mogelijk een behandeling kunnen opleveren voor aandoeningen als obesitas, metabool syndroom, chronische leverziekte en kanker.

Referenties

1. Devane, W., Hanus, L., Breuer, A., Pertwee, R., Stevenson, L., Griffin, G., Gibson, D., Mandelbaum, A., Etinger, A. & Mechoulam, R. Isolation and structure of a brain constituent that binds to the cannabinoid receptor. *Science* **258**, 1946-1949 (1992).
2. Stelt, M.v.d. & Marzo, V.D. Endovanilloids. *European Journal of Biochemistry* **271**, 1827-1834 (2004).
3. Cravatt, B.F., Demarest, K., Patricelli, M.P., Bracey, M.H., Giang, D.K., Martin, B.R. & Lichtman, A.H. Supersensitivity to anandamide and enhanced endogenous cannabinoid signaling in mice lacking fatty acid amide hydrolase. *Proceedings of the National Academy of Sciences* **98**, 9371-9376 (2001).
4. Williams, C.M. & Kirkham, T.C. Anandamide induces overeating: mediation by central cannabinoid (CB₁) receptors. *Psychopharmacology* **143**, 315-317 (1999).
5. Wang, H., Xie, H., Guo, Y., Zhang, H., Takahashi, T., Kingsley, P.J., Marnett, L.J., Das, S.K., Cravatt, B.F. & Dey, S.K. Fatty acid amide hydrolase deficiency limits early pregnancy events. *The Journal of Clinical Investigation* **116**, 2122-2131 (2006).
6. Eljaschewitsch, E., Witting, A., Mawrin, C., Lee, T., Schmidt, P.M., Wolf, S., Hoertnagl, H., Raine, C.S., Schneider-Stock, R., Nitsch, R. & Ullrich, O. The endocannabinoid anandamide protects neurons during CNS inflammation by induction of MKP-1 in microglial cells. *Neuron* **49**, 67-79 (2006).
7. Morena, M., Roozendaal, B., Trezza, V., Ratano, P., Peloso, A., Hauer, D., Atsak, P., Trabace, L., Cuomo, V., McGaugh, J.L., Schelling, G. & Campolongo, P. Endogenous cannabinoid release within prefrontal- limbic pathways affects memory consolidation of emotional training. *Proceedings of the National Academy of Sciences* **111**, 18333-18338 (2014).
8. Gobbi, G., Bambico, F.R., Mangieri, R., Bortolato, M., Campolongo, P., Solinas, M., Cassano, T., Morgese, M.G., Debonnel, G., Duranti, A., Tontini, A., Tarzia, G., Mor, M., Trezza, V., Goldberg, S.R., Cuomo, V. & Piomelli, D. Antidepressant-like activity and modulation of brain monoaminergic transmission by blockade of anandamide hydrolysis. *Proceedings of the National Academy of Sciences* **102**, 18620-18625 (2005).
9. Kathuria, S., Gaetani, S., Fegley, D., Valiño, F., Duranti, A., Tontini, A., Mor, M., Tarzia, G., Rana, G.L., Calignano, A., Giustino, A., Tattoli, M., Palmery, M., Cuomo, V. & Piomelli, D. Modulation of anxiety through blockade of anandamide hydrolysis. *Nature Medicine* **9**, 76 (2002).
10. Fanelli, F., Mezzullo, M., Repaci, A., Belluomo, I., Ibarra Gasparini, D., Di Dalmazi, G., Mastroberto, M., Vicennati, V., Gambineri, A., Morselli-Labate, A.M., Pasquali, R. & Pagotto, U. Profiling plasma *N*-acylethanolamine levels and their ratios as a biomarker of obesity and dysmetabolism. *Molecular Metabolism* **14**, 82-94 (2018).
11. Bowles, N.P., Karatsoreos, I.N., Li, X., Vemuri, V.K., Wood, J.-A., Li, Z., Tamashiro, K.L.K., Schwartz, G.J., Makriyannis, A.M., Kunos, G., Hillard, C.J., McEwen, B.S. & Hill, M.N. A peripheral endocannabinoid mechanism contributes to glucocorticoid-mediated metabolic syndrome. *Proceedings of the National Academy of Sciences* **112**, 285-290 (2015).
12. Mukhopadhyay, B., Schuebel, K., Mukhopadhyay, P., Cinar, R., Godlewski, G., Xiong, K., Mackie, K., Lizak, M., Yuan, Q., Goldman, D. & Kunos, G. Cannabinoid receptor 1 promotes hepatocellular carcinoma initiation and progression through multiple mechanisms. *Hepatology* **61**, 1615-1626 (2015).
13. Masoodi, M., Lee, E., Eiden, M., Bahlo, A., Shi, Y., Ceddia, R.B., Baccei, C., Prasit, P. & Spaner, D.E. A role for oleoylethanolamide in chronic lymphocytic leukemia. *Leukemia* **28**, 1381 (2014).
14. Caraceni, P., Viola, A., Piscitelli, F., Giannone, F., Berzigotti, A., Cescon, M., Domenicali, M., Petrosino, S., Giampalma, E., Riili, A., Grazi, G., Golfieri, R., Zoli, M., Bernardi, M. & Di Marzo, V. Circulating and hepatic endocannabinoids and endocannabinoid-related molecules in patients with cirrhosis. *Liver International* **30**, 816-825 (2010).
15. Tam, J., Hinden, L., Drori, A., Udi, S., Azar, S. & Baraghithy, S. The therapeutic potential of targeting the peripheral endocannabinoid/CB₁ receptor system. *European Journal of Internal Medicine* **49**, 23-29 (2018).

16. Hussain, Z., Uyama, T., Tsuboi, K. & Ueda, N. Mammalian enzymes responsible for the biosynthesis of *N*-acylethanolamines. *Biochimica et Biophysica Acta (BBA) - Molecular and Cell Biology of Lipids* **1862**, 1546-1561 (2017).
17. Leung, D., Saghatelian, A., Simon, G.M. & Cravatt, B.F. Inactivation of *N*-acyl phosphatidylethanolamine phospholipase D reveals multiple mechanisms for the biosynthesis of endocannabinoids. *Biochemistry* **45**, 4720-4726 (2006).
18. Tsuboi, K., Okamoto, Y., Ikematsu, N., Inoue, M., Shimizu, Y., Uyama, T., Wang, J., Deutsch, D.G., Burns, M.P., Ulloa, N.M., Tokumura, A. & Ueda, N. Enzymatic formation of *N*-acylethanolamines from *N*-acylethanolamine plasmalogen through *N*-acylphosphatidylethanolamine-hydrolyzing phospholipase D-dependent and -independent pathways. *Biochimica et Biophysica Acta (BBA) - Molecular and Cell Biology of Lipids* **1811**, 565-577 (2011).
19. Leishman, E., Mackie, K., Luquet, S. & Bradshaw, H.B. Lipidomics profile of a NAPE-PLD KO mouse provides evidence of a broader role of this enzyme in lipid metabolism in the brain. *Biochimica et Biophysica Acta (BBA) - Molecular and Cell Biology of Lipids* **1861**, 491-500 (2016).
20. Lapinsky, D.J. & Johnson, D.S. Recent developments and applications of clickable photoprobes in medicinal chemistry and chemical biology. *Future Medicinal Chemistry* **7**, 2143-2171 (2015).
21. van der Stelt, M., Hansen, H.H., Veldhuis, W.B., Bär, P.R., Nicolay, K., Veldink, G.A., Vliegthart, J.F.G. & Hansen, H.S. Biosynthesis of endocannabinoids and their modes of action in neurodegenerative diseases. *Neurotoxicity Research* **5**, 183-199 (2003).
22. Wang, J. & Ueda, N. Biology of endocannabinoid synthesis system. *Prostaglandins & Other Lipid Mediators* **89**, 112-119 (2009).
23. Uyama, T., Ikematsu, N., Inoue, M., Shinohara, N., Jin, X.-H., Tsuboi, K., Tonai, T., Tokumura, A. & Ueda, N. Generation of *N*-acylphosphatidylethanolamine by members of the phospholipase A/acyltransferase (PLA/AT) family. *Journal of Biological Chemistry* **287**, 31905-31919 (2012).
24. Zhou, J., Mock, E.D., Martella, A., Kantae, V., Di, X., Burggraaff, L., Baggelaar, M.P., Al-Ayed, K., Bakker, A., Florea, B.I., Grimm, S.H., den Dulk, H., Li, C.T., Mulder, L., Overkleeft, H.S., Hankemeier, T., van Westen, G.J.P. & van der Stelt, M. Activity-based protein profiling identifies α -ketoamides as inhibitors for phospholipase A₂ group XVI. *ACS Chemical Biology* **14**, 164-169 (2019).

List of publications

Incorporation of non-natural amino acids improves cell permeability and potency of specific inhibitors of proteasome trypsin-like sites

P. P. Geurink, W. A. van der Linden, A. C. Mirabella, N. Gallastegui, G. de Bruin, A. E. M. Blom, M. J. Voges, E. D. Mock, B. I. Florea, G. A. van der Marel, C. Driessen, M. van der Stelt, M. Groll, H. S. Overkleeft, A. F. Kisselev. *Journal of Medicinal Chemistry* **2013**, *56*, 1262-1275

Design of a highly selective quenched activity-based probe and its application in dual color imaging studies of cathepsin S activity localization

K. Oresic Bender, L. Ofori, W. A. van der Linden, E. D. Mock, G. K. Datta, S. Chowdhury, H. Li, E. Segal, M. S. Lopez, J. A. Ellman, C. G. Figdor, M. Bogyo, M. Verdoes. *Journal of the American Chemical Society* **2015**, *137*, 4771-4777

ortho-Carborane-modified N-substituted deoxynojirimycins

S. Hoogendoorn*, E. D. Mock*, A. Strijland, W. E. Donker-Koopman, H. van den Elst, R. van den Berg, J. Aerts, G. A. van der Marel, H. S. Overkleeft. *European Journal of Organic Chemistry* **2015**, 4437-4446

Enantioselective synthesis of adamantylalanine and carboranylalanine and their incorporation into the proteasome inhibitor bortezomib

G. de Bruin*, E. D. Mock*, S. Hoogendoorn, A. van den Nieuwendijk, J. Mazurek, G. A. van der Marel, B. I. Florea, H. S. Overkleeft. *Chemical Communications* **2016**, *52*, 4064-4067

Cannabinoid CB₂ receptor ligand profiling reveals biased signalling and off-target activity

M. Soethoudt, U. Grether, J. Fingerle, T. W. Grim, F. Fezza, L. de Petrocellis, C. Ullmer, B. Rothenhausler, C. Perret, N. van Gils, D. Finlay, C. MacDonald, A. Chicca, M. D. Gens, J. Stuart, H. de Vries, N. Mastrangelo, L. Z. Xia, G. Alachouzos, M. P. Baggelaar, A. Martella, E. D. Mock, H. Deng, L. H. Heitman, M. Connor, V. Di Marzo, J. Gertsch, A. H. Lichtman, M. Maccarrone, P. Pacher, M. Glass, M. van der Stelt. *Nature Communications* **2017**, *8*

Activity-based protein profiling reveals off-target proteins of the FAAH inhibitor BIA 10-2474

A. C. M. van Esbroeck, A. P. A. Janssen, A. B. Cognetta, D. Ogasawara, G. Shpak, M. van der Kroeg, V. Kantae, M. P. Baggelaar, F. M. S. de Vrij, H. Deng, M. Allara, F. Fezza, Z. Lin, T. van der Wel, M. Soethoudt, E. D. Mock, H. den Dulk, I. L. Baak, B. I. Florea, G. Hendriks, L. de Petrocellis, H. S. Overkleeft, T. Hankemeier, C. I. De Zeeuw, V. Di Marzo, M. Maccarrone, B. F. Cravatt, S. A. Kushner, M. van der Stelt. *Science* **2017**, *356*, 1084-1087

Activity-based protein profiling identifies α -ketoamides as inhibitors for phospholipase A₂ group XVI. J. Zhou, E. D. Mock, A. Martella, V. Kantae, X. Y. Di, L. Burggraaff, M. P. Baggelaar, K. Al-Ayed, A. Bakker, B. I. Florea, S. H. Grimm, H. den Dulk, C. T. Li, L. Mulder, H. S. Overkleeft, T. Hankemeier, G. J. P. van Westen, M. van der Stelt. *ACS Chemical Biology* **2019**, *14*, 164-169

Discovery of an *in vivo* active NAPE-PLD inhibitor that reduces brain anandamide levels and pain behavior

E. D. Mock, M. Mustafa, R. Cinar, V. Kantae, X. Di, Z. V. Varga, J. Paloczi, G. Donvito, A. C. M. van Esbroeck, A. M. F. van der Gracht, I. Kotsogianni, J. K. Park, A. Martella, T. van der Wel, M. Soethoudt, M. Jiang, T. J. Wendel, A. P. A. Janssen, A. T. Bakker, B. I. Florea, J. Wat, H. van den Hurk, M. Wittwer, U. Grether, M. W. Buczynski, C. A. A. van Boeckel, T. Hankemeier, P. Pacher, A. H. Lichtman & M. van der Stelt. *Manuscript submitted*

Discovery and optimization of PLAAT2 α -ketoamide inhibitors that reduce N-acyl ethanolamine production (*working title*)

J. Zhou*, E. D. Mock*, K. Al Ayed, V. Kantae, X. Di, L. Burggraaff, F. Stevens, A. Martella, F. Mohr, M. Jiang, T. van der Wel, T. Wendel, T. Ofman, Y. Tran, N. de Koster, G. van Westen, T. Hankemeier & M. van der Stelt. *Manuscript in preparation*

Optimization of pyrimidine-4-carboxamide NAPE-PLD inhibitors affords LEI-401 (*working title*)

E. D. Mock, I. Kotsogianni, J. Vooijs, C. Fonseca, C. A. A. van Boeckel, M. van der Stelt. *Manuscript in preparation*

** These authors contributed equally*

Patent

Inhibitors of N-acylphosphatidylethanolamine phospholipase D (NAPE-PLD)

E. D. Mock, A. I. Kotsogianni Teftoglou, C. A. A. van Boeckel, M. van der Stelt. PCT/EP2019/064213. Filing date: May 31, **2019**.

Curriculum vitae

Elliot David Mock was born on May 27th 1989 in Amsterdam, the Netherlands. He obtained his high school diploma (VWO-gymnasium) at the Keizer Karel College in Amstelveen in 2007. In the same year, he began his studies for a bachelor's degree in Molecular Science and Technology at Leiden University and Delft University of Technology, which he completed in 2011. In the same year, he started his studies for a master's degree in Chemistry with a specialization in 'Design and Synthesis' which he completed in 2014 *cum laude*.

As part of his master's program, he performed a research internship in the Bio-organic Synthesis group at Leiden University under the supervision of prof. dr. H. S. Overkleeft and prof. dr. G. van der Marel. The research involved synthesis and biological evaluation of glucosylcerebrosidase (GBA1) and proteasome inhibitors that incorporate *ortho*-carborane bioisosteres. A second internship was performed at Stanford University, USA under the supervision of prof. dr. M. Bogyo. Here, near-infrared quenched activity-based probes for cathepsin proteases were developed as non-invasive cancer diagnostics.

He started his doctoral studies in April 2014 in the Bio-organic Synthesis group at Leiden University. After a year he continued this research in the new Molecular Physiology group at Leiden University under the supervision of prof. dr. M. van der Stelt and prof. dr. C. A. A. van Boeckel.

The work described in this thesis was orally presented at the 28th International Cannabinoid Research Society conference (NL, 2018), CHAINS (NL, 2018) and the Oncode Masterclass Day (NL, 2019). Posters were presented at CHAINS (NL, 2014-2017), the Activity-Based Protein Profiling meeting (UK, 2015 and NL, 2017), the EMBO conference (DE, 2018) and the FIGON Dutch Medicine Days (NL, 2019).

Nawoord

Na welgeteld een decennium (afgerond) is het tijd om afscheid te nemen van de Universiteit Leiden. Maar niet voordat ik alle mensen heb bedankt die aan dit proefschrift hebben bijgedragen.

Allereerst wil ik graag mijn beide promotores bedanken, Mario van der Stelt en Stan van Boeckel. Mario en Stan, ik heb erg veel opgestoken van jullie kennis van de medicinale chemie en de ontwikkeling van kandidaat-geneesmiddelen. Mario, ik heb het bovendien altijd bijzonder gewaardeerd dat jij mij ruimte gaf om eigen onderzoeksideeën na te jagen.

Een PhD-kandidaat dient nooit te onderschatten hoeveel werk er meer kan worden verricht met een extra paar handen. Anouk, Rob, Ioli, Karol, Bert en Wouter, heel hartelijk bedankt voor de fijne samenwerking. Zonder jullie bijdrage was dit boekje substantieel dunner geweest! Ook de studenten van de MDD-practica ben ik erkentelijk voor hun inbreng, dat zelfs tot een mooie publicatie heeft geleid.

De collega's van Molphys (heden en verleden) ben ik dankbaar voor de zeer aangename werksfeer, samenwerkingen en borrels. Met plezier kijk ik terug op onze discussies waarbij we elkaars werk stevig, maar ook eerlijk bekritiseerden, wat het altijd beter maakte. Ook de (ex)-Biosyn-collega's wil ik hier bedanken voor gezelligheid in en buiten het lab. Rian, Richard, Bobby, Hans van den Elst, Nico, Hans den Dulk, Dima, Gijs, Fons, Karthick en alle AMA's, dank voor jullie ondersteuning bij al mijn vragen, zuiveringen en metingen.

Naturally, doing science is a team sport. The collaboration with Vasudev Kantae and Xinyu Di of the Thomas Hankemeier lab was instrumental for profiling our inhibitors, for which they are kindly acknowledged. I would like to thank the labs of Aron Lichtman, Pal Pacher, Matthew Buczynski and Ben Cravatt, as well as Matthias Wittwer and Uwe Grether for a fruitful collaboration. This will hopefully provide the field with new tools for an underexplored area of endocannabinoid biology. Ook Jesse Wat en Helma van der Hurk van het Pivot Park Screening Centre in Oss wil ik graag bedanken voor de prettige samenwerking. Lindsey Burggraaff, dank voor je hulp bij het bestuderen van de dockingposes van de verschillende remmers.

Afleiding van het werk kon ik vinden bij dispuutsgenoten en hun vriendinnen, evenals oud-huisgenoten in Leiden en Den Haag. Ik ben jullie allen erg dankbaar voor de onmisbare gezelligheid tijdens diners en feestjes of gewoon zomaar.

Pap, mam en Dionne, graag wil ik jullie bedanken voor jullie steun en vertrouwen.

Tot slot, lieve Eva, we hebben diepe dalen gekend de afgelopen jaren, maar daar hebben we elkaar doorheen gesleept. Ik weet zeker dat er voor ons samen nu grote hoogten zullen volgen. Ik hou van je!